INVESTIGATIONS TO DEVELOP FIELD STABILIZATION METHODS TO MITIGATE SURFICIAL SLOPE FAILURES

by

MINH LE

Presented to the Faculty of the Graduate School of

The University of Texas at Arlington in Partial Fulfillment

of the Requirements

for the Degree of

DOCTOR OF PHILOSOPHY

THE UNIVERSITY OF TEXAS AT ARLINGTON

May 2013

ACKNOWLEDGEMENTS

This project could not have been completed without the guidance and persistent help of so many important and special people.

First and foremost, I would like to express my earnest thanks to my academic advisor, Prof. Anand J. Puppala for his valuable guidance and constant motivation. He has been a philosopher, a mentor and yet a friend throughout my stay here at UTA, and the success and final outcome of this project can be directly attributed to his efforts to ensure that my research progressed successfully and smoothly. I owe my profound gratitude to him for his endless support during my time spent here at UTA.

I also heartily thank Dr. Laureano Hoyos, Dr. Xin-Bao Yu, Dr. Shih-Ho Chao and Dr. Chien-Pai Han for their willingness to serve on my examination committee. Their advice and concepts explained to me about soil mechanics, earth structures and statistical analysis of data and various other intricate concepts were vital to my research.

In addition, I would like to thank the Chair of the Civil Engineering Department and Dr. Anand J. Puppala for their financial support through EGTA fellowships and graduate assistantships.

My gratitude also goes to Al Branch, Kenneth L. McCleskey, Les Perrin and all the engineers and staff associated with the test sections at the Joe Pool Dam and Grapevine Dam. I thank the USACE for giving me uninterrupted access to the dam sites and for allowing me to use relevant information about the dam sites in my research. I thank Team Consultant for providing test procedures and recommendations for Fully Softened Shear Strength testing.

I also want to thank Dr. Dronamraju, who initiated the construction and instrumentation at the Joe Pool Dam and Grapevine Dam sites. His work has inspired and motivated me to continue in his footsteps by doing this research.

My special thanks are due to Dr. Chittoori for his help with slope stability modeling as well as reliability analysis. My extended thanks go to my colleagues Arvind, Dr. Wejrungsikul, Naga, Tom, Ranjan, Gaily, Tejo, Jeff, Justin, and Anil for their help during the field monitoring visits and during laboratory tests.

My sincere thanks to my family, including my parents, Tan Le, Van Le and my brother, Thai Le, for their moral support throughout my stay in USA.

Last, but not the least, from the bottom of my heart, I say a big THANK YOU to Christie, for her understanding and for being there to support me during the long hours that I worked on my dissertation.

April 17, 2013

ABSTRACT

INVESTIGATIONS TO DEVELOP FIELD STABILIZATION
METHODS TO MITIGATE SURFICIAL
SLOPE FAILURES

Minh Le, PhD

The University of Texas at Arlington, 2013

Supervising Professor: Anand J. Puppala

Surficial slope failures induced by rainfall have been studied for many years. Current research supported by The United States Army Corps of Engineers (USACOE) was undertaken at the University of Texas at Arlington on two sites, the Joe Pool Dam and the Grapevine Dam located in the Fort Worth district. The objective of the project was to find the stabilization method that would best mitigate those failures. A testing area of five sections (one control and four treated) was established on each site, with used admixtures of 20%compost, 4%lime with 0.30%polypropylene fibers, 8%lime with 0.15%polypropylene fibers, and 8%lime. Based on the previous analysis (Dronamraju et al., 2008), the 8%lime with 0.15%fibers was found to be the most effective admixture for preventing surficial failures. Progress has been successfully reported, based on field performance and numerical modeling, with residual saturated soil

properties. However, studies done by previous researchers have proved that the fully saturated soil conditions do not accurately describe the real soil behavior. The fully softened shear strength is most likely the dominant condition of soil exposed to the wetting and drying cycles. Furthermore, this research highlights the beneficial usage of treatments on slope stability based on the Fully Softened Shear Strength aspect. A complex reliability analysis, based on lab-testing data was also conducted to provide a better assessment of the effectiveness of all the treatments on slope stability.

TABLE OF CONTENTS

LIST OF FIGURES

LIST OF TABLES

CHAPTER 1

INTRODUCTION

1.1 Preamble

High plasticity clay soils are prevalent in the North Central Texas area, a result of weathering products of limestone material and alluvial deposits. Formations of expansive clay shale are also present in this region. Construction of several U.S. Army Corps of Engineers rolled earthfill embankment dams in the area, including Bardwell, Grapevine, and Lewisville, utilized on-site soils as borrow materials, which invariably included the high plasticity clays and clay shale. Clay soils tend to shrink during drying and swell during wetting. Repeated weathering (wetting-drying) cycles have produced desiccation cracking within high plasticity fill materials that allows greater exposure of the fill to saturation from precipitation and reduces the effective stress within the fill (McCleskey, 2005 and Dronamraju, 2008). This has resulted in numerous frequent shallow and medium “skin slide” failures at these embankments.

Historically, the skin slide failures have been repaired by removing the soil within the failure block and replacing it with the same soil with adequate compaction. Based on a review of previous skin slides at Bardwell, Grapevine, and Lewisville dams, repair costs for these failures range from $10,000 for temporary repairs to well over $100,000 per slide for more thorough repairs. The frequency and recurrence of failures increase the operation and maintenance costs for these dams resulting in a mixed success (McCleskey, 2005).

Previous research studies have investigated the effects of utilizing lime-treated fill and lime-treated fill with fibers as admixtures to mitigate slope failures. Joe Pool Dam and Grapevine Dam were selected as test sites for implementation (McCleskey, 2005 and

Dronamraju, 2008). With progress reported in field performance for the short period of time, Dronamraju (2008) also conducted a numerical analysis based on the residual strength of soil. The proposed research study would further examine this aspect to fully understand the long term slope stability issues with the treated soil covers from the fully softened shear strength point of view and, at the same time, provide continuous monitoring on the field performance. The present dissertation research is being conducted at The University of Texas at Arlington (UTA) with the financial support from the United States Army Corps of Engineers (USACE), Fort Worth district. If successful, the proposed study will establish more efficient methods to repair future slides and will also provide more efficient construction techniques for future earthfill embankments while utilizing local soil sources that will ensure long-term stability, prevent slide recurrence and reduce slope repair related maintenance costs.

1.2 Research Objectives

Slope failures in clay soils cause damage annually on dams, highway embankments and cut slopes and necessitate difficult and expensive repairs that negatively impact maintenance budgets, traffic flow, and the environment. The use of peak strength in the analysis tends to overestimate the factor of safety, and the use of residual shear strength in the analysis tends to underestimate the safety factor. The use of fully softened shear strength values results in a more accurate analysis and leads to newer design or repair methods that provide long-term stability at reasonable costs. Understanding the mechanisms of these slope failures and being able to economically predict the fully softened shear strength of clay soils is key to successful design, repair, and stabilization of clay slopes.

There are three main objectives of this research. The first objective is to study the surficial treatments on surficial slope stability by studying the instrumented test sections over longer time periods. The second objective is to study the potential utilization of fully softened shear strength measurements and their application in assessing the surficial slope stability. The third objective is to include reliability information in the present analysis. The results of this study

are expected to develop a reliable solution to address the problem of surficial slope instability for long term performance.

1.3 Research Tasks

The following tasks will be performed to accomplish the above mentioned research objectives.

- One of the research needs coming from Dronamraju's (2008) work is to address the long term performance of these surficial slope treatments. This present research has been aimed at collecting the data for this task. Data collections currently ongoing, and so far, four years of monitoring data is available for the Joe Pool Lake dam test sections and two years for the Grapevine dam test sections. The researcher has been visiting the test sites for the last 26 months for the data collection tasks. Field monitoring includes conducting elevation surveys, slope inclination, observation for cracks with the help of digital images and carrying out image analysis studies.
- Conducting tests on Fully Softened Shear Strength (FSS) to further understand the softening condition of clay soil under wetting-drying cycles. The two commonly used devices to test FSS, Direct Shear and Torsional Ring Shear apparatus were adopted to accomplish this task.
- Analyzing the field monitored data from various instrumentations, using statistical tools. Selection of the best field performing additive(s) by conducting a detailed analysis of the field monitoring data and analytical studies.
- Slope Stability analysis using SLOPE/W to assess the factor of safety (FOS) in terms of FSS. The results are compared under three conditions: no rainfall, long-term rainfall and wetting and drying cycles (FSS condition).
- Analytical and reliability analyses for slope stability based on the FSS testing results. This will address the possible variability of the results based on the outcome of FOS values.

- Final comparison of all treatments from both the field performance aspect and the reliability of FSS. Discussion of feasibility for large scale implementation in the field for prevention of surficial failures of slopes of earthfill dams and extending the results of this research to highway embankments and cut slopes.

1.4 Organization of Dissertation

The dissertation consists of 7 chapters. The units indicated are mostly English units and the results in SI units are indicated in parenthesis wherever feasible. Some of the graphs and the drawings were prepared originally in English units and the same are presented here with no alterations.

Chapter 1 consists of the introduction of the surficial failures and the proposed methodology of conducting research aimed at the mitigation of surficial failures by preventing desiccation cracking and improving the shear strength of soil.

Chapter 2 is comprised of a review of literature relevant to the problems of natural and engineered slopes, slope engineering dealing with design aspects and stability analysis. Details of previous research are also presented in the areas of rainfall-induced slope failures, influence of soil suction on slope stability, typical case studies of slope failures, slope stability methodologies and current practices of Fully Softened Shear Strength on slope stabilization.

Chapter 3 provides the entire laboratory program conducted on the borrow soil samples of Joe Pool Dam and Grapevine Dam from basic soil properties testing to more advanced test on Fully Softened Shear Strength. All the tests were repeated on the field samples obtained from test sections using standard procedures from ASTM and the recommendations of the USACE. Previous basic laboratory tests from Dronamraju (2008) were also briefly summarized in this chapter.

Chapter 4 briefly reviews the construction and instrumentation on the test sites. The main focus of Chapter 4 is the updated field data collected from the Joe Pool Dam and Grapevine Dam test sections from the period of time the researcher started his research. The

data collected from the moisture probes, temperature probes, elevation and inclinometer surveys are presented in the form of tables and figures. The nomenclature used for each test section is control, 20%compost, 4%lime with 0.30%fibers, 8%lime with 0.15%fibers and 8%lime treated sections. Observation of desiccation crack and vegetation growth on test sections is also presented. Each treatment type is ranked based on the raw field data and details summarized.

Chapter 5 presents the results of FSS testing using the Direct Shear (DS) and Torsional Ring Shear (TRS) devices. Values of FSS cohesion and FSS friction angle are interpreted using the average strength envelope recommended by most researchers. The differences in the results from the DS and TRS devices are compared and discussed. Improvement of the treated soils over the control soil is shown based on the enhancement of FSS soil properties namely FSS cohesion and FSS friction angle.

Chapter 6 presents the statistical analysis of field monitoring data collected from Joe Pool and Grapevine Dams. Statistical analysis is mainly performed to study the significant differences of field performance data between untreated and treated soils. Performance data including embedded soil temperature, soil moisture content and soil movements in both lateral and horizontal directions collected from the inclinometer and elevation surveys is analyzed. The Student's t-test using the Dunnett's procedure was chosen as the comparison test to carry out this analysis based on the amount of data points collected during the years of monitoring. A ranking summary is presented based on the results of significant difference student's t-test.

Chapter 7 presents the analytical and reliability based slope stability modeling studies using SLOPE/W software to address the slope stability issue from the deterministic and probabilistic points of view. Deterministic slope stability analysis is carried on using the FSS soil properties obtained in laboratory testing in Chapter 5. The model simulates three soil conditions: (1) No rainfall (2) Long-term rainfall and (3) Wetting and drying cycles (FSS condition) with the

application of peak undrained soil strength, residual soil strength and FSS soil strength respectively. FOS values for each condition are presented and compared in this chapter.

Chapter 7 also provides reliability analysis of FSS testing to address the variability of FSS cohesion and FSS friction angle as well as their combined effect on the outcome of FOS. Monte Carlo simulation in SLOPE/W software was utilized to complete this task. The values of the mean and standard deviation of FSS cohesion and FSS friction angle are determined from the FSS results of original tests in Chapter 5, as well as repeated tests conducted under the same conditions. Ranking analysis is conducted based on the analytical and reliability studies to compare the performance of the treated and untreated soil sections.

Chapter 8 presents the summary of the research study, conclusions drawn from the analysis of field data and the analytical/ reliability analyses, as well as recommendations for further research.

After Chapter 8, a list of references indicating the source of information for all the above chapters is presented, along with two appendices containing all the results that could not be presented in the main body of the thesis due to the space limitation.

CHAPTER 2

LITERATURE REVIEW

2.1 Introduction

Slopes may be either engineered or natural. Engineered slopes include mainly embankments, cut slopes and retaining walls (Abramson et al. 2001). Slope engineering basically involves engineering sustainable slopes made of both soil and rock material. It involves design, monitoring, construction, maintenance and repairs to the slopes in a safe, effective and economical manner (Abramson et al. 2002).

An essential part of slope engineering is a comprehensive slope stability analysis. The primary purpose of a slope stability analysis is to contribute to the safe and economic design of man-made slopes of excavations, highway and railway embankments, cut slopes, landfills and spoil heaps (Abramson et al. 2002). This chapter provides a detailed insight into the various important aspects of slope stability evaluations, including landslides and failure of dam and highway embankment slopes with a specific emphasis on the surficial failures. Also a few common methodologies to calculate slope stability based on the current state of the art are highlighted.

The cause of slope instability is also analyzed in detail with the focus on surficial failures caused by two triggering factors: desiccation cracks and rainfall. Case histories are presented to elaborate more on the phenomenon. This chapter also introduces the concept of Fully Softened Shear Strength (FSS) for clay subjected to wetting-drying cycles.

Slope failure remediation methods are also discussed. The effects of utilizing lime, fibers and compost are investigated, and, if successful will, establish more efficient methods to repair future landslides.

2.2 Engineering Slopes

Engineered slopes can be characterized into three main categories: Embankments, cut slopes and retaining walls (Abramson et al., 2001).

2.2.1 Embankments

An embankment dam is literally described as a massive water barrier, typically constructed by the placement and compaction of various compositions of soil, sand, clay and/or/rock. The engineering properties of materials used in these structures are dictated by the borrow source grain size distribution, the methods of construction and the degree of compaction (Abramson, 2001).

(a) (b)

Figure 2.1.(a) Embankment Mica Dam, Canada; (b) Tataragi Dam, Japan (www.wikipedia.org)

Embankment slopes are designed based on shear strength parameters tested on samples, which were compacted under the same design density. Slope stability issues of embankment and fill do not often associate with the same level of uncertainties and difficulties as natural slopes because fill material was used with the preselected properties (Abramson, 2001).

General construction method for embankment is layer-building. Analyses are incorporated in all steps as follows (Abramson et al. 2001):

- All phases of construction
- The end of construction, i.e. a short-term condition
- The long-term condition as represented by a slope served for a long period
- Natural disturbances such as flooding and earthquakes
- Rapid drawdown (for water-retaining structures like earth dams)

Embankment fills are most commonly made of:

- Cohesionless soils (sands and gravels)
- Cohesive soils (silts and clays)
- A mixture of cohesionless and cohesive soils, gravels, and cobbles (herein called earth-rock mixtures)

2.2.2 Cut Slopes

Shallow and deep cuts are important in civil engineering projects. The main target is to design a slope with such a height and steepness that it is stable for the required life span and with as much economy as possible. The design is influenced by the purposes of the cut, geological conditions, in situ material properties, seepage conditions, possibility of flooding and erosion, and the method of construction, as well as the purpose of a particular cutting (Abramson,2001; Chowdhury, 2010).

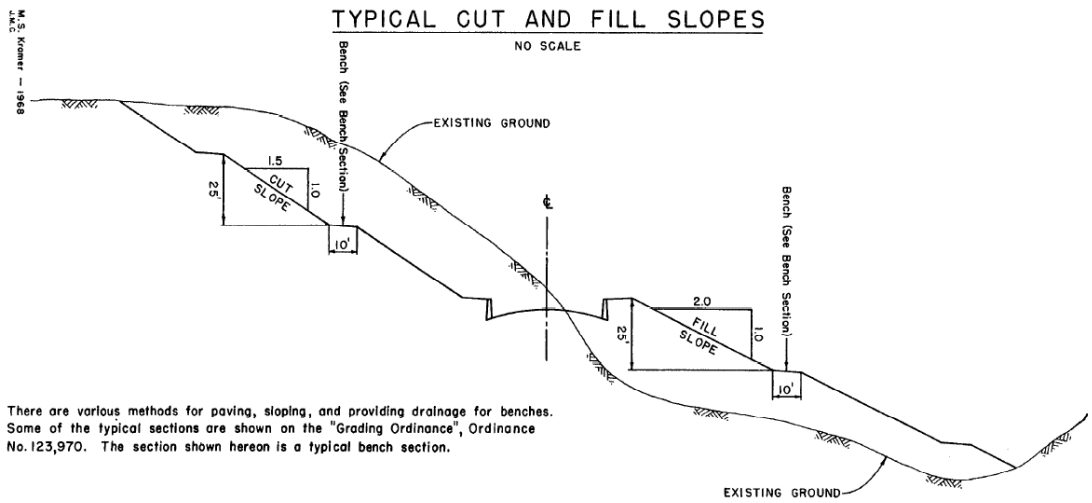

Figure 2.2. Cut and Fill Slopes (Kramer, 1968)

Steep cuts are necessary, but should always be subject to design scrutiny. In some situations, designers must consider methods to prevent immediate and sudden failure, as well as to protect the slope over the long term. The most well-known case history is the failure of a cut slope in London clay studied by Skempton (1977). The factor of safety for the slope was calculated based on undrained soil properties representing short-term loading conditions. The negative pore pressures generated during excavation dissipates with time, which means the shear strength of the soil medium will decrease at long-term drained conditions and as a result, the slope will experience failure. This loss of strength has been theorized to be time-dependent related to the rate of dissipation of negative pore pressure (Abramson, 2001). McGuffey (1982) proposed an estimation of time to failure:

$$t = \frac{h^2 \times T_{90}}{C_v} \qquad \text{Eq. 2-1}$$

where

$t -$ time to failure

$h -$ average distance from the slope surface to the depth of the maximum negative pore pressure

$T_{90} -$ time factor for 90% consolidation (0.848)

$C_v -$ coefficient of consolidation (square feet per day)

For soil cuts, it's very important to obtain soil samples in order to perform laboratory soil index tests such as grain size analysis, moisture content and Atterberg Limits. Along with in situ testing, sampling should be performed for the purpose of cut stability assessment (Samtani, 2006).

2.2.3 Retaining Structures

Earth retaining structures or systems are used to hold back the earth and maintain a difference in the elevation of the ground surface. The retaining wall is designed to withstand the forces exerted by the retained ground or "backfill" and other externally applied loads, and to

transmit these forces safely to a foundation and/or to a portion of the restraining elements, if any, located beyond the failure surface. According to Abramson (2001) there are 4 different types of retaining structures as shown in Figure 2.3.

- Gravity walls (e.g., masonry, concrete, cantilever, or crib walls) are generally in trapezoidal shape and constructed of mass concrete. The wall relies on self-weight against overturning and sliding due to lateral stresses of the retained soil. Concrete may as well be reinforced to reduce the amount needed to build the wall as in cantilever, counterforts or buttressed walls.
- Tieback or soil-nailed walls are the in-situ soil reinforcement technique in which passive inclusions (soil nails) are spaced relatively close together (3 to 6ft.) to increase the strength of the soil mass. Construction is executed in a stage manner, from top-down. After each stage of excavation, the nails are inserted, drainage systems are constructed and shotcrete is applied to the excavation face.
- Soldier pile and wooden lagging or sheet pile walls consist of driven, vibrated, or pushed interlocking steel of concrete piles sections. Based on the passive resistance of the soil in front of the wall and the flexural strength of the pile, the whole structure can resist the lateral forces from behind the wall.
- Mechanically stabilized walls employ geosynthetic, geogrid or metallic strips/bars for reinforcement. The reinforcement is placed in horizontal layers between consecutive layers of granular backfill material. Each layer of backfill has at least one compacted lift.

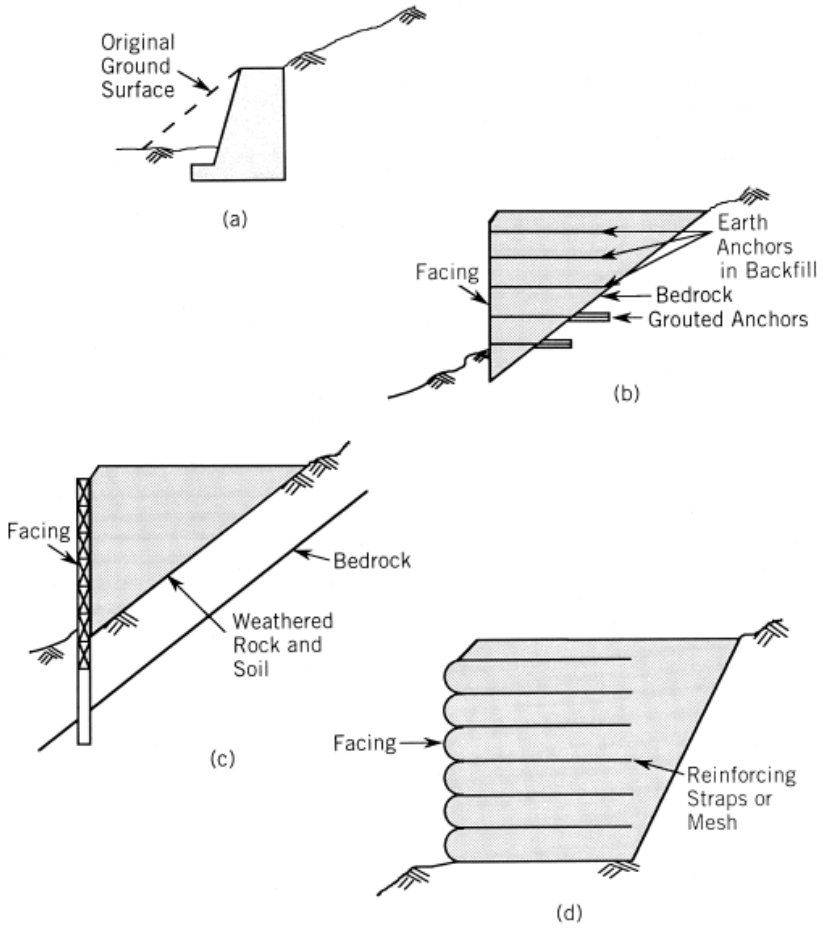

Figure 2.3 Types of retaining structures: (*a*) Gravity retaining wall. (*b*) Tieback retaining wall. (*c*) Sheet pile cantilever wall or soldier pile. (*d*) Mechanically stabilized embankment (Abramson et al, 2001)

2.3 Design of Earthfill Dams

Dams are considered an integral part of the Nation's infrastructure and are significantly beneficial in the development and management of water in river basins. The design of an embankment dam is complicated due to the uncertain factors from foundation and materials available for construction. With the help of past experience, it's confirmed that we can tailor-make the embankment dams to fit the geologic condition and operational requirements for a project. A range of variables is always presented in the detailed analyses to have a better understanding of the sensitivity of the particular analysis to the material properties and geometric characteristics. An earthfill dam is constructed from suitable soils obtained from the

borrow areas or required excavation and compacted in layers by mechanical means according to the “Slope Stability Manual” (2004) by the US Army Corps of Engineers (USACE). Some basic types of earth filled dams are shown in Figure 2.4.

2.3.1 Design Principles

Basic design requirements for earth dams are listed following USACE’s recommendations (1968):

- The embankment slope must be stable under construction and operational conditions, including rapid drawdown in the reservoir.
- The embankment must not induce excessive load on the foundation or abutments.
- Seepage flow through the embankment, foundation and abutments must be controlled so that piping, sloughing or removal of material by solution does not occur. Seepage flow quantities may also be limited by storage considerations.
- Spillways, outlet capacities and freeboard must be sufficient to prevent overtopping; freeboard must account for post construction embankment and foundation settlements.

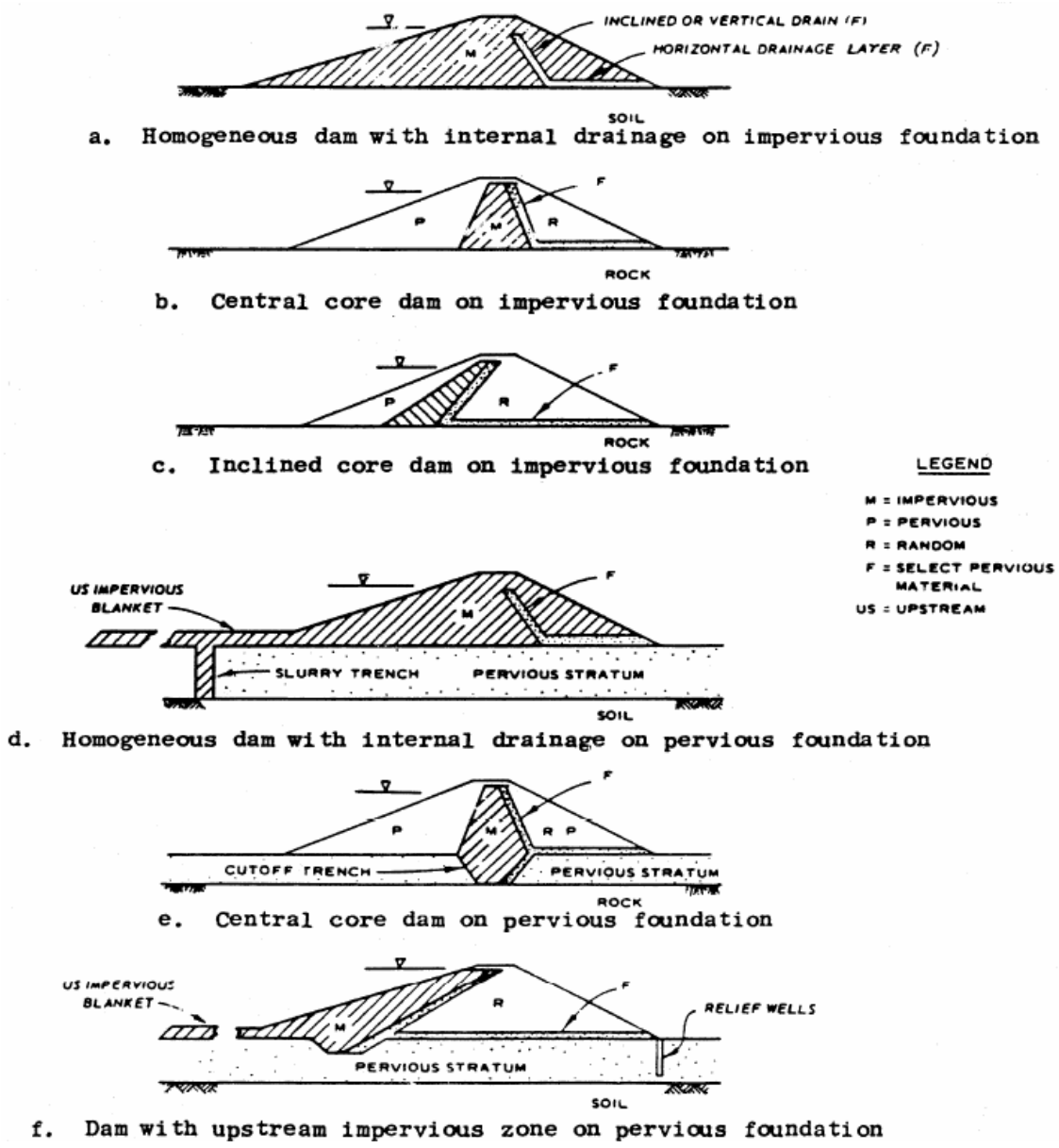

Figure 2.4.Types of earth dam sections (USACE, 2004)

2.3.2 Design Considerations

After conducting an investigation on the dam foundation as well as fill materials, design stages may commence including (but not limited to) those following check-marks:

- Stability of dam body, when slope stability analyses are performed against sliding failure of the embankment. It is also worth noticing that the evaluation of pore-water

pressure during and after construction is necessary, as the shear strength, as well as deformation characteristics of fill materials change. Seismic stability is considered as a case of liquefaction, especially if the dam is located in the seismic active zone. Additional soil dynamic tests are also performed to study soil response characteristics under seismic activities.

- Seepage through embankments and foundations includes seepage analysis on pore-water pressure, leakage through foundation, critical velocity, piping potential, hydraulic gradient and fracture.
- These features should be studied with reference to field conditions and to various alternatives before initiating detailed stability or seepage analyses (USACE).

2.3.3 Unsatisfactory Slope Performance

Unsatisfactory slope performance can occur due to varieties of reasons. Generally they are categorized into 4 types: shear failure, surficial failure, excessive deformation, piping and Internal erosion.

2.3.3.1 Shear Failure

Shear failure is a phenomenon when a soil mass of an embankment or an embankment and its foundation is sliding relative to the adjacent mass (USACE, 2004). Failure surfaces are generally considered to have a circular shape for a better estimation of its stability.

A mass movement event can happen any time when a slope becomes unstable. Triggering events can occur that cause a sudden instability to occur. Most of the time, major triggering events are the main contributors, but it should be noted that it if a slope is very close to instability, only a minor event may be necessary to cause a failure (Nelson, 2011). These major events include:

- Shocks: A sudden shock such as an earthquake, or minor shocks like heavy trucks rambling down the road, trees blowing in the wind, or human made explosions can also trigger mass movement events.

- Changes in hydrologic characteristics: heavy rains can saturate the soil and reduce grain to grain cohesion contact, thus triggering a mass movement event. Heavy rains can also saturate rock and increase its weight. Changes in the groundwater system can increase or decrease fluid pressure in rock and trigger mass movement events.
- Volcanic Eruptions: produce shocks like explosions and earthquakes. They can also cause snow to melt or crater lakes to empty, rapidly releasing large amounts of water that can be mixed with regolith to reduce the grain-to-grain contact and result in debris flows, mudflows, and landslides.

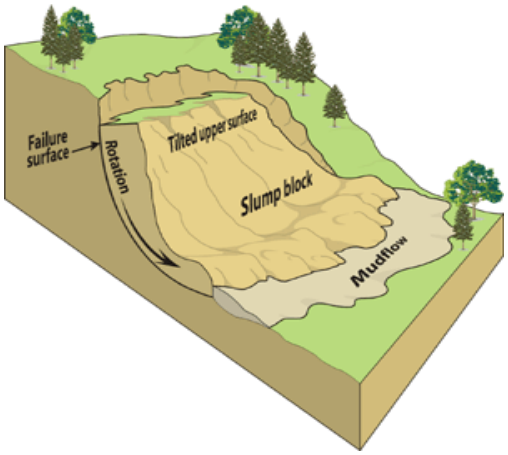

Figure 2.5. Shear Failure (Natural Resources Canada, www.nrcan.gc.ca)

2.3.3.2 Surficial Failure (surface sloughing)

Surficial failures are classified as shallow slope failures as the average depth of failure varies from 1 to 4 ft. (Day, 1996), with only a surficial portion of soil sliding downward. Rahardjo et al., (1994) proved that surficial failure occurs after wetting-drying cycles, when water infiltrates the soil through desiccation cracks and reduces the shear strength of the soil mass. Figure 2.6 shows a typical surficial failure occurred at Bardwell Dam, Texas.

Figure 2.6. Surficial failure at Bardwell Dam (USACE)

Historically, the surficial failures have been repaired by removing the soil within the failure block and replacing it with new compacted soil. The repair costs for these failures range from $10,000 for temporary repairs to well over $100,000 per slide for more thorough repairs. The frequency and recurrence of failures increase the operation and maintenance costs for these dams (McCleskey, 2005).

2.3.3.3 Excessive Deformation

Certain cohesive soils require large strains to reach their peak shear resistance. Thus, at that moment, these soils may deform excessively when loaded. According to USACE, when the strain is larger than 15%, to obtain the peak strength, deformations in embankments are considered excessive. In such cases, it is recommended to use the particular strength at 15% strain rather than the peak strength for embankment design.

Deformation of an embankment, either vertical or horizontal movement, must be estimated during the design stage and be monitored and recorded during the operation of the structure. For this reason, the instrumentation is always initiated along with construction of the embankment, and field investigations are conducted on a regular basis. These investigations may involve such items as surveying and installing movement detecting instruments. Total

station is the most commonly used instrument for observing the vertical movement of the slope. For horizontal deformation, slope indicators (inclinometers) are inserted along the embankment slope. Figure 2.7 shows the typical inclinometer and total station setup.

(a) (b)

Figure 2.7. Field Instrumentation a) Inclinometer b) Total Station

2.3.3.4 Liquefaction

Liquefaction is a phenomenon in which the strength and stiffness of the soil are reduced by shock impact, seismic activities or rapid loading. Liquefaction is responsible for tremendous amounts of damage in historical earthquakes around the world.

In civil engineering, structures are accommodated by the soil strength which they are built upon. Such projects are generally expected to have a long time span of service, with the time varying between weeks to years. Thus, the transfer of the loading from a structure to the soil is at a slow rate, when the soils have enough time to draw water into and out of the voids as they expand or shrink respectively (Coduto, 1998). In this case little or no pore water pressure is generated, as the actual rate of drainage exceeds the rate of loading.

During an earthquake event, with the rapid shaking of the ground, the rate of dynamic loading is much greater than the rate of drainage in soil. This results in the soils not having enough time to drain the water. Consequently, the positive pore water pressure is developed, leading to the decrease of effective stress and soil strength. In the end, if the shear strength

reduces even just slightly below the stress imposed by the foundations of the building, the shear failure of the soil occursd, causing severe damage and, in most instances, failures of the structure. This highlights the importance of evaluating the liquefaction of soils as one of the most critical aspects of Geotechnical Engineering (Coduto, 1998). Figure 2.8 shows the conceptual basics of liquefaction in soil.

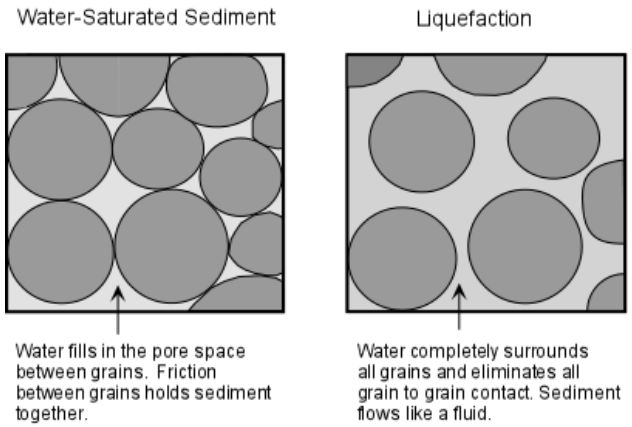

Figure 2.8. (a) Pre- and (b) Post- Liquefaction arrangement of the soil-pore water matrix (Nelson, 2011)

2.3.3.5 Piping and Internal Erosion

An internal erosion of the foundation or embankment caused by seepage is known as piping. In general, the erosion process starts at the downstream toe and goes backwards the reservoir, forming channels or pipes under the dam. The channels or pipes follow paths of maximum permeability and may not develop until many years after construction. If the seepage force is large enough, soil will be carried from the embankment and deposited as sediments in the shape of a cone around the outlet. Sinkholes may develop on the surface of the embankment as internal erosion happens. Emergency procedures, including downstream evacuation, should be initiated if this condition is noted (Ohio Department of Natural Resources, 1994).

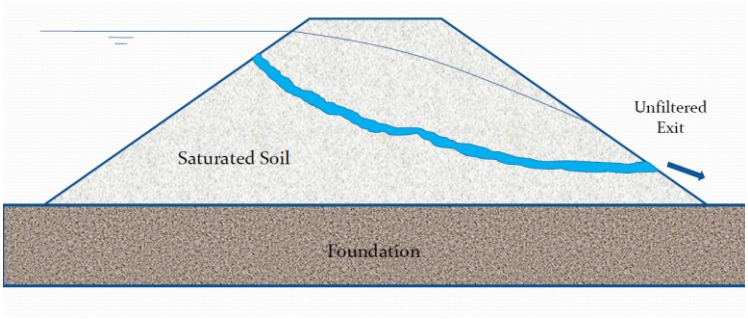

Figure 2.9. Backward Erosion (piping) (Richards, 2012)

The most common case study for piping is the Teton Dam catastrophic failure on June 5, 1976 as it was filling for the first time. The collapse of the dam resulted in the deaths of 11 people and 13000 head of cattle. The dam cost about $100 million to build, and the federal government paid over $300 million in claims related to its failure. Total damage estimates have ranged up to $2 billion (Bureau of Reclamation, 2011)

Figure 2.10. Failure in Teton Dam, 1976 (Bureau of Reclamation, www.usbr.gov)

2.4 Slope Stability Analyses

Evaluation of the slope stability is an important but challenging aspect of civil engineering. Through experiences involving failures important lessons are learned which aid in understanding the causes of failure. As a result better methods are developed. Even though methods may have a solid logical background in mechanics and understanding of the behavior of soils and rocks, it is important to remember that these methods are semi-empirical in nature and they are always subject to further development (Duncan and Wright, 2005).

There has been a tremendous increase in the power of computers and considerable progress has been made in the development of specialized software based on both traditional and sophisticated methods of analysis relevant to slope stability. Nevertheless, choosing an appropriate method to study the slope failure is very crucial to the analysis (Chowdhury, 2010). Efforts should be made to collect field conditions and the failure observations in order to define the failure mechanisms, which determine the method to be used in the analysis.

Slope stability methods can be categorized into the limit equilibrium approach and the numerical solutions, including finite element approach or the finite difference method (Duncan, 2013). The limit equilibrium approach first defines assumed slip surfaces, then the slip surfaces are studied and examined to obtain the factor of safety, which is defined as the ratio between the available resisting moments and the driving moments along the surface. The most critical slip surface is the one that yields the lowest factor of safety. A fFactor of safety that is lower than 1 is considered a failure. The limit equilibrium approach has been established since the early 19th century and is considered the fundamental basis of slope stability. Since then, the approach has been used by most researchers and practitioners. By geometric characteristics of problems, methods using the limit equilibrium approach are subdivided into two-dimensional (2D) and three-dimensional (3D) methods.

Slope stability analysis using numerical solution has a similar failure definition as the limit equilibrium method for the soil mass and does not need simplifying assumptions as it has

the ability to simulate physical behaviors using computational tools. Many methods for slope stability analysis using finite element approach have been studied and presented during the last two decades. Among all those methods, the gravity increase method (Swan and Seo, 1999) and the strength reduction method (Matsui and San, 1992; Griffiths and Lane, 1999) are most commonly used. In the gravity increase method, gravity forces are increased gradually until the slope fails (g_f), then the factor of safety is defined as the ratio between the gravitational acceleration at failure (g_f) and the actual gravitational acceleration (g). In the case of the strength reduction method, soil strength parameters are reduced until the slope reaches an unstable condition; therefore, the factor of safety is determined as the ratio between the initial strength parameter and the critical strength parameter. The gravity increase method is applied to study the stability of embankments during construction since it gives more reliable results in studying the stability of existing slopes. In order to compare the results of limit equilibrium methods with finite element analysis results, the strength reduction method is more suitable since it resembles the limit equilibrium approach more than the gravity increase method (Albataineh, 2006).

In this present research, the limit equilibrium approach from both two-dimensional (2D) and three-dimensional (3D) aspects are thoroughly studied and presented.

2.4.1 2D method

Two dimensional slope stability methods are the most commonly used methods for geotechnical engineers due to their simplicity in calculations. These methods are based on simplifying the 3D problem to a 2D problem, assuming the side effects won't be significant in the third dimension. As a result, the accuracy of two dimensional analyses varies depending on the demand of the geotechnical practitioners.

The method based on limit equilibrium analyzes the stability of the failing soil mass taking into consideration the static equilibrium of the slices as an individual as well as the whole mass overall. The static equilibrium can be obtained in Force, Moment or both of them. Two-

dimensional slope stability methods using the limit equilibrium technique can be divided into circular methods (Swedish Method), the method of slices and noncircular methods.

2.4.1.1 Circular Method (Swedish Method)

A series of trial slip surfaces are generated, with various centers of rotation O and radii R (Figure 2.11) along the slope. Each of the surfaces is analyzed to determine the most critical circle with the lowest factor of safety. This simple circular analysis is suitable to analyze the short-term stability of both homogeneous and inhomogeneous slopes based on the assumptions that a soil mass will fail by rotation about the center and the friction angle is zero so the shear strength is assumed to be obtained only from cohesion. The factor of safety can be determined by calculating the ratio of the resisting moment over driving moment about the center of the circular surface:

$$F = \frac{Resisting\ moment}{Driving\ moment} = \frac{c_u \times L \times R}{W \times x} \qquad \text{Eq. 2-2}$$

where:

c_u - undrained shear strength

R - radius of circular surface

L - length of circular arc

W - weight the soil mass above the circular slip surface

x - horizontal distance between circle center, O, and the center of the gravity of the soil mass

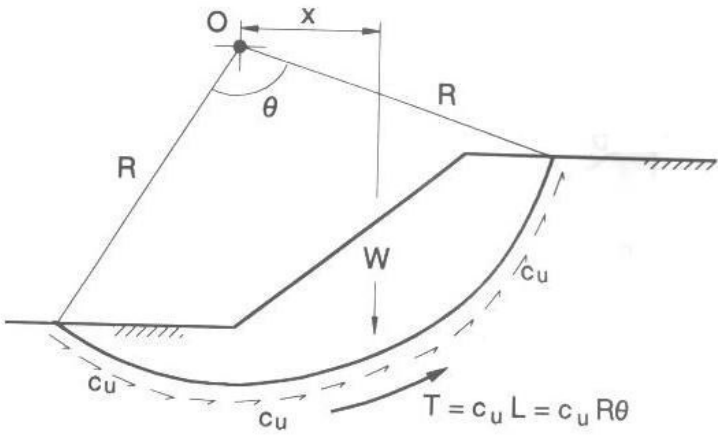

Figure 2.11. Swedish Circle Method (Abramson et al., 1996)

The Circular Method (Swedish Method) has a statically determinate solution with respect to moment equilibrium by assuming that the normal stresses act through the center of the circle and the shear stresses act at the same distance from the center of the circle. Therefore their moment arm is constant and independent of their solution (Albataineh, 2006).

The undrained shear strength around the slip surface is assumed to be constant and independent of the normal stress from the slope surface. In an effective stress analysis, the shear strength on the slip surface is calculated using the effective normal stress by the Mohr-Coulomb failure criterion; therefore, the variation of the normal stress around the failure surface must be considered. This is achieved by the following methods by dividing the failure mass into a number of slices.

2.4.1.2 Method of Slices

The method of slices is the only general method of analysis available for dealing with irregular slopes in non-homogenous soil and rocks in which the values of c and φ are not constant (Chowdhury et al., 2010). The method was created by Fellenius (1927) and Taylor (1937) and has since been modified in many ways in order to extend its practicability and accuracy. In the method of slices, the soil mass above the slip surface is subdivided into a certain number of vertical slices, and the static equilibrium of each of these slices is considered

(Albataineh, 2006). In most variations of the method, the subdivision is based on vertical boundaries of slices, and their widths are not necessarily equal (Chowdhury et al., 2010). The actual number of the slices depends on the slope geometry and, soil profile, as well as the degree of accuracy the analysis requires. However, breaking up the mass into a series of vertical slices does not make the problem statically determinate. The number of unknowns always exceeds the number of known factors. In order to get the factor of safety by using the method of slices, it is necessary to make assumptions to remove the extra unknowns, and these assumptions are the distinguishing aspects of different methods of slices. Some of the most popular methods are described below.

2.4.1.3 Ordinary Method of Slices (Fellenius' method)

This method is also referred to as "Fellenius' Method", and it is the simplest method of slices to use. Slip surface, as shown in Figure 2.12 (a), is subdivided into a number of imaginary vertical slices. Each slice is acted upon by its own weight, W, and by the boundary interslice forces which have both tangential components T and normal components E. The forces acting on the base of a slice of inclination α and length l are the shear resistance S and the normal force P. According to Chowdhury (2010), a rigorous solution to the problem of stability involving the soil mass requires the following:

- The forces on each slice must satisfy the equilibrium conditions.
- The forces acting on the sliding mass, as a whole, must satisfy the conditions of equilibrium.

The method assumes that the resultant force of the interslice forces acting between two consecutive slices is parallel to its base; therefore the interslice forces E and T are neglected (Fellenius, 1936). Bishop (1955) expressed the assumption as regards the overall equilibrium of the sliding mass consisting of n slices:

$$\sum tan(\varphi')\{(T_n - T_{n-1})cos(\alpha) - (E_n - E_{n+1})sin(\alpha)\} = 0 \qquad \text{Eq. 2-3}$$

where

α – the angle between the tangent of the center of the base of the slice and the horizontal.

For the slice shown in Figure 2.12 below, the Mohr-Coulomb failure criteria is:

$$s = c' + (\sigma - u)\, tan(\varphi') \qquad \text{Eq. 2-4}$$

where

σ – the total normal stress, u, is the pore pressure

c' – the effective cohesion

φ' – the effective friction angle, and s is the shear stress.

From neglecting the interslice forces, the normal force P on the base of the slice can be expressed as:

$$P = W \times cos(\alpha) \qquad \text{Eq. 2-5}$$

where

W – the weight of the slice

Taking moments about the center of the slip circle, the following equation is obtained for the factor of safety and is defined as a ratio of resisting and disturbing moments:

$$F = \frac{\sum\{c \times l + tan\varphi'(W \times cos(\alpha) - u \times l\}}{\sum W \times sin(\alpha)} \qquad \text{Eq. 2-6}$$

where

u –pore water pressure

Because only the moment equilibrium is satisfied, the factors of safety calculated by this method are typically underestimated. The inaccuracy is large for deep critical circles with a large variety of α. It is also not accurate for high pore water pressure. Factors of safety calculated for flat slopes and/or slopes with high pore pressures can be on the conservative side by as much as 60 percent, when compared with values from more exact solutions (Whitman and Baily, 1967). For this reason this method is not used much today (Albataineh, 2006).

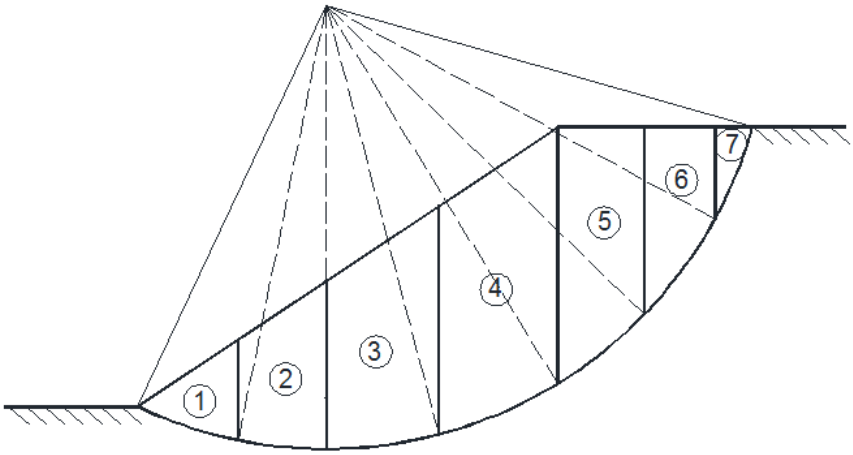

(a)

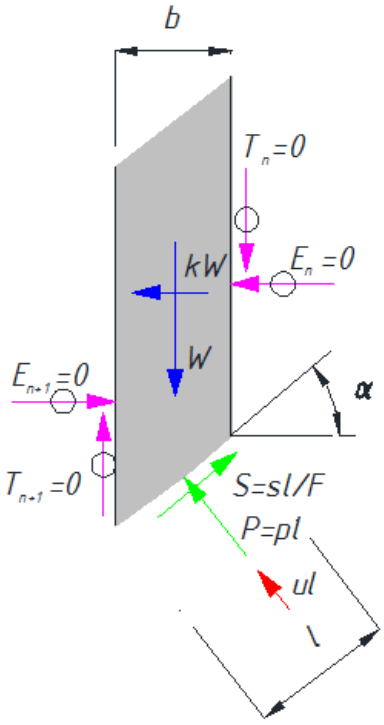

(b)

Figure 2.12. Ordinary Method of Slices (Fellenius' Method) (a) Slices (b) Forces acting on single slice

2.4.1.4 Bishop's Method

Bishop (1955) studied the problem rigorously by including the inter-slice forces in the equations of equilibrium for a typical slice. He proposed that a simplified calculation can be made, which gives fairly accurate results even though the inter-slice forces are ignored (Chowdhury, 2010). The simplified Bishop method uses the method of slices to find the factor of safety for the soil mass with several assumptions made as follows:

- The failure is assumed to occur by rotation of a mass of soil on a circular slip surface centered on a common point as in the Fellenius' method. Thus, Bishop's method should not be used to compute the factor of safety for non-circular surfaces unless a frictional center of rotation is used (Anderson and Richards, 1987).
- The forces on the sides of the slice are assumed to be horizontal; thus, there are no shear stresses between slices (Bishop, 1955). In Figure 2.13, shear force components T are ignored.
- The total normal force is assumed to act at the center of the base of each slice, and is derived by summing forces in a vertical direction.

Value of shear resistance s is calculated using this expression, including the unknown factor of safety F as:

$$s = \frac{c' + \left(\frac{W}{b} - u\right) tan(\varphi')}{1 + tan(\alpha) \times tan(\varphi')/F} \quad \text{Eq. 2-7}$$

The equation is a consequence of calculating p by considering the vertical equilibrium of the slice, as mentioned above. The total force, P, on the slice base, the product of p and the length of the base, l is given by this expression:

$$P = \frac{\frac{W}{b} - \frac{tan(\alpha)}{F}(c' - u \times tan(\varphi'))}{1 + tan(\alpha) \times tan(\varphi')/F} \quad \text{Eq. 2-8}$$

Taking moments of all forces about the center of the circular slip surface, the equilibrium of the entire sliding mass in terms of forces requires that:

$$\sum W \times sin\alpha = \sum \frac{s \times l}{F} \quad \text{Eq. 2-9}$$

$$F = \sum \frac{s \times l}{W \times sin(\alpha)} \quad \text{Eq. 2-10}$$

Combining Eq. 2-9 and Eq. 2-10 we have:

$$F = \frac{\sum\{c' \times b + (W - u \times b) \times tan(\varphi')\}/m_\alpha}{\sum W \times sin(\alpha)} \quad \text{Eq. 2-11}$$

where

$$m_\alpha = \left(1 + \frac{tan(\alpha) \times tan(\varphi')}{F}\right) cos(\alpha) \quad \text{Eq. 2-12}$$

As Eq. 2-11 contains the factor of safety F on both sides, it has to be solved iteratively. Although computer softwares are now routinely used for slope analysis, the iterative process and convergence are usually quick. Thus this method can be adopted for hand calculation (Bishop, 1955 and Chowdhury, 2010).

Although the simplified Bishop method does not satisfy complete static equilibrium and the methodology is still based on assumptions, the procedure gives considerably accurate values for the factor of safety, FOS. Bishop (1955) proved that the Simplified Bishop method is more accurate than the Ordinary Method of Slices, especially in case of effective stress analysis with high pore water pressure. Also, Wright et al., (1973) have shown that the factor of safety calculated by the Simplified Bishop method agrees favorably (within about 5%) with the factor of safety calculated using finite element approach. The primary limitation of the Simplified Bishop method is that it is limited to circular slip surface (Albataineh, 2006).

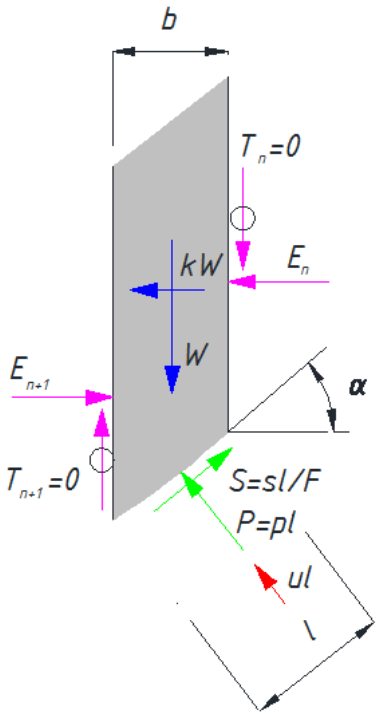

Figure 2.13. Bishop's Method

2.4.1.5 Janbu's Simplified Method

In general, a slip surface may not necessarily be circular in the cross section. The Janbu's simplified method is applicable to non-circular slip surfaces. Janbu (1956) considered the force and moment equilibrium of a typical vertical slice and the force equilibrium of the sliding mass as a whole (Chowdhury, 2010). Using the overall horizontal equilibrium as a stability criterion, the factor of safety is expressed as:

$$F = \frac{\sum b \times s \times sec^2(\alpha)}{\sum (W + d \times T) \times tan(\alpha)} \quad \text{Eq. 2-13}$$

In which dT is the difference of tangential or shear forces in between two consecutive slices

$$dT = T_{n+1} - T_n \quad \text{Eq. 2-14}$$

$$s = \frac{\left\{c' + \left(\frac{W + dT}{b} - u\right) tan\varphi'\right\}}{1 + tan\alpha tan\varphi'/F} \quad \text{Eq. 2-15}$$

The calculations can only be made with an assumption about the magnitude and orientation of the interslice forces. The Janbu's method imposes a stress distribution on each slice. The interslice stress distribution is often assumed hydrostatic and the resultant is assumed to act on the lower third point along the side of the slice. A line which passes through the interslice force resultants on either side of the slice is known as the line of thrust (Figure 2.14 and Figure 2.15). The new term was introduced in Janbu's rigorous (or generalized) method.

The behavior of the Janbu's method points out that limit equilibrium approach based purely on static can, in some circumstances, over-constrain the problem, resulting in unrealistic conditions (Krahn, 2004)

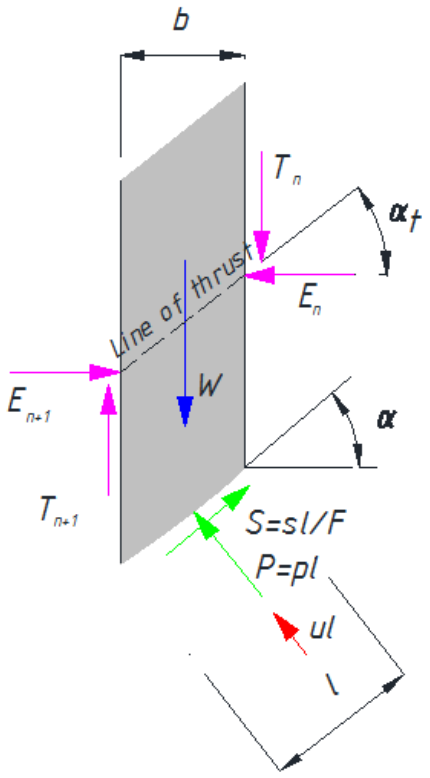

Figure 2.14. Janbu's Simplified Method

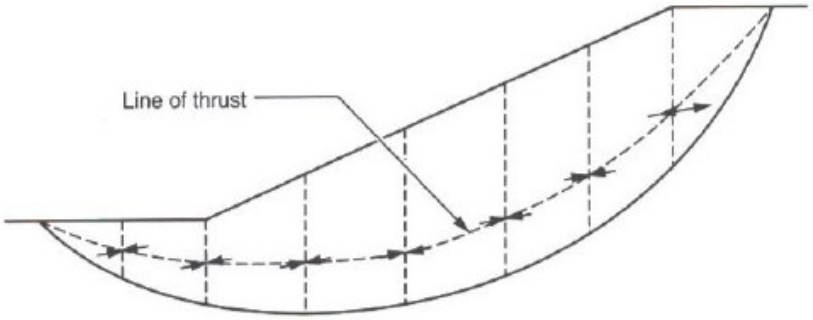

Figure 2.15. Line of thrust describing the locations of the interslice forces on the slice (Duncan and Wright, 2005)

2.4.1.6 Morgenstern-Price's Method

This method was introduced by Morgenstern and Price (1965), and considers not only the normal and tangential equilibrium but also the moment equilibrium for each slice in circular and non-circular slip surfaces. This method is a modification of the general limit equilibrium (GLE) approach by Fredlund (1977, 1981). The GLE formulation is based on two factors of safety equations and allows for a range of interslice shear-normal force assumptions. One equation gives the factor of safety with respect to moment equilibrium, while the other equation gives the factor of safety with respect to horizontal force equilibrium (Krahn, 2004).

In this method, an arbitrary mathematical function is assumed to describe the direction of the interslice forces (Albataineh, 2006). The relationship between the interslice shear forces (T) and the interslice normal forces (E) is determined as:

$$T = \lambda \times f(x) \times E \qquad \text{Eq. 2-16}$$

where,

$f(x)$- an assumed function that varies continuously across the slip with respect to x

λ – an unknown scaling factor that is solved for as part of the unknowns.

The specified function giving variations of $f(x)$ with slice position may be assumed as constant or given by forms (half-sine, clipped-sine, trapezoidal…). Figure 2.16 shows the typical function $f(x)$ as proposed by Fredlund and Krahn (1976). The unknowns that are solved in the

Morgenstern and Price method are the factor of safety (F), the scaling factor λ, the normal forces on the base of the slice (P), the horizontal interslice force (E), and the location of the interslice forces (line of thrust). The above unknowns are calculated using the equilibrium equations, then the shear component of the interslice forces (T) is calculated from Eq. 2-16.

The factor of safety F depends on the assumed side force function $f(x)$. It does not have a unique value, although the variations in F are normally very small (Chowdhury, 2010).

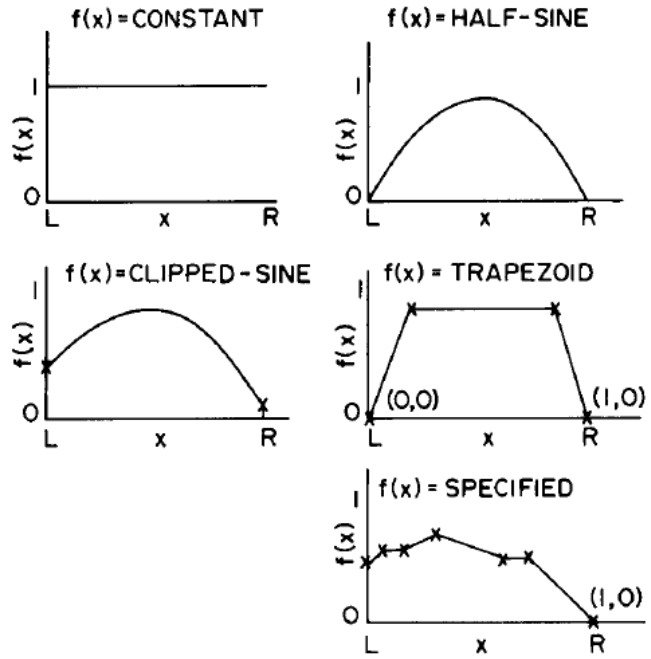

Figure 2.16. Functional variation of the direction of the side force with respect to the x direction (Fredlund and Krahn, 1976)

Morgenstern and Price's method for slope stability is considered to be more robust as it satisfies both force and moment equilibriums and accounts for interslice forces. The method is applicable to failure surfaces of arbitrary shape and arbitrary boundary conditions. Considerable experience and judgment is required to use the method reliably, to assume the right side force function $f(x)$, which gives acceptable results, and to interpret the results (Chowdhury, 2010).

2.4.1.7 Method of Block Analysis

Block analysis may be used to estimate the Factor of Safety (FOS) against sliding in situations where the shearing strength of an embankment fill is greater than that of the foundation soil, as shown in Figure 2.17. In these particular cases, it's necessary to investigate the stability along the failure surface of weak soil passing through the foundation of the embankment.

A planar failure surface is expected to develop if the foundation soil layer is relatively thin. The block analysis is rather simple and straightforward and can be performed merely by hand calculation (Abramson, 1996).

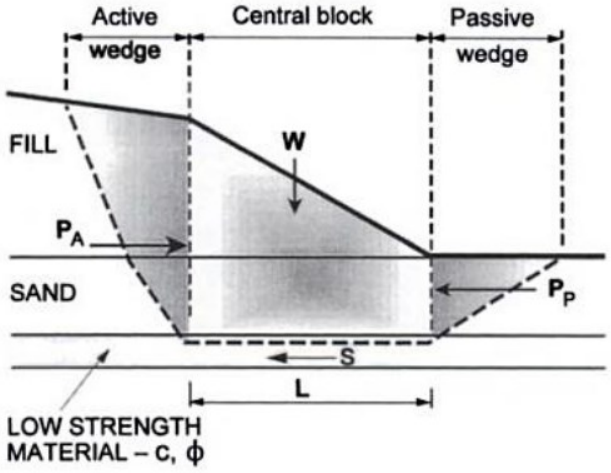

Figure 2.17. Sliding block analysis (Abramson, 1996)

For the analysis, the potential sliding block is subdivided into three parts (Figure 2.17): (1) an active wedge at the left head of the slide, (2) a central block, and (3) a passive wedge at the toe. The FOS is defined by summing the horizontal forces as:

$$F = \frac{Horizontal\ resistance\ forces}{Horizontal\ driving\ forces} = \frac{P_p + c'_m \times L + (W \times cos(\alpha) - U)tan(\varphi'_m)}{P_a} \qquad \text{Eq. 2-17}$$

where

P_a –active force (driving)

P_p –passive force (resisting)

L −resisting force due to the cohesion of clay

α −inclination of the base of the central block

c'_m and φ'_m − cohesion and friction angle of the soil at the base of the central bock, with effective weight $(W - U)$

The active and passive lateral earth pressures used in the block analysis are calculated using

$$\sigma_{A/P} = K_{A/P} \times \sigma'_v \mp 2 \times c_m \sqrt{K_{A/P}} \quad \text{Eq. 2-18}$$

where

K_A −active earth pressure coefficient

K_P − passive earth pressure coefficient

σ'_v −vertical effective stress

c_m −mobilized cohesion parameter

The earth pressure coefficients may be calculated using the Ranking expression:

$$K_A = \frac{1 - sin(\varphi_m)}{1 + sin(\varphi_m)} \quad \text{Eq. 2-19}$$

$$K_P = \frac{1 + sin(\varphi_m)}{1 - sin(\varphi_m)} \quad \text{Eq. 2-20}$$

Several trial locations of the active and passive wedges must be tested to determine the minimum FOS. In case of weak layer having considerable thickness, the failure plane must be checked at different depths to find the critical condition with the lowest FOS (Abramson, 1996).

The sliding block method can be used for typical non-circular failure surface (bi-planar and tri-planar. It is well suited to many rock slope problems and some soil slope problems. The inclination of inter-wedge forces is crucial especially for short deep failure masses with high pore water pressures (Chowdhury, 2010)..

2.4.1.8 Other special cases-Infinite Slope

A slope that extends for a relatively long distance and has a consistent subsoil profile may be analyzed as an infinite slope. The failure plane in this case is parallel to the surface of the slope and the limit equilibrium method can be used (Abramson, 1996).

A typical slice for a slope in dry sand is shown in Figure 2.18 with its free body diagram. The weight of the slice (with a unit dimension into the page) is given by:

$$W = \gamma \times b \times h \quad \text{Eq. 2-21}$$

$$N = W \times cos(\beta) \quad \text{Eq. 2-22}$$

$$T = W \times sin(\beta) \quad \text{Eq. 2-23}$$

The frictional strength along the failure surface will depend only on the friction angle φ of sand given by:

$$S = N \times tan(\varphi) \quad \text{Eq. 2-24}$$

The factor of safety is the ratio of available strength to strength required to maintain stability as:

$$F = \frac{N \times tan(\varphi)}{W \times sin(\beta)} = \frac{tan(\varphi)}{tan(\beta)} \quad \text{Eq. 2-25}$$

The FOS is independent of the slope height and depth, z, and depends only on the angle of internal friction, φ, and the slope angle, β.

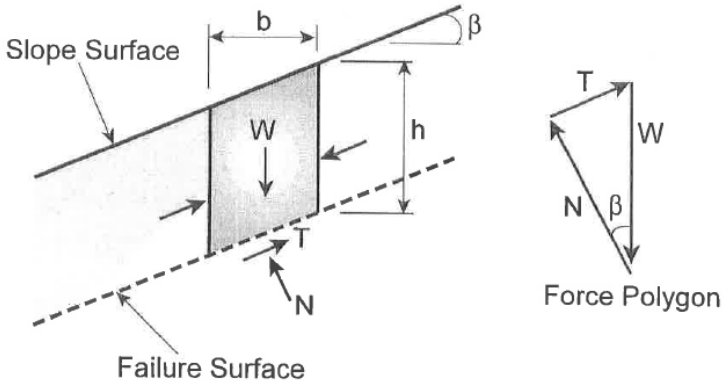

Figure 2.18. Infinite slope failure in dry sand (Abramson, 1996)

The infinite slope analysis approach can also be applied in $c - \varphi$ soil with seepage. The factor of safety is calculated accounting for the presence of moist and saturated unit weights, as well as its location as:

$$F = \frac{c' + h \times cos^2(\beta)[(1-m) \times \gamma_m + m \times \gamma'] \times tan(\varphi')}{h \times sin(\beta) \times cos(\beta) \times [(1-m) \times \gamma_m + m \times \gamma_{sat}]} \quad \text{Eq. 2-26}$$

where

γ_{sat} −saturated unit weight

γ_m −moist unit weight

m −ratio of the water level and the total height of soil.

2.4.1.9 Conclusion between limit equilibrium methods

The factor of safety equations for all methods of slices can be expressed in the same kind of format if it represents moment and (or) force equilibrium (Fredlund and Krahn, 1977). The normal force equation has the same forms between all methods except for the ordinary (Fellenius') method. The only distinguished difference comes from the way interslice forces are being interpreted between methods.

Each method will best fit in some special cases. The analytical aspects of slope stability can be satisfied with one factor of safety with moment equilibrium and satisfying force equilibrium. Table 2.1 presents basis characteristics of all limit equilibrium methods mentioned in this research, and Table 2.2 depicts the applicable cases for each of those methods.

Table 2.1.Characteristics of Commonly Used Methods of Limit Equilibrium Analysis (after Duncan and Wright, 2005; Albataineh, 2006).

Method	Equilibrium	Slip surface	Assumptions	Unknowns solved
Swedish ($\varphi = 0$)	Overall moment about center circle	Circular	• Friction angle is zero	1 factor of safety = 1 total unknown
Ordinary Method of Slices (Fellenius's Method)	Overall moment about center circle	Circular	• Forces on the side are neglected • The normal force on the base is $Wcos\alpha$ and the shear force is $Wsin\alpha$	1 factor of safety = 1 total unknown
Simplified Bishop's Method	Vertical force and overall moment	Circular	• All interslice shear forces are zero	1 factor of safety and n normal forces on the base of slices $(N) = n + 1$ total unknowns
Janbu's Simplified Method	Force equilibrium (vertical and horizontal)	Any Shape	• The side forces are horizontal	1 factor of safety and n normal forces on the base of slices (N), $n - 1$ resultant interslice forces and $Z = 2n$ total unknowns
Morgenstern and Price's	All conditions of equilibrium (forces	Any shape	• Interslice shear forces is related to interslice normal	1 factor of safety, 1 interslice force inclination "scaling factor" λ, n Normal forces on the base

Method	and moment)		force by $T = \lambda \times f(x) \times E$ • The normal force acts at the center of the base of the slice.	of slices (N), n- 1 Horizontal interslice forces E, n-1 location of interslice forces (line of thrust) =3n total unknowns

Table 2.2. Summary of applicable cases for different Limit Equilibrium Slope Stability methods (after Duncan and Wright, 2005; Albataineh, 2006)

Method	Applicable cases
Swedish ($\varphi = 0$)	To slopes where $\varphi = 0$ (i.e undrained analyses of slopes in saturated clays)
Ordinary Method of Slices (Fellenius's Method)	Applicable to non-homogeneous slopes and $c - \varphi$ soils where slip surface can be approximated by a circle. Very convenient for hand calculations. Inaccurate for effective stress analyses with high pore water pressures.
Simplified Bishop's Method	Applicable to non-homogeneous slopes and $c - \varphi$ soils where slip surface can be approximated by a circle. More accurate than Ordinary Method of slices, especially for analyses with high pore water pressures. Calculations feasible by hand or spreadsheet.
Janbu's Simplified Method	Applicable to non-circular slip surfaces. Also for shallow, long planar failure surfaces that are not parallel to the ground surface.
Morgenstern and Price's Method	An accurate procedure applicable to virtually all slope geometries and soil profiles. Rigorous, well established complete equilibrium procedure.

2.4.2 3D method

Idealization of real three-dimensional (3D) slope problems as two dimensional (2D) problems is often valid. However, in some certain cases, the effect of 3D may be significant and can't be ignored. It is also very important to do back-analysis when the factor of safety for the failure is calculated and compared from both 2D and 3D aspects. In general, a 2D back analysis provides lower factor of safety due to underestimating the shear strength of soil (Chowdhury, 2010).

Three-dimensional analysis methods use the 3D shapes of slip surface. These methods, like 2D methods, have the assumptions to achieve a statically determinate definition of the problem. There are several ways to do that; some methods do it by decreasing the number of unknowns, and others by increasing the number of equations or both, so that the two numbers can be equal (Albataineh, 2006).

In particular, the 3D analysis becomes prevalent in cases where the slope geometry is rather complex, which makes it difficult to select a typical two-dimensional section to analyze. The geometry of the slope and slip surface varies significantly in the lateral direction. Moreover, in case of the material properties highly inhomogeneous or anisotropic, or when the slope is locally surcharged, the slope with a complicated shear strength or pore-water pressure requires combining the effects of slope geometry and shear strength to determine the direction of movement that leads to a minimum factor of safety. In these situations, a 3D analysis may be necessary (Albataineh, 2006).

A large number of three-dimensional slope stability analysis methods based on the limit equilibrium concept have been developed since the 1960s, ranging from the relatively simple to the most sophisticated. Duncan (1992), in a review, noted that most researchers reported 3D values of FOS to be greater than the corresponding ones in 2D. But some investigators reported instances or examples with the opposite outcome (Chowdhury, 2010).

Some aspects of different approaches for 3D analyses are presented in the following sub-sections. Here, the emphasis is on relatively simple approaches. Many of them are valid only under certain conditions. These methods have been reviewed extensively to understand the limitations of each. A comprehensive comparison between these methods is reported by Duncan (1996), as shown in Table 2.3.

2.4.2.1 Hovland's Method

Hovland (1977) proposed a general but simplified (approximate) approach for 3D slope stability analyses aimed at finding a factor of safety, F ,defined as the ratio of the total available resistance along a failure surface and the total mobilized resistance along it. The method is an extension of the initial assumptions associated with the 2D traditional method, but instead of using slices, columns were used. In Hovland's method, all inter-column forces acting on the sides of the columns are ignored. The normal and shear forces acting on the base of each column are calculated as components of the weight of the column itself. Another assumption is that there is motion only in one direction. The equilibrium of the system was calculated for this direction.

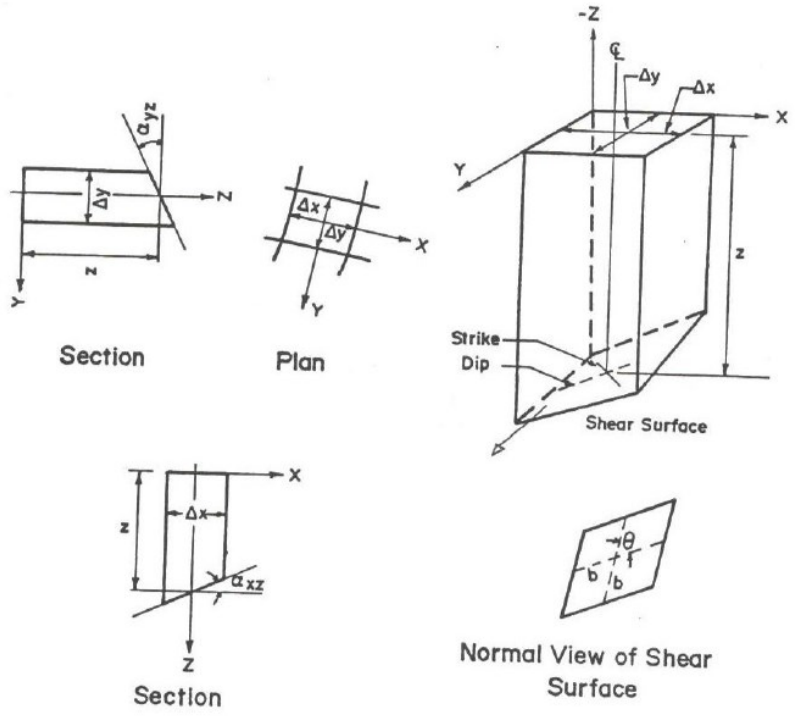

Figure 2.19. Plan, Section and 3D views of one Soil column (Hovland, 1977)

From the simple definition adopted above, the 2D factor of safety F_2 for a slope of height *h* may be expressed as follows (Chowdhury, 2010):

$$F_2 = \frac{c}{\gamma \times h} \times A_2 + tan(\varphi) \times B_2 \qquad \text{Eq. 2-27}$$

where

$$A_2 = \frac{\sum sec(\alpha)}{\sum \frac{z}{h} \times sin(\alpha)} \qquad \text{Eq. 2-28}$$

$$B_2 = \frac{\sum z \times cos(\alpha)}{\sum z \times sin(\alpha)} \qquad \text{Eq. 2-29}$$

In which α is the inclination of the base of any slice and z its height and the column width is considered constant. A_2 and B_2 are functions only of geometry and determine how cohesion and friction components of resistance are influenced by geometry (Chowdhury, 2010).

The 3D the factor of safety, F_3, may be presented by dividing the soil mass above the failure surface into a number of vertical soil columns, assuming the x- and y- coordinates are perpendicular and are in the horizontal plane, the z- coordinate is vertical and the y-coordinate is to be in the direction of down slope movement (Chowdhury, 2010). Let Δx and Δy define the cross section of the soil column in the x-y plane and both of them are constant for all columns. The factor of safety can be expressed as:

$$F_3 = \frac{c}{\gamma \times h} \times A_3 + tan(\varphi) \times B_3 \qquad \text{Eq. 2-30}$$

where

$$A_3 = \frac{\sum_x \sum_y sec(\alpha_{xz}) \times sec(\alpha_{yz}) \times sin(\theta)}{\sum_x \sum_y \frac{z}{h} \times sin(\alpha_{yz})} \qquad \text{Eq. 2-31}$$

$$B_3 = \frac{\sum_x \sum_y z \times cos(DIP)}{\sum_x \sum_y z \times sin(\alpha_{yz})} \qquad \text{Eq. 2-32}$$

In which α_{xz} and α_{yz} are the dip angles in the xz and yz planes respectively and DIP and θ are given by:

$$\cos(DIP) = \left(1 + tan^2(\alpha_{xz}) + tan^2(\alpha_{yz})\right)^{-1/2} \qquad \text{Eq. 2-33}$$

$$cos\theta = (sin(\alpha_{xz}) \times sin(\alpha_{yz})) \qquad \text{Eq. 2-34}$$

The factors A_3 and B_3 represent the influence of the problem geometry including the shape of the 3D failure surface.

Hovland (1977) found that 3D factors of safety (FOS_3) are usually higher than 2D factors of safety (FOS_2) after a number of 2D and 3D cases. In his studies, he also pointed out that landslides in cohesive soils may follow a wide shear surface geometry similarly resembling 2D case. However, failures in cohesionless soil may follow a 3D wedge type surface. In general, the ratio of FOS_3/FOS_2 is very sensitive to the values of c and φ, as well as the geometric shape of the 3D failure surface. Hovland's approach is against the 2D traditional way of ignoring the intercolumn forces, as they do not represent the realistic scenario since 3D effects are not

accounted for (Chowdhury, 2010). As shown in Figure 2.20 with the 3D effect presented, all the side forces will create more friction and thus prevent the soil mass from sliding downward. This will result in greater factor of safety from 3D calculation over 2d calculation.

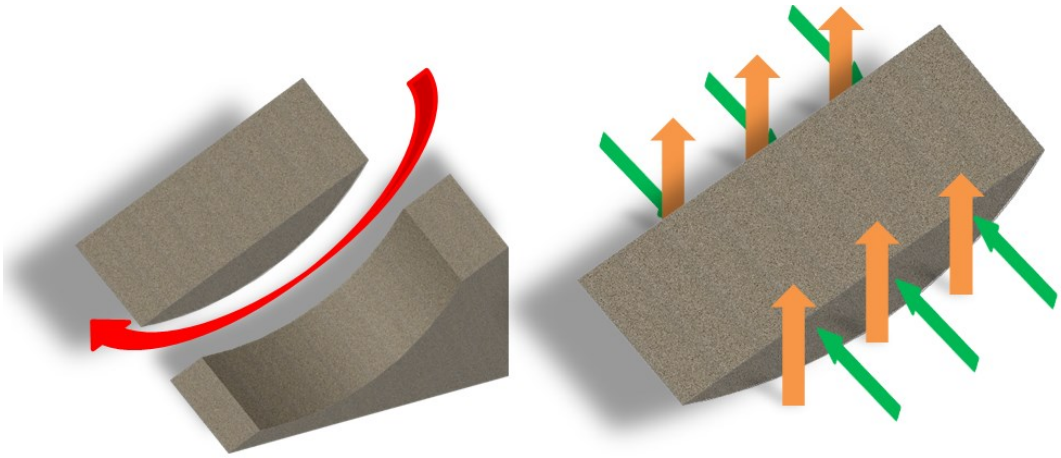

Figure 2.20. Hovland's 3D effects criticism

2.4.2.2 Method by Chen (1981) and Chen and Chameau (1983)

Chen (1981) and Chen and Chameau (1983) developed a comprehensive study of the three dimensional effects on the slope stability of a large variety of soil parameters. They suggested methods for the analysis of the three-dimensional block surfaces (Figure 2.21), as well as for the rotational surfaces (Figure 2.22). The method showed Hovland's method (1977) to be conservative and derived from an extension of Spencer's (1967).

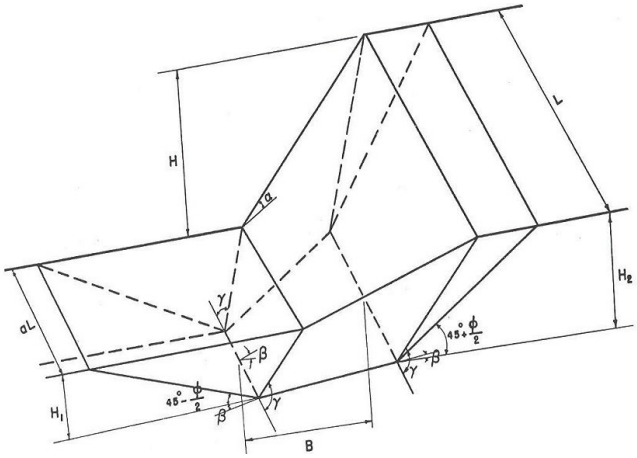

Figure 2.21. 3D Block Type failure (Chen, 1981)

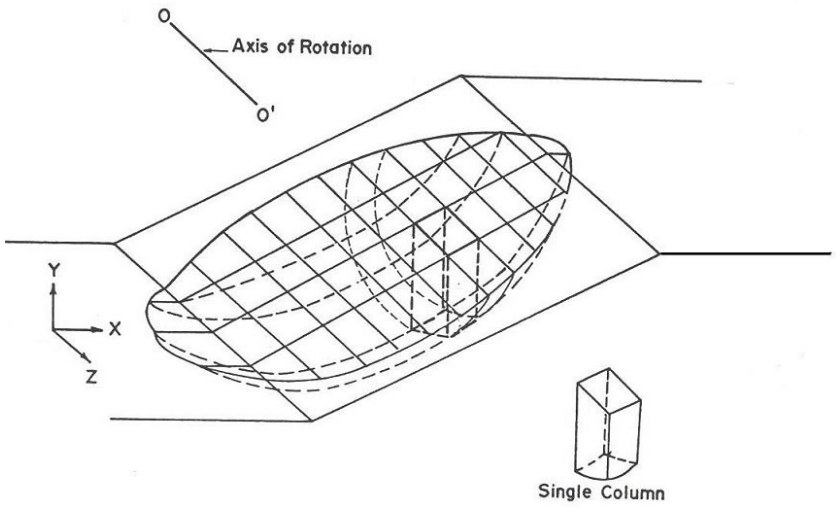

Figure 2.22. Spoon shaped failure in the Embankment (Chen, 1981)

Factor of safety is calculated using computer software BLOCK3. The rotational 3D failure surface was assumed to have homogeneous soil and composed of a central cylinder attached by two semi-ellipsoids at the two ends. A computer program, LEMIX, using the limit equilibrium method, was generated to achieve the required analysis (Albataineh, 2006).

Chen's 3D method requires certain assumptions to be made. The failure mass is assumed to be symmetrical and divided into many vertical columns. The intercolumn shear forces are parallel to the base of the column and are a function of their positions. The intercolumn normal stress distribution is assumed to be linear with depth. The inclination of the interslice forces is assumed to be the same throughout the whole failure mass.

With the use of the rotational slides, Chen (1983) concluded that the 3D effects are more significant at smaller lengths of the failure mass. For application, the 3D effects are most significant for soils of high cohesion intercept and low friction angle. For soils of low cohesion intercept and high friction angle, the 3D factor of safety may be slightly less than that for the 2D case. The effect of pore water pressures may also promote the effect of 3D slope analysis over 2D.

2.4.3 Conclusions on 2D and 3D approaches

Duncan (1996) summarized the studies of 3D slope stability as shown in Table 2.3. Based on his report, the following conclusions were noted (Albataineh, 2006):

- The factor of safety for 3D analysis is greater than the factor of safety for 2D analyses. The only studies that found the otherwise cases are those by Hovland (1977), Chen and Chameau (1983), and Seed et al. (1990). Hovland's analyses were based on an extension of the Ordinary Method of slices, which is inaccurate because it assumes zero normal stress on vertical surfaces. Azzouz and Baligh (1978) showed that results calculated using this method are illogical for some conditions, and that extension of the Ordinary Method of Slices is not an adequate approach to 3D analysis. Hutchison and Sarma (1985), Cavounidius (1987), and Hungr (1987) questioned some of the assumptions used by Chen and Chameau, and found that Factor of safety for 3D analysis was greater than the factor of safety for 2D analysis rather than smaller, as Chen and Chameau had found. Seed et al. (1990) compared the results of 2D and 3D analyses that did not satisfy all conditions of equilibrium. The horizontal force imbalance in their approximate 3D analysis was 3.7% of the weight of the sliding mass. Because the friction angles along the slip surface they studied were so small (8º to 9º), this force imbalance could result in as much as a 25% difference in the calculated factor of safety. Thus, all of the cases where the factor of safety for 3D analysis was found to be smaller than the factor of safety for 2D analysis appear to involve significant potential inaccuracies.
- Hutchinson and Sarma (1985) and Leshchinsky and Baker (1986) pointed out that 2D and 3D analyses should give the same factor of safety for slopes in homogeneous cohesionless soils, because the critical slip surface is a shallow plane parallel to the surface of the slope.

- Azzouz et al. (1981), and Leshchinsky and Huang (1992) noted that if 3D effects are neglected in analyses to back calculate shear strengths, the back calculated strengths will be too high.

Table 2.3. Methods of analyzing 3D Slope Stability (Duncan, 1996)

Authors (1)	Method (2)	Strength (3)	Geometry of slope/slip surface (4)	3D effects found (5)
Anagnosti (1969)	Extended Morgenstern and Price	c, ϕ	Unrestricted/unrestricted	$F_3 = 1.5\ F_2$ in one case
Baligh and Azzouz (1975)	Extended circular arc	$\phi = 0$	Simple slopes/surfaces of revolution	$F_3 > F_2$
Giger and Krizek (1975)	Upper bound theory of perfect plasticity	c, ϕ	Slopes with corners/log spiral	$F_3 > F_2$
Giger and Krizek (1976)	Upper bound theory of perfect plasticity	c, ϕ	Slopes with corners/log spiral (with loads on top of slope)	$F_3 > F_2$
Baligh et al. (1977)	Extended circular arc	$\phi = 0$	Simple loaded slopes/surfaces of revolution	$F_3 > F_2$
Hovland (1977)	Extended ordinary method of slices	c, ϕ	Unrestricted/unrestricted	$F_3 < F_2$ for some cases
Azzouz et al. (1981)	Extended Swedish circle	$\phi = 0$	Four real embankments/surfaces of revolution	$F_3 = 1.07\ F_2$ to $1.3\ F_2$
Chen and Chameau (1982)	Extended Spencer, and finite element	c, ϕ	Unrestricted/unrestricted	Spencer results are similar to FEM
Chen and Chameau (1983)	Extended Spencer	c, ϕ	Unrestricted/unrestricted	$F_3 < F_2$ for some cases
Azzouz and Baligh (1983)	Extended Swedish circle	$\phi = 0$	Same as Baligh and Azzouz with loads on top	$F_3 > F_2$
Dennhardt and Forster (1985)	Assumed s on slip surface	c, ϕ	Slopes with loads/unrestricted	$F_3 > F_2$
Leshchinsky et al. (1985)	Limit equilibrium and variational analysis	c, ϕ	Unrestricted	$F_3 > F_2$
Ugai (1985)	Limit equilibrium and variational analysis	$\phi = 0$	Vertical slopes/cylindrical	$F_3 > F_2$
Leshchinsky and Baker (1986)	Limit equilibrium and variational analysis	c, ϕ	Slopes constrained in 3rd dimension/ unrestricted	$F_3 > F_2$ for $c > 0$, $F_3 = F_2$ for $c = 0$
Baker and Leshchinsky (1987)	Limit equilibrium and variational analysis	c, ϕ	Conical heaps/unrestricted	$F_3 > F_2$
Cavounidis (1987)	Limit equilibrium	c, ϕ	Unrestricted/unrestricted	F_3 must be $> F_2$
Hungr (1987)	Extended Bishop's modified	c, ϕ	Unrestricted/surfaces of revolution	$F_3 > F_2$
Gens et al. (1988)	Extended Swedish circle	$\phi = 0$	Simple slopes/surfaces of revolution	$F_3 > F_2$
Leshchinsky and Mullet (1988)	Limit equilibrium and variational analysis	c, ϕ	Vertical slopes with corners/unrestricted	$F_3 > F_2$
Ugai (1988)	Extended ordinary method of slices, Bishop's modified, Janbu, and Spencer	c, ϕ	Unrestricted/unrestricted	$F_3 > F_2$, except for OMS
Xing (1988)	Limit equilibrium	c, ϕ	Unrestricted/ellipsoidal	$F_3 > F_2$
Michalowski (1989)	Kinematical theorem of limit plasticity	c, ϕ	Unrestricted/unrestricted	$F_3 > F_2$
Seed et al. (1990)	Ad hoc 2D and 3D	c, ϕ	One particular case, the Kettleman Hills failure	$F_3 < F_2$
Leshchinsky and Huang (1991)	Limit equilibrium and variational analysis	$c. \phi$	Unrestricted/unrestricted	$F_3 > F_2$

2.5 Surficial Failures

Surficial failures are quite common in the United States (Day and Axten, 1989). It is also categorized as one of the more frequently occurring landslides, also known as surficial slumps. It is a phenomenon involving a relatively thin zone of soil, generally parallel to the slope face sliding down the slope (Day, 1996). Evan (1972), in his study, pointed out the surficial failures usually reach to the depth of 4ft. or less after collecting data from all slope failure cases in America. Figure 2.23 presents the concept of surficial failure.

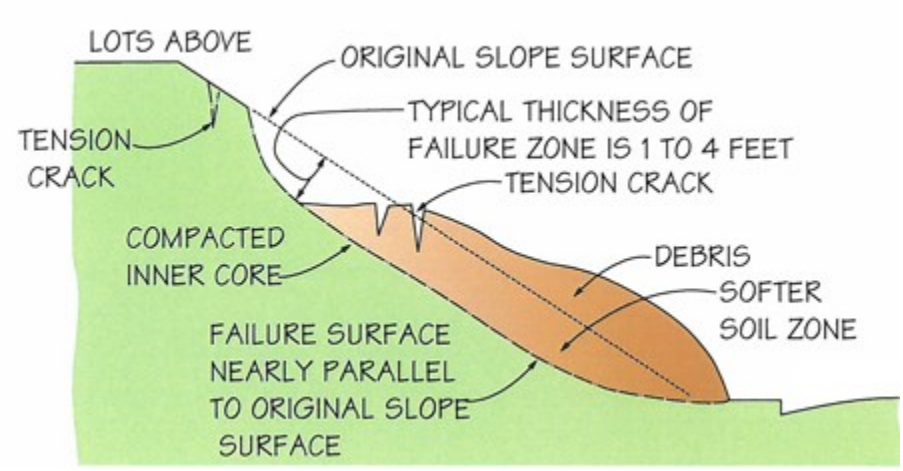

Figure 2.23. Surficial failure conceptual illustration (American Geotechnical, Inc.)

The failure area of a soil mass generally has the shape of an oval. In natural slopes, this form of instability is usually limited to the surface soil layer. In graded slopes, the problem typically occurs in the weathered soil zone near the surface where the soil is subject to wetting and drying cycles. Similarly, the problem in graded slopes is more common in compacted fill slopes composed of expansive clayey soil. When the outer face of an expansive fill material swells even slightly, soil particles in the swelling zone move apart ever so slightly. Nonetheless, as the soil porosity increases even slightly, the permeability of the soil parallel to the slope face increases significantly.

Once permeability differences develop between the outer zone of the slope and the compacted inner core, seepage occurs parallel to the slope face in response to prolonged heavy rainfall. When this seepage does occur, the buoyant effect is triggered, the soil strength is roughly cut in half, and the slumping begins. Occasionally, granular fill slopes and bedrock slopes may be impacted by surficial slumping. The failure mechanism is controlled by the steepness of the slope, permeability differences, and the soil or rock strength characteristics. In order to initiate a failure, sufficient water is required to saturate the soil and cause seepage to develop essentially parallel to the slope surface.

Pradel and Raad (1993) studied the effects of precipitation on shallow slope failures in southern California. In their report, they concluded that the observed rainfall could not lead to saturation conditions to a depth of 4 ft. for soils with a permeability of more than 3.94×10^{-3} in. /sec. Thus, clayey and silty soils are more prone to surficial failures in southern California. Day and Axten (1989), in their study of a southern California surficial failure case, summarized the common characteristics of the surficial failure mechanism:

- Desiccation cracks are formed during the hot and dry summer periods as the soil on the slope shrinks. The extent of desiccation depths depends on the nature of the soil as well as outside factors like temperature, humidity and the presence of vegetation.
- During the rainfall season, water infiltrates through the cracks causing the slope surface to swell and be fully saturated. This will lead to the reduction of shear strength as the effective parameters of soil decreases.
- Permeability of soil parallel to the slope increases, and with the extension of rainfall, seepage will eventually develop parallel to the slope surface.
- Failure occurs when the shear strength decreases lower than the critical value.

2.5.1 Slope case histories

2.5.1.1 Highway Slopes and Embankments, Wisconsin

Titi and Helwany (2007), in their report for the Wisconsin Highway Research Program, investigated two slope failures in newly constructed embankments and slopes (cut sections). Figure 2.24 and Figure 2.25 show the cases of surficial failures along the State Trunk Highway STH-164 cut slope in Waukesha County and on the County Trunk Highway CTH A embankment near Burlington, Wisconsin. In Wisconsin, shallow slope failures often occur after prolonged and heavy rainfall, and sometimes these failures worsen during the spring thaw period (snowmelt) (Titi and Helwany, 2007)

(a) (b)

Figure 2.24. Pictures (a and b) of surficial slope failure along STH-164 in Waukesha County, Wisconsin (cut slope) (Titi and Helwany, 2007)

(a) (b)

Figure 2.25. Pictures (a and b) of surficial slope failure along CTH A near Burlington, Wisconsin (embankment slope) (Titi and Helwany, 2007)

Field observations by the Wisconsin Department of Transportation (WisDOT) engineers at sites of shallow slope failures provided the evidence that the failure surface depth ranges from approximately 2 to 4 ft. The research team performed field measurements of the depth of a shallow slope failure at STH-164 in Waukesha County and found that the average depth of failure surface is about 2 ft.

The surficial slope failure on the CTH A embankment near Burlington, Wisconsin is considered a typical case study for surficial failure as the reason was the soil being saturated

due to prolonged rainfall and snowmelt. A field visit approximately two weeks after the failure clearly showed that the surficial soil from the slope was fully saturated with frozen water in some locations. Under the top soil, there was a thin clay layer with apparent lower permeability. This layer may act as a drainage barrier, allowing the water to stay on it and rise in the upper surficial soil. When the water rose in the upper surficial soil, the effective shear strength of the soil was reduced due to the pore water pressure presence, causing the instability of the surficial soil. Also, Wisconsin climate data for the month of December 2006 had above-average precipitation and thus, it provided a continuous wetting of the slope that was under construction. Therefore, this prolonged rainfall led to the saturation of the upper soil and the subsequent surficial failure of the slope (Titi and Helwany, 2007).

2.5.1.2 Shallow landslide in Blackhawk, California.

Short et al (2005) reported some instances of shallow rainfall-induced landslides in the residential community of Blackhawk, California, located east of the San Francisco Bay (Figure 2.26). Given the real threat to property values in residential and commercial infrastructures and the constant maintenance problem posed to lifeline structures such as utilities, roadways, and pipelines, new methods to deal with these landslides are needed. Currently, research is being conducted by Short et al., (2005) based on plate pile mitigation for shallow landslides. The plate pile technique provides a sound, cost-effective methodology and in general shows a 20% increase in the factor of safety against failures.

Figure 2.26. One of 60 shallow landslides occurring on December 15, 2002 in Blackhawk, California (Short et al., 2005)

2.5.1.3 Cut Slopes in Poway, California

Figure 2.27 shows a picture of a surficial slope failure in a cut slope located in Poway, California that happened in 1991 due to cutting down the hillside during the construction of the adjacent road. The cut slope has an area of about $4000\ ft^2$, a maximum height of 20 ft. and a slope inclination that varies from 1.5:1 (34^o) to 1:1 (45^o). The failure mechanism is a series of thin surficial failures, about 0.5 ft. thick.

The cause of the surficial slope failures was weathering of the Friars formation. Weathering breaks down the rock and reduces the effective shear strength of the material. The weathering process also opens up fissures and cracks, which increases the permeability of the near surface rock and promotes seepage of water parallel to the slope face (Ortigao et al., 1997). Failure will eventually occur when the material has weathered to such a point that the effective cohesion approaches zero.

Surficial failures are most common for cut slopes in soft sedimentary rocks, such as claystones or weakly cemented sandstones. As mentioned earlier, the most common reason for the surficial failure is because a relatively steep slope (such as 1.5:1 or 1:1) is excavated into

the sedimentary rock. Then, with time, as vegetation is established on the slope face and the face of the cut slope weathers, the probability of surficial failures increases. The surficial failure usually develops during or after a period of heavy and prolonged rainfall.

Figure 2.27. Surficial failure, cut slope for road in Poway, California (Day, 2010)

2.5.1.4 Fill slope in Southern California

Pradel and Raad (1993), in their study, showed that in southern California, fill slopes made of clayey or silty soils are more susceptible to surficial instability than slopes made of sand or gravel. This is due to the fact that in granular fill, water tends to migrate downward rather than parallel to the slope face. Figure 2.28 (a) shows a surficial failure in a fill slope. Such failures can cause extensive damage to landscaping and can even carry large trees downslope. Besides the landscaping, there can be damage to the irrigation and drainage lines. The surficial failure can also damage appurtenant structures, such as fences, walls, or patios.

A particularly dangerous condition occurs when the surficial failure mobilizes itself into a debris flow. In such cases, severe damage can occur to any structure located in the path of the debris flow. Figure 2.28 (b) shows partial mobilization of the surficial failure, which flowed over the sidewalk and into the street. Surficial failures, such as the failure shown in Figure 2.28, can be sudden and unexpected, without any warning of potential failure. In cases of clays, there may be characteristic signs of imminent failure, as a clay slope has a series of nearly continuous semicircular ground cracks. After this picture was taken (during the rainy season), this slope failed in a surficial failure mode.

(a) (b)

Figure 2.28. Surficial slope failure in a fill slope, California (Day, 2010)

2.5.1.5 Grapevine and Joe Pool Dams, Texas

Surficial failures are often witnessed at a number of earthfill dam sites, levees, highway embankments, and cut slopes. Both Joe Pool Dam and Grapevine Dam are located in the Dallas Fort Worth Metroplex in the state of Texas, USA. Both the dams selected have experienced a huge number of surficial failures since their inception (McCleskey 2005). At Joe Pool Dam, the first failure occurred within two years of its construction, followed by number of

surficial failures. At Grapevine Dam, there were more than 20 surficial failures within 40 years of its construction (McCleskey, 2005). Most of the failures were attributed to prolonged rainfall events followed by droughts (McCleskey et al., 2008). Analysis of these failures reveals that the highest number of failures occurred during the hotter months between March and July and the lower number during the coldest months of December and January. The failures have sometimes repeated either at the same location or close by.

Maintenance of the slopes costs millions of dollars annually. In order to mitigate these failures, a research study was undertaken by The University of Texas at Arlington (UTA), in cooperation with the U.S. Army Corps of Engineers (USACE), Fort Worth District (SWF), with the objective of exploring the best field stabilization method to mitigate desiccation cracks in the upper embankment soils of the two dams. Four admixtures selected and used to treat surficial soils were 20%compost, 4%lime with 0.30%polypropylene fibers, 8%lime with 0.15%polypropylene fibers, and 8%lime. Five test sections, including four treated sections and one control section without any surface treatment, were constructed at each dam site. The test sections were instrumented with moisture probes, temperature probes, and inclinometers. The sites have been monitored for a period of 3.5 years at Joe Pool Dam and 2.5 years at Grapevine Dam. With the different types of soil at each dam site, the result is expected to give a better insight into the aspects of the behavior of clayey soils when treated with chemical admixtures.

(a) (b)

Figure 2.29. Surficial Failures at Grapevine Dam (a) and Joe Pool Dam (b)

2.5.2 Standard Codes for Shallow stability

Abramson et al (2007) introduced the well-known set of standard codes in the County of Los Angeles for surficial failure analysis. The Minimum Standards for Slope Stability Analysis, pertinent aspects of these standards are:

- Calculation should be based on analysis for the stability of an infinite slope with seepage parallel to the failure surface, which would yield the lowest factor of safety.
- The equation used for calculation is :

$$FOS = \frac{c' + (y_t - y_w) \times z_w \times cos^2(\alpha) \times tan(\varphi')}{y_t \times z_w \times sin(\alpha) \times cos(\alpha)} \quad \text{Eq. 2-35}$$

Where

c' –the effective cohesion

φ' –the effective friction angle

α –the slope angle

z_w –the vertical depth of saturated soil

γ_t –the total unit weight

γ_w –the unit weight of water

- The minimum acceptable vertical depth of soil saturation shall be 4ft.

- The minimum factor of safety for surficial stability shall be 1.50
- Shear strength parameters (cohesion and friction angle) determined for use in analyzing the gross stability of the same slope will be considered acceptable for surficial stability analysis without specific justification. The consultant must justify application of higher shear strength values.

Eq. 2-35 was proposed by Skempton and Delory (1957) for analyzing the slope stability of infinite slopes with seepage parallel to the face in clay slopes. For cohesionless soils with $c' = 0$, Eq. 2-35 is reduced to:

$$FOS = \left(1 - \frac{\gamma_w}{\gamma_t}\right) \times \frac{tan(\varphi')}{tan(\alpha)} \qquad \text{Eq. 2-36}$$

Abramson et al. (2002) presented an evaluation of the use of these equations in the analysis of surficial slope stability. The results showed that Eq. 2-36 will withstand slopes being constructed flatter than the ratio of 3.5:1 (H:V), assuming the angle of internal friction range for sand is between 28^o and 40^o and $FOS = 1.50$. Eq. 2-36 also proves that slopes steeper than 2.5:1 would potentially fail under heavy rainfall ($FOS = 1$). Abramson et al. (2002) stated that this is a contradiction to the observations that many 1.5:1 and 2:1 cohesionless soil slopes remained stable after prolonged intense rainfall. In addition, a small increase in cohesion value in Eq. 2-35 can increase the factor of safety. Therefore, Eq. 2-35 suggests that slopes made of cohesive soils (silt and clay) will have a higher factor of safety and will be less susceptible to surficial instabilities than cohesionless soils (sand and gravel). A study by Hollingsworth and Kovacs (1981) on surficial slope failures after intense rainfall showed that clayey and silty soils are more prone to failure than gravelly and sandy soils due to the loss of cohesion between particles, which is more prominent for strength in clayey and silty soils (Titi and Helwany, 2007)

2.6 Desiccation cracks

Desiccation cracks in clay are also known as syneresis cracks. The cracks can have different orientations and different degrees of completeness. Syneresis cracks are formed from

shrinkage of sediment. The shrinkage can be due to the salinity of water around it. The syneresis cracks are described as discontinuous, sinuous, and spindle in shape.

Physico-chemically induced cracking may be divided in to three groups: syneresis cracks, cracks induced by freeze-thaw cycles and cracks induced by desiccation (drying of the material) (Omidi et al. 1996). Syneresis cracks are generated by changes of the inter-particle forces resulting from replacement of interstitial water with a low dielectric organic solvent or highly aqueous solution (Brown and Anderson, 1983; Omidi et al. 1996). Various Studies have also shown that freeze-thaw cycles result in the formation of cracks, and the net result is increased in hydraulic conductivity of soils. During summer or periods of drought, desiccation cracks are induced by evaporation of water and the consequent shrinkage of the soil (Omidi et al. 1996; Othman et al. 1994; Bowders and McClelland, 1994).

2.6.1 Mechanism of Desiccation Cracking

The shrinkage and ambient temperature are the vital factors involved in the formation of cracks in soil-cement mixture (Westergaard, 1926). George (1969) pointed that effect of temperature on cracking is insignificant compared to the influence of change in moisture content. He found that tensile stresses develop in the soil due to shrinkage and shrinkage stresses reach the maximum value in the early stage of drying near the surface and the shrinkage stresses decrease rapidly with depth. He stated that the stress is relieved either by surface cracking or plastic flow in materials. George (1969) explained the mechanism of desiccation cracking as a failure of the material in tension. That indicates that when the tensile stresses due to shrinkage exceed the tensile strength of soil, the desiccation cracks form.

Evaporation of water from the soil surface initiates shrinkage by generating tensile stresses exceeding the soil strength, thus the cracks form (Costa et al, 2008). This is a very complex process due to the interactions that take place among different factors such as material, ambience, and boundary conditions. The process is summarized as during evaporation, the soil water content decreases, soil material properties change, affecting the rate

of moisture flow and water evaporation, soil tensile strength, modulus and fracture toughness, and the boundary adhesion. Thus, understanding and modeling of the cracking process need to be developed.

Towner (1987), in his research, pointed out that when drying clays are prevented from shrinking in one direction, desiccation won't form until the stress induced in that direction is equal to or greater than the corresponding tensile strength. With the presence of matric suction and with decreasing water content in soil the tensile stress and the tensile strength increase. The tensile stress generated during isotropic shrinkage of a saturated soil is equal to the change in soil-water suction, but considerably less for enforced anisotropic shrinkage. Furthermore, the induced stress in the constrained direction is approximately a function only of the water content, independent of the state of anisotropy (Cyrus, 2008).

Morris et al. (1992) reported that macro cracks were produced by the growth of micro cracks under tensile loading at the crack tips as a result of increased soil matrix suction. The soil matrix suction is inversely proportional to the radius of the capillaries and hence to the particle size. The capillary forces associated with soil moisture loss to the atmosphere cause a soil mass to shrink. He also concluded that soil macro cracks due to soil suction are more readily produced in fine grained soils than in coarse grained soils. This is because fine grained soils have a smaller particle size and hence smaller inter-particle voids. The smaller voids provide large soil suction. He also reported that conditions for crack propagation are more favorable at the ground surface where pore water suctions are generally largest and self-weight stresses are zero. The depth to which the crack extends is ultimately constrained by the increasing stresses due to self-weight of soil, and the planar length of the crack is limited by intersection with other cracks (Cyrus, 2008).

Albrecht and Benson (2001), studied the effect of desiccation on compacted natural clays. They found the volumetric shrinkage strain occurring in compacted natural clays during desiccation to be a direct function of the volume of water/volume of soil when the soil was

saturated. Soils with higher clay content and higher plasticity index generally are more susceptible to large volumetric shrinkage strains during drying. In addition, specimens compacted near the optimum water content with a higher compaction effort have less water/unit volume when saturated and lower volumetric shrinkage strains (Tahas, 2011).

Fang (1994) reported that when water is lost from surface soil mass, tensile forces are established in the drying surface layer. Due to the water loss, soil loses its ability to relieve tensile forces. These stresses are finally relieved by the formation of shrinkage cracks. As soil particles move closer, the surface layer is broken up into pieces of more or less distinct geometric shapes. These geometric shapes of the cracks depend on the clay mineral composition, the heating process, and the pore fluids.

Costa et al. (2008) conducted a research on desiccation crank patterns using Merri-Creek clay. The evolution of cracks was captured by automated digital photography. They concluded that under the conditions tested, the cracks occurred sequentially subdividing the overall surface area into cells.

2.6.2 Extent of Desiccation Cracking

Clay soils tend to shrink during drying due to development of substantial matric suction in the pore structure of fine grained soils. Nahlawi and Kodikara (2006) reported that soil dries faster when the humidity is lower, and the depth of desiccation cracks is expected to be varied from as low as few inches to as high as 33 ft.

Zein El Abedine and Robinson (1971) reported on desiccation cracking characteristics of swelling clay soil (vertisols) in Sudan. The drying period for the test lasted about three to six months. They found that the average crack spacing varied from 0.28 m (0.91 ft.) for soils under natural conditions to about 0.5 m (1.64 ft.) for soils located in delta areas, where flooding conditions were predominant. Also they noticed that the soil in grassy areas cracked at a wider spacing (0.51 m/1.64 ft.) than soils under treed areas. The depths of cracking were found to be between 0.65 m (2.14 ft.) in irrigated soils to 1.35 m (4.42 ft.) in non-irrigated soils. Observation

on grassy areas seemed to have shallow cracking, whereas areas under trees developed deep cracks. They concluded that the crack spacing and crack depth are related to the amount of precipitation and irrigation, the kind and density of vegetation and the history of soil development.

The extent and depth of cracks depend on various factors like temperature, humidity, plasticity of clay, and extraction of moisture from plant roots. Day (1996) classified surficial failures as shallow slope failures as the average depth varies from 1 ft. to 4 ft. (0.31 m to 1.22 m).

Blight and Williams (1971) measured opened shrinkage cracks in South Africa to a depth of 0.65m (2.14 ft.), with closed cracks extending to 1.45 m (5.41 ft.). Desiccation cracks up to 3 cm (1.18 in.) wide and 2 m (6.6 ft.) deep were reported (Ritchie and Adams, 1974; Bronswijk, 1988). Lecocq and Vandewalle (2002) reported that widest cracks are those that appear first when crack patterns were observed successively.

Dronamraju (2008) conducted a research at the University of Texas of Arlington on two clayey soils at Grapevine and Joe Pool dams. During the field visits, he noticed the presence of desiccation cracks along the slope surface on the downstream side despite the help of vegetation. A few cracks were as wide as 3 inches and as deep as 18 inches. A 3 foot long crack along with few other cracks, was also noticed in the middle and near the top of the slope. In order to assess the extent of cracking, digital image analysis was carried out using digital image software.

Figure 2.30. Cracking on the slope of Joe Pool dam (Dronamraju, 2008)

Lau (1987) attempted to predict the depth of desiccation cracks using elastic and plastic equilibrium analyses. The mode of failure of desiccated soils is believed to follow the elastic equilibrium, as it resembles the physical behavior of desiccation cracking in soils.

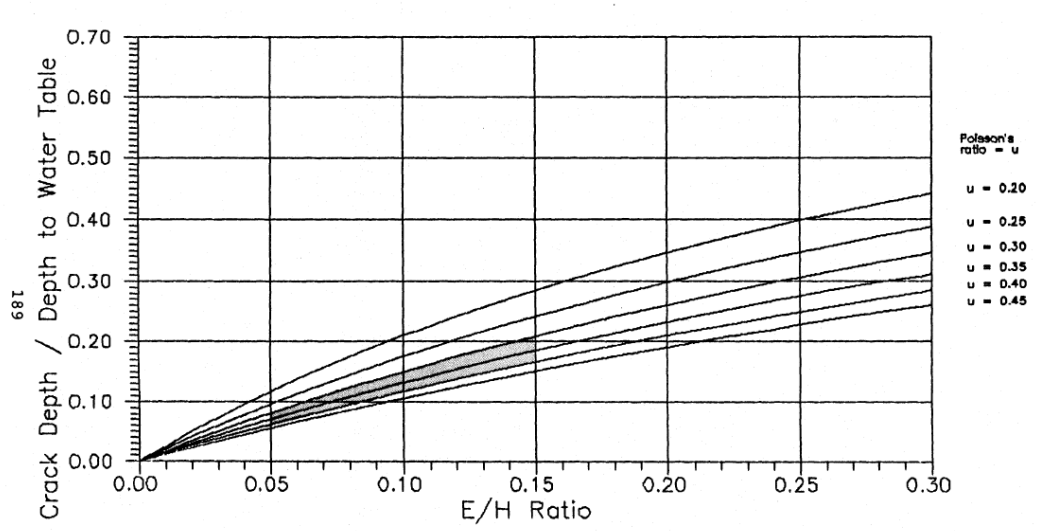

Figure 2.31. The range of predicted crack depth of Indian head Till, using elastic equilibrium analysis, suction profile "A" (i.e. matric suction varies linearly with depth), $F_w = 1.0$, $\gamma = 18.5 kN/m^3$

With the absence of complete data on the soil parameters, matric suction profile and the actual depth of cracks in the field, the validity of the elastic and plastic equilibrium analyses cannot be verified (Lau, 1987).

2.6.3 Effect of Desiccation Cracks

2.6.3.1 Effect on Soil Permeability

Vipulanandan and Leung (1990) simulated cracks and paths of preferential flow in soil samples by inserting syringe needles of various lengths into the compacted samples. Their data shows that simulated cracks increased hydraulic conductivity five times with water (after Omini et al, 1996).

Omidi et al. (1996) conducted research on the effect of desiccation cracks on the hydraulic conductivity of the compacted soil. The hydraulic conductivity of soil was measured using replicated fixed wall permeameters. Figure 2.32 illustrates that permeability increases with desiccation.

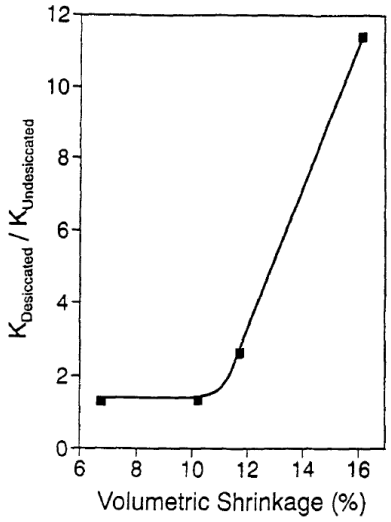

Figure 2.32. Changes in the hydraulic conductivity of soils caused by desiccation (Omidi et al. 1996)

The ratio of the desiccated permeability to that of the undesiccated permeability ($K_{desiccated}/K_{undesiccated}$) indicates that the desiccation caused a 1.3 to 11.5 fold increase in hydraulic conductivity due to crack formation. It appears that soils with a high volumetric shrinkage are most severely impacted by desiccation after compaction. Also the hydraulic conductivity of soils with a volumetric shrinkage of 11% or less will only be slightly affected by

desiccation, while soils with greater than 11% volumetric shrinkage will be greatly affected by desiccation (Omidi et al, 1996)

Laboratory experiments on different combinations of soil mixtures were conducted by Dronamraju (2008) with the help of permeameters, and he arrived at a conclusion that soils with high volumetric shrinkage are more susceptible to desiccation (Dronamraju, 2008).

2.6.3.2 Effect on Tensile Strength of Soils

Lau (1987) in the study of the desiccation cracking of clay noted that soils in general are weak in tension. Most practitioners neglect the tensile strength of soils in the design of earth structures. A limited amount of research has been conducted on the tensile properties of soils.

It is reasonable to assume that soil cracking is a result of the application of tensile stresses. A number of researches conducted in the past suggested that tensile strains-at-failure increase with increases in water content (Lau, 1987).

Fang and Chen (1972) showed that tensile strength increases but unconfined compressive strength to tensile strength ratio decreases as the plasticity index increases (Figure 2.33 and Figure 2.34)

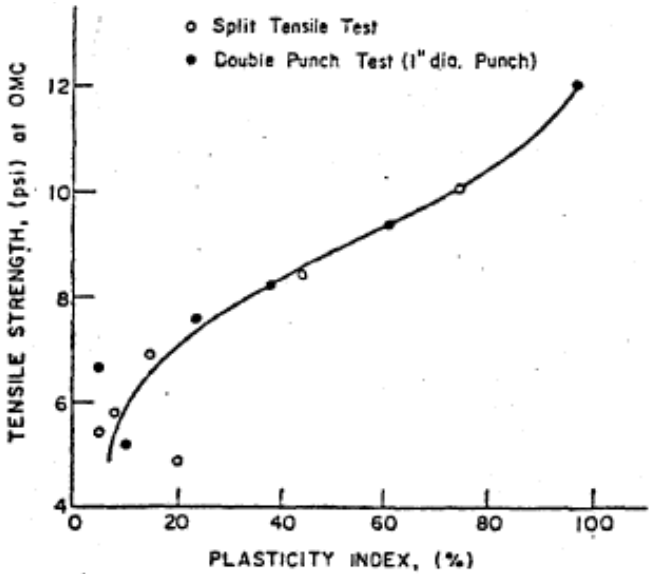

Figure 2.33. Relationship between tensile strength and plasticity index (Fang and Chen, 1972)

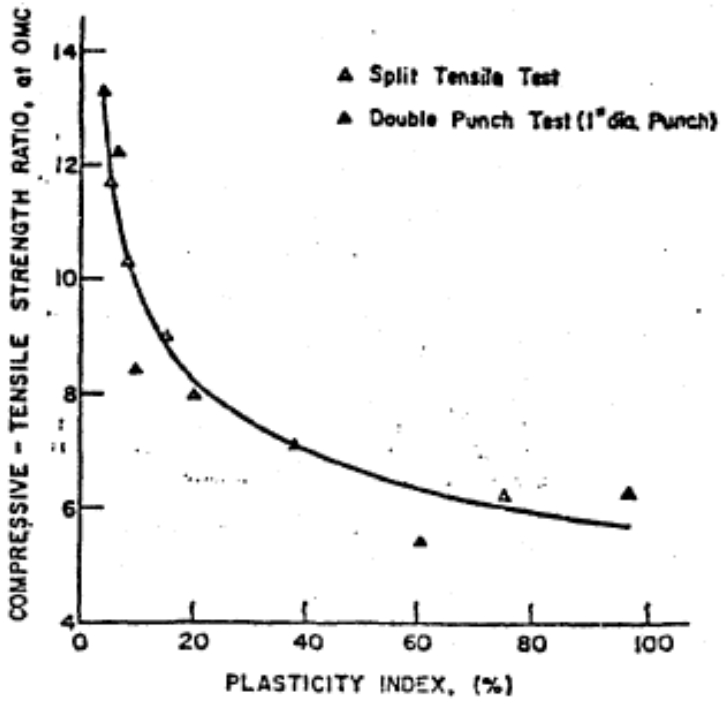

Figure 2.34. Relationship between unconfined compressive strength- tensile strength ratio to plasticity index (Fang and Chen, 1972)

2.6.3.3 Effect on Soil Suction

Most of the cracking patterns observed in the cracking tests were initiated within the 0 to 85kPa (0 to 12.33 psi) range of soil suction (Lau, 1987). At higher soil suction, there is least likelihood of any new desiccation cracks, but the cracks are widened as a result of further soil shrinkage.

Lau (1987), from his research study, concluded that desiccation cracks are expected to form in soils at low soil suction conditions (below 10kPa/1.45psi). The matric suction at cracking for silty soils is expected to be higher than that for clayey soils. Silty soils have greater compressibility than clayey soils and thus require higher matric suction at cracking than clayey soils. Some of the test results are shown in Table 2.4.

Table 2.4. A summary of the cracking test results along with matric suctions (Lau, 1987)

Cracking Test No.	Time elapsed	Average matric suction	w%	Average vert. strain
T01	43.0 hrs	3.6 kPa	32.3%	6.3%
T02	34.5 hrs	3.6 kPa	32.6%	6.3%
T03	4.0 hrs	1.8 kPa	28.8%	1.0%
T04	22.5 hrs	4.5 kPa	33.0%	6.9%
T05	56.5 hrs	5.9 kPa	71.6%	4.7%
T06	81.5 hrs	11.9 kPa	27.6%	9.3%

2.6.3.4 Effect of Tension Cracks on Slope Stability

Abramson (2001), in his research, also highlighted the importance of additional water due to rainfall in tension cracks, as it will add hydrostatic pressure and increase the tendency for a slip to occur. He used the fundamental equation based on Rankin's earth pressure theory to calculate the depth of tension cracks as:

$$z_c = \frac{2 \times c}{\gamma} \times tan^2\left(45 + \frac{\varphi}{2}\right) \qquad \text{Eq. 2-37}$$

Where

z_c −depth of tension crack

c −cohesion

φ −angle of friction

γ −unit weight of the soil material

The depth of a tension crack based on c' and φ' is likely to be much less than that using $c = s_u$ and $\varphi = 0$, because c' is considerably less than s_u. For embankments and undisturbed natural slopes, it is recommended to use effective parameters $c'$and φ' to calculate depth of tension cracks because undrained conditions due to sudden removal of lateral support may have not occurred (Abramson, 2001). Chowdhury (2010) pointed out that Eq. 2-37, based on the assumption of an active Rankin state, is only applicable to homogeneous soil. It does not take into account the geometrical effect of a slope, including pore water pressure within it and, more importantly, the factor of safety of the slope.

Spencer (1973) assumed that the factor of safety of a slope as FOS and proposed another similar equation in terms of mobilized effective stress parameters and the pore pressure ratio r_u as;

$$z_c = \frac{2 \times c'_m}{\gamma \times (1 - r_u)} \times tan^2\left(45 + \frac{\varphi'_m}{2}\right) \quad \text{Eq. 2-38}$$

where

$$c'_m = \frac{c'}{FOS} \quad \text{Eq. 2-39}$$

$$\tan(\varphi'_m) = \frac{tan(\varphi')}{FOS} \quad \text{Eq. 2-40}$$

$$r_u = \frac{u}{\gamma \times z} \quad \text{Eq. 2-41}$$

When the pore pressure is zero, Eq. 2-37 and Eq. 2-38 are identical except that one is expressed in terms of total stress parameters and the other in terms of mobilized effective stress parameters. The factor of safety, FOS, is unknown and therefore, the stability analysis can be carried out to determine a new value of F, which may then be used again for a new analysis. Thus, through iterative analysis it will lead to the correct values of z_c and FOS.

McCarthy (2002) has explained the effect of tension crack as illustrated in Figure 2.35 below.

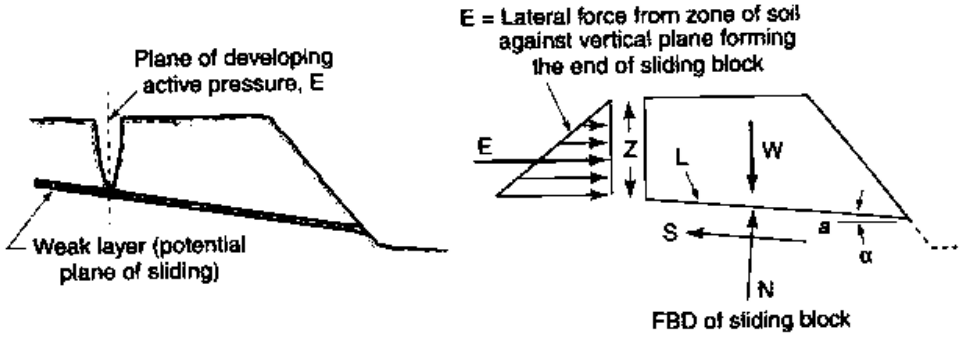

(a)

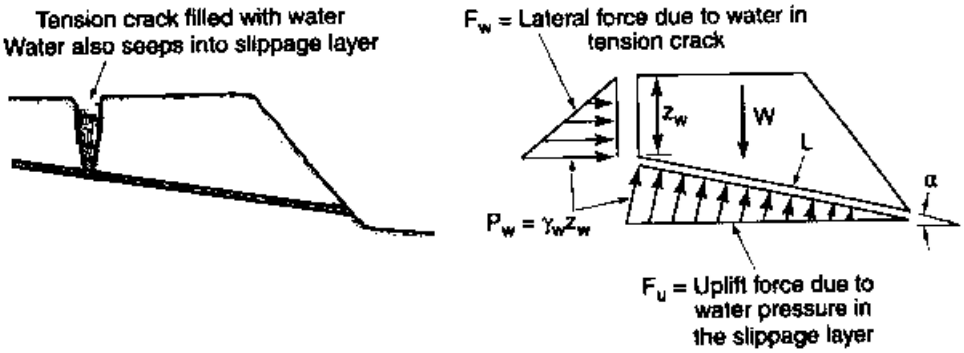

(b)

Figure 2.35. Block failure (a) Contribution to failure along weak plane by active pressure zone at top of sliding block (b) Contribution to failure where water pressure develops in the tension crack and slippage layer (McCarthy, 2002)

The shrinkage cracks formed due to desiccation during the dry season get filled up during precipitation, and the water exerts hydrostatic pressure, resulting in sliding of the block away from the crack, duly causing an increase of the width of shrinkage cracks.

McCarthy (2002) has come up with two formulae for both the cases described in Figure 2.35, considering the water pressures in the tension crack and uplift pressure exerted by seepage forces along the slippage layer. Eq. 2-42 is for case (a) and Eq. 2-43 is for case (b) as illustrated above respectively.

$$FS = \frac{c \times L + (W \times \cos(\alpha) + E \times \sin(\alpha)) \times \tan(\phi)}{W \times \sin(\alpha) + E \times \cos(\alpha)} \quad \text{Eq. 2-42}$$

$$FS = \frac{c \times L + (W \times \cos(\alpha) - F_u + F_w \times \sin(\alpha)) \times \tan(\phi)}{W \times \sin(\alpha) + F_w \times \cos(\alpha)} \quad \text{Eq. 2-43}$$

where

α –the slope angle and other notations are as shown in Figure 2.35.

The importance of tension cracks and their effect on stability (particularly when filled with water) is not always emphasized in soil mechanics (Chowdhury, 2010). This may be due, in

part, to conclusions reached by some workers that the effect of tension cracks on the factor of safety of the embankments is negligible (e.g., Spencer, 1968, 1973). Such conclusions only apply for the small depth of tension cracks predicted by using c and φ (Eq. 2-37 and Eq. 2-38). In cut slopes, tension cracks could extend to considerable depths and exert significant influence on the value of *F* as in the case of the slips at Bradwell (Skempton and La Rochelle, 1965).Tension cracks can also cause a consequence of the initiation of progressive shear failure. As such,the existence of tension cracks deserves careful attention.

2.6.4 Consideration of Tension Crack during Slope Stability Analysis

It is a common practice to neglect the resistance offered by the slip circle near the tension crack as shown in Figure 2.36 (EM 1110-2-1902, dated 31st October, 2003).

When a strength envelope with a significant cohesion intercept is used in slope stability computations, tensile stresses appear in the form of negative forces on the sides of the slices and sometimes on the bases of slices.

Such tensile stresses are almost always located along the upper portion of the shear surface, near the crest of the slope, and should be eliminated unless the soil possesses significant tensile strength because of cementing, which will not diminish over time (EM 1110-2-1902, dated 31st October, 2003).

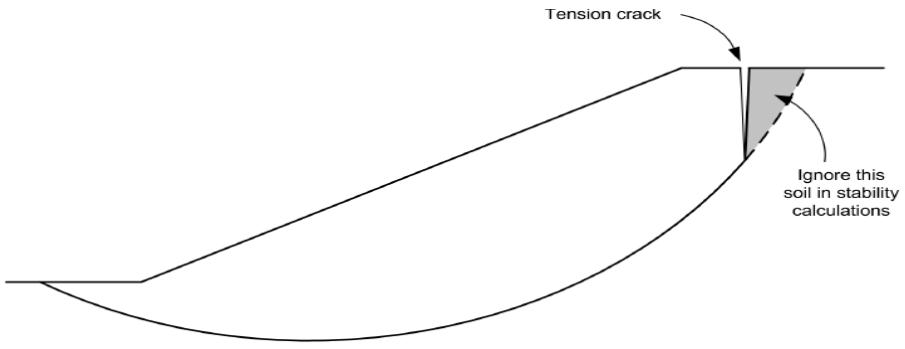

Figure 2.36. Introduction of vertical tension crack to avoid tensile stresses In cohesive soils (USACE)

When a strength envelope with a significant cohesion intercept is used in slope stability computations, tensile stresses appear in the form of negative forces on the sides of the slices and sometimes on the bases of slices.

Such tensile stresses are almost always located along the upper portion of the shear surface, near the crest of the slope, and should be eliminated unless the soil possesses significant tensile strength because of cementing which will not diminish over time (EM 1110-2-1902, dated 31st October, 2003).

The tensile stresses are easily eliminated by introducing a vertical crack of an appropriate depth as shown in Figure 2.36. The soil upslope from the crack (to the right of the crack in Figure 2.36) is then ignored in the stability computations.

This is accomplished in the analyses by terminating the slices near the crest of the slope, with a slice having a vertical boundary, rather than the usual triangular shape, at the upper end of the shear surface (EM 1110-2-1902, dated 31st October, 2003).

2.6.5 Crack treatments

There are different types of treatments for old materials, such as cement and lime, and new materials, such as fiber. From Table 2.5, the treatment with fiber for high-plasticity index silty soil was powerful, while for clay soil, the powerful material for treatment was a lime and silica fume. From the study conducted by Guney, Sari *et al*., (2007) on the impact of cyclic wetting-drying on the swelling behavior of lime-stabilized soil, it was observed that lime-stabilized soils are negatively affected by the wetting-drying cycles. In other words, the beneficial effect of lime stabilization in controlling the swelling potential of lime-treated samples is partially lost upon subjecting them to cycles of wetting and drying. The results of the study showed that lime-stabilized, expansive, clayey soil must not be used in the regions where wetting and drying cycles are significant. Another study showed that soils with a plasticity index above 20 are not suited to cement stabilization using manual presses because of problems with

excessive drying shrinkage, inadequate durability and low compressive strength (Walker, P.J., 1995).

Table 2.5. The effect of different treatment materials on the shrinkage strain, swelling strain, and hydraulic conductivity (Tahas, 2011)

Soil properties			Treatment Material	Reduction in shrinkage strain	Reduction in swelling (%)	Change in hydraulic conductivity (%)	Impact of cyclic wetting and drying on treated soil	Reference
Sand	Silt	Clay	0.4% Polypropylene Fiber (RCP17T)	Low	-	-	-	Hariant, Hayashi *et al.*, (2008)
			0.6% Polypropylene Fiber (RCP17T)	Low	-	-		
35%	52%	13%	0.8% Polypropylene Fiber (RCP17T)	Medium	-	-		
PI = 80.3		1%	High Polypropylene Fiber (RCP17T)	-	-			
			1.2% Polypropylene Fiber (RCP17T)	Medium	-	-		
Sand	Silt	Clay	4% lime	Medium	-	Large increase	-	Omidi (1993)
			7% lime	High	-	Large increase		
16.2%	31.4%	52.4%	9% lime	High	-	Large increase		
			4% cement	Medium	-	Large increase		
			7% cement	High	-	Medium decrease		
PI = 36.6			12% cement	Medium	-	Large decrease		
			0.25% fiber	Low	-	Small decrease		
			0.5% fiber	Low	-	Small increase		
Sand	Silt	Clay	4% lime	Medium	-	Large increase	-	
			7% lime	Medium	-	Large increase		
5.1%	49.6%	45.3%	9% lime	Medium	-	Large increase		
			4% cement	Low	-	Large decrease		
			7% cement	Medium	-	Large decrease		
PI = 19.7			12% cement	Medium	-	Large decrease		
			0.25% fiber	Low	-	Small increase		
			0.5% fiber	Low	-	Small increase		
Sand	Silt	Clay	4% lime	Medium	-	Large increase	-	Omidi (1993)
			7% lime	Medium	-	Large increase		
			9% lime	Medium	-	Large increase		
63.8%	12.7%	23.5%	4% cement	Low	-	Large decrease		
			7% cement	Low	-	Large decrease		
			12% cement	Medium	-	Large decrease		
PI = 5.2			0.25% fiber	Low	-	Small increase		
			0.5% fiber	Low	-	Small increase		
Sand	Silt	Clay	3% Lime	High			The maximum swelling potential reduction occurred at the first cycle, but the swelling potential of lime-treated samples is partially lost upon subjecting them to cycles of wetting and drying.	Guney, Sari et. al., (2007)
4%	15%	81%						
PI= 350			6% Lime	High				
Sand	Silt	Clay	3% Lime	High				
9%	18%	73%						
PI= 315			6% Lime	Medium				
Sand	Silt	Clay	3% Lime	High				
7%	18%	75%						
PI= 208			6% Lime		Negative effect			
Clayey soil with PI=9.9			5% Blast furnace slag	Low	-	-	The maximum shrinkage strain at the first cycle and the difference between treated and untreated samples is partially lost upon subjecting them to cycles of wetting and drying.	Osinubi and Nwaiwu Kalkan (2009)
			10% Blast furnace slag	Medium	-	-		
			15% Blast furnace slag	Low	-	-		
Clayey soil with PI=37			10% Silica Fume	-	Medium	Medium decrease	-	
			20% Silica Fume	-	High	Medium decrease		
			30% Silica Fume	-	High	Large decrease		

Furthermore, from the study by Rifai and Miller, (2009) on the theoretical assessment of the increased tensile strength of fibrous soil undergoing desiccation, a theoretical model was developed to describe the mechanism of the increased tensile strength due to fiber inclusion in the soil. Fiber inclusion increased the tensile strength of the fiber-soil composite significantly. This increase in tensile strength is expressed as a function of fiber and soil-water contents.

Fiber content increases the tensile strength of the soil because of the increase in the number of fibers crossing the crack plane, which in turn increases the soil's resistance to cracking.

Previous studies by Viswanadham, Phanikumar et al., (2009) on the swelling behavior of a geofiber-reinforced expansive soil showed that reinforced expansive clay specimens with polypropylene fiber reduced heave, swelling, and swelling pressure.

The results of the study of the influence of freeze-thaw cycles on the unconfined compressive strength of fiber-reinforced clay by Ghazavi and Roustaie (2010) showed that the unconfined strength of all reinforced and unreinforced samples decreased by 20%-25% when the number of freeze-thaw cycles increased. The addition of 3% fibers increased the unconfined compression strength of soil for polypropylene fibers by 160% and 60% before and after applying cycles, respectively. For steel fibers, these increases are approximately 7% and 6% before and after applying cycles, respectively.

2.7 Effect of Rainfall on Surficial Failures

Rahardjo (1994) highlighted the importance of quantifying the contribution of negative pore-water pressure to the shear strength of soil. During a rainfall event, water penetrates into the soil through the desiccation cracks. The wetting front is created and slowly advances into the slope. With the increase of pore water pressure, shear strength reduces, which leads to triggering the failure (Cho et al. 2002).

Day (1996) also emphasized the importance of the wetting front, as it increases the permeability parallel to slope increases, and thus the seepage occurs parallel to them. Apart from rainfall intensity, other factors such as rainfall characteristics, antecedent precipitation, soil characteristics and topography also contribute to the failure of any slope (Church and Miles, 1987). The problem is aggravated as the weight of moist soil acts as a surcharge. The resisting factors are the drained cohesion and internal friction, which attenuate during rainfall as pore-water pressure rises.

The vegetation on the slopes contributes to safety against failures. Reduction of soil moisture content due to transpiration helps in gaining strength especially during rainfall. It has also been discovered that the plant roots enhance the shear strength of soil as reinforcement (Waldron, 1977; Day, 1993). Studies of natural and synthetic fiber reinforcement in sand proved an increase in shear strength due to the reinforcing effect (Gray and Ohashi, 1983; Day, 1996).

Many unsaturated slopes fail during heavy rains following reduction in matric suction and the increase in pore water pressures (Lim et al.. 2006).

Rainfall infiltration is an important factor affecting slope stability. Tan et al. (2011) showed that during a rainfall event, the unsaturated zone decreased, while the transient saturated zone increased. The pore-water pressure, displacements and the negative shear stress on the slope surface grew proportionally with increasing rainfall intensity and duration. The safety factors of the slope also decreased with the rising of the rainfall intensity and duration, and were all lower than 1.0.

2.7.1 Case studies

2.7.1.1 Antecedent rainfall in Singapore

Rahardjo (2001) studied the effect of antecedent rainfall on slope stability in Singapore, where there were more than twenty surficial failures after a storm event. A finite element model was carried on to imitate the situation. Soil permeability was calculated using the indirect method outlined by Fredlund and Rahardjo (1993), as shown in Figure 2.37, in conjunction with Matric Suction:

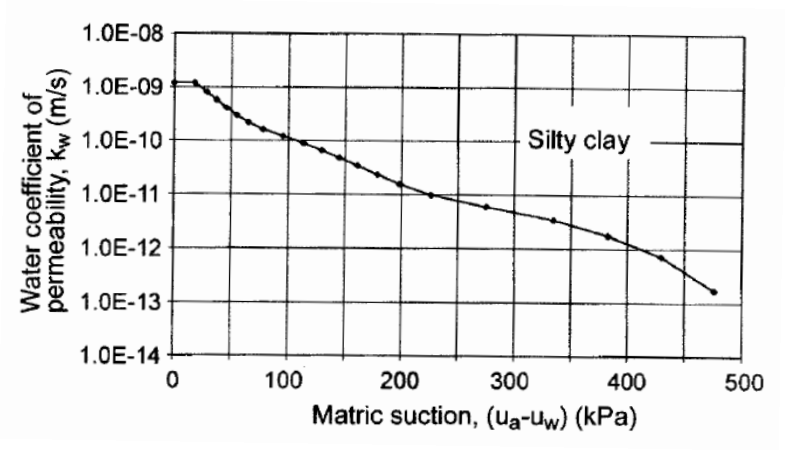

Figure 2.37. Soil-Water Characteristic curve for a residual soil from the Jurong Sedimentary Formation (Fredlund and Rahardjo, 1993)

Results of modeling showed that the water table rises rapidly during rainfall, causing the pore-water pressure to increase or the matric suction to decrease. The antecedent rainfall prior to the storm event has decreased the matric suction in the slope causing the coefficient of permeability of the soil to increase, making the soil more permeable to infiltration. As a result, the shear strength decreases and consequently, the factor of safety of the slope decreases during rainfall. It is interesting to note that the water table continues to rise after the rain has stopped, as shown in all the three cases indicating that infiltrating water continues to percolate downward even when the rain has stopped (Rahardjo, 2001).

2.7.1.2 Study of the Effect of Antecedent Rainfall in Surficial Failures at Grapevine Dam, Texas

McCleskey et al. (2005) reported various failures occurred at the Grapevine Dam in the state of Texas, USA. A study has been carried out by referring to rainfall data. It was observed that almost all the failures were preceded by rainfall events, as shown in Table 2.6.

Table 2.6. History of surficial slope failures at Grapevine Dam (McCleskey, 2008)

Date of slide	Slide Width × Length (m)	Rainfall observations during the month (and preceding month where necessary)
26 Feb 1965	30 x 12	157 mm- Feb
05 Jun 1970	38 x 14	16 mm - June, 92 mm- May
09 Feb 1973	24 x 5	49 mm-Feb, 83 mm-Jan
23 Apr 1973	23 x 11	154 mm-Apr,
03 Apr 1974	60 x 21	64 mm-Apr, 58 mm-Mar
10 Apr 1974	15 x 11	64 mm-Apr, 58 mm-Mar
--Jun 1976	18 x 21	36 mm-June, 153 mm-May
-- Jun 1976	27 x 21	36 mm-June, 153 mm-May
17 Jan 1977	45 x 20	61 mm-Jan
17 Jan 1977	15 x 15	61mm-Jan
07 Feb 1977	42 x 15	43 mm-Feb
-- Jun 1977	46 x 15	17.5 mm-June, 25 mm-May
27 Oct 1981	16 x 21	360 mm-Oct
27 Oct 1981	16 x 18	360 mm-Oct
10 Jan 1982	46 x 21	59 mm-Jan,4 mm-Dec81
19 May 1982	70 x 18	347 mm-May
19 May 1982	32 x 18	347 mm-May
09 July 1982	33 x 21	69 mm-July, 109 mm-July
13 Mar 1989	30 x --	95 mm-Mar, 94 mm-Feb
04 Nov 2004	45 x 23	127 mm-Nov, 145 mm-Oct

Dronamraju (2008) studied the effect of rainfall intensity and duration regarding the slope stability issue on Grapevine Dam. A numerical modeling was conducted under three cases: a) no rainfall, b) short-term rainfall and c) long-term rainfall. Desiccation cracks were assumed to happen up to 4ft. depth. Residual soil properties were used for soil in the wet front as it expanded through desiccation cracks. Figure 2.38 and Figure 2.39 show the expansion of wetting front in case of short and long rainfall events. The results showed that with increasing of intensity and duration, the factor of safety dropped from approximately 3.14 to 0.8. This

explained the reason of surficial failures happening frequently in North Texas embankment slopes because rainfall effect on soil strength was not included in the original designs.

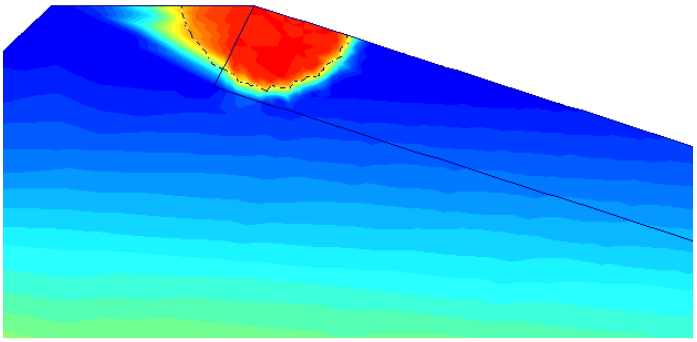

Figure 2.38.Saturation of soil near the crest high intensity rainfall for 1 day (Case 2) (Dronamraju, 2008)

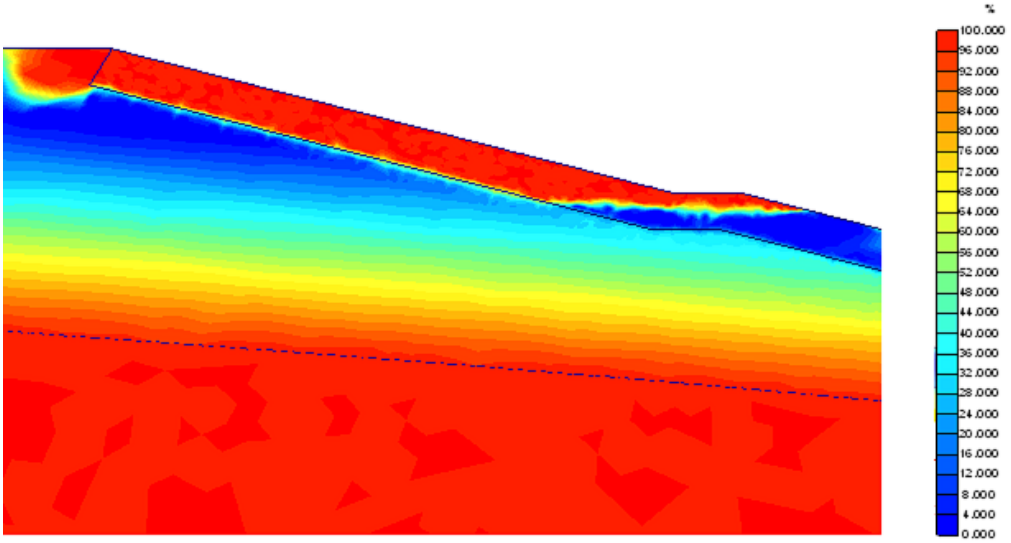

Figure 2.39.Complete saturation of soil for case 3 – desiccation and high intensity rainfall for a long time (Dronamraju, 2008)

2.7.2 Suction Measurements at a Slope

Lim et al. (1996) conducted suction studies in Singapore, with respect to the effect of rainfall at different depths on a soil having a plasticity index of about 30%. The average effective cohesion and friction angle were reported to be 30 kPa (0.62 ksf) and 26º, respectively. The field and laboratory coefficient of permeability measured was 1.0x 10^{-6} m/sec (3.3 x 10^{-6} ft./sec) and 1.0x 10^{-9} m/sec (3.3 x 10^{-9} ft./sec), respectively at depths of 1.7 m to 1 m (5.6 – 3.3 ft.).

Higher value of permeability in the field was attributed to the desiccation cracks in the soil. The field section had a width of 15 m (49 ft.) and a length of 25 m (82 ft.) along the slope, with a slope of 30º and reducing to 12º to 15º near the toe. The site originally had grass. Three test sections, each of 5 m (16.4 ft.) width were constructed, as shown in Figure 2.21.

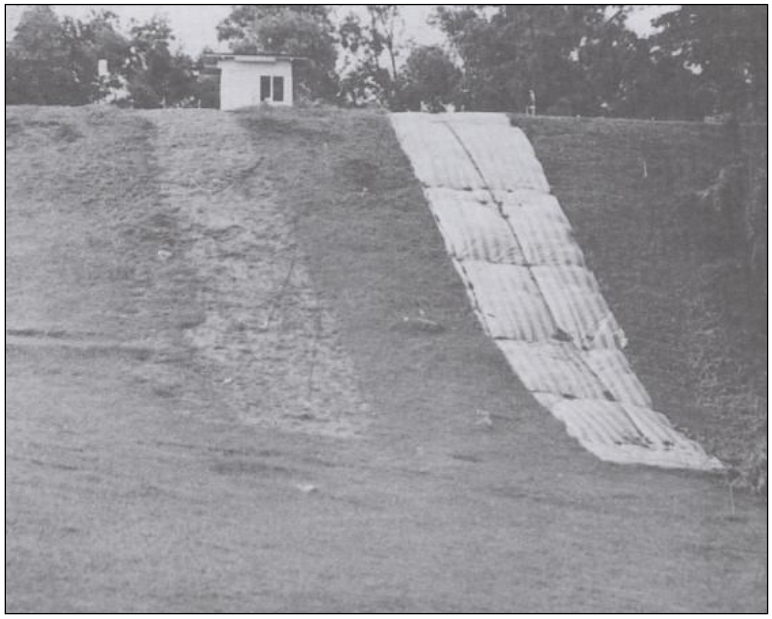

Figure 2.40. Influence of varying ground surface conditions (Lim et al. 1996)

The test sections from left to right are

1. Bare ground surface
2. Grassed surface and
3. Canvas over grass surface
4. The progressive change in the field matric suction was shown in Figure 2.22. Changes in the matric suction profile under the bare surface were reported to be more significant than below the grass surface. There was very little variation of matric suction under the canvas covered surface.

For grass covered surface, the change in the matric suction near the surface was reported to be more significant than at deeper depths because of evaporation and evapo-

transpiration. The presence of grass accelerated the removal of water and prevented the advancement of water front.

For bare slopes, there was only surface evaporation, and the wetting front continued to greater depths at the end of each rainstorm. The propagation was up to a depth of 1.5 m (5 ft.) or more. It was also observed that the matric suction measured at 1.5 m (5 ft.) depth was relatively low.

It could be seen that the soil started showing the trend of changing to the saturated condition from the unsaturated condition at depths of about 1.5m (5 ft.). Piezometric observations showed that a perched water table probably developed at 1.5 m (5 ft.) below the ground surface. It can be concluded that with continued rainfall, the soil in the top few meters get saturated and pore pressures increased.

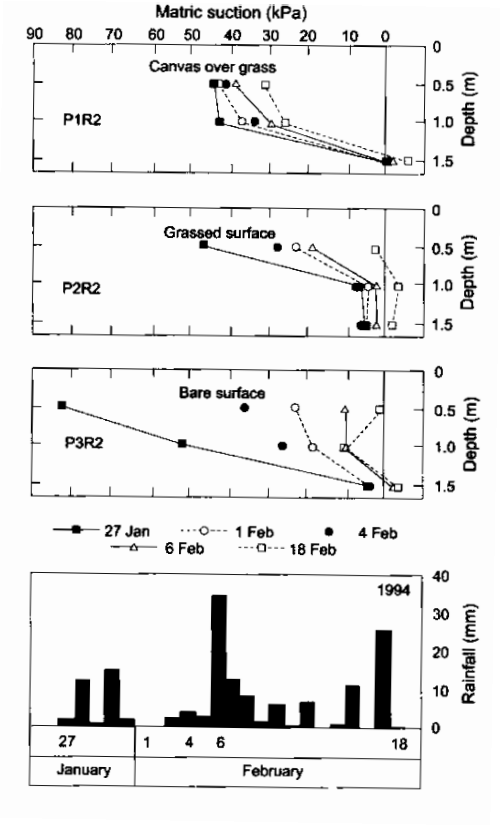

Figure 2.41. In-situ changes in suction due to rainfall (Lim et al. 1996)

2.8 Fully Softened Shear Strength

In design of embankments or cut slopes, the use of peak strength in the analyses tends to overestimate the factor of safety (stability), and the use of residual shear strength in the analysis tends to underestimate the factor of safety (stability). With the surficial failures associated with soil being exposed to wetting and drying cycles, clay soils become "fully softened" due to shrink-swell action. The use of fully softened shear strength values results in a more accurate analysis and leads to designs or repair methods that provide long-term stability at reasonable costs. Slope analyses using either peak or residual strength properties do not properly model most slope failure or potential failure conditions. Understanding the mechanisms of these slope failures and being able to economically predict the fully softened shear strength of clay soils is the key to successful design, repair, and stabilization of clay slopes.

2.8.1 Background

Skempton (1970) introduced the concept of fully softened shear strength, which is between the peak strength and residual strength (Figure 2.42). He concluded that softening over time decreases clay strength to the "critical state strength, which is approximately equal to the strength of the clay when normally consolidated. He suggested that the FSS soil parameters c' and φ' are equal numerically to the peak strength parameters of the normally consolidated clay. Chandler and Skempton (1974), in their research of slides in London clay, emphasized the importance of c' in FSS. In shallow slides, even small values of c' result in significant differences in calculated factors of safety.

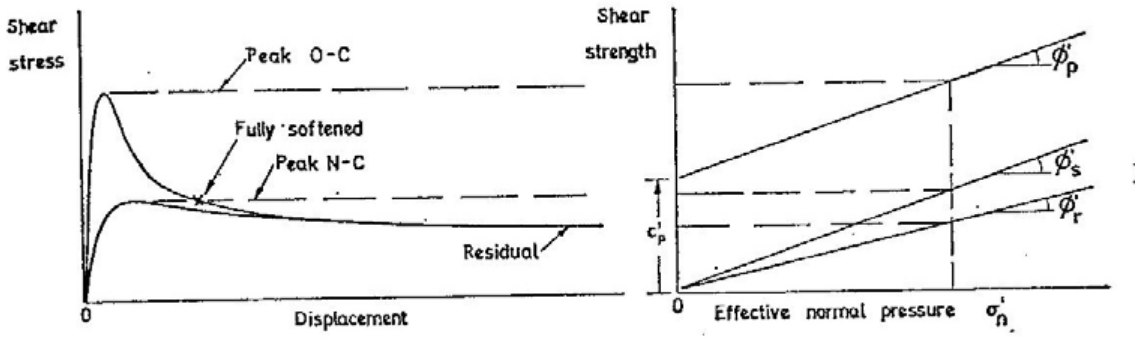

Figure 2.42. Comparison of Peak, Residual and Fully Softened Shear Strength envelopes (Skempton,1970).

Terzaghi et al. (1996) described fully softened shear strength (FSS) as a drained shear strength of an overconsolidated clay developed under highly fissured and jointed conditions without the presence of a preexisting shear surface. Friction angle of FSS is equal to the friction angle φ' of clay of the same composition in a normally consolidated state, such as produced by a laboratory consolidation from a slurry soil condition. He also highlighted the unique feature of FSS failure envelope that has a slightly nonlinear characteristic. Figure 2.43 presents the failure envelope of London clay (after Terzaghi, 1996).

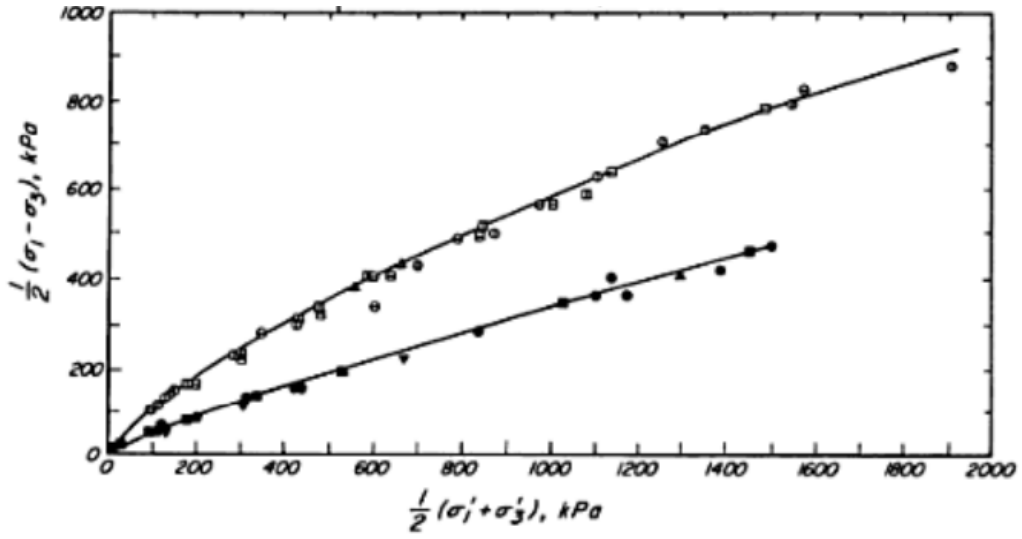

Figure 2.43. Intact and fully softened strengths of samples of London clay from depth of 35m (Bishop et al., 1965 and Terzaghi, 1996)

Skempton (1970) recommended the FSS as the applicable strength for first-time slides in excavations of homogeneous stiff fissured clays. However, Mesri and Shahien (2003) suggested that part of the slip surface may still be at the residual strength condition even for first-time slides in excavated stiff clays and shale. The reason is anisotropy and bedding planes due to geologic deposition, as it may naturally provide residual strength conditions within slopes. They argued that if part of the slip surface is not already at the residual condition prior to excavation, the residual strength can develop by progressive failure.

Kayyal and Wright (1991) conducted a study of Paris and Beautmont Clays on long-term strength properties. They found that the shear strengths at the time of occurrence of these slides, determined by back analysis, were much smaller than the strength of the compacted clay measured in laboratory tests. After a number of wetting and drying cycles, the strength of the clay decreased close to the value of FSS (or normally consolidated). Originally the FSS was considered to apply only to slope failures in stiff fissured over-consolidated natural clay and shale deposits. The authors suggested that the reduction of strength was due to the formation of shrinkage cracks during period of droughts, followed by water permeating through those cracks during rainfall resulting in the clay being softened, They recommended that the long-term strength of clay soil, under wetting and drying cycles, can be measured using the strength of remolded, normally consolidated test specimens. Saleh and Wright (1997) defined the FSS as the strength to eventually develop in clays after a long period of exposure to environmental conditions (shrink-swell, wetting-drying, etc.) FSS is considered to happen for first-time slides in both excavated and fill slopes in highly plastic clays.

Day and Axten (1990) suggested applying the FSS concept to shallow failures (up to 4ft. deep) in compacted clay slopes in Southern California that were similar to those in Texas. The failures occurred after prolonged rainfall, causing swelling and reduction in strength of clay soil. McCook (1997) in his investigation of shallow slides in embankments of highly plastic clays,

concluded that the slide depth was limited by the depth of desiccation cracks, and the shear strength at failures was between the peak and the residual strength.

2.8.2 Current Testing Methodologies for FSS

Based on background research of FSS characteristics, FSS can be measured by testing either specimens that are normally consolidated or compacted specimens that have been subjected to repeated wetting and drying with corresponding shrinkage and expansion (Wright, 2005). While normally consolidated clay specimens can be prepared by forming slurry and consolidating at a slow pace to fully achieve normal consolidation, preparing compacted specimens under wetting-drying cycles can be a very time consuming process. Accordingly, laboratory testing for FSS is most commonly in the former way of preparing samples.

Stark et al. (2005) developed the Fully Softened Shear Strength (FSS) testing procedure using Torsional Ring Shear apparatus. This was later adopted as ASTM standards for testing FSS of clayey soil in the 2010 ASTM Compilation. However, using the FEM model in ABAQUS, Meehan (2007) pointed out the effect of side friction in increasing the frictional resistance of soil during the measurement of FSS with torsional apparatus and thus yielding higher values of FSS. This was proven by Tiwari (2010) with friction angles measured with ring shear devices that consistently exhibited higher values than those obtained from Direct Shear apparatus.

Wright et al, (2007) performed a series of consolidated-undrained triaxial compression tests on specimens of Eagle Ford Shale. The slurry of soil was poured into a cylindrical piston, and incremental load was applied until the desired pressure was reached. Each load increment came after the verification of the previous load's primary consolidation. Each specimen required approximately 25-30 days to consolidate due to the specific high of specimen required to perform the triaxial test.

Tiwari (2010) performed testing on FSS using Direct Shear apparatus. Because of its ability to allow specimens to fully drain, direct shear apparatus can measure the FSS under drained (long-term) conditions with the proper shearing rate.

To date, the literature on testing FSS using Direct Shear apparatus is limited, and the proposed research is one of the earlier attempts. The results of testing FSS on both Direct Shear and Torsional Ring Shear are presented and compared in later Chapters.

2.9 Slope Stabilization Methods

Stabilizing surficial slope failures often faces great challenges due to the site access limitations and the difficulties of working on sloped surfaces. A number of ground improvement methods have been studied and partially applied to prevent surficial slope failure. The most commonly used method to repair surficial failures is to rebuild the failed area by digging the failed soil and recompacting it. In this chapter, we briefly introduce some other methods including Pipe Piles and Wood Lagging, Lime-Cement Column, Soil Nailing and Anchoring, Aggregate Rammed Pier, Recycled Plastic Pins and Drilled Shafts. Some of these methods were initially developed for a deep seated slope failure scenario but they can also be applied to surficial slope failures.

2.9.1 Pipe Piles and Wood Lagging Method

Day (1997) recommended the use of pipe piles and wood lagging as the most commonly used repair method. The pipe pile and wood lagging method consists of disposing of the failed debris and cutting benches into the slope below the failure surface, as shown in Figure 2.44.

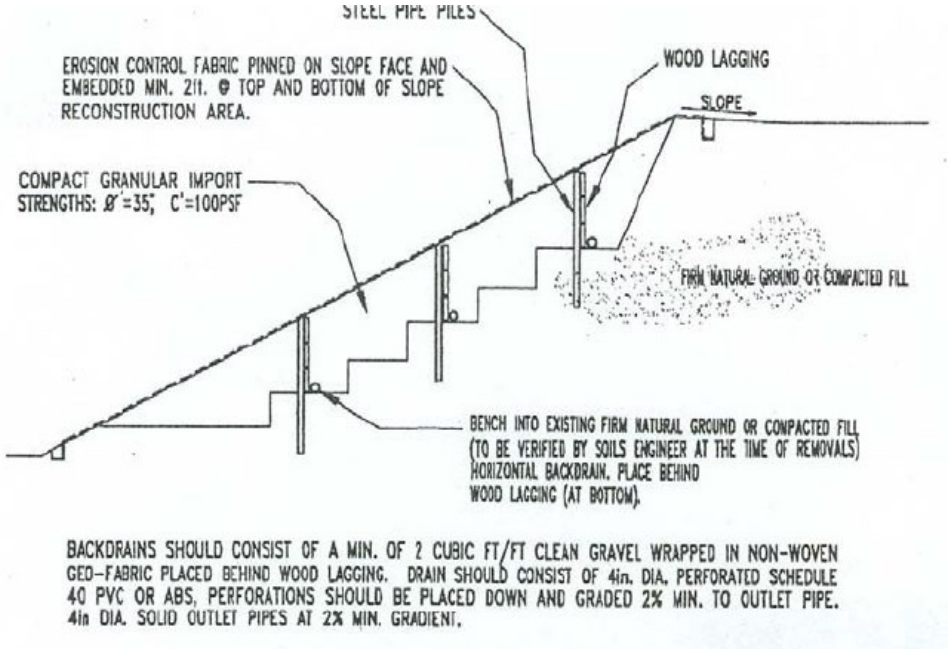

Figure 2.44. Pipe pile and wood lagging repair (Day, 1997)

Wood lagging was placed behind the piles and a drainage system was then built behind the wood. A select fill was compacted in layers and the face of the slope was protected with erosion control fabric and vegetation. Titi and Helwany (2007) pointed out that the disadvantage of this method was that the soil pressure against wood lagging was transferred directly to pipe piles. This resulted in failure of the pile in bending.

2.9.2 Geogrid repair

Using geogrid against slope surficial failures is considered an innovative and cost-effective method. The open structure of geogrids provides good interlocking with granular materials and thus, improves soil retention on a vulnerable slip plane surface. Its tensile strength carries the loading forces imposed on the anchorage zone. Because geogrids also utilize inferior in-situ materials and waste, it is also called a sustainable construction method.

Day (1997) discussed the repair of surficial slope failures using geogrid. The process starts with the complete removal of the failed soil mass. Benches are then cut down into the undisturbed soil below the slip surface, as shown in Figure 2.45. Drains (vertical and horizontal)

are designed to collect water from the slope and dispose of it off-site. The slope is built on constructing layers of geogrid and compacted granular material (Day, 1997).

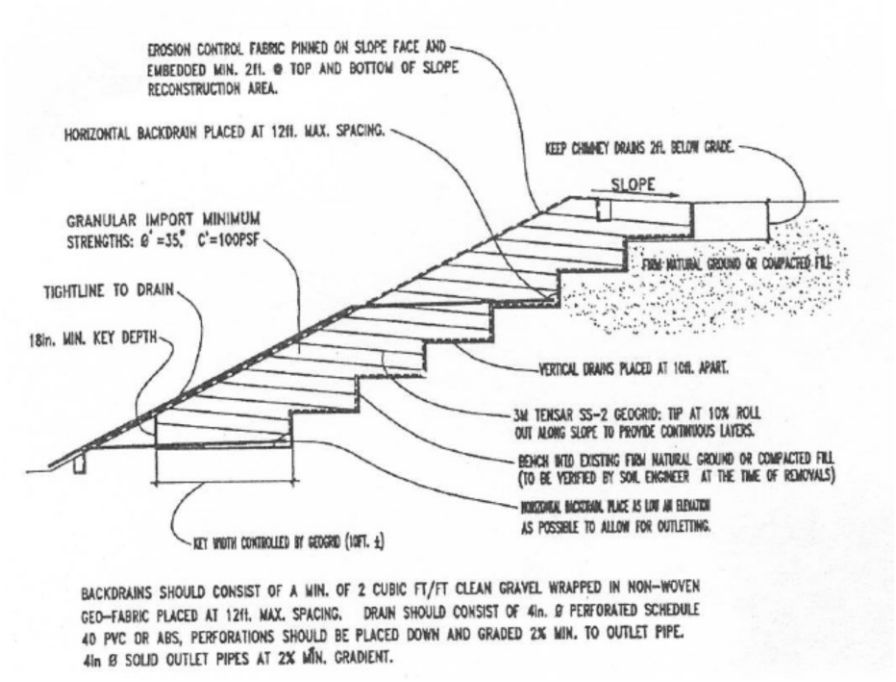

Figure 2.45. Repair of surficial slope failure by geogrid (Day, 1997)

2.9.2 Lime-Cement Column Stabilization Method

Watn et al. (1999) has successfully developed a principle for a Deep Soil Mixing method in stabilizing slope failures using effective strength parameters. A continuous series of lime-cement columns constructed in the configuration of the ribs have been reported to increase the shear capacity of the slope rather than withstanding the vertical load when constructed in a single column configuration. The stabilization principle of a slope with lime-cement columns proposed by Watn (1999) is illustrated in Figure 2.46.

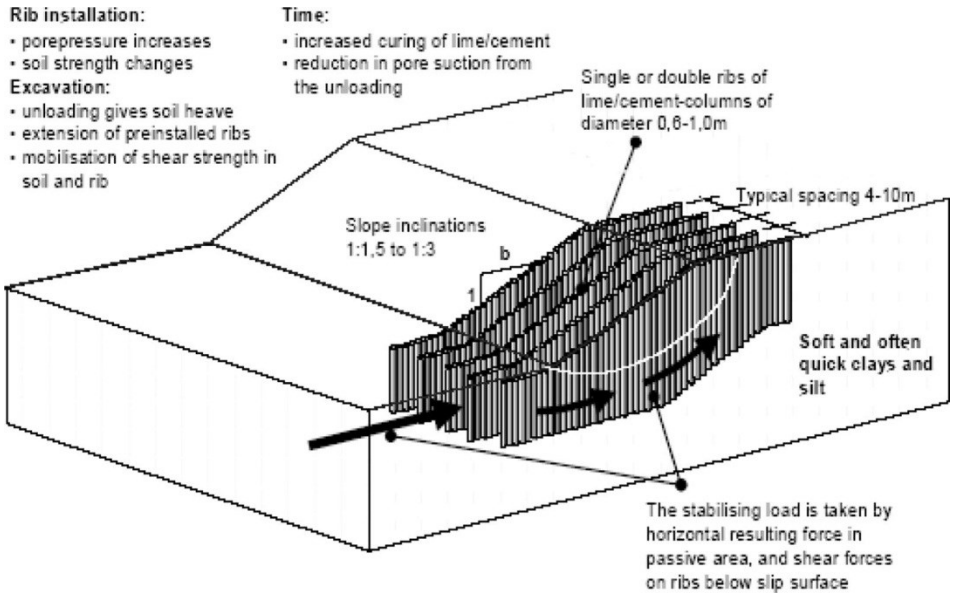

Figure 2.46. Principle for stabilization of a slope with lime-cement columns configured in ribs (Watn et al., 1999)

2.9.3 Use of Nailing and Anchor Techniques to Improve Surficial Slope Stability

Titi and Helwany (2007) have carried out extensive research for the Wisconsin Department of Transportation to repair the surficial slides that occurred on the highway embankments and cut slopes. They have documented the use of vertical members for slope stabilization to prevent surficial failures. The study team of the University of Wisconsin, Milwaukee visited various sites of surficial failures. One of the locations of surficial failure was along STH-164 in Waukesha County, Wisconsin, as shown in Figure 2.47. The team concluded that the cause of failure was prolonged rainfall and snowmelt. When a small hole was dug at another surficial failure site near Burlington, it got filled up with water quickly, as shown in Figure 2.48, indicating presence of abundant quantity of water near the failure surface.

Figure 2.47. Surficial failure on a cut slope along STH-164, Wisconsin
(Titi and Helwany, 2007)

Figure 2.48. Perched water on a failure surface through seepage
(Titi and Helwany, 2007)

2.9.3.1 Soil Nailing

Titi and Helwany (2007) recommended launching of soil nails beyond the failure surface under pressure using Soil Nail Launchers. Soil nails are inserted into the slope face at a high speed, utilizing high pressure compressed air. Figure 2.49 shows the process of soil nail

launching on slopes. It was observed that top portion of the soil did not move when it was stabilized with soil nails.

Figure 2.49. Installation of soil nails (Titi and Helwany, 2007)

The technique with the use of a soil nail launcher provides quick installation with minimal impact on the site environment. The depth of penetration depends on the compressed air pressure and the properties of the soil on slopes.

2.9.3.2 Repairs Using Earth Anchors

The earth anchoring system consists of a mechanical earth anchor, wire rope and end plate with accessories. The method was recommended for slope stabilization and repairs of surficial failure locations. The technique involves the grading of the failed slope, providing a turfing mat and then installing earth anchors as shown in the Figure 2.50 (Titi and Helwany, 2007)

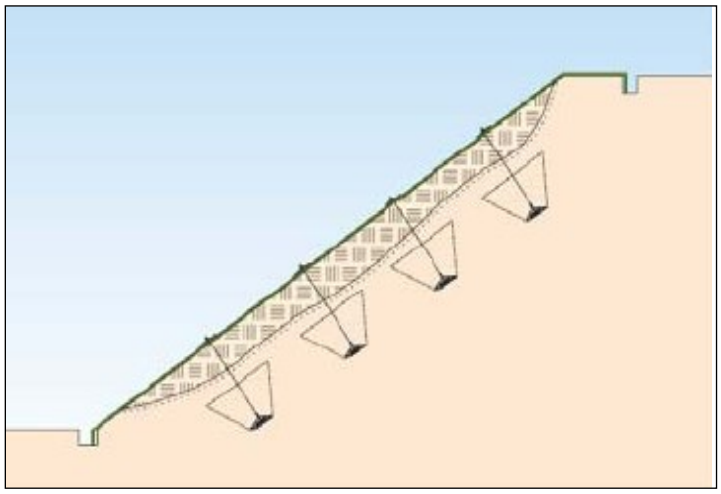

Figure 2.50. Installation of earth anchor (Titi and Helwany, 2007)

For installing the earth anchors, the anchor is first inserted into the soil below the failure surface. The wire of the tendon of the anchor is pulled to move the anchors to its full working position. The wire tendon is locked against the end plate, and the system is tightened.

2.9.4 Rammed Aggregate Pier

Parra et al. (2007) demonstrated successful use of rammed aggregate pier to repair two deep seated slope failure sites on US Highway 71 (Figure 2.51) and US Highway 167. Aggregate was placed at the bottom of the drilled hole and then compacted by a high-energy beveled impact tamper. The piers are completed by ram loading aggregate to form undulated-sided shaft (Figure 2.52).

Figure 2.51. Slope Failure at US-71 (Parr, 2007)

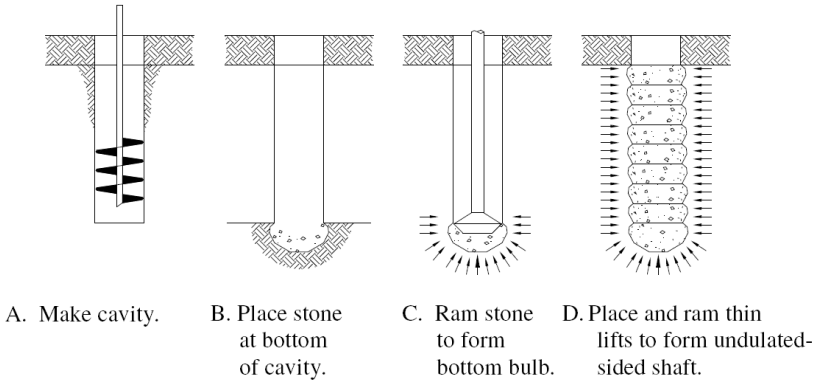

Figure 2.52. Rammed Aggregate Pier Reinforcement Installation Procedure (Fox and Cowell, 1998)

The result monitored during the post-construction period shows that the progressive lateral displacement of slope was minimized completely. The Rammed Aggregate Pier Stabilization Method was found to be simple and cost-effective compared to other traditional slide repair solutions.

2.9.5 Use Of Recycled Plastic Pins To Improve Surficial Slope Stability

Loehr and Bowders (2007) conducted research for the Missouri Department of Transportation to repair the surficial slides that occurred on the highway embankments and cut slopes. The use of recycled plastic pins for slope stabilization to prevent surficial failures was

documented by the Missouri Transportation Institute and Missouri Department of Transportation (OR07.006). A schematic of using recycled plastic pins as reinforcing members is shown in Figure 2.53.

Recycled plastic pins are manufactured from industrial or post-consumer waste consisting of polymeric materials like high density polyethylene (HDPE), low density polyethylene (LDPE), polystyrene, polypropylene, polyethylene-terephthalate (PET) and varying amounts of additives like sawdust, fly ash and other waste materials. The average compressive strength ranges from 10 to 21 MPa (1500 psi to 3000 psi).

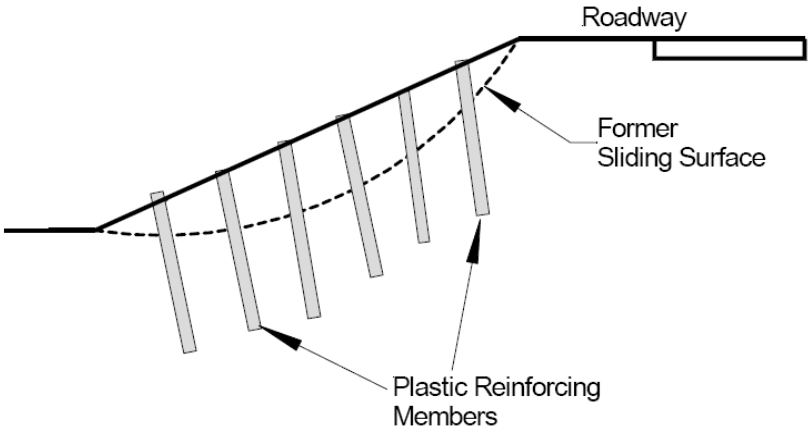

Figure 2.53.Stabilization of surficial slope failures with recycled plastic pins

(Loehr and Bowders, 2007)

The measured flexural strengths of specimens loaded to failure or 2% strain ranged from 9 MPa to 25 MPa (1300 psi to 3600 psi). The material was found to be resilient to a broad range of exposure in typical environmental conditions.

The eight test sites selected had embankment slopes varying from 1.7H:1V to 3.2H:1V and the slope heights varying from 4.5 m (15 ft.) to 14 m (46 ft.). The test sections were instrumented with inclinometers to measure lateral displacements.

Several reinforcing members were instrumented with strain gages and force-sensing resistors to monitor the loads mobilized. Figure 2.54 shows a typical instrumented recycled plastic member. Figure 2.55 shows the sectional view of the installation of these pins. The sites

were also instrumented to measure pore pressures and matric suction using piezometers, thetaprobes and equitensiometers.

(a)

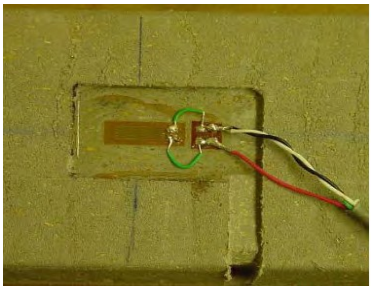

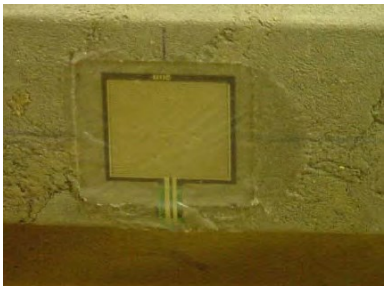

(b) (c)

Figure 2.54.Instrumentation (a) An instrumented recycled plastic pin, (b) Electric resistance strain gage (c) Force-Sensing resistor (Loehr and Bowders, 2007)

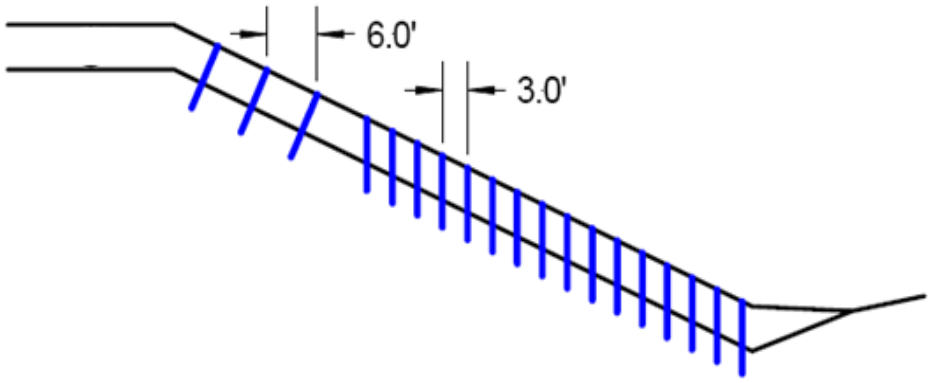

Figure 2.55.Sectional view of installation of plastic pins (Loehr and Bowders, 2007)

Various observations made during the study are summarized below.

- Pins provided at two slide areas at I70-Emma site were proved to be successful, but two control sections failed later.

- For a third slide area at I70–Emma site, observations were made over a period of about two years, and there was a failure in the test section. The failure was preceded by displacements of sections ranging from 6 cm to 12 cm (2.5 in. to 5 in.).
- It was concluded based on the investigation, that the failure did not occur in sections where the pins were closely spaced. Failure occurred where the pins were placed at a spacing of 1.8 m (6 ft.).
- Various other sites were tested with different spacing of recycled plastic pins. The performance of recycled plastic pins was reported to be satisfactory with a spacing of 0.9m (3 ft.) to prevent surficial failures.

2.9.6 Using Drilled Shafts

Two continuous research studies were conducted by Liang and Zeng (2002) and Liang and Yamin (2007) at The University of Akron on a single row of drilled shafts at the State Route ATH-124 (Figure 2.56). A series of extensive instrument sensors were installed on both sides of the drilling shafts and on the slope to monitor the performance during the ramp surcharge loading period at the crest area. The testing also provided field data to calibrate the finite element model rendered in ABAQUS (Figure 2.57) to further simulate different catastrophic situations.

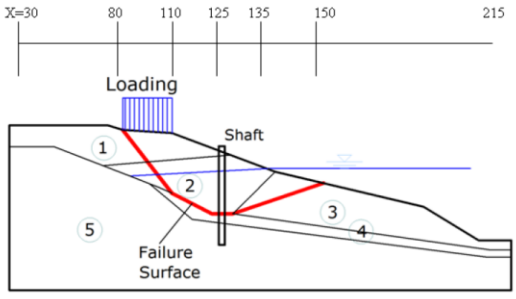

Zone	Description
1	Cohesive fill
2	Granular fill
3	Colluvium/Alluvium
4	Cohesive soil
5	Rock

Figure 2.56. Simplified Cross-Section of ATH-124 Landslide (Liang 2010)

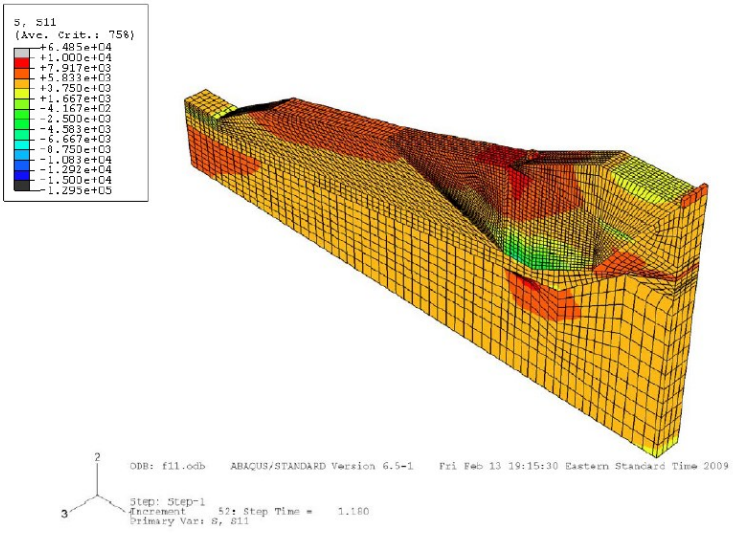

Figure 2.57. FEM Computed Stress at Failure Condition of soil reaction within a drilled shafts row (Liang 2010)

The research result was then adopted and applied to three ODOT slope stabilization projects in Jefferson County (JEF-152) (Figure 2.58 and Figure 2.59), Washington County (WAS-7) and Morgan Country (MRG-376).

Figure 2.58. JEF-152 Failed Slope under Repair (Liang 2010)

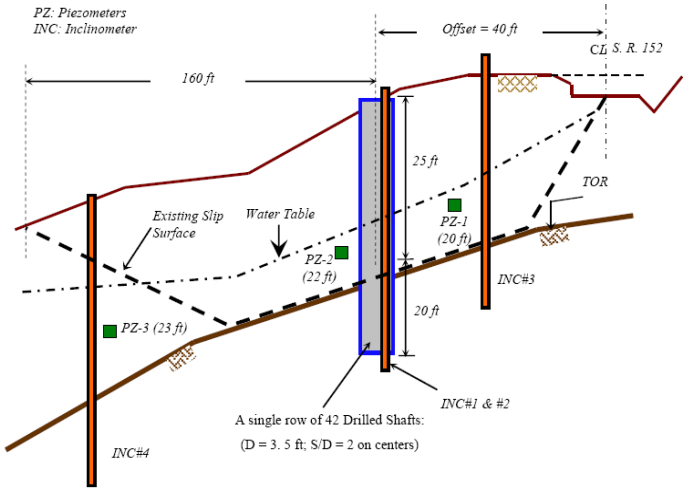

Figure 2.59. Schematic Cross section at JEF-152 (Liang, 2010)

Based on the analysis of the result obtained, drilled shafts can be a practical and effective means for stabilizing landslides. However, further research still needs to be conducted to fully establish design guideline for this slope stabilization method.

2.9.7 On-Going Research at the University of Texas at Arlington

Two sites, Joe Pool dam and Grapevine Dam located in the Fort Worth district were selected for the research, where surficial slope failures have occurred in the past. The slope testing area on each site was divided into five sections including four treated sections and one control section. The admixtures used to treat the embankment soil were 20%compost, 4%lime with 0.30%polypropylene fibers, 8%lime with 0.15%polypropylene fibers and 8%lime (Figure 2.60)

During the construction of the dam, the core soil was overlain by a topsoil of about 23 cm (9 in.) thick for the purpose of vegetation growth. The treatment of admixtures was intended to be mixed with the core soil of the dam. First, the top soil was excavated using a back hoe then stockpiled aside for reuse to place it back over the treated section after compaction of the 45 cm (18 in.) thick soil layer mixed with admixtures on the slope surface. The core dam soil was excavated and placed in the level pad area. It was then pulverized, moistened and mixed with admixtures before being transported and placed back in the embankment.

(a) (b)

Figure 2.60. Construction of test section at Grapevine Dam

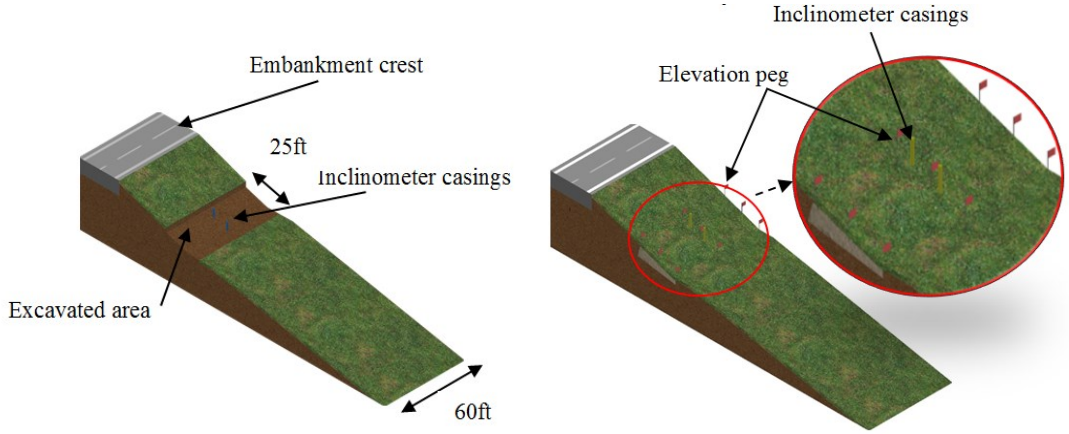

(a) (b)

Figure 2.61. Instrumentation on test section

To monitor the performance of the admixture, each section was instrumented with moisture probes, temperature probes and inclinometers (casings were placed during construction periods). The vertical movements of the test sections were also monitored by conducting periodical inclinometer surveys. A series of nine (9) elevation pegs were positioned on each section (red flags shown in Figure 2.61) as spots for elevation survey.

Based on the analysis of the data, the image studies, and the analytical model studies, the 8%lime with 0.15%fibers was found to be the most effective admixture, followed by the 8%lime to prevent desiccation cracking and surficial failures of high plasticity clays. Currently,

the research is exploring both durability and long term field performance monitoring of the test sections. We anticipate the research to produce design and construction methodologies for shallow slope treatments.

2.10 Use of Lime, Fibers and Compost to Improve Surficial Slope Stability

Expansive soils usually have the properties of moderate to high plasticity, low to moderate strength and high swell and shrinkage (Puppala et al. 2006). Chemical stabilization of expansive soils using calcium based stabilizers like lime and cement improved soil strength, stiffness, durability and a reduction in soil plasticity and swell/shrinkage potential (Hoyos et al. 2004). University of Texas at Arlington (UTA) has been conducting research studies of problematic slopes and distressed pavements laid on expansive clays. The studies revealed that lime, fibers and compost were very promising for slope stabilization or mitigation of desiccation cracking of expansive soils. McCleskey (2005) conducted laboratory studies on soils obtained from dam sites of Joe Pool Lake Dam and Grapevine Lake Dam using lime, compost and fibers as the chemical admixtures to treat the soil and found that these admixtures were quite promising for mitigating the desiccation cracking.

2.10.1 Use of Lime as a Soil Admixture

The use of lime stabilization of clay in construction is 5000 years old (Khattab et al. 2006). The pyramids of Shersi in Tibet were built using a compacted mixture of clay and lime (Greaves, 1996; Little, 1995). Lime stabilization is one of the oldest methods to improve soil properties economically (Schoute, 1999). Lime treatment is classified into two processes viz., soil modification and soil stabilization (Source: INDOT manual, Indiana). Soil modification aims at creating a working platform for construction equipment, and soil stabilization targets enhancing the strength of soil and improving other desirable properties.

2.10.1.1 Chemistry of Lime Treatment

Lime used for soil treatment can be in the form of quicklime (calcium oxide, CaO), hydrated lime (calcium hydroxide, $Ca[OH]_2$ or lime slurry (Lime manual, 2004). Quicklime is

manufactured by chemically transforming calcium carbonate (lime stone, $CaCO_3$) into calcium oxide. Hydrated lime is created when quicklime chemically reacts with water.

$$CaCO_3 \rightarrow (Heating\ at\ 900^oC)CaO + CO_2 \quad \text{Eq. 2-44}$$

$$CaO + H_2O \rightarrow Ca[OH]_2 \quad \text{Eq. 2-45}$$

Lime cannot react with soils containing as little as 7% clay and Plasticity Indices as low as 10 (Lime manual, 2004). INDOT recommends the following guidelines for classifying the soil as a reactive soil.

1. For Modification, % soil passing sieve No. 200 > 35 and PI > 5
2. For Stabilization, PI > 10 and minimum clay content > 10%

When lime is added to a reactive soil, both short term and long term reactions occur. Short term reactions include cation exchange, flocculation and agglomeration; whereas, long term reactions included pozzolanic reaction and carbonation (Khattab et al. 2006). These reactions result in mineralogical and micro structural changes in the stabilized soils, altering the properties of expansive soil (Khattab et al. 2007). A brief description of various reactions involved with lime stabilization is indicated below.

2.10.1.1.1 Short Term Reactions

Clay particles have negatively charged ions and lime has positively charged ions. After initial mixing, the positively charged calcium ions (Ca^{++}) migrate to the surface of the clay particles and displace the water and other ions adhered to the surface like Mg, K or Na ions. At this stage, the Plasticity Index (PI) of soil decreases and the tendency of soil to swell and shrink reduces (Lime manual, 2004). With a mere addition of 1 to 2% of soil, the reactions start immediately and the clay particles are electrically attracted and flocs are formed. The process is called flocculation and agglomeration and occurs within a few hours. The workability of soil increases and this process accounts for soil modification.

2.10.1.1.2 Long Term Reactions

Carbonation and Pozzolanic reactions are time dependent which may take a few days to years (Ola, 1978). Carbonation reaction is very slow during which the CaO reacts with atmospheric CO_2 and forms $CaCO_3$. The addition of an adequate quantity of lime beyond the quantity of lime required for soil modification causes a rapid increase of pH of the soil water due to partial dissolution of $Ca(OH)_2$ (Ola, 1978).

Lime reacts with clay minerals and complex chemical reactions or pozzolanic reactions take place, forming cementitious products in the form of a water insoluble gel of calcium silicate hydrates. With time, the gel gradually crystallizes into cementing agents such as calcium silicate hydrates (CSH) (tobermorite and hillebrandite) and calcium aluminate hydrates (CAH) (Ingles and Metcalf, 1972; Galvao et al. 2004, Lime manual 2004). CSH and CAH are cementitious products similar to those formed in Portland cement. The reaction occurs only when the water is present, and it carries calcium and hydroxyl ions to the clay surface (Galvao et al. 2004). This process results in soil stabilization, improving strength of soil significantly besides altering various other properties of the soil like swelling, shrinkage, permeability etc.

2.10.1.2 Selection of Type of Lime

The type of lime selected for stabilization should be based on several important considerations like type of soil, site conditions, the experience of a contractor, availability of equipment and a water source (Lime manual, 2004). Quicklime or hydrated lime is usually used for lime stabilization, as detailed below.

- Quicklime contains 20 to 24% more available lime oxide content than hydrated lime and hence is economical to use (Lime manual, 2004). Dry quicklime is ideal for drying wet soils. However, quicklime requires more water (about 32% of its weight) for reactions and time for mellowing. Quicklime also raises lots of dust, causing environmental concerns.

- Hydrated Lime or Lime Slurry Dry hydrated lime can be used for drying clay, but it is not as effective as quicklime (Lime manual, 2004). Lime slurry is a hydrated lime mixed with water. The main advantage of slurry lime is that it ensures a dust free application. It is easier to achieve an even distribution (Lime manual, 2004). However, this method is not suitable for wet soils.

2.10.1.3 Effect of Lime Treatment on Properties of Soil

It is generally known that the addition of lime reduces the plasticity index of soil and in most of the cases the liquid limit decreases significantly and plastic limit increases slightly. Studies (Bell, 1996; Osinubi, 1998) have shown that the addition of lime to soil results in a significant increase in optimum moisture content and decrease of dry density. The compressive strength of soil increases many times.

2.10.1.3.1 Permeability of Lime Treated Soils

Permeability of soil increases with the addition of lime due to the effects of flocculation and agglomeration. Townsend and Klym (1966) reported an increase of permeability of CH soils from 2 x 10^{-8} cm/s to 4 x 10^{-6} cm/s (0.79 x 10^{-8} in./s to 1.6 x 10^{-6} in./s) with the addition of lime.

The permeability also depends on the type of soil, gradation of soil, dry density and optimum moisture content (OMC). The permeability of compacted clay samples on the dry side of OMC was many times higher than on the wet side (Mitchell and Dermatas, 1992; Osinubi, 1998). This phenomenon is due to random particle orientations and a large average pore size than when compacted on the wet side of OMC. Osinubi (1998) conducted permeability studies on a CL soil.

It was found that the permeability increased up to 4% with the addition of lime and then decreased with further addition of lime. The increase of permeability was attributed to flocculation and an increase of pore size. The decrease in permeability due to the addition of more than 4% of lime was attributed to the increase of pH value as a result of partial dissociation of calcium hydroxide.

It was also opined that the formation of insoluble CAH or CSH gels obstructed the flow through the voids. The presence of an excess amount of lime was also said to be responsible for long term pozzolanic reactions.

Galvao et al. (2004) reported that the permeability of lime-treated soil decreased with an increase of lime content up to 8%. However, the permeability reported by various researchers at 8%lime was still higher than the permeability of untreated soils.

Compressibility of Lime Treated Soils

Studies of Galvao et al. (2004), using one dimensional consolidation tests, indicated that the soils, when treated with lime exhibited significant resistance to compressibility.

However, the increase of lime content from 4% to 8% did not have much impact on the resistance to compressibility. This can be attributed to the fact that even with the addition of 1% to 2% of lime, the process of cation exchange starts, and changes take place in the physico chemical characteristics of soil surfaces (Galvao et al. 2004).

2.10.1.3.2 Collapsibility of Lime Treated Soils

Collapsible soils refer to the category of soil deposits that undergo significant decrease in volume when exposed to water (McCarthy, 2002). Tests were conducted by Galvao et al. (2004) using the double odometer method for evaluating wet induced collapse. Samples were prepared at densities lower than the maximum dry density and OMC values obtained from proctor test in favor of collapse. For a given pressure intensity, the difference in strain between samples tested normally and under soaked condition was considered to be the amount of wetting induced collapse. For untreated soils, the wetting-induced collapse increased with an increase in pressure intensity. Lime treated soils exhibited greater resistance to strains and it was found to be very useful for reducing wetting-induced collapse of low density lateritic soils (Galvao et al., 2004).

2.10.1.3.3 Long Term Stability Characteristics of Lime Treated Soils

Long term stability characteristics of lime treated soils can also be referred to as durability of lime treated soils. Durability criteria are important when a soil is subjected to wetting and drying cycles, freezing-thawing cycles and leaching. Studies pertaining to durability against these environmental factors are not extensive (Khattab et al. 2007). Various aspects of the durability of lime treatment are discussed briefly below.

Malhotra and Bhasker (1983) and Little (1995) show that leaching has a significant effect both on treated and untreated soils that contain highly soluble salts and minerals. However, leaching has limited detrimental effects on soils that do not contain soluble salts (Khattab et al. 2007).

Various studies further report that leaching has little influence in the case of poorly drained soils, and detrimental effects were the least at an optimum lime content of 4-6% (McCallister et al. 1990; Parsons and Milburn 2003; McCleskey, 2005). Khattab et al. (2007) conducted leaching tests for 60 days in the laboratory and measured pH, Ca^{++} and flow of water in the leachate. He noticed a slight decrease in pH, Ca^{++} and permeability.

It was concluded that leaching does not reduce the efficiency of treatment as the quantity of lime displaced by the water flow was small, compared to the quantity of lime added initially during treatment.

2.10.1.3.4 Influence of Wetting and Drying Cycles

Khattab et al. (2007) conducted experiments on FoCa soil (Clayey soil from France) by oven drying at 60º C and submerging in water. The untreated specimen experienced a swelling of about 75%, with a corresponding void ratio of about 2.5 during wetting. During the drying phase, the settlement was about 25%, with a corresponding void ratio of about 0.5. The effect of wetting and drying on the treated and untreated specimen is shown in Figure 2.62. It was concluded that due to wetting and drying, lime treated soils have shown reduction in swelling characteristics.

It was emphasized that the efficiency was maximized when the soil was first subjected to wetting. The authors recommended that lime stabilized soils should not be immediately subjected to drying conditions as soon as the curing is completed during the hot season.

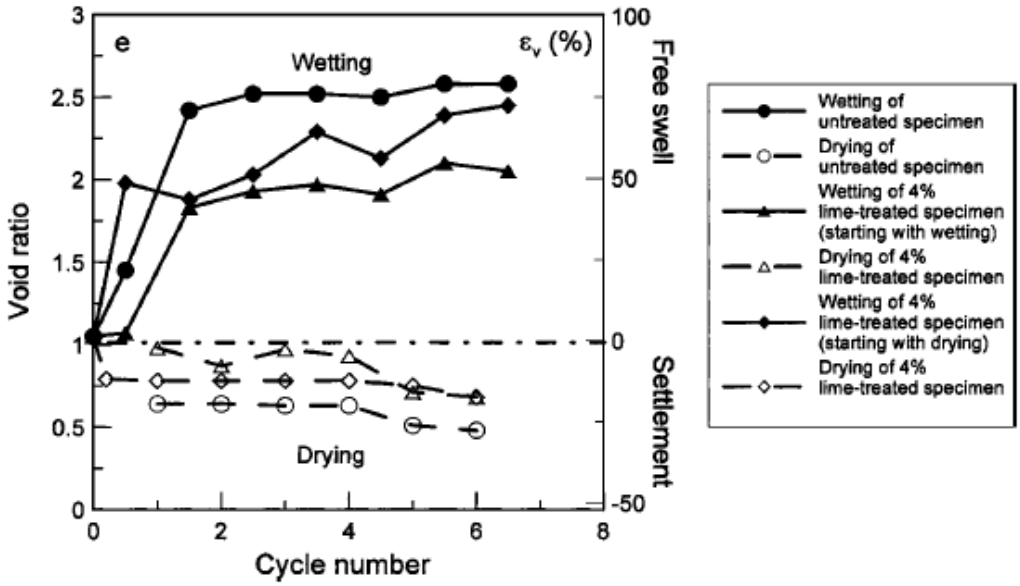

Figure 2.62. Volumetric changes of lime treated and untreated specimens during wetting and drying cycles. (Khattab et al. 2007)

Guney et al. (2007) investigated the impact of cyclic wetting and drying on the swelling behavior of lime stabilized clayey soils. With cyclic wetting and drying, the swelling potential of unstabilized clays was reduced.

The maximum swelling potential was reduced during the first cycle and then reduced gradually with subsequent cycles, reaching equilibrium after 4 to 6 cycles.

In the case of lime stabilized soils, the stabilization effect was found to be lost with the increase in the number of cycles of wetting and drying. The clay content of the cycled samples increased, which affected the plasticity index, shrinkage limit and swell potential of the lime treated expansive soil.

Gunery et al (2007) recommended that the lime treatment may not be used in regions susceptible to severe wetting and drying cycles.

2.11 Use of Compost as a Soil Admixture

Texas is one of the largest producers of waste materials in the USA (EPA, 1997; Puppala et al, 2004). TxDOT uses recycled asphaltic pavement (RAP) and cemented quarry fines (CFQ) for pavement base or sub base materials (Puppala et al. 2008). Other waste materials or recycled materials used for pavement applications in highway construction include blast furnace slag, steel slag, and coal combustion by products and compost materials (Schroeder, 1994).

Desiccation cracks are noticed on the unpaved shoulders of highways in longitudinal and transverse directions. The intrusion of surface runoff or rainfall infiltration into the cracks further weakens the base and subgrade layers (Puppala et al, 2004). Moisture affinity (hydrophilic characteristics) and the presence of fibrous material in the compost help reduce the shrinkage of natural expansive subgrades when stabilized with compost.

Compost materials are capable of maintaining a uniform moisture level by absorbing moisture from the atmosphere, which in turn will help prevent desiccation cracking (Puppala et al, 2004).

Compost is a relatively stable and decomposed organic material obtained from the composting of different types of wastes (Puppala et al, 2004). Composting is recognized as one of the innovative methods of recycling organic waste materials.

Composting is a natural process of aerobic, thermophilic, microbiological degradation of organic wastes into a stabilized and useful product that is free of odors and pathogens (Girovich, 1966). The benefits of using compost have been identified by various agencies, as shown in Table 2.7.

Table 2.7. Benefits of addition of compost identified by various Agencies / Researchers (modifired from Jennings et al., 2003)

	USCC	US EPA	Mitchell, D.	Univ. of Georgia	Univ. of Florida
Improves soil structure, porosity, bulk density	✓		✓		
Increases water holding capacity of soil	✓	✓		✓	✓
Increases infiltration and permeability of soils	✓		✓	✓	
Erosion control	✓		✓	✓	
Helps moderate soil temperatures					✓
Adds organic bulk and humus to regenerate poor soils		✓	✓	✓	✓
Helps suppress plant diseases and pests		✓			

2.11.1 Application of Compost

Various applications of compost are landscaping, land reclamation, erosion control, and top dressing of golf course / parks, agriculture, residential gardening and nurseries. Intharasombat (2005) conducted research using various types of compost, as shown in Figure 2.45. These composts were used to treat the top layer of shoulder soil test sections, and the performance was monitored with heavy instrumentation, digital imaging and elevation survey for a period of more than 2.5 years.

The studies have shown that the correct selection of compost helped mitigate shoulder cracking of highway pavements by reducing shrinkage cracking. It was also concluded that out of the various types of composts used for study bio-solids compost and Cotton Burr compost were found to be more suitable for enhancing properties of expansive clayey soils. Dairy manure was not found to be very suitable for preventing shoulder cracking. All the composts, in general, were found to be good at promoting vegetation growth. However, compost amended

soils have shown high swell strains which were attributed to the hydrophilic characteristics of ingredients of compost (Puppala et al., 2004).

Studies by Xiao et al. (2006) have shown that compost has a good potential of rainfall erosion control. For a roadside embankment, filtered compost and vegetated compost were used. Compost of three different pellet sizes was laid on up-slope, mid-slope, and down-slope with the finer compost on up-slope and coarse compost on down-slope. Vegetated compost has the composted surface vegetated with grass. The filtered compost application significantly reduced the soil erosion, and the vegetated compost showed the capability of sustaining repeated rainfall and acting like a promising long term erosion control blanket (Xiao et al., 2006). The results also showed that the soil loss due to erosion was within the tolerable limits.

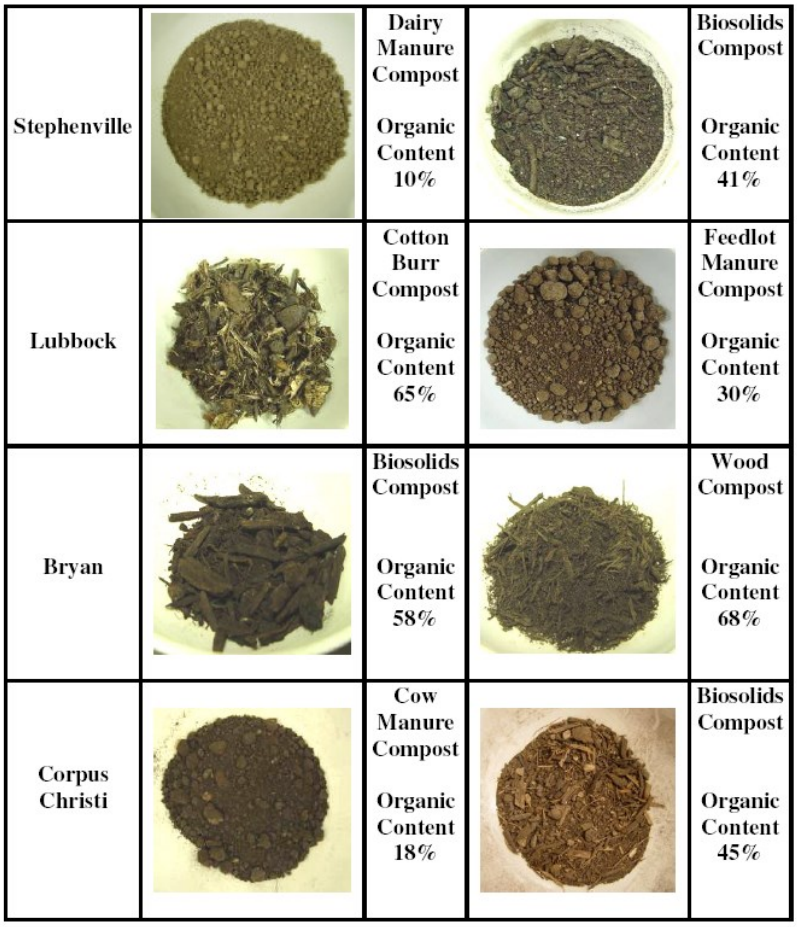

Figure 2.63.Various types of compost used for research (Intharasombat, 2005)

2.12 Use of Fibers as a Soil Admixture

Deterioration of concrete structures owing to corrosion called for a new quest of an ideal and durable material which has the desired properties of low shrinkage, good thermal expansion, substantial modulus of elasticity, high tensile strength, improved fatigue and impact resistance. This led to emergence of fiber reinforcement in concrete applications (Brown et al., 2002). Soon, the application found place in the geotechnical engineering field.

Soil reinforcement implies inclusion of strips, sheets, nets, mats and synthetic fiber to reduce tensile strain (Kumar and Singh, 2008). Strips, geosynthetics consist of continuous inclusions into earth mass whereas fiber reinforcement is injected in a random pattern. These inclusions act to interlock particles as a coherent matrix and the main advantage is the increase in strength of soil (Maher and Gray, 1990).

The mechanism of strength improvement is similar to that of root reinforcement. Roots mechanically reinforce a soil by the transfer of shear stress in the soil to tensile resistance of roots (Gray and Sotir, 1996). When shear occurs in the soil, the root fiber or synthetic fiber deforms causing an elongation of fiber provided there is sufficient interface friction along the length of fiber and confining stress to lock the fibers in place and prevent slipping or pulling (Gray and Sotir, 1996).

The laboratory experiments revealed that the shear strength increase was linear with increase in fiber content. The fiber aspect ratio, L/d, has an influence on the shear strength. The higher the L/d ratio, the higher is the contribution of fiber to the shear strength (Maher and Gray, 1990).

2.12.1 Types of Fibers

Various natural and synthetic fibers are used for soil reinforcement. The most commonly used natural fiber is coir (Babu and Vasudevan, 2008). Natural Fibers mixed with soil have applications in irrigation and drainage projects such as river levees, bunds, and temporary canal diversions, check dams etc., (Babu and Vasudevan, 2008). Studies by Babu and

Vasudevan (2008) using natural coir fiber have shown that with the increase of fiber content, seepage velocity decreased and piping resistance of soil increased. Wood pulp or wood fibers present in the compost also cause similar effect of soil reinforcement. Most commonly used synthetic fibers are polypropylene fibers, polyvinyl chloride and glass. Fibrous carpet waste was also used in some countries like Iran for soil reinforcement (Ghiassain, 2004). Latest developments include the use of adhesive-coated natural or synthetic fibers to prevent erosion and strength loss in berms and embankments.

2.12.2 Properties of Polypropylene Fibers

The most commonly used synthetic fiber for concrete or soil reinforcement is polypropylene fibers. Polypropylene fibers are available in the form of fibrillated films and tapes or woven meshes. They have a better bond than chopped monofilament fibers (Brown et al. 2002). Propylene is an unsaturated hydrocarbon, containing only carbon and hydrogen atoms. Polypropylene is a versatile thermoplastic material which is produced by polymerizing monomer units of polypropylene molecules into very long polymer molecules or chains in the presence of a catalyst (Brown et al. 2002). The mechanical properties of polypropylene are as indicated below (Brown et al. 2002).

- Tensile Strength: 25 - 33 MPa (522-689 ksf)
- Flexural Modulus: 1200 - 1500 MPa (25,062-31,328 ksf)
- Elongation at break: 150 – 300%
- Strain at yield: 10 – 12%

2.12.3 Various Findings and Recommendations by Researchers

Puppala and Musenda (2000) reported that the fibers improved unconfined compressive strength and reduction in volumetric shrinkage strains and swell pressures of expansive clays. Heineck et al. (2005) conducted ring shear tests and bender element tests and concluded that the contribution of polypropylene fiber reinforcement is more effective after a certain level of shear strain.

Tingle et al. (2002), after conducting a series of field studies concluded that discrete geofiber stabilization of sand was a viable alternative to traditional stabilization techniques for low volume road applications.

Miller and Rifai (2004) recommended use of fiber reinforcement for waste containment liners, as they found the use of fiber reinforcement reduced the desiccation cracking phenomenon of clay liners. However, an increase of fiber content beyond 1% significantly increased the hydraulic conductivity of clay liners.

Welker and Josten (2005) carried out direct shear tests and suggested an optimum dosage of 0.2% for reinforcing clayey soil.

2.13 Mixing of Soil, Fibers and Cement / Lime

Consoli et al. (1998) have conducted experiments on fibers and cement mixed with cohesion less soil and compared relative performance. The peak friction angle of uncemented cohesion less soil increased from 35º to 46º due to fiber inclusion. The addition of cement to soil increased stiffness and peak strength. Fiber reinforcement increased both peak and residual triaxial strengths. Three percent of fiber reinforcement of soil mixed with 1% cement decreased stiffness and changed the brittle behavior of cemented soil to a more ductile one. Cai et al. (2006) conducted experiments on soil mixed with different proportions of lime and fibers and reported beneficial changes in the properties of soil. It was reported that the unconfined strength, cohesion and friction angle increased with an increase in the length of the curing period. The fiber-lime-soil exhibited high strength, and mproved toughness, and swell and shrinkage properties.

2.14 Summary

With the focus on surficial failures, a detailed overview of various kinds of slope stabilization studies was reviewed from the available literature in this chapter. A number of important research literatures from various authors, including case studies, were discussed, which assisted greatly in carrying out the present research tasks.

CHAPTER 3

LABORATORY EXPERIMENTAL PROGRAMS

3.1 Introduction

A research study was undertaken at the University of Texas at Arlington with an objective of exploring the best field stabilization methods to diminish desiccation cracks in the upper embankment soils, thereby enhancing surficial slope stability. Two dams in North Texas, Joe Pool and Grapevine Dams, maintained and operated by the U.S. Army Corps of Engineers, Fort Worth District, were selected as test sites for the research. The admixtures used to treat surficial soils were annotated as 20%compost, 4%lime with 0.30%polypropylene fibers, 8%lime with 0.15%polypropylene fibers, and 8%lime as were used in this research. These stabilizers were selected based on a comprehensive laboratory testing program by McCleskey (2005) and Dronamraju (2008). Five test sections, including four treated sections and one control section, were constructed at each dam site.

Borrow soil obtained from Joe Pool Dam and Grapevine Dam sites were subjected to a basic laboratory testing program that included sieve analysis, hydrometer analysis and Atterberg limits tests. The results were compared with the test results performed earlier by McCleskey (2005) and Dronamraju (2008). More advanced testing was also conducted focusing mainly on testing of Fully Softened Shear Strength, utilizing Direct Shear and Torsional Ring Shear tests. Details of testing procedures are presented in this chapter and test procedures are as per ASTM and procedures outlined by the US Army Corps of Engineers (USACE).

Dronamraju (2008) performed earlier laboratory investigations on soil of these two dam sites. Laboratory studies were carried out on all the basic engineering tests, required

mineralogical tests, strength tests, and swell and shrinkage tests on the field construction samples. The summarized results of these tests are presented at the end of this chapter.

3.2 Laboratory Test Procedures

3.2.1 Sieve Analysis Test

In order to classify a soil for engineering purposes, the distribution of the grain sizes in a given soil mass needs to be identified. Due to the nature of the soil as clay, the grain size distribution of the soil was determined using ASTM standard procedure for sieve analysis of Fine and Coarse Aggregates with Designation C136-01.

The tests were carried out on the control soil samples obtained from both the dam sites for the purpose of classification of soil. Field soil was first air-dried for 7 days. The vegetation roots were then picked out by hand, and the soil was pulverized with a rubber tipped pestle and kept in the oven to the constant mass at a temperature of $230 \pm 9^{o}F$. After it was dry, the soil was passed through a set of sieves.

The stack of sieves was kept in a mechanical shaker shown in Figure 3.1 for 15 minutes. The mechanical sieve shaker creates motion of the sieves to cause the particles to bounce, tumble, or otherwise turn so as to present different orientations to the sieving surface. The percentage of soil retained was calculated.

Figure 3.1.Stack of sieves in a mechanical shaker

Wet analysis was carried out as for the cohesive soil by washing the soil retained on sieve No. 200. Soil passing through 75 micron size was dried and hydrometer analysis was conducted as explained in the section 3.2.2.

3.2.2 Hydrometer Analysis

Hydrometer analysis is the procedure generally adopted for determining the particle-size distribution in a soil for the fraction that is greater than No. 200 sieve size (0.075mm) (Das, 2009). The test was carried out to study the micro level distribution of finer particles as silt and clay fraction present in the field soil of the Joe Pool Dam and Grapevine Dam. The testing used the ASTM 152 H type hydrometer as shown in Figure 3.2.

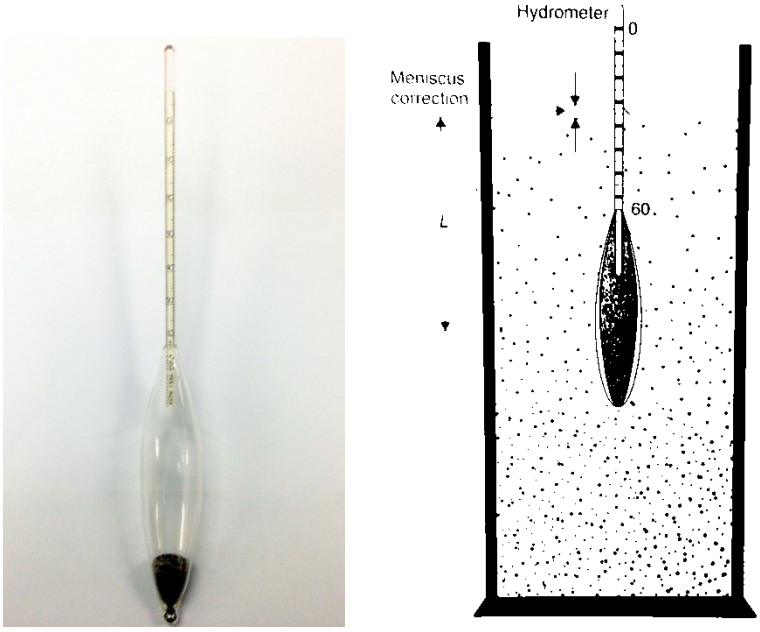

Figure 3.2. ASTM 152 H hydrometer (Das, 2009)

At first, 0 g of oven dried and well pulverized soil was mixed with a solution of 4% deflocculating agent (sodium hexametaphosphate $(NaPO_3)_6$ or Calgon) and soaked for about 8 to 12 hours.

A 1000 cm^3 graduated cylinder was kept ready with 875 cm^3 of distilled water mixed with 125 cm^3 of deflocculating agent. The temperature of the bath was recorded. Meniscus correction and zero corrections were observed.

The prepared soil was thoroughly mixed in a mixer cup and all the soil solids inside the mixing cup were transferred to a 1000 cm^3 graduated cylinder. The graduated cylinder was filled with distilled water up to the 1000 cm^3 mark. The hydrometer readings were recorded at cumulative times of 0.25 min., 0.5 min., 1 min, 2 min., 4 min., 8 min., 15 min., 30 min., 1 hr., 2 hr., 4 hr., 8 hr., 12 hr., 24 hr., 48 hr., and 72 hr.

After taking the readings initially for the first 2 minutes, the hydrometer was taken out and kept in another cylinder filled with distilled water. Necessary temperature corrections, zero corrections and meniscus corrections were made to the hydrometer readings as per procedure.

3.2.3 Atterberg liquid limit Test

Liquid limit state of the soil represents the condition of Fully Softened Soil. Atterberg liquid limit test was conducted as per ASTM D-4318 standard test method using the Casagrande liquid limit device. The device consists of a brass cup that can be raised and dropped through a distance of 0.394 in. (10 mm) on a hard rubber base by a cam operated by a crank (see Figure 3.3a). Figure 3.3b shows the schematic diagram of a grooving tool.

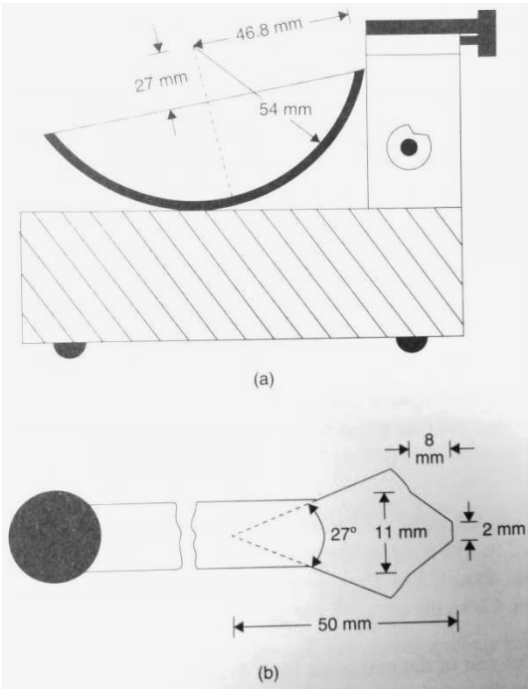

Figure 3.3. Schematic diagrams: a) Liquid limit device b) Grooving tool (Das, 2009)

About 250g of air-dried soil is sieved through No.40 sieve then water is added and mixed to form a slurry uniform paste. A portion of the paste is placed in the brass cup to the maximum depth of the soil about 8mm. A groove along the centerline of the soil pat in the cup is cut using the grooving tool (Figure 3.4). The crank is turned at the rate of 2 revolutions per second. The soil from the two sides of the cup will begin to flow toward the center. The moisture sample from the soil is collected if the number of blows N about 25 to 35. The test is repeated 3-4 times to determine the exact liquid limit corresponding to 25 blow count.

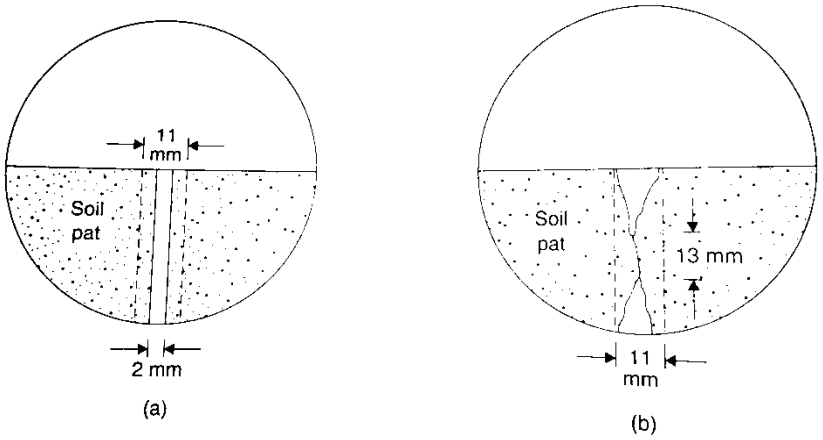

Figure 3.4. Schematic diagram (plan) of soil pat in cup of liquid limit device a) Beginning of test b) End of test (Das, 2009)

3.2.4 Fully Softened Shear (FSS) Test

Current state of the art for FSS testing involves using either direct shear equipment or rotational ring shear equipment. Both require significant care to achieve quality test results for analysis of FSS results. Regardless of the test methods, the sample must be sheared at a slow rate to avoid excess pore pressure developed during shearing.

3.2.4.1 Sample Preparation

Soil samples used for FSS testing were prepared under the same procedures for both test methods. Borrow soil obtained from both Grapevine and Joe Pool dams was air-dried and then passed through No.40 sieve. Fine soil was kept in the oven for 24 hours to completely eliminate existing moisture in the soil. The soil was then mixed with water equivalent to the moisture content close to the liquid limit to form slurry. The specimen was then transferred to a zip-lock bag and kept in the moisture room for 24 hours for hydration.

Soil samples with admixtures containing lime are required to have a specific amount of time for curing. In this particular case, the samples were mixed with moisture content at optimum moisture content value obtained from standard Proctor compaction test and then kept in the moisture room for at least one week for curing. The specimen was brought to liquid limit state by adding more water before being put into the shear devices.

3.2.4.2 Direct Shear Apparatus

The testing protocol for determining FSS using direct shear equipment was followed by the procedure recommended by the US Army Corps of Engineers (USACE). The protocol was used previously on some USACE projects as a part of the USACE technical guidance. The testing method followed closely the ASTM D3080 procedure for standard direct shear test. Since the device involves testing a much larger specimen than rotational or ring shear equipment, it seems to be less susceptible to sample artifacts.

The direct shear machine used in UTA laboratory provides improvement in electronic deformation devices and automation of data acquisition system over the traditional direct shear device with manual measurements.

3.2.4.2.1 Description of Test Apparatus

A direct shear machine consists primarily of a direct shear box, which is split into two halves (top and bottom) and which holds the soil specimen. Digishear shear box has a cylindrical shape of 2.5 in. diameter and 1 in. height. The sample is sheared after the completion of consolidation. The shear resistance comes from the surface of sliding during the shearing process, and this is detected by the load cell and recorded in the data acquisition system (Figure 3.5). The automatic data acquisition system also facilitates recording vertical and horizontal movements during the test. The Digishear device is fully programmable from loading schedule, consolidation schedule to recording the shear resistance.

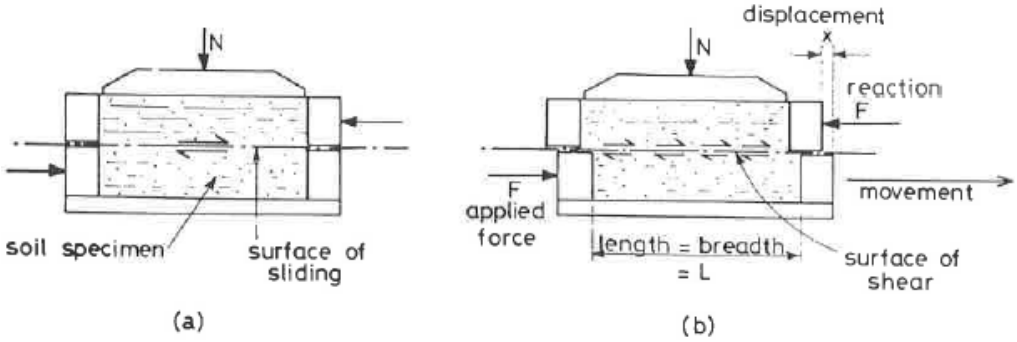

Figure 3.5. Principle of shearbox test a) Start of test, b) During relative displacement (ASTM D-3080)

3.2.4.2.2 Test Procedure

The preparation of the soil specimen is described in 3.2.4.1 Sample Preparation section. The soil specimen, at the liquid limit after hydration, is placed in the shear box (Figure 3.6). The shear box is then tapped to eliminate air bubbles trapped in the specimen. The specimen was pre-consolidated under a water bath at a load increment ratio of one from the minimum applied normal stress of 12.5 kPa (0.26 ksf) until the desired normal stress was applied. Care was taken to prevent soil from oozing out of the shear box. For each load increment, it was verified that the primary consolidation was complete by checking the vertical displacement versus time graph (ASTM D2435). During the consolidation stage of testing, the upper and lower shear box halves were held in contact with each other with alignment screws. Four normal stresses (50 kPa, 100 kPa, 200 kPa and 400 kPa) were chosen to characterize the failure envelope for FSS.

Figure 3.6. Placement of soil paste into the shear box

After completion of the normal load, guiding and fixed screws joining the two halves of the shear box were removed leaving a gap of approximately 0.025 in. The slow rate of displacement allowed dissipation of pore pressures and helped obtain realistic drained shear

strength values. The following equation (ASTM 3080) was used as a guide in determining the estimated minimum time required from the start of the test to failure:

$$t_f = 50 \times t_{50} \qquad \text{Eq. 3-1}$$

Where

t_f –total estimated elapsed time to failure, min

t_{50} –time required for the specimen to achieve 50 percent consolidation under the specified normal stress (or increments thereof), min

This rate was adjusted for each test run on the GeoTac devices, but because of the difficulty of changing the rate of shear for every normal stress, we use a lower bound rate of 0.0051 mm/min (0.0002 in./min)

As the analysis was focused on shallow slope failures, the results obtained at lower normal stresses is discussed as it simulates the field condition. The initial time as well as vertical and shear displacements, were monitored during the test. Shear forces were converted from analog signal and processed to yield numerical values using the software built-in the system. The magnitude of the estimated displacement at failure is dependent on many factors including the type of soil used in testing.

Figure 3.7. Direct Shear box with sheared sample

3.2.4.3 Bromhead Torsional Ring Shear Apparatus

The test protocol for determining FSS using rotational or ring shear apparatus was prepared by Stark (2005) and adopted as ASTM D7608-10 method. This test method is performed by shearing a normally consolidated, reconstituted soil specimen at a controlled displacement rate until the peak shear resistance has been obtained. Generally, drained fully softened failure envelope is determined by using results at three or more effective normal stresses.

In this research, Bromhead ring shear test apparatus available in the UTA laboratory was used to determine the FSS of untreated soil and treated soils. The test procedure prescribed by the ASTM D 7608-10 method was followed. Four normal stresses of 50 kPa, 100 kPa, 200 kPa and 400 kPa were chosen to represent the strength envelope for FSS.

3.2.4.3.1 Description of Test Apparatus

The equipment contains a shear device which holds the specimen securely between two porous inserts and provides a means of applying normal stress to the faces of the specimen, permitting drainage of water through the top and bottom boundaries of the specimen. The device is capable of applying a torque to the specimen along a shear plane parallel to the faces of the specimen. At the inner and outer walls of the specimen container, friction is developed during shearing. The device is capable of shearing the specimen at a uniform rate of displacement. The rate of displacement can be selected using a combination of gear wheels from 44.52 mm/min. travel to 0.018 mm/min. travel.

The specimen container is annular in shape, with an inner diameter of 70 mm and outer diameter of 100 mm. The container radially confines the 5 mm thick soil specimen. Due to this confinement, wall friction is developed at the inner and outer circumference of the specimen. The magnitude of the wall friction is the least at the top porous stone and the soil interface and increases with the depth of the specimen. Thus the failure plane occurs at the surface of the top

porous stone where the wall friction is the least. This type of failure condition is referred to as *smear* condition. Figure 3.8 shows a schematic illustration of the Bromhead Ring Shear device.

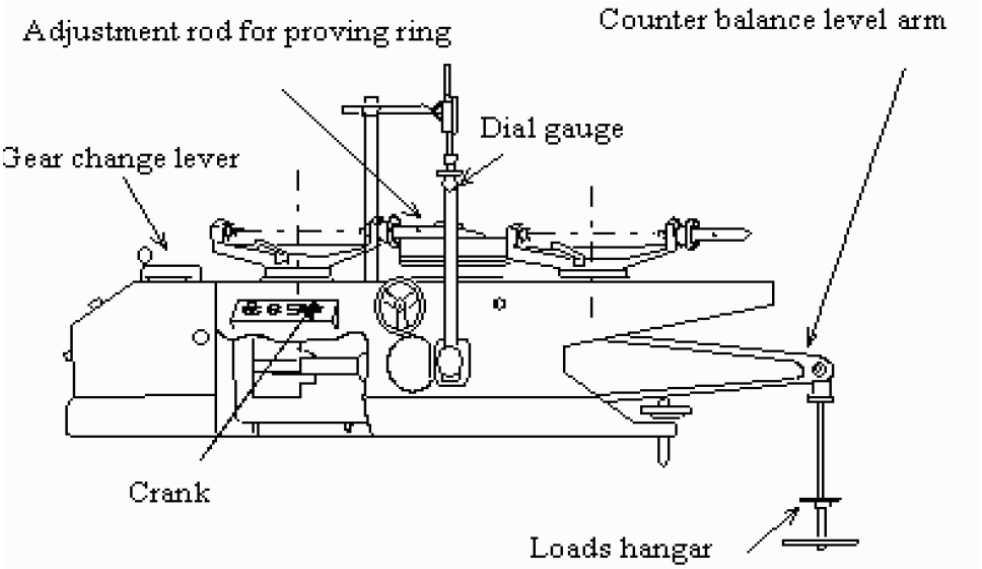

Figure 3.8. Bromhead Ring Shear Device

3.2.4.3.2 Test Procedure

The preparation of soil specimen is described in 3.2.4.1 Sample Preparation section. Soil specimen at the liquid limit after hydration was placed in the annular space of the bottom platen and the top platen was placed over it. The specimen was pre-consolidated under a water bath at a load increment ratio of one at the minimum applied normal stress of 12.5 kPa (261 psf) until the desired normal stress was reached to avoid soil “bleeding” through the gap of top cap and the annular mold. For each load increment, it was verified that primary consolidation was complete by checking the vertical displacement versus time graph (ASTM D2435). After applying normal load, identical soil specimens were sheared at various normal stresses and at a very slow rate of displacement of 0.018 mm/min (0.0007 in./min).

The slow rate of displacement allows dissipation of pore pressures and helps obtain realistic drained shear strength values. As the analysis was focused on shallow slope failures, the results obtained at lower normal stresses is discussed as it simulates the field condition. The initial time, as well as vertical and shear displacements were recorded during the test.

Shear forces were converted from the readings of both ring gauges. The magnitude of the estimated displacement at failure was dependent on many factors including the type of soil.

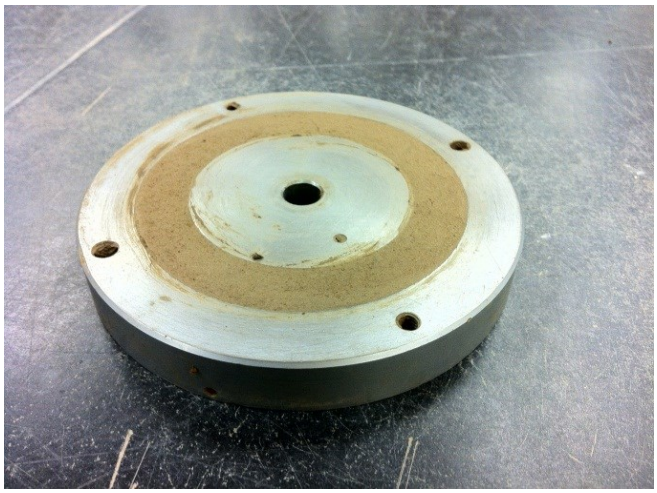

Figure 3.9.Placement of soil paste to the annular mold

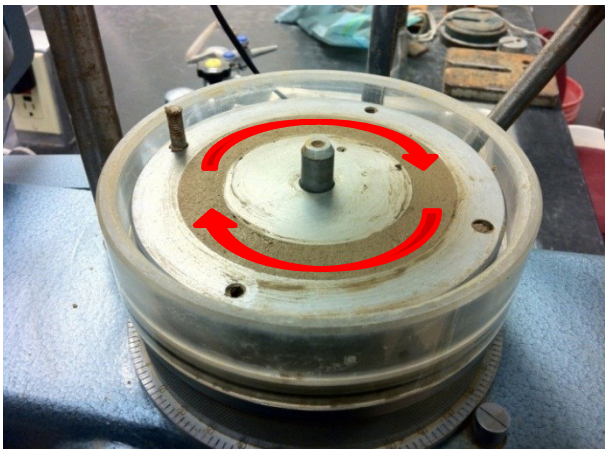

Figure 3.10. Shearing direction in Bromhear Ring Shear

3.3 Research Conducted by Dronamraju (2008)

Early works of Dronamraju (2008) involved basic laboratory testing. This section briefly summarizes all the experimental programs conducted on the soil samples obtained from borrow sites of Joe Pool and Grapevine Dams.

3.3.1 Results of Laboratory Tests

3.3.1.1 Specific gravity test

Specific gravity is defined as the ratio of the density of a given volume of material to the density of an equal volume of distilled water. It is an important parameter for calculating the weight-volume relationship. Specific gravity G_s is defined as:

$$G_s = \frac{density\ of\ soil\ solids}{density\ of\ water} = \frac{\rho_s}{\rho_w} \qquad \text{Eq. 3-2}$$

The specific gravity was determined as per ASTM standard method D854-06.

3.3.1.2 Standard Proctor Tests

Dronamraju (2008) used Tex-114-E procedure for standard proctor test to determine moisture content versus dry density relationships. The optimum moisture content of the soil is the water content at which the soils are compacted to a maximum dry unit weight condition. The optimum moisture content and maximum dry density values were initially obtained by conducting proctor tests on the borrow soils of both the dam sites. Standard Proctor tests were conducted on both control and treated soils. By adding the stabilizer agent such as lime or compost to the control soil, both physical and chemical properties of the mixed soils changed. In order to ensure quality control during construction, the optimum moisture content and maximum dry unit weight required to be achieved were specified in the specifications supplied to the contractor before commencement of test section construction.

3.3.1.3 Linear Shrinkage Bar Test

The Linear shrinkage bar test used in this research was based on the procedure established by the Texas Department of Transportation (Tex-107-E standard method). This test measures the volumetric shrinkage (width, depth, and height) of the soil samples in the shrinkage mold shown in Figure 3.11.

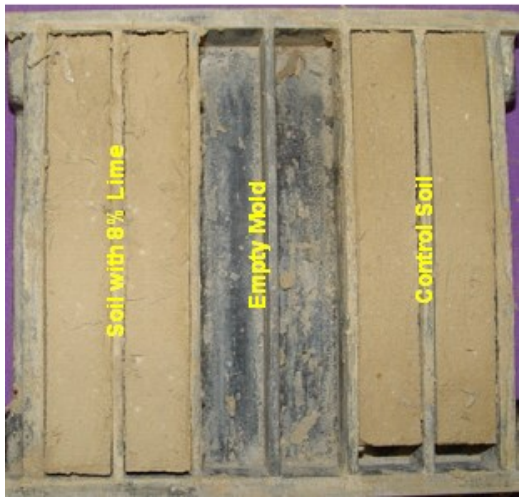

Figure 3.11. Linear shrinkage test setup (Dronamraju, 2008)

Soil samples were first mixed with a water level corresponding to the liquid limit state, and then the samples were molded and placed in a linear shrinkage block, which are 12.7 cm (5 in.) long and 1.9 cm (0.75 in.) wide and deep. Soil samples were kept at room temperature condition for twelve hours. Then, the soil samples were dried in the oven at 110°C. The length, width and height of the dried sample were measured by vernier calipers and the volumetric shrinkage was calculated and expressed as a percent of its original volume (Dronamraju, 2008)

3.3.1.4 Free Swell Test

One dimensional free swell test represents the field condition of a dam slope. The result of the test gives the heave potential of soil. Samples of control soil and treated soils were obtained from both the dam sites and remolded samples were prepared to fit a conventional Oedometer steel ring of size 64 mm (2.5 in.) in diameter and 25 mm (1 in.) in height.

The free swell was measured by observing the change in the dial gage readings for a period of 24 hours. The free swell was measured from the dial gage having a least count of 0.001 in. the swell measured is presented in the form of percentage over the thickness of 1 in. of soil sample.

3.3.1.5 Suction Measurements by Pressure Plate and Filter Paper Method

Several test methods, including the filter paper and the pressure plate method are commonly used to develop Soil Water Characteristic Curves (SWCCs) of unsaturated soils studies. The limitation of the pressure plate device is that it can measure matric suction up to only 1000 kPa (20885 ksf) to 1500 kPa (31328 ksf). The capacity is sometimes limited by the availability of a pressure plate and the capacity of the compressor. Therefore, the filter paper method was used to measure soil suction ranging more than 1000 kPa (20885 ksf). Hence, both pressure plate and filter paper methods were employed in the development of a complete SWCC of the present soils. Figure 3.12 shows the schematic of a typical pore water extraction testing setup using a pressure plate apparatus

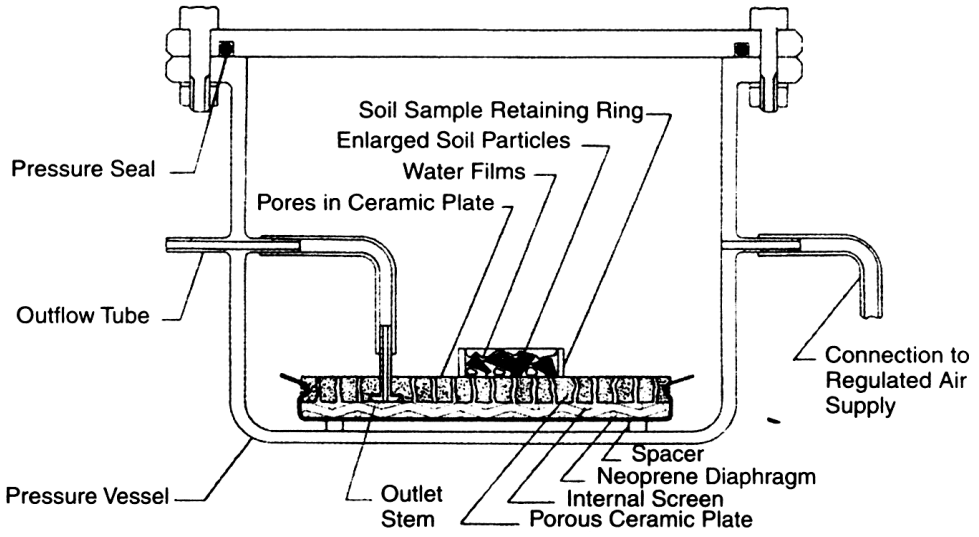

Figure 3.12. Schematic drawing of pressure plate (Soil-Moisture Equipment Corp., 2003)

3.3.1.6 Permeability Test

The falling head permeability test was conducted on all the soil samples from both control and treated sections to determine their hydraulic conductivity. The Grapevine Dam soil was found to have a higher hydraulic conductivity than the Joe Pool Dam soil. The treated soils were found to have higher permeability than the control soil (Dronamraju, 2008).

3.3.2 Recommendations from Dronamraju (2008)

Important interpretations of the laboratory tests conducted and conclusions based on the analysis of data are discussed here. The control soil from Joe Pool Dam and Grapevine Dam was classified as Sandy Lean Clay (CL) and Sandy Fat Clay (CH), respectively. Swell test results indicated that the lime and lime with fiber treatment reduced the swelling potential of the soil. The addition of fibers to the soil did not improve the swell propertiehs of soil. Swelling was also observed to be high in the case of soil specimens prepared with compost-amended soil. Shrinkage test results indicated that both lime and lime with fibers were proven to be an effective treatment in preventing shrinkage cracks in the soil. The addition of lime has significantly improved the shear strength of soil. The addition of fibers to the soil has also improved the tensile strength of soil mixtures.

Dronamraju (2008), based on laboratory study and field performance observations, made the following recommendation with respect to field additive treatments to construct test sections at Joe Pool Dam and Grapevine Dam sites:

- Additional data (moisture and slope movement) needs to be collected from the field performance to make a relative comparison of the test sections for long term effect of the treatments.
- Statistical analysis of field data must be carried out to assess the reliability of the data collected and may well be the way to predict the soil behavior for future research.

3.4 Summary

This chapter summarizes a complete description of various test procedures used in the experimental program. Earlier research findings of Dronamraju (2005) based on the laboratory tests conducted on the soil samples obtained from borrow sites of Joe Pool Dam and Grapevine Dam, were presented along with his recommendations for future research tasks.

Also, descriptions of Fully Softened Shear Strength tests are provided along with use of Direct Shear and Torsional Ring Shear tests to measure FSS of soils. The results from both

methods are compared, and these results are described in Chapter 5. These results are used to provide a better judgment for the effectiveness of the admixtures against surficial slope instability issues.

CHAPTER 4

LONG-TERM MONITORING OF INSTRUMENTED EMBANKMENT SECTIONS

Research conducted by McCleskey (2005) on soil samples obtained from Joe Pool Dam and Grapevine Dam has suggested that the use of lime, lime mixed with fibers and compost as admixtures helpes improve the shrinkage and swelling properties of soil. Based on these laboratory study recommendations, Dronamraju (2008) studied the effectiveness of the treatments in the field studies by construction of test sections on the same two test sites at Joe Pool Dam and Grapevine Dam. The test sections were specifically selected to have virgin soil and had not been previously subjected any kind of failure. Five test sections were constructed at each site with field additive treatments following McCleskey's recommendations:

- Control section to compare the performance
- 20%compost
- 4%lime with 0.30%fiber
- 8%lime with 0.15%fiber
- 8%lime

Field instrumentation was also implemented and this included the use of moisture and temperature sensors, inclinometer surveys and elevation surveys. As part of future research needs, Dronamraju recommended that the field monitoring should continue to further examine the long term effect of the applied admixtures.

In this chapter, the researcher briefly reviewed the construction stages and the instrumentation on each test site. Updated long term data collected from moisture and temperature sensors, inclinometer surveys and elevation surveys are presented in a chronological order following the work of Dronamraju in 2008. Visual observation for the surface cracking pattern and vegetation growth were also monitored and reported in this section.

4.1 Construction of Test Sections

The dam sites have a close proximity to The University of Texas at Arlington. The Joe Pool Dam test section site is at a distance of about 15 miles south of Arlington and the Grapevine Dam test section is at a distance of 25 miles north of Arlington from UTA. A map depicting the location of these two dams is shown in Figure 4.1.

Figure 4.1. Location of Joe Pool Dam and Grapevine Dam (source: google.com)

On each dam, five sections of 25 ft. x 60 ft. each were selected to be treated with compost, lime and fibers in McCleskey's recommended proportions. First, the grass and other vegetation on the surface were removed by mowing. Then the top soil was excavated using a backhoe and stockpiled aside to be placed back over the treated section after the compaction of the 18 in. soil layer with admixtures on the slope surface. After the excavation of the top soil, the core soil of the dam was removed as per the plan. The depth of excavation near the top surface

was about 42 in., as shown in Figure 4.2. The excavated core soil was loaded into the trucks and transported to the soil processing area called level pad, where the soil was placed in a layer of 6 to 8 in. thickness (Figure 4.3). The soil in the level pad area was then pulverized, moistened and mixed with compost, lime and fibers. Figure 4 shows the mixing process for lime and fibers. The treated soil with admixtures was transported and placed back in the embankment immediately. The test sections with treated soil were properly compacted with a sheep foot roller. Finally, after the completion of construction, the embankment area, level pad and borrow pit were fertilized and seeded to provide a good vegetation surface.

(a) (b)

Figure 4.2. Excavation of top soil (left) and core soil (right) (Dronamraju, 2008)

Figure 4.3. Soil processing area at Joe Pool dam (Dronamraju, 2008)

(a) (b)

Figure 4.4. Mixing of lime (left) and fibers (right) on a level pad (Dronamraju, 2008)

A layout showing the details of the proposed construction of test sections is shown in Figure 4.5. The sequence of construction operations for each test section was illustrated in Figure 4.6.

Figure 4.5. Layout for construction of test section 60 ft. x 25 ft. (Dronamraju, 2008)

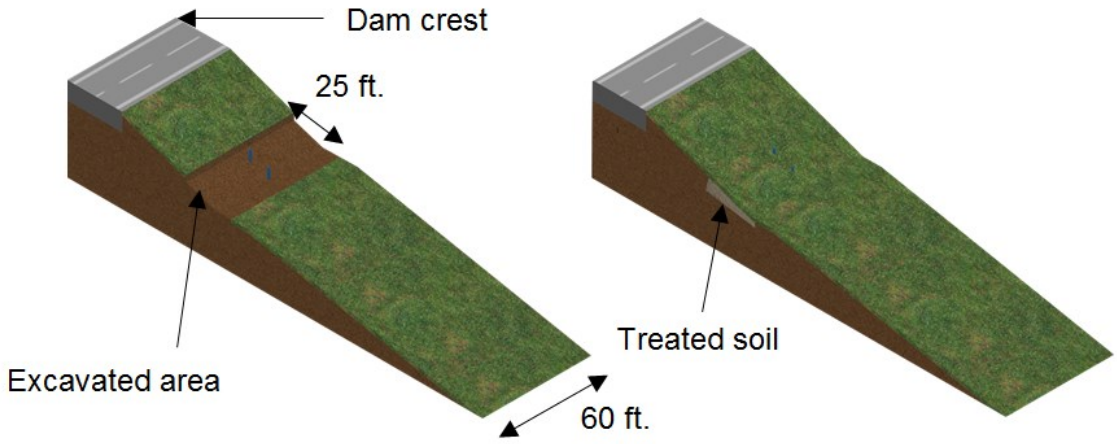

(a) (b)

Figure 4.6. Construction on one test section

4.2 Instrumentation

In order to analyze the effectiveness of the treatments, test sections were instrumented with moisture and temperature sensors to observe the fluctuation of soil water content and temperature. Lateral displacement of the slope was monitored by conducting inclinometer

surveys, while vertical movement of the slope was recorded by elevation surveys. With respect to the previous work of Dronamraju (2008), field performance of the admixtures was continuously monitored to further assess the reliability of the treatment compared to the untreated soil in the control section.

The treated sections were also monitored visually to detect the shrinkage crack development, as well as its propagation. The ability to promote growth of vegetation on the test sites treated with admixtures was also verified during the field visits.

4.2.1 GroPoint Moisture Probes

In order to monitor the soil moisture content and soil temperature, two moisture probes were placed in each treated test section. The moisture sensor works on the principle of 'Time Domain Transmission' or (TDT) technology and provides volumetric moisture contents.

The bottom probe was placed at a depth of 20 in. from the top of the surface, i.e., at the middle of the thick treated section. The second moisture probe was placed at the top of the treated section near the interface, with a top soil at a depth of 10 in. from the top surface of the slope. The temperature probe was placed in the treated section nearer to the top moisture probe in the treated portion of the soil. Both moisture and temperature probes provide real time volumetric moisture content and temperature data.

The data was recorded and stored in a data logger stationed at each test site, and the data was downloaded to a laptop computer periodically during site visits by connecting to the data cable and using the GroGraph software program. The moisture content and temperature data recorded every hour was transferred to an excel file for further analysis. Figure 4.7 shows the schematic indicating the working principle of moisture probes and their positions with respect to the slope surface.

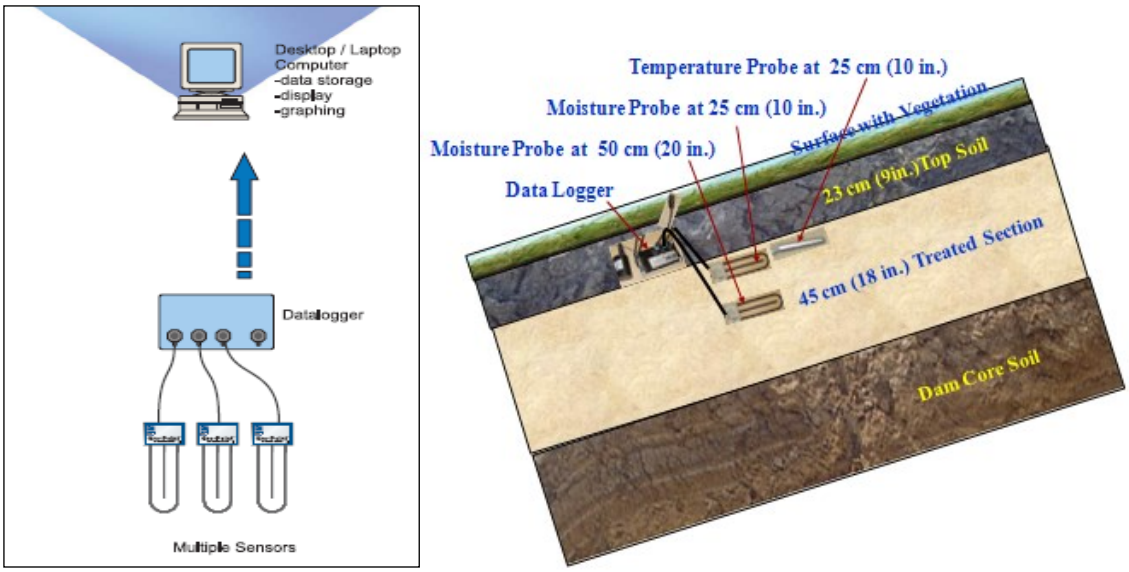

Figure 4.7. The working principles of moisture probes (left) (ESI) and their positions (Dronamraju, 2008)

4.2.2 Installation of Inclinometer Casings

Each test section was instrumented with two inclinometer casing of 15 ft. long and 2.75 in. diameter. Using the vertical inclinometer probe, lateral movement of the slope was recorded perodically in every 2 ft. of depth. The data obtained was then analyzed with the help of computer software DMMWin and DigiPro, as provided by the manufacturer of the inclinometer probe. Figure 4.8 shows the installation of the inclinometer casing and inclinometer probe used for field measurement.

(a) (b)

Figure 4.8. Installation of inclinometer casings (a) and Inclinometer Probe (b)

4.2.3 Elevation Surveys

For the purpose of monitoring the vertical movement of the slope, a series of elevation pegs were installed on each dam site to serve as spots for elevation surveys. With 9 pegs in each test section, a total of 45 pegs were inserted in 5 sections on both Joe Pool Dam and Grapevine Dam sections. The schema positioning elevation pegs is shown in Figure 4.9. The benchmark point was set on top of the embankment crest with the known elevation magnitude. Leica TCR 305 total station was used to conduct the surveys (Figure 4.10).

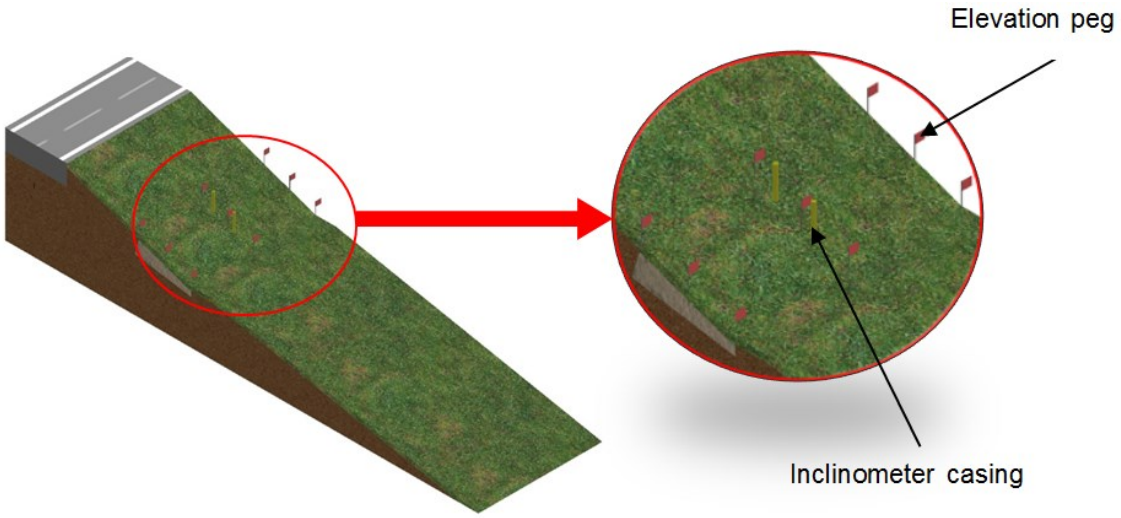

Figure 4.9. Positions of Elevation pegs on each test section

Figure 4.10. Total Station Leica TCR 305

4.3 Updated Field Data

After initiating the construction and instrumentation on both Joe Pool Dam and Grapevine Dam, Dronamraju (2008) started monitoring the early performance of the admixtures and recorded the moisture, temperature of the soil as well as conducted regular inclinometer and elevation surveys to analyze the slope movement. With the early positive responses collected from the treatments and test sections, he recommended further extending the

monitoring period to explore the long term effects of those chosen treatments on the overall slope performance of the two dam sites. This research has investigated this aspect as the researcher has been constantly visiting the test sites for a period of two and a half years (since 2010) to gather the field data from instrumentation and surveys. This section provided the collected data on all the aforementioned aspects.

4.3.1 Moisture Sensors Data

4.3.1.1 Rainfall Data

While studying the moisture content fluctuations and the temperature variations of the test sections, site precipitation details over the same period were also collected. The data of rainfall was collected with the information provided by the Western Regional Climate Center (WRCC) (www.wrcc.dri.edu) from Joe Pool Dam's and Grapevine Dam's weather stations located at the sites. Data pertaining to monthly accumulated precipitation was presented in reverse chronological order. In the process of collecting the data for each month, the amount of missing days did not exceed five, resulting in the interpolation of data for some particular months. Table 4.1 and Table 4.2 present the monthly total rainfall data for Joe Pool Dam and Grapevine Dam.

Table 4.1. Monthly Total Precipitation at Joe Pool Dam (WRCC)

Year	Monthly Total Precipitation (in)											
	Jan	Feb	Mar	Apr	May	Jun	Jul	Aug	Sep	Oct	Nov	Dec
2012	7.15	2.49	3.88	1.3	2.5	2.56	0.42	1.78	0.05	2.17	0.05	1.95
2011	2.41	1.4	0.07	3.97	4.77	1.31	0	0.21	2.16	5.33	0.87	5.3
2010	2.9	2.38	4.11	1.87	2.85	2.91	4.42	2.4	9.4	0	3.48	1.92
2009	1.46	1.08	4.99	4.98	3.55	3.9	5.71	2.57	6.43	10.95	2.45	2.21
2008	0.76	1.74	8.07	6.43	3.33	1.52	1.97	2.83	0.87	0.84	3.29	0.2
2007	0	0.79	5.34	0.99	6.73	12.27	4.38	2.96	5.14	2.7	1.72	2.44

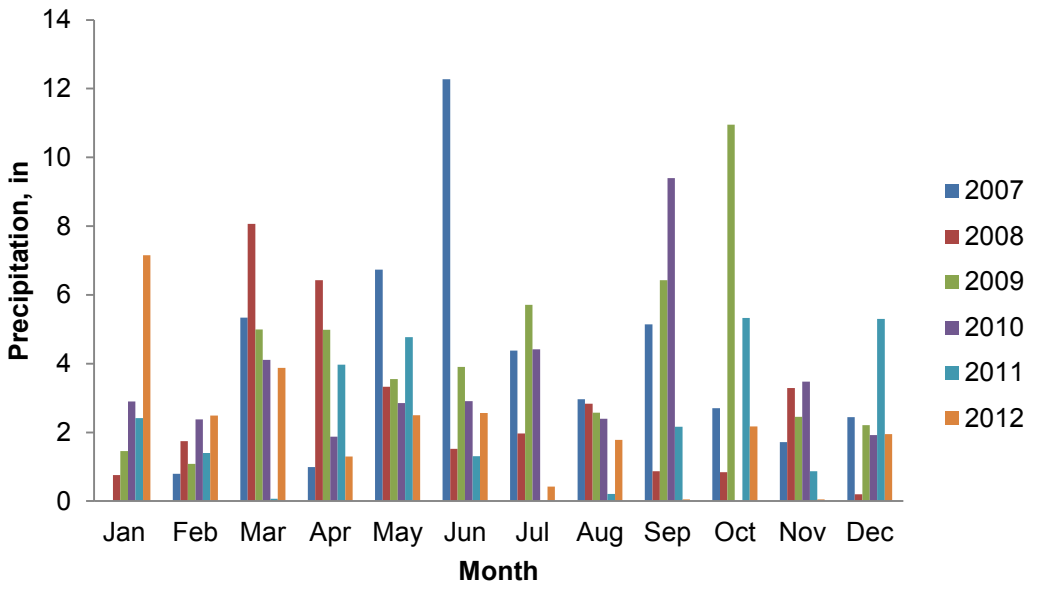

Figure 4.11. Comparison of monthly total precipitation from 2007 to 2012 at Joe Pool Dam

Table 4.2. Monthly Total Precipitation at Grapevine Dam (WRCC)

Year	Monthly Total Precipitation (in)											
	Jan	Feb	Mar	Apr	May	Jun	Jul	Aug	Sep	Oct	Nov	Dec
2012	5.88	2.21	6.64	3.9	2	2.37	1.2	3.71	1.84	1.01	0.3	2.09
2011	1.88	0.44	0.13	4.47	7.78	4.08	0.05	0.91	0.85	3.63	1.38	5.2
2010	2.66	2.26	4.35	2.2	2.14	3.54	3.6	0.27	13.25	0	1.54	1.65
2009	0.54	0.87	7.69	2.91	4.87	3.55	3.59	0.45	6.75	8.75	2.11	2.1
2008	0.28	1.49	6.48	4.86	2.98	1.14	0.25	2.67	2.56	1.43	3.91	0.8
2007	5.09	0.52	3.95	2.84	9.58	10.33	3.25	1.55	6.27	3.24	1.34	2.36

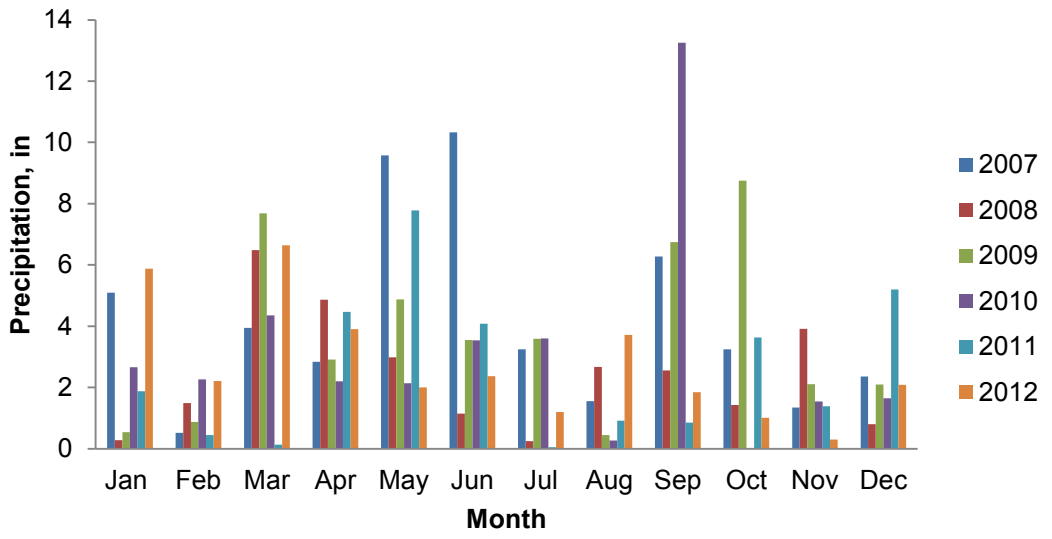

Figure 4.12. Comparison of monthly total precipitation from 2007 to 2012 at Grapevine Dam

4.3.1.2 Moisture Data

Volumetric moisture content data was recorded at two different depths of 10 in. and 20 in. with respect to the slope surface from the TDT moisture sensors. Data collected was analyzed to study the response of soil moisture content variations to different weather conditions, involving changes in precipitation and air ambient temperature conditions at the site. This was further discussed in the field data analysis in Chapter 5. Figure 4.13 to 4.22 present the soil moisture data on both Joe Pool Dam and Grapevine Dam sites.

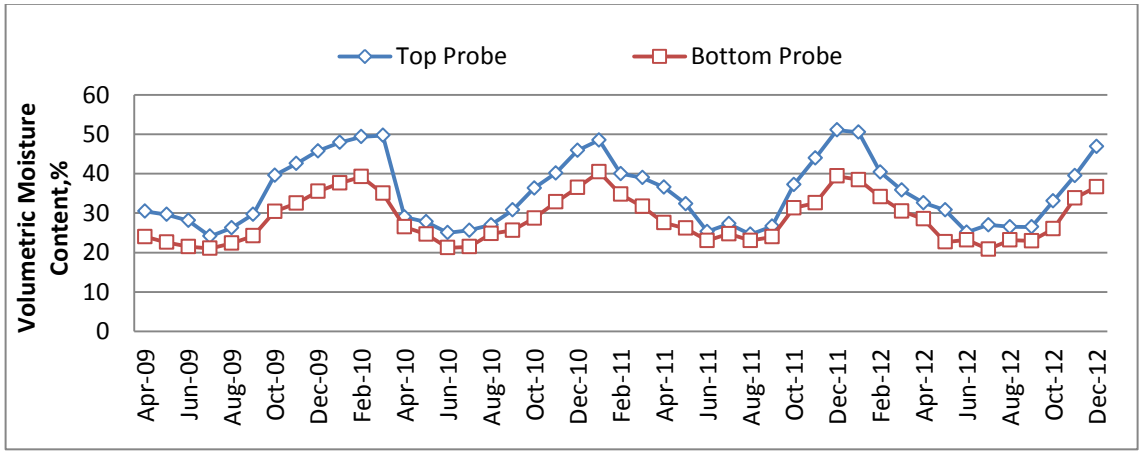

Figure 4.13. Moisture Content Data for Control Section at Joe Pool Dam

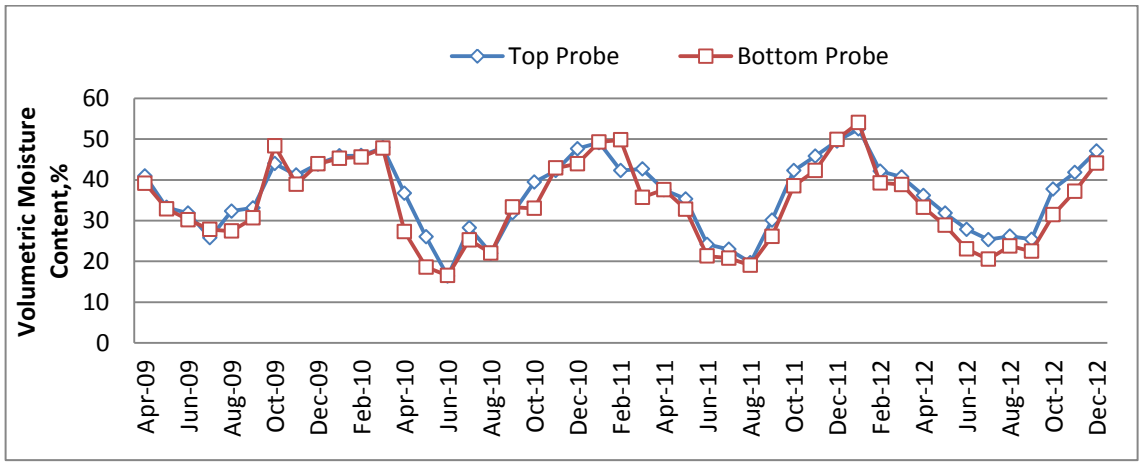

Figure 4.14. Moisture Content Data for 20%compost Section at Joe Pool Dam

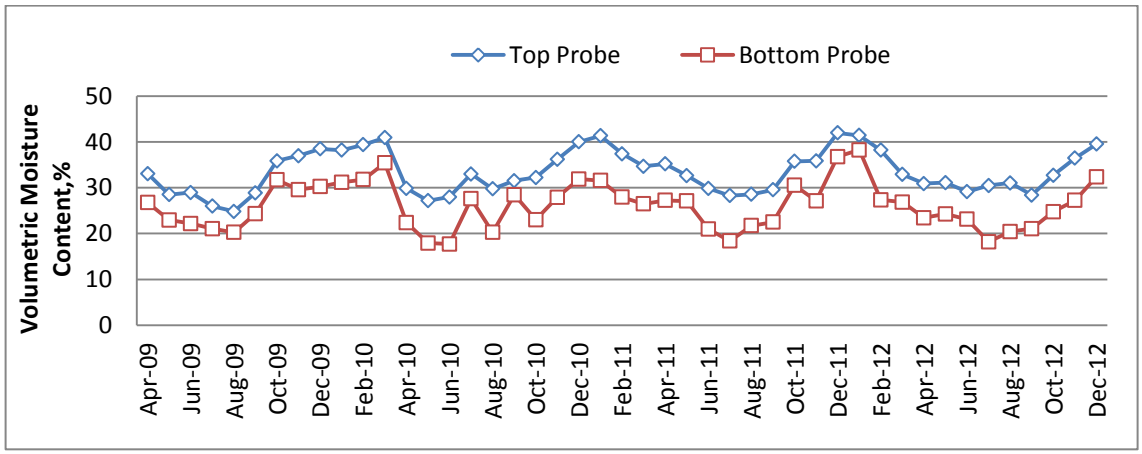

Figure 4.15. Moisture Content Data for 4%lime and 0.3%fibers Section at Joe Pool Dam

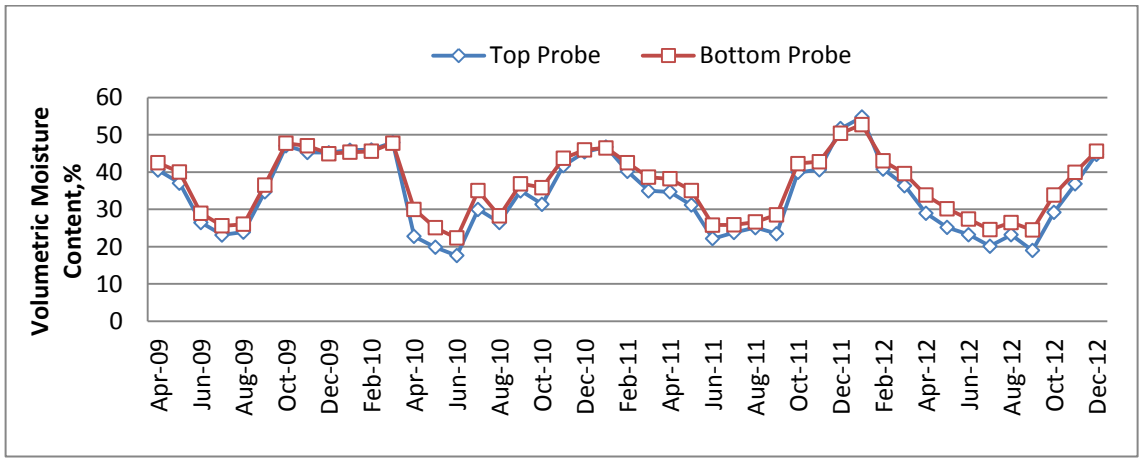

Figure 4.16. Moisture Content Data for 8%lime and 0.15%fibers Section at Joe Pool Dam

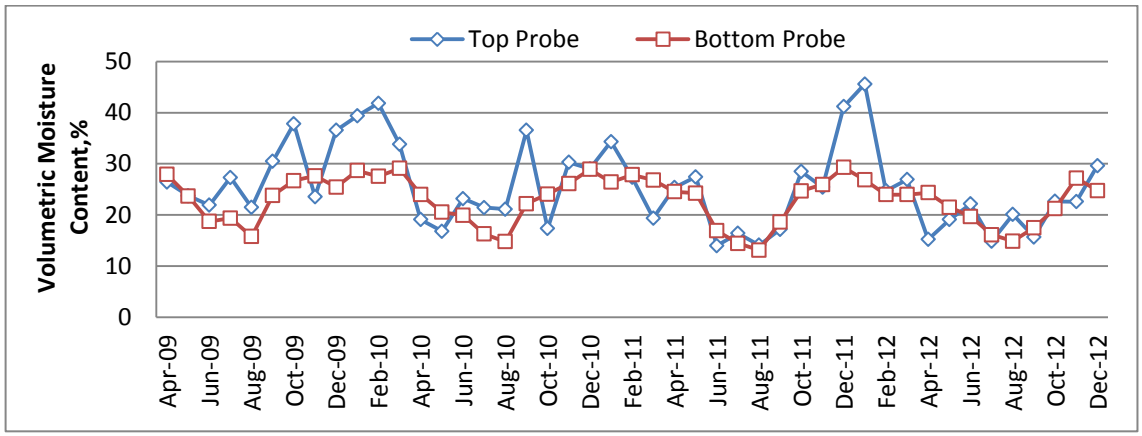

Figure 4.17. Moisture Content Data for 8%lime Section at Joe Pool Dam

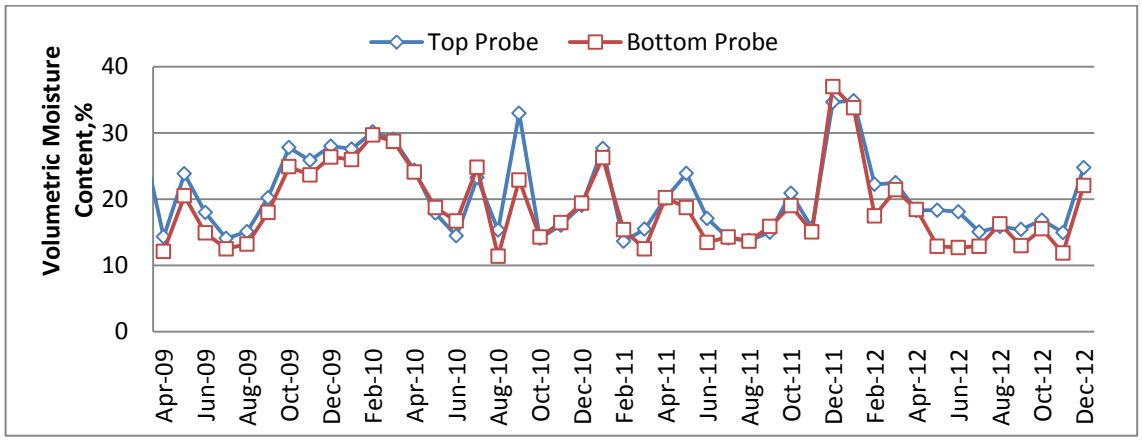

Figure 4.18. Moisture Content Data for Control Section at Grapevine Dam

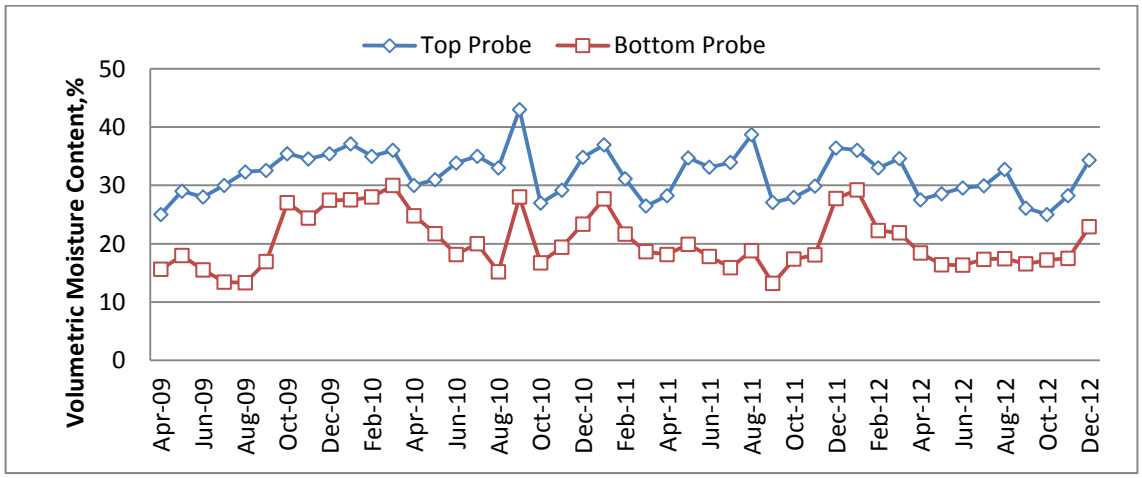

Figure 4.19. Moisture Content Data for 20%compost Section at Grapevine Dam

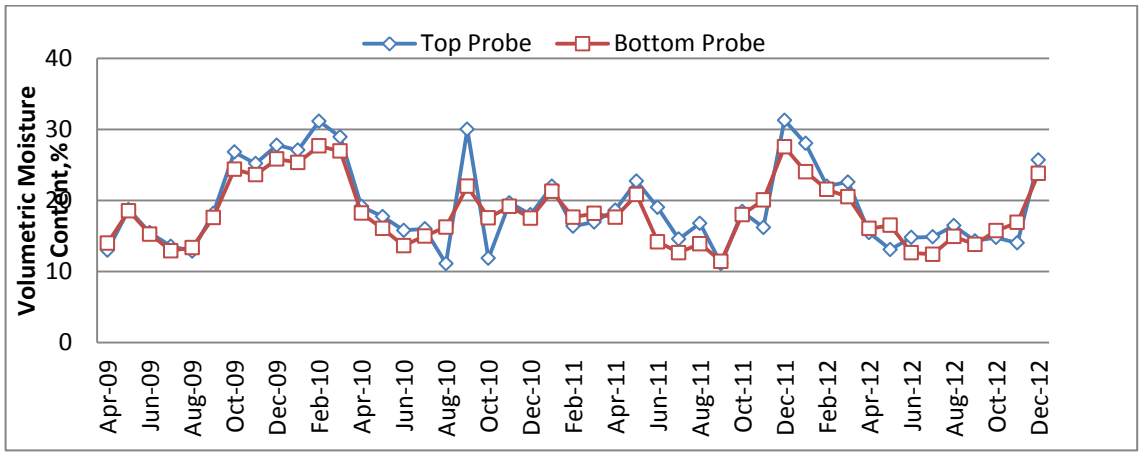

Figure 4.20. Moisture Content Data for 4%lime+0.30%fibers Section at Grapevine Dam

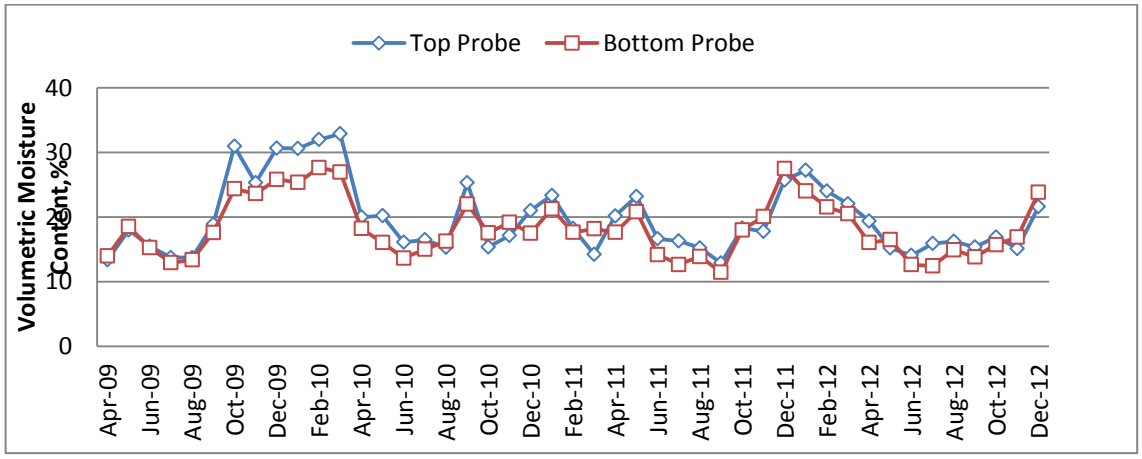

Figure 4.21. Moisture Content Data for 8%lime+0.15%fibers Section at Grapevine Dam

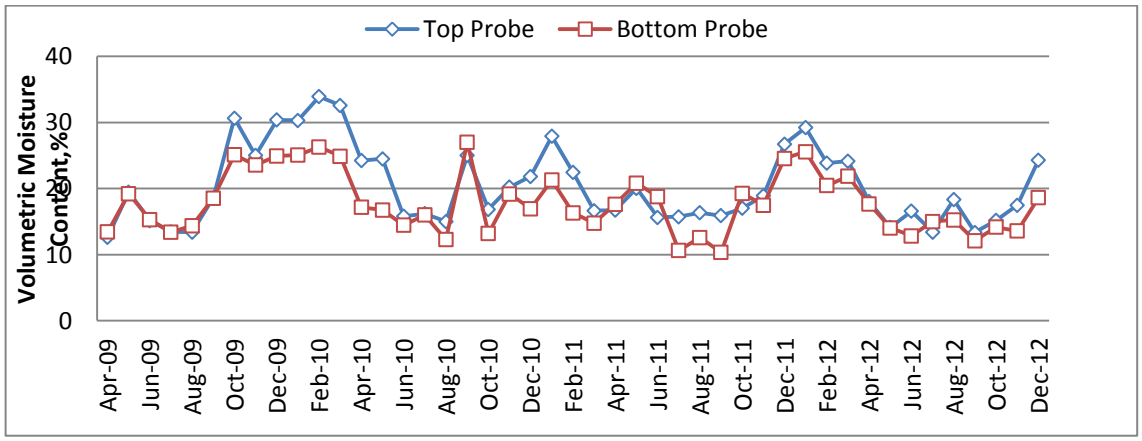

Figure 4.22. Moisture Content Data for 8%lime Section at Grapevine Dam

4.3.2 Soil Temperature Data

4.3.2.1 Air Temperature Data

For the purpose of field data analysis, the air temperature was collected based on the information provided by WRCC. The data is shown in Table 4.3 - Table 4.4 and Figure 4.23-Figure 4.24. It can be seen from the data on both Joe Pool Dam and Grapevine Dam sites that the changes of air temperature in every year follow the pattern of typical wetting and drying seasons in Texas with the peak of temperature in July-August and lowest temperature in December-January periods.

Table 4.3. Monthly Average Temperature at Joe Pool Dam (source: WRCC)

Year	Monthly Average Temperature (°F)											
	Jan	Feb	Mar	Apr	May	Jun	Jul	Aug	Sep	Oct	Nov	Dec
2012	46.96	58	65.03	68.11	75.4	82.89	84.95	86.54	81.34	69.45	57.9	51.2
2011	45.13	56.58	59.94	66.88	72.3	86.12	90.56	91.32	77.59	63.92	54.89	46.4
2010	43.24	40.95	54.23	66.33	75.66	84.95	85.29	89.37	79.68	63.5	58.85	49.58
2009	47.26	56.11	58.29	62.48	72.82	81.46	86.02	85.05	75.27	63.14	59.75	42.66
2008	41.16	47.07	53.79	62.08	69.36	80.03	83	85.21	76.59	65.22	60.08	44.29
2007	46.4	45.5	61.66	61.6	69.95	76.15	75.11	81.13	75.8	64.78	56.97	45.14

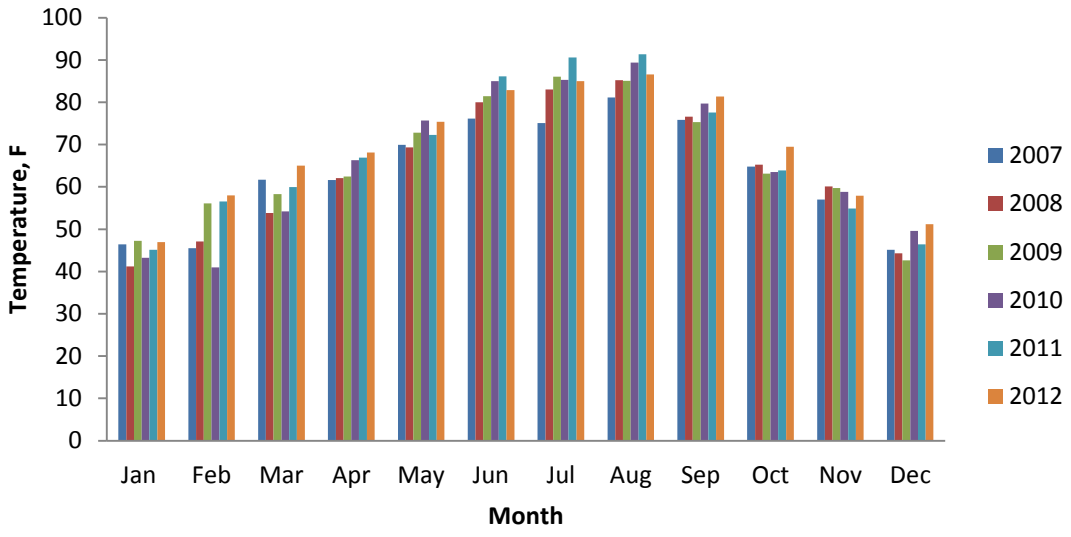

Figure 4.23. Monthly Average Temperature at Joe Pool Dam (2007-2013)

Table 4.4. Monthly Average Temperature at Grapevine Dam (2007-2013) (WRCC)

Year	Monthly Total Precipitation (in)											
	Jan	Feb	Mar	Apr	May	Jun	Jul	Aug	Sep	Oct	Nov	Dec
2012	48.7	51.57	63.98	69.33	75.89	83.22	87.1	85.83	73	66.61	58.3	47.2
2011	41.11	53.52	60.08	68.67	71.52	85.78	90.59	92.18	79.12	65.14	57.17	45.38
2010	42.79	40	53.58	65.53	74.45	84.93	84.69	88.9	79.13	64.8	56.75	47.39
2009	44.65	54.21	56.26	63.04	70.46	82.27	84.97	84.24	74.45	60.98	58.77	40.47
2008	42.5	53.75	58.86	66.34	75.79	85.07	87.47	86.16	74.93	67	59	45.79
2007	42.66	48	65.45	61.05	73.44	78.93	81.79	86.3	78.71	67.98	59.43	48.74

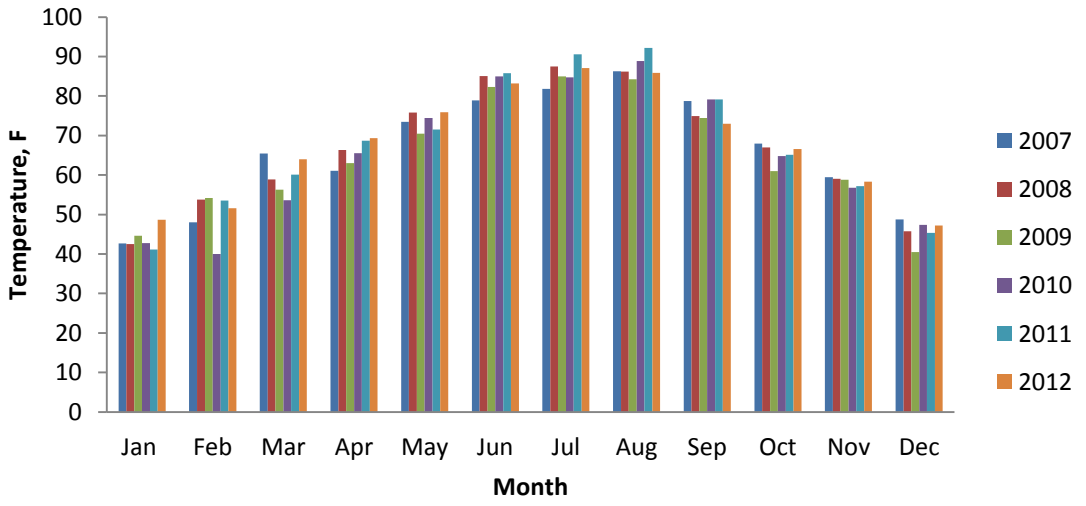

Figure 4.24. Monthly Average Temperature at Grapevine Dam (2007-2013)

4.3.2.2 Soil Temperature Data

A soil temperature sensor was installed at a depth of 10 in. from the top of the slope surface, just right beneath the edge of the treated soil layer. Due to the proximity of the sensor to the surface, the changes of temperature highly resembled the changes of the air temperature thorough the year with the highest temperature in June-August and lowest temperature in December-January on both Joe Pool and Grapevine sites. Details are shown in Figures 4.25 to 4.34.

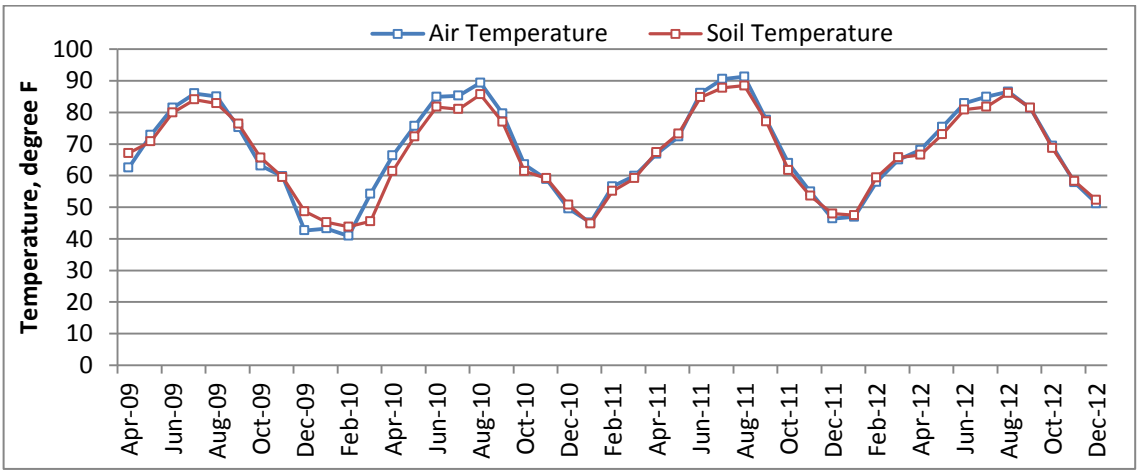

Figure 4.25. Soil Temperature at Control Section at Joe Pool Dam

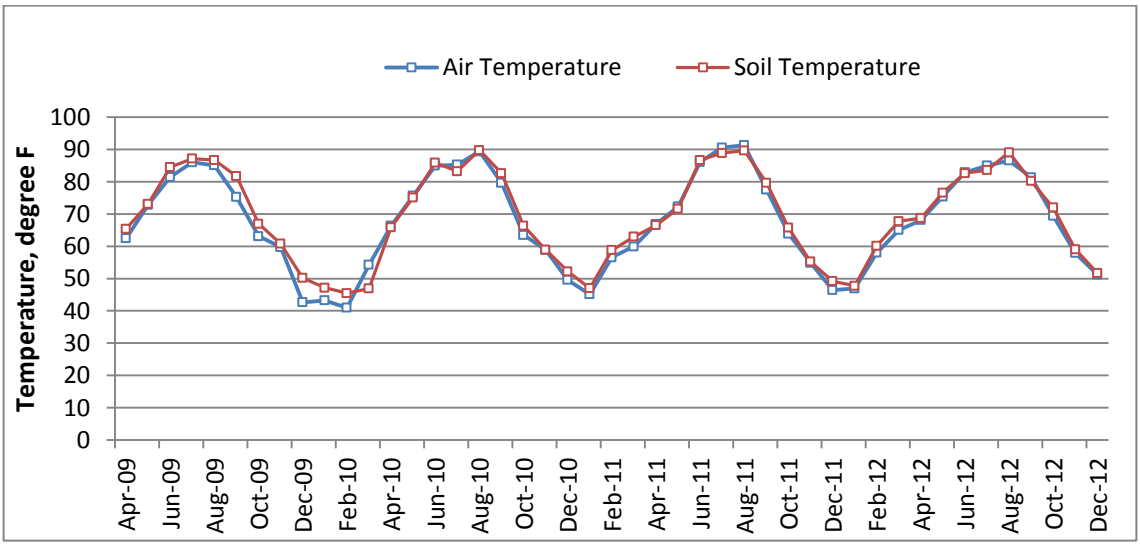

Figure 4.26. Soil Temperature at 20%compost Section at Joe Pool Dam

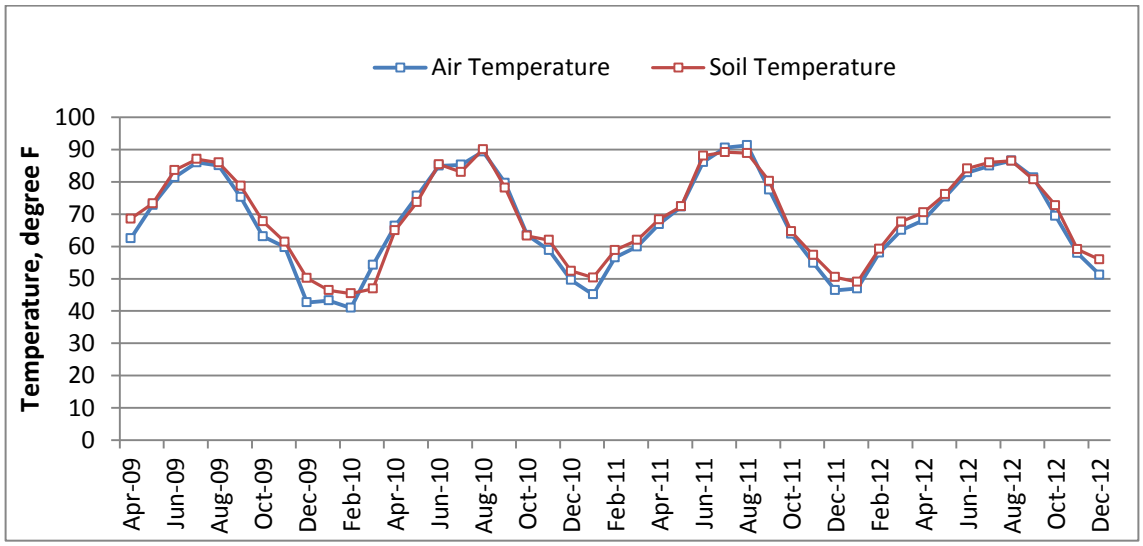

Figure 4.27. Soil Temperature at 4%lime+0.3%fibers Section at Joe Pool Dam

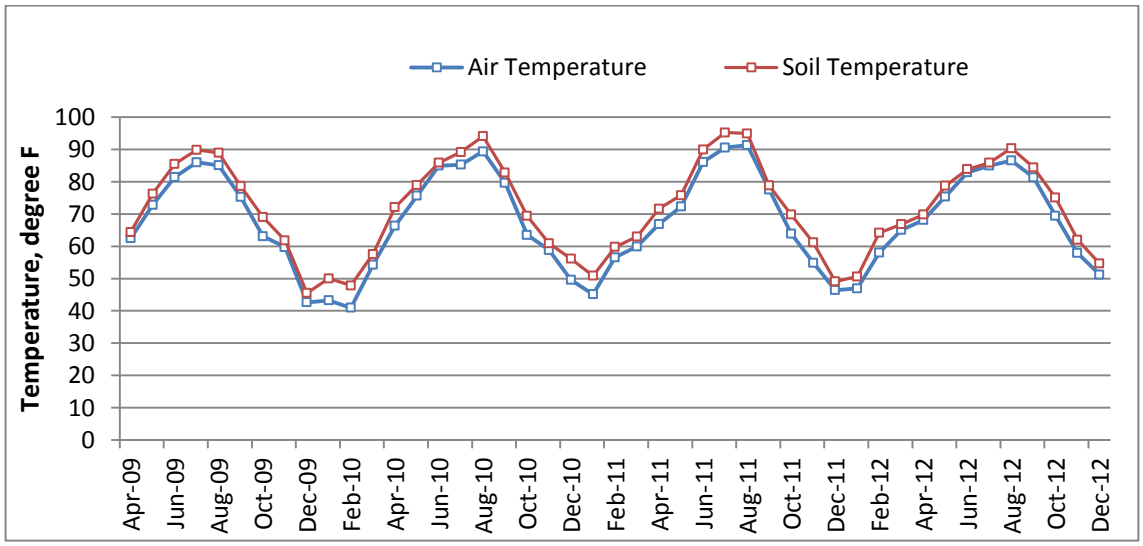

Figure 4.28. Soil Temperature at 8%lime+0.15%fibers Section at Joe Pool Dam

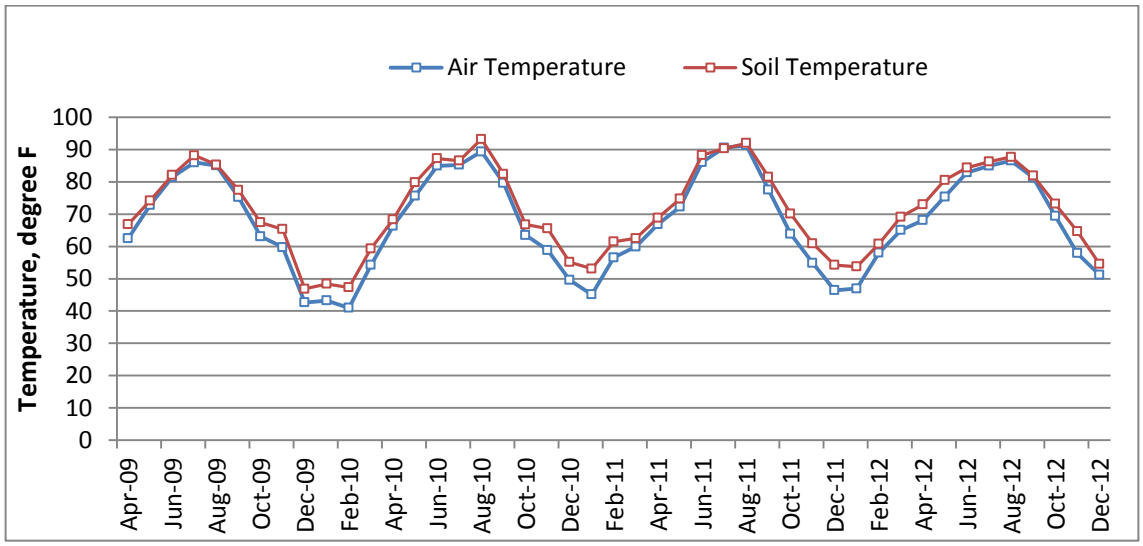

Figure 4.29. Soil Temperature at 8%lime Section at Joe Pool Dam

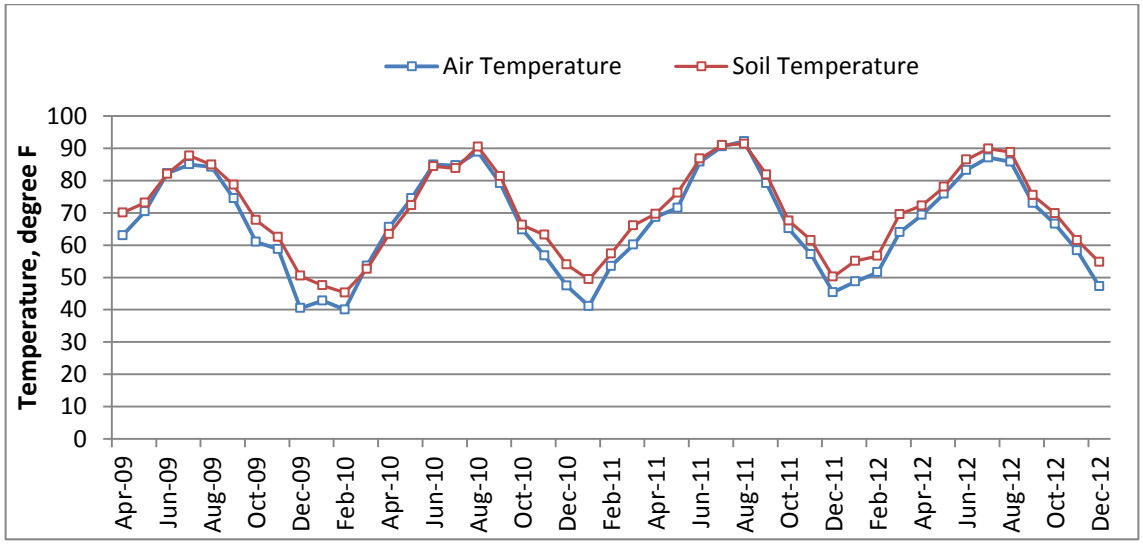

Figure 4.30. Soil Temperature at Control Section at Grapevine Dam

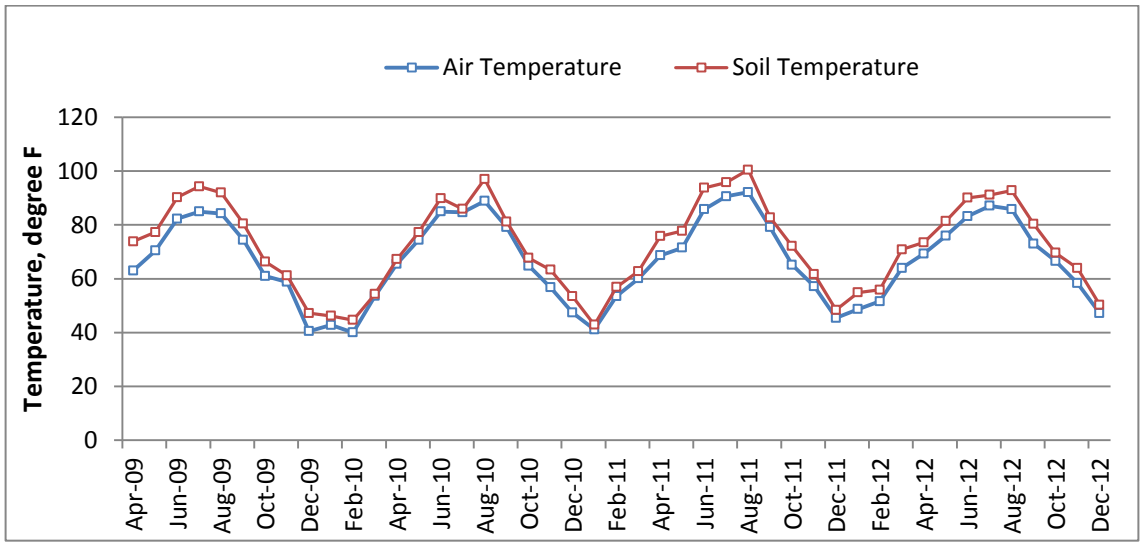

Figure 4.31. Soil Temperature at 20%compost Section at Grapevine Dam

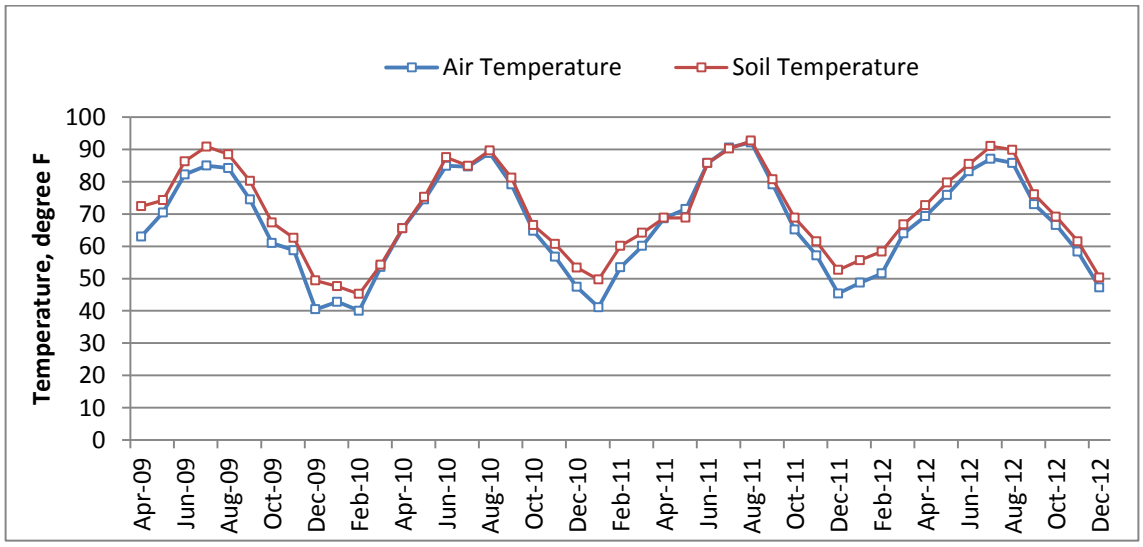

Figure 4.32. Soil Temperature at 4%lime+0.30%fibers Section at Grapevine Dam

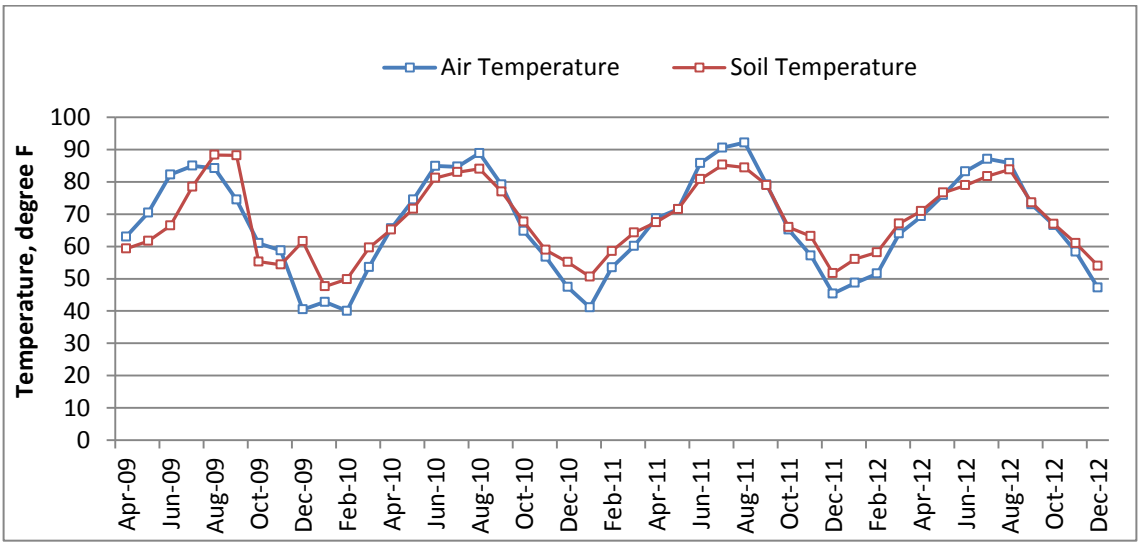

Figure 4.33. Soil Temperature at 8%lime+0.15%fibers Section at Grapevine Dam

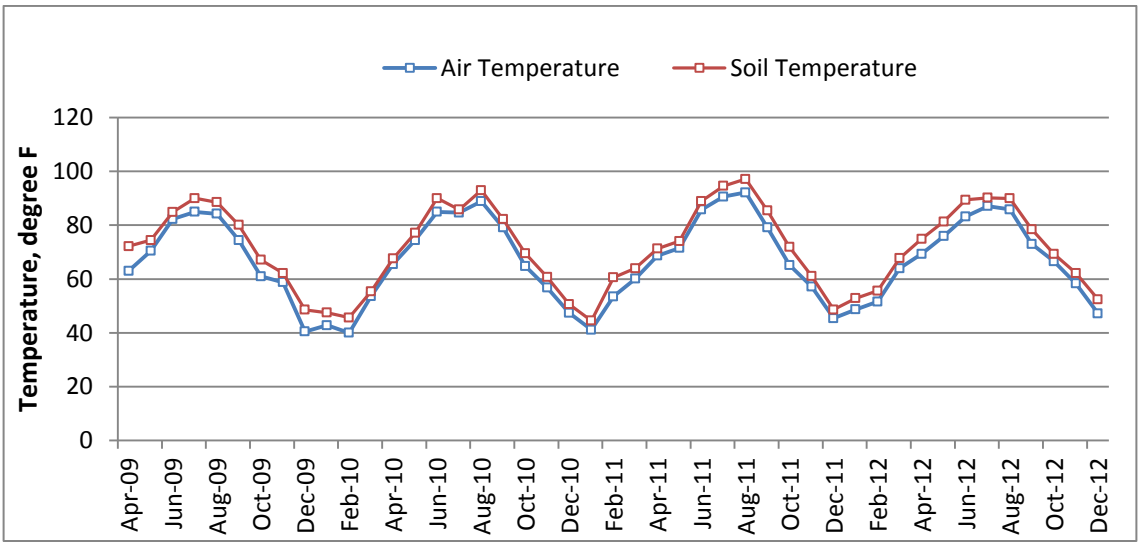

Figure 4.34. Soil Temperature at 8%lime Section at Grapevine Dam

4.3.3 Inclinometer Surveys

Lateral movement of the slope was recorded on a monthly basis with the help of the inclinometer instrument. Each test section had two rows of inclinometer casings installed with the numerical notation XY (X: row number, Y: section number). Readings were taken every 2 ft.

depth in both slope directions A-axis and cross slope direction B-axis. Figure 4.35 shows the notation of the inclinometers casing and the reading directions.

Figure 4.35. Notations of inclinometer casings and movement directions on test sections

Data was continuously recorded since the researcher started visiting the test sites from September 2010. Due to the amount of the data recorded, Figures 4.36 to 4.55 only highlight the significant soil movement at various time periods.

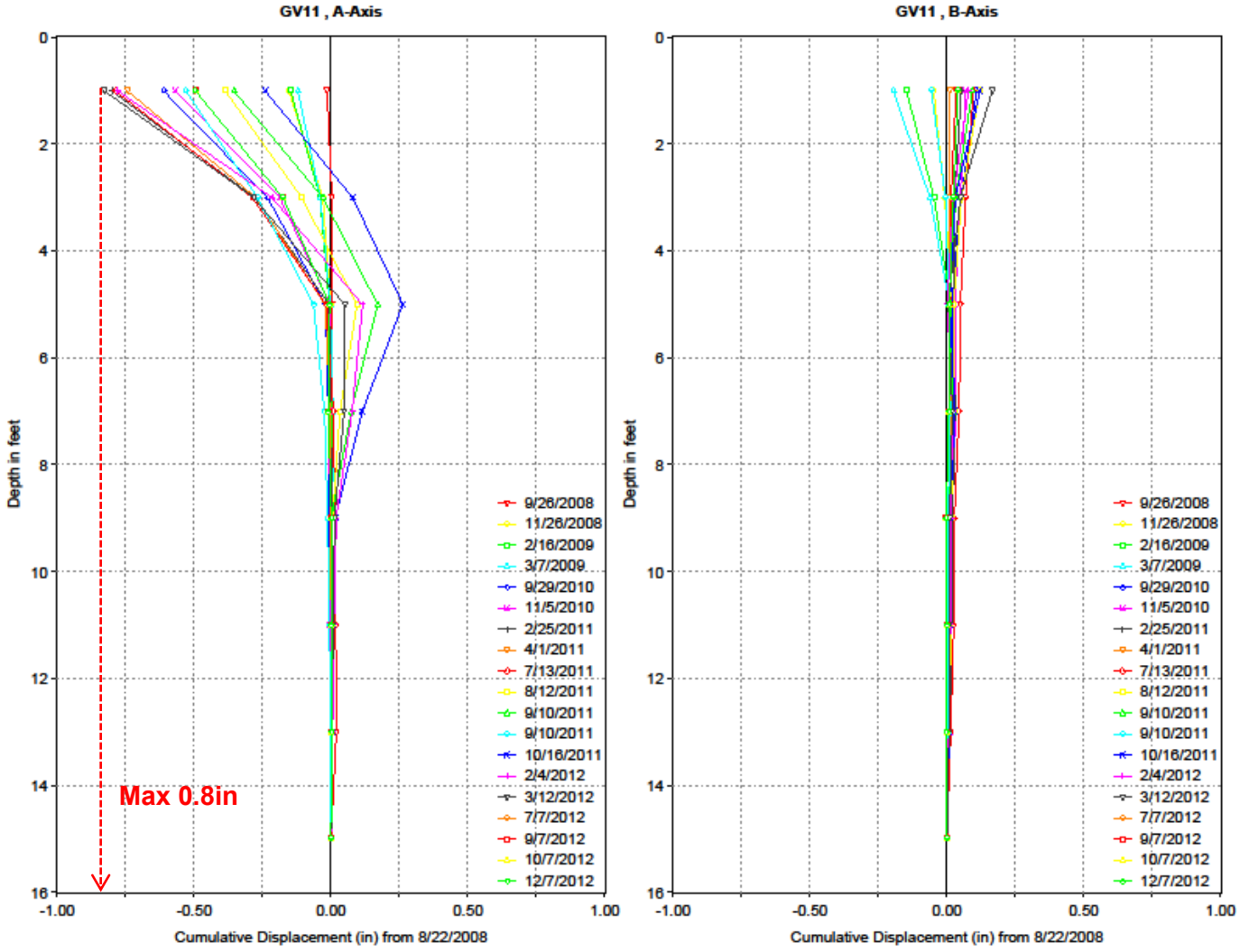

Figure 4.36. Inclinometer data for top Control Section at Grapevine Dam

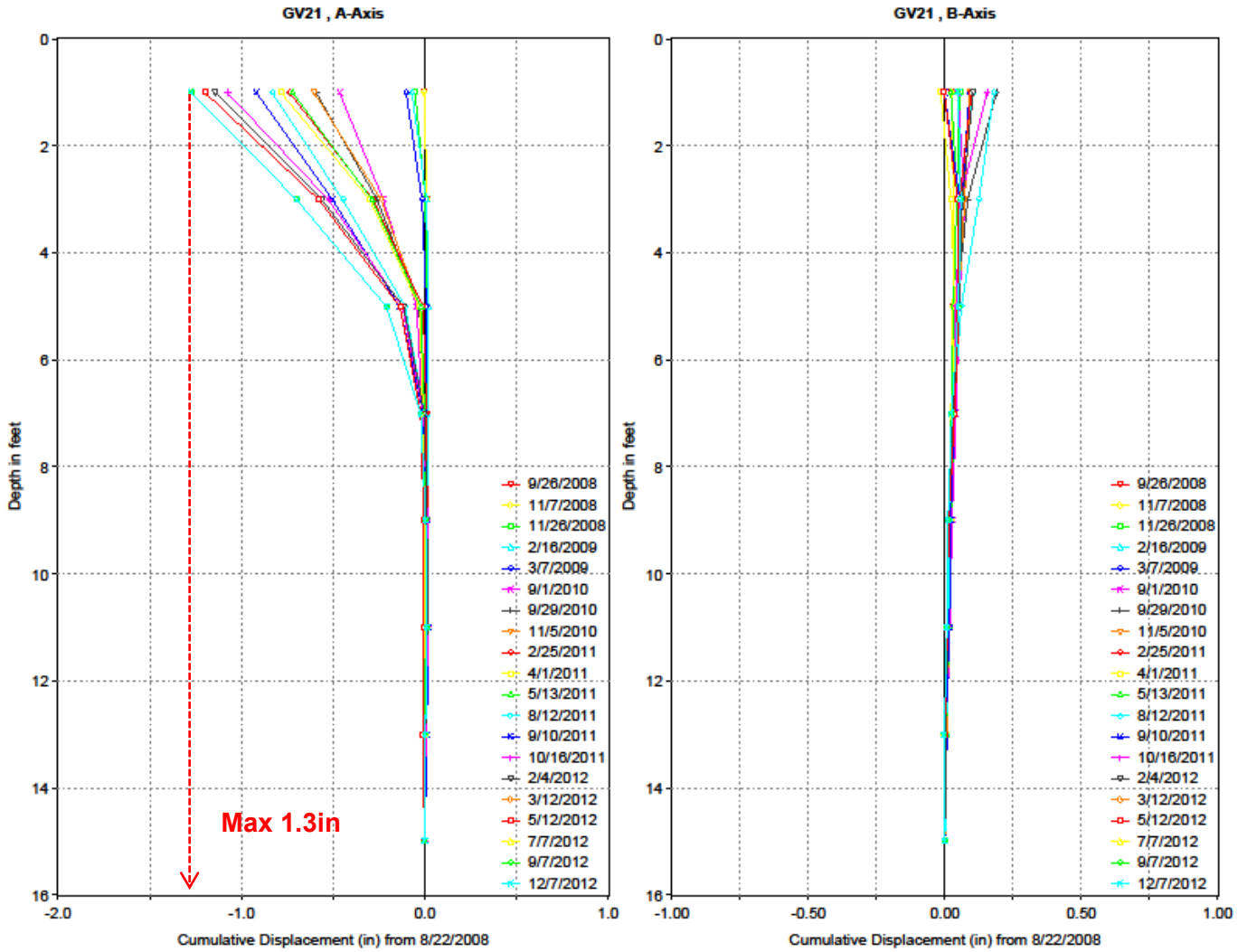

Figure 4.37. Inclinometer data for bottom Control Section at Grapevine Dam

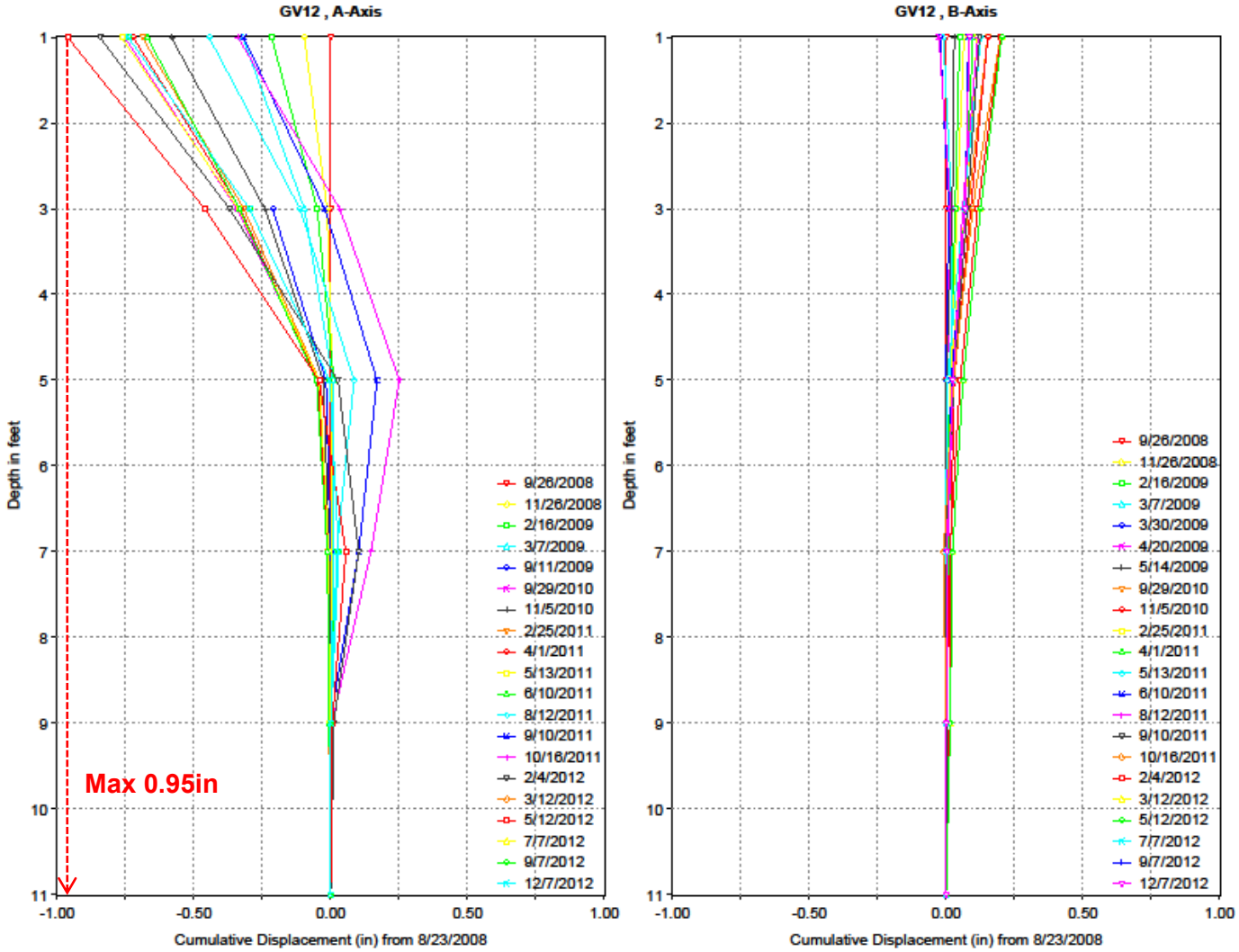

Figure 4.38. Inclinometer data for top 20%compost Section at Grapevine Dam

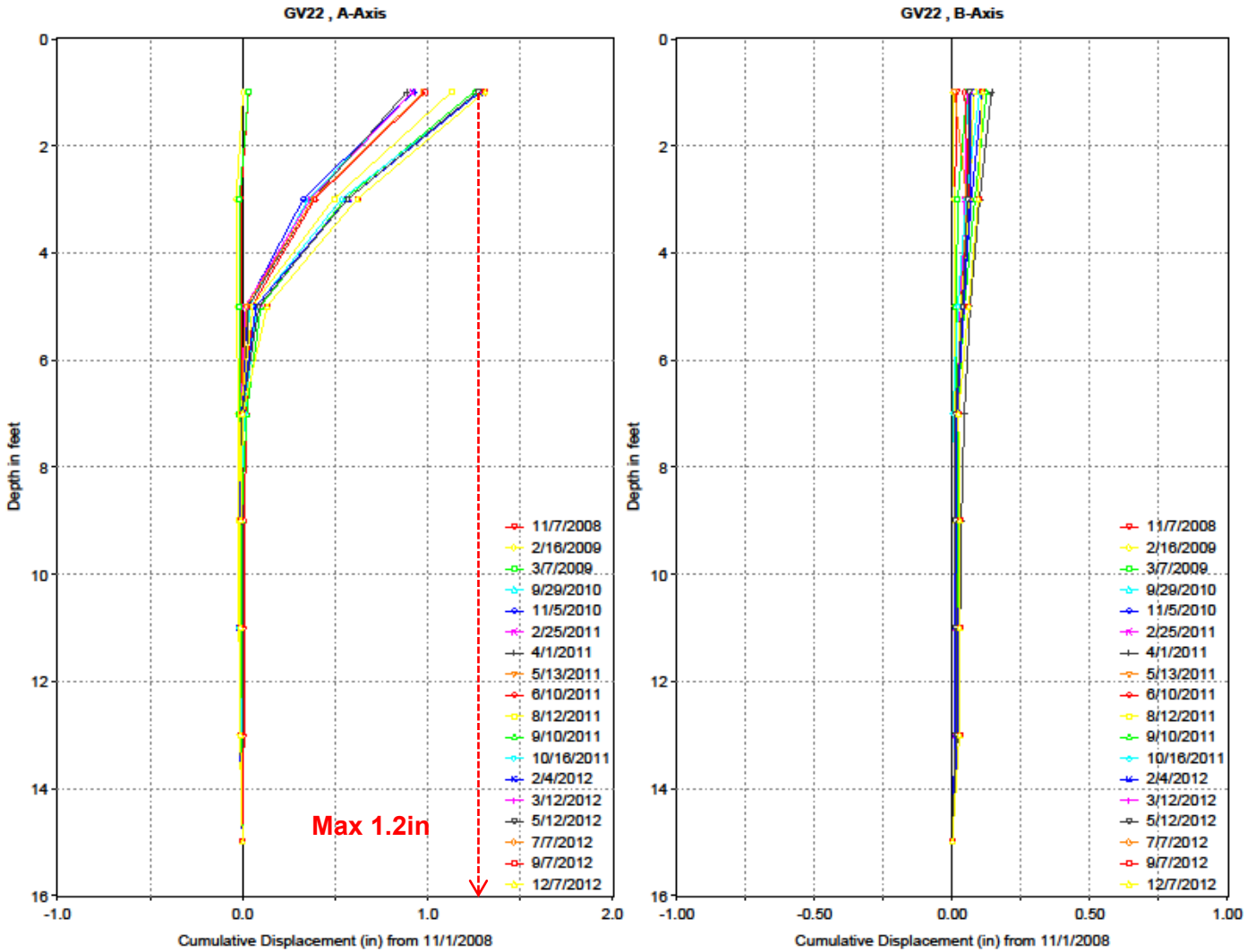

Figure 4.39. Inclinometer data for bottom 20%compost Section at Grapevine Dam

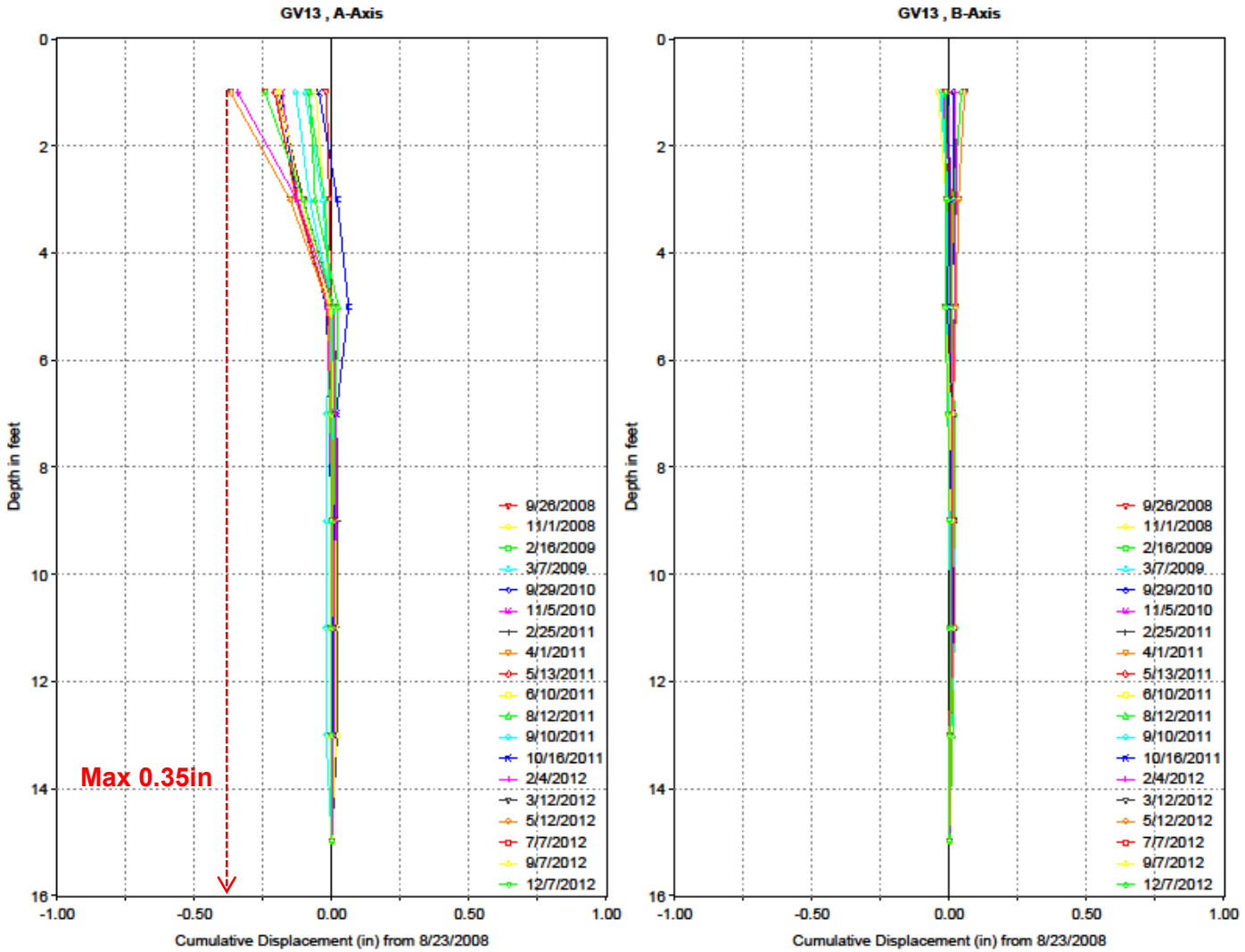

Figure 4.40. Inclinometer data for top 4%lime+0.30%fibers Section at Grapevine Dam

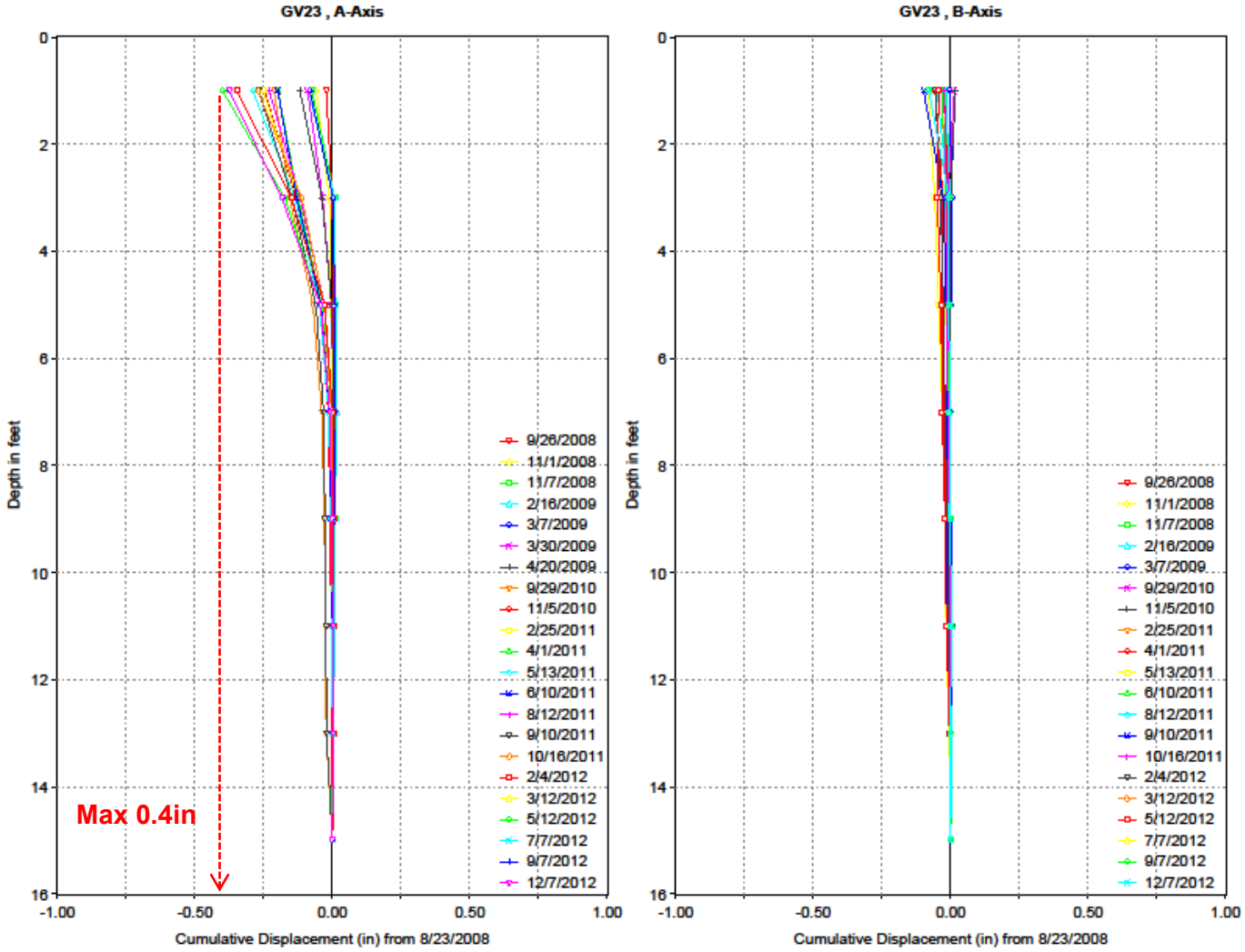

Figure 4.41. Inclinometer data for bottom 4%lime+0.30%fibers at Grapevine Dam

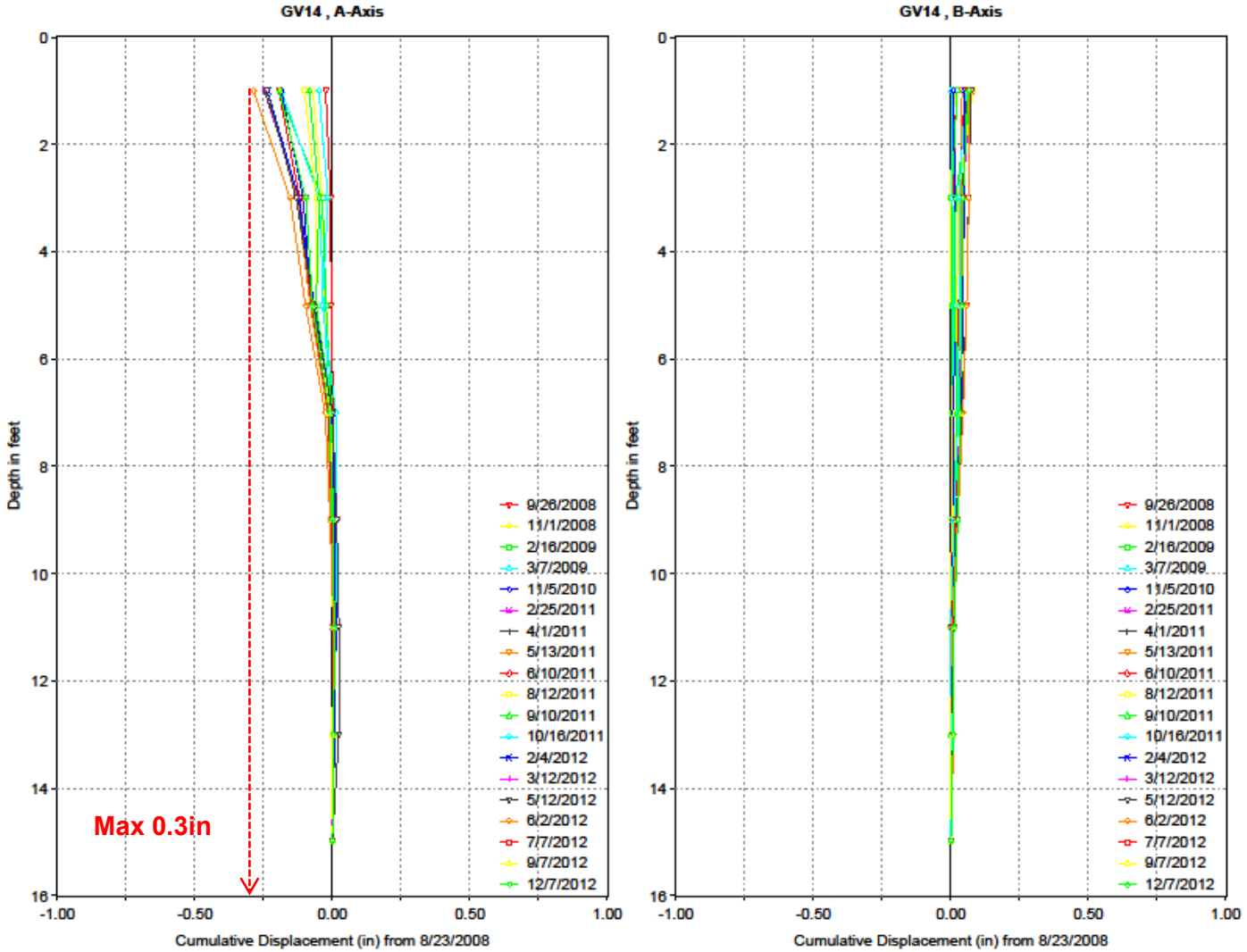

Figure 4.42. Inclinometer data for top 8%lime+0.15%fibers Section at Grapevine Dam

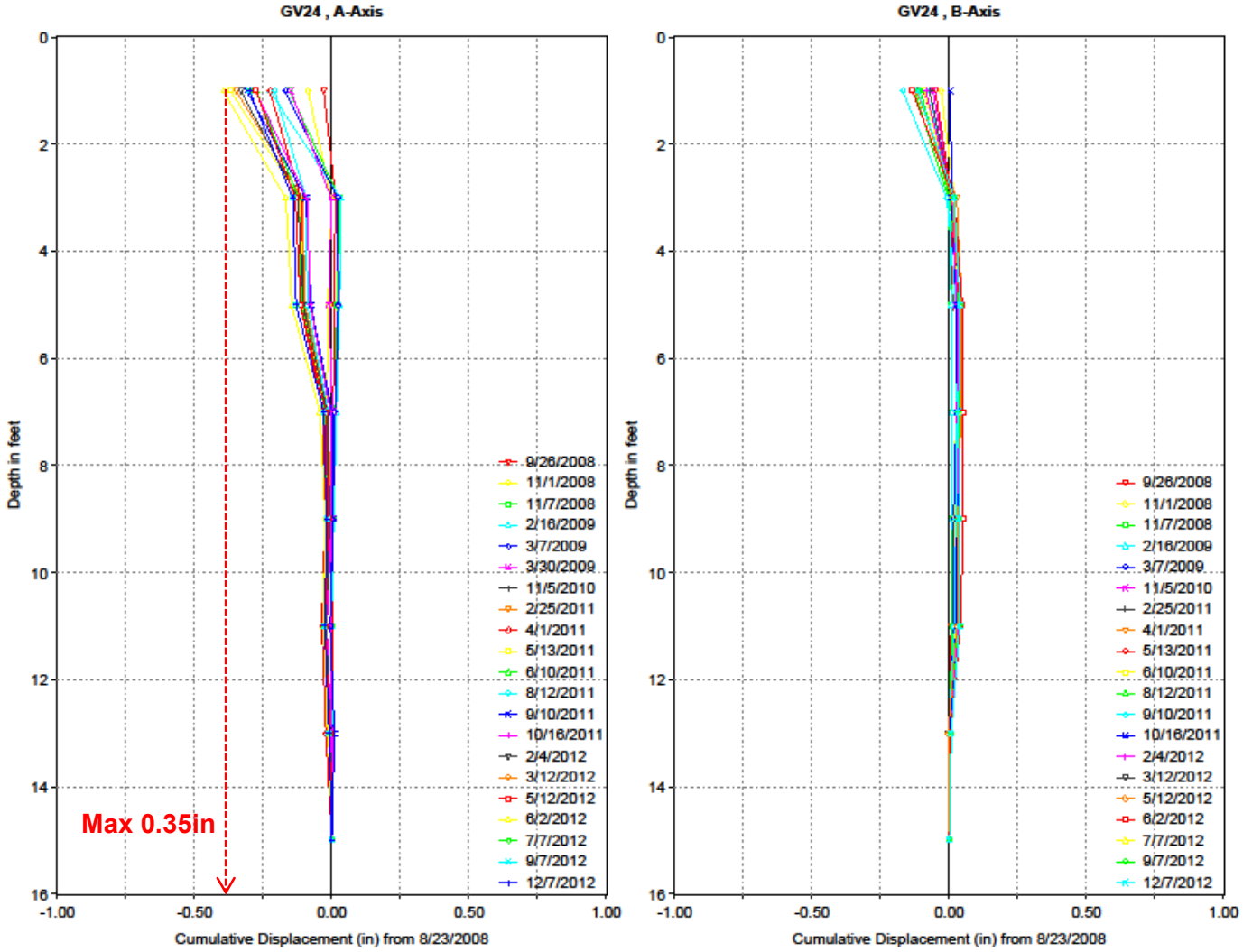

Figure 4.43. Inclinometer data for bottom 8%lime+0.15%fibers Section at Grapevine Dam

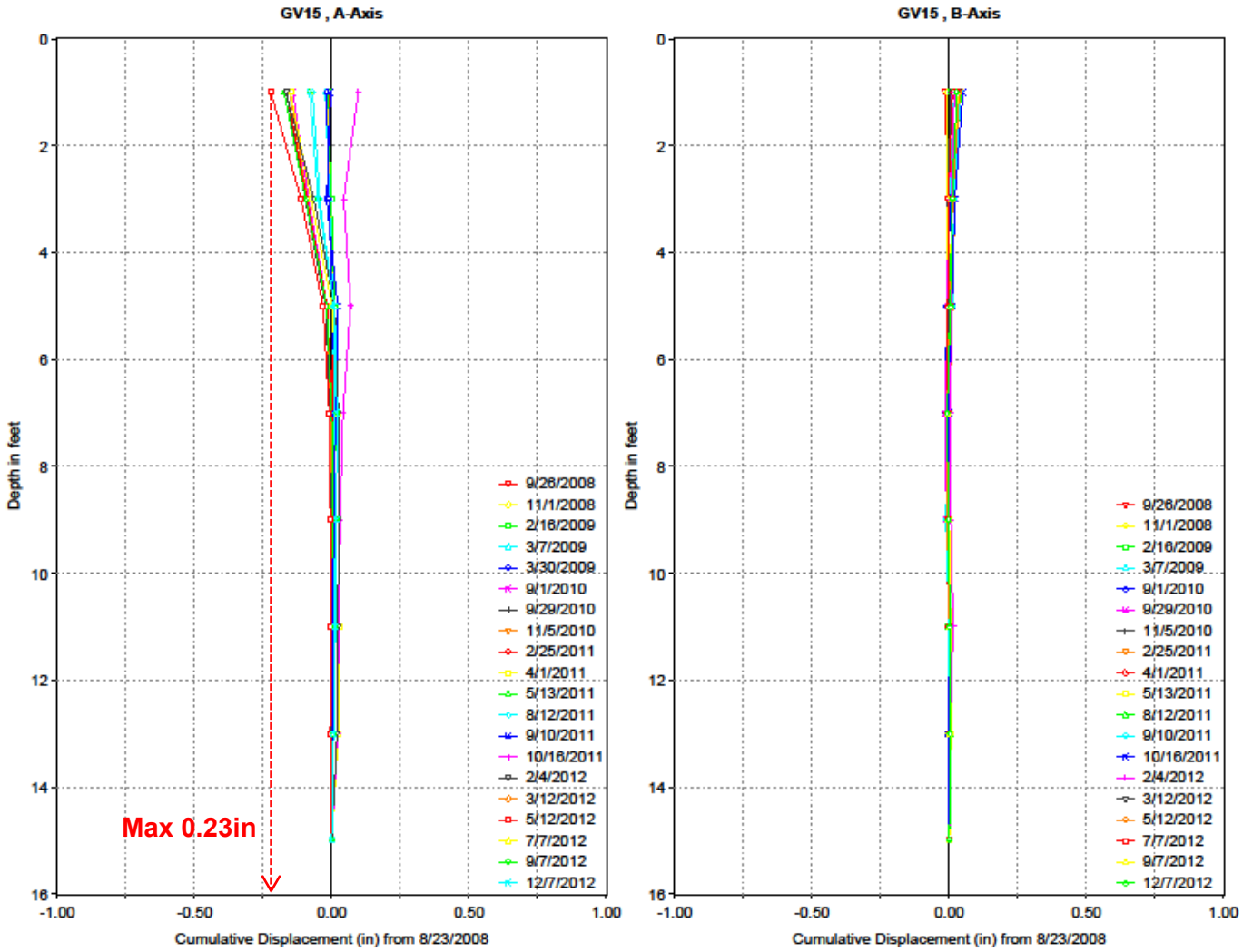

Figure 4.44. Inclinometer data for top 8%lime Section at Grapevine Dam

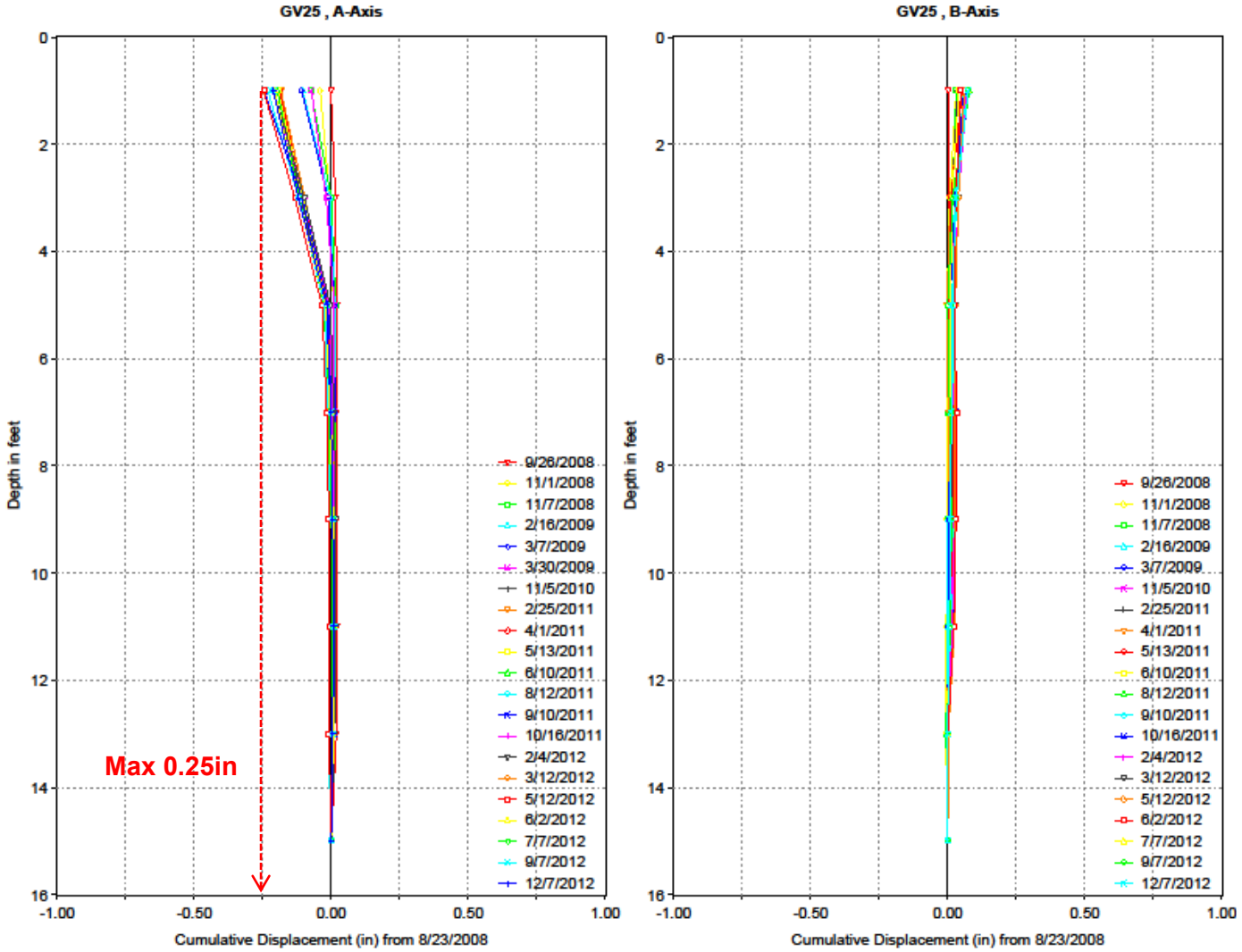

Figure 4.45. Inclinometer data for bottom 8%lime Section at Grapevine Dam

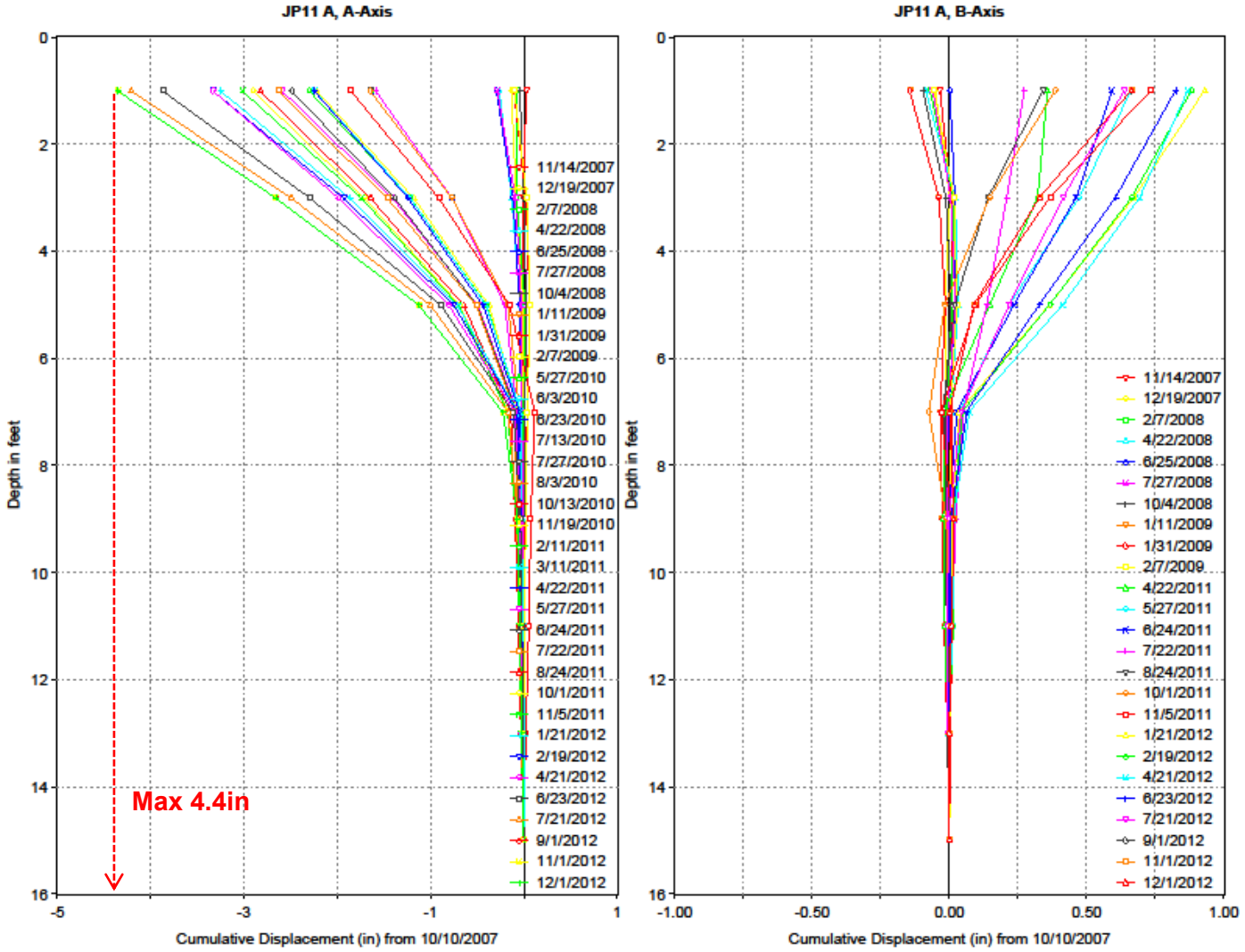

Figure 4.46. Inclinometer data for top Control Section at Joe Pool Dam

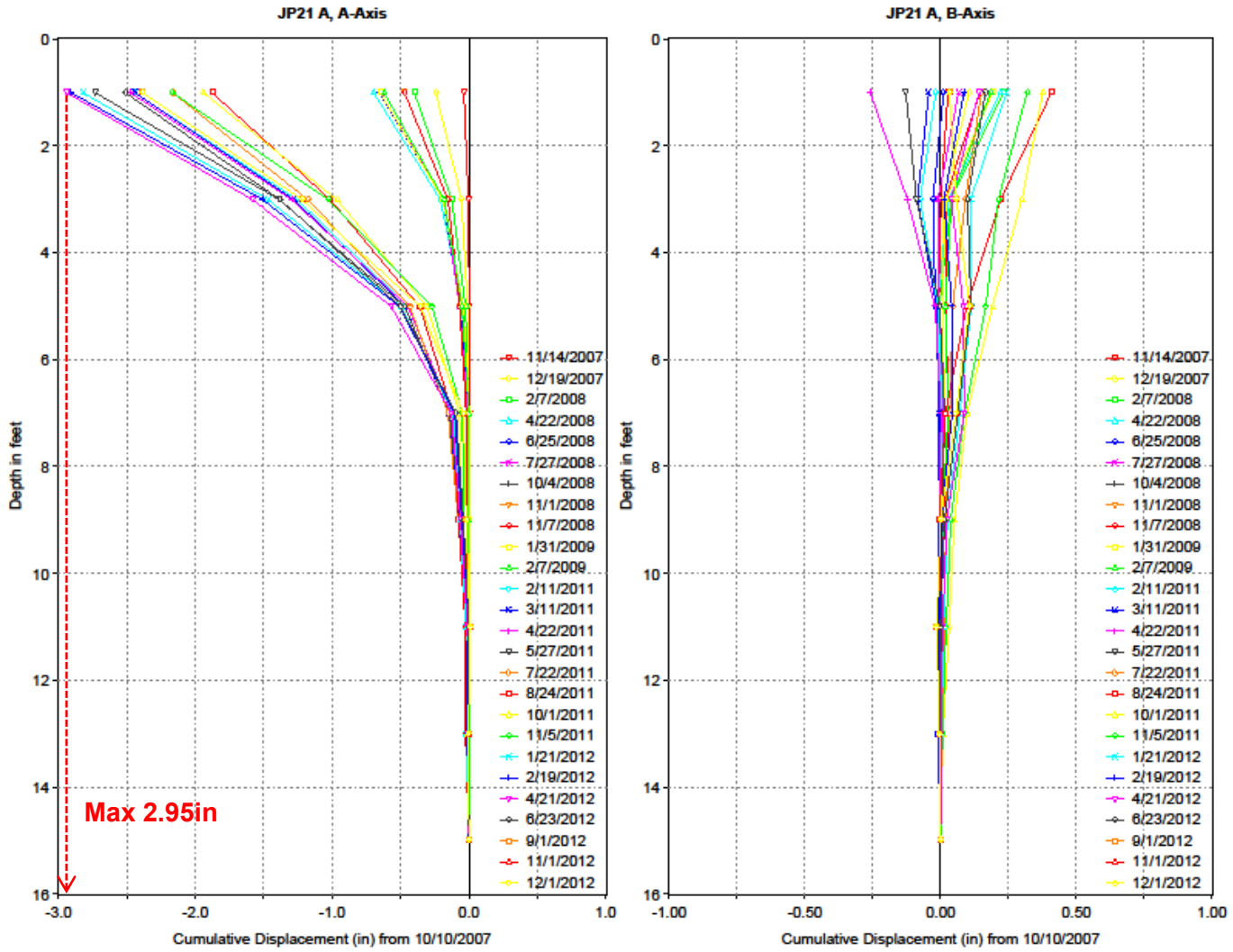

Figure 4.47. Inclinometer data for bottom Control Section at Joe Pool Dam

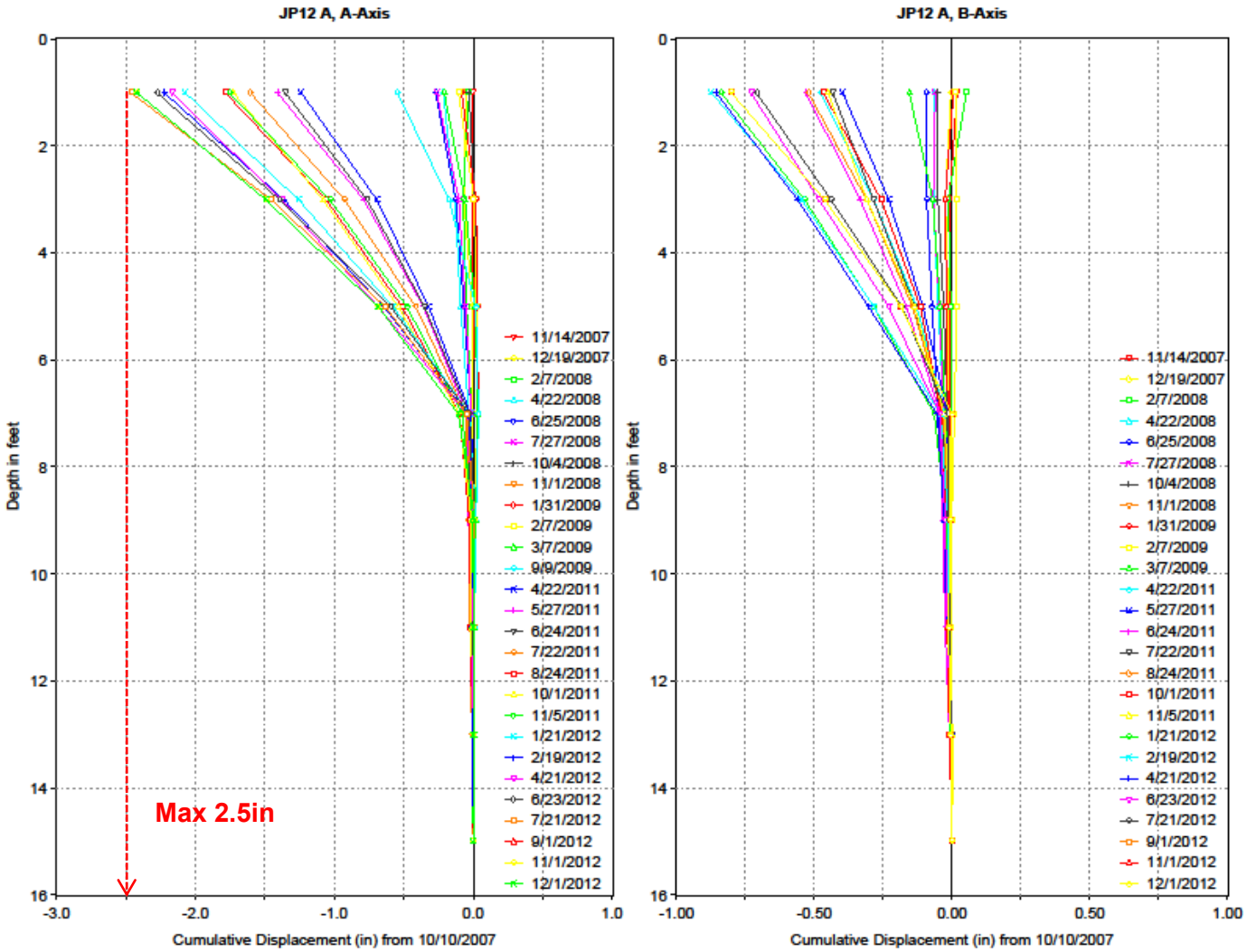

Figure 4.48. Inclinometer data for top 20%compost Section at Joe Pool Dam

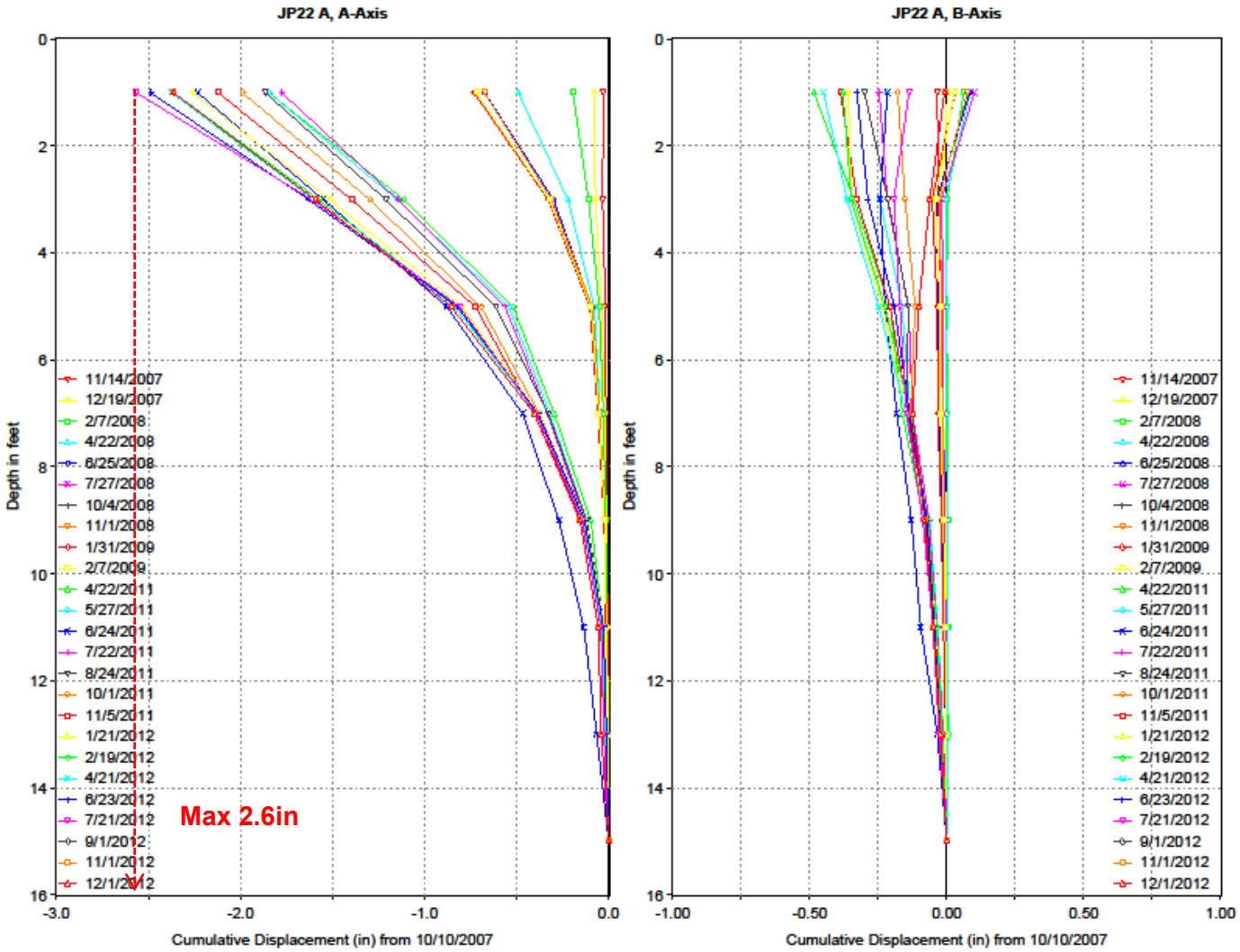

Figure 4.49. Inclinometer data for bottom 20%compost Section at Joe Pool Dam

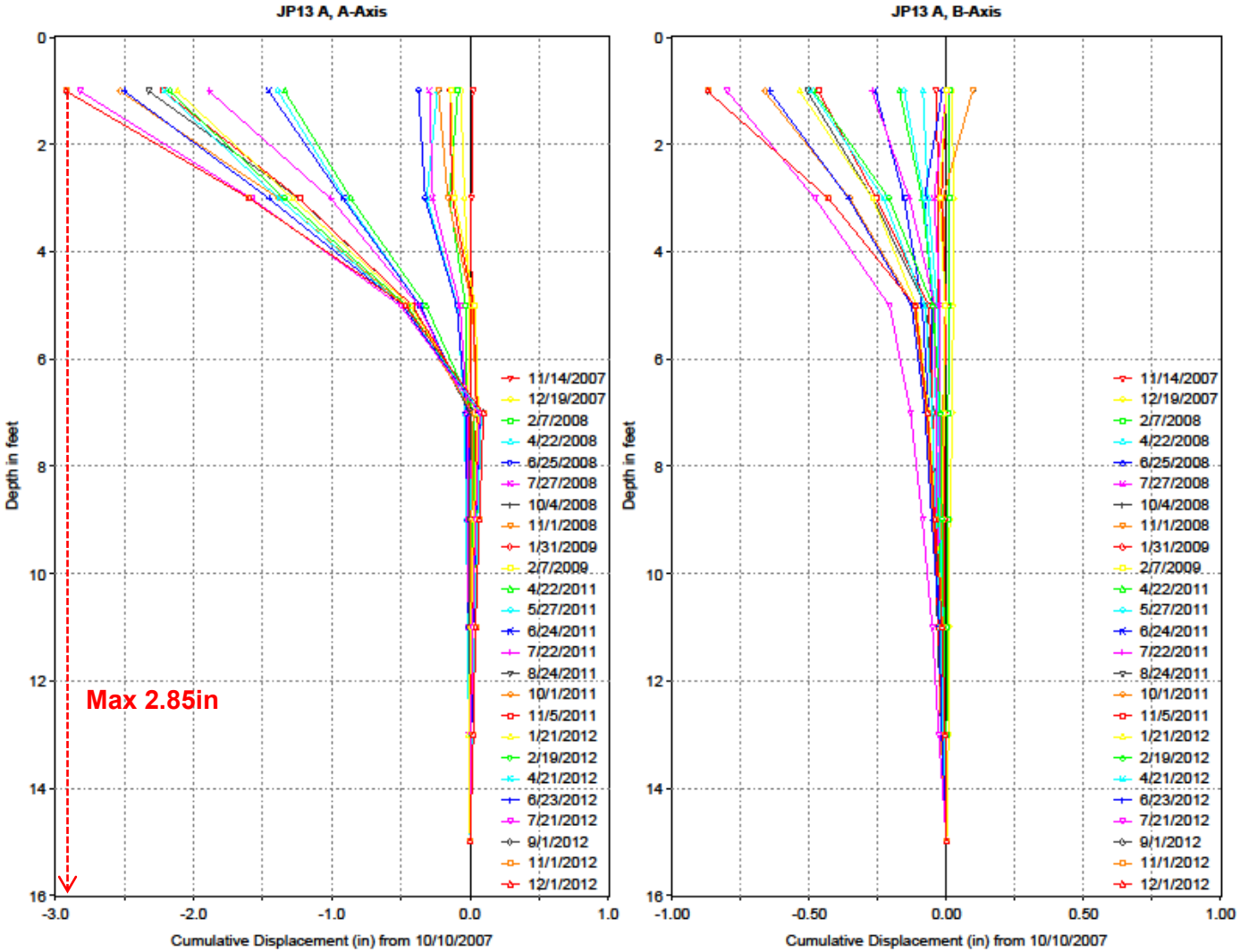

Figure 4.50. Inclinometer data for top 4%lime+0.30%fibers Section at Joe Pool Dam

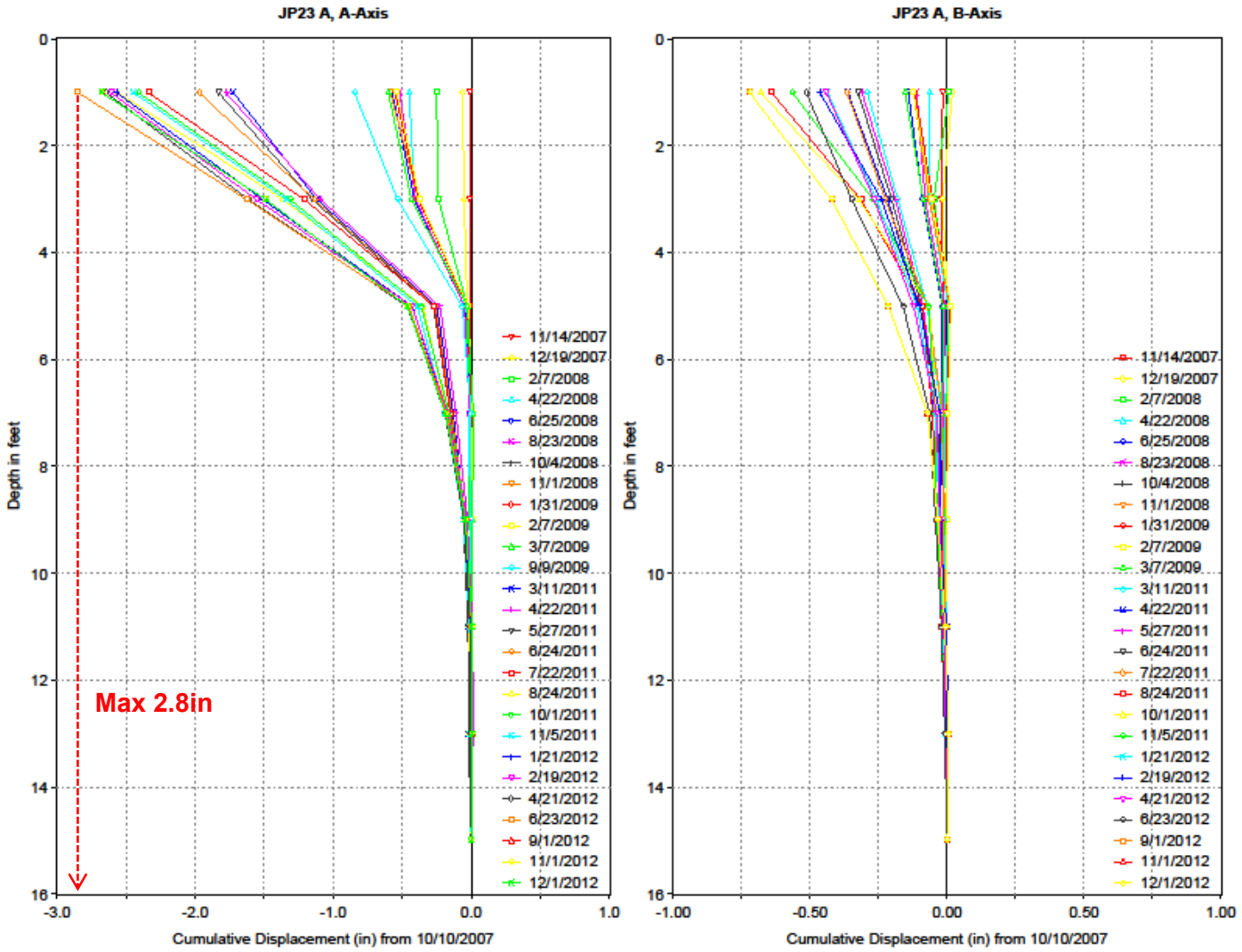

Figure 4.51. Inclinometer data for bottom 4%lime+0.30%fibers Section at Joe Pool Dam

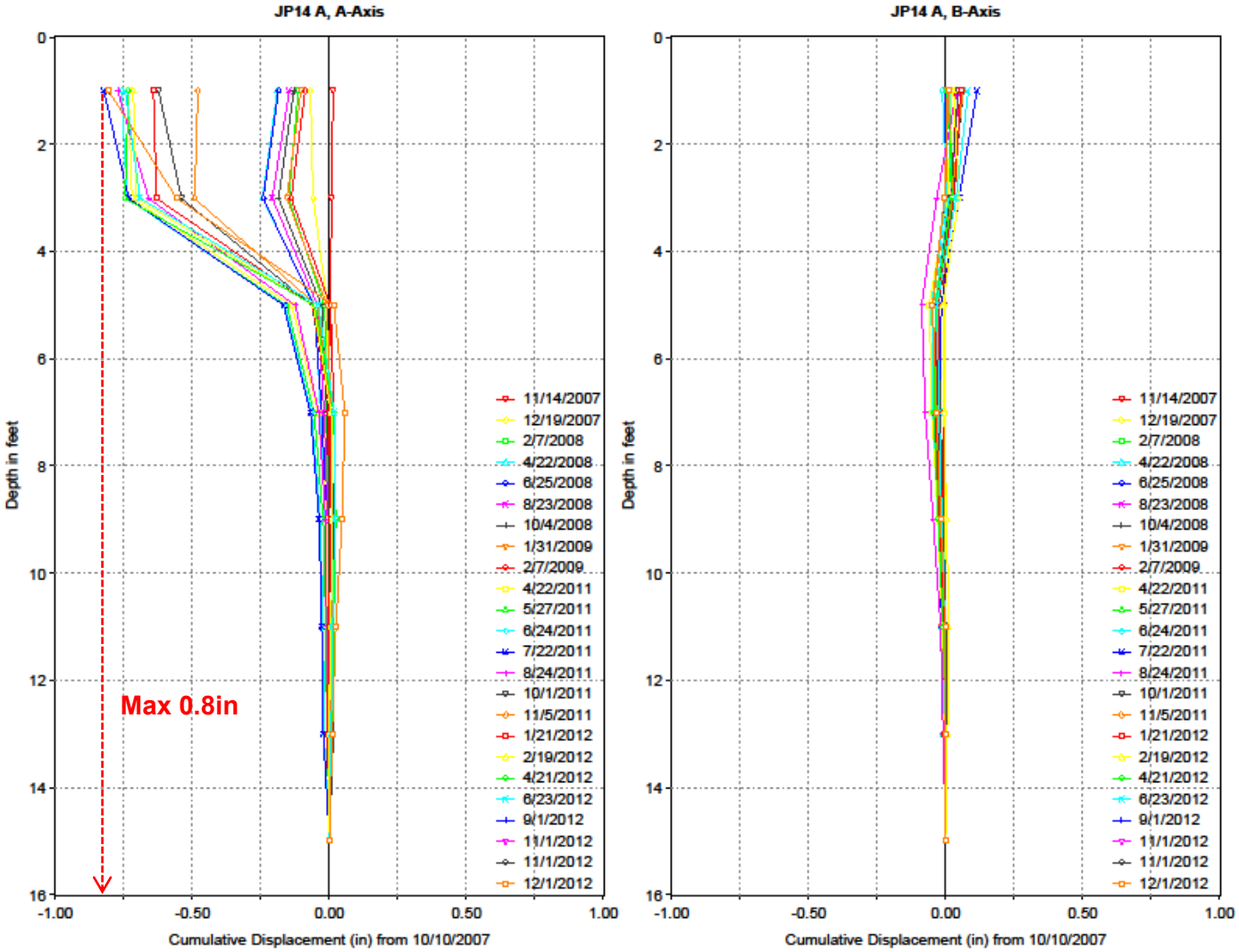

Figure 4.52. Inclinometer data for top 8%lime+0.15%fibers Section at Joe Pool Dam

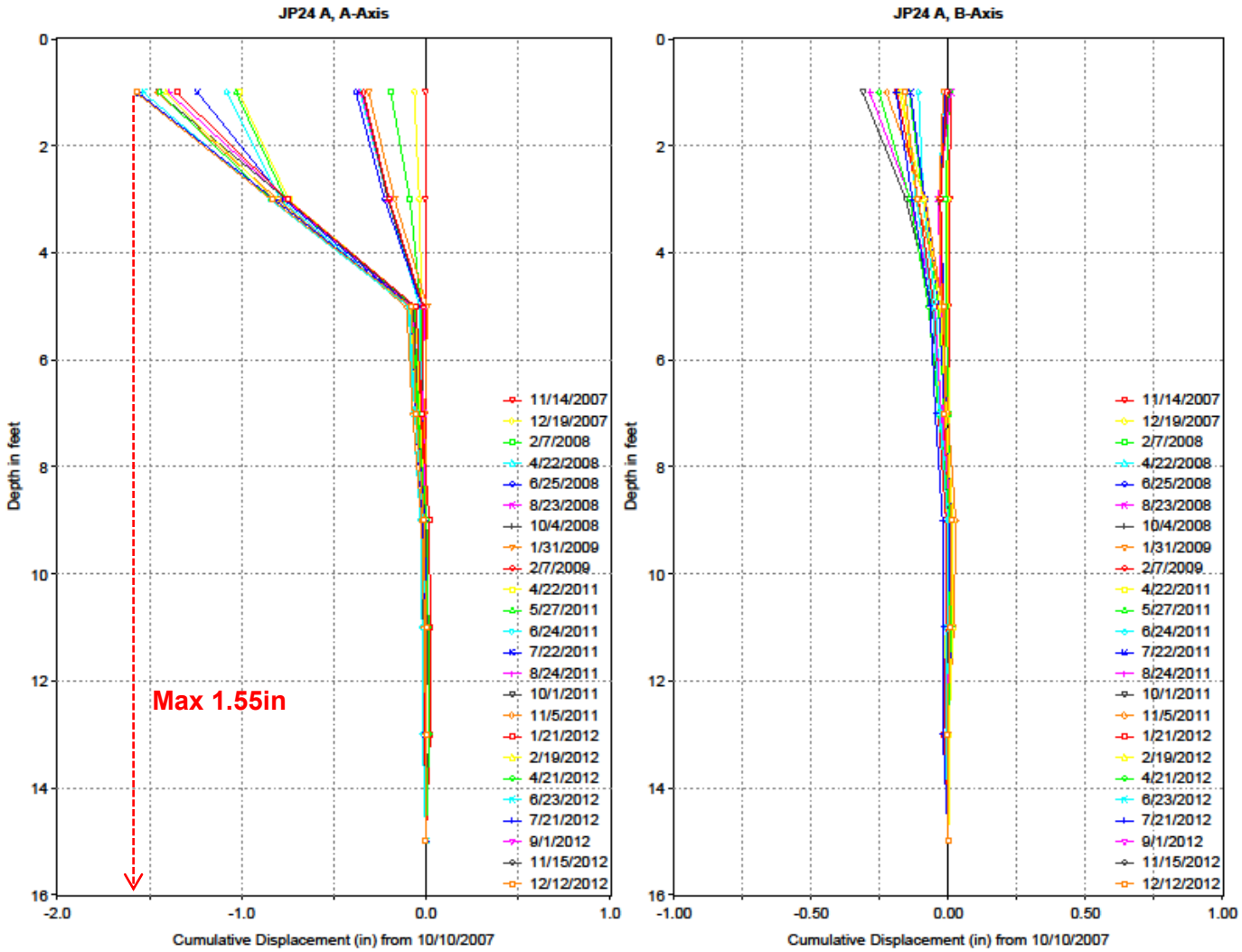

Figure 4.53. Inclinometer data for bottom 8%lime+0.15%fibers Section at Joe Pool Dam

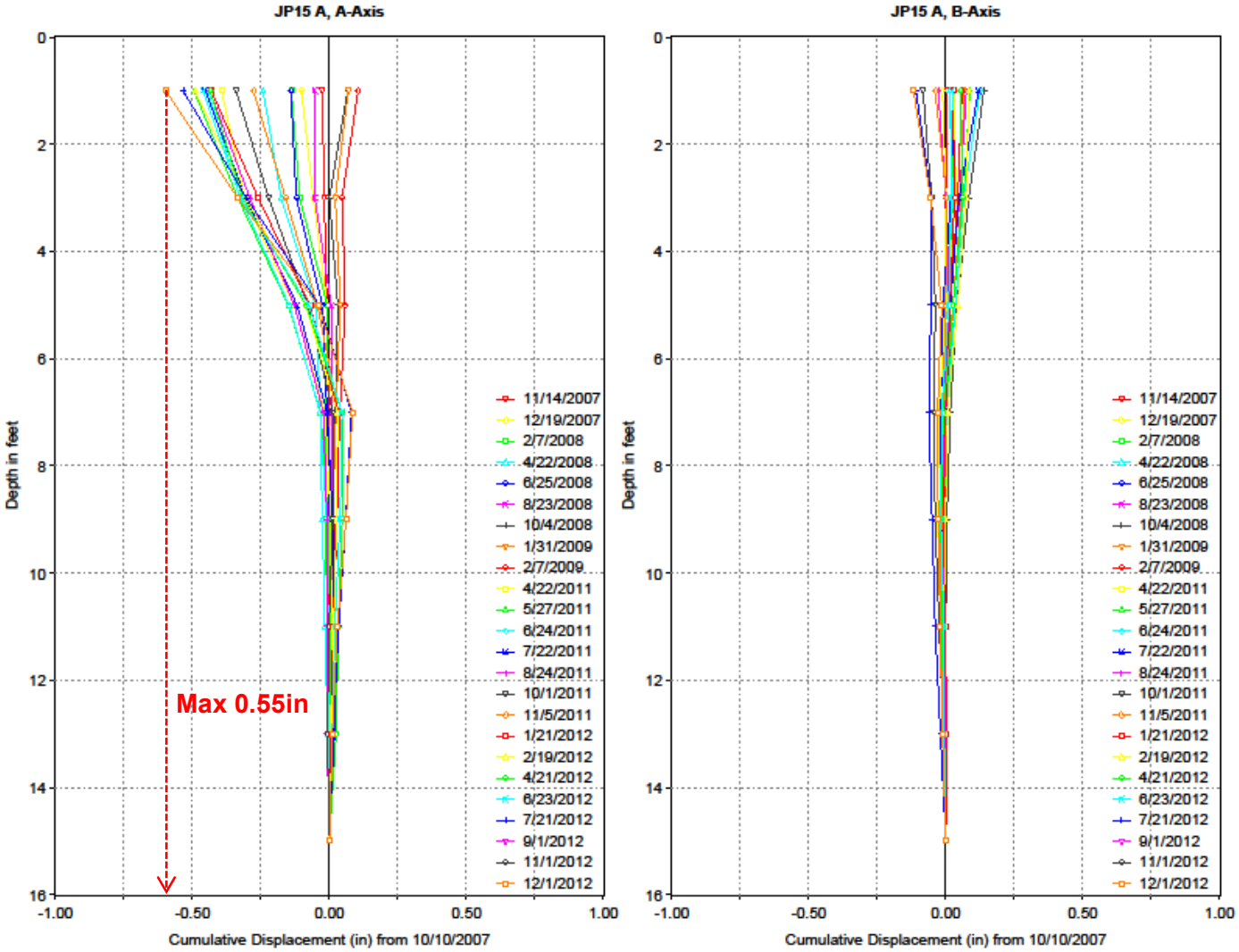

Figure 4.54. Inclinometer data for top 8%lime Section at Joe Pool Dam

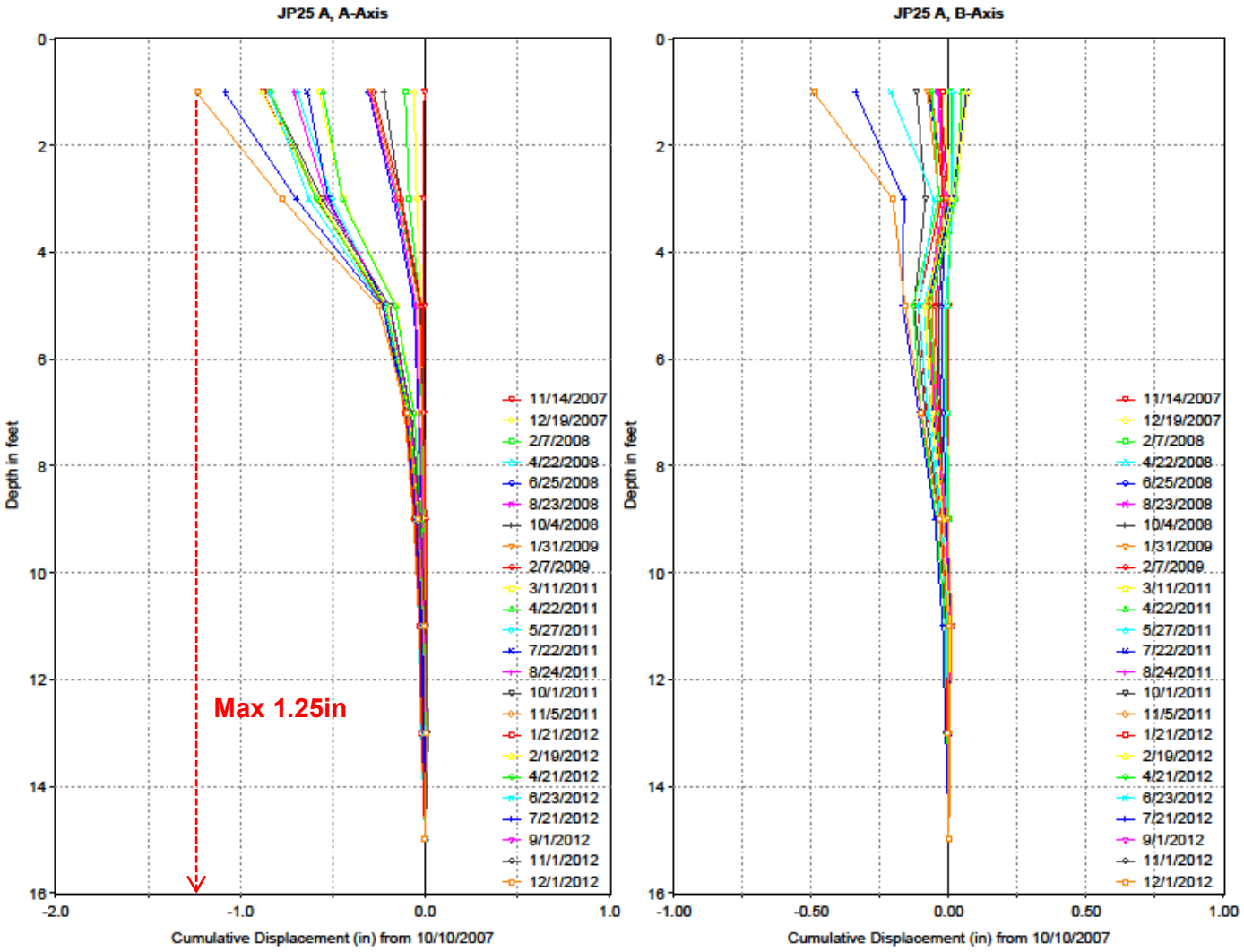

Figure 4.55. Inclinometer data for bottom 8%lime Section at Joe Pool Dam

Table 4.5. Maximum lateral movement (in) at Grapevine Dam

Probe	Control	20% compost	4%lime+0.30%fibers	8%lime+0.15%fibers	8%lime
Top	0.8	0.95	0.35	0.3	0.23
Bottom	1.3	1.2	0.4	0.35	0.25

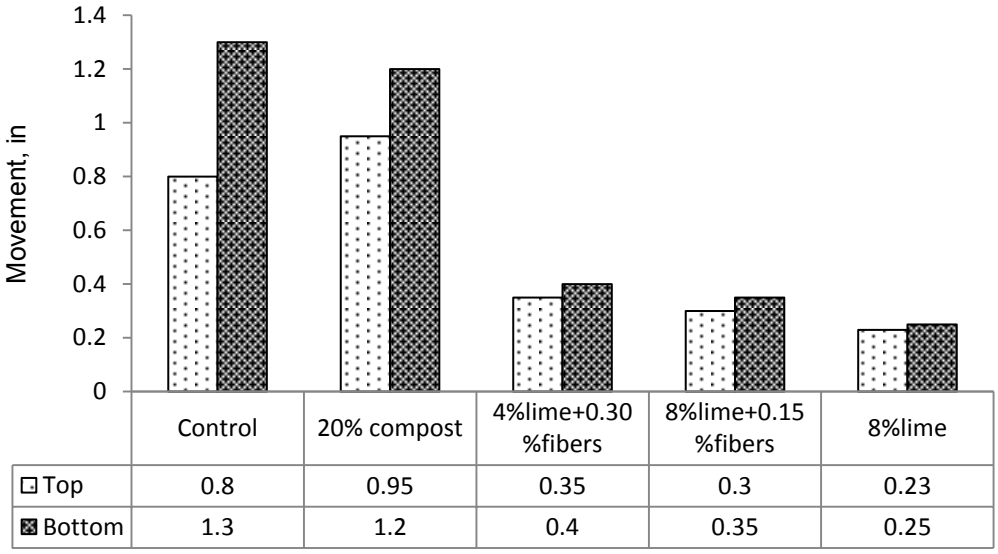

Figure 4.56. Comparison between movements of different test sections at Grapevine Dam

Table 4.6. Maximum lateral movement (in) at Joe Pool Dam

Probe	Control	20% compost	4%lime+0.30%fibers	8%lime+0.15%fibers	8%lime
Top	4.4	2.5	2.85	0.8	0.55
Bottom	2.95	2.6	2.8	1.55	1.25

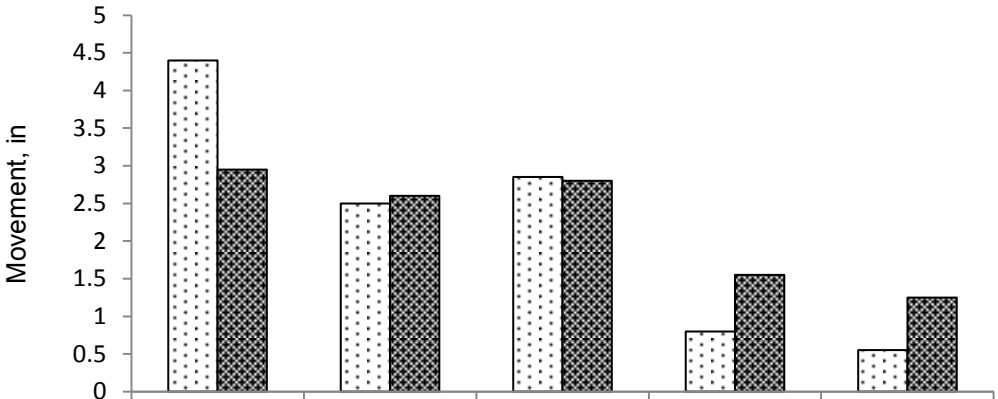

	Control	20% compost	4%lime+0.30 %fibers	8%lime+0.15 %fibers	8%lime
Top	4.4	2.5	2.85	0.8	0.55
Bottom	2.95	2.6	2.8	1.55	1.25

Figure 4.57. Comparison between movements of different test sections at Joe Pool Dam

It can be seen that the lateral displacements of soil monitored in the bottom row of inclinometers are higher than the top row in all cases (except for control soil at the Joe Pool dam site). Also, the displacement in the slope direction A-axis was more significant than the displacement in the cross slope direction B-axis

In most cases the displacement was heading downwards and more prominent from the slope surface to the depths of 3-4 ft. from the surface. From the depths of 7-8 ft. and deeper the movement was considerably negligible.

Among all sections, the control soil continued to show the lack of resistance against shrinking and swelling phenomenon, resulting in the maximum movement compared to other treated sections at both Joe Pool Dam and Grapevine Dam. 20% compost and 4%lime+0.30%fibers treated sections started displaying their inconsistencies in long term performance. 4%lime+0.30%fibers performed well on Grapevine Dam soil but not successfully at Joe Pool Dam soil (with the lateral movement at the bottom row almost as high as in control section). 8%lime+0.15%fibers and 8%lime treated sections showed the best performance with the least amount of lateral slope movement during the monitoring period.

4.3.4 Elevation Surveys

Elevation surveys were conducted on the test sections during every field visit. Steel flags were inserted on the slope with the density of 9 in. each test section, making it a total of 45 flags on each Joe Pool and Grapevine dam site. Elevation pegs were fixed so that the observations were to be taken at the same point every time to observe the pattern of vertical slope movement patterns.

The total station instrument was always positioned in the middle of the entire length in front of the test sections and on a firm concrete pedestal to yield the highest accuracy. Apart from the fixed station points, benchmark points were set up on the crest of the dam on the bitumen paved surface. The readings of the total stations were used to calculate the movement of each point on the treated sections.

Figure 4.58 shows the schematic positioning elevation pegs and total station in the field.

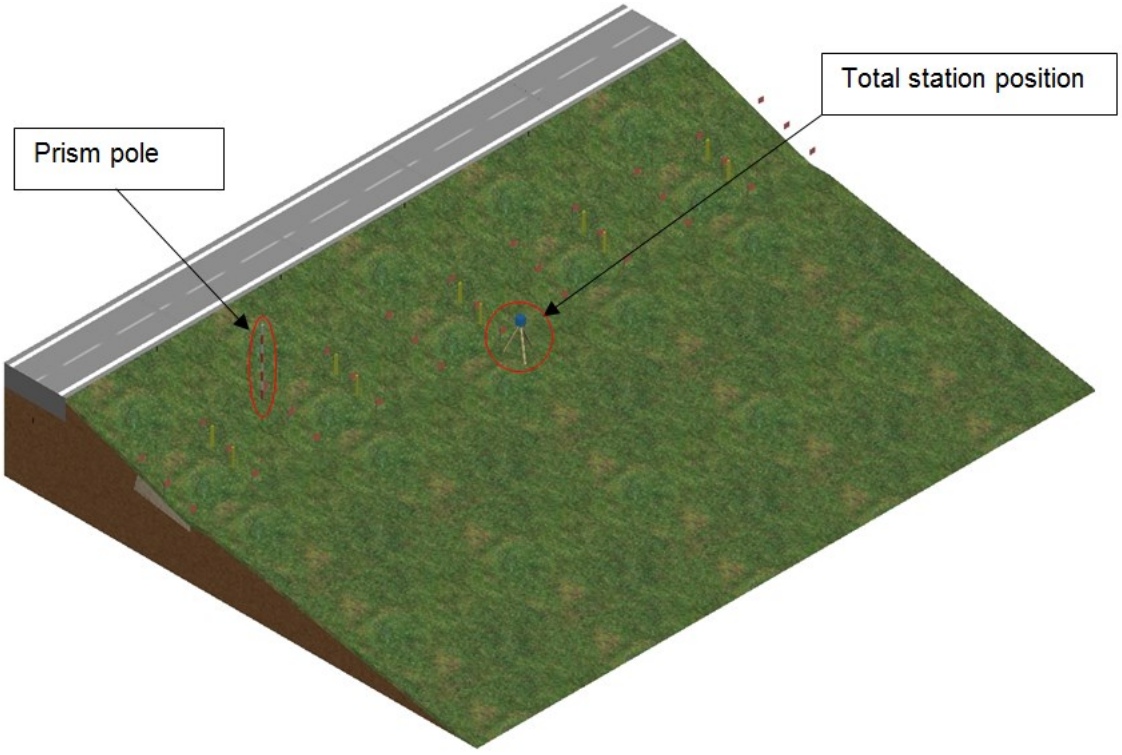

Figure 4.58. Total station position in the field for elevation surveys

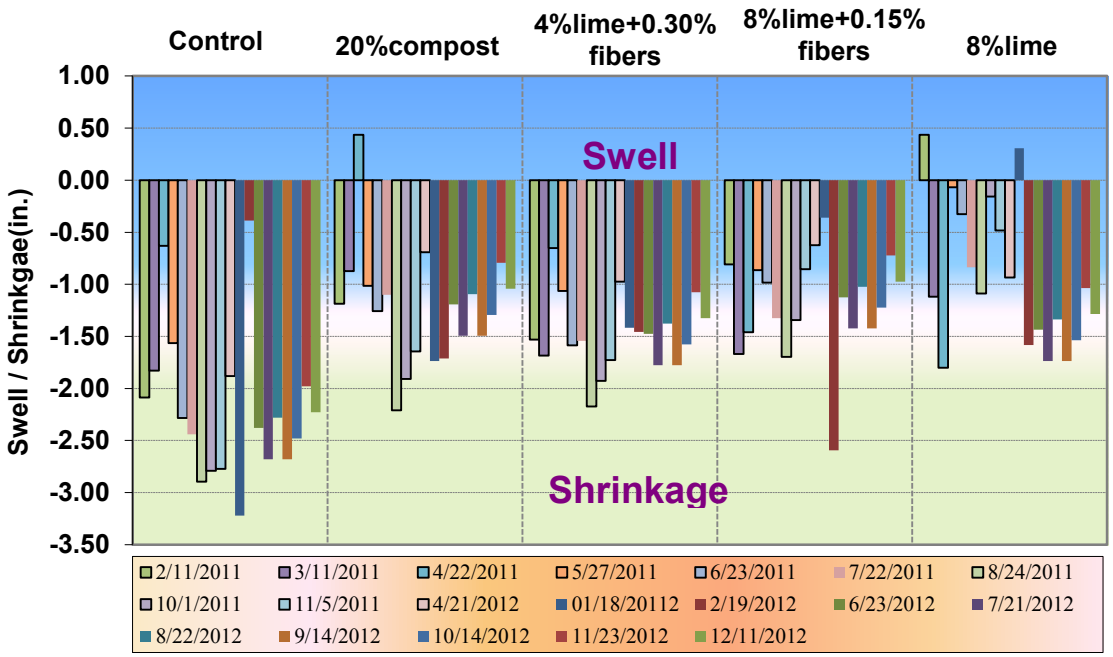

Figure 4.59. Elevation survey for slope movement at Joe Pool Dam

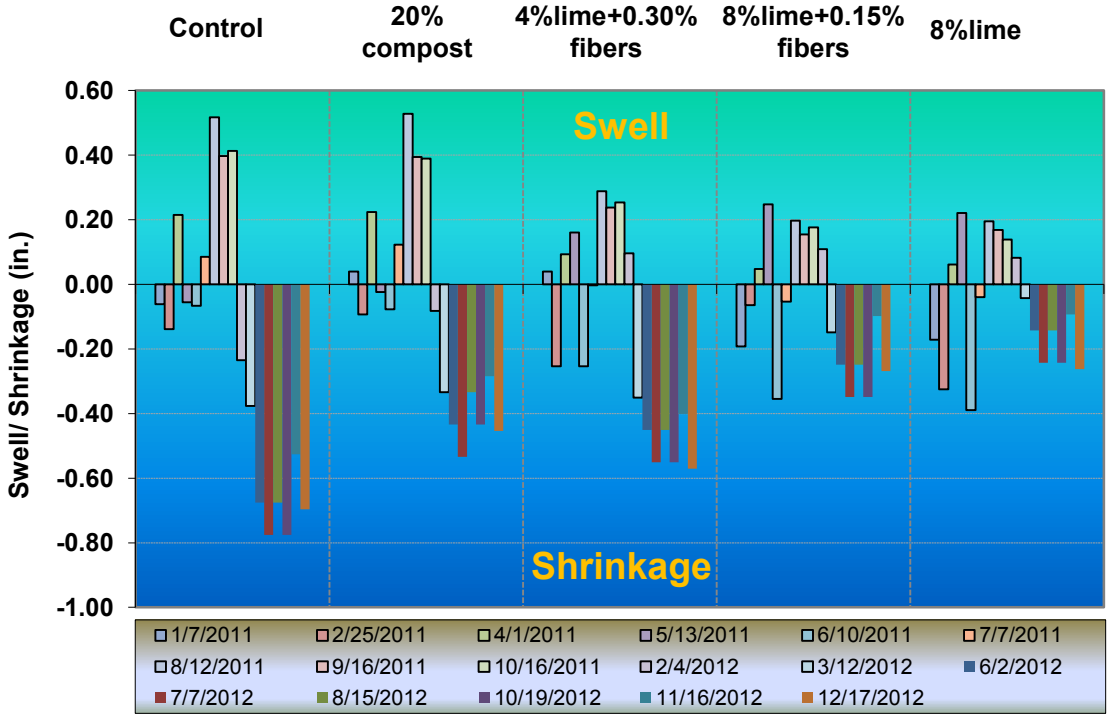

Figure 4.60. Elevation survey for slope movement at Grapevine Dam

It may be inferred from the above graphs that the shrinkage tendency of the soil from both sites exceeded swelling, specifically at Joe Pool Dam site. The control section continued to exhibit the highest movement in comparison with other treated sections.

Compared to the previous observation of Dronamraju (2008), the 20%compost and 4% lime+0.30%fibers treated sections started to show the inconsistent performance. At the Grapevine Dam site, 4%lime+0.30%fibers section exhibited second highest shrinkage magnitude among all other treatments while it still performed reasonably well at the Joe Pool Dam site. Overall, both 8%lime+0.15%fibers and 8%lime treated sections still continued to perform the best with the lowest vertical deformations recorded on both Joe Pool and Grapevine sites.

4.3.5 Vegetation Growth

Due to the streak of continuous hot days from June to August (above 100 degrees F) in North Texas, vegetation on each dam was exposed to excessive amount of heat from sunlight during this time period. This resulted in the change of grass color, as shown in Figures 4.61 to 4.63. Vegetation in the first two sections (Control and compost-treated) still had good nutrition to maintain green color, while grass in the other sections was dying out. This showed the visible benefit of using compost as a treatment as it helps the growth of vegetation during hot weather. And, since the vegetation also plays a role in absorbing excessive rainfall water and strengthening the soil with its roots, this may pay off for the downside of compost decomposing with time.

Figure 4.61. Vegetation on control and compost treated section (JoePool Dam)

Figure 4.62. Vegetation on 4%lime + 0.3%fiber, 8%lime + 0.15%fiber and 8%fiber sections (Joe Pool Dam)

Figure 4.63. Vegetation distribution on different sections (Joe Pool's dam Aug 24, 2011)

4.3.6 Surfical Crackings Observations

Surficial cracks were observed on the majority of the control and compost sections during the driest months of summer 2011. While soil on the control section was not treated to increase strength, the compost decomposing characteristic attributed to the loss of its ability to reduce shrinkage cracks. On the other hand, little or no cracks were found on the remaining 3 sections (lime and lime- fibers treated) as the combined chemical and mechanical effects from lime and fibers helped the soil to increase in strength, stiffness, durability and reduce swell/shrinkage potential.

On the control section of Grapevine Dam, a 4 ft. long crack along with a few other cracks was noticed in the middle of the section and also near the top inclinometer casing in summer 2011. The compost section had fewer cracks on the surface but had severe cracks along the construction joint on the top side. Figure 4.64-Figure 4.68 show cracks appearing at Grapevine Dam during summer time of 2011.

At Joe Pool dam site, a 24 ft. long crack appeared on the control section near the bottom inclinometer casing. This had huge potential of failure. Another noticeable 2.3 ft. long crack was found on the compost section. A schematic view of Joe Pool's dam with the 24 ft. long crack is shown in Figure 4.70 and Figure 4.71.

Figure 4.64. Surficial crack 4 ft. length on control section (Grapevine Dam August 12, 2011)

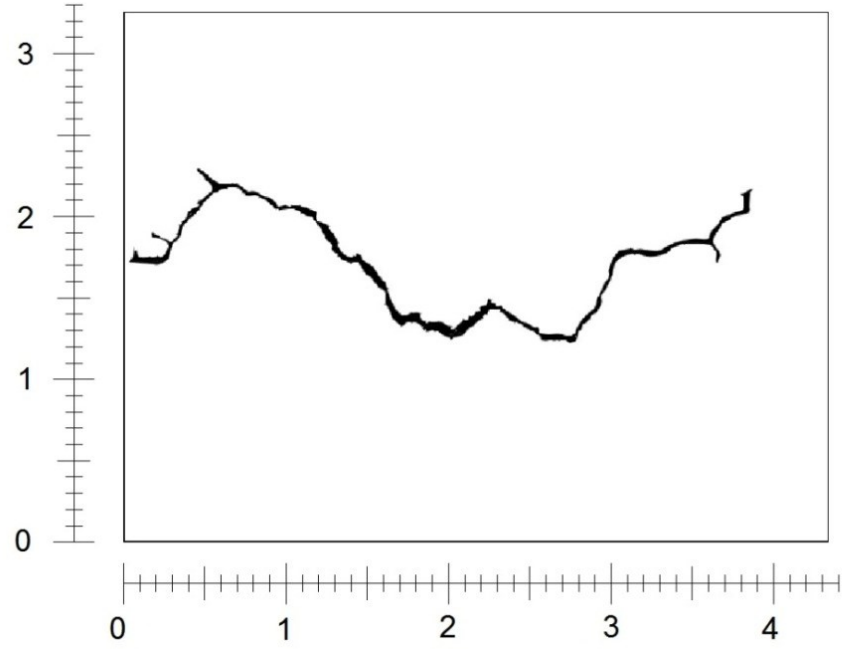

Figure 4.65. Threshold image on control section (Grapevine Dam August 12, 2011)

Figure 4.66. Surficial crack 10.5 in depth on control section (Grapevine Dam August 12, 2011)

Figure 4.67. Surficial crack 2.3 ft. length on compost treated section (Grapevine Dam August 12, 2011)

Figure 4.68. Surficial crack 4in depth on compost section (Grapevine Dam August 12, 2011)

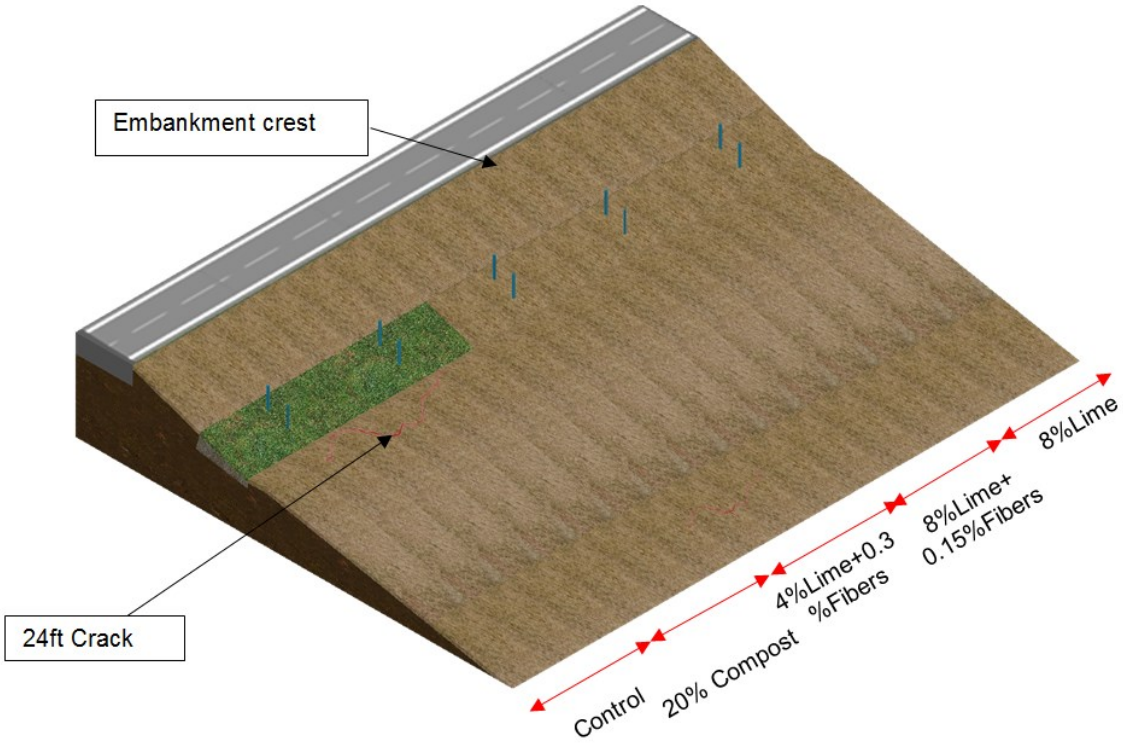

Figure 4.69. Position of major cracks on Joe Pool's dam

Figure 4.70. 24ft. crack at Joe Pool Dam

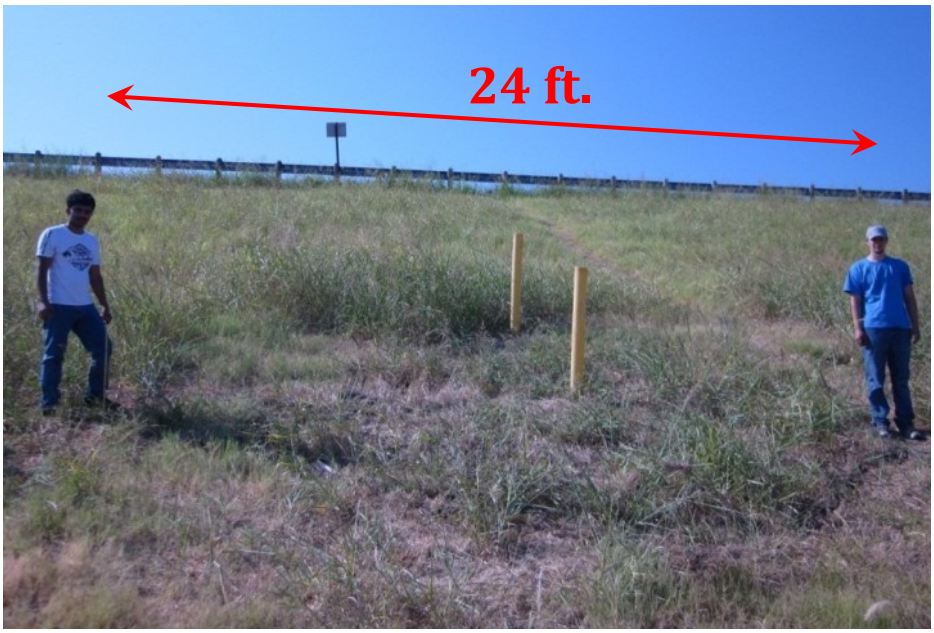

Figure 4.71. 24 ft. long crack at Joe Pool Dam

4.4 Ranking Summary

The performance of the test sections at Grapevine Dam and Joe Pool Dam has been evaluated based on field performance aspects including: soil moisture content, lateral movement, vertical movement, vegetation growth and surficial cracks. The ranking of each test

section based on those considered factors is shown in Table 4.7 and Table 4.8 . Points were allotted from 1 to 5, with 1 being for the best performance and 5 for the worst. With respect to all aspects, every single category was equally weighed and the total summary reflected the overall performance of all the sections.

Table 4.7. Initial ranking of field performance for Joe Pool Dam soils

Soil	Soil Moisture	Lateral movement	Vertical Movement	Vegetation Growth	Surficial Cracks	Total
Control soil	5	5	5	2	5	22
20%compost treated soil	2	3	3	1	4	13
4%lime+0.30%fibers treated soil	4	4	4	3	3	18
8%lime+0.15%fibers treated soil	1	2	1	5	1	10
8%lime treated soil	3	1	2	4	2	12

Table 4.8. Initial ranking of field performance for Joe Pool Dam soils

Soil	Soil Moisture	Lateral movement	Vertical Movement	Vegetation Growth	Surficial Cracks	Total
Control soil	5	5	5	2	5	22
20%compost treated soil	4	4	3	1	4	16
4%lime+0.30%fibers treated soil	3	3	4	3	3	16
8%lime+0.15%fibers treated soil	2	2	2	5	1	12
8%lime treated soil	1	1	1	4	2	9

From the ranking of test sections shown in the tables above, the combined lime and fibers treatment namely 8%lime+0.15%fibers method was proven to be the best treatment method on Joe Pool Dam site soils and 8%lime was the best treatment for Grapevine dam site soils. 4%lime+0.30%fibers and 20%compost treatments were ranked 3 and 4 over the control untreated soil.

4.5 Summary

Field data was collected and processed to analyze the performance of treated sections with respect to control sections at both Joe Pool Dam and Grapevine Dam. The performance was studied based on the soil moisture, elevation surveys, inclinometer surveys, desiccation cracking and vegetation growth. The performance ranking between all sections was presented including all the aforementioned aspects, to give a better judgment. The result showed the dominance in almost all categories of 8%lime+0.15%fibers and 8%lime treated sections among other admixtures.

CHAPTER 5

FULLY SOFTENED SHEAR STRENGTH TEST RESULTS AND ANALYSIS

A total of 120 tests were conducted to measure Fully Softened Shear Strength (FSS) property using both Direct Shear (DS) and Torsional Ring Shear (TRS) devices. All soil samples were reconstituted at the liquid limit and kept in the moisture room for at least 24 hours to achieve the uniform hydration condition. Soil samples treated with lime remained in the master room for at least 7 days curing period before being subject to testing.

Soil specimens were carefully placed in the shear mold and tapped to eliminate trapped air bubbles. The consolidation process followed by ramping loads starting from 12.5 kPa (261 psf) with a load increment ratio of 1, which means no more than the amount of existing load was added in the next loading step. This was done to reduce soil bleeding. Primary consolidation completion was checked before each loading step by observing the consolidation reading. Shearing rate was maintained at a slow pace of 0.002 in/min to ensure that the drained condition of soil prevailed during shearing. Readings were recorded automatically in the DS machine and manually in the TRS testing machine.

Due to the number of DS machines (two in UTA laboratory compared to one TRS), more tests were performed using the DS device. A total of 80 tests was conducted on soils from both the Joe Pool Dam and Grapevine Dam sites at different effective normal stresses (σ'_n) of 50 kPa (1044.3 psf), 100 kPa (2088.5 psf), 200 kPa (4177.1 psf) and 400 kPa (8354.2 psf) while 40 tests were conducted using the TRS test device for the same specific effective normal stresses.

Due to the sensitivity of the FSS test results, a profound statistical analysis was performed and these results were analyzed in Chapter 6. In this chapter, FSS test results are presented,

analyzed and compared to evaluate the effects of chemical stabilizers on test results. Also, the influence of testing methods on the test measurements is studied.

5.1 Joe Pool Dam Soil

5.1.1 Direct Shear Test Results

Figures 5.1 to 5.5 present the FSS test results in the form of shear stress versus horizontal displacement curves and the corresponding vertical deformation versus horizontal displacement curves for both untreated and treated soils.

The shear displacement rate was set to a constant value of 0.002 in/min (0.05 mm/min) and continued to the maximum horizontal displacement. The tests were terminated if the shear stress-horizontal displacement curve showed the plateau condition, indicating that maximum shear stress was attained. Readings were recorded by the automatic data acquisition system. For the purpose of simplicity, the author opted not to show the data points as they clustered the graphs.

Also due to the stroke length of the GeoTac DS device, the maximum shear displacement was capped at 0.5 in. (12.5 mm). Because of this limitation, testing of soil specimens with effective normal stresses (σ'_n) over 400 kPa (8354.2 psf) were difficult to perform in the present test facility. However, this is not a limitation for the present experimental research as such high effective normal stresses are not needed for characterizing the large dam embankment materials.

It is important to mention that a shear stress-horizontal strain relationship may be obtained from the FSS results by DS. However, a shear stress-horizontal strain relationship or any associated quantity, such as modulus, cannot be determined from the TRS apparatus due to the possible soil extrusion, and volume change prevents defining the height needed in the shear strain calculations (ASTM D7608-10). As a result, shear stress versus horizontal strain are not presented; rather, the shear stress–horizontal displacement relations are shown for the sake of comparison between the two testing methods.

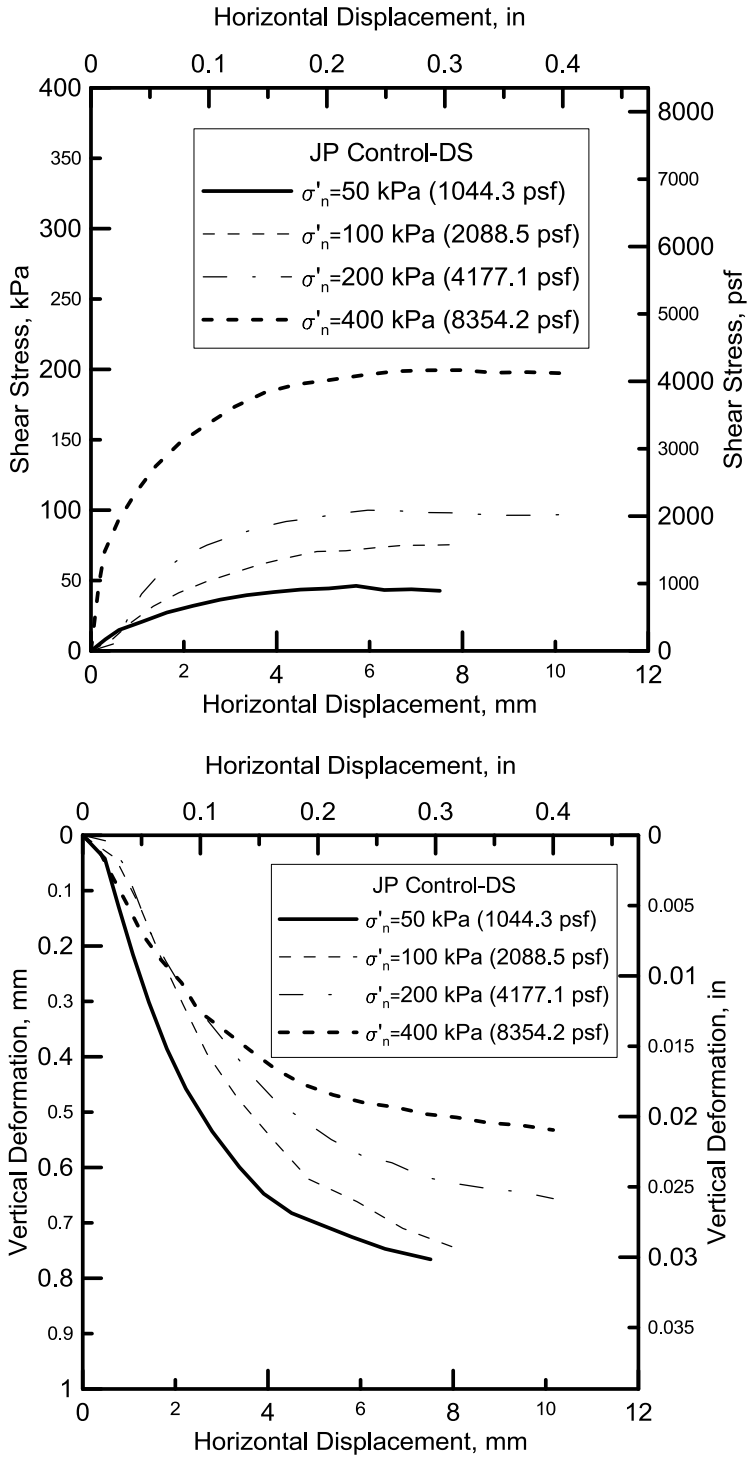

Figure 5.1 FSS results for the Joe Pool Dam Control soil

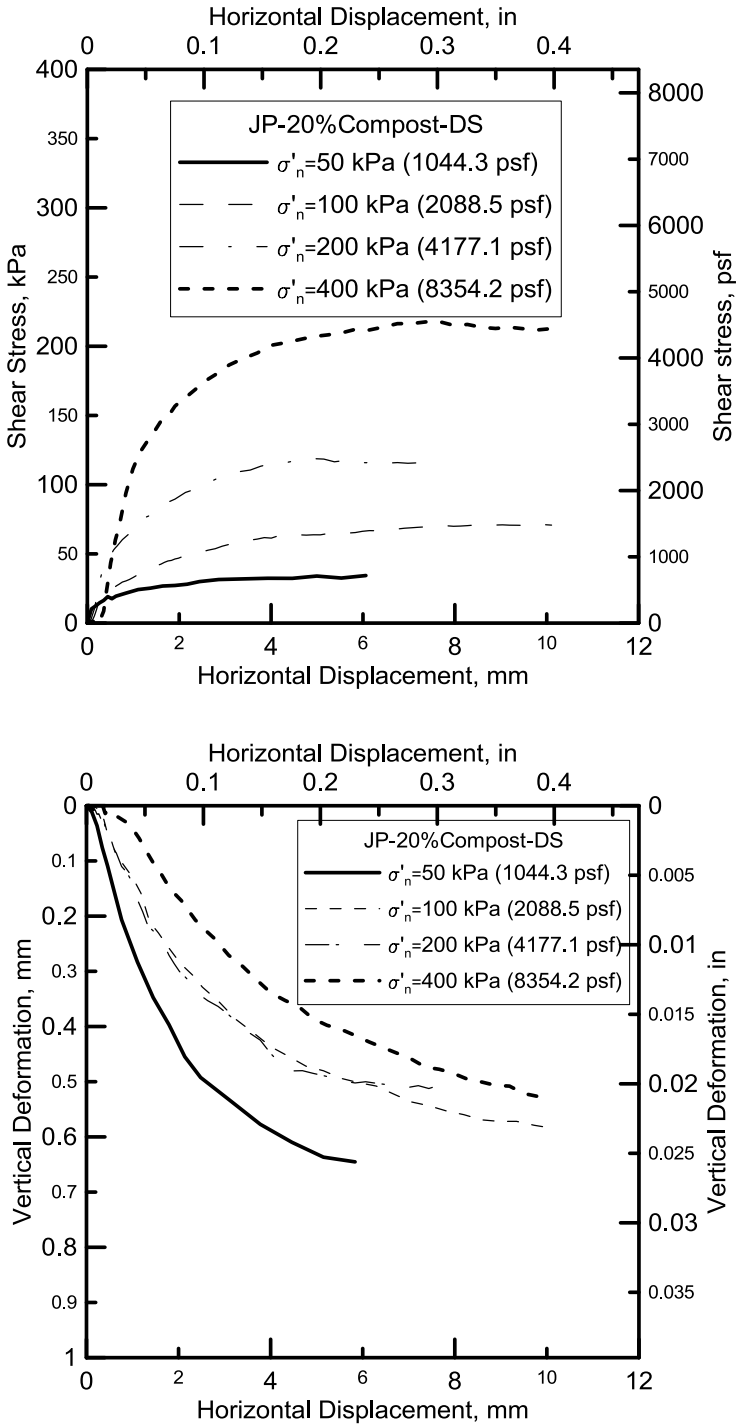

Figure 5.2. FSS results for the Joe Pool Dam 20%compost treated soil

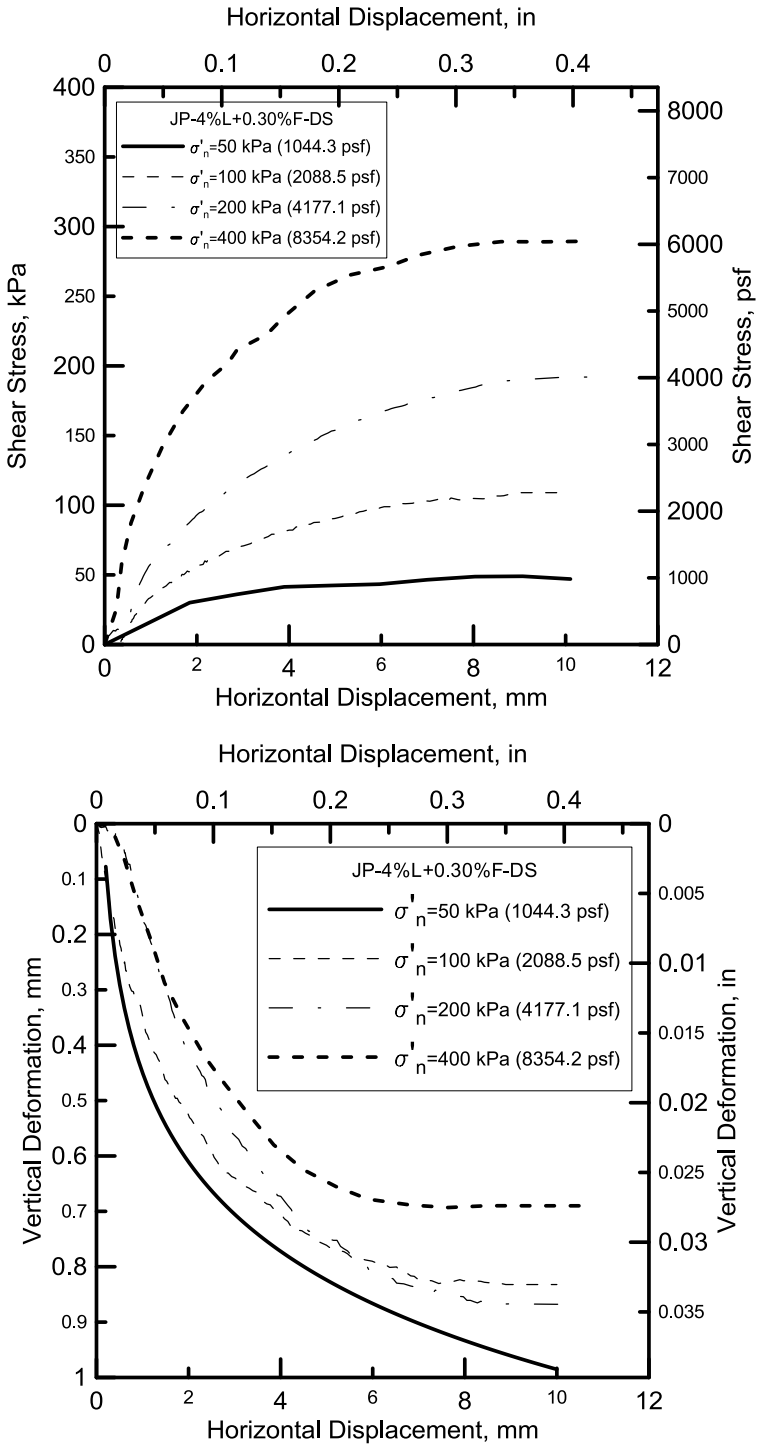

Figure 5.3. FSS results for the Joe Pool Dam 4%lime+0.30%fibers treated soil

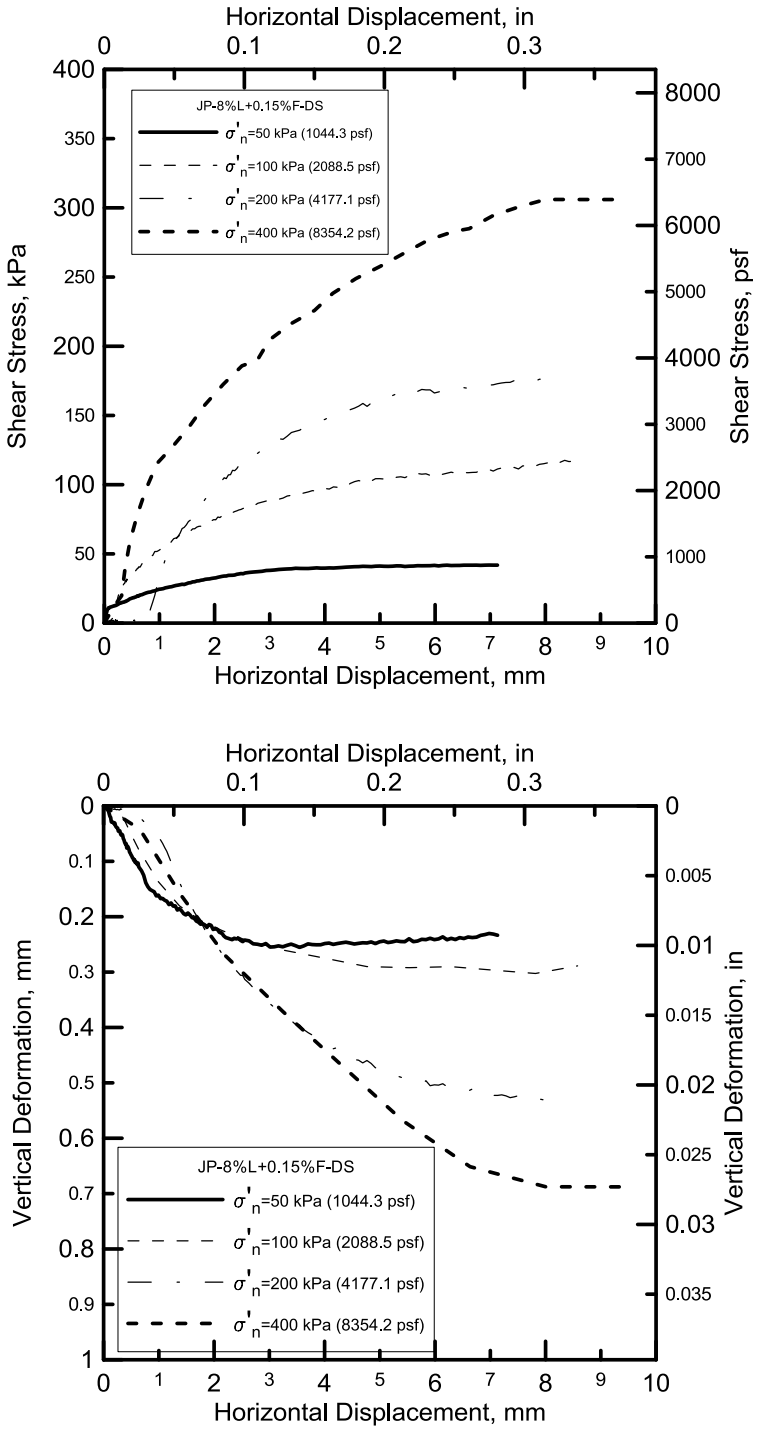

Figure 5.4. FSS results for the Joe Pool Dam 8%lime+0.15%fibers treated soil

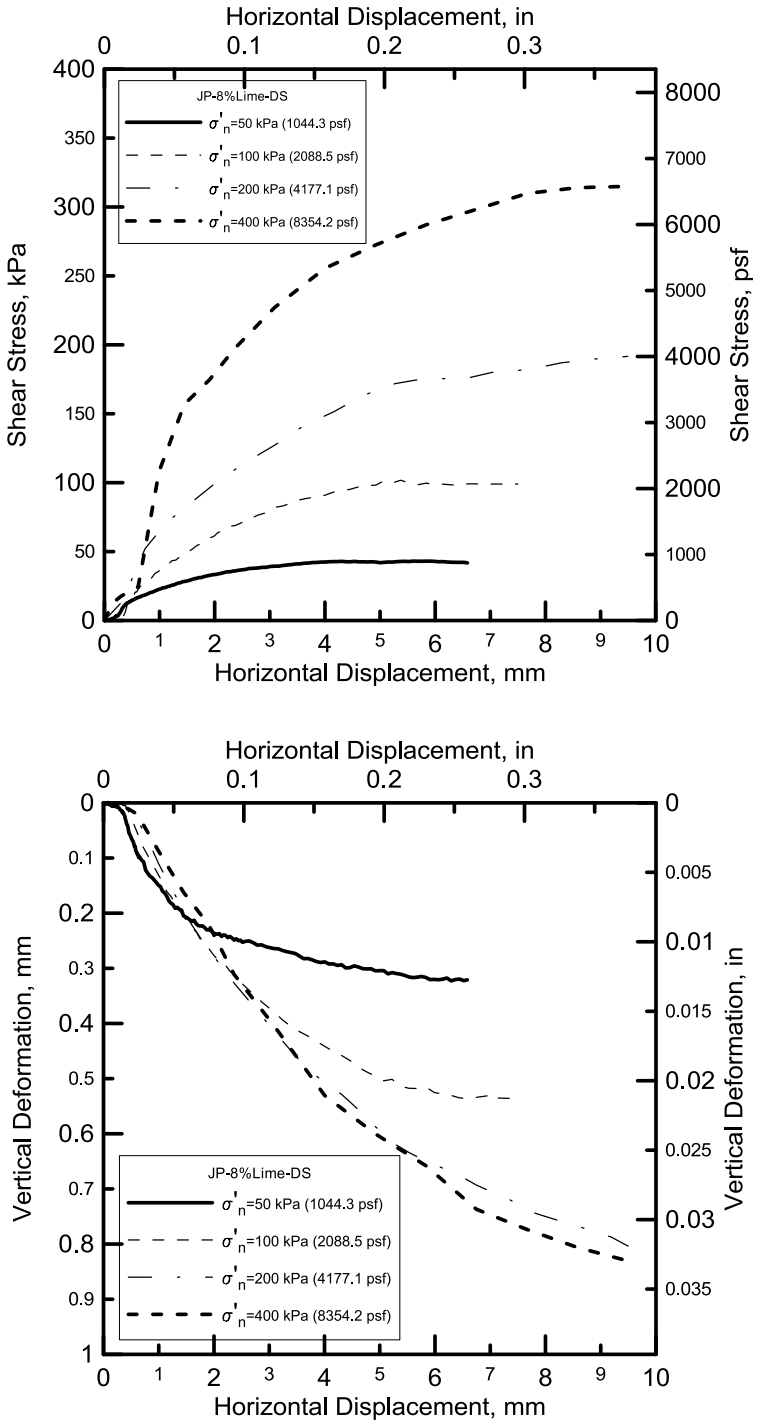

Figure 5.5. FSS results for the Joe Pool Dam 8%lime treated soil

Vertical deformations of the soil sample during the testing were recorded within the range of 1 mm. In a few instances, due to the long testing process, soil specimens submerged in water experienced the swelling phenomenon, which is a common characteristic of soils in the North Texas area. Overall, the vertical deformation varied from 0.2 to 1 mm and did not always folow the consistent trend with the the effective normal stresses.

The shear stress vs. horizontal displacement graphs presented did not show peak values; rather they reached the straight plateau condition while being sheared. The lower the effective normal stresses, the less displacement was required for the specimen to attain its maximum shear stress. Overall, failure of soil specimens happened at 4 mm (0.17 in.) of horizontal displacement and beyond. Test results of lime treated soils (4%lime+0.30%fibers, 8%lime+0.15%fibers and 8%lime) did require more displacements to fail the specimens than those of 20%compost treated and control soil specimens.

Ultimate shear stress of all test specimens are presented graphically in Figure 5.6 to show the variations of untreated and treated soil test results at various effective normal stresses.

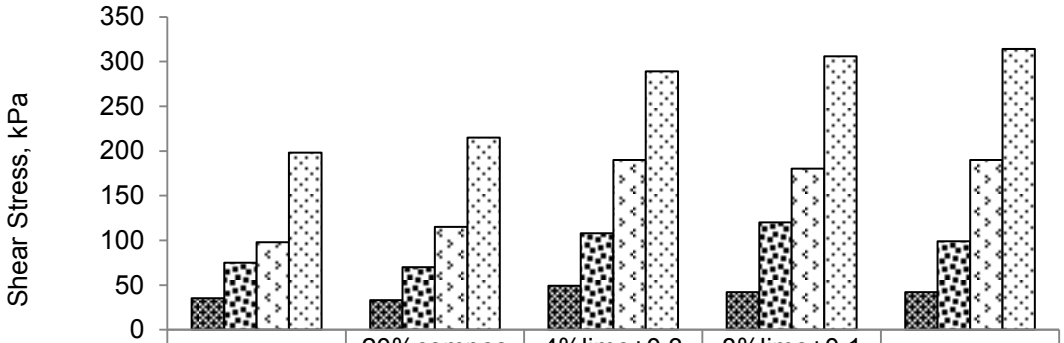

	Control Soil	20%compost Treated Soil	4%lime+0.30%fibers Treated Soil	8%lime+0.15%fibers Treated Soil	8%lime Treated Soil
σ'n=50 kPa	35	33	49	42	42
σ'n=100 kPa	75	70	108	120	99
σ'n=200 kPa	98	115	190	180	190
σ'n=400 kPa	198	215	289	306	314

Figure 5.6. Shear Stress comparison by DS for the Joe Pool Dam soils

It could be seen from the test data that among all stabilizers, the differences among shear strengths were more pronounced at effective normal stress (σ'_n) more than 100 kPa (2088.5 psf) than at effective normal stresses (σ'_n) less than 100 kPa. Between all treatments, 4%lime+0.30%fibers, 8%lime+0.15%fibers and 8%lime treated soils yielded higher strength than the 20%compost amendment. Particularly, at effective normal stress (σ'_n) of 400 kPa (8354.2 psf), these above mentioned stabilizers provided the highest shear strength over the untreated soil test results. The 20% compost-amended soil did not show much improvement over the untreated soil.

5.1.2 Torsional Ring Shear Test Results

Figures 5.7 to 5.11 present the FSS test results using the Bromhead TRS device. Soil specimens were sheared at drained conditions, using annular bronze porous stones secured to the top and bottom of the loading platens. The 5 mm thickness soil specimen in the TRS apparatus provided a faster primary consolidation, which is one of the advantages of the TRS test over the DS test for the FSS measurements.

Because readings were recorded manually off the strain gauges, results from the TRS machine provided more discrete point data than the DS tests. In addition, with the ability to perform unlimited shear displacements, shearing in the TRS device was continued for a longer time to guarantee the measurement of the ultimate shear stress of the soils.

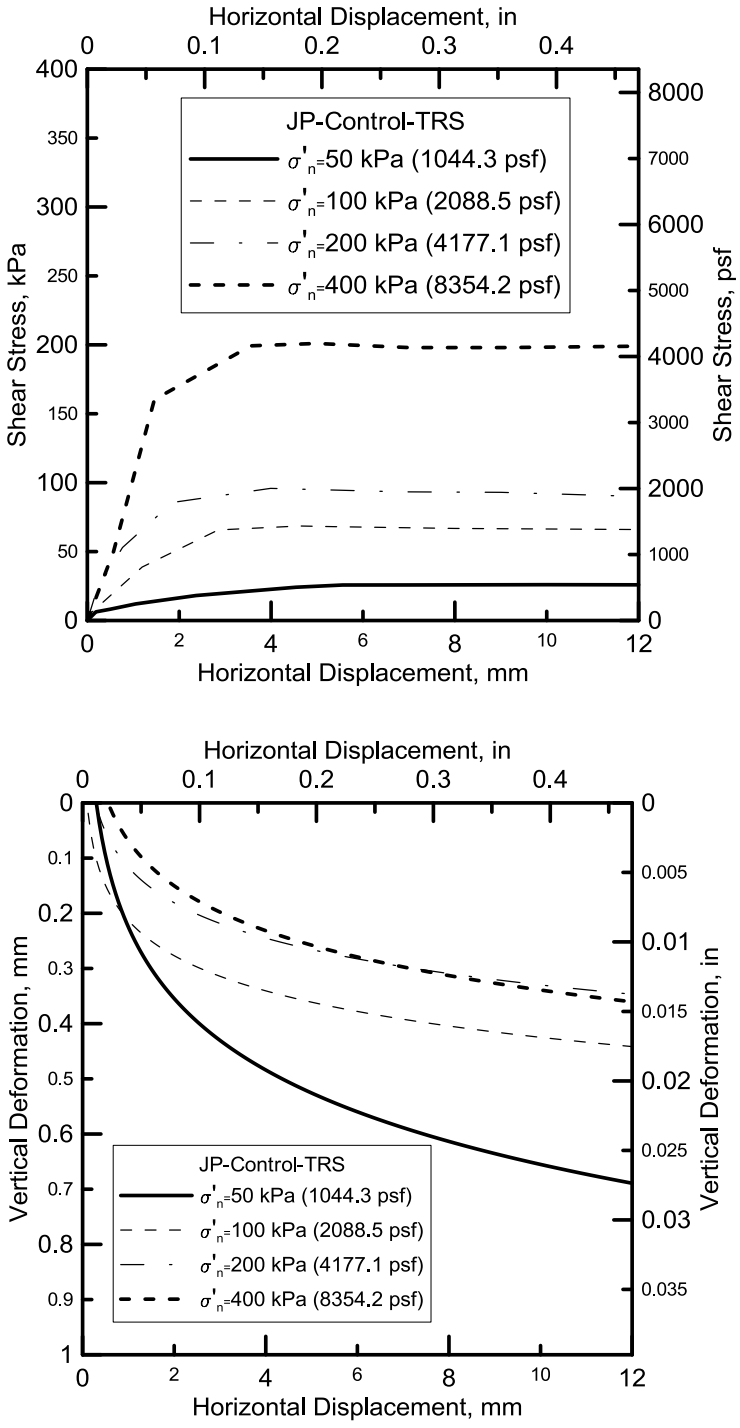

Figure 5.7. FSS results for the Joe Pool Dam Control soil

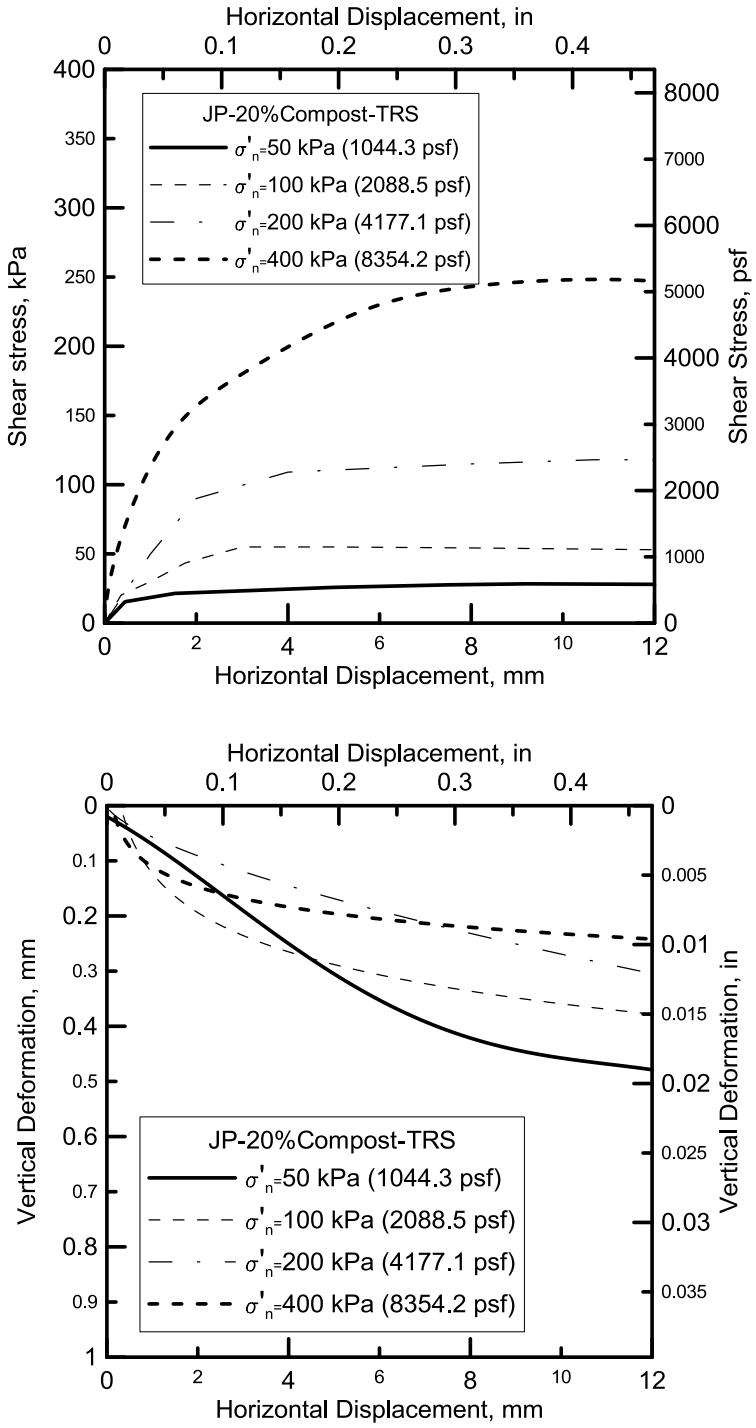

Figure 5.8. FSS results for the Joe Pool Dam 20%compost treated soil

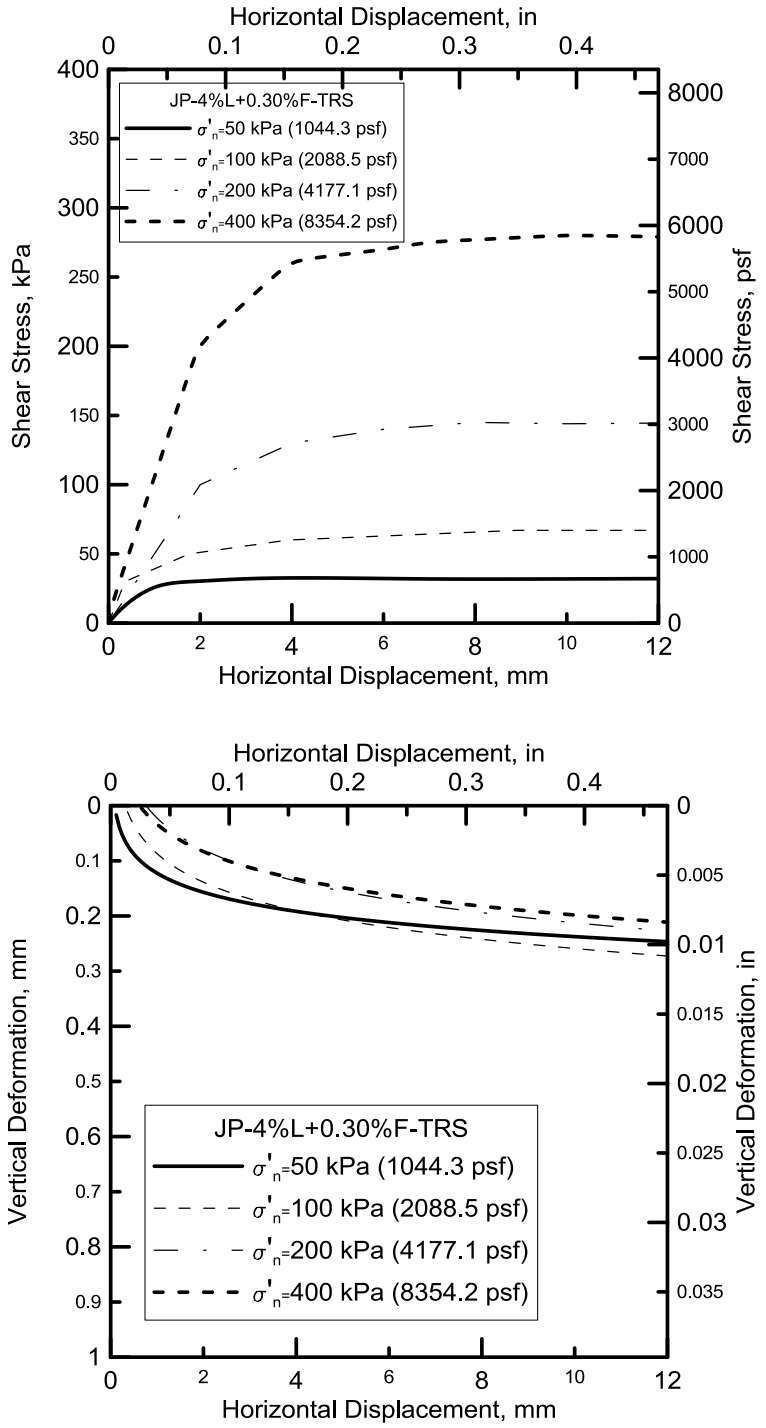

Figure 5.9. FSS results for the Joe Pool Dam 4%lime+0.30%fibers treated soil

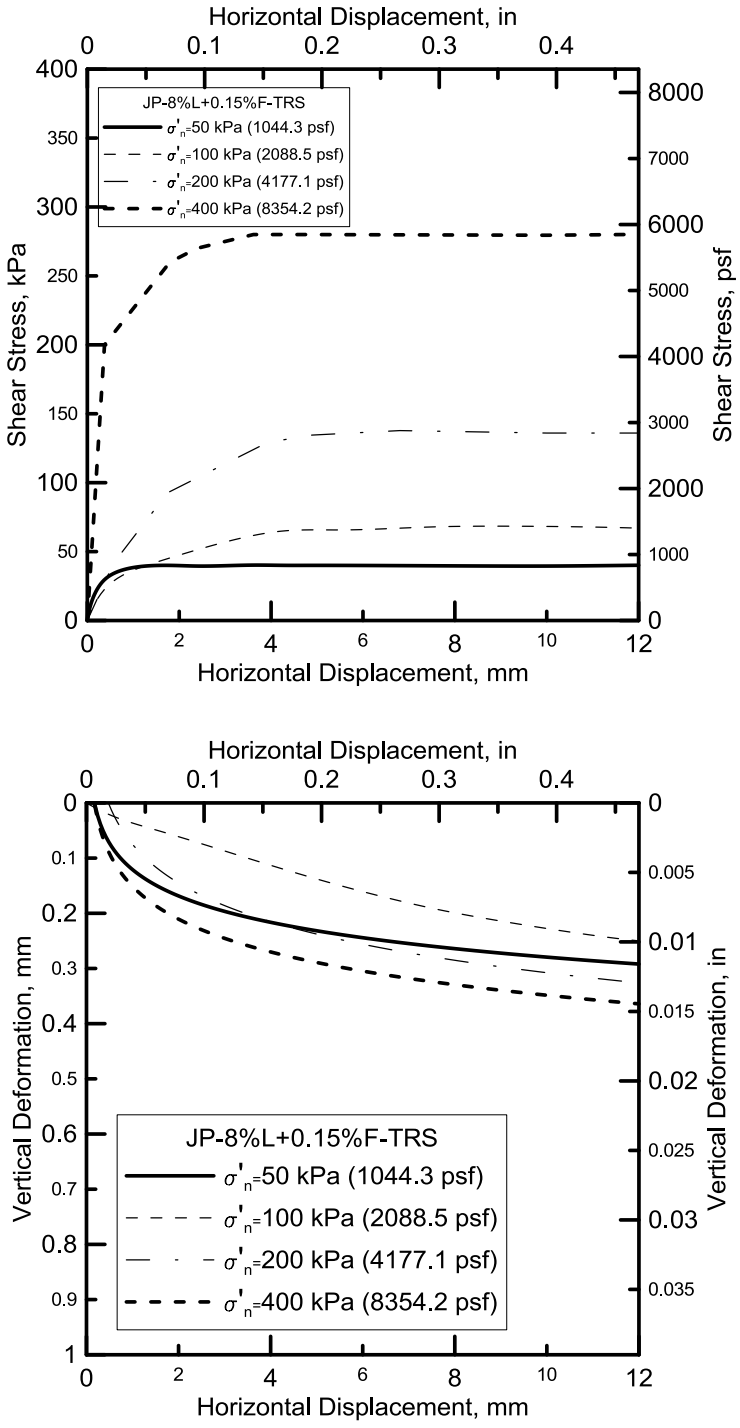

Figure 5.10. FSS results for the Joe Pool Dam 8%lime+0.15%fibers treated soil

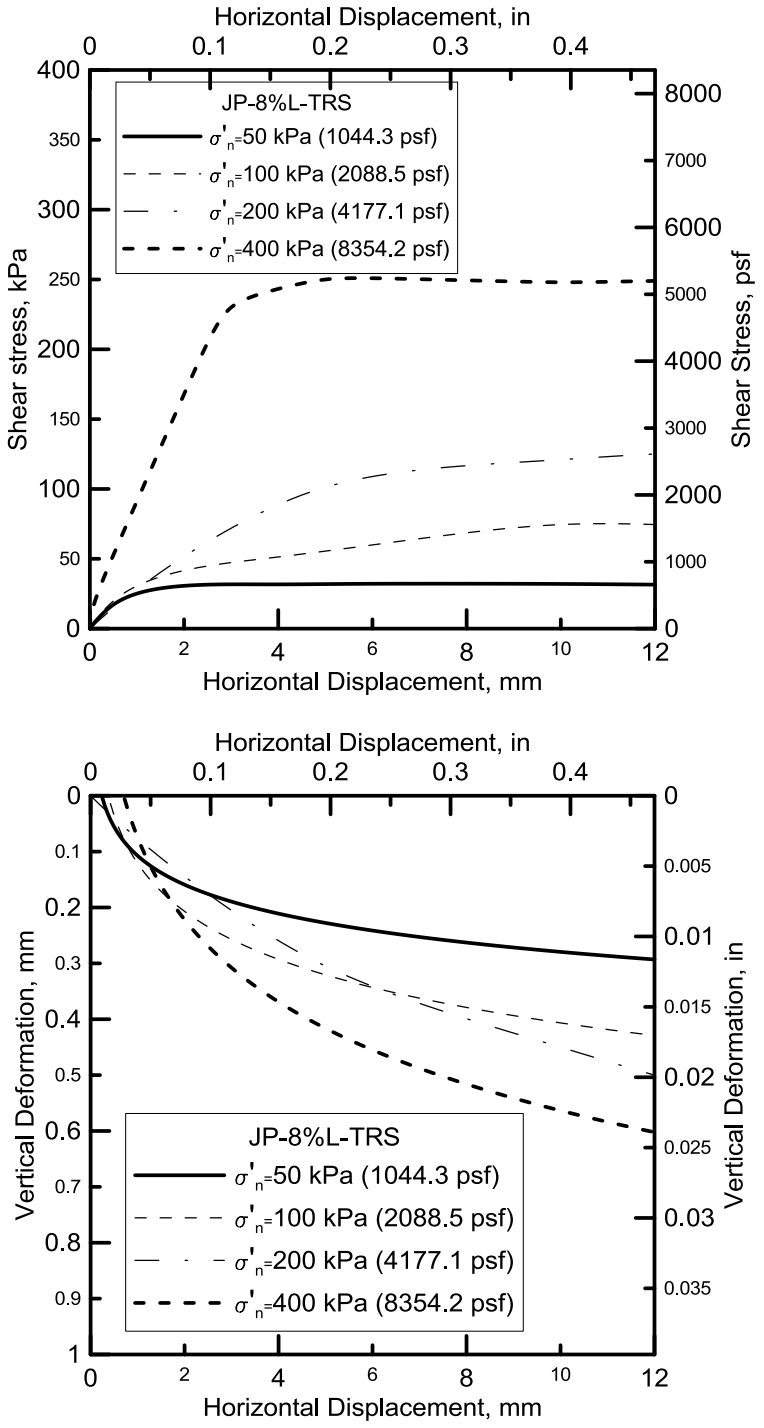

Figure 5.11. FSS results for the Joe Pool Dam 8%lime treated soil

The shear strength – horizontal displacement graphs, plotted using data from TRS tests show that the FSS values were generally reached at relatively low displacement of 5 mm (0.2

in.). At lower effective normal stresses, smaller displacements were required for the soil specimens to reach their maximum shear strength. Chemically treated soils namely 4%lime+0.30%fibers, 8%lime+0.15%fibers and 8%lime treated soils did undergo larger displacements to experience failure; these values were more than those of the 20%compost treated and control soils.

Figure 5.12 presents the shear stress response comparison among untreated and treated soils at various effective normal stresses. All treatments showed considerable improvements over the control soil. Comparisons between the performance of the treatment additives, 4%lime+0.30%fibers, 8%lime+0.15%fibers stabilizers were ranked as the top two treatments gained 40 to 50% higher strength over the control untreated soil.

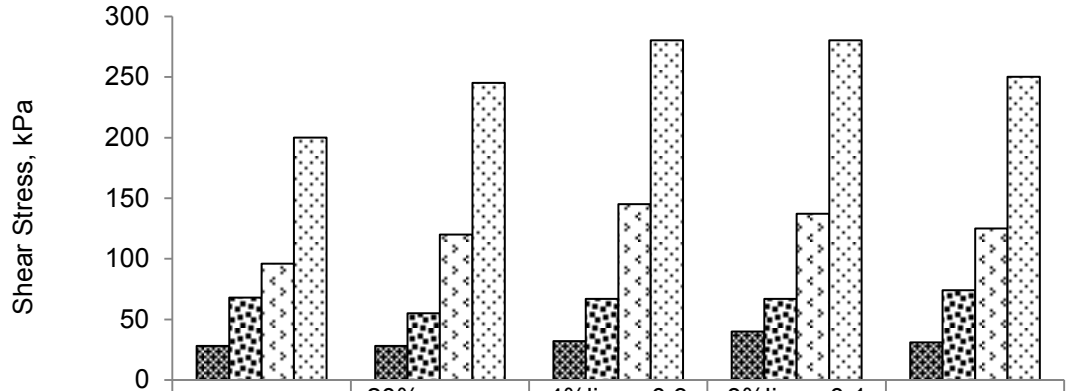

	Control Soil	20%compost Treated Soil	4%lime+0.30%fibers Treated Soil	8%lime+0.15%fibers Treated Soil	8%lime Treated Soil
σ'n=50 kPa	28	28	32	40	31
σ'n=100 kPa	68	55	67	67	74
σ'n=200 kPa	96	120	145	137	125
σ'n=400 kPa	200	245	280	280	250

Figure 5.12. Shear stress comparison for the Joe Pool Dam soils

5.2 Grapevine Dam Soil

5.2.1 Direct Shear Test Results

Figures 5.13 to 5.17 present FSS test results by the DS device conducted on the Grapevine Dam control and treated soils.

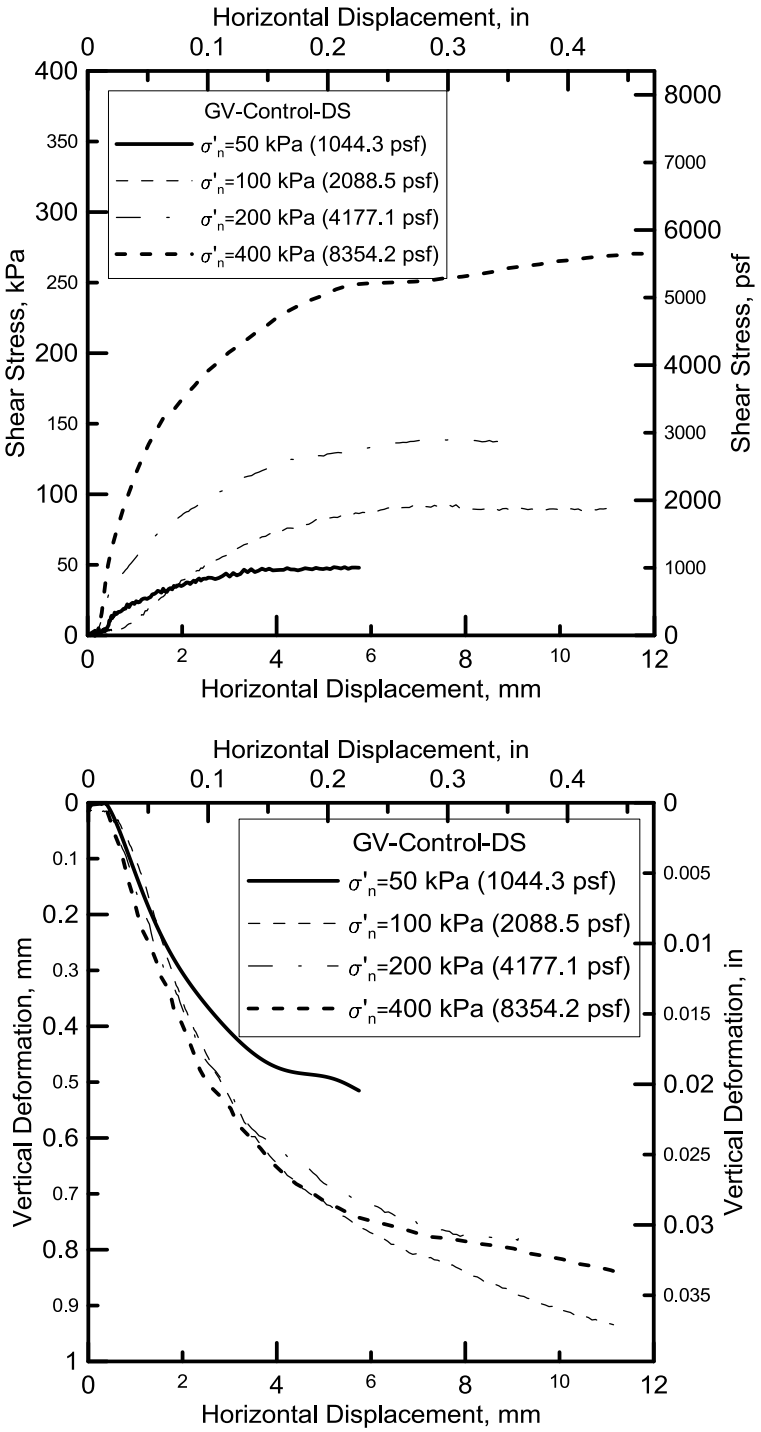

Figure 5.13. FSS results for the Grapevine Dam Control soil

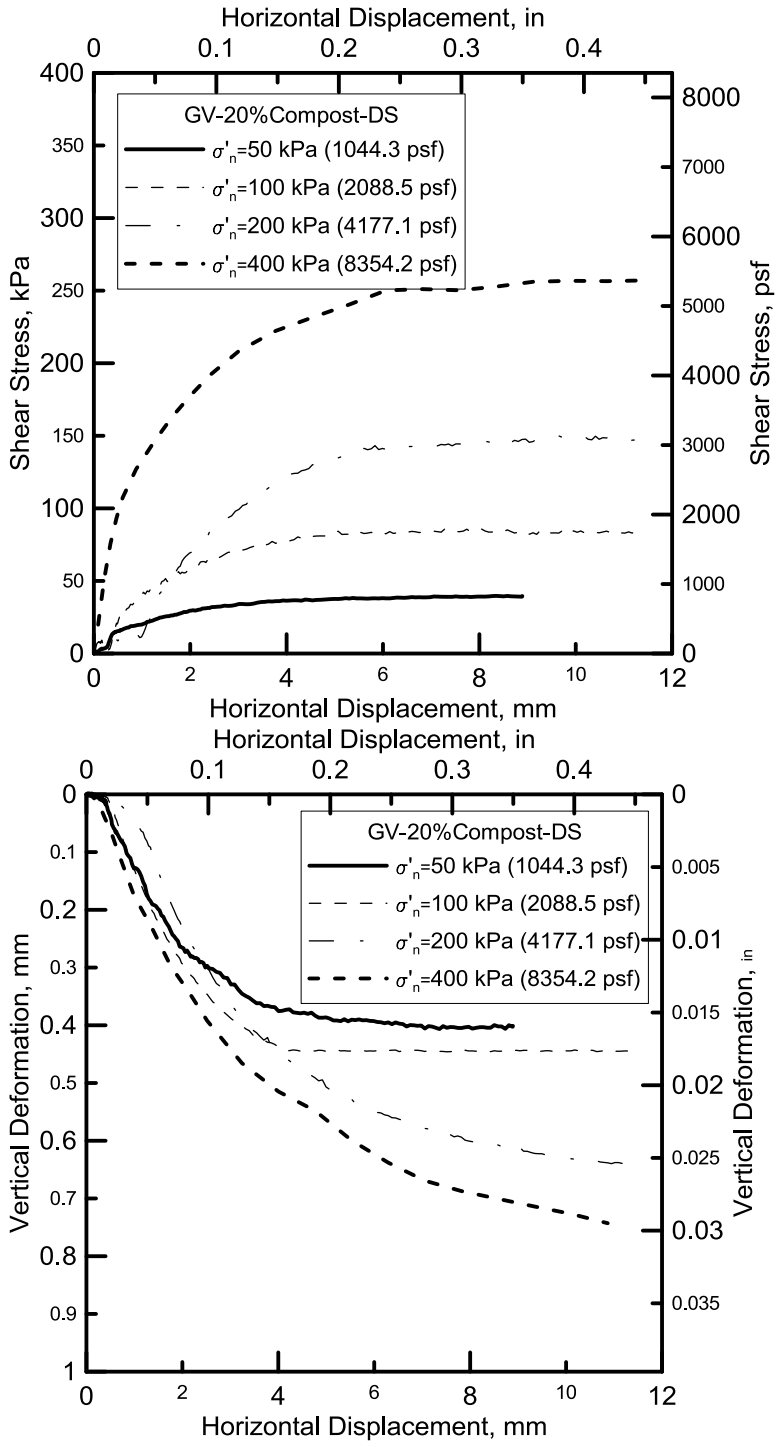

Figure 5.14. FSS results for the Grapevine Dam 20%compost treated soil

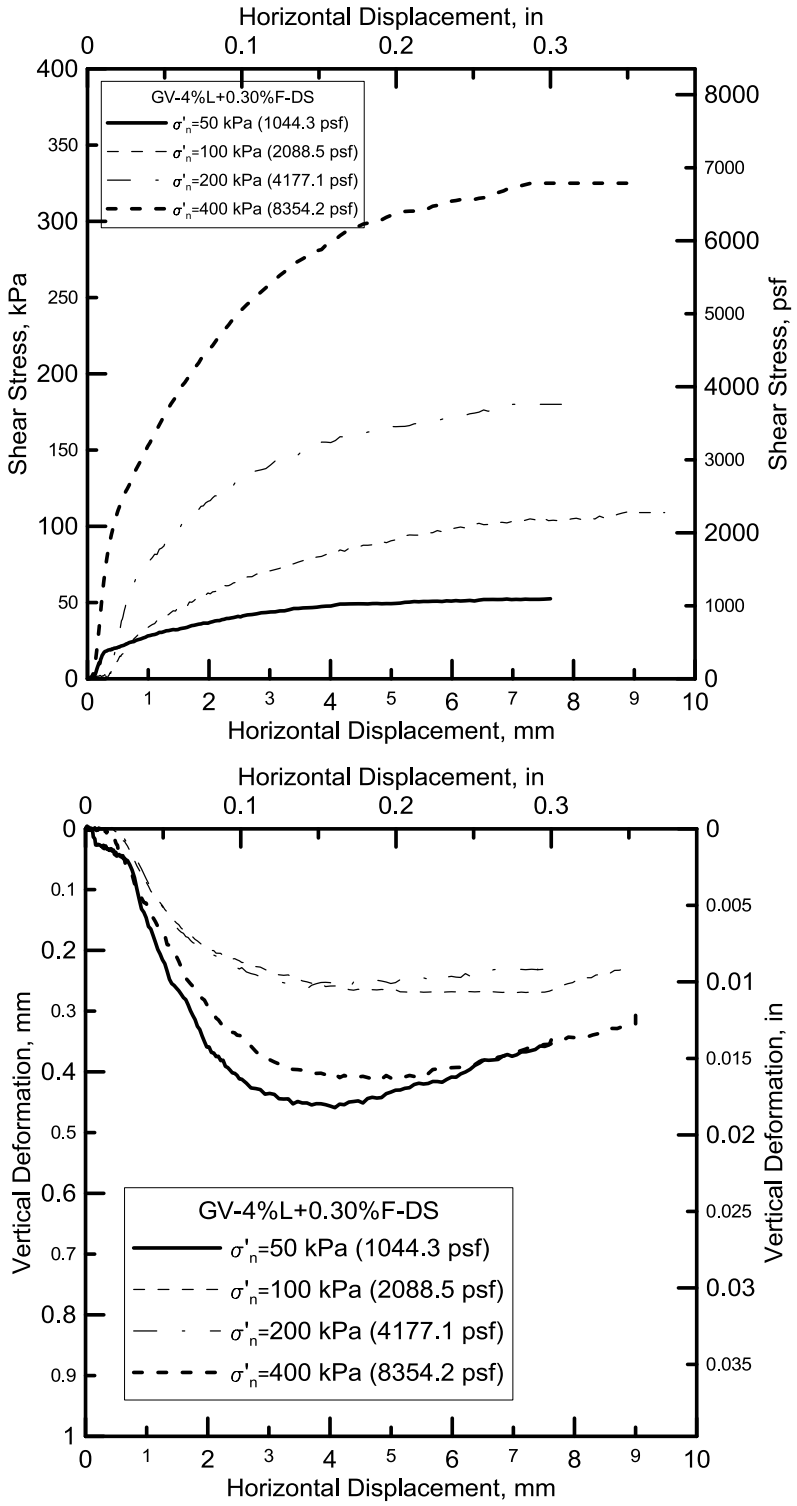

Figure 5.15. FSS results for the Grapevine Dam 4%lime+0.30%fibers treated soil

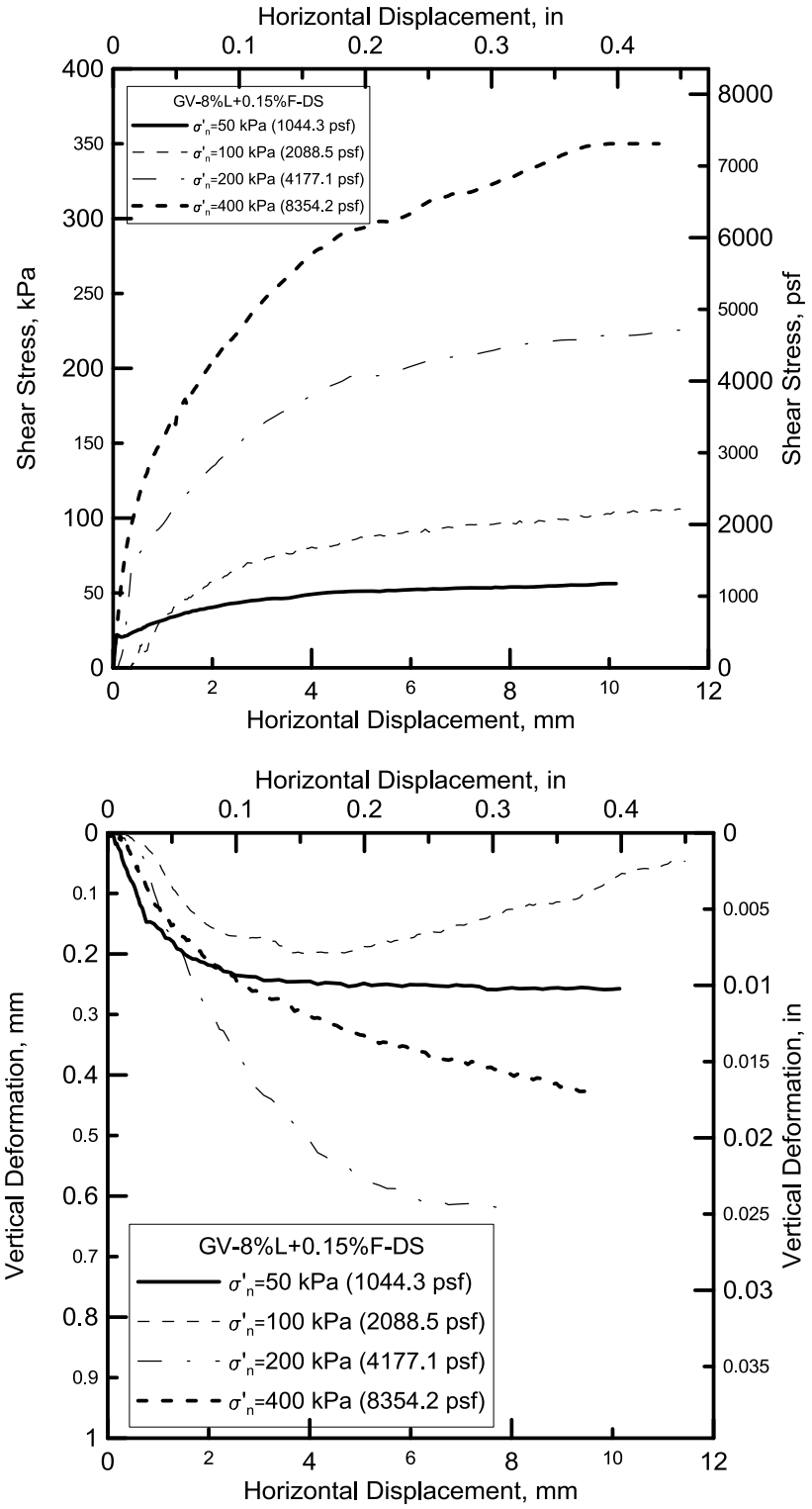

Figure 5.16. FSS results for the Grapevine Dam 8%lime+0.15%fibers treated soil

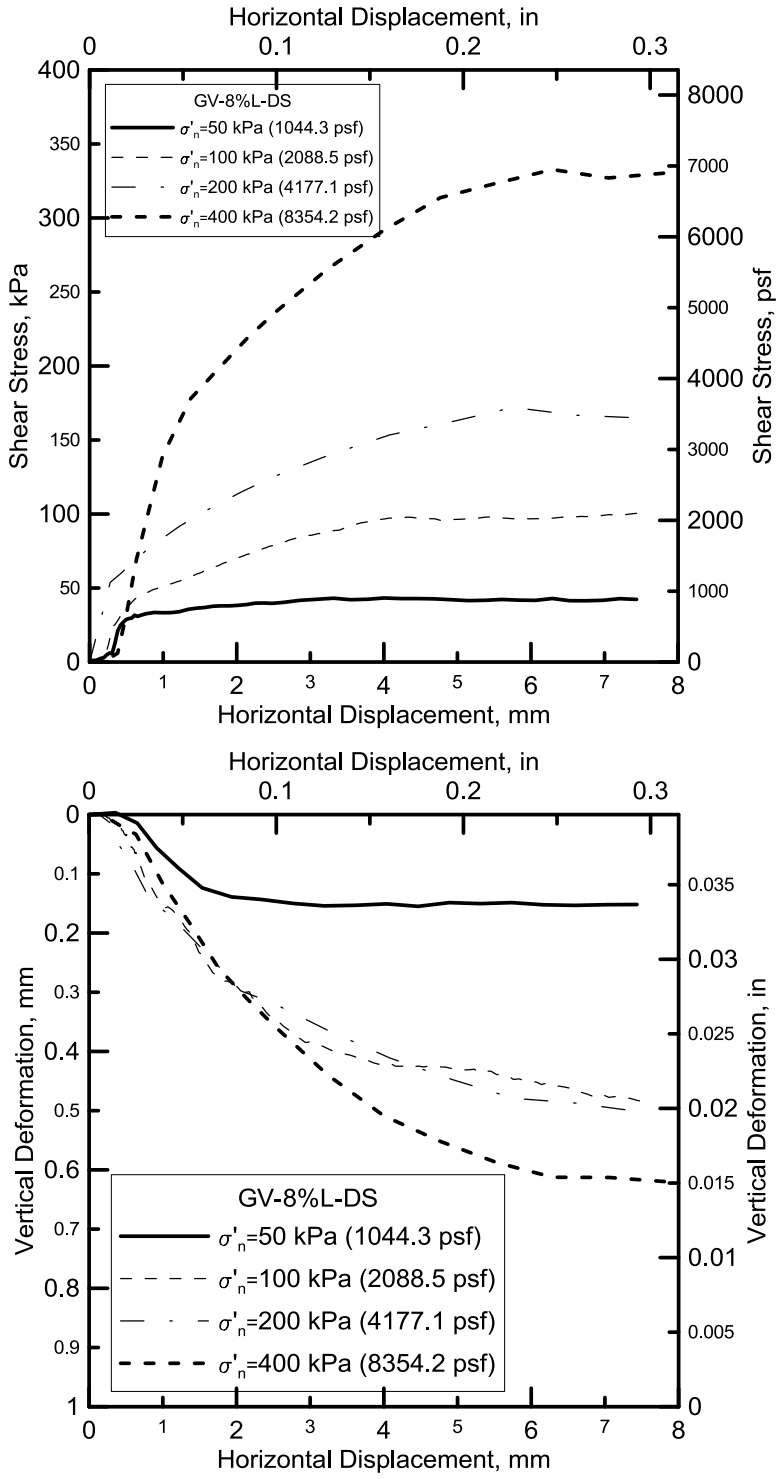

Figure 5.17.FSS results for the Grapevine Dam 8%lime treated soil

Experimental data from 4%lime+0.30%fibers and 8%lime+0.15%fibers treated soils indicated that the stroke length of the DS device might not be capable of capturing the maximum shear stress under 400 kPa (8354.1 psf) normal stress and beyond. This resulted in the ultimate maximum strength obtained from some of the tests as extrapolated values. Similar to the Joe Pool Dam soil, shear stress of the Grapevine Dam soil did not experience the peak value during the shearing process.

Figure 5.18 illustrates the shear stress responses of treated and untreated soil under different normal stresses. Among all stabilizers except the 20%compost treated soil, soil strength improvement was achieved as high as 20 to 30%. Testing results showed the inconsistency of the 20%compost treatment, as it could not outperform the original treated soil in any of the effective normal stresses. In comparison with treatment effect on the Joe Pool Dam soil, the results of the Grapevine Dam soil displayed less improvement and consistency. This could be attributed to the difference between in the soil nature of each site, including plasticity and mineralogy aspects.

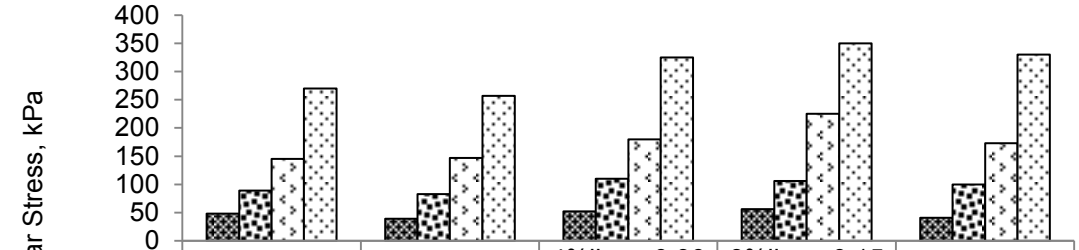

	Control Soil	20%compost Treated Soil	4%lime+0.30 %fibers Treated Soil	8%lime+0.15 %fibers Treated Soil	8%lime Treated Soil
σ'n=50 kPa	48	39	52	56	41
σ'n=100 kPa	89	83	110	106	100
σ'n=200 kPa	145	147	180	225	173
σ'n=400 kPa	270	257	325	350	330

Figure 5.18. Shear Stress comparison for the Grapevine Dam soils

5.2.2 Torsional Ring Shear Test Results

Figures 5.19 to 5.23 present the FSS test results using the DS apparatus for the Grapevine Dam control and treated soils.

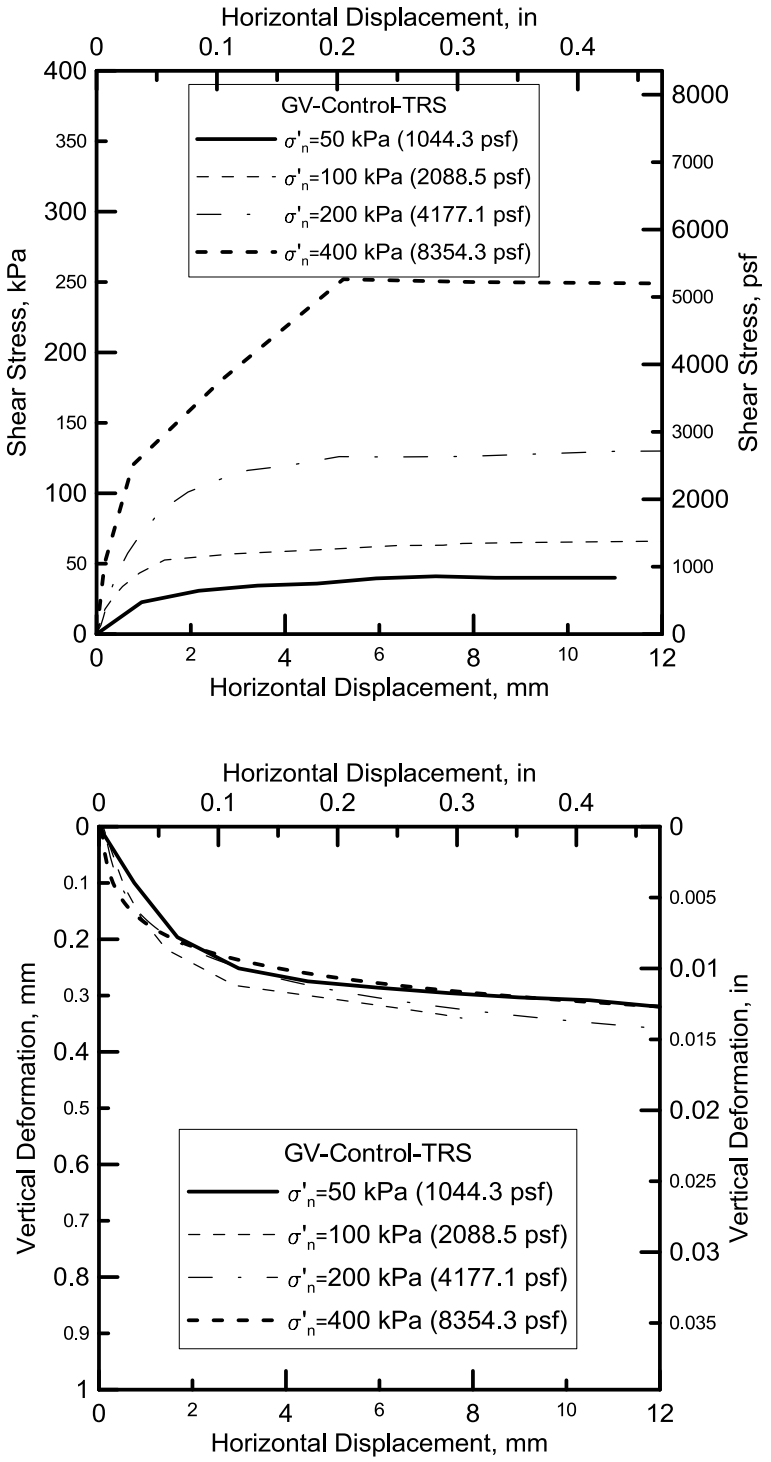

Figure 5.19. FSS results for the Grapevine Dam Control soil

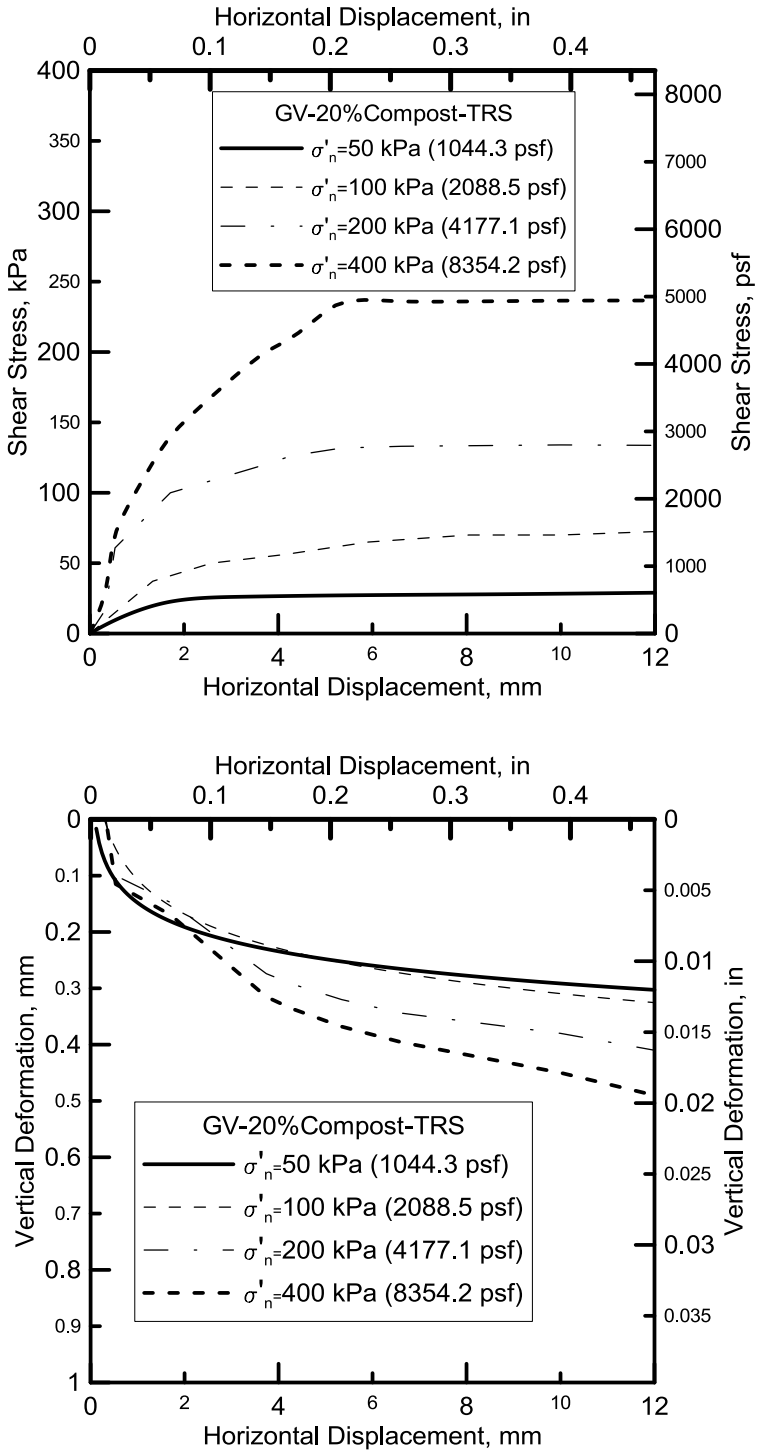

Figure 5.20. FSS results for the Grapevine Dam 20%compost treated soil

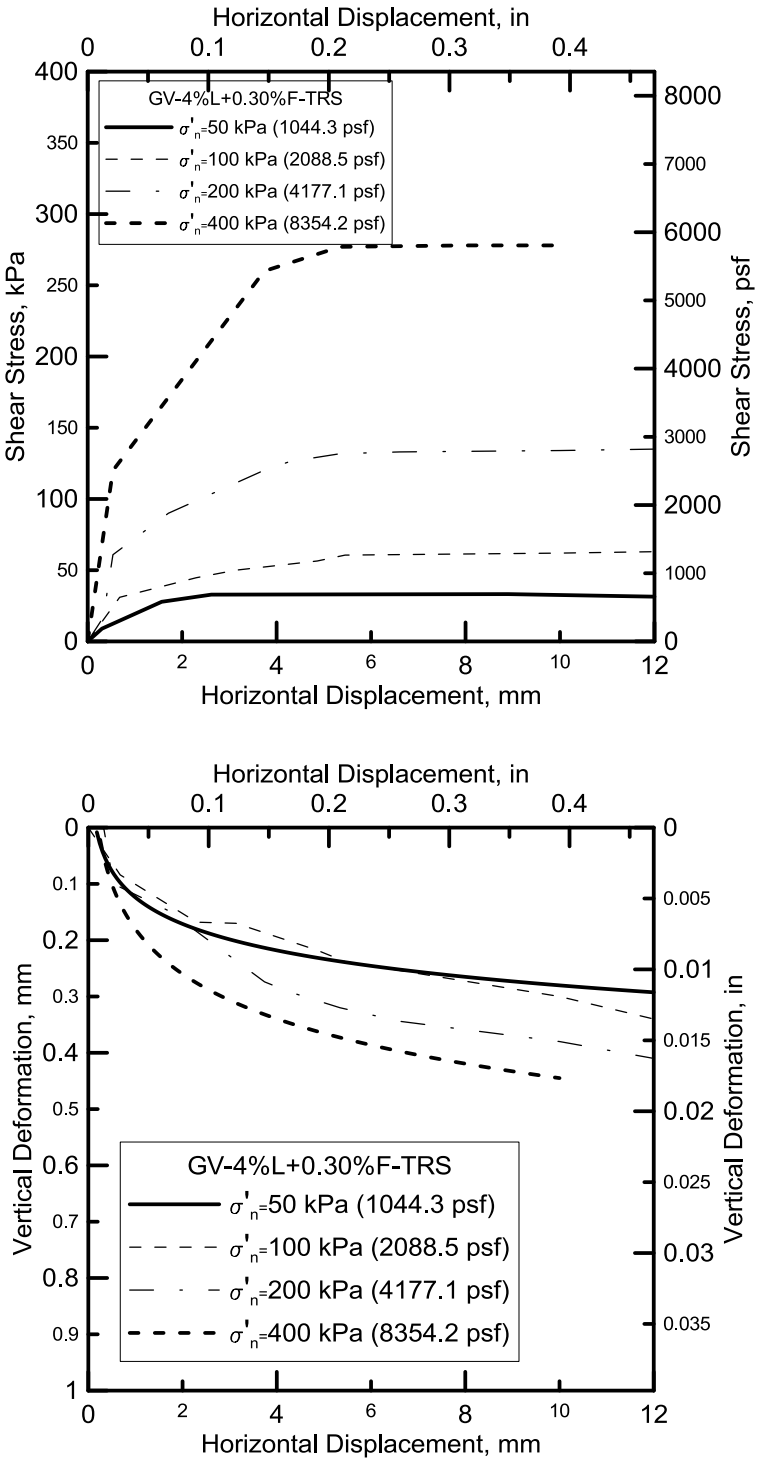

Figure 5.21. FSS results for the Grapevine Dam 4%lime+0.30%fibers treated soil

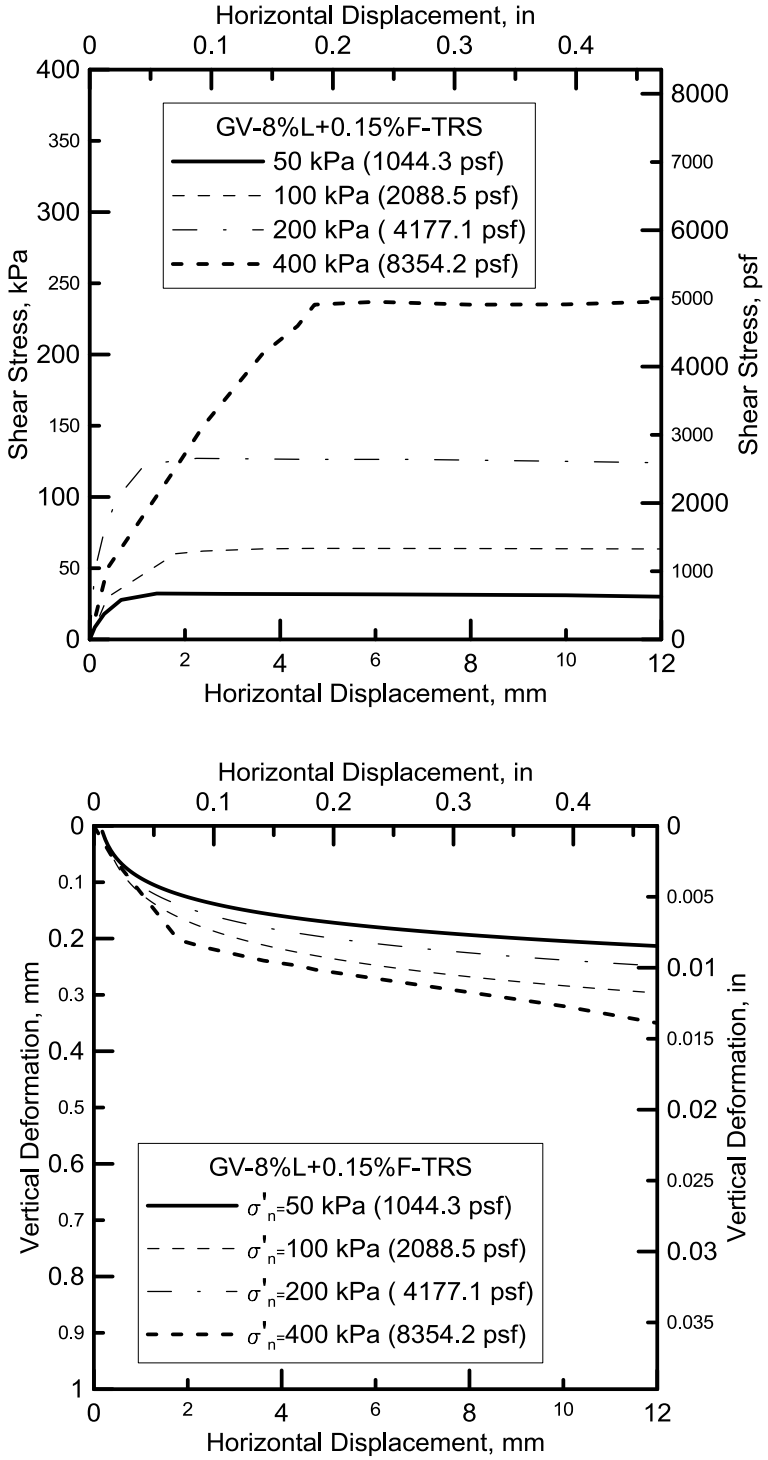

Figure 5.22. FSS results for the Grapevine Dam 8%lime+0.15%fibers treated soil

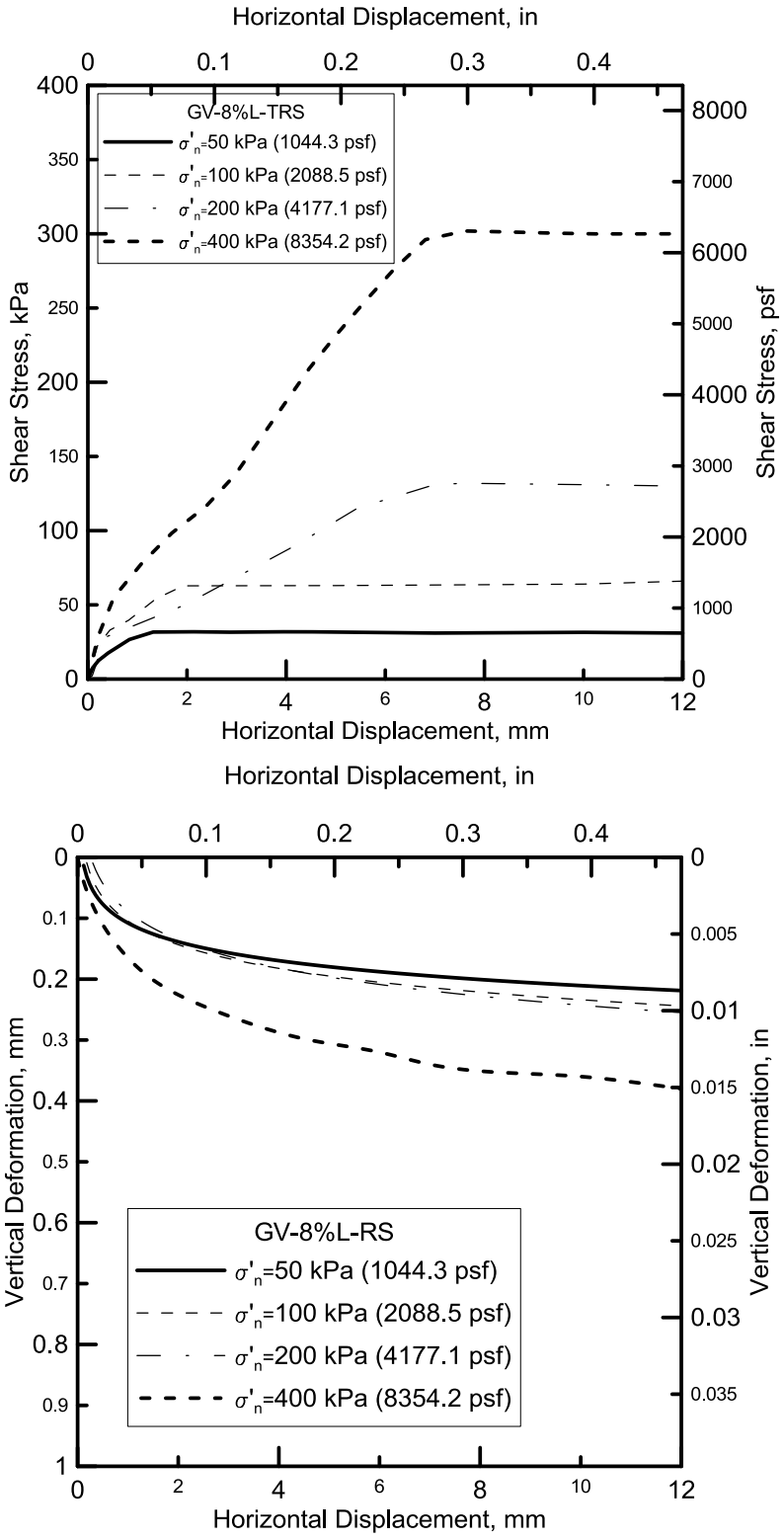

Figure 5.23. FSS results for the Grapevine Dam 8%lime treated soil

Based on the Shear Stress-Displacement plots, shear strength of soils was determined graphically and shown in Figure 5.24. Data interpretation emphasized that little or no improvement of the stabilizers was seen for effective normal stresses σ'_n under 200 kPa (4177.1 psf). However, at 400 kPa (8354.2 psf) 8%lime+0.15%fibers and 8%lime treated soils still increased the peak strength of the soil by 10 to 20%.

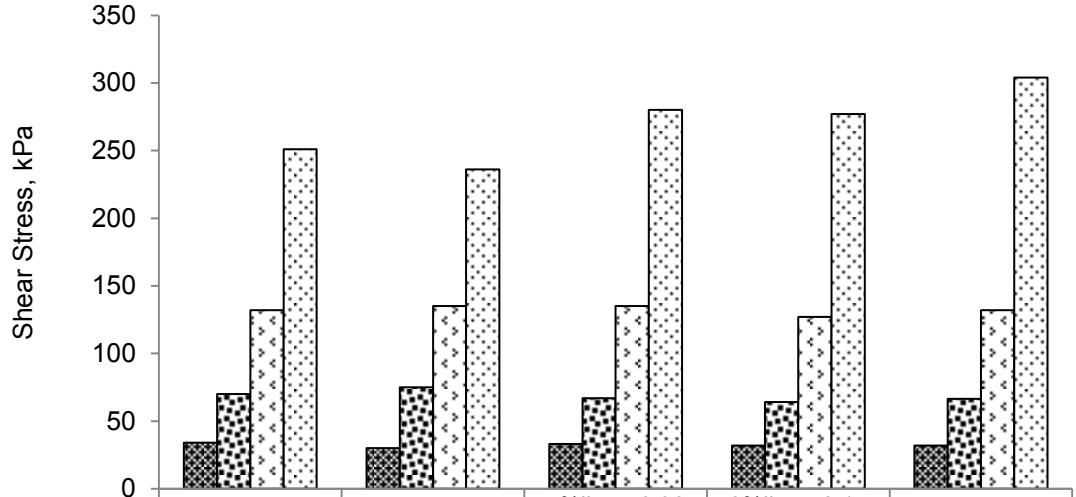

	Control Soil	20%compost Treated Soil	4%lime+0.30 %fibers Treated Soil	8%lime+0.15 %fibers Treated Soil	8%lime Treated Soil
σ'n=50 kPa	34	30	33	32	31.9
σ'n=100 kPa	70	75	67	64	66.5
σ'n=200 kPa	132	135	135	127	132
σ'n=400 kPa	251	236	280	277	304.1

Figure 5.24. Shear Stress comparison for the Grapevine Dam soils

5.3 Data Comparisons and Analysis

5.3.1 Shear Stress comparisons between Direct Shear and Torsional Ring Shear tests

Figure 5.25 and Figure 5.26 show the shear stress comparison between the DS and TRS test results for the Joe Pool Dam and Grapevine Dam soils. DS test results were plotted on the x-axis and TRS test results were plotted on y-axis. For the purpose of comparisons, both axes were drawn to the same scale in both SI and English units.

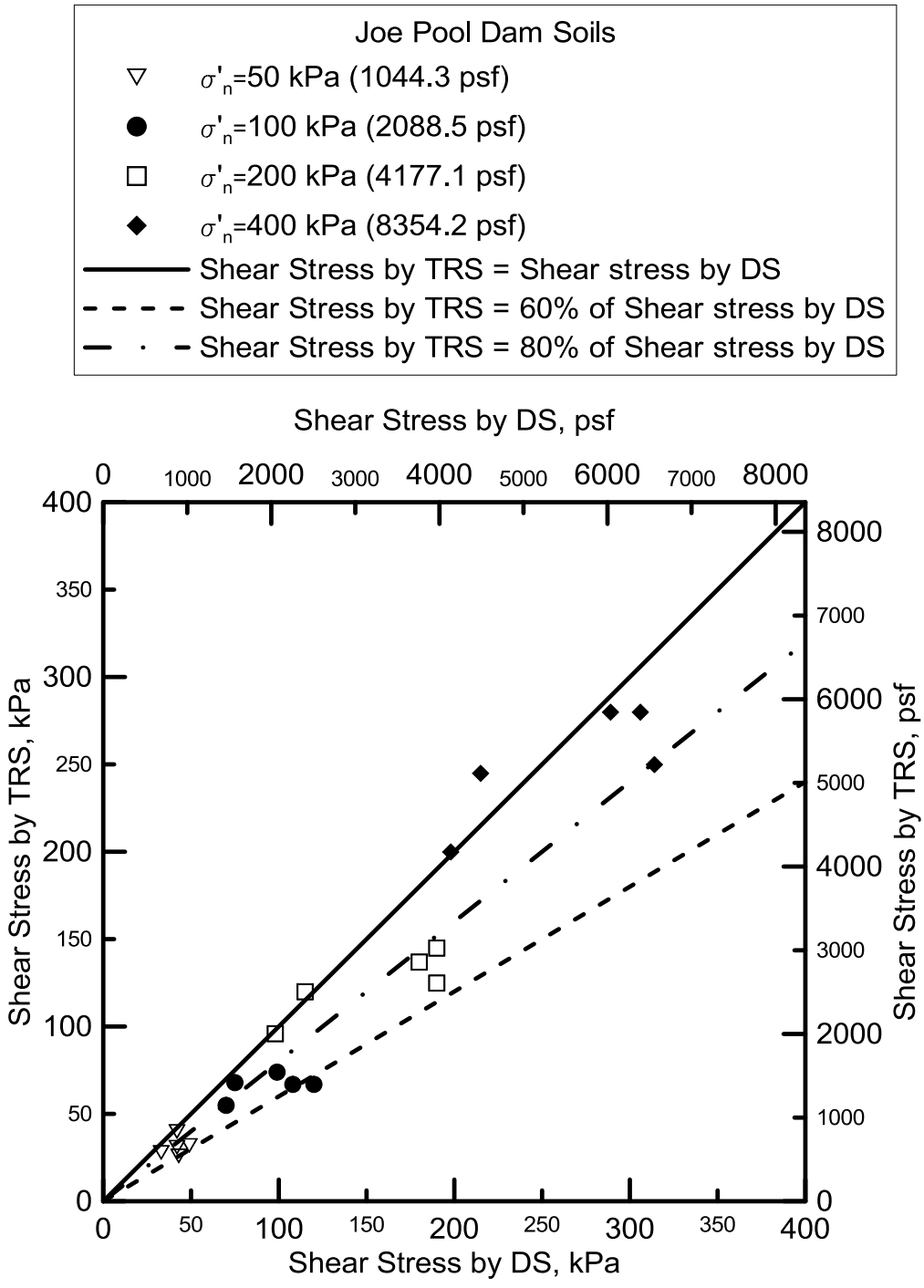

Figure 5.25. Shear stress comparison between the DS and TRS test results for the Joe Pool Dam soils

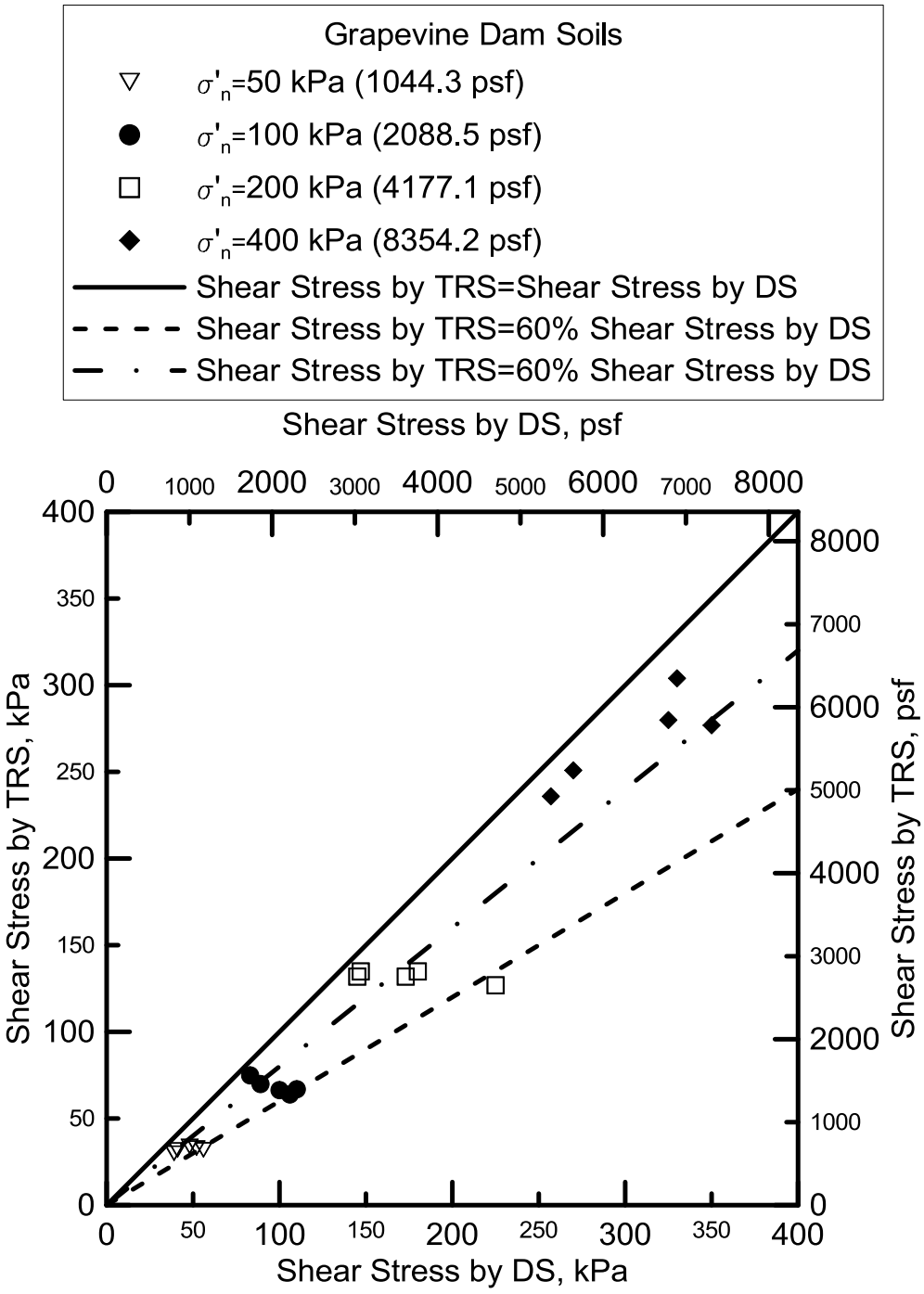

Figure 5.26. Shear stress comparison between the DS and TRS test results for the Grapevine Dam soils

It can be noted from the graphs that all data points plotted lie below the equality line, indicating that the FSS test results by DS slightly exceeded the FSS test results by TRS. In an attempt to quantify the difference between the shear stress responses, two linear functions were plotted to characterize the boundaries of the shear stress by TRS over shear stress by DS ratio. Results showed that for lower effective normal stresses (σ'_n) of 50 kPa (1044.3 psf) and 100 kPa (2088.5 psf), shear stresses captured by the TRS device are only equal to as low as 60% of the DS test results, while at (σ'_n) of 400 kPa (8354.2 psf) this ratio increased to the minimum of 80%. This also indicated that the difference between the two methods is more distinct at lower effective normal stresses than at the higher effective normal stresses. Overall, the TRS measurements ranged from 60% to 100% compared to the DS results.

Results of shear stresses are also tabulated for the purpose of quantitative comparisons as shown in Table 5.1.

Table 5.1. Shear Stress comparison for the Joe Pool Dam soils

Soil	Direct Shear Results τ_{DS}, kPa				Torsional Ring Shear Results τ_{TRS}, kPA			
	50 kPa	100 kPa	200 kPa	400 kPa	50 kPa	100 kPa	200 kPa	400 kPa
Control Soil	35	76	98	198	28	68	96	200
20%compost Treated Soil	33	70	115	215	28	55	120	245
4%lime+0.30%fibers Treated Soil	49	108	190	289	32	67	145	280
8%lime+0.15%fibers Treated Soil	42	120	180	306	40	67	137	280
8%lime Treated Soil	43	102	190	310	31	74	125	250

Table 5.2. Shear Stress comparison for the Grapevine Dam soils

Soil	Direct Shear Results τ_{DS}, kPa				Torsional Ring Shear Results τ_{TRS}, kPa			
	50 kPa	100 kPa	200 kPa	400 kPa	50 kPa	100 kPa	200 kPa	400 kPa
Control Soil	48	89	145	270	34	70	132	251
20%compost Treated Soil	39	83	147	257	30	75	135	236
4%lime+0.30%fibers Treated Soil	52	110	180	325	33	67	135	280
8%lime+0.15%fibers Treated Soil	56	106	225	350	32	64	127	277
8%lime Treated Soil	41	100	173	330	31.9	66.5	132	304.1

Results of FSS from the Joe Pool Dam and Grapevine Dam soils are compared with the work of Castellanos et al. (2013), who studied the differences of the FSS test results from the DS and TRS devices on ten different clays that covered a wide range of liquid limits, plasticity indices and clay-sized fractions. Data for control soil from Table 5.1 and Table 5.2 are used to calculate the ratio of the shear stress by DS (τ_{DS}) over the shear stress measured by the TRS device (τ_{TRS}). Table 5.3 presents the ratio (τ_{DS}/τ_{TRS}) for the Joe Pool Dam and Grapevine Dam test results on Control soil. These results are then plotted on the same graph illustrated by Castellanos in his study as shown in Figure 5.27.

Table 5.3. τ_{DS}/τ_{RS} for the Joe Pool Dam and Grapevine Dam Test results

Soil	Joe Pool Dam Test Results τ_{DS}/τ_{TRS}				Grapevine Dam Test Results τ_{DS}/τ_{TRS}			
	50 kPa	100 kPa	200 kPa	400 kPa	50 kPa	100 kPa	200 kPa	400 kPa
Control Soil	1.25	1.12	1.02	0.99	1.41	1.27	1.10	1.08

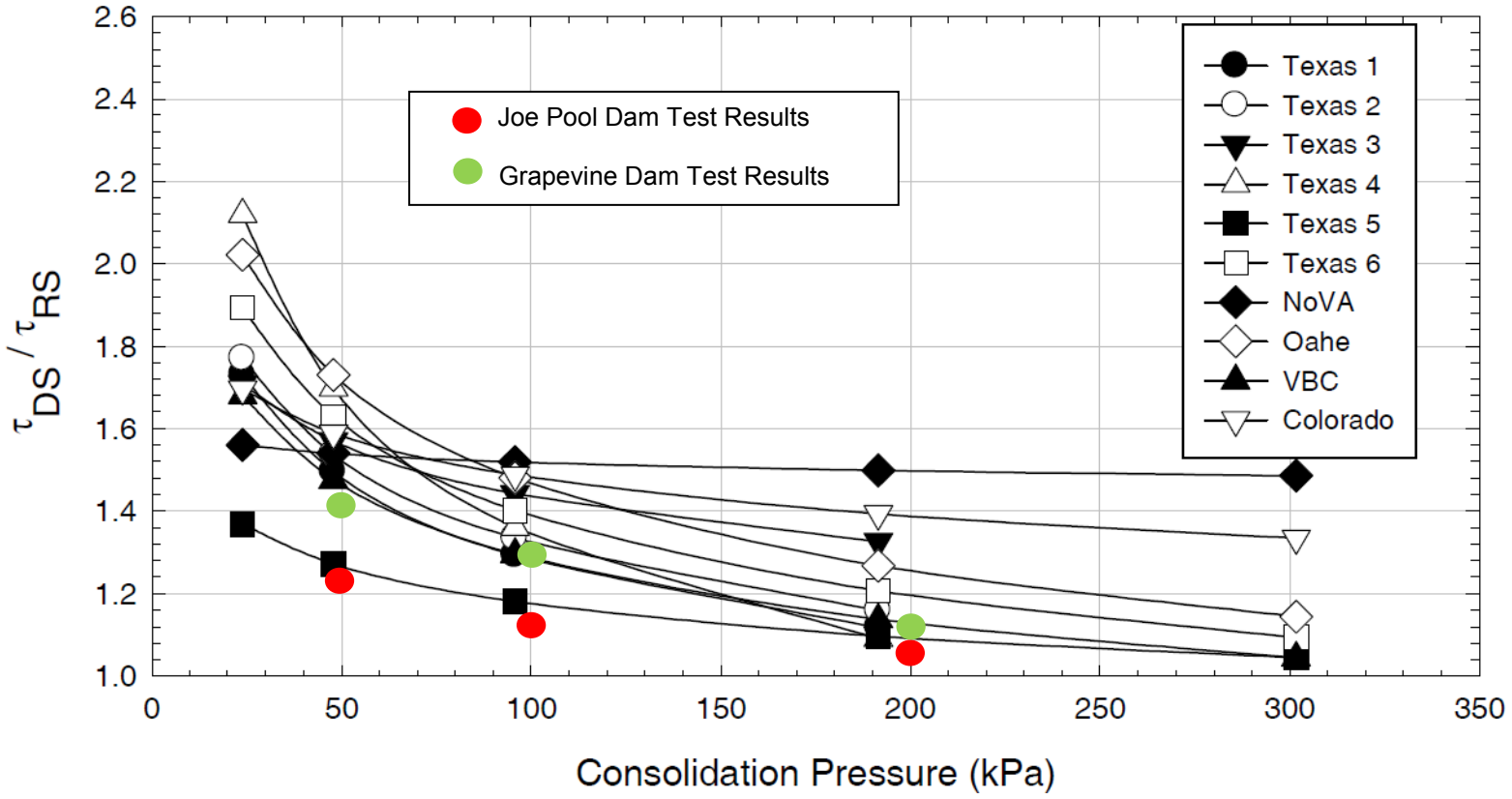

Figure 5.27. Ratio of the FSS measured with the DS and TRS devices (Castellanos et al., 2013)

As shown in Figure 5.27, results from the Joe Pool Dam and Grapevine Dam soils are in a good agreement with Castellanos's research results. The majority of the test data coincided within the ranges of the results from the tested specimens in Castellanos's work. It is noteworthy to mention that none of the soil used in Castellanos's study perfectly matched in terms of Liquid Limit, Plastic Limit, Plasticity Indices and Clay-Sized Fraction with the Joe Pool Dam and Grapevine Dam soils used in this study. For comparison, soil properties from both Castellanos's study and Joe Pool Dam and Grapevine Dam are provided in Table 5.4 and Table 5.5.

Table 5.4. Index properties of soils tested in Castellanos's study (Casterllanos et al., 2013)

Sample	Non-blenderized				Blenderized			
	LL	PL	PI	Clay-sized Fraction	LL	PL	PI	Clay-sized Fraction
Texas 1[a]	68	25	43	63	76	25	51	N/A
Texas 2[a]	66	23	43	58	74	21	53	N/A
Texas 3[a]	65	21	44	55	71	22	49	N/A
Texas 4[a]	66	24	42	67	76	23	53	N/A
Texas 5[a]	76	28	48	59	84	27	57	N/A
Texas 6[a]	73	26	47	51	77	25	52	N/A
Colorado Clay	42	22	20	24	42	22	20	55
NOVA	66	28	38	17	79	28	51	35
Oahe	N/A	N/A	N/A	N/A	126	26	100	75
VBC	78	26	52	69	94	26	68	65

NOTES: [a] Index properties obtained by ERDC.

Table 5.5. The Joe Pool Dam and Grapevine Dam soil index properties (McCleskey, 2005)

Soil	LL	PL	PI	Clay-sized Fraction %
Joe Pool Dam	55	24	34	10.5
GrapeVine Dam	32	17	12	15.5

5.3.2 Fully Softened Soil Parameters comparison

Previous researchers have presented the fully softened shear strength envelopes in slightly curved trend and hence used the secant fully softened friction angles to address the curvature of the failure envelope. Figure 5.28 illustrates the concept of using the secant friction angle by Wright et al. (2011).

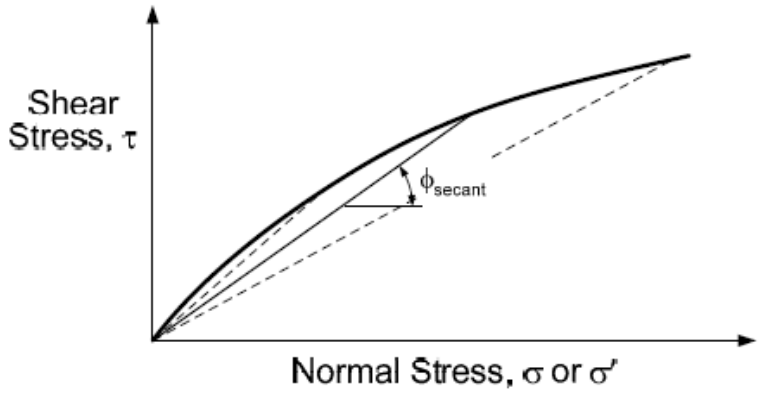

Figure 5.28. Secant Friction Angle concept (Wright et al., 2011)

However, Stark et al., (1997) in his study pointed out that the nonlinearity is not significant for cohesive soils with a clay-size fraction (CSF) less than 25%. In his research, for soil specimens with CSF less than 20% and liquid limit less than 80% the reduction of secant fully softened friction angle from a normal stress of 50-400 kPa is less than 2-3 degrees. Joe Pool Dam soil was classified as a CH soil with a liquid limit value of 58 and CSF of 10.5 and the Grapevine Dam soil was classified as a CL soil with a liquid limit value of 30 and CSF of 15.5 (Dronamraju,2008). Both match with soil descriptions by Stark's results.

Tiwari (2011) suggested the use of average friction angles for the tested range of normal stresses, which simplifies the analyses using the FSS parameter. The fully softened soil parameters are estimated using the best fit linear trend lines for the strength envelopes. The equation for the trend line is shown below:

$$y = b + m \times x \qquad \text{Eq. 5.5-1}$$

representing the FSS equation as:

$$\tau_{fs} = c'_{fs} + \sigma'_n \times tan(\varphi'_{fs}) \quad \text{Eq. 5-2}$$

where

τ_{fs} –fully softened shear strength

c'_{fs} –fully softened cohesion

σ'_n –effective normal stress

φ'_{fs} –fully softened friction angle

Following Tiwari's approach, FSS results for both the Joe Pool Dam and Grapevine Dam soils from Table 5.1 and Table 5.2 are analyzed by plotting with the strength envelope over the experimental results. Linear regression analysis was used to characterize the strength envelopes with the best fit functions possible. The statistical report exhibited a good correlation with the least coefficient of determination R^2 of 0.98.

5.3.2.1 Joe Pool Dam Soil

Figure 5.29 and Figure 5.30 present the FSS strength envelopes by DS and TRS for the Joe Pool Dam untreated and treated soils under various effective normal stresses. For the purpose of quantitative comparison, the corresponding FSS parameters for all test specimens are also presented in a tabular form as shown in Table 5.6.

Table 5.6. FSS parameters determined from the DS and TRS test results for Joe Pool Dam soils

Soil	DS Results		TRS Results	
	c'_{fs}, kPa	φ'_{fs}, degrees	c'_{fs}, kPa	φ'_{fs}, degrees
Control Soil	0.0	27.0	0.0	26.8
20%compost Treated Soil	13.1	26.9	0.0	31.2
4%lime+0.30%fibers Treated Soil	34.8	33.5	0.0	35.1
8%lime+0.15%fibers Treated Soil	29.0	35.4	0.0	34.9
8%lime Treated Soil	21.9	36.6	0.0	32.2

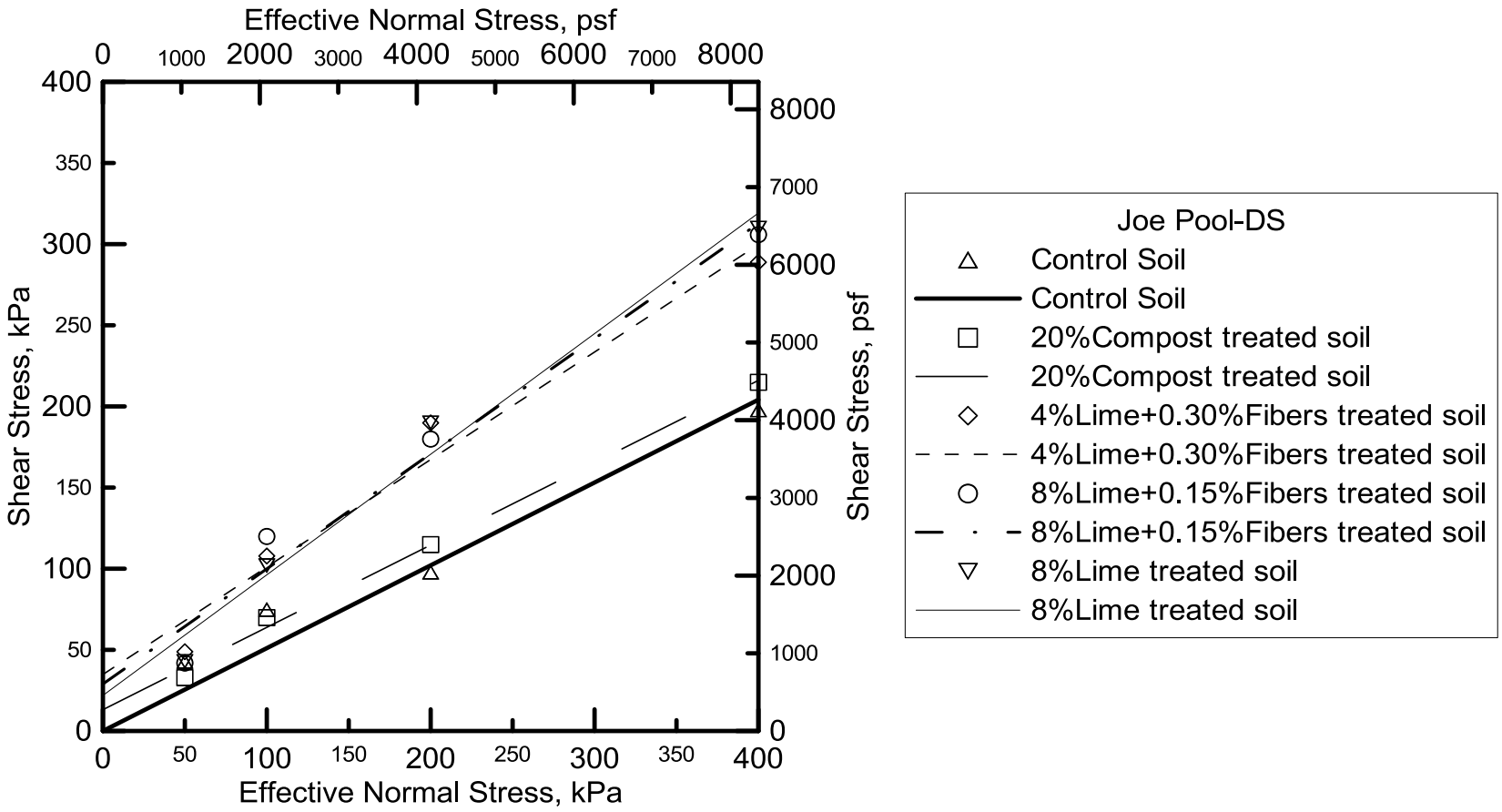

Figure 5.29. FSS Strength envelopes by DS for the Joe Pool Dam soils

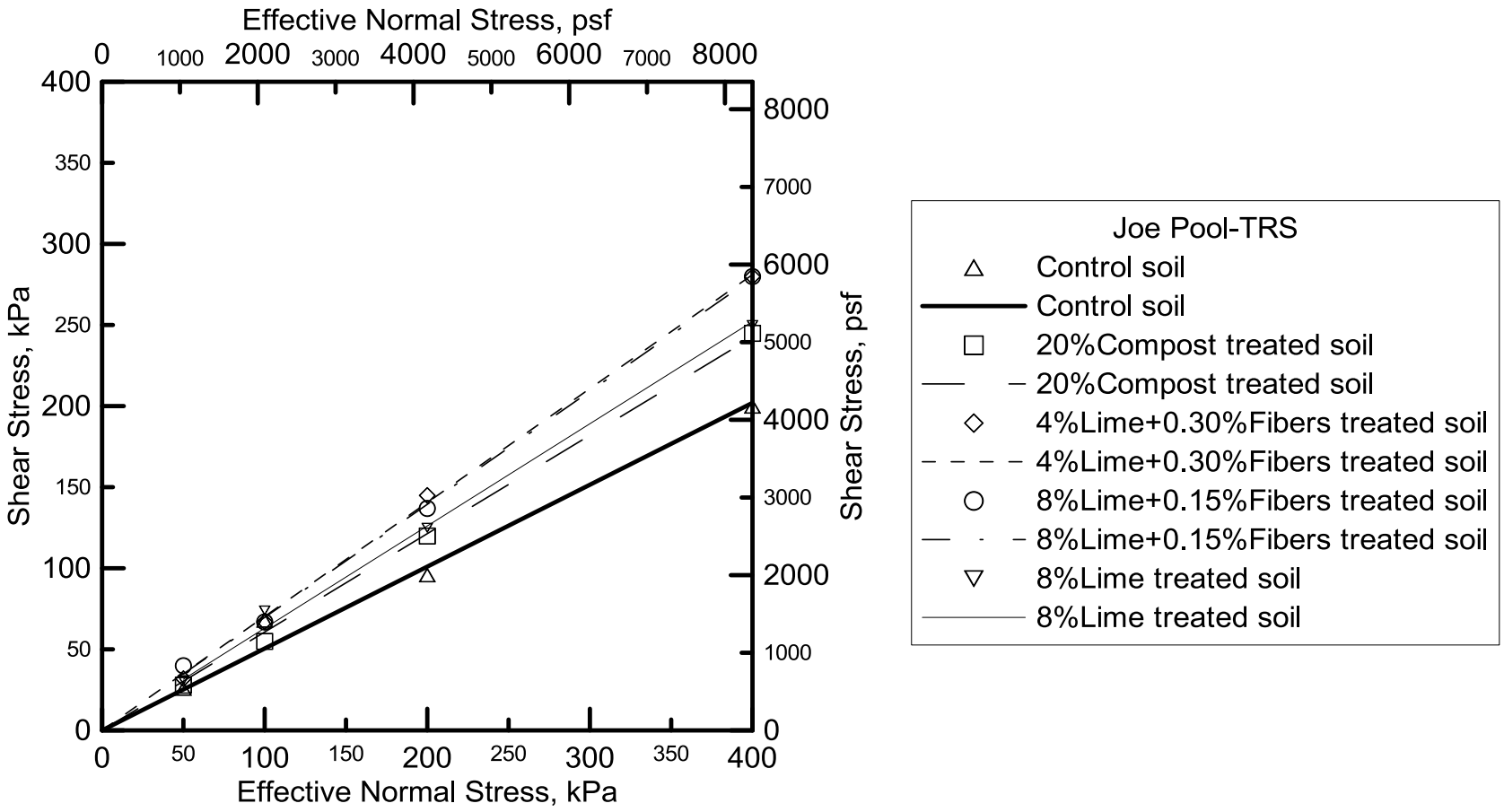

Figure 5.30. FSS Strength envelopes by TRS for the Joe Pool Dam soils

Direct Shear results

Based on the results, it can be concluded that all soil treatments improved soil strength. Results of 4%lime+0.30%fibers, 8%lime+0.15%fibers and 8%lime treated soils showed that both FSS friction angle (φ'_{fs}) and FSS cohesion intercepts (c'_{fs}) were improved while the 20% Compost treatment resulted in enhancement of FSS cohesion but reduction of the FSS friction angle of the soil.

All lime treated soils exhibited significant improvement in FSS cohesion intercept (c'_{fs}) by the stabilizers with a maximum FSS cohesion of 34.8 kPa (726.8 psf) obtained for 4%lime+0.30%fibers treatment. In the case of FSS friction angle (φ'_{fs}), 4%lime+0.30%fibers, 8%lime+0.15%fibers and 8%lime treatments showed the most improvements by enhancing this value by 20-35% when compared to the same of the untreated soil.

Torsional Ring Shear results

Contrary to the DS results, the TRS testing did not show improvement in cohesion in any of the treatment additives as all strength envelopes passed through the origin indicating the absence of FSS cohesion (c'_{fs}). Nevertheless, the admixtures displayed considerable improvement on FSS friction angle (φ'_{fs}) over the control soil with the slopes of the strength envelope for the treated soils steeper than the solid line representing control soil as shown in Figure 5.30.

It was found that the stabilizers increased the FSS friction angle (φ'_{fs}), of the untreated soil by 20-30%. Between all treatments, the 4%lime+0.30%fibers, 8%lime+0.15%fibers provided the greatest FSS friction (φ'_{fs}), followed by 8%lime and 20%compost additives.

5.3.2.2 Grapevine Dam Soil

Figure 5.31 and Figure 5.32 show the FSS strength envelopes by the DS and TRS results for the Grapevine Dam untreated and treated soils. Based on the strength envelope, soil parameters are determined using linear regression analysis. Values of FSS parameters, cohesion (c'_{fs}) and friction angle (φ'_{fs}) are determined and presented in Table 5.7.

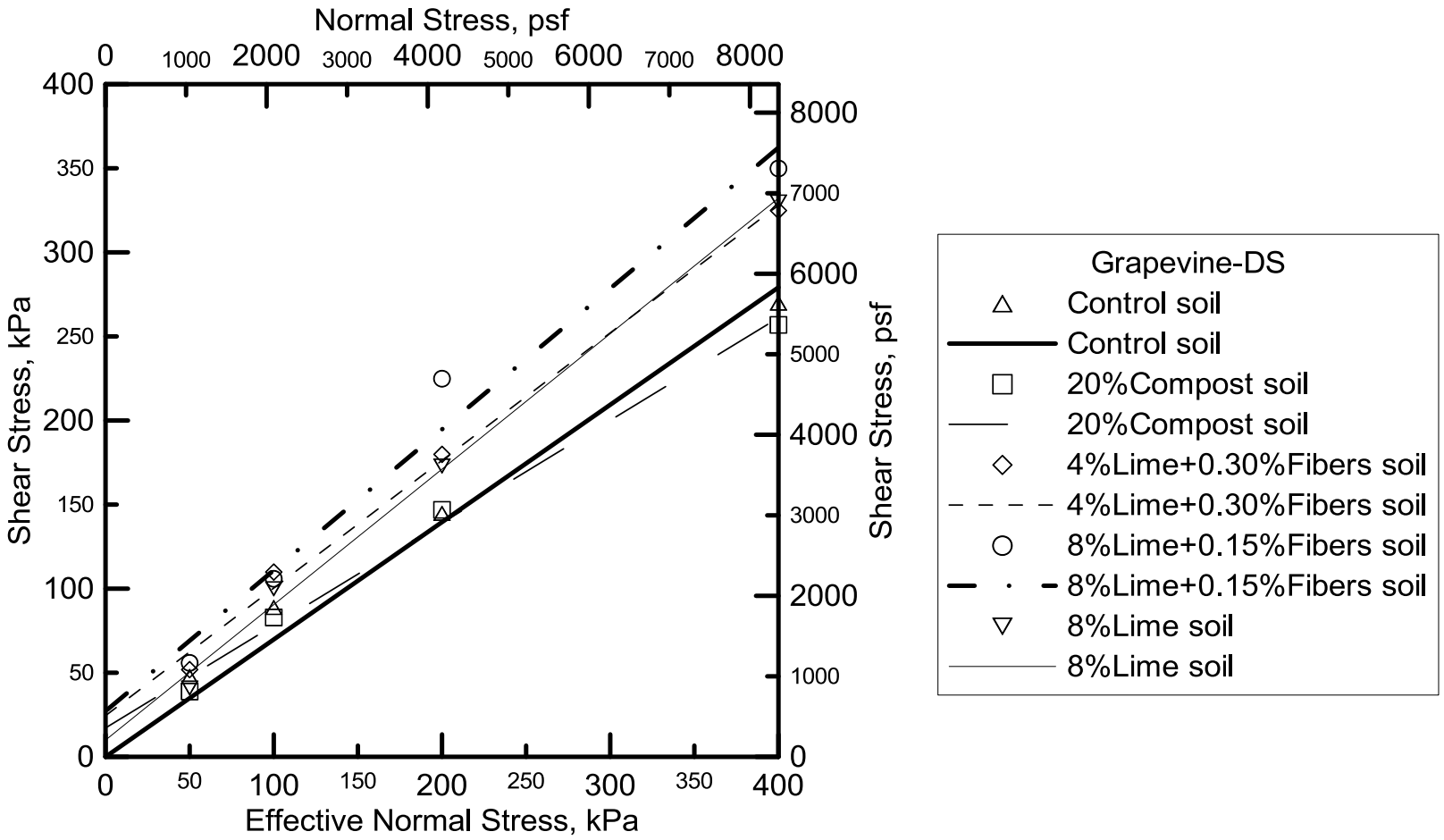

Figure 5.31. FSS strength envelopes by DS for the Grapevine Dam soils

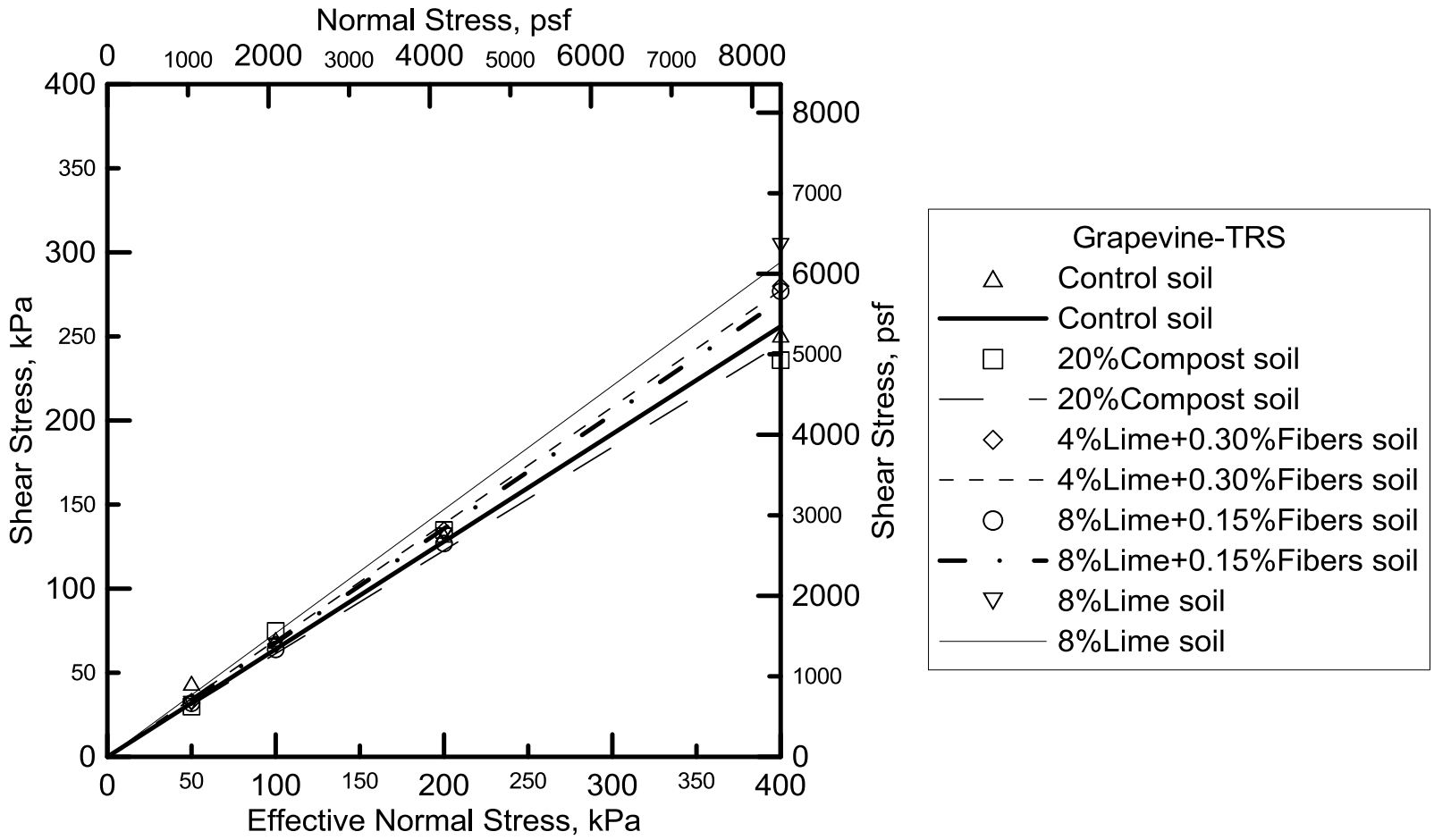

Figure 5.32. FSS strength envelopes by TRS for the Grapevine Dam soils

Table 5.7. Fully Softened Shear Strength Parameters determined from Direct Shear and Torsional Ring Shear tests for the Grapevine Dam soils

Soil	DS Results		TRS Results	
	c'_{fs}, kPa	φ'_{fs}, degrees	c'_{fs}, kPa	φ'_{fs}, degrees
Control Soil	0.0	34.8	0.0	32.6
20%compost Treated Soil	17.2	31.4	0.0	31.5
4%lime+0.30%fibers Treated Soil	24.5	37.2	0.0	34.7
8%lime+0.15%fibers Treated Soil	27.2	40.0	0.0	34.2
8%lime Treated Soil	10.0	38.9	0.0	36.3

.

Direct Shear Results

Failure envelope results clearly showed the improvement of admixtures over the control untreated soil. The FSS cohesion (c'_{fs}) enhancement was observed as this parameter ranged from 10 kPa (209 psf) to 25 kPa (1044 psf), which is considered a significant improvement as this value will be a vital role in strengthening the soil against slope instability under rainfall conditions.

However, the FSS friction angle increase is more subtle when compared to the Joe Pool Dam soil test results as all the treatments except 20%compost provided almost identical friction angle value similar to that of the control soil. Percent of increase of FSS friction angle approximately ranges from 8-15%.

Overall, 4%lime+0.30%fibers, 8%lime+0.15%fibers soils did perform the best in these tests based on both FSS cohesion (c'_{fs}) and FSS friction angle property enhancement aspects. 8%lime treatment improved the FSS friction angle of the soil but did not provide much of FSS cohesion compared to other admixtures. The 20%compost treatment helped the soil gain more

cohesion but reduced the FSS friction angle (φ'_{fs}), similar to the results of the Joe Pool Dam soil that was discussed earlier in this Chapter.

Torsional Ring Shear Results

Comparing the results from the Joe Pool Dam soil, similar observations can be made for the Grapevine Dam soils. FSS cohesion property enhancements are minimal in these test results. The effect of stabilizers was seen more in terms of FSS friction angle. However, not all the treated soil increased the friction of the soil as shown in Figure 5.32. The result of the 20% compost treated soil indicated that it underperformed the control soil resulting in the deduction of FSS friction angle (φ'_{fs}) from 32.6 kPa (681.3 psf) to 31.5 kPa (658.7 psf). 8% Lime provided the most enhancements to FSS friction angle among all treatments with a 10% increase of the FSS friction angle of the control soil.

Based on the results of the Joe Pool Dam and Grapevine Dam soils, it could be concluded that test results from the TRS device are slightly less when compared to the test results using the DS device. Moreover, the absence of cohesion in the TRS result of FSS strength may result in the underestimation of the FSS of the soil, which could reduce the factor of safety values for slope under heavy rainfall condition.

5.4 Summary and Conclusions

Based on the testing data, the FSS results of the Joe Pool Dam and Grapevine Dam soils displayed consistency in terms of numerical values for shear strength between all the treatment additives. The peak shear strength was mobilized at a minimum shear displacement of 4 mm for the DS test and 2 mm for the TRS test on soils from both sites. At higher effective normal stresses, the higher horizontal displacement was required to achieve the plateau condition than at lower effective normal stresses. Comparing between all stabilizers, lime treated soil did experience more horizontal displacement strain than the 20%compost treated soil as well as the untreated soil at any effective normal stresses. Also it could be concluded

that as the effective normal stresses increased, changes of shear strength became more distinguishable between untreated and treated soil.

Testing results are analyzed with linear regression analysis to interpret the FSS soil parameters from the strength envelope as suggested by Stark (2008) for soils that are not prone to have stress-dependent failure envelopes.

Tiwari (2011) conducted a research on correlating relating the FSS of reconstituted soil to the clay mineral content. Results for the FSS friction angle (φ'_{fs}) of the control soils from Joe Pool Dam and Grapevine Dam were compared to Tiwari's empirical equations as shown in Figure 5.33. The four points proved fairly close to the prediction of Tiwari's study.

Between the two testing methods, the DS results provided higher values for the FSS than those obtained by using the TRS device. This is in agreement with the majority of studies conducted by the past researchers:

- Castelanos et al. (2013) recommended the use of DS for measurement of the FSS. In his study, the FSS results using the TRS were lower than those determined using the DS apparatus, with the difference being greatest at low effective normal stresses. Furthermore, he suggested that the difference between the results of the two apparatus may be due to the small test specimen thickness of the TRS device with less than 5 mm thickness after consolidation. It also could be attributed to the proximity of the failure plane to the top platen in the Bromhead TRS device. In the TRS apparatus, the failure plan was observed to be close to the top platen while in DS device the failure plane was located at about 0.5 in (12 mm) from the end platen. Hvorslev (1960) also highlighted the effect of failure plane proximity to the end platens as well as the platen roughness on the test outcomes.
- Tiwari (2011) pointed out that the ring shear device is not considered a suitable device to capture the FSS due to the unequal shear strains at the inner and outer edges of the annular soil specimens. Bishop et al. (1971) and La Gatta (1970) suggested that the nonuniformity of shear displacements radially across the specimen in TRS mold affects the

measurement of the shear stress. Tiwari and Marui (2004) in their study concluded that the shearing process in the TRS device significantly changed the particle degradation.

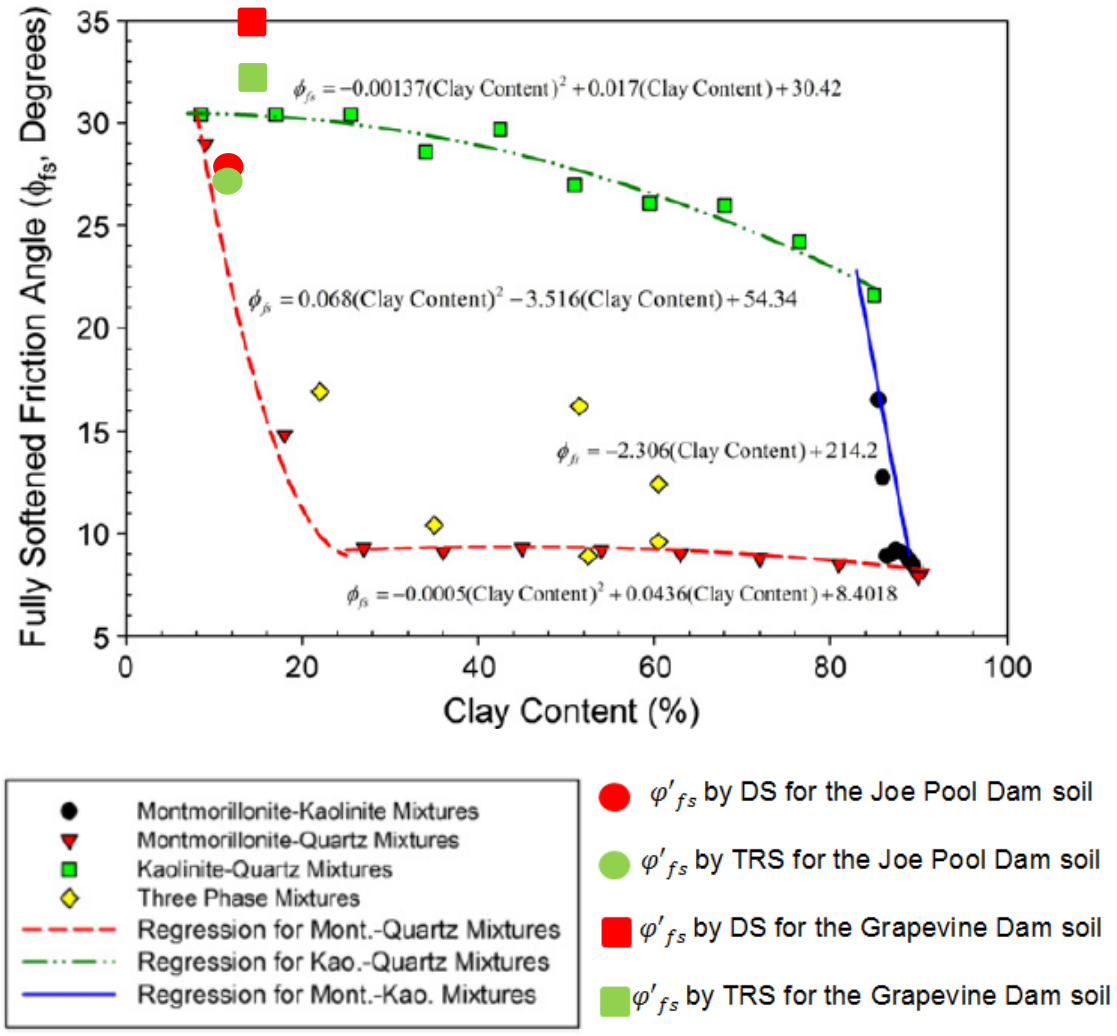

Figure 5.33. Variation of the FSS friction angle with the clay mineral content (Tiwari et al., 2011)

It should also be mentioned that the area of soil-to-soil contact during the shearing process may affect the FSS testing results. **Error! Reference source not found.** shows the reduction of contact area transpiring during the DS testing. Shear displacement (horizontal displacement) was captured at 0.1 to 0.5 in. magnitude with 0.1 in. increment along with the corresponding contact area of soil between the two halves of the DS shear box. The reduction follows the linear trend as shown in Figure 5.35. With the reduction of the soil contact area and

constant normal load, the normal stress induced on the soil increased and hence could yield higher shear stress as a consequence.

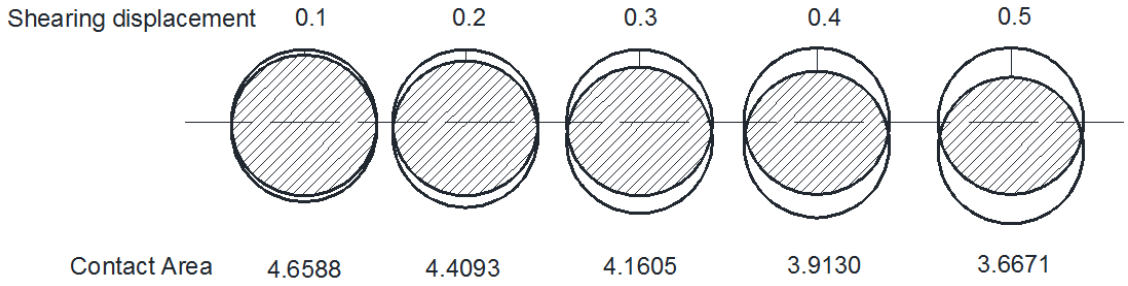

Figure 5.34. Contact area reduction in DS device during shearing

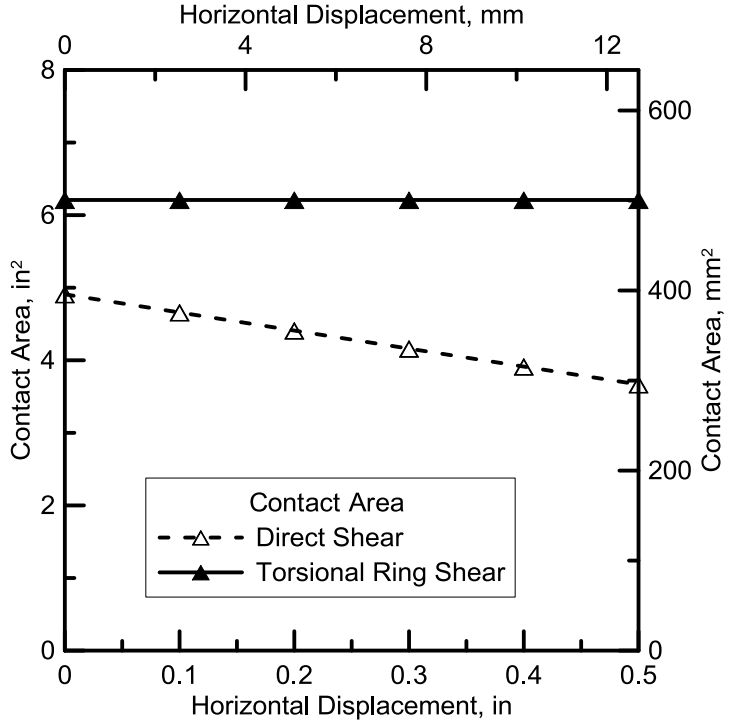

Figure 5.35. Contact area comparison between DS and TRS devices during shearing

The DS results were able to show the improvement in the cohesion aspect while the TRS did not provide such information. It was hypothesized that the 5 mm sample thickness of the TRS device, which helped speed up the consolidation process, affected the FSS cohesion of soil body as compared to 25.4 mm (1 in.) thickness of the sample in the DS machine. On the other hand, it could be attributed to the proximity of shearing zone to the top platen and the top

platen's roughness resulting in the top platen slipping on the soil surface during testing. Thus, this has resulted in impacting the contact area of soil to soil. Figure 5.36 presents the schematic of ring shear test mechanism for Bromhead TRS apparatus as depicted by Sadrekarimi and Olson (2009).

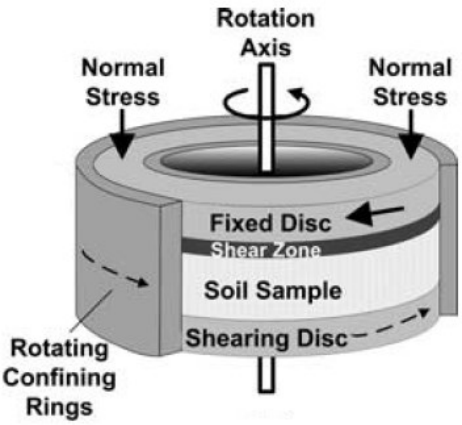

Figure 5.36. Shear Zone in Bromhead TRS device (Sadrekarimi and Olson, 2009)

Since the improvement of cohesion was not properly observed in the TRS results, the effect of side friction of this device cannot be fully explained. Also the strains imposed during TRS testing for FSS conditions are much higher than those induced in DS testing due to the difference of sample thickness that could have affected the results.

As the majority of researchers, including Castellanos et al. (2013), Tiwari et al. (2011) and Skempton (1985) have recommended the use of the DS machine for the FSS testing, a total of 80 tests of FSS tests using the DS device were incorporated for analytical modeling and reliability studies in Chapter 7.

CHAPTER 6

STATISTICAL ANALYSIS OF FIELD MONITORING DATA

6.1 Introduction

In Chapter 4, field monitored data was compiled and reduced to month wise data. In this chapter, these results are analyzed with statistical analysis tools. Statistical analysis is mainly performed to study the significant differences of field performance data between untreated and treated soils. Performance data including embedded soil temperature, soil moisture content as well as soil movements in both lateral and horizontal directions collected from the inclinometer and elevation surveys is analyzed.

The Student's t-test using the Dunnett's procedure was chosen as the comparison test to carry out this analysis based on the amount of data points collected during the years of monitoring. A t-test is a statistical hypothesis test in which the test statistic follows a Student's t distribution to evaluate if the null hypothesis is supported. With the ability to compare multiple treatments at the same time, t-test using the Dunnett's procedure, can determine if the treatment effects induce a significance difference in the field performance characteristics of the treated soils with those of the control soil.

In using the t-test procedure we make the assumption that samples drawn from independent populations can be interpreted by a normal distribution. Normality of a sample can be tested using various methods; one of them is the graphical interpretation through probability plot. Probability plotting is a graphical technique for determining whether sample data conforms to a hypothesized distribution based on a subjective visual examination of the data. The normality test procedure was described in Montgomery's "Design and Analysis of Experiments" (5th Edition, 2000). First, the observations are ranked from smallest to largest. For example the sample $y_1, y_2 \ldots, y_n$ is arranged as $y_{(1)}, y_{(2)} \ldots y_{(n)}$ where $y_{(1)}$ is the smallest observation and $y_{(n)}$

is the largest. The ordered observations are then plotted against their observed frequency $(j-0.5)/n$, also known as the cumulative normal probability. The cumulative frequency scale has been arranged so that if the hypothesized distribution adequately describes the data, the plotted points will fall approximately along a straight line; if the plotted points deviate significantly from a straight line, the hypothesized model is not appropriate. Figure 6.1 illustrates an example of adequate evidence for data normal distribution as described by Montgomery (2000).

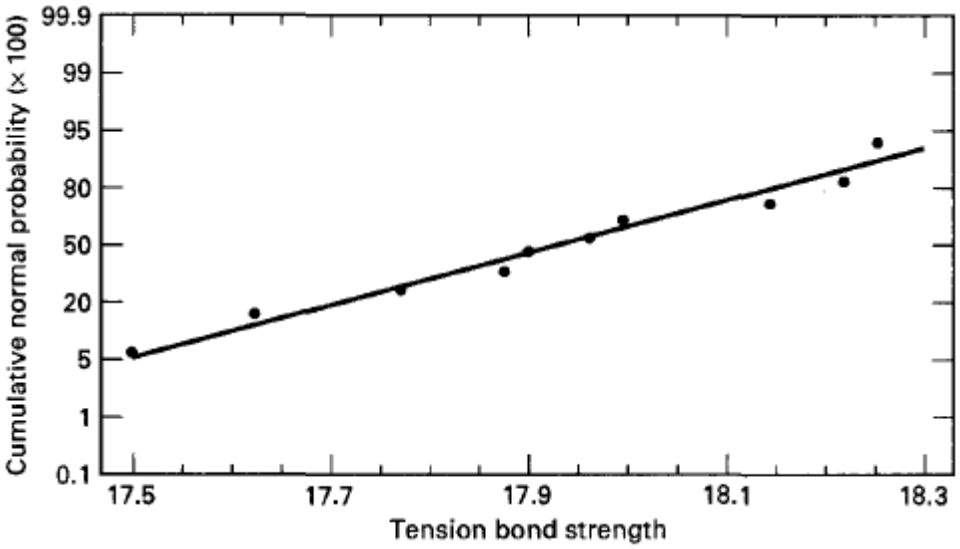

Figure 6.1. Normality probability plot of tension bond strength in the Portland cement experiment (Montgomery, 2000)

After the normality is confirmed for the presented data, the student's t-test using the Dunnett's procedure can be executed. The Dunnett's procedure was described by Montgomery (2000). Suppose we have a treatments we wish to compare. The observed response from each of the a treatments is a random variable. A statistical hypothesis may be stated formally as:

$$H_o: \mu_i = \mu_a \qquad \text{Eq. 6-1}$$

$$H_1: \mu_i \neq \mu_a \qquad \text{Eq. 6-2}$$

Where μ_a is the mean value of the "control" and μ_i is the mean value of the i-th treatment.To initiate the analysis, the data would be first tabulated as in Table 6.1.

Table 6.1. Typical Data for a Single-Factor Experiment (Montgomery, 2000)

Treatment (level)	Observations				Totals	Averages
1	y_{11}	y_{12}	$\cdots$	y_{1n}	$y_{1.}$	$\bar{y}_{1.}$
2	y_{21}	y_{22}	$\cdots$	y_{2n}	$y_{2.}$	$\bar{y}_{2.}$
$\vdots$	$\vdots$	$\vdots$	$\cdots$	$\vdots$	$\vdots$	$\vdots$
a	y_{a1}	y_{a2}	$\cdots$	y_{an}	$y_{a.}$	$\bar{y}_{a.}$
					$y_{..}$	$\bar{y}_{..}$

where

a is the number of treatments. In this research, there are five sections including one untreated and four treated soil sections representing five different treatments. A control section was termed as a "control" or untreated section, thus all the results of other treated sections are analyzed by comparing their results with the "control".

y_{ij} is an entry representing the j-th observation taken under factor level or treatment i. Observations are readings taken from the equipment and sensors embedded in the field. Slope movements (horizontal and vertical directions), soil moisture content (from the top and bottom probes), soil temperature (from thermocouple) are the parameters analyzed in this research.

n represents the number of observations for each treatment. In general there will be the same number of observations for each type of treatments.

$y_{i.}$ is the total number of the observations under the i-th treatment:

$$y_{i.} = \sum_{j=1}^{n} y_{ij} \qquad \text{Eq. 6-3}$$

$\bar{y}_{i.}$ is the average of the observations under the i-th treatment:

$$\bar{y}_{i.} = y_{i.}/n \quad \text{Eq. 6-4}$$

$y_{..}$ is the grand total of all the observations:

$$y_{..} = \sum_{i=1}^{a}\sum_{j=1}^{n} y_{ij} \quad \text{Eq. 6-5}$$

$\bar{y}_{..}$ is the grand average of all the observations:

$$\bar{y}_{..} = \frac{y_{..}}{N} \quad \text{Eq. 6-6}$$

N is the total number of observations:

$$N = n \times a \quad \text{Eq. 6-7}$$

For $i = 1,2, \dots, a-1$ comparisons, we form an individual hypothesis for each comparison test. In each hypothesis, we compute the observed differences in the average of the observations $|\bar{y}_{i.} - \bar{y}_{a.}|$

The null hypothesis $H_o: \mu_i = \mu_a$ is rejected using a type I error with significance level α if:

$$|\bar{y}_{i.} - \bar{y}_{a.}| > d_\alpha(a-1, f) \times \sqrt{MS_E \times \left(\frac{1}{n_i} + \frac{1}{n_\alpha}\right)} \quad \text{Eq. 6-8}$$

where

$d_\alpha(a-1, f)$ is the critical values for the Dunnett's test, which is provided in a Table format with f as a degree of freedom.

The critical values of $d_\alpha(a-1, f)$ for value of significance level $\alpha = 0.05$ can be found from Montgomery (2000). The significance level α represents the probability of incorrectly rejecting the null hypothesis $H_o: \mu_i = \mu_a$ when it is true. The lower the significance level, the more the data must diverge from the null hypothesis to be significant. Generally, researchers use 0.05 (5%) as an adequate number for significance level (Montgomery, 2000).

MS_E is the mean square error and can be calculated as:

$$MS_E = \frac{SS_E}{a \times (n-1)} \quad \text{Eq. 6-9}$$

SS_E is called the sum of squares due to error. SS_E can be determined through the Analysis of Variance (ANOVA). ANOVA is a collection of statistical models, which provides a statistical test of whether or not the means of several groups are significantly different. Table 6.2 shows a typical ANOVA table with all the necessary components.

Table 6.2. ANOVA table for Single-Factor, Fixed Effects Model (Montgomery, 2000)

Source of Variation	Sum of Squares	Degrees of Freedom	Mean Square	F_0
Between treatments	$SS_{\text{Treatments}} = n\sum_{i=1}^{a}(\bar{y}_{i.} - \bar{y}_{..})^2$	$a - 1$	$MS_{\text{Treatments}}$	$F_0 = \frac{MS_{\text{Treatments}}}{MS_E}$
Error (within treatments)	$SS_E = SS_T - SS_{\text{Treatments}}$	$N - a$	MS_E	
Total	$SS_T = \sum_{i=1}^{a}\sum_{j=1}^{n}(y_{ij} - \bar{y}_{..})^2$	$N - 1$		

where

SS_T is the total corrected sum of squares:

$$SS_T = \sum_{i=1}^{5}\sum_{j=1}^{n_i} y_{ij}^2 - \frac{y_{..}^2}{N} \qquad \text{Eq. 6-10}$$

$SS_{Treatments}$ is the sum of squares due to treatments (i.e., between treatments):

$$SS_{Treatments} = \sum_{i=1}^{5}\frac{y_{i.}^2}{n_i} - \frac{y_{..}^2}{N} \qquad \text{Eq. 6-11}$$

$$SS_E = SS_T - SS_{Treatments} \qquad \text{Eq. 6-12}$$

In this chapter, all the field data collected previously are first checked for normality to assure the validity of t-test. The student's t-test using the Dunnett's procedure is then utilized to compare the performance of the control soil with each of the treated amendments for significant difference induced by the treatment. A total of 4 field performance categories are analyzed including soil moisture, soil temperature and soil movement (horizontal and vertical directions) data. First, data points from each category are tabulated as presented in Table 6.1. Based on the tabulated values, ANOVA components are then calculated to determine the mean square

error MS_E as shown in Table 6.2. Value of the critical value $d_\alpha(a-1, f)$ can be found by using the Appendix table provided by Montgomery (2000) with the corresponding degree of freedom f and default significance level $\alpha = 0.05$. This value is used with the mean square error MS_E to calculate the critical difference $d_\alpha(a-1, f)\sqrt{MS_E\left(\frac{1}{n_i}+\frac{1}{n_\alpha}\right)}$. Mean value differences between the performance of the control soil and each of the treatment amendments are compared with the critical difference value to detect the presence of significant differences.

For the sake of simplicity, test results are presented in tabular forms starting with the normality check for each of the field data categories.

6.2 Normality Check

Normality checks were performed on the field data as a preliminary requirement to conduct Student's t-test. Observations (data points) were first sorted from the smallest to largest and plotted against their corresponding cumulative normal probability. Figures 6.1 to 6.13 present the normality checks for the Joe Pool Dam and Grapevine Dam soil moisture content, soil temperature, soil vertical movement and soil horizontal movement. Due to the limitation of space, only results of one treated section (8%lime+0.15%fibers) along with the untreated section are presented for each dam site. The remaining results for other sections can be found in the Appendix A section.

Best fit trend lines were drawn along with the statistical report of coefficient of determination R^2, to describe how well the regression lines fitted the data.

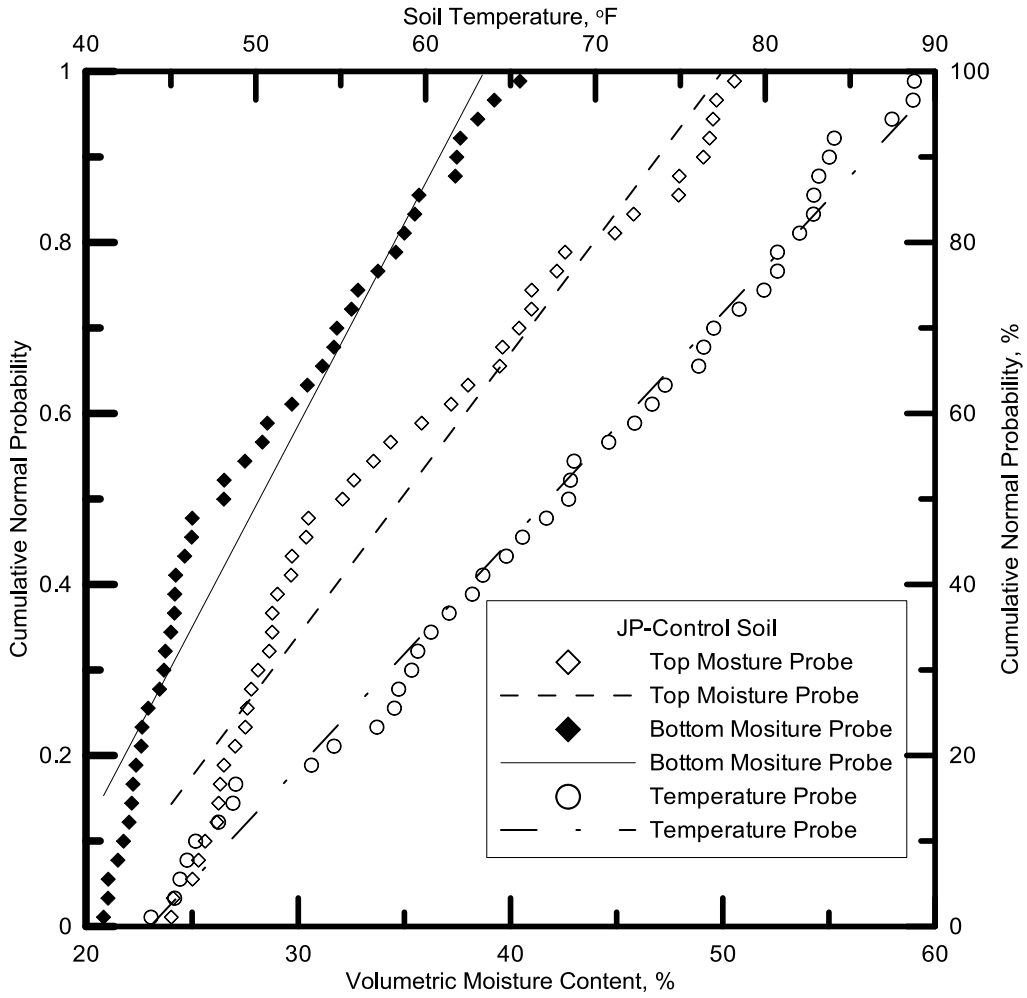

Fit Results

Top Moisture Probe
Equation Y = 0.03299610879 * X - 0.6493237767
Number of data points used = 45
Average X = 34.8321
Average Y = 0.5
Residual sum of squares = 0.204234
Regression sum of squares = 3.54391
Coef of determination, R-squared = 0.945511
Residual mean square, sigma-hat-sq'd = 0.00474964

Fit Results

Bottom Mositure Probe
Equation Y = 0.04723136615 * X - 0.8306997652
Number of data points used = 45
Average X = 28.1741
Average Y = 0.5
Residual sum of squares = 0.200546
Regression sum of squares = 3.5476
Coef of determination, R-squared = 0.946495
Residual mean square, sigma-hat-sq'd = 0.00466386

Fit Results

Temperature Probe
Equation Y = 0.02128296119 * X - 0.9316775542
Number of data points used = 45
Average X = 67.2687
Average Y = 0.5
Residual sum of squares = 0.0328893
Regression sum of squares = 3.71526
Coef of determination, R-squared = 0.991225
Residual mean square, sigma-hat-sq'd = 0.000764867

Figure 6.2 Normality check for soil moisture and temperature of the Joe Pool Dam Control soil

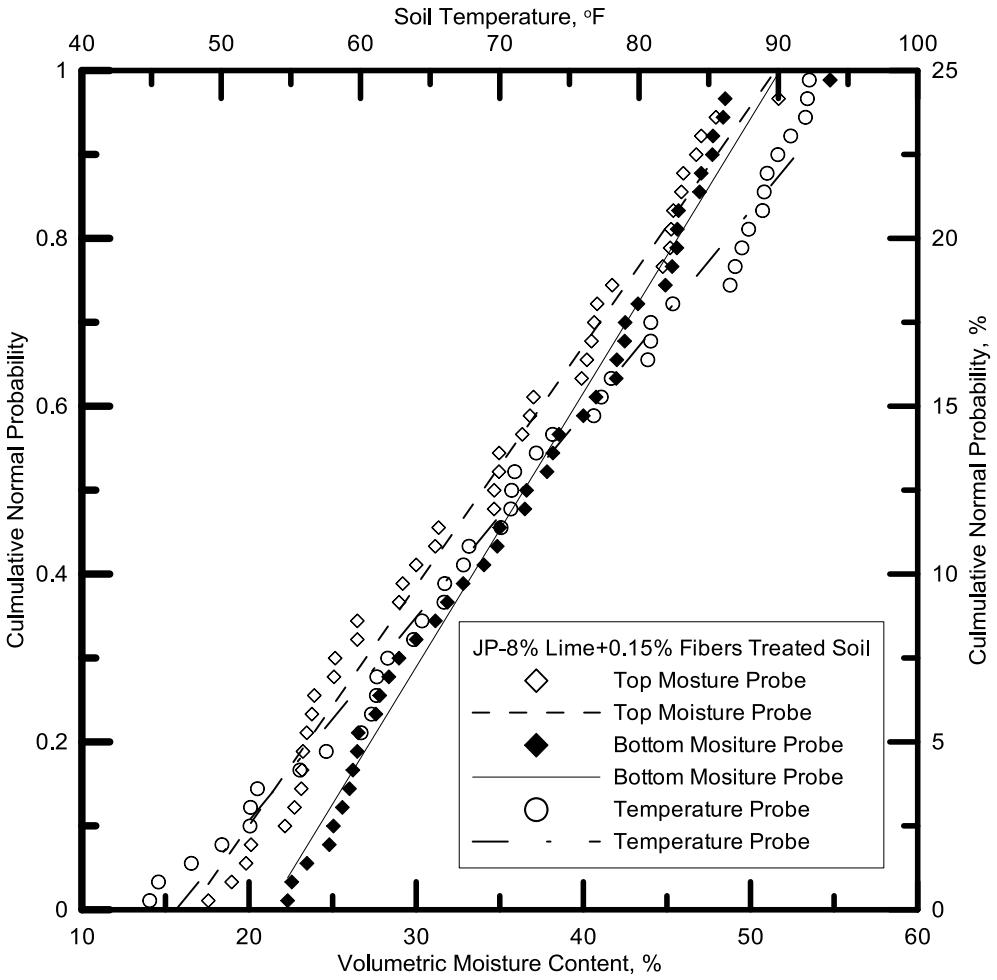

Fit Results

Top Moisture Probe
Equation Y = 0.02857505069 * X - 0.4713134432
Number of data points used = 45
Average X = 33.9917
Average Y = 0.5
Residual sum of squares = 0.0563431
Regression sum of squares = 3.69181
Coef of determination, R-squared = 0.984968
Residual mean square, sigma-hat-sq'd = 0.0013103

Fit Results

Bottom Mositure Probe
Equation Y = 0.0326592172 * X - 0.6904719589
Number of data points used = 45
Average X = 36.4513
Average Y = 0.5
Residual sum of squares = 0.0478625
Regression sum of squares = 3.70029
Coef of determination, R-squared = 0.98723
Residual mean square, sigma-hat-sq'd = 0.00111308

Fit Results

Temperature Probe
Equation Y = 0.02019669069 * X - 0.9440985685
Number of data points used = 45
Average X = 71.5017
Average Y = 0.5
Residual sum of squares = 0.0391318
Regression sum of squares = 3.70902
Coef of determination, R-squared = 0.98956
Residual mean square, sigma-hat-sq'd = 0.000910042

Figure 6.3 Normality check for soil moisture and temperature of the Joe Pool Dam 8%lime+0.15%fibers treated soil

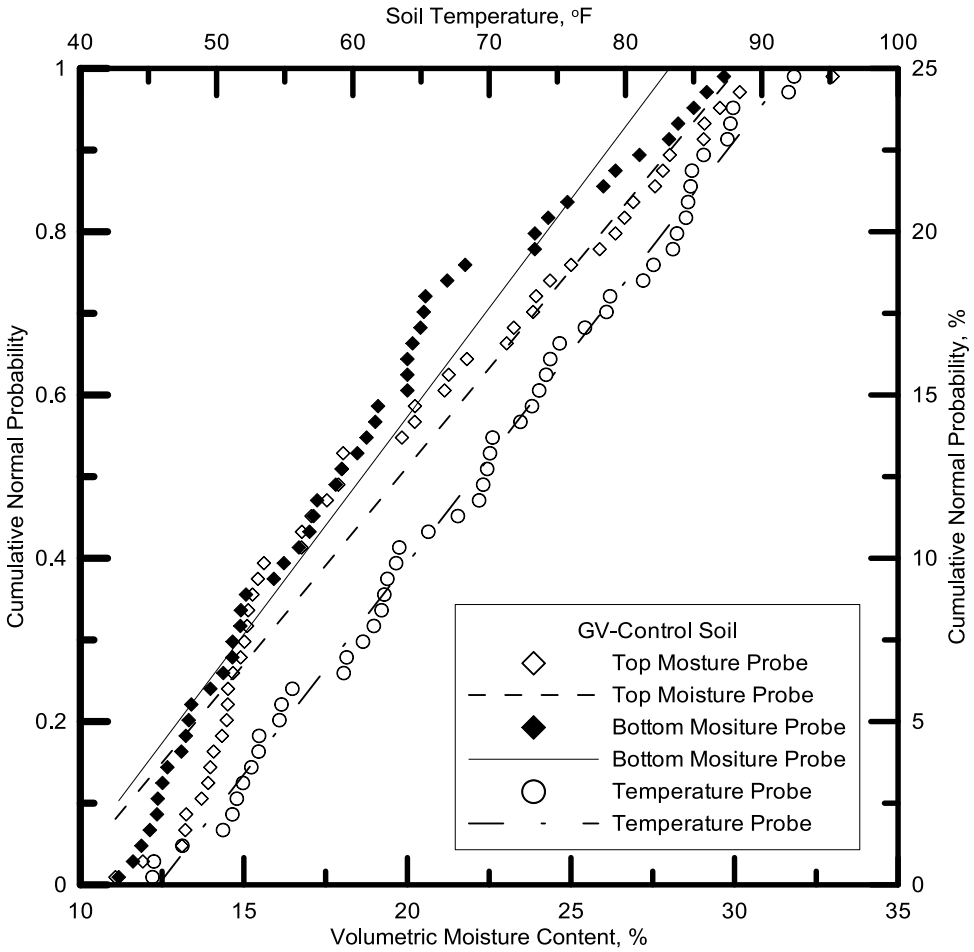

Fit Results

Top Moisture Probe
Equation Y = 0.04830269514 * X - 0.4541730203
Number of data points used = 52
Average X = 19.754
Average Y = 0.5
Residual sum of squares = 0.208185
Regression sum of squares = 4.12355
Coef of determination, R-squared = 0.95194
Residual mean square, sigma-hat-sq'd = 0.0041637

Fit Results

Bottom Mositure Probe
Equation Y = 0.05328795509 * X - 0.4924560926
Number of data points used = 52
Average X = 18.6244
Average Y = 0.5
Residual sum of squares = 0.183992
Regression sum of squares = 4.14774
Coef of determination, R-squared = 0.957525
Residual mean square, sigma-hat-sq'd = 0.00367984

Fit Results

Temperature Probe
Equation Y = 0.0215613031 * X - 0.9859383282
Number of data points used = 52
Average X = 68.9169
Average Y = 0.5
Residual sum of squares = 0.024775
Regression sum of squares = 4.30696
Coef of determination, R-squared = 0.994281
Residual mean square, sigma-hat-sq'd = 0.0004955

Figure 6.4 Normality check for soil moisture and temperature of the Grapevine Dam Control soil

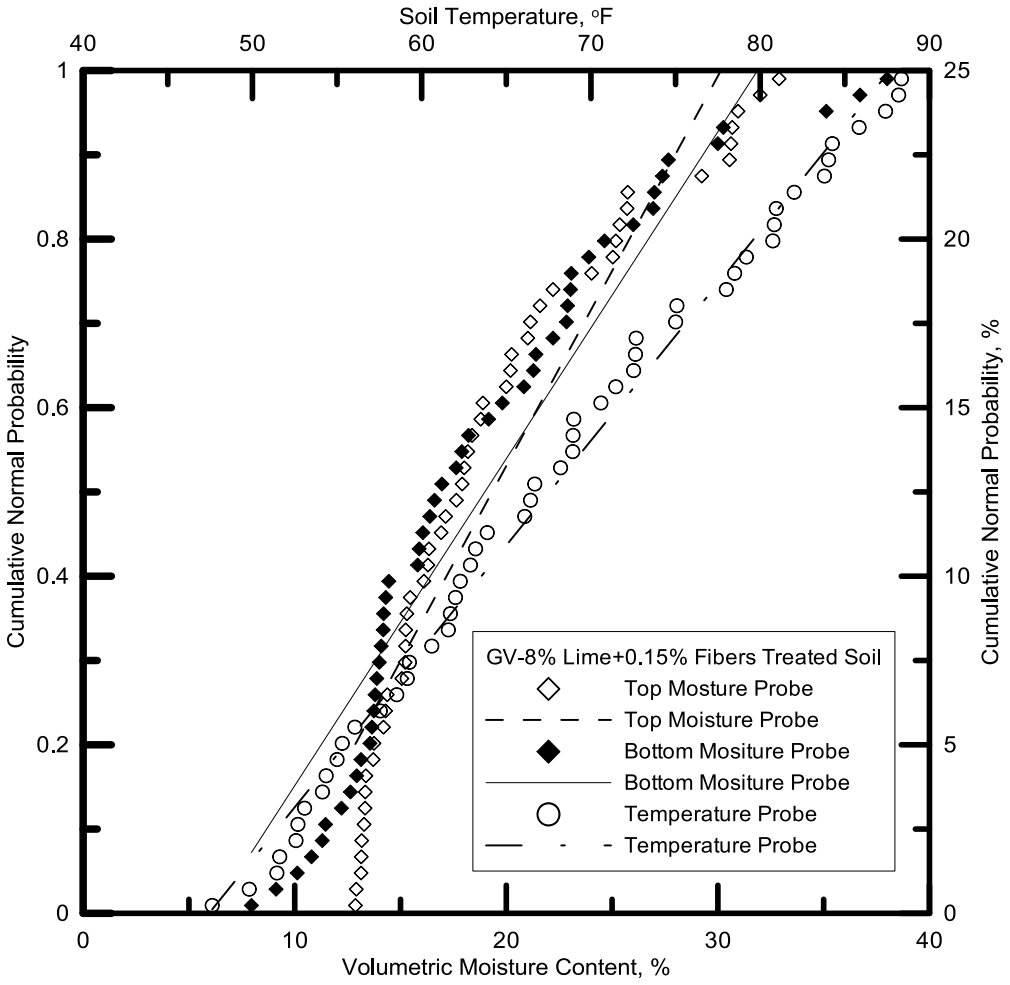

Fit Results

Top Moisture Probe
Equation Y = 0.04625753641 * X - 0.3943568436
Number of data points used = 52
Average X = 19.3343
Average Y = 0.5
Residual sum of squares = 0.442462
Regression sum of squares = 3.88927
Coef of determination, R-squared = 0.897856
Residual mean square, sigma-hat-sq'd = 0.00884924

Fit Results

Bottom Mositure Probe
Equation Y = 0.03879188117 * X - 0.2364124109
Number of data points used = 52
Average X = 18.9837
Average Y = 0.5
Residual sum of squares = 0.398138
Regression sum of squares = 3.93359
Coef of determination, R-squared = 0.908088
Residual mean square, sigma-hat-sq'd = 0.00796275

Fit Results

Temperature Probe
Equation Y = 0.02485746611 * X - 1.179124127
Number of data points used = 52
Average X = 67.5501
Average Y = 0.5
Residual sum of squares = 0.0351146
Regression sum of squares = 4.29662
Coef of determination, R-squared = 0.991894
Residual mean square, sigma-hat-sq'd = 0.000702292

Figure 6.5 Normality check for soil moisture and temperature of the Grapevine Dam 8%lime+0.15%fibers treated soil

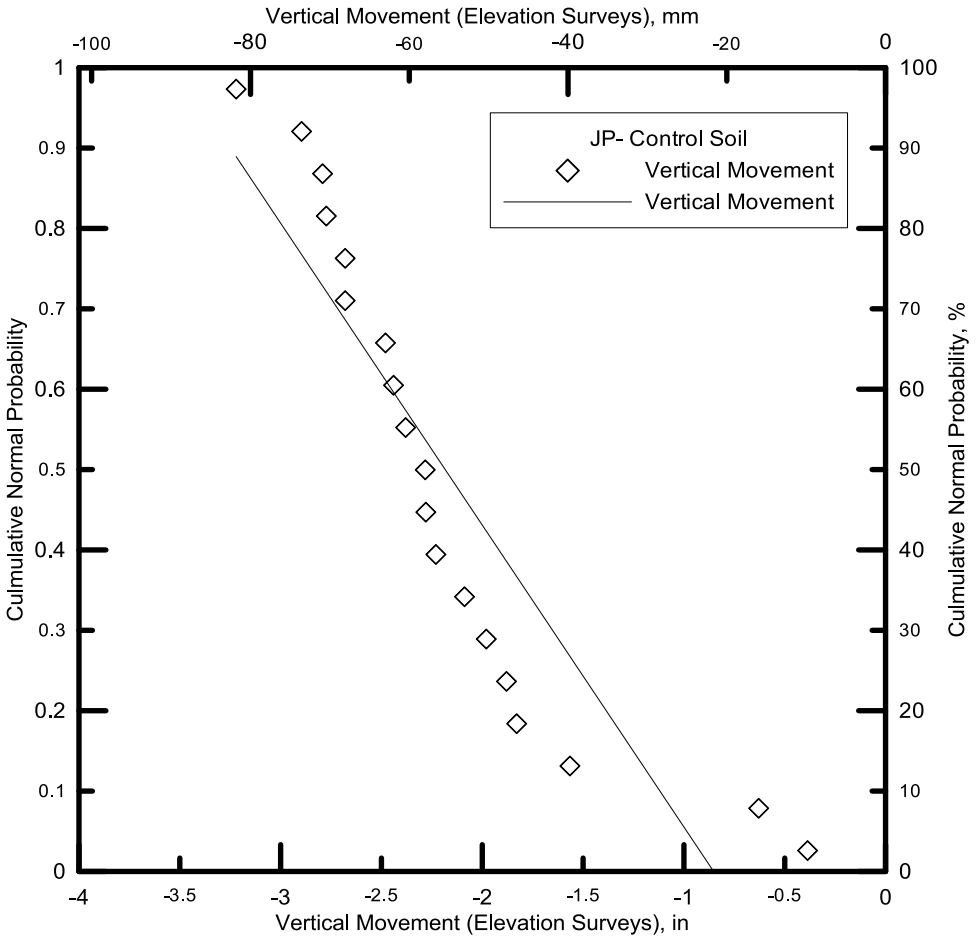

Fit Results

Vertical Movement
Equation Y = -0.3756073965 * X - 0.3202694442
Number of data points used = 19
Average X = -2.18385
Average Y = 0.5
Residual sum of squares = 0.266615
Regression sum of squares = 1.31233
Coef of determination, R-squared = 0.831144
Residual mean square, sigma-hat-sq'd = 0.0156832

Figure 6.6 Normality check for vertical movement of the Joe Pool Dam Control Soil

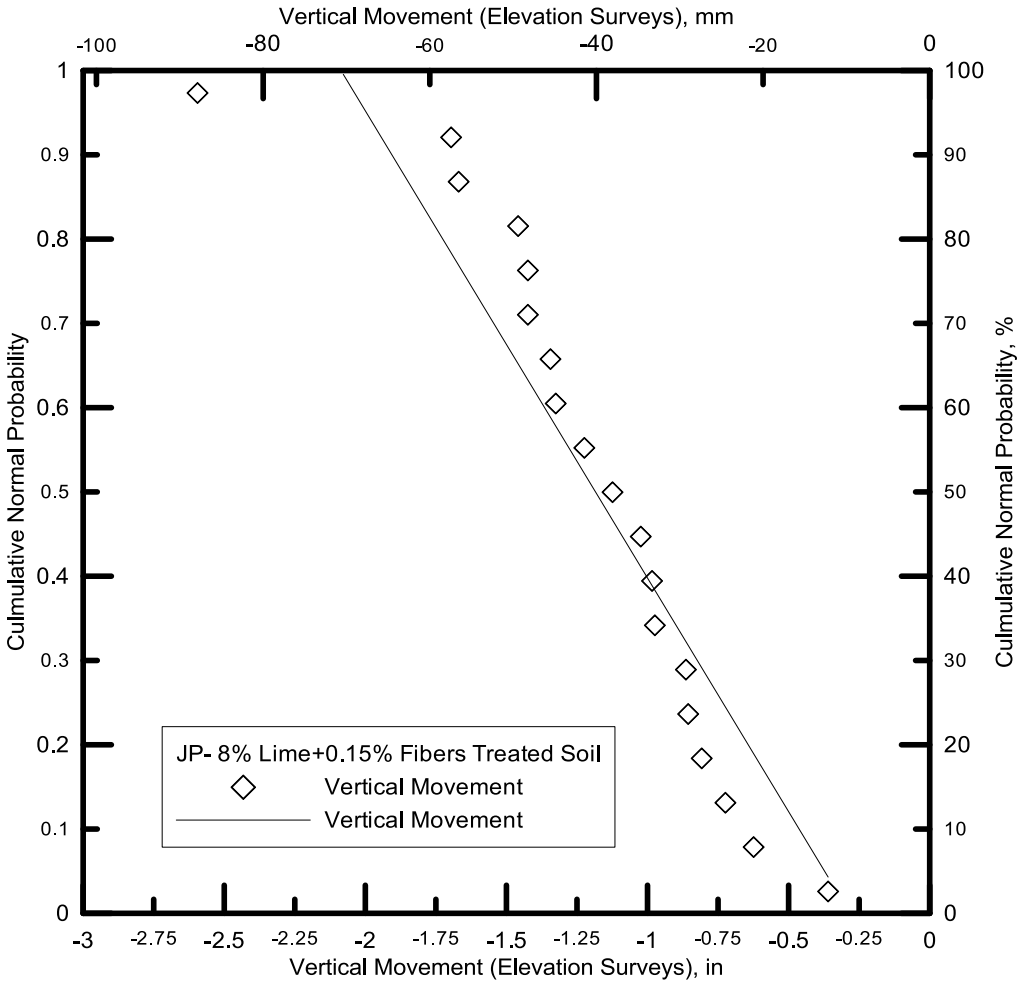

Fit Results

Vertical Movement
Equation Y = -0.5543275374 * X - 0.1564988551
Number of data points used = 19
Average X = -1.18432
Average Y = 0.5
Residual sum of squares = 0.228664
Regression sum of squares = 1.35028
Coef of determination, R-squared = 0.85518
Residual mean square, sigma-hat-sq'd = 0.0134508

Figure 6.7 Normality check for vertical movement of the Joe Pool Dam 8%lime+0.15%fibers Treated Soil

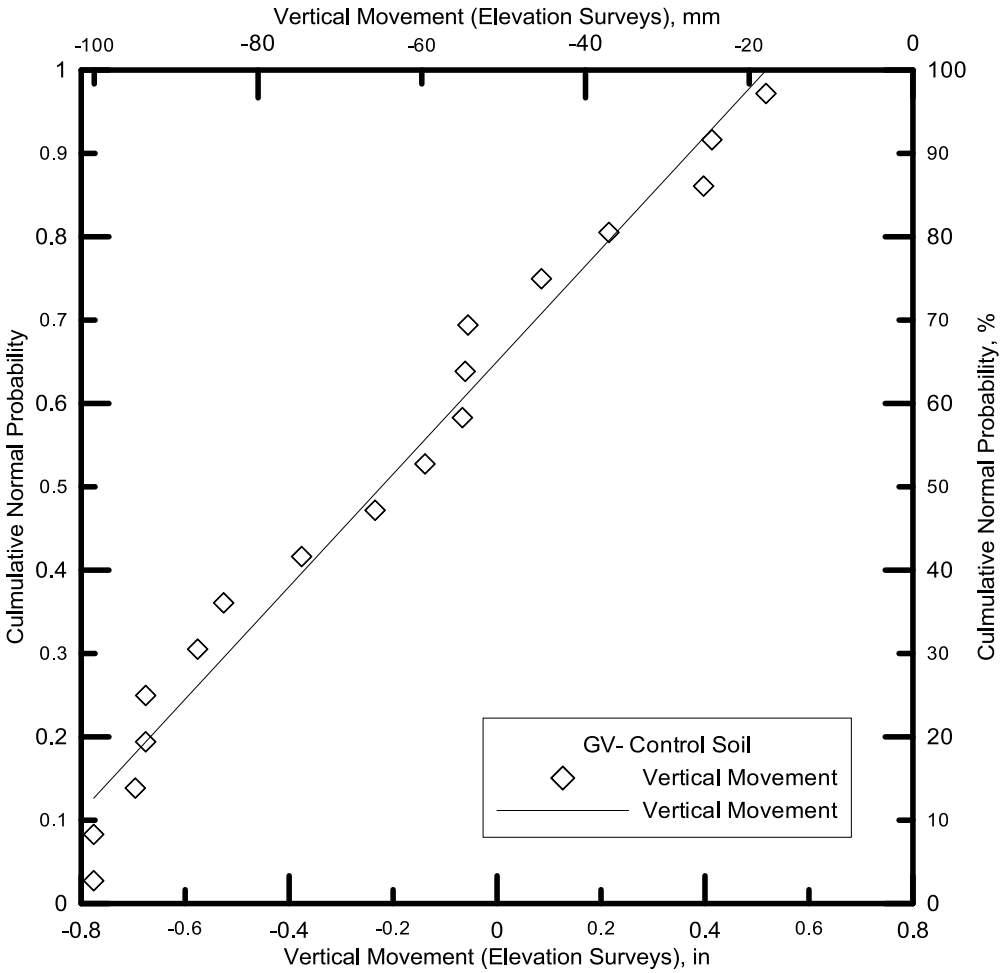

Fit Results

Vertical Movement
Equation Y = 0.6751254076 * X + 0.6502829157
Number of data points used = 18
Average X = -0.2226
Average Y = 0.5
Residual sum of squares = 0.0385523
Regression sum of squares = 1.45682
Coef of determination, R-squared = 0.974219
Residual mean square, sigma-hat-sq'd = 0.00240952

Figure 6.8 Normality check for vertical movement of the Grapevine Dam Soil

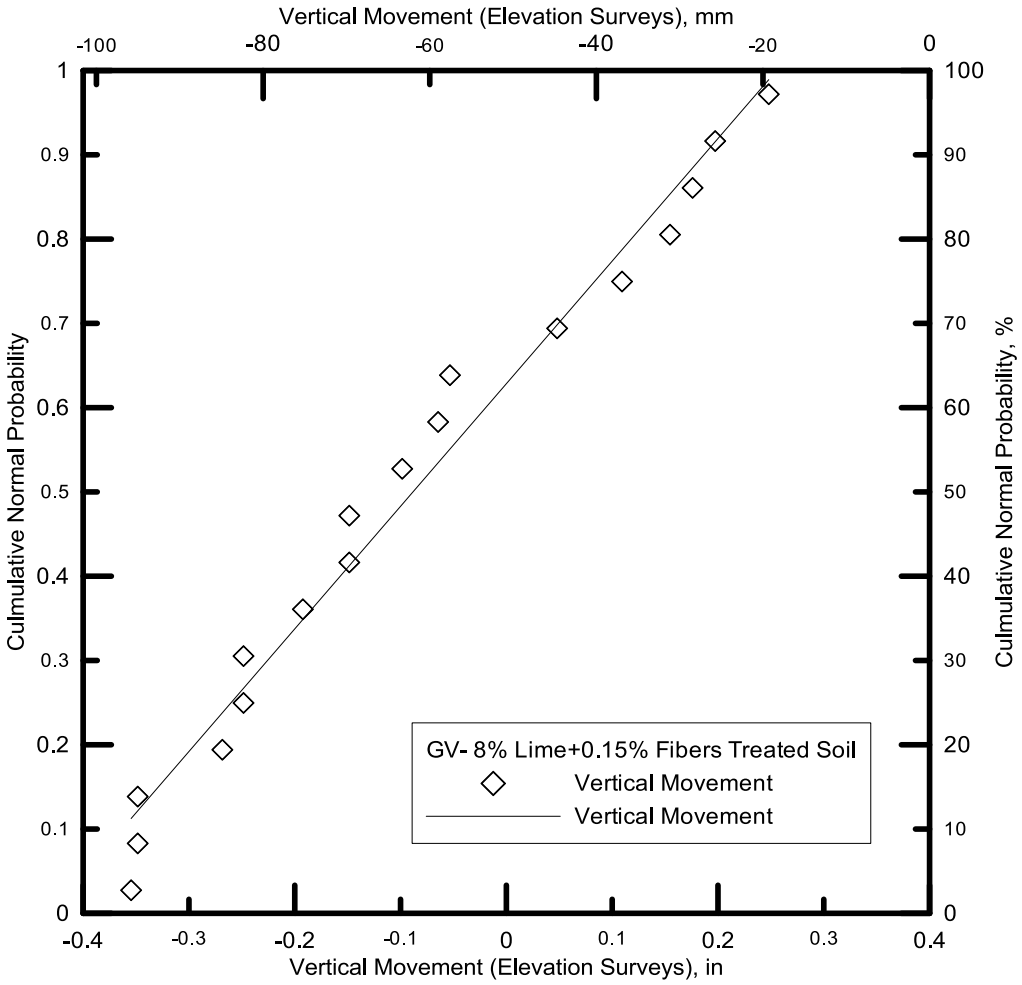

Fit Results

Vertical Movement
Equation Y = 1.454625498 * X + 0.6284182898
Number of data points used = 18
Average X = -0.0882827
Average Y = 0.5
Residual sum of squares = 0.0328315
Regression sum of squares = 1.46254
Coef of determination, R-squared = 0.978045
Residual mean square, sigma-hat-sq'd = 0.00205197

Figure 6.9 Normality check for vertical movement of the Grapevine Dam 8%lime+0.15%fibers Treated Soil

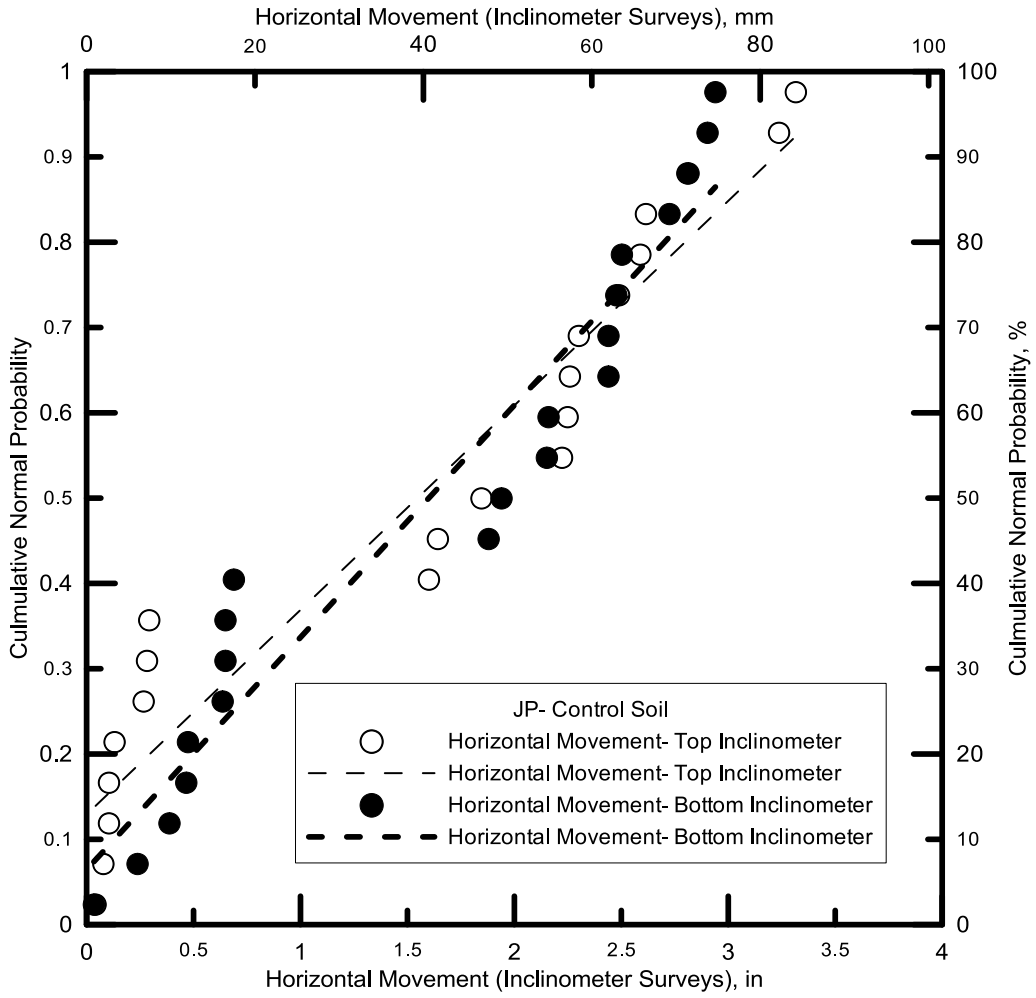

Fit Results

Horizontal Movement- Top Inclinometer
Equation Y = 0.2397675421 * X + 0.1291700448
Number of data points used = 21
Average X = 1.54662
Average Y = 0.5
Residual sum of squares = 0.123695
Regression sum of squares = 1.62234
Coef of determination, R-squared = 0.929156
Residual mean square, sigma-hat-sq'd = 0.00651029

Fit Results

Horizontal Movement- Bottom Inclinometer
Equation Y = 0.2721891875 * X + 0.06457194674
Number of data points used = 21
Average X = 1.59973
Average Y = 0.5
Residual sum of squares = 0.120768
Regression sum of squares = 1.62526
Coef of determination, R-squared = 0.930833
Residual mean square, sigma-hat-sq'd = 0.00635623

igure 6.10 Normality check for horizontal movement of the Joe Pool Dam Control Soil

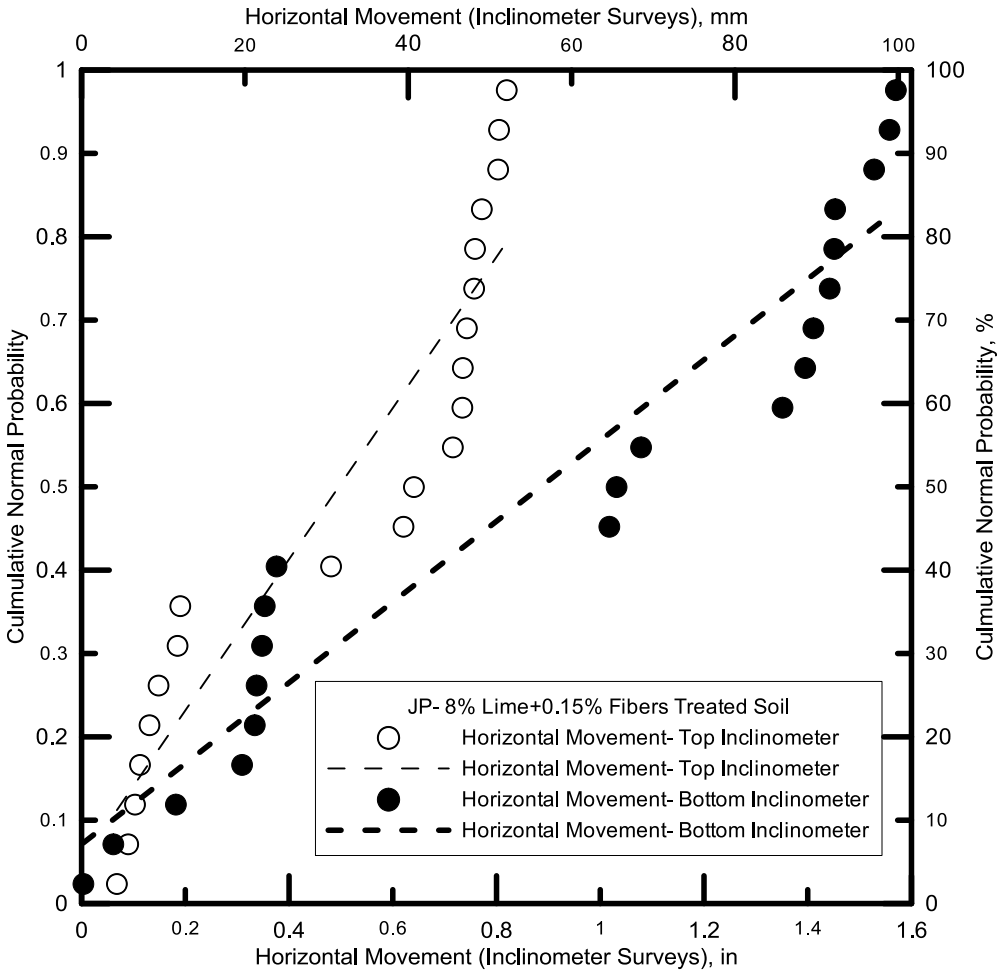

Fit Results

Horizontal Movement- Top Inclinometer
Equation Y = 0.9068476474 * X + 0.05032067679
Number of data points used = 21
Average X = 0.495871
Average Y = 0.5
Residual sum of squares = 0.215637
Regression sum of squares = 1.53039
Coef of determination, R-squared = 0.876499
Residual mean square, sigma-hat-sq'd = 0.0113493

Fit Results

Horizontal Movement- Bottom Inclinometer
Equation Y = 0.4843784923 * X + 0.07118873735
Number of data points used = 21
Average X = 0.885281
Average Y = 0.5
Residual sum of squares = 0.142445
Regression sum of squares = 1.60359
Coef of determination, R-squared = 0.918418
Residual mean square, sigma-hat-sq'd = 0.00749712

Figure 6.11 Normality check for horizontal movement of the Joe Pool Dam 8%lime+0.15%fibers Treated Soil

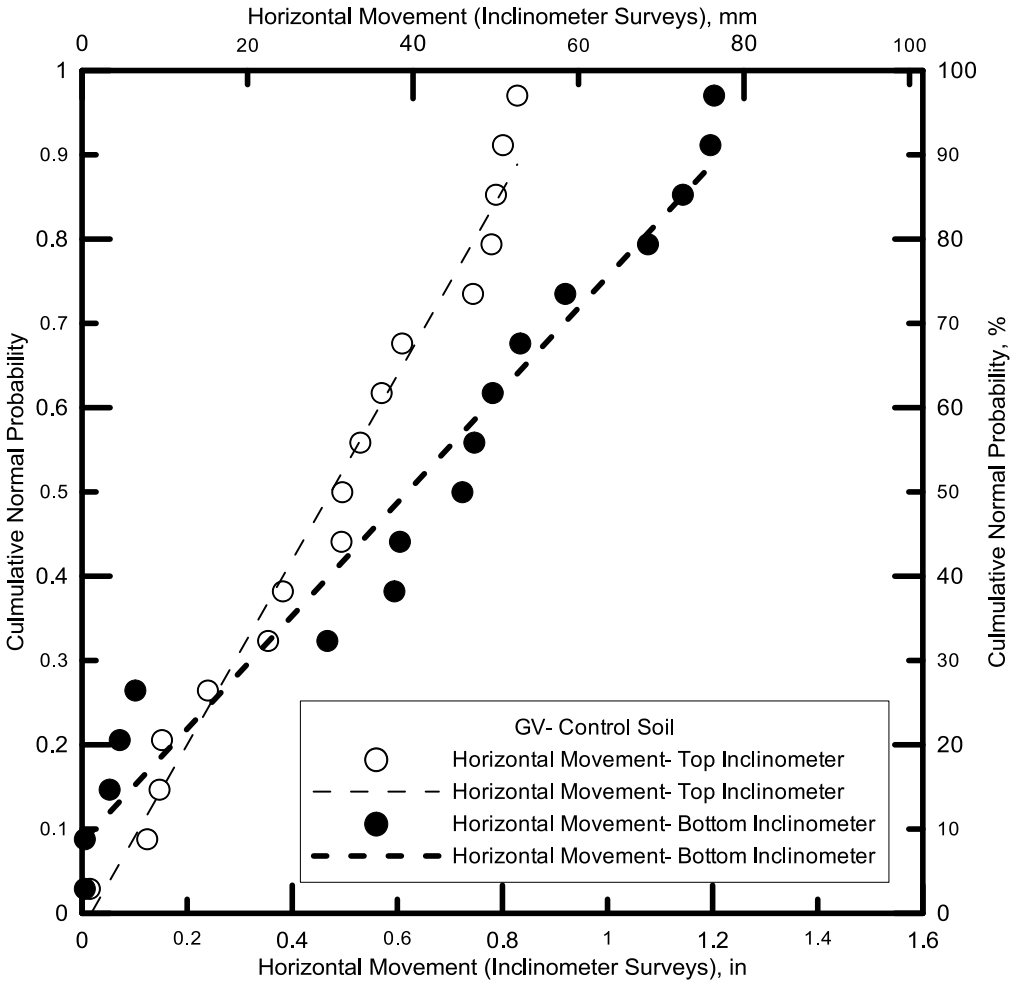

Fit Results

Horizontal Movement- Top Inclinometer
Equation Y = 1.095849788 * X - 0.01902323846
Number of data points used = 17
Average X = 0.473626
Average Y = 0.5
Residual sum of squares = 0.0311046
Regression sum of squares = 1.38066
Coef of determination, R-squared = 0.977968
Residual mean square, sigma-hat-sq'd = 0.00207364

Fit Results

Horizontal Movement- Bottom Inclinometer
Equation Y = 4.344743174 * X - 0.08273349321
Number of data points used = 17
Average X = 0.134124
Average Y = 0.5
Residual sum of squares = 0.140645
Regression sum of squares = 1.27112
Coef of determination, R-squared = 0.900376
Residual mean square, sigma-hat-sq'd = 0.00937635

Figure 6.12 Normality check for horizontal movement of the Grapevine Dam Control Soil

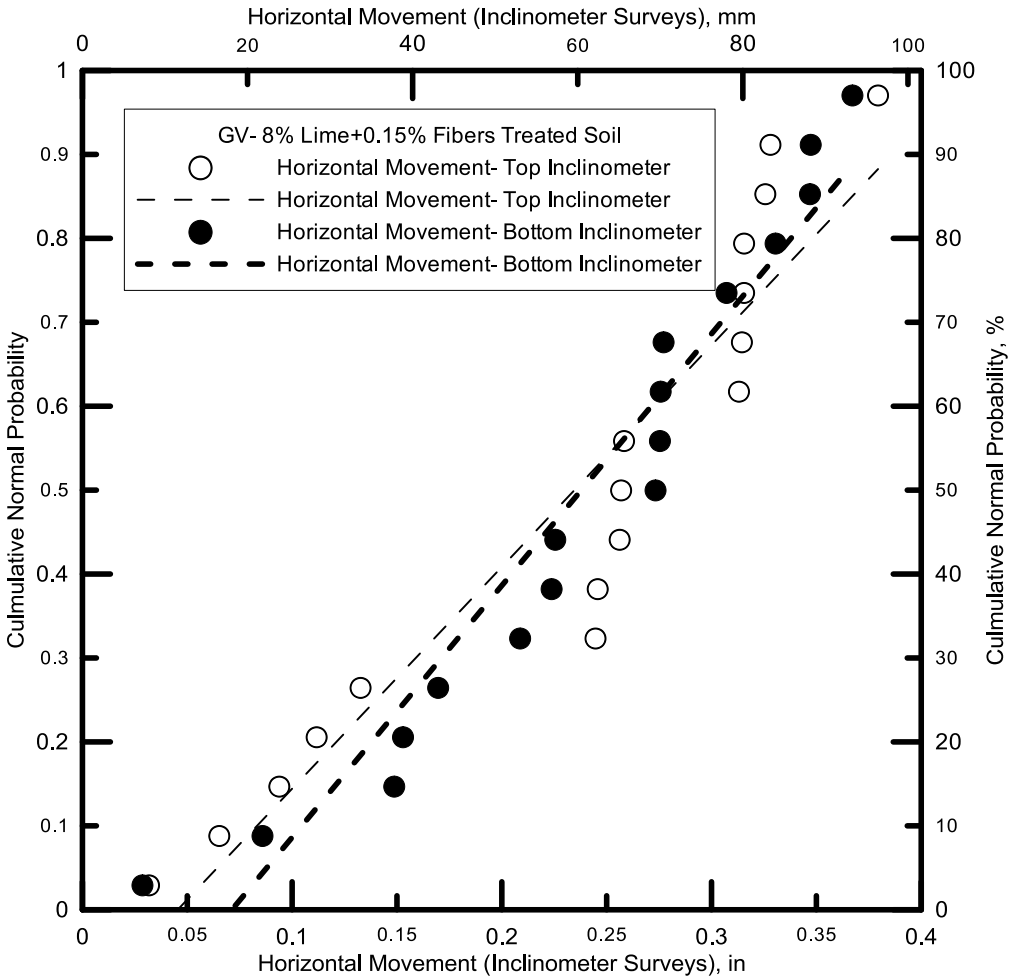

Fit Results

Horizontal Movement- Top Inclinometer
Equation Y = 2.642351804 * X - 0.1199937669
Number of data points used = 17
Average X = 0.234637
Average Y = 0.5
Residual sum of squares = 0.151433
Regression sum of squares = 1.26033
Coef of determination, R-squared = 0.892735
Residual mean square, sigma-hat-sq'd = 0.0100955

Fit Results

Horizontal Movement- Bottom Inclinometer
Equation Y = 4.344743174 * X - 0.08273349321
Number of data points used = 17
Average X = 0.134124
Average Y = 0.5
Residual sum of squares = 0.140645
Regression sum of squares = 1.27112
Coef of determination, R-squared = 0.900376
Residual mean square, sigma-hat-sq'd = 0.00937635

Figure 6.13 Normality check for horizontal movement of the Grapevine Dam 8%lime+0.15%fibers Treated Soil

Results from the probability graphs show that the field data fairly resembled the normal distribution in each category of the field performance. Coefficient of determination R^2 was achieved at a reliable level of approximately 0.83 and above. This indicated that the t-test could be performed on the data collected to further analyze the treatment effects using the Dunnett's procedure.

It is noteworthy to mention that the number of observations has also affected the outcome of the normality check. The more data points we have, the more reliable the judgment on normality can be. Data shown in Figures 6.1 to 6.13 exhibited a higher level of deviation in the slope movement measurements from the trend lines (for both vertical and horizontal directions). The results could be more accurately interpreted with more data points. Nevertheless the present collected data has proven to be more than sufficient to draw conclusions from the analysis.

6.3 Results Comparison using the Dunnett's t-test procedure

The student's t-test using the Dunnett's procedure was carried out by comparing each of the treated soils with the control untreated soil. Details of the calculations are not provided; rather the test results and a summary of all the analysis components are presented and tabulated. Tables 6.3 to 6.38 summarize the reports on ANOVA and conclusions for the presence of significance difference on each of the data comparison categories on the Joe Pool Dam and Grapevine Dam soils.

Table 6.3. Components for ANOVA test results for the Joe Pool Dam soil moisture from the Top probe

Soil	n_i	Totals $y_{i.}$	Averages $\bar{y}_{i.}$	$y_{..}$	$\bar{y}_{..}$	SS_T	$SS_{Treatments}$	SS_E
Control Soil	45	1567.44	34.83	7397.07	32.88	17996.69	3224.96	14771.73
20%compost Treated Soil	45	1644.10	36.54					
4%lime+0.30%fibers Treated Soil	45	1503.80	33.42					
8%lime+0.15%fibers Treated Soil	45	1529.62	33.99					
8%lime Treated Soil	45	1152.10	25.60					

Table 6.4. Components for ANOVA test results for the Joe Pool Dam soil moisture from the Bottom probe

Soil	n_i	Totals $y_{i.}$	Averages $\bar{y}_{i.}$	$y_{..}$	$\bar{y}_{..}$	SS_T	$SS_{Treatments}$	SS_E
Control Soil	45	1267.83	28.17	6655.87	29.58	17268.18	5848.65	11419.53
20%compost Treated Soil	45	1547.88	34.40					
4%lime+0.30%fibers Treated Soil	45	1169.55	25.99					
8%lime+0.15%fibers Treated Soil	45	1640.31	36.45					
8%lime Treated Soil	45	1030.30	22.90					

Table 6.5. ANOVA test results for the Joe Pool Dam soil moisture from the Top probe

Source of variation	Sum of Squares	Degree of freedom	Mean square
Soil treatments	3224.96	4	806.24
Error	14771.73	220	67.14
Total	17996.69	224	

Table 6.6. ANOVA test results for the Joe Pool Dam soil moisture from the Bottom probe

Source of variation	Sum of Squares	Degree of freedom	Mean square
Soil treatments	5848.65	4	1462.16
Error	11419.53	220	51.91
Total	17268.18	224	

.

Table 6.7. Moisture comparison of treated sections with the control section for the Joe Pool Dam soils from the Top Probe

Treatment	Mean difference		Critical difference	Is the difference significant?
Control soil vs. 20%compost treated soil	$\lvert\bar{y}_{1.} - \bar{y}_{2.}\rvert$	1.70	4.21	No
Control soil vs. 4%lime+0.30%fibers treated soil	$\lvert\bar{y}_{1.} - \bar{y}_{3.}\rvert$	1.41	4.21	No
Control soil vs. 8%lime+0.15%fibers treated soil	$\lvert\bar{y}_{1.} - \bar{y}_{4.}\rvert$	0.84	4.21	No
Control soil vs. 8%lime treated soil	$\lvert\bar{y}_{1.} - \bar{y}_{5.}\rvert$	9.23	4.21	Yes

Table 6.8. Moisture comparison of treated sections with the control section for the Joe Pool Dam soil from the Bottom Probe

Treatment	Mean difference		Critical difference	Is the difference significant?
Control soil vs. 20%compost treated soil	$\lvert\bar{y}_{1.} - \bar{y}_{2.}\rvert$	6.22	3.7	Yes
Control soil vs. 4%lime+0.30%fibers treated soil	$\lvert\bar{y}_{1.} - \bar{y}_{3.}\rvert$	2.18	3.7	No
Control soil vs. 8%lime+0.15%fibers treated soil	$\lvert\bar{y}_{1.} - \bar{y}_{4.}\rvert$	8.28	3.7	Yes
Control soil vs. 8%lime treated soil	$\lvert\bar{y}_{1.} - \bar{y}_{5.}\rvert$	5.28	3.7	Yes

Table 6.9. Components for ANOVA test results for the Grapevine Dam soil moisture from Top probe

Soil	n_i	Totals $y_{i.}$	Averages $\bar{y}_{i.}$	$y_{..}$	$\bar{y}_{..}$	SS_T	$SS_{Treatments}$	SS_E
Control Soil	52	1027.21	19.75	5697.12	21.91	14091.67	6142.63	7949.03
20%compost Treated Soil	52	1644.52	31.63					
4%lime+0.30%fibers Treated Soil	52	999.11	19.21					
8%lime+0.15%fibers Treated Soil	52	1005.38	19.33					
8%lime Treated Soil	52	1020.90	19.63					

Table 6.10. Components for ANOVA test results for the Grapevine Dam soil moisture from Bottom probe

Soil	n_i	Totals $y_{i.}$	Averages $\bar{y}_{i.}$	$y_{..}$	$\bar{y}_{..}$	SS_T	$SS_{Treatments}$	SS_E
Control Soil	52	968.47	18.62	4863.58	18.71	7664.34	165.85	7498.49
20%compost Treated Soil	52	1040.03	20.00					
4%lime+0.30%fibers Treated Soil	52	954.73	18.36					
8%lime+0.15%fibers Treated Soil	52	987.15	18.98					
8%lime Treated Soil	52	913.20	17.56					

Table 6.11. ANOVA test results for the Grapevine Dam soil moisture from the Top probe

Source of variation	Sum of Squares	Degree of freedom	Mean square
Soil treatments	6142.63	4	1535.66
Error	7949.03	255	31.17
Total	14091.67	259	

Table 6.12. ANOVA test results for the Grapevine Dam soil moisture from the Bottom probe

Source of variation	Sum of Squares	Degree of freedom	Mean square
Soil treatments	165.85	4	41.46
Error	7498.49	255	29.41
Total	7664.34	259	

Table 6.13. Moisture comparison of treated sections with the control section for the Grapevine Dam soil from the Top Probe

Treatment	Mean difference		Critical difference	Is the difference significant?
Control soil vs. 20%compost treated soil	$\lvert\bar{y}_{1.} - \bar{y}_{2.}\rvert$	11.87	2.67	Yes
Control soil vs. 4%lime+0.30%fibers treated soil	$\lvert\bar{y}_{1.} - \bar{y}_{3.}\rvert$	0.54	2.67	No
Control soil vs. 8%lime+0.15%fibers treated soil	$\lvert\bar{y}_{1.} - \bar{y}_{4.}\rvert$	0.42	2.67	No
Control soil vs. 8%lime treated soil	$\lvert\bar{y}_{1.} - \bar{y}_{5.}\rvert$	0.12	2.67	No

Table 6.14. Moisture comparison of treated sections with the control section for the Grapevine Dam soil from the Bottom Probe

Treatment	Mean difference		Critical difference	Is the difference significant?
Control soil vs. 20%compost treated soil	$\lvert\bar{y}_{1.} - \bar{y}_{2.}\rvert$	1.38	2.60	No
Control soil vs. 4%lime+0.30%fibers treated soil	$\lvert\bar{y}_{1.} - \bar{y}_{3.}\rvert$	0.26	2.60	No
Control soil vs. 8%lime+0.15%fibers treated soil	$\lvert\bar{y}_{1.} - \bar{y}_{4.}\rvert$	0.36	2.60	No
Control soil vs. 8%lime treated soil	$\lvert\bar{y}_{1.} - \bar{y}_{5.}\rvert$	1.06	2.60	No

Table 6.15. Components for ANOVA test results for the Joe Pool Dam soil temperature

Soil	n_i	Totals $y_{i.}$	Averages $\bar{y}_{i.}$	$y_{..}$	$\bar{y}_{..}$	SS_T	$SS_{Treatments}$	SS_E
Control Soil	45	3027.09	67.27	15752.34	70.01	43462.41	616.98	42845.43
20%compost Treated Soil	45	3131.50	69.59					
4%lime+0.30%fibers Treated Soil	45	3138.84	69.75					
8%lime+0.15%fibers Treated Soil	45	3217.58	71.50					
8%lime Treated Soil	45	3237.32	71.94					

Table 6.16. Components for ANOVA test results for the Grapevine Dam soil temperature

Soil	n_i	Totals $y_{i.}$	Averages $\bar{y}_{i.}$	$y_{..}$	$\bar{y}_{..}$	SS_T	$SS_{Treatments}$	SS_E
Control Soil	52	3583.68	68.92	18075.90	69.52	50795.97	412.10	50383.87
20%compost Treated Soil	52	3691.62	70.99					
4%lime+0.30%fibers Treated Soil	52	3609.28	69.41					
8%lime+0.15%fibers Treated Soil	52	3512.60	67.55					
8%lime Treated Soil	52	3678.72	70.74					

Table 6.17. ANOVA test results for the Joe Pool Dam soil temperature

Source of variation	Sum of Squares	Degree of freedom	Mean square
Soil treatments	616.98	4	154.25
Error	42845.43	220	194.75
Total	43462.41	224	

Table 6.18. ANOVA test results for the Grapevine Dam soil temperature

Source of variation	Sum of Squares	Degree of freedom	Mean square
Soil treatments	412.10	4	103.02
Error	50383.87	255	197.58
Total	50795.97	259	

Table 6.19. Temperature comparison of treated sections with the control section for the Joe Pool Dam soil

Treatment	Mean difference		Critical difference	Is the difference significant?
Control soil vs. 20%compost treated soil	$\lvert\bar{y}_{1.} - \bar{y}_{2.}\rvert$	2.32	7.18	No
Control soil vs. 4%lime+0.30%fibers treated soil	$\lvert\bar{y}_{1.} - \bar{y}_{3.}\rvert$	2.48	7.18	No
Control soil vs. 8%lime+0.15%fibers treated soil	$\lvert\bar{y}_{1.} - \bar{y}_{4.}\rvert$	4.23	7.18	No
Control soil vs. 8%lime treated soil	$\lvert\bar{y}_{1.} - \bar{y}_{5.}\rvert$	4.67	7.18	No

Table 6.20. Temperature comparison of treated sections with the control section for the Grapevine Dam soil

Treatment	Mean difference		Critical difference	Is the difference significant?
Control soil vs. 20%compost treated soil	$\lvert\bar{y}_{1.} - \bar{y}_{2.}\rvert$	2.08	6.73	No
Control soil vs. 4%lime+0.30%fibers treated soil	$\lvert\bar{y}_{1.} - \bar{y}_{3.}\rvert$	0.49	6.73	No
Control soil vs. 8%lime+0.15%fibers treated soil	$\lvert\bar{y}_{1.} - \bar{y}_{4.}\rvert$	1.37	6.73	No
Control soil vs. 8%lime treated soil	$\lvert\bar{y}_{1.} - \bar{y}_{5.}\rvert$	1.83	6.73	No

Table 6.21. Components for ANOVA test results for the Joe Pool Dam soil vertical movement (Elevation Surveys)

Soil	n_i	Totals $y_{i.}$	Averages $\bar{y}_{i.}$	$y_{..}$	$\bar{y}_{..}$	SS_T	$SS_{Treatments}$	SS_E
Control Soil	19	41.49	2.18	135.54	1.43	41.20	15.77	25.43
20%compost Treated Soil	19	24.18	1.27					
4%lime+0.30%fibers Treated Soil	19	28.12	1.48					
8%lime+0.15%fibers Treated Soil	19	22.50	1.18					
8%lime Treated Soil	19	19.24	1.01					

Table 6.22. Components for ANOVA test results for the Grapevine Dam soil vertical movement (Elevation Surveys)

Soil	n_i	Totals $y_{i.}$	Averages $\bar{y}_{i.}$	$y_{..}$	$\bar{y}_{..}$	SS_T	$SS_{Treatments}$	SS_E
Control Soil	18	7.26	0.40	24.10	0.27	3.17	0.64	2.53
20%compost Treated Soil	18	5.02	0.28					
4%lime+0.30%fibers Treated Soil	18	5.36	0.30					
8%lime+0.15%fibers Treated Soil	18	3.46	0.19					
8%lime Treated Soil	18	3.00	0.17					

Table 6.23. ANOVA test results for the Joe Pool Dam soil vertical movement (Elevation Surveys)

Source of variation	Sum of Squares	Degree of freedom	Mean square
Soil treatments	15.77	4	3.94
Error	25.43	90	0.28
Total	41.20	94	

Table 6.24. ANOVA test results for the Grapevine Dam soil vertical movement (Elevation Surveys)

Source of variation	Sum of Squares	Degree of freedom	Mean square
Soil treatments	0.64	4	0.16
Error	2.53	85	0.03
Total	3.17	89	

Table 6.25. Comparison of treated sections with the control section for the Joe Pool Dam soil vertical movement (Elevation Surveys)

Treatment	Mean difference		Critical difference	Is the difference significant?
Control soil vs. 20%compost treated soil	$\lvert\bar{y}_{1.} - \bar{y}_{2.}\rvert$	0.91	0.43	Yes
Control soil vs. 4%lime+0.30%fibers treated soil	$\lvert\bar{y}_{1.} - \bar{y}_{3.}\rvert$	0.70	0.43	Yes
Control soil vs. 8%lime+0.15%fibers treated soil	$\lvert\bar{y}_{1.} - \bar{y}_{4.}\rvert$	1.00	0.43	Yes
Control soil vs. 8%lime treated soil	$\lvert\bar{y}_{1.} - \bar{y}_{5.}\rvert$	1.17	0.43	Yes

Table 6.26. Comparison of treated sections with the control section for the Grapevine Dam soil vertical movement (Elevation Surveys)

Treatment	Mean difference		Critical difference	Is the difference significant?
Control soil vs. 20%compost treated soil	$\lvert\bar{y}_{1.} - \bar{y}_{2.}\rvert$	0.12	0.14	No
Control soil vs. 4%lime+0.30%fibers treated soil	$\lvert\bar{y}_{1.} - \bar{y}_{3.}\rvert$	0.11	0.14	No
Control soil vs. 8%lime+0.15%fibers treated soil	$\lvert\bar{y}_{1.} - \bar{y}_{4.}\rvert$	0.21	0.14	Yes
Control soil vs. 8%lime treated soil	$\lvert\bar{y}_{1.} - \bar{y}_{5.}\rvert$	0.24	0.14	Yes

Table 6.27. Components for ANOVA test results for the Joe Pool Dam soil horizontal movement (Inclinometer Surveys) from the Top Inclinometer

Soil	n_i	Totals $y_{i.}$	Averages $\bar{y}_{i.}$	$y_{..}$	$\bar{y}_{..}$	SS_T	$SS_{Treatments}$	SS_E
Control Soil	21	32.48	1.55	99.09	0.94	94.16	24.73	69.43
20%compost Treated Soil	21	20.16	0.96					
4%lime+0.30%fibers Treated Soil	21	29.51	1.41					
8%lime+0.15%fibers Treated Soil	21	10.41	0.50					
8%lime Treated Soil	21	6.53	0.31					

Table 6.28. Components for ANOVA test results for the Joe Pool Dam soil horizontal movement (Inclinometer Surveys) from the Bottom Inclinometer

Soil	n_i	Totals $y_{i.}$	Averages $\bar{y}_{i.}$	$y_{..}$	$\bar{y}_{..}$	SS_T	$SS_{Treatments}$	SS_E
Control Soil	21	33.59	1.60	127.13	1.21	85.59	16.98	68.61
20%compost Treated Soil	21	33.45	1.59					
4%lime+0.30%fibers Treated Soil	21	28.97	1.38					
8%lime+0.15%fibers Treated Soil	21	18.59	0.89					
8%lime Treated Soil	21	12.53	0.60					

Table 6.29. ANOVA test results for the Joe Pool Dam soil horizontal movement (Inclinometer Surveys) from the Top Inclinometer

Source of variation	Sum of Squares	Degree of freedom	Mean square
Soil treatments	69.43	4	17.36
Error	24.73	100	0.25
Total	94.16	104	

Table 6.30. ANOVA test results for the Joe Pool Dam soil horizontal movement (Inclinometer Surveys) from the Bottom Inclinometer

Source of variation	Sum of Squares	Degree of freedom	Mean square
Soil treatments	68.61	4	17.15
Error	16.98	100	0.17
Total	85.59	104	

.

Table 6.31. Horizontal Movement comparison of treated sections with the control section from the Top Inclinometer for Joe Pool Dam

Treatment	Mean difference		Critical difference	Is the difference significant?
Control soil vs. 20%compost treated soil	$\lvert\bar{y}_{1.} - \bar{y}_{2.}\rvert$	0.59	0.38	Yes
Control soil vs. 4%lime+0.30%fibers treated soil	$\lvert\bar{y}_{1.} - \bar{y}_{3.}\rvert$	0.14	0.38	No
Control soil vs. 8%lime+0.15%fibers treated soil	$\lvert\bar{y}_{1.} - \bar{y}_{4.}\rvert$	1.05	0.38	Yes
Control soil vs. 8%lime treated soil	$\lvert\bar{y}_{1.} - \bar{y}_{5.}\rvert$	1.24	0.38	Yes

Table 6.32. Horizontal Movement comparison of treated sections with the control section from the bottom Inclinometer for Joe Pool Dam

Treatment	Mean difference		Critical difference	Is the difference significant?
Control soil vs. 20%compost treated soil	$\lvert\bar{y}_{1.} - \bar{y}_{2.}\rvert$	0.01	0.32	No
Control soil vs. 4%lime+0.30%fibers treated soil	$\lvert\bar{y}_{1.} - \bar{y}_{3.}\rvert$	0.22	0.32	No
Control soil vs. 8%lime+0.15%fibers treated soil	$\lvert\bar{y}_{1.} - \bar{y}_{4.}\rvert$	0.71	0.32	Yes
Control soil vs. 8%lime treated soil	$\lvert\bar{y}_{1.} - \bar{y}_{5.}\rvert$	1.00	0.32	Yes

Table 6.33. Components for ANOVA test results for the Grapevine Dam soil horizontal movement (Inclinometer Surveys) from the Top Inclinometer

Soil	n_i	Totals $y_{i.}$	Averages $\bar{y}_{i.}$	$y_{..}$	$\bar{y}_{..}$	SS_T	$SS_{Treatments}$	SS_E
Control Soil	18	8.05	0.47	26.60	0.31	5.79	2.75	3.04
20%compost Treated Soil	18	9.76	0.57					
4%lime+0.30%fibers Treated Soil	18	3.01	0.18					
8%lime+0.15%fibers Treated Soil	18	3.99	0.23					
8%lime Treated Soil	18	1.79	0.11					

Table 6.34. Components for ANOVA test results for the Grapevine Dam soil horizontal movement (Inclinometer Surveys) from the Bottom Inclinometer

Soil	n_i	Totals $y_{i.}$	Averages $\bar{y}_{i.}$	$y_{..}$	$\bar{y}_{..}$	SS_T	$SS_{Treatments}$	SS_E
Control Soil	18	10.53	0.62	35.68	0.42	14.80	8.03	6.77
20%compost Treated Soil	18	15.80	0.93					
4%lime+0.30%fibers Treated Soil	18	3.03	0.18					
8%lime+0.15%fibers Treated Soil	18	4.04	0.24					
8%lime Treated Soil	18	2.28	0.13					

Table 6.35. ANOVA test results for the Grapevine Dam soil horizontal movement (Inclinometer Surveys) from the Top Inclinometer

Source of variation	Sum of Squares	Degree of freedom	Mean square
Soil treatments	2.75	4	0.69
Error	3.04	80	0.04
Total	5.79	84	

Table 6.36. ANOVA test results for the Grapevine Dam soil horizontal movement (Inclinometer Surveys) from the Bottom Inclinometer

Source of variation	Sum of Squares	Degree of freedom	Mean square
Soil treatments	8.03	4	2.01
Error	6.77	80	0.08
Total	14.80	84	

.

Table 6.37. Horizontal Movement comparison of treated sections with the control section from the Top Inclinometer for Grapevine Dam

Treatment	Mean difference		Critical difference	Is the difference significant?
Control soil vs. 20%compost treated soil	$\lvert\bar{y}_{1.} - \bar{y}_{2.}\rvert$	0.10	0.17	No
Control soil vs. 4%lime+0.30%fibers treated soil	$\lvert\bar{y}_{1.} - \bar{y}_{3.}\rvert$	0.30	0.17	Yes
Control soil vs. 8%lime+0.15%fibers treated soil	$\lvert\bar{y}_{1.} - \bar{y}_{4.}\rvert$	0.24	0.17	Yes
Control soil vs. 8%lime treated soil	$\lvert\bar{y}_{1.} - \bar{y}_{5.}\rvert$	0.37	0.17	Yes

Table 6.38. Horizontal Movement comparison of treated sections with the control section from the bottom Inclinometer for Grapevine Dam

Treatment	Mean difference		Critical difference	Is the difference significant?
Control soil vs. 20%compost treated soil	$\lvert\bar{y}_{1.} - \bar{y}_{2.}\rvert$	0.31	0.25	Yes
Control soil vs. 4%lime+0.30%fibers treated soil	$\lvert\bar{y}_{1.} - \bar{y}_{3.}\rvert$	0.44	0.25	Yes
Control soil vs. 8%lime+0.15%fibers treated soil	$\lvert\bar{y}_{1.} - \bar{y}_{4.}\rvert$	0.38	0.25	Yes
Control soil vs. 8%lime treated soil	$\lvert\bar{y}_{1.} - \bar{y}_{5.}\rvert$	0.49	0.25	Yes

The final summary of significance difference testing for both Dam sites for all field performance categories is presented in Table 6.39 and Table 6.40. When the difference is significant, the mean values of the treatment performance from ANOVA components tables are used to determine whether the performance is better or poorer compared to the control soil. Upward arrows ↑ are assigned for treatments with significantly better performance and downward arrows are added to those with poorer performance. Treatments with the majority of significantly better performance marks (Yes↑) are recommended for future slope stabilization.

Table 6.39. Summary of significance difference testing for the Joe Pool Dam soils

Soil	Moisture		Temperature	Vertical movement	Horizontal movement		Is the treatment recommended?
	Top Probe	Bottom Probe			Top Inclinometer	Bottom Inclinometer	
Control soil vs. 20%compost treated soil	No	Yes↑	No	Yes↑	Yes↑	No	**Yes**
Control soil vs. 4%lime+0.30%fibers treated soil	No	No	No	Yes↑	No	No	**No**
Control soil vs. 8%lime+0.15%fibers treated soil	No	Yes↑	No	Yes↑	Yes↑	Yes↑	**Yes**
Control soil vs. 8%lime treated soil	Yes↓	Yes↓	No	Yes↑	Yes↑	Yes↑	**Yes**

Note: For 'Yes' cases, the improvement is noted by the symbols ↑ (soil property in test section better than control); ↓(soil property in test section poorer than control);

Table 6.40. Summary of significance difference testing for the Grapevine Dam soils

Soil	Moisture		Temperature	Vertical movement	Horizontal movement		Is the treatment recommended?
	Top Probe	Bottom Probe			Top Inclinometer	Bottom Inclinometer	
Control soil vs. 20%compost treated soil	Yes↑	No	No	No	No	Yes↓	**No**
Control soil vs. 4%lime+0.30%fibers treated soil	No	No	No	No	Yes↑	Yes↑	**No**
Control soil vs. 8%lime+0.15%fibers treated soil	No	No	No	Yes↑	Yes↑	Yes↑	**Yes**
Control soil vs. 8%lime treated soil	No	No	No	Yes↑	Yes↑	Yes↑	**Yes**

Note: For 'Yes' cases, the improvement is noted by the symbols ↑ (soil property in test section better than control); ↓(soil property in test section poorer than control);

Joe Pool Dam soils

Results of t-test using the Dunnett's procedure reveal that the treatments did affect the moisture content of the soil. As the bottom probe is located within the treated zone (at the depth of 20 in. from the slope) as shown in Figure 6.14, its measurement directly reflects the treatment effects on the soil's ability to hold moisture. Significance differences were found at almost all treated sections except for 4%lime+0.30%fibers treated soil.

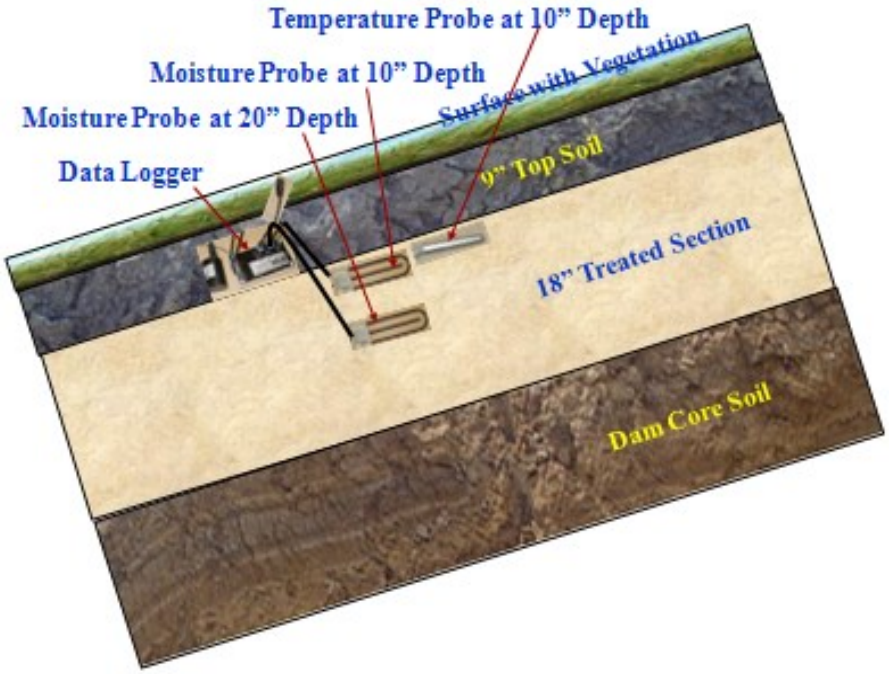

Figure 6.14. Instrumentation position in the field (Dronamraju, 2008)

The t-test data indicated that there was no significance difference between the temperatures recorded for the treated sections and those of control sections. The result is in good agreement with the early work of Dronamraju (2008), when data was recorded at the initial stage of the post-construction period in the field.

In regard to the vertical movement, results show the presence of significance difference between the performances of the test sections. Among the treatments, 8%ime+0.15%fibers and 8%lime amendments are ranked the top two as they exhibited 50 to 60% less vertical movement than the control untreated soil.

The t-test data for horizontal movement shows no significance difference between the control soil and the 4%lime+0.30%fibers treated soil while less movement was reported on other treated sections. 8%lime+0.15%fibers and 8%lime treated sections outperformed other sections experiencing only 20 to 50% of lateral movement compared to the control untreated soil.

Grapevine Dam soils

In comparison with the Joe Pool Dam soils, results of t-test for the Grapevine Dam soils did not show the effects of the treatment additives regarding soil moisture content and temperature. With the absence of the significance difference in the temperature aspect of both Dam sites, it can be concluded that temperature cannot be used to identify the best treatment to be adopted for dam slopes. Hence, temperature data is not considered for further analyses in this research.

Soil movement in vertical and horizontal directions shows the consistency of the 8%lime+0.15%fibers and 8%lime treated amendments as they yield 30 to 50% less movement than the control untreated soil in both directions.

Results indicate that for the Joe Pool Dam and Grapevine Dam soils, 8%lime+0.15%fibers and 8%lime amendments are the most suitable additives. 20%compost treatment is recommended to be implemented only for the Joe Pool Dam soil. For the purpose of quantitative comparison, results from Table 6.39 and Table 6.40 are enhanced with a field performance ranking analysis.

6.4 Ranking Analysis

Final field performance is ranked based on the results of the significance difference analysis and also based on the engineering property improvement or performance improvement criteria. To further explain the ranking results, the following rules and criteria are applied:

- Ranking points are given on a scale of 1 to 5 with 1 being indicating the best performance and 5 for the worst ranked section. Thus, test section with the lowest total score is the best section and vice versa.
- In soil moisture content, a section that can hold more moisture thorough the year is the best performing section (1) as it helped the soil to reduce soil shrinkage cracking during dry season.
- In soil temperature, the difference is not significant. Thus, the analysis will not use it as a criterion for ranking.
- In the soil movement category (both directions), soil that experiences the least amount of movement is given a best rank of 1.
- There are a total of three categories of comparison: moisture content, vertical movement and horizontal movement. All points are weighed equally for each category. However, there are two readings for each compaction moisture content (from the top and bottom probes) and horizontal movements (from the top and bottom inclinometers). In this case, average points are used to better assess the overall performance of the sections.
- For all categories (except temperature), even in case of lacking significance difference, all treated sections are ranked based on the mean value of all observations ($y_{i.}$). Applying all the rules mentioned above, a quantitative criterion is used to compare the performance and assign the right points for all the treatments. However, it is important to note that ranking based on the average values with the lack of significance difference may appear reasonable, but those average values can't be statically detected with the significance level α of 0.5.

Table 6.41 and Table 6.42 present the final field performance ranking for the Joe Pool Dam and Grapevine Dam untreated and treated soils.

Table 6.41. Final Field Performance ranking for the Joe Pool Dam soils

Soil	Moisture			Vertical movement	Horizontal movement			Total
	Top Probe	Bottom Probe	Avg.		Top Inclinometer	Bottom Inclinometer	Avg.	
Control soil	2	3	2.5	5	5	5	5	12.5
20%compost treated soil	1	2	1.5	3	3	4	3.5	8
4%lime+0.30%fibers treated soil	4	4	4	4	4	3	3.5	11.5
8%lime+0.15%fibers treated soil	3	1	2	2	2	2	2	6
8%lime treated soil	5	5	5	1	1	1	1	7

Note: Red numbers indicate that the difference is not significant.

Table 6.42. Final Field Performance ranking for the Grapevine Dam soils

Soil	Moisture			Vertical movement	Horizontal movement			Total
	Top Probe	Bottom Probe	Avg.		Top Inclinometer	Bottom Inclinometer	Avg.	
Control soil	2	3	2.5	5	4	4	4	11.5
20%compost treated soil	1	1	1	3	5	5	5	9
4%lime+0.30%fibers treated soil	5	4	4.5	4	2	2	2	10.5
8%lime+0.15%fibers treated soil	4	2	3	2	3	3	3	8
8%lime treated soil	3	5	4	1	1	1	1	6

Note: Red numbers indicate that the difference is not significant.

6.5 Summary

Field data was collected and statistically analyzed using the Student's t-test following the Dunnett's procedure to compare the performance of treated sections with respect to the control section at the Joe Pool Dam and Grapevine Dam sites. Significance difference was reported on almost all field performance categories except for temperature. Based on the ranking results of field data presented in this Chapter, the 8%lime+0.15%fibers and 8%lime amendments performed the best for both Joe Pool Dam and Grapevine Dam soils. The results of this chapter will be enhanced by the ranking of soil properties based on laboratory testing and modeling in Chapter 7.

CHAPTER 7

ANALYTICAL AND RELIABILITY BASED SLOPE STABILITY MODELING STUDIES

7.1 Introduction

In Chapter 5, results of laboratory testing on fully softened shear strength (FSS) showed the preliminary improvements of treated soils over control untreated soils. The judgment was based solely on the quantitative comparison of soil components: FSS cohesion (c'_{fs}) and FSS friction angle (φ'_{fs}). In order to assess the combined effect of those soil properties on soil strength, an analytical slope stability analysis based on the FSS test results was conducted and presented in this chapter. The soil stability issue was tackled by evaluating the factor of safety (FOS) for the present Joe Pool Dam and Grapevine Dam sites using the obtained (c'_{fs}) and (φ'_{fs}) from FSS testing.

Dronamraju (2008) studied the effects of rainfall-induced slope failures on the Joe Pool Dam site. In this research, an analytical modeling was studied to address surficial failure for three cases representing three different scenarios: no rainfall, short-term rainfall and long-term rainfall conditions. FOS for each case was calculated using GSTABLE7 software, which uses limit equilibrium approach. Test results of slope stability analyses indicated that the FOS value was found to be the highest in the no rainfall condition and is the least for slopes subjected to rainfall events for long-term conditions. In this chapter, results of those two critical conditions from Dronamraju's research study are compared with the scenario of slopes subjected to wetting and drying cycles, i.e. using fully softened shear strength or FSS condition. FSS soil parameters obtained from Chapter 5 are used as input parameters for slope stability analysis and modeling.

Software SLOPE/W was chosen and used in the present modeling task for the calculation of FOS values. Two previously studied cases of no rainfall and long-term rainfall conditions were also repeated with the same soil input parameters used in Dronamraju's study to analyze the difference between GSTABL7 and SLOPE/W modeling tools.

Due to the sensitivity of FSS testing, slope stability analysis is also enhanced with a profound reliability study to address the variability of FSS soil parameters. As discussed early in Chapter 5, FSS results from DS device were adopted for this analysis, as the DS machine better represents the genuine values of FSS soil properties. Average values of FSS cohesion (c'_{fs}) and FSS friction angle (φ'_{fs}) were calculated and presented. To account for the fluctuation of the obtained FSS cohesion (c'_{fs}) and FSS friction angle (φ'_{fs}), a series of repeated tests were conducted on the control and treated soils using the DS apparatus for each effective normal stress (σ'_n) of 50 kPa (1044.3 psf), 100 kPa (2088.7 psf), 200 kPa (4177.1 psf) and 400 kPa (8354.2 psf). For the uniformity of the analysis of test results, all repeated tests used the same soil prepared from the same batch, where the soil was taken to conduct the original tests. Also soil specimens were tested on both DS setups to avoid equipment's default inaccuracies.

The approach of averaging the FSS cohesion $\left(c'_{fs}\right)$ and FSS friction angle (φ'_{fs}) was then utilized to analyze the results. Slight changes were observed in both FSS soil parameters and the standard deviation was determined by characterizing how much results of each test deviated from the total average values. The results were first interpreted and standard deviation was calculated. Normality check on the obtained soil properties was performed to assure the requirement for reliability study. Monte Carlo simulation was utilized to conduct the probabilistic analysis. Reliability index (β) and probability of failure (p_f) were calculated based on the safety margin for FOS of 1.5 as recommended for surficial failure on embankment dams by most researchers.

7.2 Slope stability studies using SLOPE/W

SLOPE/W is one component in a complete suite of geotechnical slope related analysis software called GeoStudio; this original software was developed by Prof. Fredlund at the University of Saskatchewan. SLOPE/W was one of the early geotechnical software products developed for analyzing slope stability. It features the limit equilibrium approach, which is suitable for solving numerous cases of slope failures including surficial skinslide type failures. Furthermore, slope stability analyses in SLOPE/W can be performed using both deterministic and probabilistic input parameters, which in turns helps to address the variability of soil strength properties as input parameters. With this comprehensive range of features, the SLOPE/W was adopted to carry on the slope stability studies in this chapter.

Based on the information provided by USACE, the cross sections with the corresponding geometries and positions of approximate phreatic surfaces for Joe Pool Dam and Grapevine Dam sites are presented in Figure 7.1 and Figure 7.2. Pool levels were used at the normal elevation of 522 ft. for Joe Pool Dam and 535 ft. for Grapevine Dam (Source: USACE). From the graphs, it could be inferred that seepage was found to be far under the surficial slope boundary, which is shallow and local in nature (Day, 1997). Therefore the effect of porewater pressure is negligible and will not be addressed in this slope stability analysis.

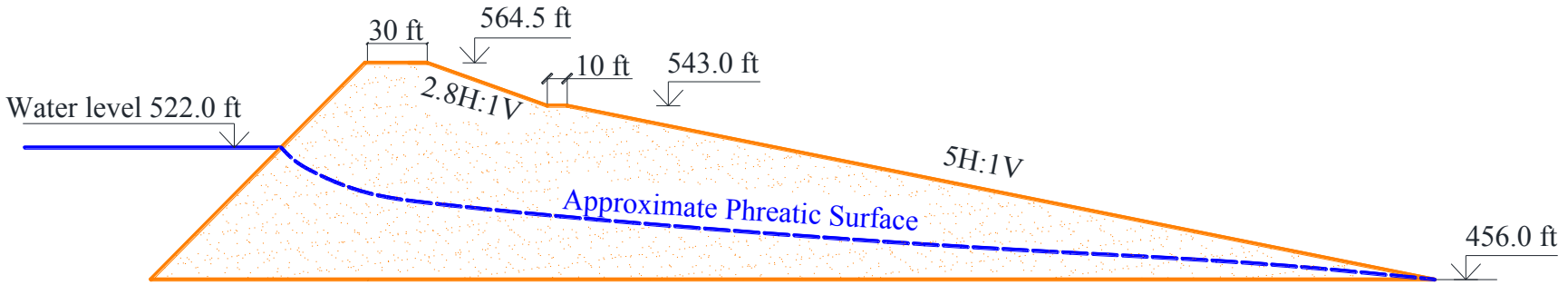

Figure 7.1. Geometries and approximate phreatic surface of Joe Pool Dam

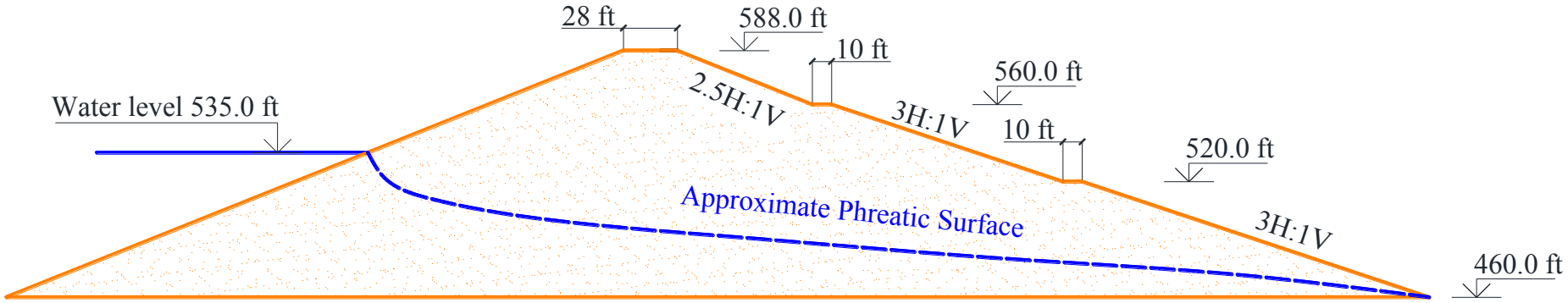

Figure 7.2. Geometries and approximate phreatic surface of Grapevine Dam

It can be noticed from the geometries of Joe Pool Dam and Grapevine Dam provided in Figure 7.1 and Figure 7.2 that the upper part of the downstream side close to the dam crest has a steeper slope with the ratio of 2.8H:1V for Joe Pool Dam and 2.5H:1V for Grapevine Dam. Thus, surficial failure is more likely to occur in these zones rather than other parts along the downstream side slope. Actual models used for slope stability analysis in SLOPE/W are shown in Figure 7.3 and Figure 7.4, analyzing only the critical part of the slope where the soil is more prone to failure.

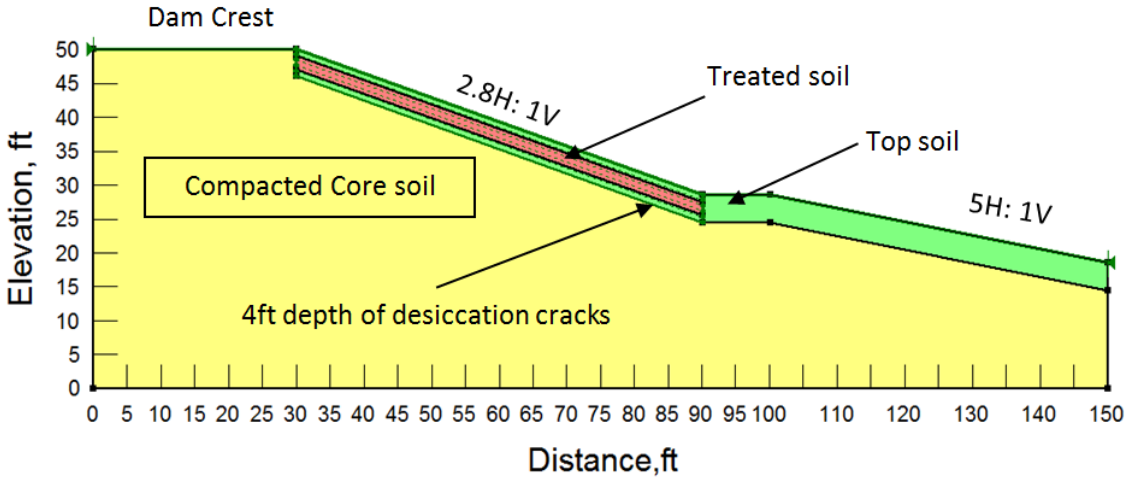

Figure 7.3. Cross-section of Joe Pool Dam modeled in SLOPE/W

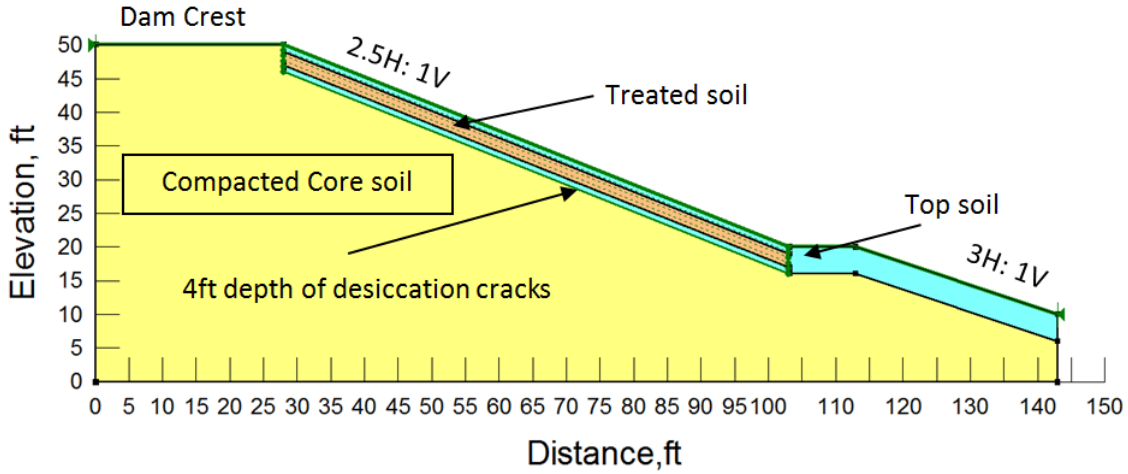

Figure 7.4. Cross-section of Grapevine Dam modeled in SLOPE/W

Both models of Joe Pool Dam and Grapevine Dam have three different soil regions: compacted core soil, top soil within 4 ft. from the surface and treated soil. The compacted core soil located within 4 ft. from the slope surface is subject to wetting and drying cycles, which alters the soil parameters. Thus, it was colored differently than the core soil of the embankment. Soil properties will be assigned properly to the soil regions based on the three case scenarios and their corresponding strength parameters.

Due to the nature of surficial slope failure, slip circles are determined using the grid and radius method. Figure 7.5 illustrates the Grid and Radius method in SLOPE/W. The center grid contains all possible center points of slip surfaces. Radii of slip surfaces are determined by the Tangential Points grid, which limits the failure surfaces to go within the desiccation crack depth of 4 ft.

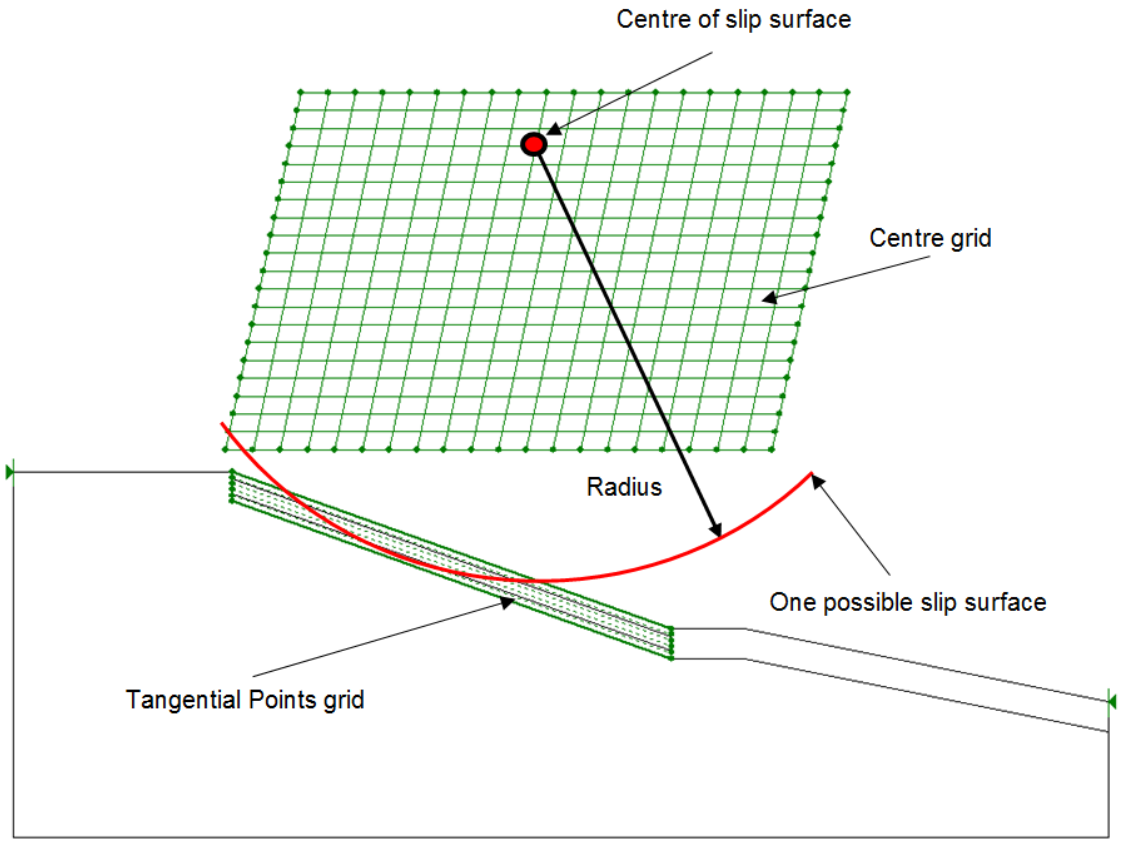

Figure 7.5. Grid and Radius Method in SLOPE/W

SLOPE/W generates all possible slip surfaces that meet the conditions of centre grid and tangential point grid and reports the lowest possible value of FOS. The Morgenstern-Price method was considered a suitable method to calculate FOS as it yields less value of safety compared to other methods like Bishop, Janbu and Ordinary Method of Slices.

7.2.1 Material Inputs

7.2.1.1 Unit weight

Mohr-Coulomb material model was adopted for this analysis with the basic soil parameters of unit weight, cohesion and friction angle as inputs. McCleskey (2005), in his research, studied the maximum dry unit weight of the control and treated soils from both Joe Pool Dam and Grapevine Dam. Table 7.1 and Table 7.2 show the results of McCleskey's work.

Table 7.1. Maximum dry unit weight for Joe Pool Dam soils (McCleskey, 2005)

Description	Unit Weight (pcf)
Control soil	93.5
20%compost treated soil	86
4%lime+0.30%fibers treated soil	98
8%lime+0.15 %fibers treated soil	95
8 %lime treated soil	97.5

Table 7.2. Maximum dry unit weight for Grapevine Dam soils (McCleskey, 2005)

Description	Unit Weight (pcf)
Control soil	108
20%compost treated soil	89
4%lime+0.30%fibers treated soil	103
8%lime+0.15 %fibers treated soil	102
8 %lime treated soil	103.5

In this analysis, maximum dry unit weight of soils was used for control and treated soils in all three cases regarding the saturation condition of the soils. The unit weight change upon the transition of soil from being unsaturated to being fully saturated is believed to have little impact on the outcome of slope stability analysis.

7.2.1.2 Cohesion and Friction Angle

Cohesion and friction angle inputs vary upon the soil conditions and will be determined specifically for each of the cases as (1) No rainfall condition, (2) Long-term rainfall condition and (3) Wetting and Drying Cycles-FSS condition

Case 1. No rainfall condition

McCleskey (2005) studied the undrained strength soil properties for short term loading on soils from the Joe Pool Dam and Grapevine Dam sites. Soils were compacted at optimum moisture content and tested in the DS machine. Undrained strength parameters namely undrained cohesion (c_u) and friction angle (φ_u) were determined from the DS testing data for both control and treated specimens. Test results are shown in Table 7.3 and Table 7.4.

Table 7.3. Undrained Strength Parameters for the Joe Pool Dam soils (McCleskey, 2005)

Treatment	Undrained Strength Parameters (DS Test)	
	Undrained Cohesion c_u kPa (psf)	Undrained Friction Angle φ_u (degrees)
Control soil	75.46 (1576)	37.6
20%compost treated soil	92.94 (1941)	42.9
4%lime+0.30%fibers treated soil	55.83 (1166)	28.1
8%lime+0.15 %fibers treated soil	55.40 (1157)	34.3
8 %lime treated soil	140.58 (2936)	23.5

Table 7.4. Undrained Strength Parameters for the Grapevine Dam soils (McCleskey, 2005)

Treatment	Undrained Strength Parameters (DS Test)	
	Undrained Cohesion c_u kPa (psf)	Undrained Friction Angle φ_u (degrees)
Control soil	38.50 (800)	16.9
20%compost treated soil	90.21 (1880)	38.8
4%lime+0.30%fibers treated soil	49.75 (1040)	38.4
8%lime+0.15 %fibers treated soil	46.97 (980)	42.3
8 %lime treated soil	94.52 (1970)	32.8

During the construction of both Joe Pool Dam and Grapevine Dam, embankment body was constructed on the borrow soil compacted to the optimum moisture content. Thus, the undrained strength parameters should be used to represent the soil state in the post-construction condition. The properties are also applicable to the compacted soil within 4 ft. of desiccation crack in case of no rainfall as it was originally excavated from the embankment core.

Case 2. Long-Term rainfall condition

Dronamraju (2008) in his study pointed out that long-term rainfall infiltration leads to saturation of the desiccated zone along the slope and the drained conditions typically prevail in the desiccation zone parallel to the slope. The residual shear strength parameters were considered relevant and adopted to carry out the slope analysis for this scenario. Residual strength testing on both Joe Pool Dam and Grapevine Dam soils was conducted using the Bromhead TRS device. The obtained residual cohesion (c'_r) and friction angle (φ'_r) parameters were applied to the top 4 ft. of desiccation zone including the compacted core soil and the treated soils. The undrained strength parameters from the DS test results of the control

soil were used for the soil below the desiccation zone. Table 7.5 and Table 7.6 report the TRS test results on residual strength parameters of Joe Pool Dam and Grapevine Dam soils. It should be noted that the Case 2 of this research is similar to Case 3 of the Dronamraju's (2003) study.

Table 7.5 Results of TRS test on Joe Pool Dam soils (Dronamraju, 2008)

Treatment	Residual Cohesion c'_r kPa (psf)	Residual Friction Angle φ'_r (degrees)
Control soil	0 (0)	20
20%compost treated soil	2.9 (60)	19
4%lime+0.30%fibers treated soil	10.5 (220)	33
8%lime+0.15 %fibers treated soil	16.8 (350)	39
8 %lime treated soil	12.5 (260)	36

Table 7.6 Results of TRS test on Grapevine Dam soils (Dronamraju, 2008)

Treatment	Residual Cohesion c'_r kPa (psf)	Residual Friction Angle φ'_r (degrees)
Control soil	0 (0)	18
20%compost treated soil	3.4 (70)	20
4%lime+0.30%fibers treated soil	10.5 (220)	35
8%lime+0.15 %fibers treated soil	16.3 (340)	40
8 %lime treated soil	12.9 (270)	38

Case 3. Under repeated wetting and drying conditions (Fully Softened condition)

Wright (2005) studied shallow slope failures in embankments and suggested that after several wetting and drying cycles, softening will take place in the soil. This reduces the drained strength of clays nearly to the normally consolidated strength values. The softening phenomenon starts from the formation of shrinkage cracks during periods of drought, followed

by water entering these cracks during rainfall. Wright recommended the long-term soil strengths for embankment of compacted clay be characterized by the Fully Softened Shear (FSS) strength parameters.

Tiwari (2011) recommended the use of linear average result to characterize the FSS based on the tested effective normal stresses. This approach simplifies the analyses and is commonly used by the most researchers. Wright (2005) also suggested that the strength envelope for FSS can be represented by an equivalent linear envelope with the condition that strengths are not extrapolated beyond the range of tested effective normal stresses. In this study, one of the main objectives is to address the shallow surficial failure where effective normal stresses are well below 400 kPa (8354.2 psf). Thus, the use of curved strength envelope for FSS is not necessary; rather average strength envelope is sufficient and hence adopted. Two FSS soil properties, namely the FSS cohesion (c'_{fs}) and FSS friction angle (φ'_{fs}) obtained from Chapter 5 are used as input parameters.

Results of FSS testing by the DS device in Chapter 5 were used for this analysis over TRS testing data, as the DS device is believed to provide the FSS strength that are more expected for treated soils and shear strain levels. Table 7.7 and Table 7.8 present the FSS soil parameters from the Joe Pool Dam and Grapevine Dam test site soils.

Table 7.7. FSS parameters determined from the DS test results for Joe Pool Dam soils

Soil	DS Results	
	c'_{fs} kPa (psf)	φ'_{fs} Degrees
Control soil	0 (0)	27.0
20%compost treated soil	13.13 (274.2)	26.9
4%lime+0.30%fibers treated soil	34.8 (726.8)	33.5
8%lime+0.15 %fibers treated soil	29.0 (605.7)	35.4
8 %lime treated soil	21.9 (457.4)	36.6

Table 7.8. FSS parameters determined from the DS test results for Grapevine Dam soils

Soil	DS Results	
	c'_{fs} kPa (psf)	φ'_{fs} Degrees
Control soil	0.0 (0)	34.8
20%compost treated soil	17.2 (359.2)	31.4
4%lime+0.30%fibers treated soil	24.5 (511.7)	37.2
8%lime+0.15 %fibers treated soil	27.2 (568.1)	40.0
8 %lime treated soil	10.0 (208.9)	38.9

FSS soil parameters were applied to the top 4 ft. of soil, where wetting and drying cycles prevailed. Compacted core soil properties were adopted for embankment core materials which are similar to those used in Case 2 analysis.

7.2.2 Results and Discussion from Slope Stability Analysis

Figures 7.6 to 7.11 present the results of present slope stability analyses of both embankment sections. FOS values are highlighted in each case along with the position of the critical slip surface. Only the results of control untreated soil and one treated soil (8%lime+0.15%fibers amendment) from Joe Pool Dam and Grapevine Dam are presented in this chapter. The remaining results for other surficial slope treatments can be found in the Appendix B section.

The results of slope stability analysis from SLOPE/W software for all three cases are summarized in Table 7.9 and Table 7.10.

.

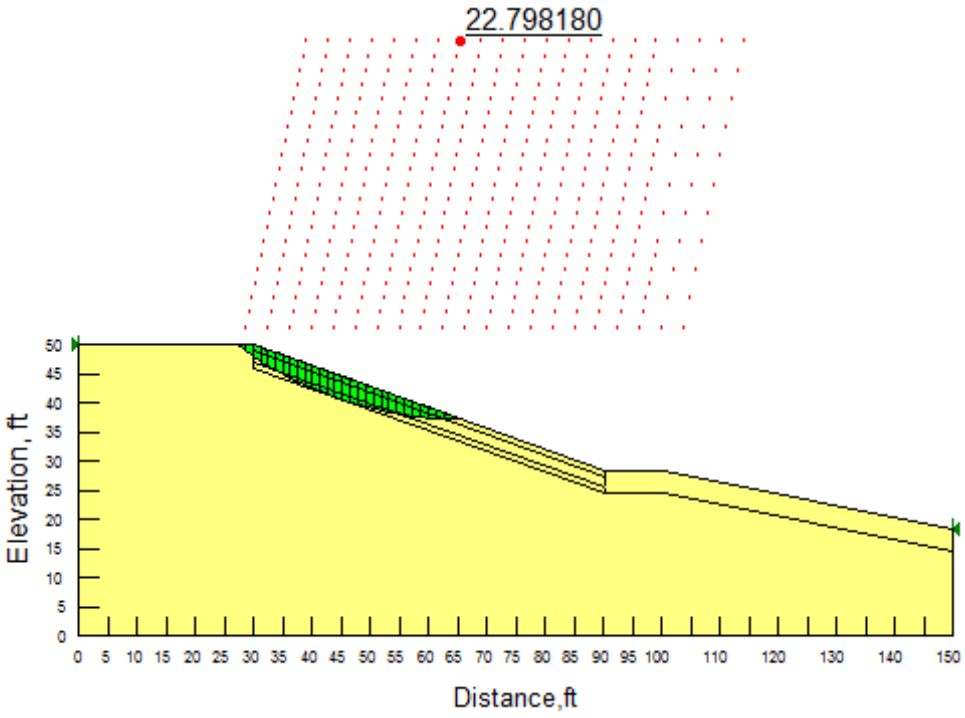

Figure 7.6. Case 1 result for Joe Pool Dam Control soil

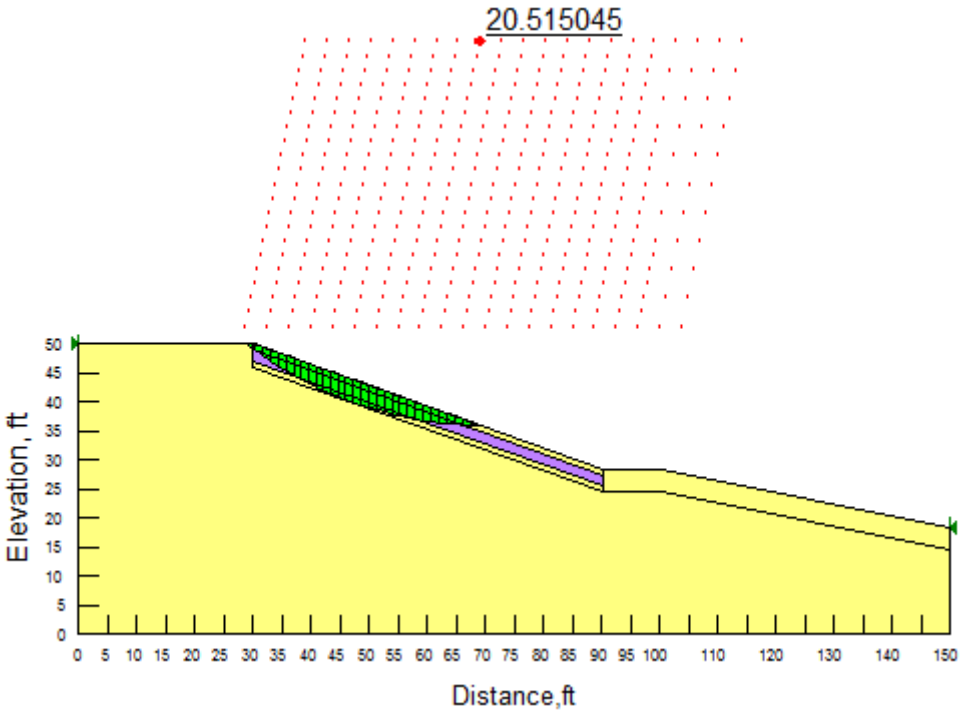

Figure 7.7. Case 1 result for Joe Pool Dam 8%lime+0.15%fibers treated soil

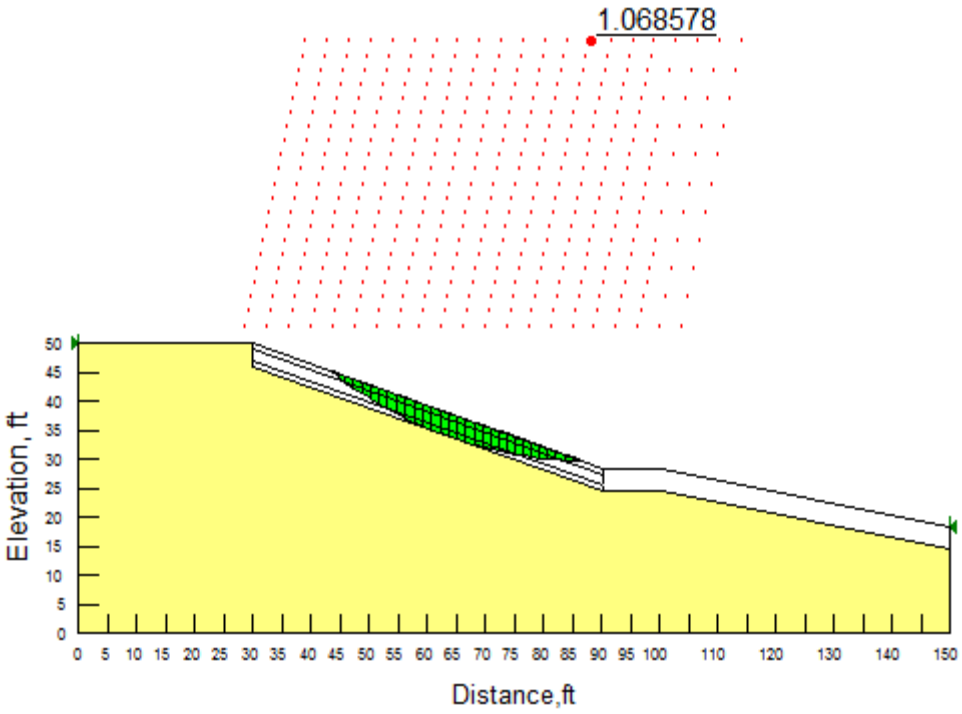

Figure 7.8. Case 2 result for Joe Pool Control Dam soil

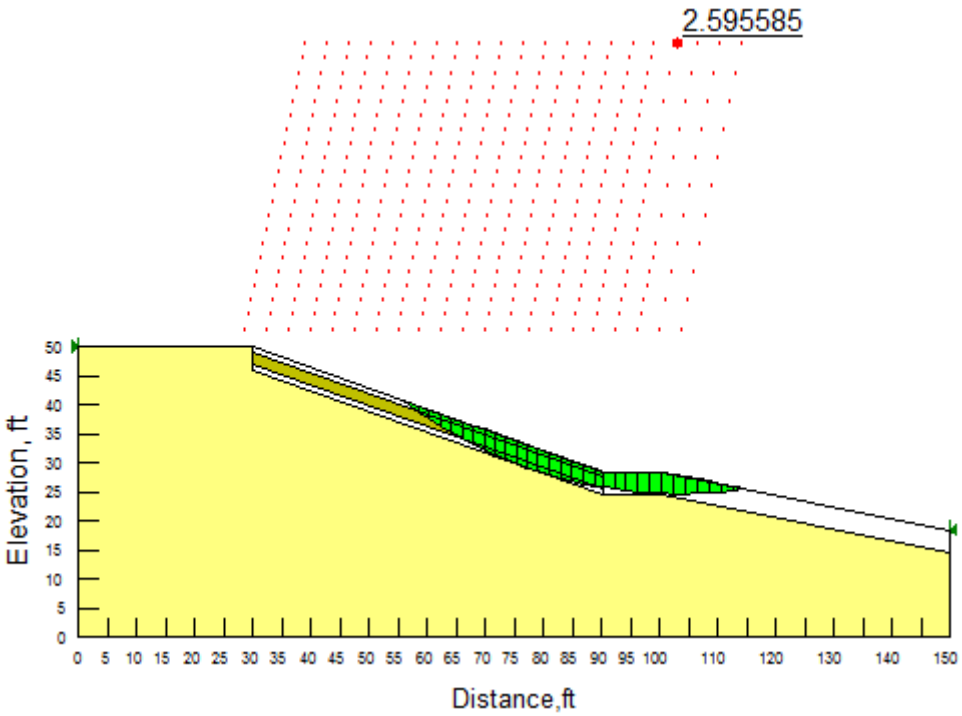

Figure 7.9. Case 2 result for Joe Pool Dam 8%lime+0.15%fibers treated soil

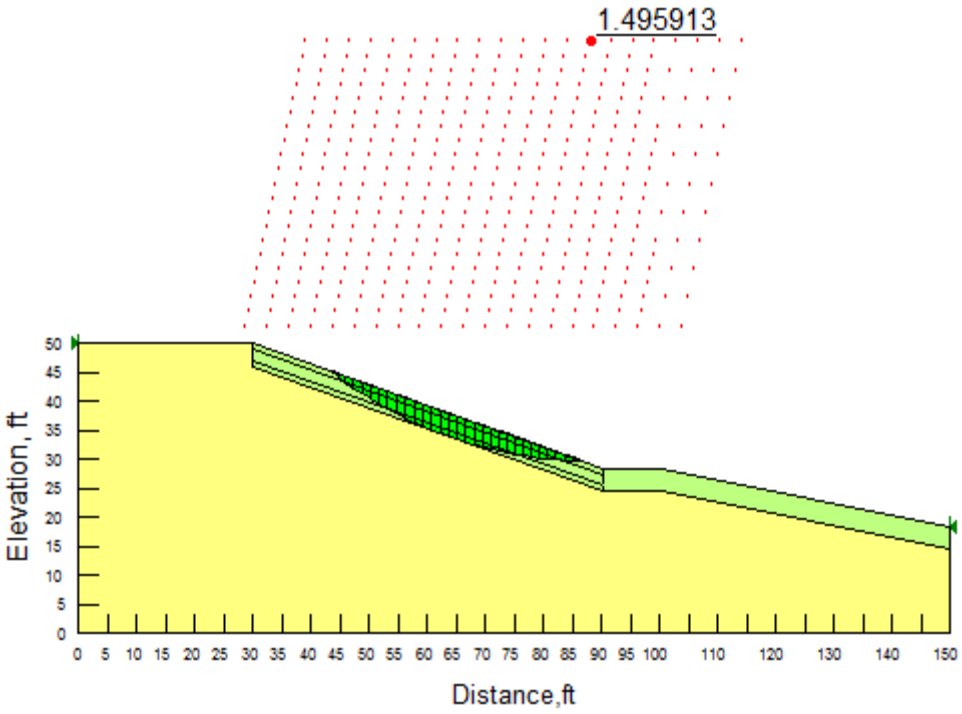

Figure 7.10. Case 3 result for Joe Pool Dam Control soil

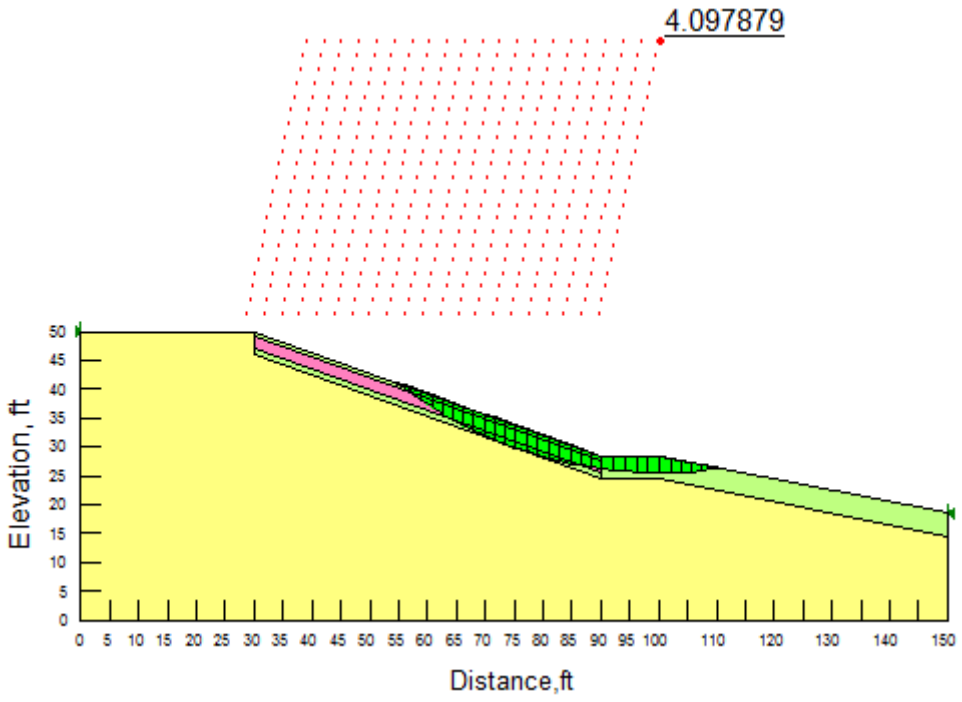

Figure 7.11. Case 3 result for Joe Pool Dam 8%lime+0.15%fibers treated soil

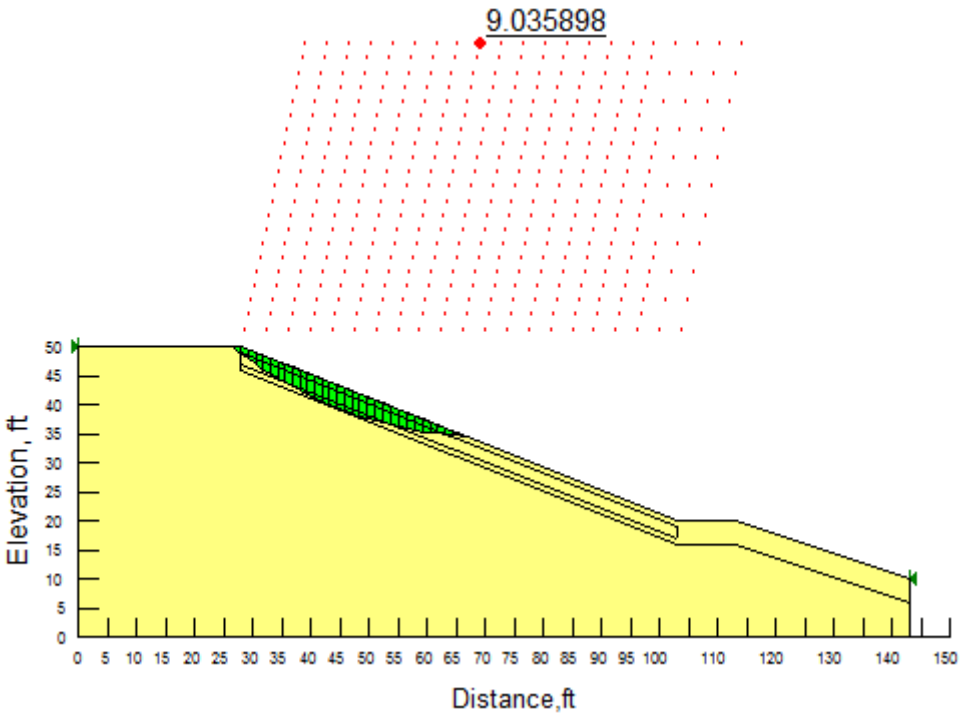

Figure 7.12. Case 1 result for Grapevine Dam Control soil

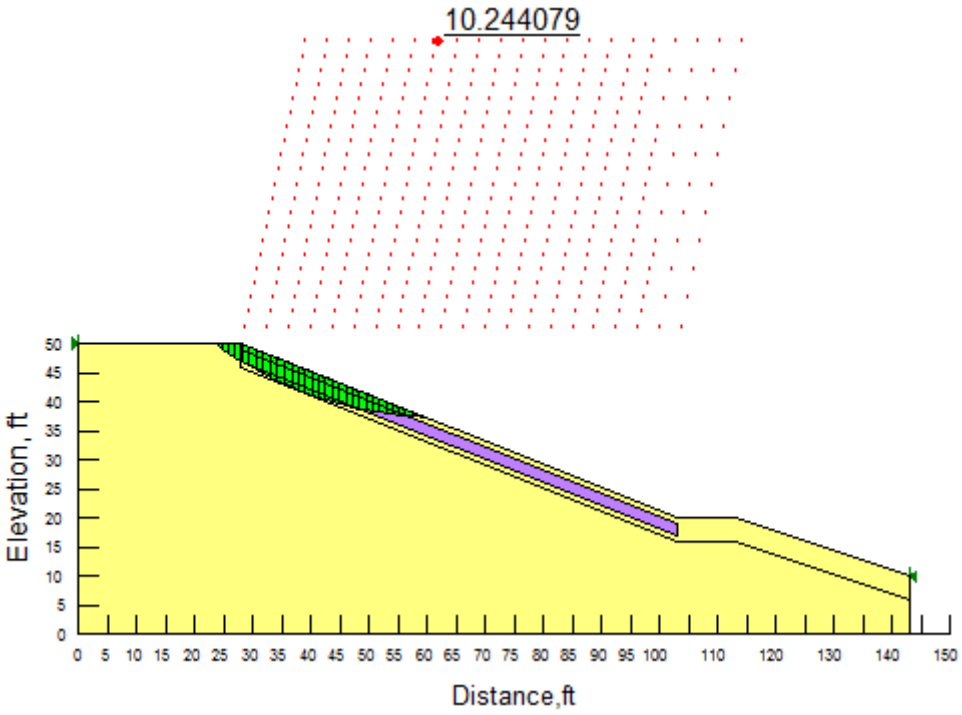

Figure 7.13. Case 1 result for Grapevine Dam 8%lime+0.15%fibers treated soil

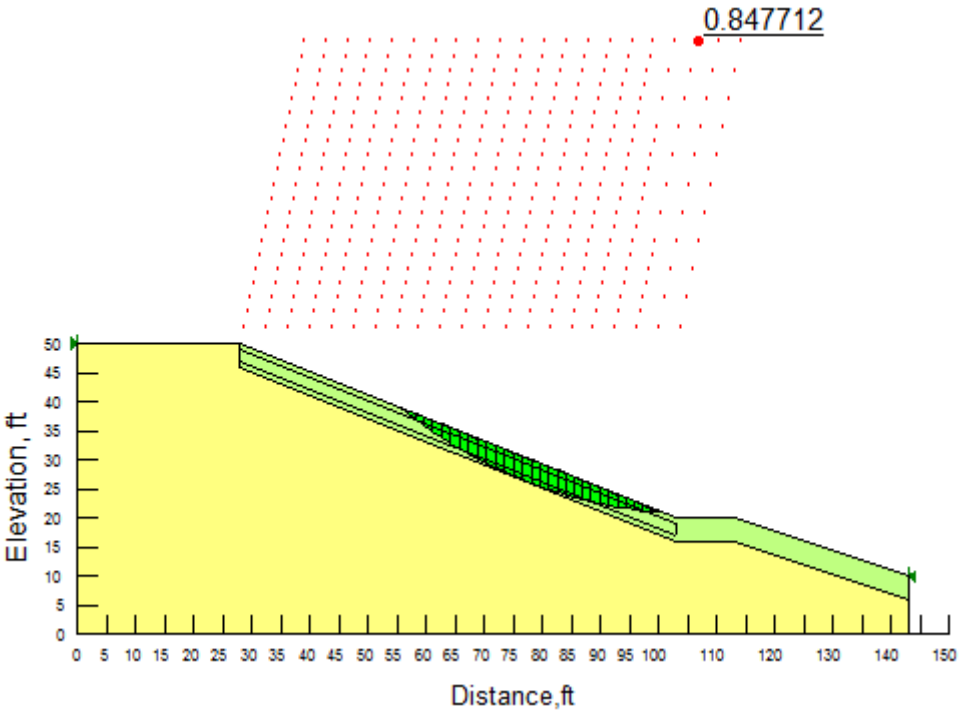

Figure 7.14. Case 2 result for Grapevine Dam Control soil

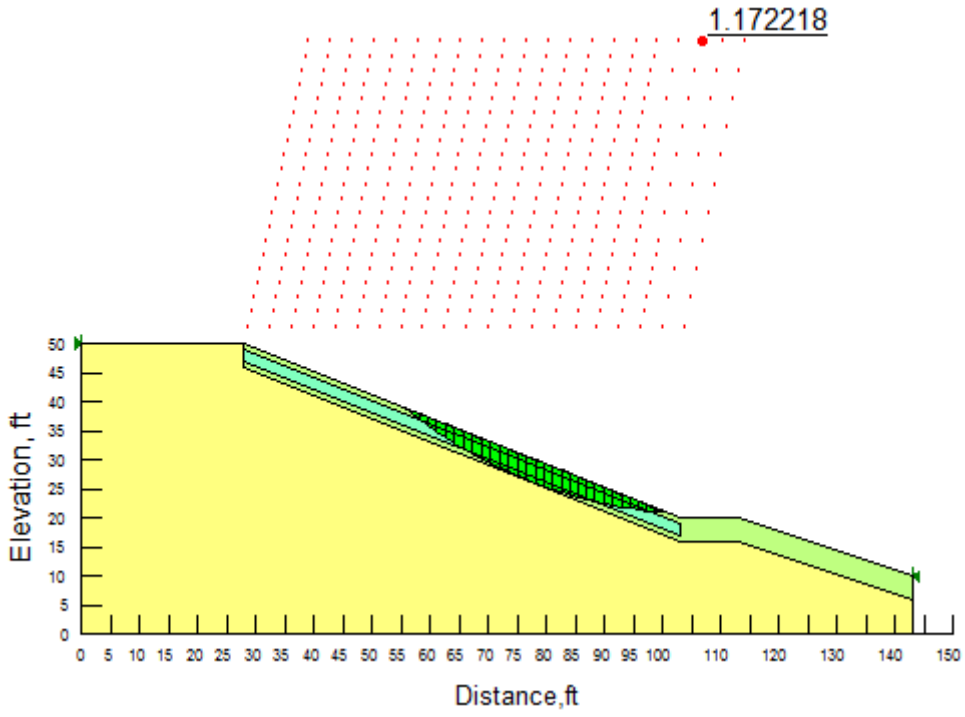

Figure 7.15. Case 2 result for Grapevine Dam 8%lime+0.15%fibers treated soil

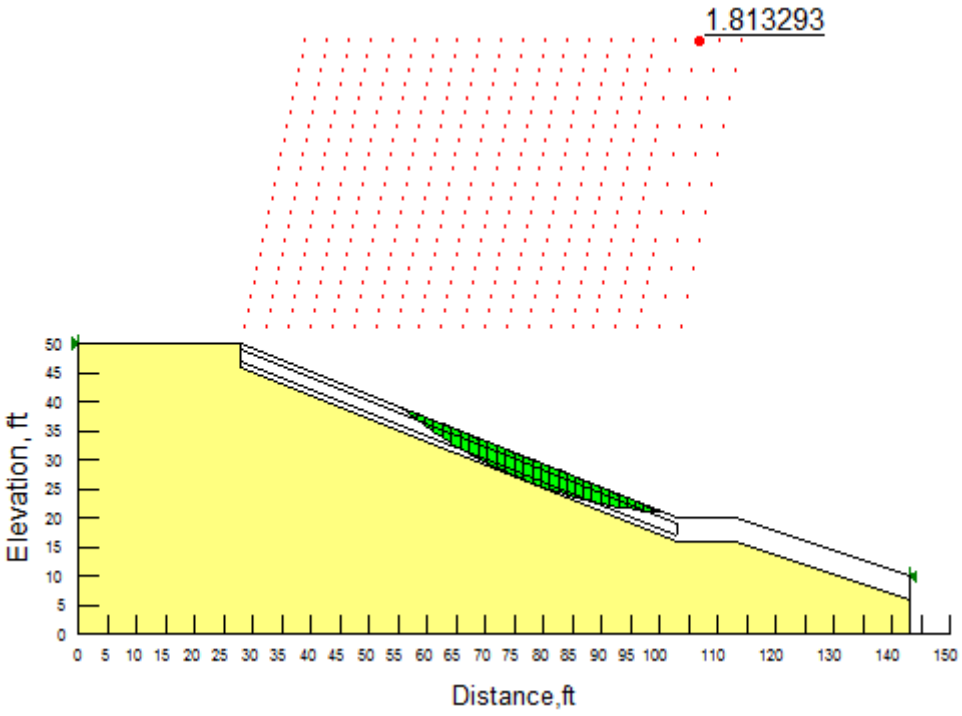

Figure 7.16. Case 3 result for Grapevine Dam Control soil

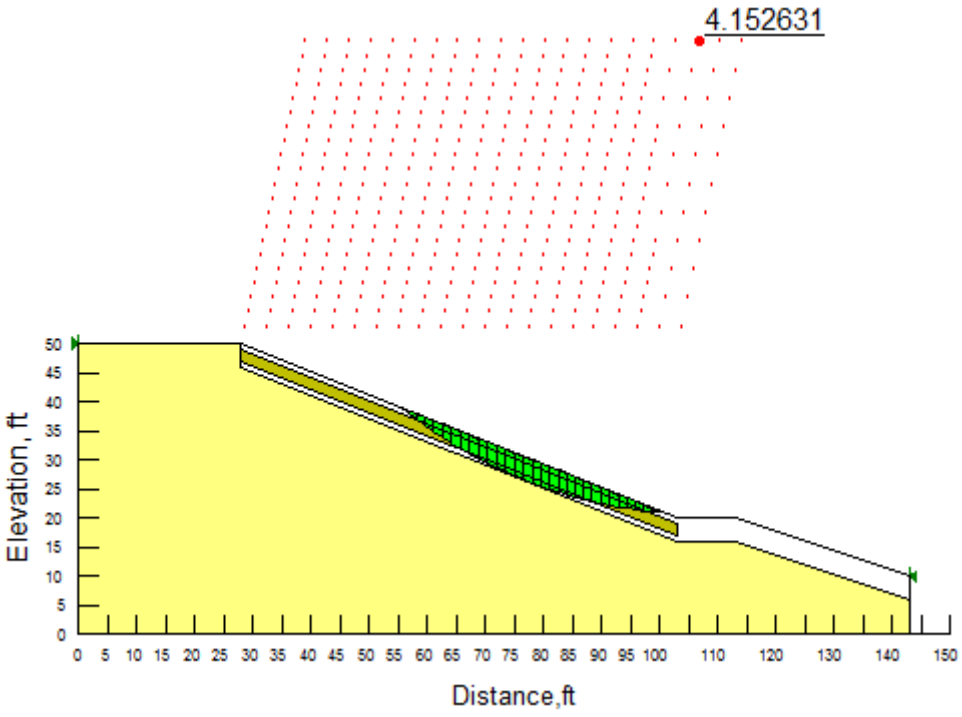

Figure 7.17. Case 3 result for Grapevine Dam 8%lime+0.15%fibers treated soil

Table 7.9. FOS for different cases for Joe Pool Dam soils – Surficial Slope Failures

Soil	Case 1. No Rainfall Condition	Case 2. Long-term Rainfall Condition	Case 3. Wetting and Drying Cycles -FSS Condition
Control Soil	22.8 (9.0)	1.1 (1.8)	1.5
20%compost Treated Soil	25.3 (9.2)	1.4 (2.3)	2.9
4%lime+0.30%fibers Treated Soil	20.1 (8.9)	2.12 (4.7)	4.4
8%lime+0.15%fibers Treated Soil	20.5 (9.0)	2.56 (6.7)	4.1
8%lime Treated Soil	26.8 (9.4)	2.3 (5.9)	3.4

Note: FOS in parenthesis were reported from GSTABL and for Deep Seated Soil Failure by Dronamraju (2008)

Table 7.10. FOS for different cases for Grapevine Dam soils

Soil	Case 1. No Rainfall Condition	Case 2. Long-term Rainfall Condition	Case 3. Wetting and Drying Cycles -FSS Condition
Control Soil	9.0	0.9	1.8
20%compost Treated Soil	12.9	1.2	3.3
4%lime+0.30%fibers Treated Soil	10.3	1.9	3.9
8%lime+0.15%fibers Treated Soil	10.2	2.5	4.2
8%lime Treated Soil	12.3	2.2	2.7

Note: Red numbers indicate that the FOS is not satisfied. Failure is prominent.

Generally, the minimum FOS required for embankment to prevent surficial failure is 1.5. Results show that the failure will occur for Case 2 of long-term rainfall events for both Joe Pool Dam and Grapevine Dams in untreated soil condition. In the case of Case 3 – FSS under wetting and drying cycle scenario, failure is likely for the control section from Joe Pool Dam site when the FOS value is close to 1.49. Overall, FOS is higher for the sections in which soil admixtures were used for surficial soil treatments.

Case 1. No Rainfall Condition

The results from the slope stability analysis indicate that under undrained conditions, the slope is safe against failure when there is no rainfall. FOS values obtained are well beyond the safety margin with FOS of Joe Pool Dam soils above 20 and FOS of Grapevine Dam soils above 9.

The treatment admixtures appear to have minor influence on the factor of safety values. Results from Table 7.9 for Joe Pool Dam soils indicate that in case of no rainfall, 8%lime+0.15%fibers and 8%lime amendments have slightly lower FOS compared to the control untreated soil. Overall, for case 1, all sections showed effective performance.

However, compared to the values of FOS values reported by Dronamraju (2008), the present SLOPE/W analysis yields higher FOS values. This is attributed to the fact that the model used in Dronamraju's study of Case 1 had explored for deep-seated soil failure; whereas, the present SLOPE/W analysis has only considered surficial slope failures for a depth restriction of 4 ft. from the slope surface.

Case 2. Long-Term Rainfall Condition

Among all cases, long-term rainfall condition yielded the lowest FOS. 8%lime+0.15%fibers and 8%lime treatments provided the highest FOS values on both Joe Pool Dam and Grapevine Dam sites. Enhanced FOS values from these two sections (8%lime+0.15%fibers and 8%lime sections) have the ratios are two to four times those of the FOS calculated for control soil section, respectively. FOS of control section and 20%compost

treated section are well below the safety margin of 1.5 and will most likely result in failure on both Joe Pool Dam and Grapevine Dam sites. Also, results for SLOPE/W appear to be more conservative (lower) than the values of FOS in Dronamraju's study (2008), which used GSTABLE7 software. The variation could be attributed to the nature of the slope stability analysis method used in the respective analyses and also more realistic simulation of layer properties used in the surficial layer modeling.

Case 3. Wetting and Drying Cycles-FSS Condition

FOS values obtained from this scenario are in between those of case 1 and case 3. Nevertheless, unsafe levels are reached on control soil at Joe Pool Dam (FOS of 1.49) and it is close to unsafe zone for Control soil at Grapevine Dam (FOS of 1.81). Both 4%lime+0.30%fibers and 8%lime+0.15%fibers treatments have improved the strength and hence the related FOS values, which are 2 to 3 times that of FOS of control soil section. Based on the FOS values presented in Table 7.9 and Table 7.10, the improvement of FOS of the admixtures over the control soil is plotted and shown in Figure 7.18 and Figure 7.19, the improvement of FOS of the admixtures over the control soil is plotted and shown in Figure 7.18 and Figure 7.19.

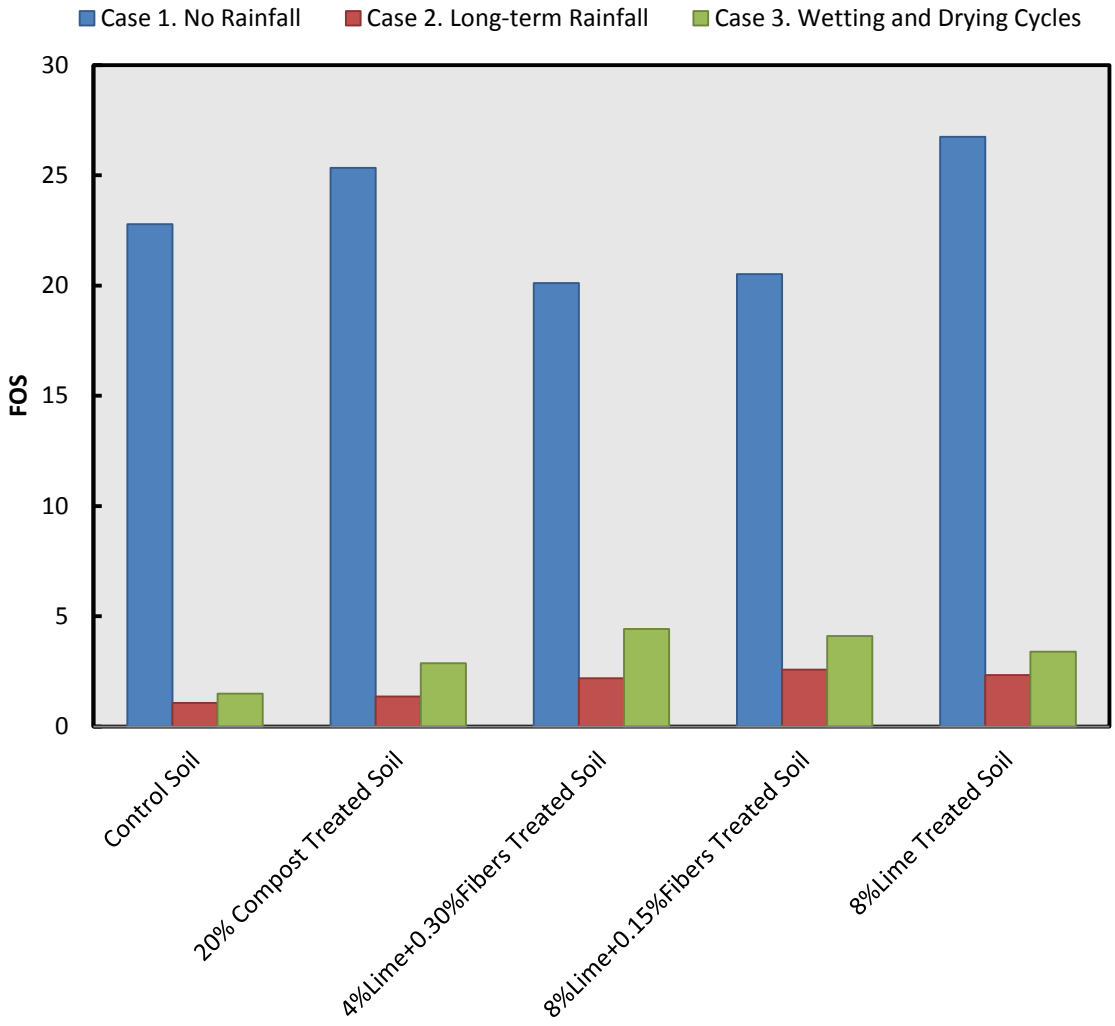

Figure 7.18. FOS comparison between 3 cases for Joe Pool Dam soils

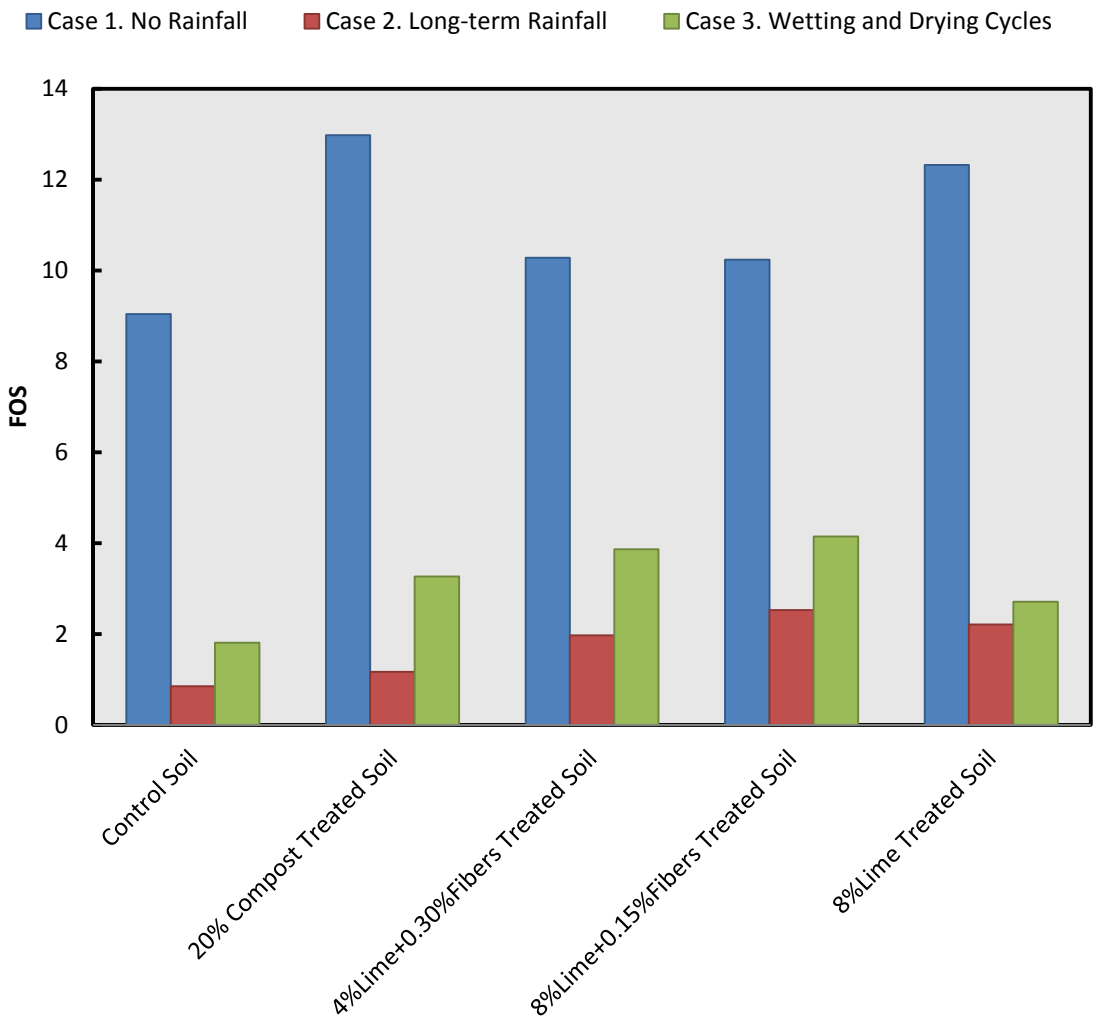

Figure 7.19. FOS comparison between 3 cases for Grapevine Dam soils

Skempton (1977), in his case study research involving slopes in brown London clay, suggested that slopes of fissured clay that have not undergone previous sliding (first-time slides) could be designed based on FSS soil parameters. Using residual drained soil properties for design is appropriate for slopes that have already undergone 1-2 m of shear displacement (Skempton, 1964; Skempton, 1977). Wright (2005) also highlighted the importance of using FSS soil properties to depict slopes being exposed to wetting and drying cycles. His studies suggested that the formation of desiccation cracks during drought, followed by rainfall water

entering these cracks, softens the clay and reduces its strength from the as-compacted strength value to the fully softened strength value. Thus, the use of the FSS approach is considered relevant for the design of both Joe Pool Dam and Grapevine Dam sites, where the slopes experience wetting and drying cycles, and surficial failures have been commonly experienced.

Slope modeling results in this chapter are in agreement with the results of Chandler and Skempton's study (1974) as they pointed out that the FSS cohesion (c'_{fs}) is vital to slope stability against surficial slope failure and it is excessively conservative to ignore the small cohesion value. The amendment admixtures used on both the Joe Pool Dam and Grapevine Dam surficial soils provided an increase in cohesion intercept of 40 kPa (835 psf) and this has increased the FOS values significantly when compared to the control or untreated soil slope section. This reconfirms the observation from Dronamraju's study that drained cohesion at the surface due to soil treatment will play a major role in enhancing surficial slope stability.

7.3 Reliability Analysis

Duncan (2013) in his state of the art study for slope stability emphasized the use of probabilistic analysis as it reflects the effects of uncertainties and provides a viewpoint for geotechnical engineers in comparing the probabilistic uncertainties that can happen in real field conditions. Present researchers have been using the concept of FSS from a deterministic point of view. However, variability and reliability of the FSS are still important objectives to explain the importance of this failure in the field in probabilistic terms. Due to the sensitivity of FSS testing, the results could be exposed to a certain level of variability. In an attempt to quantify the variability of the FSS test results namely the interpreted average values of FSS cohesion (c'_{fs}) and FSS friction angle (φ'_{fs}), a reliability study is conducted here in this chapter to assess the effects of variable uncertainty on the outcome of FOS from slope stability analysis.

To establish accurate and realistic results, several identical tests were conducted on both control and treated soil of Joe Pool Dam and Grapevine Dam sites, using the DS device. Average values of FSS cohesion (c'_{fs}) and FSS friction angle (φ'_{fs}) were calculated based on

the combined data from the original tests and the repeated tests. Variability of these FSS soil parameters is characterized by their standard deviation and average values, which were calculated from the same FSS test results.

Results of interpreted FSS cohesion and FSS friction angle values are first subjected to normality checks. Reliability analysis is then conducted using the Monte Carlo simulation method as a built-in feature of the SLOPE/W software.

7.3.1 Data interpretation

Data in Chapter 5 indicated that the FSS of soils can be characterized by two equations, using linear regression modeling on the test results:

For control untreated soil $$\tau_{fs} = \sigma'_n \times tan(\varphi'_{fs})$$ Eq. 7-1

For treated soils $$\tau_{fs} = c'_{fs} + \sigma'_n \times tan(\varphi'_{fs})$$ Eq. 7-2

Data interpretation is described in the following sections for control and treated soils.

Control soil

Based on the 8 tests (including 4 repeated tests to ascertain the deviation and variability), linear strength envelope is established by analyzing test results with a linear regression modeling. The average FSS friction angle is then determined and is reported as (φ'_{fs}). The standard deviation of the FSS friction angle (Δ_φ) is then determined from individual test data.

Figure 7.20 presents the concept of determining an average FSS friction angle for each data point (φ'_{fsi}). Data points having coordinates of $(\sigma'_{ni},\tau'_{fsi})$ represent the FSS test results conducted under effective normal stress (σ'_{ni}) with the value of corresponding shear stress(τ'_{fsi}). Line (a) is drawn through the origin and the data point $(\sigma'_{ni},\tau'_{fsi})$ as shown in Figure 7.20. As described in Eq. 7-1, FSS strength (τ_{fs}) is directly proportional to the tangent of FSS friction angle (φ'_{fs}), thus the average FSS friction angle (φ'_{fsi}) for that particular data point is determined as:

$$\varphi'_{fsi} = tan^{-1}\left(\frac{\tau'_{fsi}}{\sigma'_{ni}}\right)$$ Eq. 7-3

Standard deviation for FSS friction angle (Δ_φ) is calculated based on the results of all the individual average FSS friction angles (φ'_{fsi}) calculated from all testing data points. Table 7.11 summarizes the calculations for standard deviation of the FSS friction angle (φ'_{fs}).

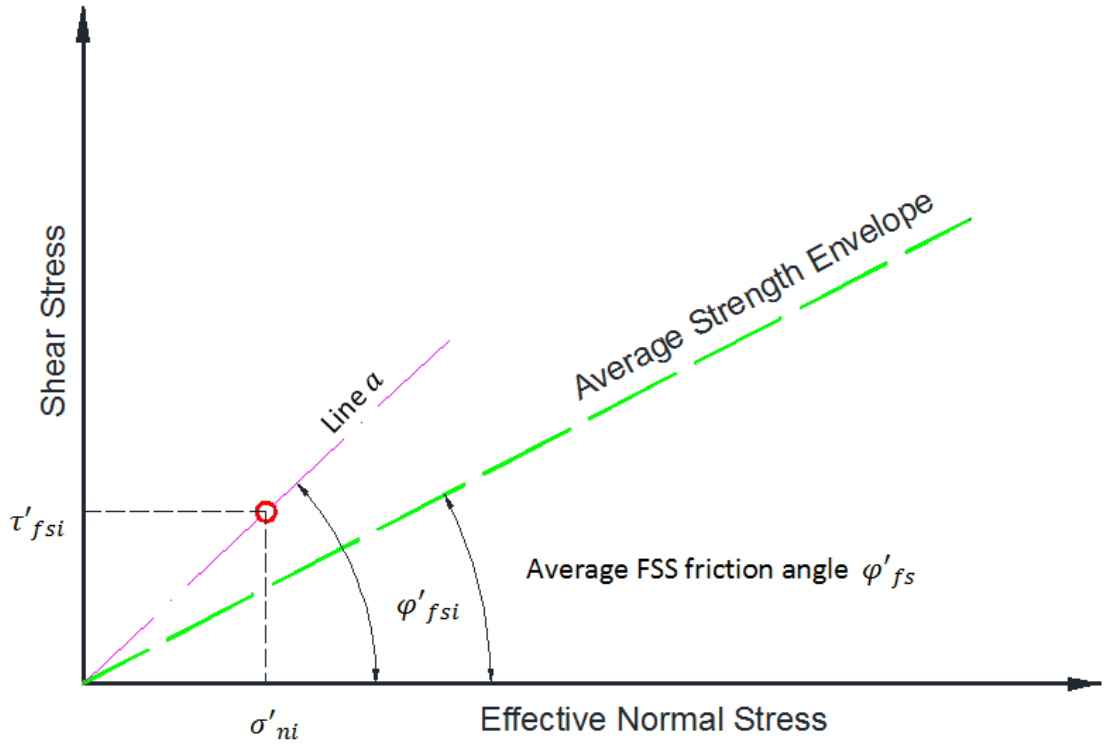

Figure 7.20. Data interpretation for Control soil

Table 7.11. Standard deviation calculation for FSS friction angle for Control soil

$No.$	σ'_{ni}	τ'_{fsi}	$\varphi'_{fsi} = tan^{-1}\left(\frac{\tau'_{fsi}}{\sigma'_{ni}}\right)$	Δ_φ
1	σ'_{n1}	τ'_{fs1}	φ'_{fs1}	$\Delta_\varphi = \sqrt{\frac{\sum_{i=1}^{a}(\varphi'_{fsi} - \varphi'_{fs})^2}{a-1}}$
2	σ'_{n2}	τ'_{fs2}	φ'_{fs2}	
3	σ'_{n3}	τ'_{fs3}	φ'_{fs3}	
...				
a	σ'_{na}	τ'_{fsa}	φ'_{fsa}	

Note: Average FSS friction angle (φ'_{fs}) is determined by the result of linear regression analysis

Treated soil

In Chapter 5, the preliminary results show the presence of cohesion as part of the additive effect on the control soil. The procedure to interpret average and standard deviation data is similar to the procedure used in the case of control soil, except that this calculation is attempted for both cohesion and friction angle components. With the 8 test results, the average strength envelope is plotted by using the linear regression analysis. Values of average FSS cohesion (c'_{fs}) and FSS friction angle (φ'_{fs}) are determined based on the statistic report of the best fit functions.

In order to calculate standard deviation for FSS cohesion (c'_{fs}) and FSS friction angle (φ'_{fs}), the average FSS soil parameters (φ'_{fsi}) and (c'_{fsi}) for each data point should be estimated as well.

Figure 7.21 illustrates the concept of estimating FSS soil parameters (φ'_{fsi}) and (c'_{fsi}) from each test result. Each test result is depicted by one data point $(\sigma'_{ni}, \tau'_{fsi})$ representing the shear stress obtained as (τ'_{fsi}) from the effective normal stress (σ'_{ni}) as marked as a red circle in Figure 7.21. To obtain the corresponding values of FSS cohesion (c'_{fsi}) and FSS friction angle (φ'_{fsi}) for that data point, the procedure is as follows:

- For FSS friction angle (φ'_{fsi}) , line (a) joining the average FSS cohesion (c'_{fs}) and the current data point $(\sigma'_{ni}, \tau'_{fsi})$ is drawn. With the value FSS cohesion fixed to the average FSS cohesion (c'_{fs}), the FSS friction angle for the current data point is the slope of line (a) and thus value of (φ'_{fsi}) can be determined as:

$$\varphi'_{fsi} = tan^{-1}\left(\frac{\tau'_{fsi} - c'_{fs}}{\sigma'_{ni}}\right) \qquad \text{Eq. 7-4}$$

- For FSS cohesion c'_{fsi}, line (b) parallel to average strength envelope found above is drawn through the data point $(\sigma'_{ni}, \tau'_{fsi})$ (Figure 7.21). Hence the value of FSS friction angle is fixed with average FSS friction angle (φ'_{fs}) as line (b) has the same slope value as the average

Strength Envelope. The intercept of the drawn line with Shear Stress axis (vertical axis) is the FSS cohesion (c'_{fsi}). Value of (c'_{fsi}) can be numerically calculated as:

$$c'_{fsi} = \tau'_{fsi} - \sigma'_{ni} \times tan(\varphi'_{fs}) \qquad \text{Eq. 7-5}$$

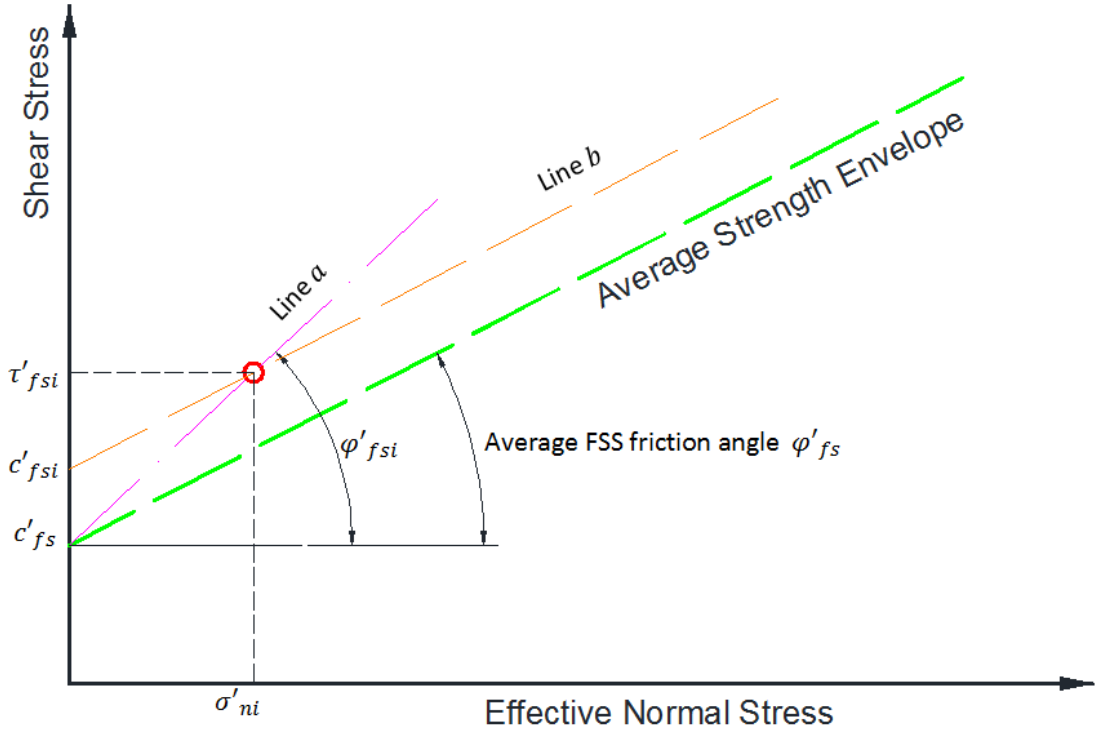

Figure 7.21. Data interpretation for Treated soil

Standard deviation values for FSS friction angle (Δ_φ) and FSS cohesion (Δ_c) are calculated based on the results of all the individual average FSS friction angles (φ'_{fsi}) and FSS cohesion (c'_{fsi}) values calculated from all test data points. Table 7.12 summarizes calculations for standard deviation of the FSS friction angle (Δ_φ) and FSS cohesion (Δ_c) .

Figure 7.22 to Figure 7.25 present the average shear strength envelopes developed using linear regression based analysis on the original and repeated tests. From the strength envelopes, average values of FSS Cohesion (c'_{fs}) and FSS Friction Angle (φ'_{fs}) are determined and used to calculate the (c'_{fsi}) and (φ'_{fsi}) for each data point, which in turn is utilized to calculate the standard deviations as shown in Table 7.13 toTable 7.16. Due to space

limitation, only results of control soil and 8%lime+0.15%fibers treated soil sections are presented. The remaining results of other treatments can be found in Appendix B section.

Table 7.12 Standard deviation calculation for FSS friction angle and FSS cohesion for Treated soil

$No.$	σ'_{ni}	τ'_{fsi}	$\varphi'_{fsi} = tan^{-1}\left(\frac{\tau'_{fsi} - c'_{fs}}{\sigma'_{ni}}\right)$	$c'_{fsi} = \tau'_{fsi} - \sigma'_{ni} \times tan(\varphi'_{fs})$	Δ_{φ}	Δ_c
1	σ'_{n1}	τ'_{fs1}	φ'_{fs1}	c'_{fs1}	$\Delta_{\varphi} = \sqrt{\frac{\sum_{i=1}^{a}(\varphi'_{fsi} - \varphi'_{fs})^2}{a-1}}$	$\Delta_c = \sqrt{\frac{\sum_{i=1}^{a}(c'_{fsi} - c'_{fs})^2}{a-1}}$
2	σ'_{n2}	τ'_{fs2}	φ'_{fs2}	c'_{fs2}		
3	σ'_{n3}	τ'_{fs3}	φ'_{fs3}	c'_{fs3}		
...						
a	σ'_{na}	τ'_{fsa}	φ'_{fsa}	c'_{fsa}		

Note: Average FSS friction angle φ'_{fs} and FSS cohesion c'_{fs} are determined from the result of linear regression analysis

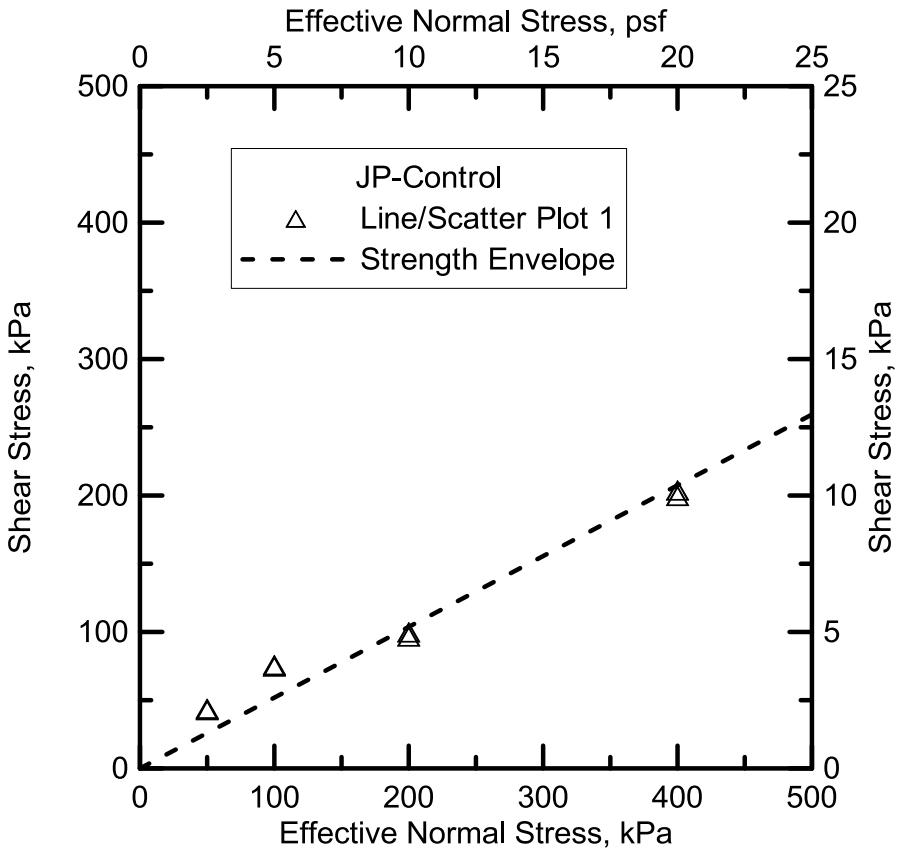

Fit Results

Strength Envelope
Equation Y = 0.5187058824 * X
Number of data points used = 8
Average X = 187.5
Average Y = 104.875
Residual sum of squares = 1862.29
Coef of determination, R-squared = 0.983975
Residual mean square, sigma-hat-sq'd = 266.041

Figure 7.22. Strength Envelope for Joe Pool Dam Control soil

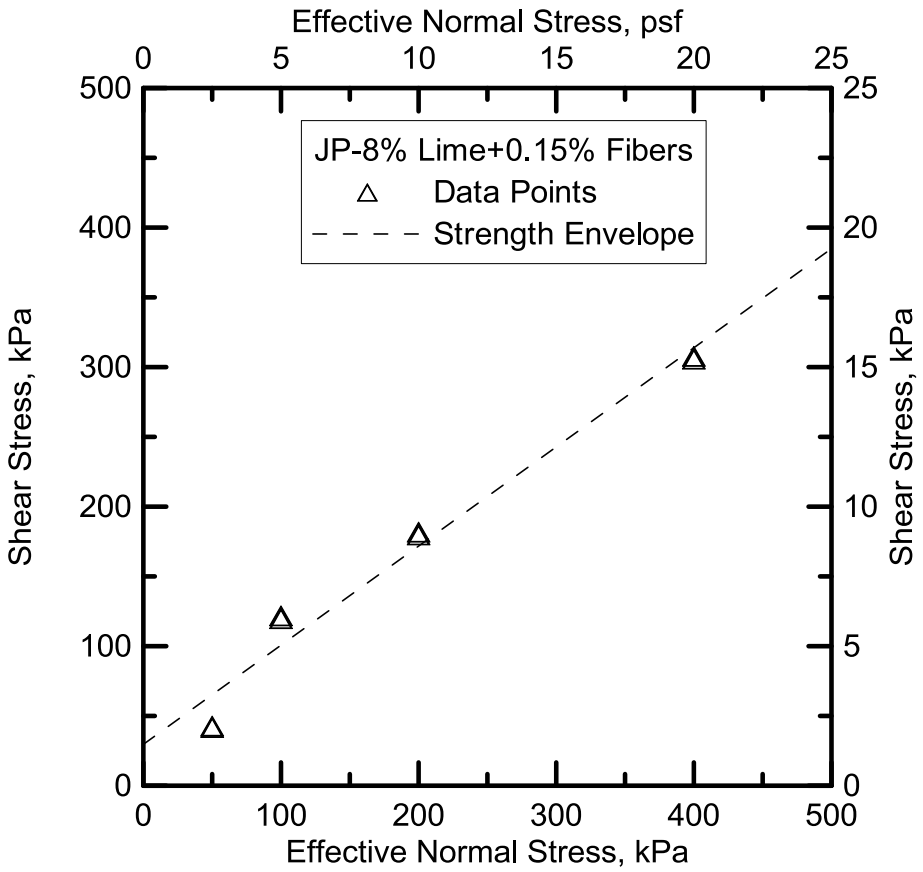

Fit Results

Strength Envelope
Equation Y = 0.7105217391 * X + 29.65217391
Number of data points used = 8
Average X = 187.5
Average Y = 162.875
Residual sum of squares = 2123.96
Regression sum of squares = 72570.9
Coef of determination, R-squared = 0.971565
Residual mean square, sigma-hat-sq'd = 353.993

Figure 7.23. Strength Envelope for Joe Pool Dam 8%lime +0.15%fibers treated soil

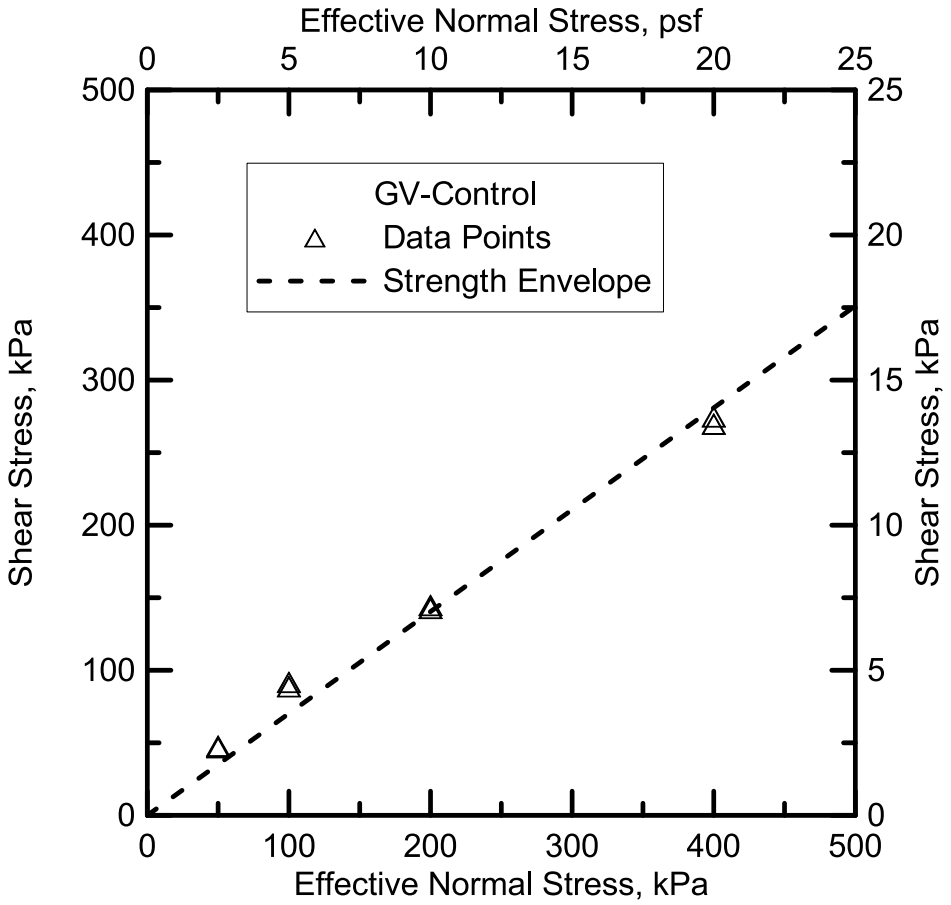

Fit Results

Strength Envelope
Equation Y = 0.7022352941 * X
Number of data points used = 8
Average X = 187.5
Average Y = 138.625
Residual sum of squares = 1314.88
Coef of determination, R-squared = 0.993765
Residual mean square, sigma-hat-sq'd = 187.839

Figure 7.24. Strength Envelope for Grapevine Dam Control soil

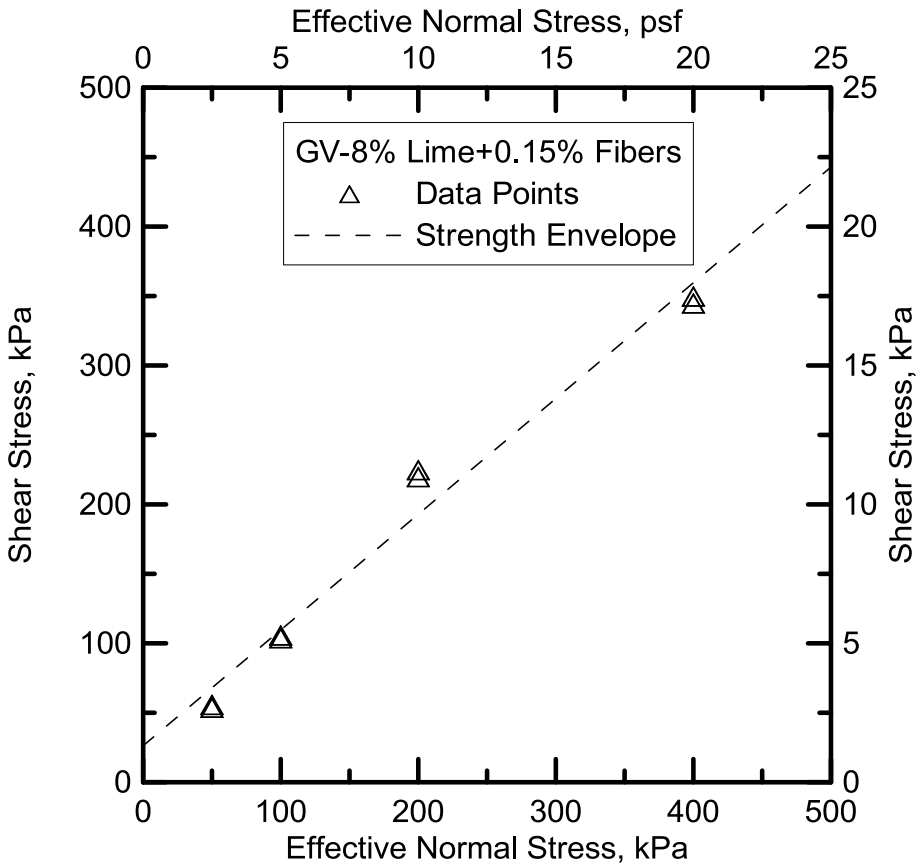

Fit Results

Strength Envelope
Equation Y = 0.8330434783 * X + 26.30434783
Number of data points used = 8
Average X = 187.5
Average Y = 182.5
Residual sum of squares = 2447.04
Regression sum of squares = 99757
Coef of determination, R-squared = 0.976057
Residual mean square, sigma-hat-sq'd = 407.841

Figure 7.25. Strength Envelope for Grapevine Dam 8%lime +0.15%fibers treated soil

Table 7.13. Results of data interpretation for Joe Pool Dam Control soil

Test No.	Effective Normal Stress σ'_{ni} kPa	FSS Shear Stress τ'_{fsi} kPa	FSS friction angle φ'_{fsi} degree
1	50	44	41.35
2	50	43	40.70
3	100	75	36.87
4	100	76	37.23
5	200	100	26.57
6	200	97	25.87
7	400	200	26.57
8	400	204	27.02
$\varphi'_{fs} = tan^{-1}(0.5187) = 27.37^o$		$\Delta_\varphi = 7.02$	

Table 7.14. Results of data interpretation for Joe Pool Dam 8%lime+0.15%fibers treated soil

Test No.	Effective Normal Stress σ'_{ni} kPa	FSS Shear Stress τ'_{fsi} kPa	FSS cohesion c'_{fsi} kPa	FSS friction angle φ'_{fsi} degree
1	50	42	6.47	13.87
2	50	43	7.47	14.95
3	100	120	48.95	42.09
4	100	122	50.95	42.72
5	200	180	37.90	36.93
6	200	182	39.90	37.29
7	400	306	21.79	34.64
8	400	308	23.79	34.83
$\varphi'_{fs} = tan^{-1}(0.7105217) = 35.39^o$		$\Delta_\varphi = 11.36$	$c'_{fs} = 29.65$	$\Delta_c = 17.42$

Table 7.15. Results of data interpretation for Grapevine Dam Control soil

Test No.	Effective Normal Stress σ'_{ni} kPa	FSS Shear Stress τ'_{fsi} kPa	FSS friction angle φ'_{fsi} degree
1	50	47	43.23
2	50	48	43.83
3	100	89	41.67
4	100	92	42.61
5	200	145	35.94
6	200	143	35.56
7	400	270	34.02
8	400	275	34.51
$\varphi'_{fs} = tan^{-1}(0.70) = 35.02^o$		$\Delta_\varphi = 4.27$	

Table 7.16. Results of data interpretation for Grapevine Dam 8%lime+0.15%fibers treated soil

Test No.	Effective Normal Stress σ'_{ni} kPa	FSS Shear Stress τ'_{fsi} kPa	FSS cohesion c'_{fsi} kPa	FSS friction angle φ'_{fsi} degree
1	50	56	14.35	30.70
2	50	54	12.35	28.98
3	100	106	22.70	38.55
4	100	104	20.70	37.84
5	200	225	58.39	44.81
6	200	220	53.39	44.08
7	400	350	16.78	38.98
8	400	345	11.78	38.54
$\varphi'_{fs} = tan^{-1}(0.83) = 39.79^o$		$\Delta_\varphi = 5.6$	$c'_{fs} = 26.30$	$\Delta_c = 18.70$

Due to the number of tests increasing from 4 to 8, the statistical linear regression analysis yielded a slight difference in values of average FSS cohesion (c'_{fs}) and FSS Friction Angle (φ'_{fs}) compared to those parameters reported in Chapter 5. Table 7.17 presents the average values of FSS cohesion and FSS friction angles, as well as their standard deviations.

Table 7.17. Summary of Average FSS soil parameters and their standard deviation

Soils	Joe Pool Dam				Grapevine Dam			
	φ'_{fs} degree	Δ_{φ} degree	c'_{fs} kPa	Δ_c kPa	φ'_{fs} degree	Δ_{φ} degree	c'_{fs} kPa	Δ_c kPa
Control soil	27.07	7.02			35.02	4.27		
20%compost treated soil	26.99	3.15	13.43	4.59	31.59	4.22	17.41	7.22
4%lime+0.30%fibers treated soil	33.49	9.52	35.67	17.49	36.79	4.74	25.89	8.24
8%lime+0.15 %fibers treated soil	35.39	11.36	29.65	17.42	39.79	5.6	26.30	18.70
8 %lime treated soil	36.61	7.30	22.91	14.72	39.09	3.54	9.65	6.65

7.3.2 Normality Checks

Normality checks are performed on the interpreted data of FSS cohesion and FSS friction angle to ensure the validity of reliability analysis. The probability plotting method was utilized to graphically judge the normality trend of FSS soil parameters. First data was sorted by the values from the smallest to the largest. Then sorted data was plotted against their Cumulative Normal Distribution values. Details of the method can be found in Chapter 6.

Results of normality check are shown in Figures 7.26 to 7.29 for control soil and 8%lime+0.15%fibers treated soil from the Joe Pool Dam and Grapevine Dam. The remaining results for other sections can be found in Appendix B section.

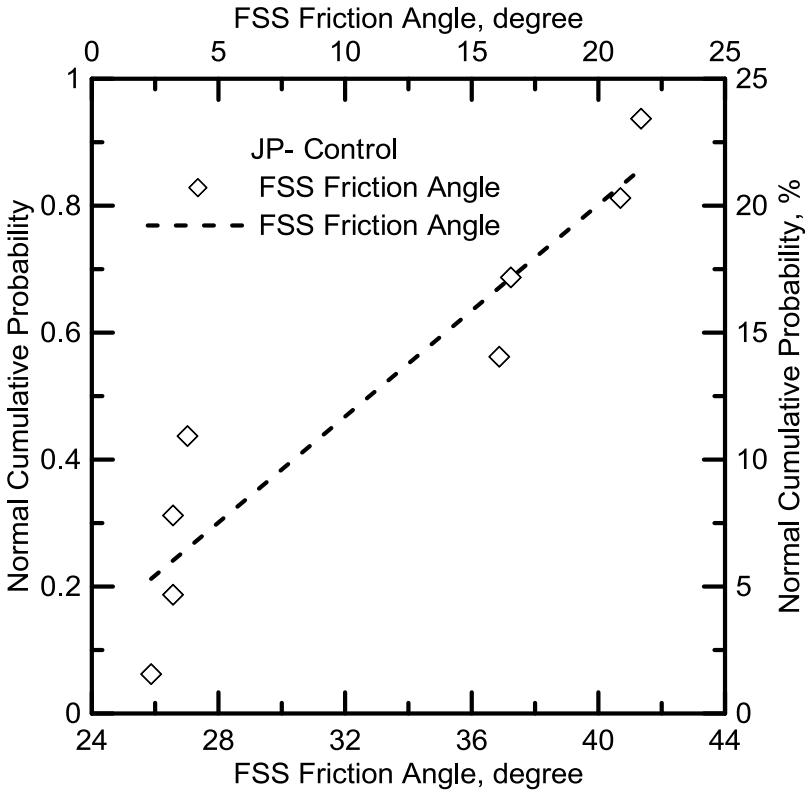

Fit Results

FSS Friction Angle
Equation Y = 0.04172960967 * X - 0.8675476879
Number of data points used = 8
Average X = 32.7716
Average Y = 0.5
Residual sum of squares = 0.080301
Regression sum of squares = 0.575949
Coef of determination, R-squared = 0.877637
Residual mean square, sigma-hat-sq'd = 0.0133835

Figure 7.26. Normality check for FSS friction angle of Joe Pool Dam Control soil

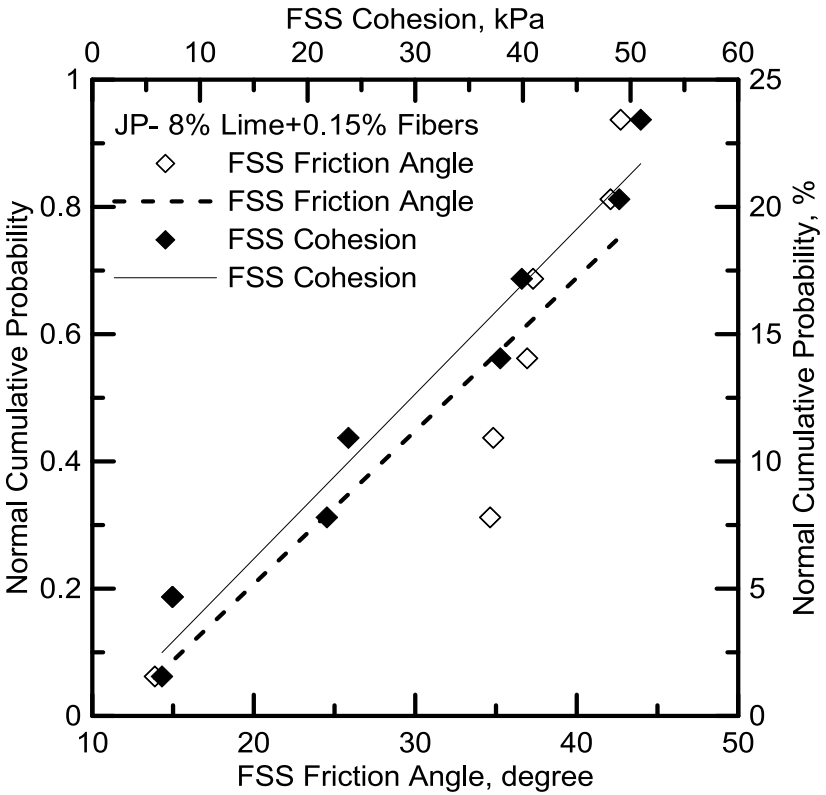

Fit Results

FSS Friction Angle
Equation Y = 0.02405954465 * X - 0.2738624879
Number of data points used = 8
Average X = 32.1645
Average Y = 0.5
Residual sum of squares = 0.133345
Regression sum of squares = 0.522905
Coef of determination, R-squared = 0.796808
Residual mean square, sigma-hat-sq'd = 0.0222241

Fit Results

FSS Cohesion
Equation Y = 0.01727622305 * X - 0.01227757054
Number of data points used = 8
Average X = 29.6522
Average Y = 0.5
Residual sum of squares = 0.0223159
Regression sum of squares = 0.633934
Coef of determination, R-squared = 0.965995
Residual mean square, sigma-hat-sq'd = 0.00371932

Figure 7.27. Normality check for FSS friction angle and FSS cohesion of Joe Pool Dam 8%lime+0.15%fibers Treated soil

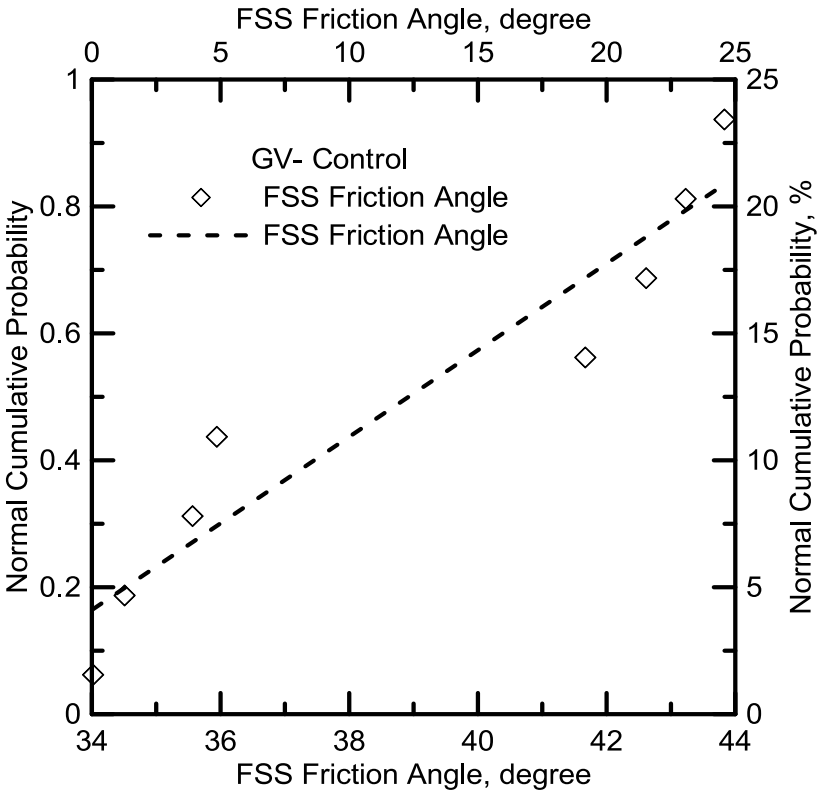

Fit Results

FSS Friction Angle
Equation Y = 21.03150549 * X + 22.25588588
Number of data points used = 8
Average X = 0.5
Average Y = 32.7716
Residual sum of squares = 40.4713
Regression sum of squares = 290.275
Coef of determination, R-squared = 0.877637
Residual mean square, sigma-hat-sq'd = 6.74522

Figure 7.28. Normality check for FSS friction angle of Grapevine Dam Control soil

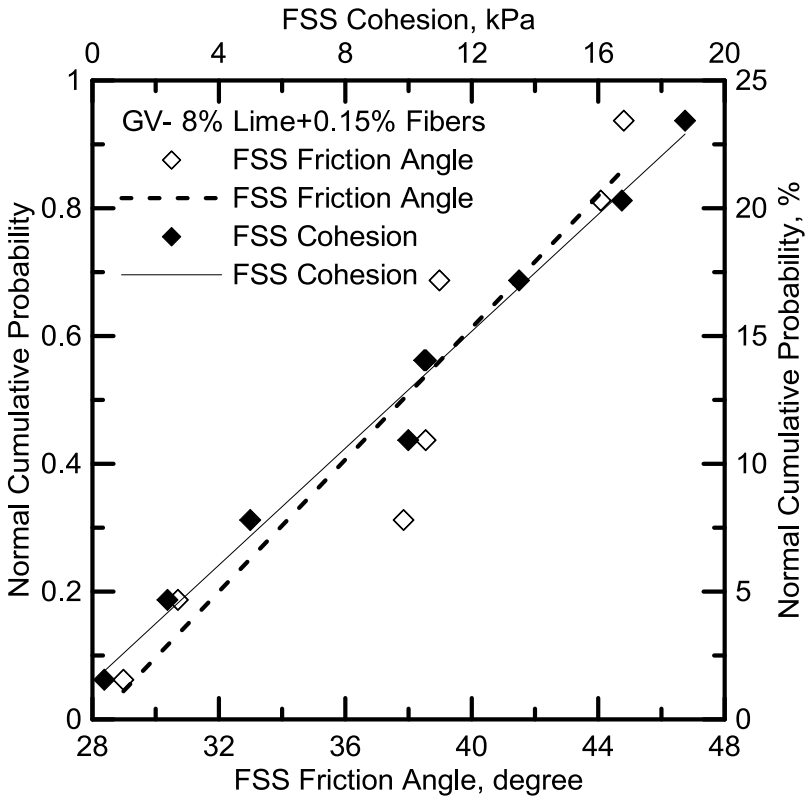

Fit Results

FSS Friction Angle
Equation Y = 0.05163622712 * X - 1.452363906
Number of data points used = 8
Average X = 37.81
Average Y = 0.5
Residual sum of squares = 0.0718409
Regression sum of squares = 0.584409
Coef of determination, R-squared = 0.890528
Residual mean square, sigma-hat-sq'd = 0.0119735

Fit Results

FSS Cohesion
Equation Y = 0.045745757 * X + 0.05845399768
Number of data points used = 8
Average X = 9.65217
Average Y = 0.5
Residual sum of squares = 0.0086492
Regression sum of squares = 0.647601
Coef of determination, R-squared = 0.98682
Residual mean square, sigma-hat-sq'd = 0.00144153

Figure 7.29. Normality check for FSS friction angle and FSS cohesion of Grapevine Dam 8%lime+0.15%fibers Treated soil

7.3.3 Results of Reliability Analysis

Since the average values of FSS soil parameters and their corresponding standard deviations as well as their normal distributions, are well established, a probabilistic analysis was possible here. Hence the researcher performed a comprehensive slope stability using this data. SLOPE/W software that has Monte Carlo simulation was utilized to conduct the probabilistic slope stability analysis. In geotechnical engineering, this method along with other probabilistic methods has rendered more practical results due to the use of the computer. As the application of studying uncertainties in geotechnical analyses has been of major focus, probabilistic methods like the Monte Carlo simulation are being used more frequently these days (Duncan, 2013).

The Monte Carlo simulation (also known as Monte Carlo method) was developed in 1949 by John von Neumann and Stanislav Ulam (Peterson, 1999). It is a computerized mathematical technique that can determine risk in quantitative analysis and decision making. First, Monte Carlo simulation is formulated based on a deterministic model where multiple inputs are used to calculate a single value outcome. In slope stability analysis, unit weight, cohesion and friction angle are the commonly used input variables. However, within the zone of surficial failure (i.e. 4 ft. from the slope surface) the change of unit weight is believed to be minimal. Thus, for the purpose of analyzing the variability of FSS soil parameters, unit weight of soil and the strength parameters of compacted core soil are considered constant. Two input variables are the FSS cohesion and FSS friction angle.

After all input variables are identified, the probability distribution for each independent variable is established for the simulation model (i.e. normal, beta, log normal, etc.). FSS cohesion and FSS friction angle variables were subjected to normality checks and were proved to follow a normal distribution model as discussed earlier in this chapter.

A random trial process generated a probability distribution function for the deterministic situation being modeled. In each trial, a random value obtained from the distribution function for

each parameter was used for calculation. Numerous problems were solved by running multiple trials to obtain a solution for each pass. In SLOPE/W, based on the average values of FSS soil parameters, Monte Carlo simulation allows users to specify the range of variability based on the values of mean and standard deviation. In this research, three different ranges of variability were analyzed as follows:

- **Case A:** Within the range of $(mean - standard\ deviation)$ to $(mean + standard\ deviation)$. Practical implication of Case A means the strength results used in the analysis will be 68% of the raw test results for FSS cohesion and FSS friction angle values.
- **Case B:** Within the range of $(mean - 2 \times standard\ deviation)$ to $(mean + 2 \times standard\ deviation)$. Practical implication of Case B means the strength results used in the analysis will be 97% of the raw test results for FSS cohesion and FSS friction angle values.
- **Case C:** Within the range of $(mean - 3 \times standard\ deviation)$ to $(mean + 3 \times standard\ deviation)$. The practical implication of Case C means the strength results used in the analysis will be 99% of the raw test results for FSS cohesion and FSS friction angle values.

Monte Carlo simulation generates all possible pairs of FSS cohesion and FSS Friction Angle, each of which is used as inputs for the SLOPE/W program to calculate FOS values. Ranges for values of FSS cohesion and Friction Angle used in this analysis are shown in Table 7.18 and Table 7.19.

The appropriate number of trials for an analysis is a function of the number of input parameters, the complexity of the modeled situation, and the desired precision of the output (Peterson, 1999). In general, the more Monte Carlo trials that were run, the more accurate the results were. However, in this research, preliminary tests were run at 500, 1000, 2000 and 5000 trials. Results showed no major difference for 1000 trials and above, thus the number of trials was selected to be 1000 and this is also used for restricting the time for analysis.

Table 7.18. FSS parameters input range for Monte Carlo Simulation on Joe Pool Dam soils

Soil	Case A				Case B				Case C			
	$\varphi'_{fs} - \Delta_\varphi$ degree	$\varphi'_{fs} + \Delta_\varphi$ degree	$c'_{fs} - \Delta_c$ psf	$c'_{fs} + \Delta_c$ psf	$\varphi'_{fs} - 2 \times \Delta_\varphi$ degree	$\varphi'_{fs} + 2 \times \Delta_\varphi$ degree	$c'_{fs} - 2 \times \Delta_c$ psf	$c'_{fs} + 2 \times \Delta_c$ psf	$\varphi'_{fs} - 3 \times \Delta_\varphi$ degree	$\varphi'_{fs} + 3 \times \Delta_\varphi$ degree	$c'_{fs} - 3 \times \Delta_c$ psf	$c'_{fs} + 3 \times \Delta_c$ psf
Control soil	20.05	34.09			13.03	41.11			6.01	48.13		
20%compost treated soil	23.84	30.14	184.6	376.4	20.69	33.29	88.8	472.2	17.54	36.44	0.0	568.1
4%lime+0.30%fibers treated soil	23.97	43.01	379.7	1110.3	14.45	52.53	14.4	1475.6	4.93	62.05	0.0	1840.8
8%lime+0.15 %fibers treated soil	24.03	46.75	255.4	983.1	12.67	58.11	0.0	1346.9	1.31	69.47	0.0	1710.7
8 %lime treated soil	29.31	43.91	171.1	785.9	22.01	51.21	0.0	1093.4	14.71	58.51	0.0	1400.8

Note: Red numbers indicate that the cohesion cannot go beyond 0. Minimum value of 0 is used instead.

Table 7.19. FSS parameters input range for Monte Carlo Simulation on Grapevine Dam soils

Soil	Case A				Case B				Case C			
	$\varphi'_{fs} - \Delta_\varphi$ degree	$\varphi'_{fs} + \Delta_\varphi$ degree	$c'_{fs} - \Delta_c$ psf	$c'_{fs} + \Delta_c$ psf	$\varphi'_{fs} - 2 \times \Delta_\varphi$ degree	$\varphi'_{fs} + 2 \times \Delta_\varphi$ degree	$c'_{fs} - 2 \times \Delta_c$ psf	$c'_{fs} + 2 \times \Delta_c$ psf	$\varphi'_{fs} - 3 \times \Delta_\varphi$ degree	$\varphi'_{fs} + 3 \times \Delta_\varphi$ degree	$c'_{fs} - 3 \times \Delta_c$ psf	$c'_{fs} + 3 \times \Delta_c$ psf
Control soil	30.75	39.29			26.48	43.56			22.21	47.83		
20%compost treated soil	27.37	35.81	212.8	514.4	23.15	40.03	62.0	665.2	18.93	44.25	0.0	816.0
4%lime+0.30%fibers treated soil	32.05	41.53	368.6	712.8	27.31	46.27	196.5	884.9	22.57	51.01	24.4	1057.0
8%lime+0.15 %fibers treated soil	34.19	45.39	158.7	939.8	28.59	50.99	0.0	1330.4	22.99	56.59	0.0	1721.0
8 %lime treated soil	35.55	42.63	62.7	340.4	32.01	46.17	0.0	479.3	28.47	49.71	0.0	618.2

Note: Red numbers indicate that the cohesion cannot go beyond 0. Minimum value of 0 is used instead.

Figures 7.30 to 7.41 present the Probability Density Functions and Probability Distribution Functions for Joe Pool Dam and Grapevine Dam soils based on the FOS values calculated using Monte Carlo trials. Due to the space limitation, only results of control soil and 8%lime+0.15%fibers Treated soil are presented. The remaining results can be found in Appendix B section.

It can be seen from the results that the outcome of FOS values fairly resembled the normal distribution function as the Probability Density Function graphs imitated the bell-curve shape. The resemblance was more defined in Case B and Case C where the variability was greater for both soil parameters cohesion and friction angle (as shown in Table 7.18 and Table 7.19).

Based on the Probability Distribution Function graphs, probability of failure can be determined graphically. Control soil from both Joe Pool Dam and Grapevine Dam exhibited higher probability of failure than the 8%lime+0.15%fibers treated soil. By default by SLOPE/W, the margin of safety for FOS was set at 1.

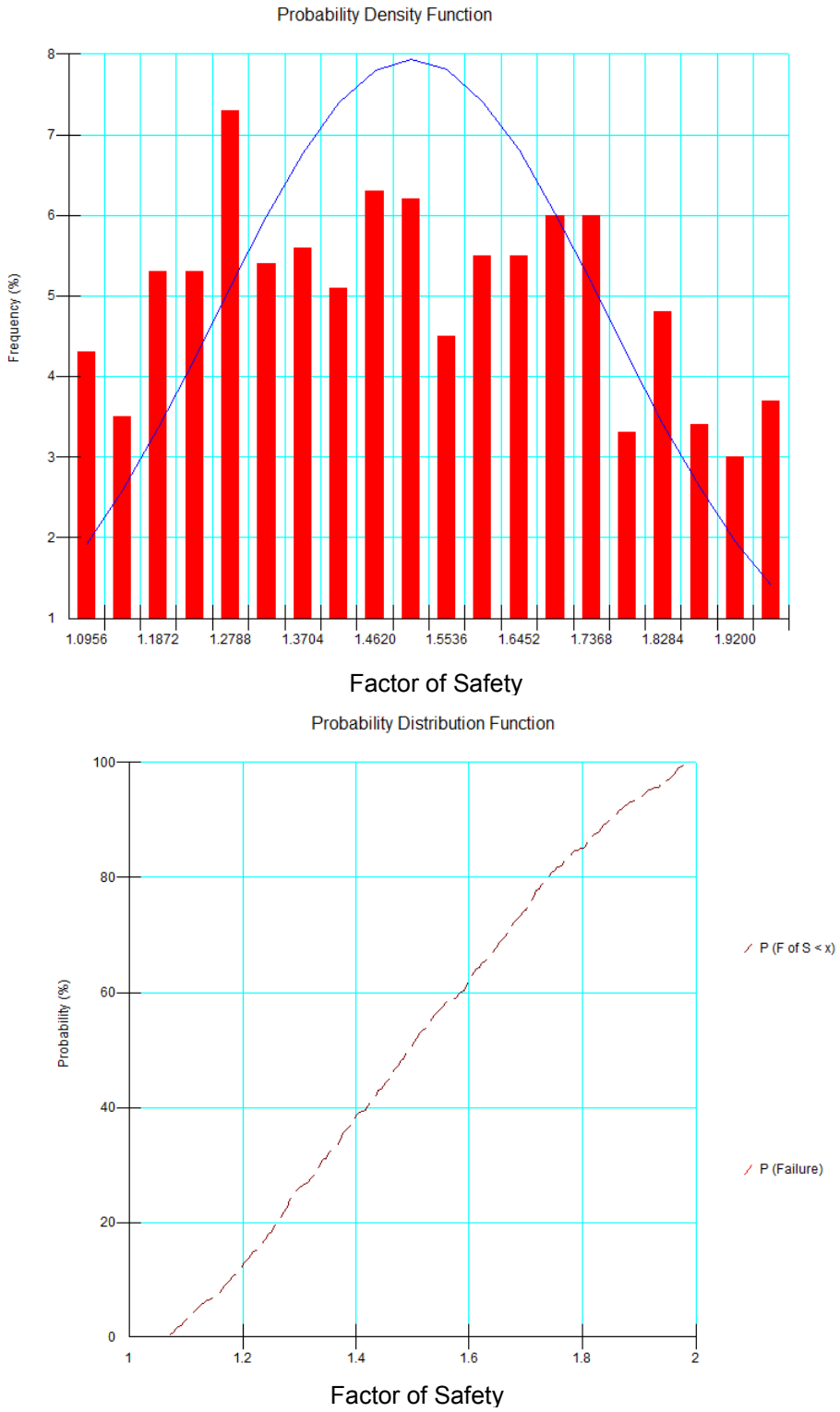

Figure 7.30. Probability Density Function (above) and Probability Distribution Function (below) of FOS for Joe Pool Dam Control Soil (Case A)

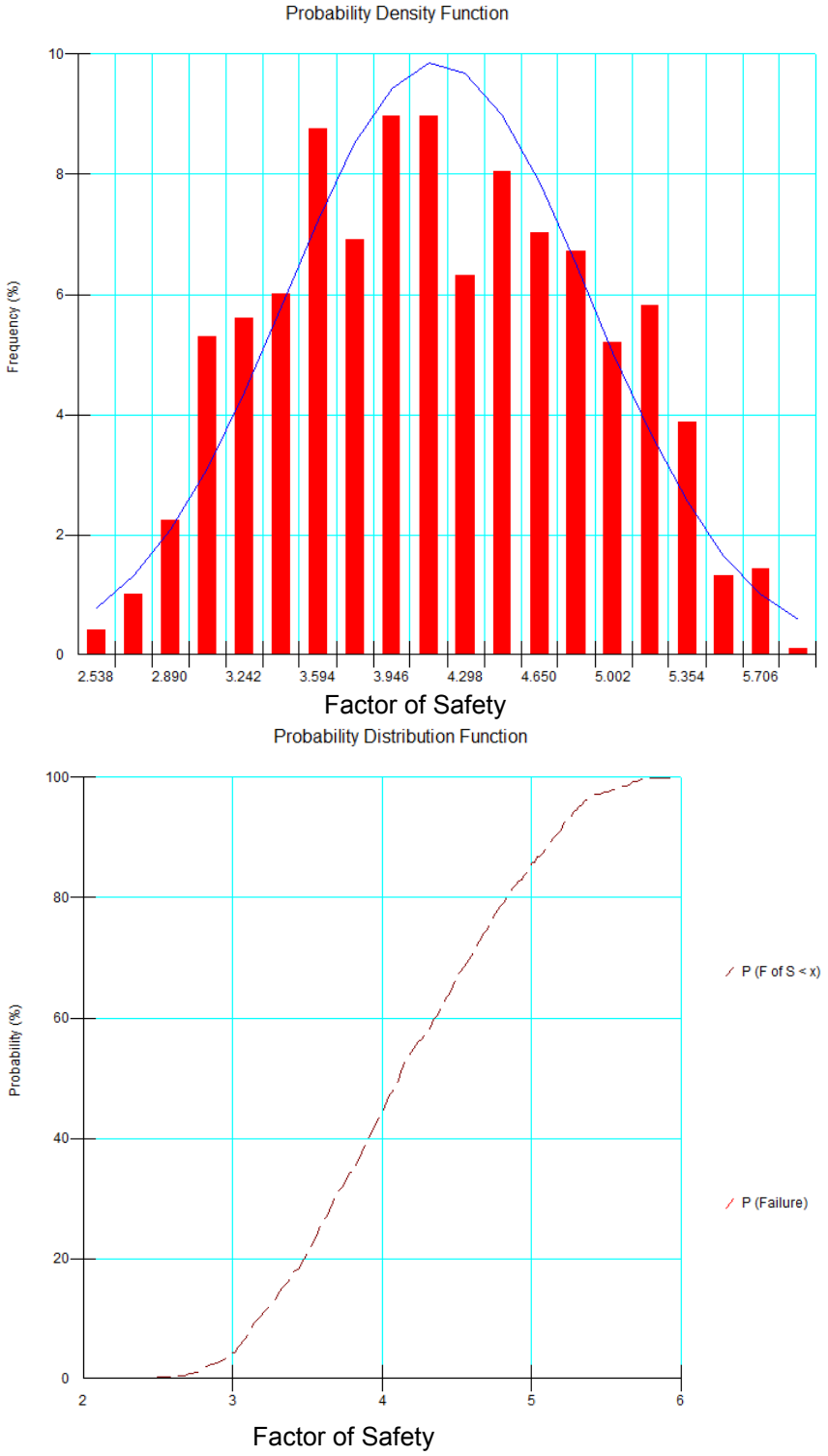

Figure 7.31. Probability Density Function (above) and Probability Distribution Function (below) of FOS for Joe Pool Dam 8%lime+0.15%fibers treated Soil (Case A)

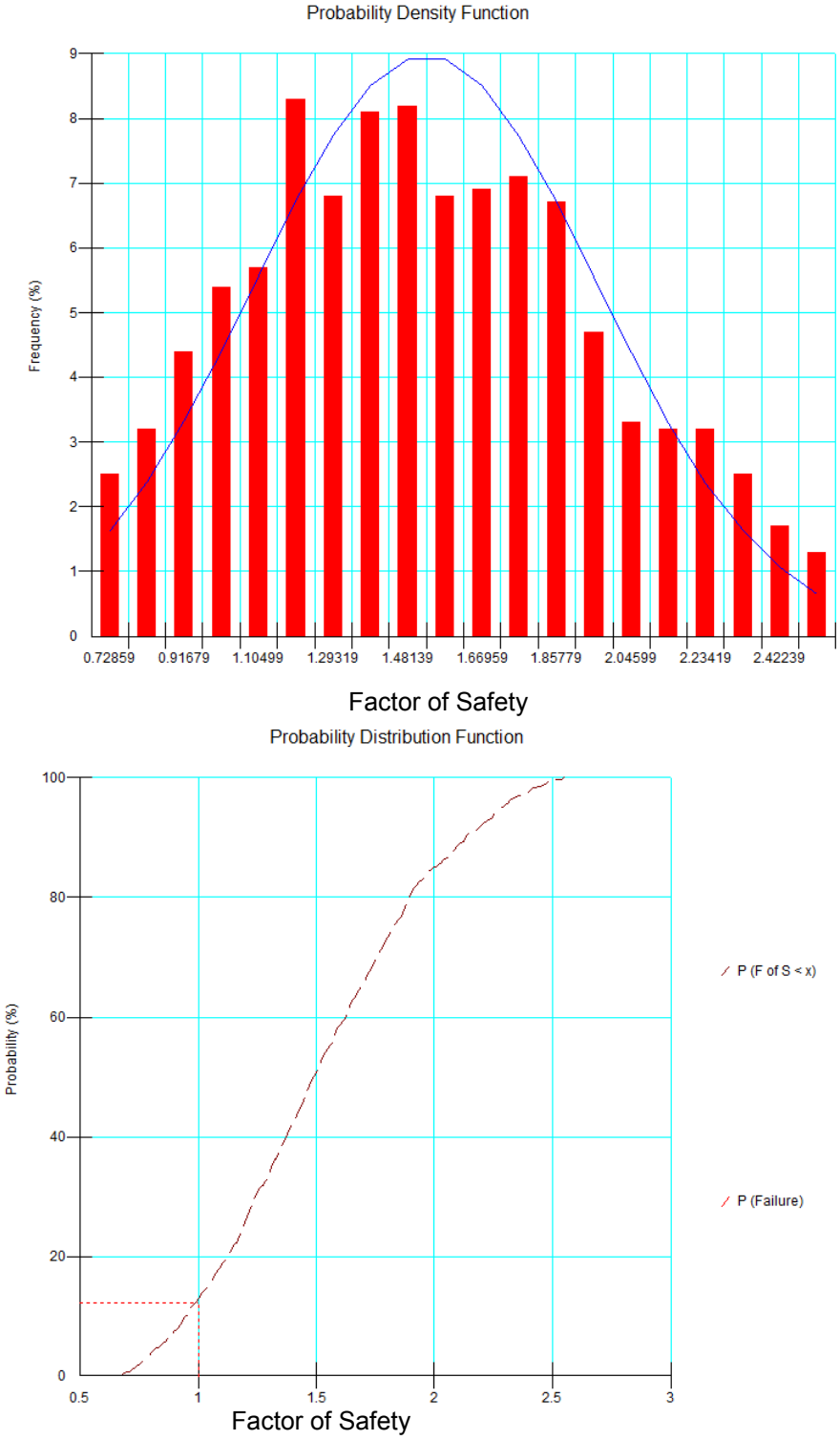

Figure 7.32. Probability Density Function (above) and Probability Distribution Function (below) of FOS for Joe Pool Dam Control Soil (Case B)

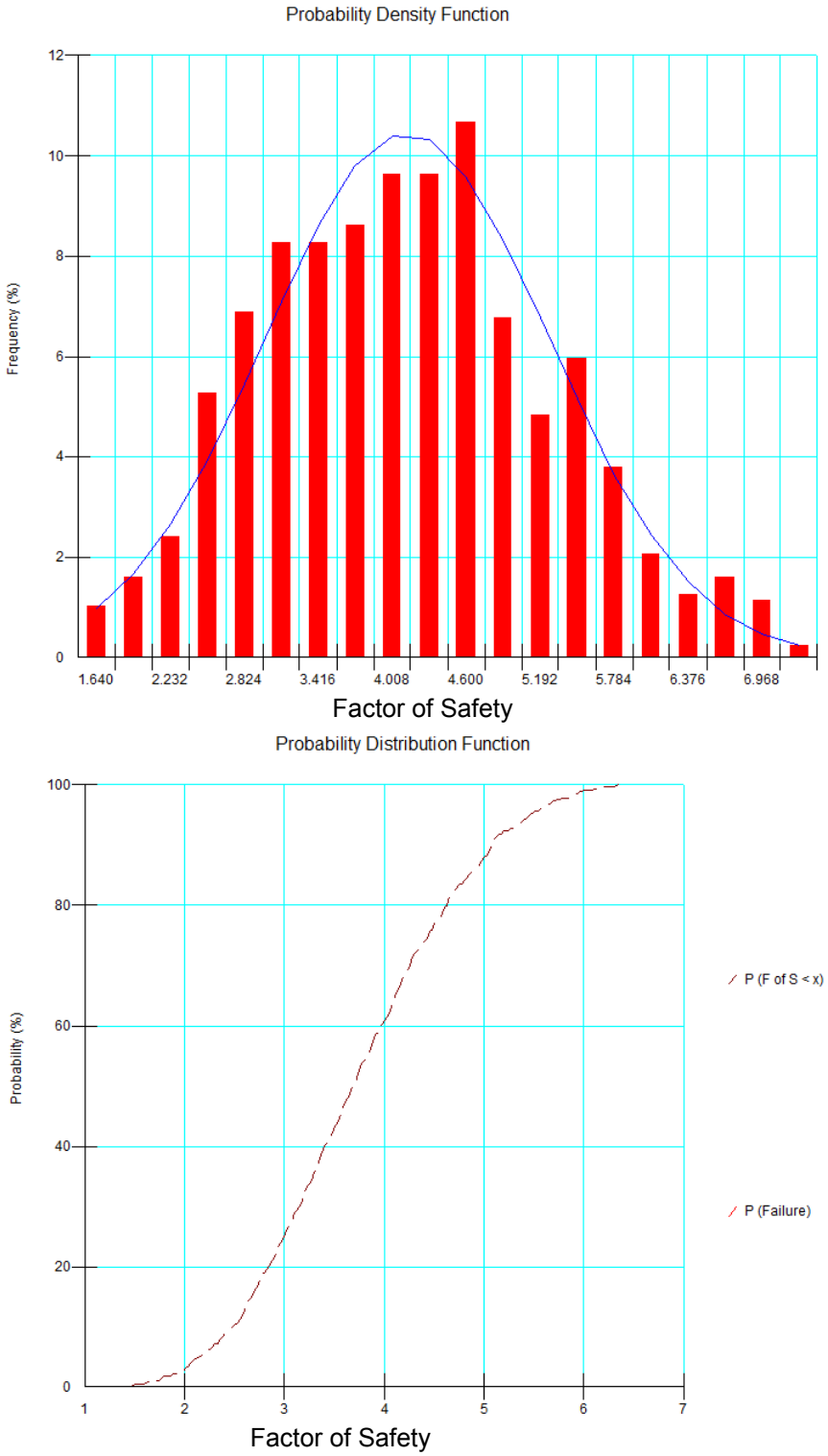

Figure 7.33. Probability Density Function (above) and Probability Distribution Function (below) of FOS for Joe Pool Dam 8%lime+0.15%fibers treated Soil (Case B)

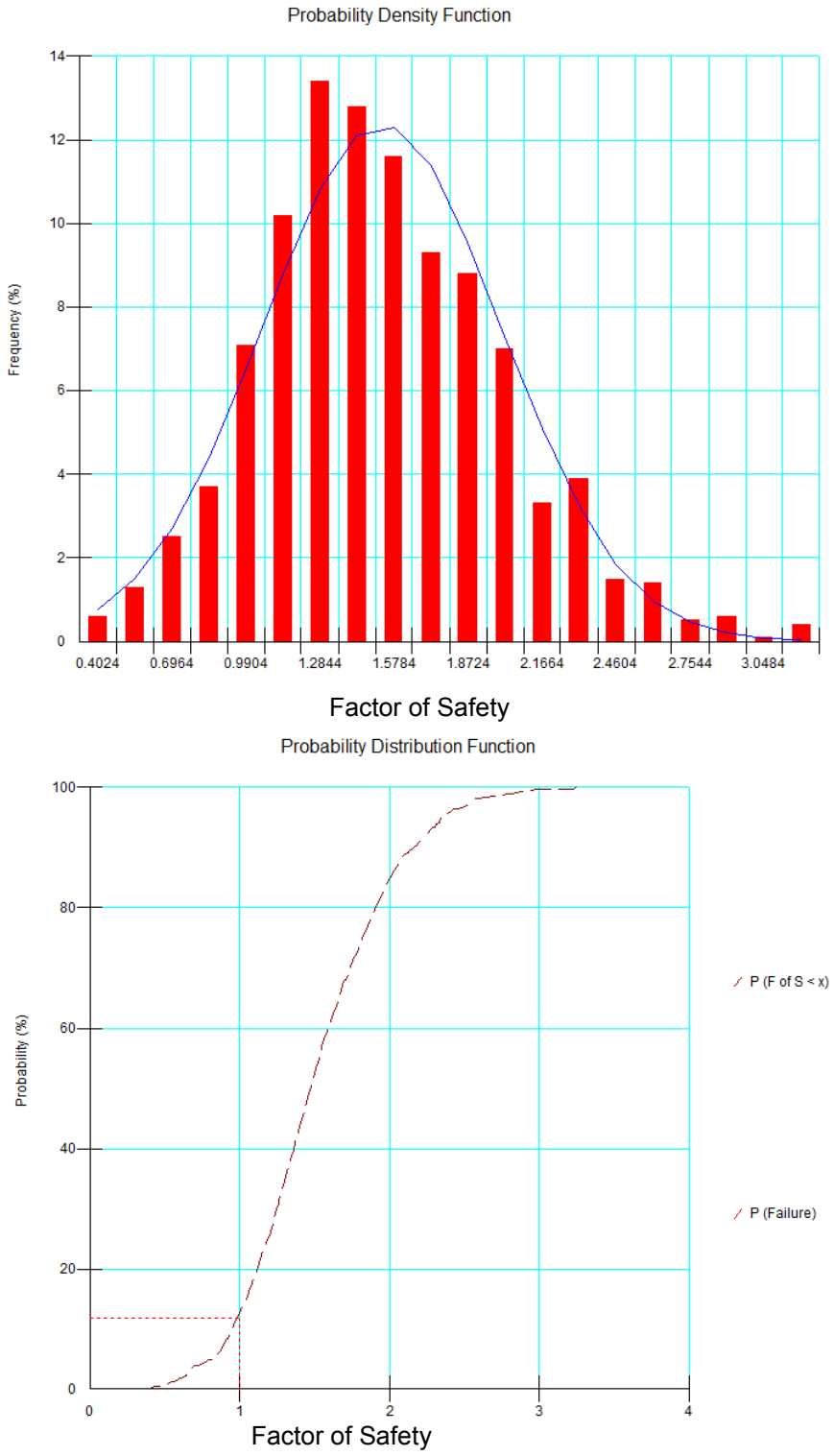

Figure 7.34. Probability Density Function (above) and Probability Distribution Function (below) of FOS for Joe Pool Dam Control Soil (Case C)

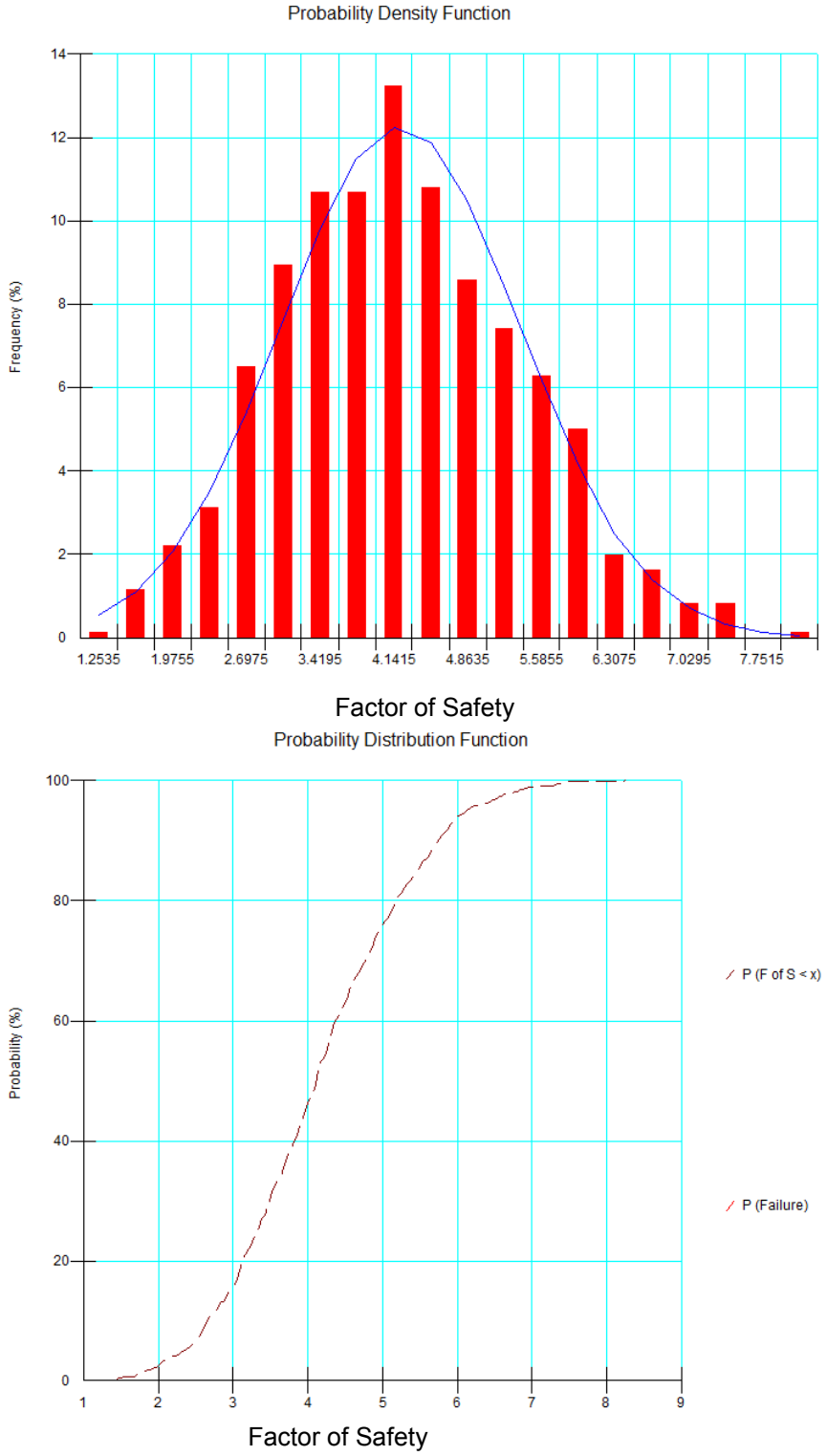

Figure 7.35. Probability Density Function (above) and Probability Distribution Function (below) of FOS for Joe Pool Dam 8%lime+0.15%fibers treated Soil (Case C)

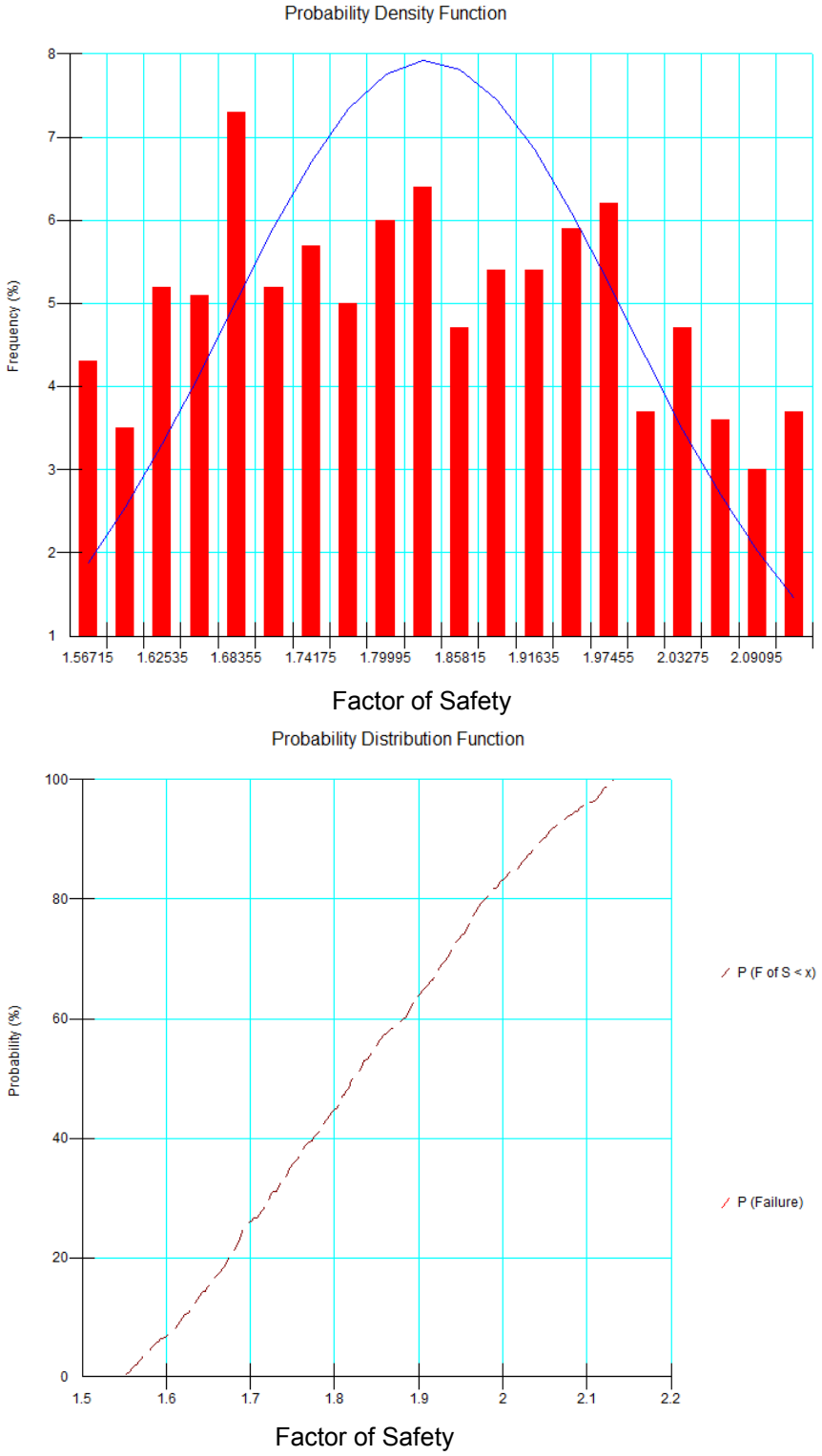

Figure 7.36. Probability Density Function (above) and Probability Distribution Function (below) of FOS for Grapevine Dam Control Soil (Case A)

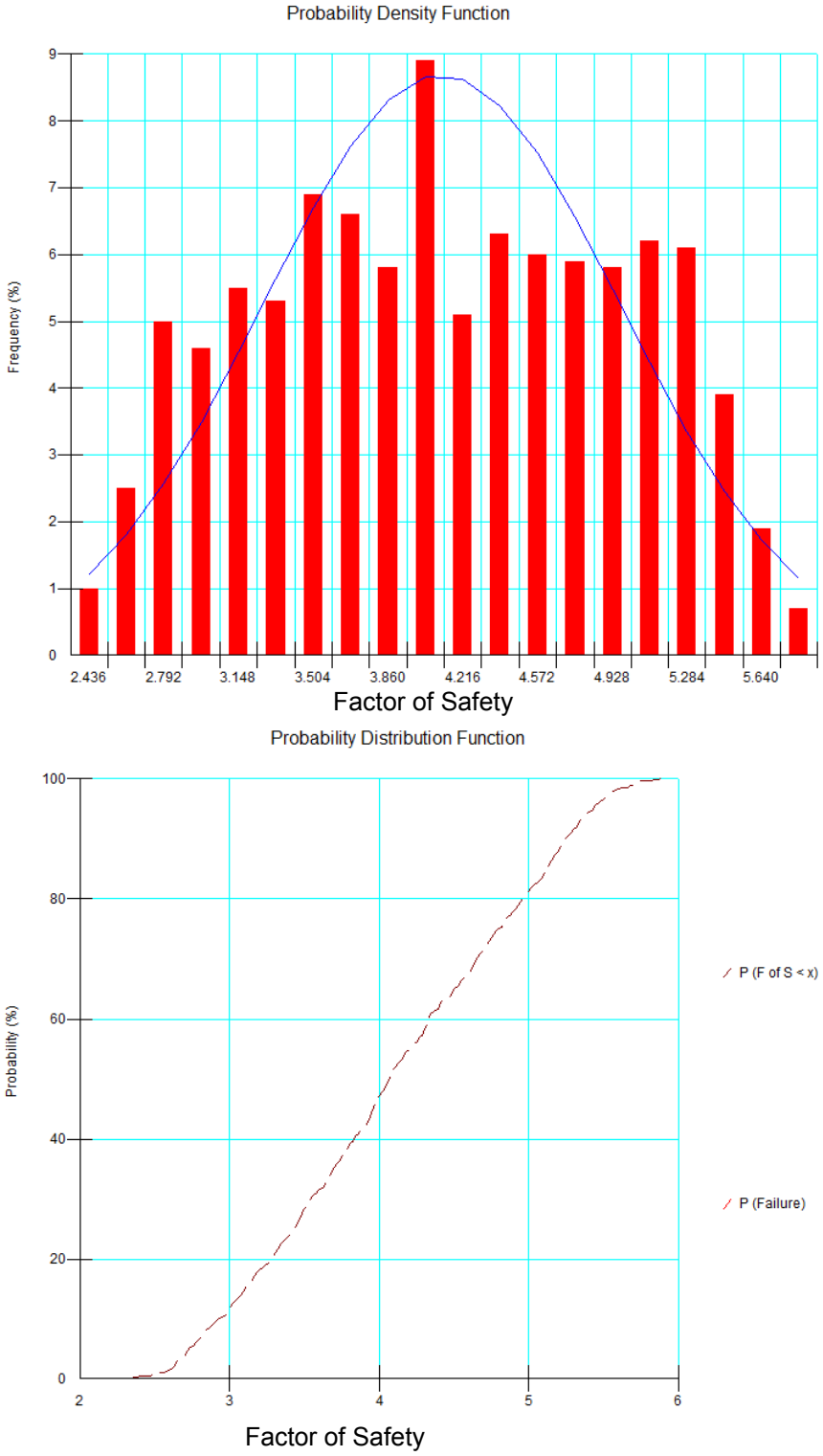

Figure 7.37. Probability Density Function (above) and Probability Distribution Function (below) of FOS for Grapevine Dam 8%lime+0.15%fibers treated Soil (Case A)

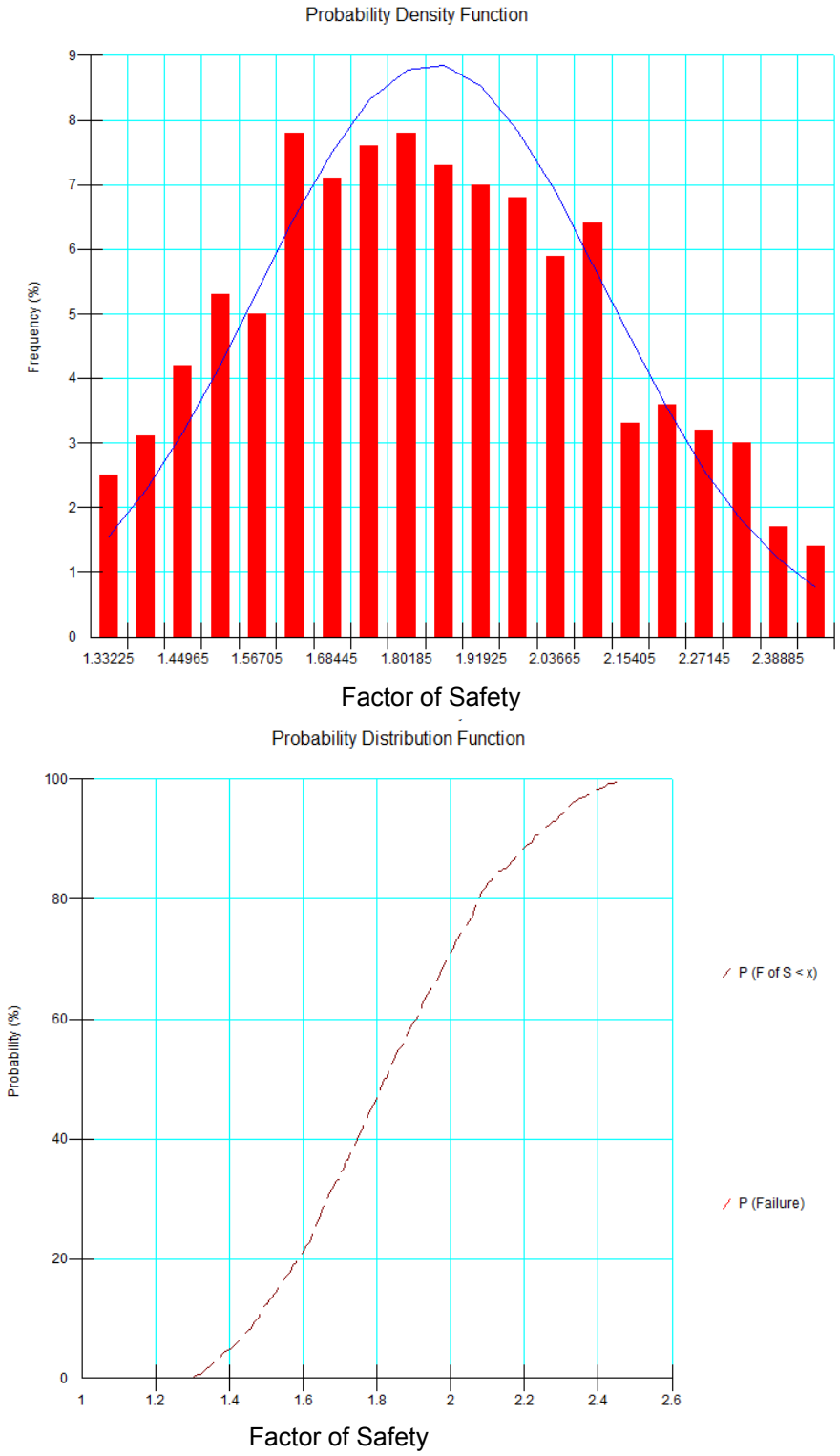

Figure 7.38. Probability Density Function (above) and Probability Distribution Function (below) of FOS for Grapevine Dam Control Soil (Case B)

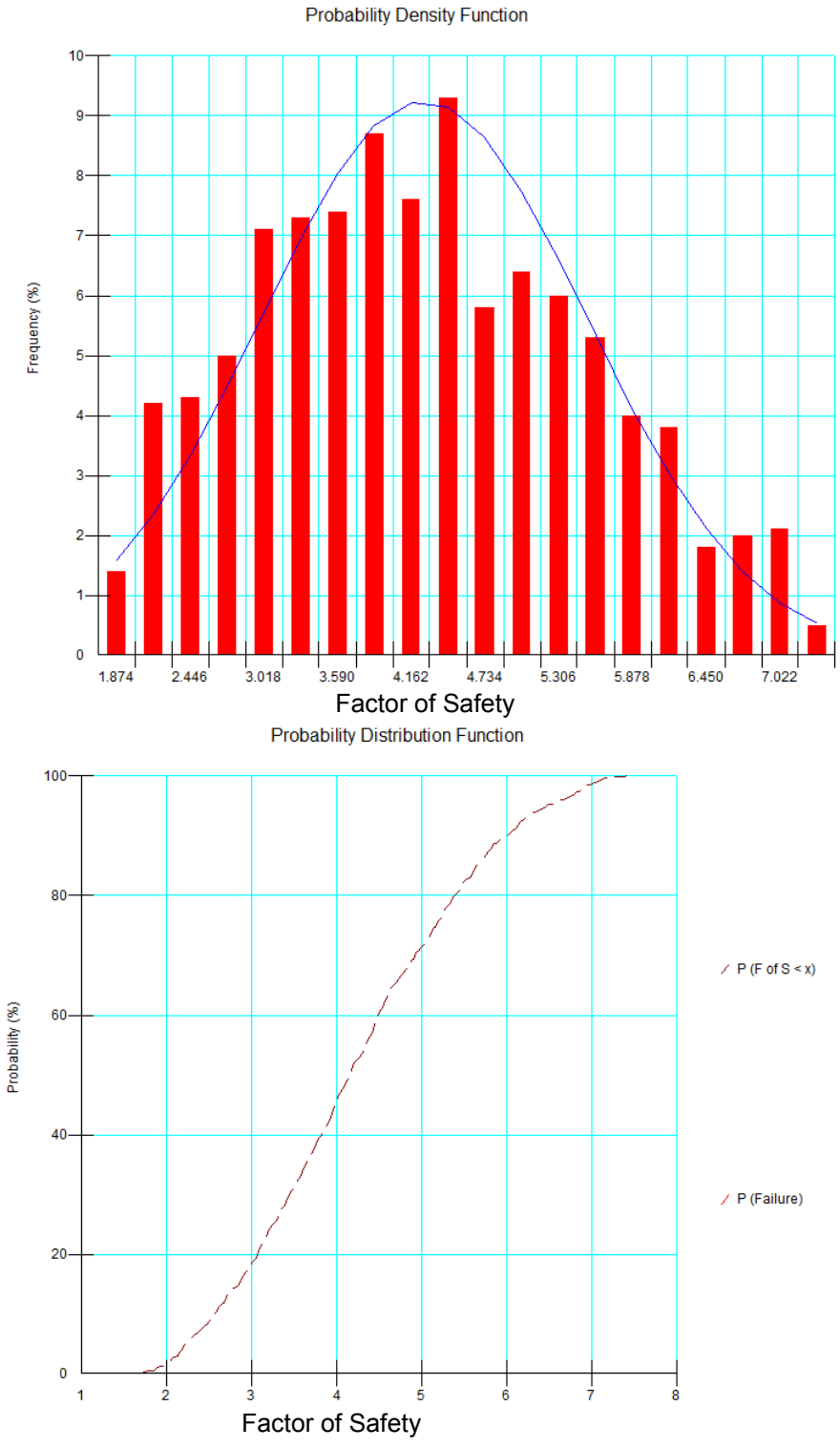

Figure 7.39. Probability Density Function (above) and Probability Distribution Function (below) of FOS for Grapevine Dam 8%lime+0.15%fibers treated Soil (Case B)

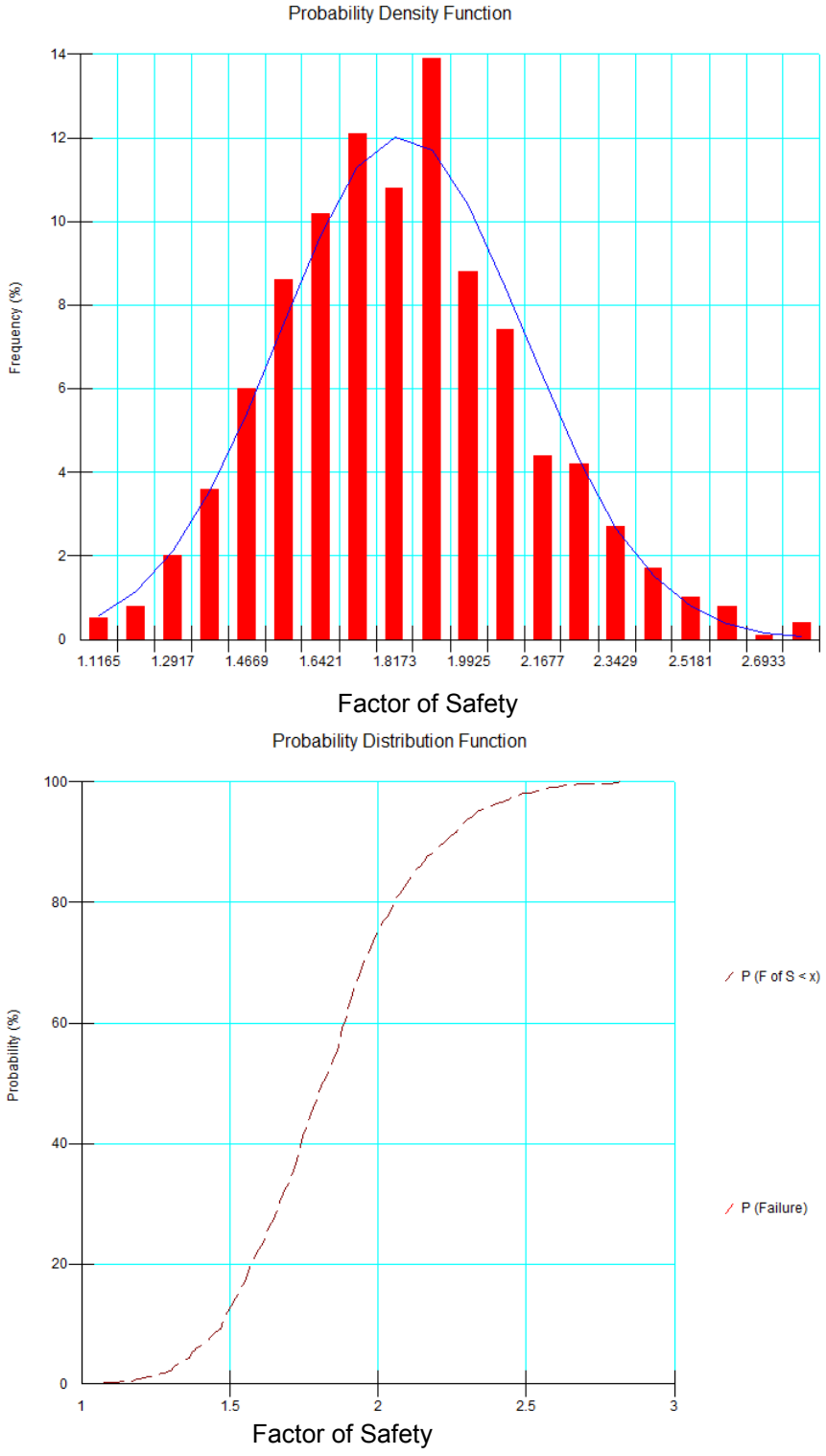

Figure 7.40. Probability Density Function (above) and Probability Distribution Function (below) of FOS for Grapevine Dam Control Soil (Case C)

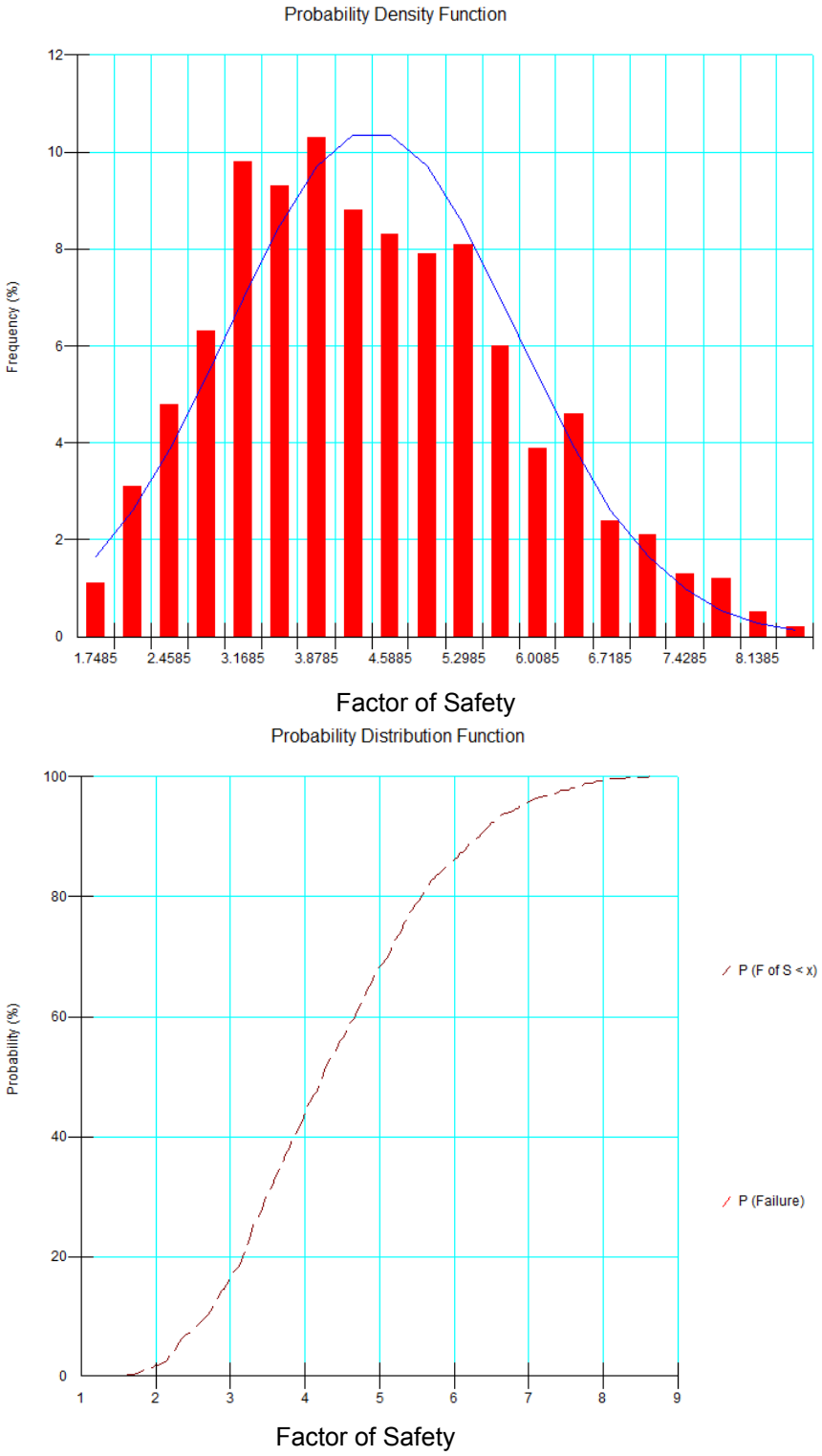

Figure 7.41. Probability Density Function (above) and Probability Distribution Function (below) of FOS for Grapevine Dam 8%lime+0.15%fibers treated Soil (Case C)

In addition, Monte Carlo simulation in SLOPE/W also reports minimum values of FOS, maximum values of FOS, mean values of FOS and its standard deviation. These parameters are used to calculate the reliability index (β).

Reliability index (β) is defined as the margin of safety normalized with the respect to its standard deviation. Value of (β) for default margin of safety of 1.0 in SLOPE/W is calculated as:

$$\beta = \frac{\mu_{FOS} - 1}{\sigma_{FOS}} \qquad \text{Eq. 7-6}$$

where (μ_{FOS}) is the mean value of factor of safety and (σ_{FOS}) is the standard deviation of factor of safety. Probabilistic analysis using Monte Carlo simulation in SLOPE/W reports values of (μ_{FOS}) and (σ_{FOS}) based on the FOS of all cases generated by the given ranges for FSS soil parameters.

However, the majority of researchers recommend the use of minimum FOS as 1.5 for dams experiencing first time slides (Stark et al., 2011; USACE). Thus, results of reliability parameters calculated by SLOPE/W are converted to depict 1.5 as a safe-unsafe boundary as follows:

$$\beta = \frac{\mu_{FOS} - 1.5}{\sigma_{FOS}} \qquad \text{Eq. 7-7}$$

Probability of failure (p_f) is another important index in reliability analysis. It is the probability of obtaining a factor of safety less than the safety margin namely 1.5 for surficial failure. In Monte Carlo simulation, probability of failure is calculated as the ratio of frequency that FOS obtained below 1.5 over the total trial of 1000.

Figure 7.42 to Figure 7.46 presents the comparisons of average value of FOS, minimum of FOS, maximum of FOS, reliability indices and standard deviation for FOS for Joe Pool Dam and Grapevine Dam soils.

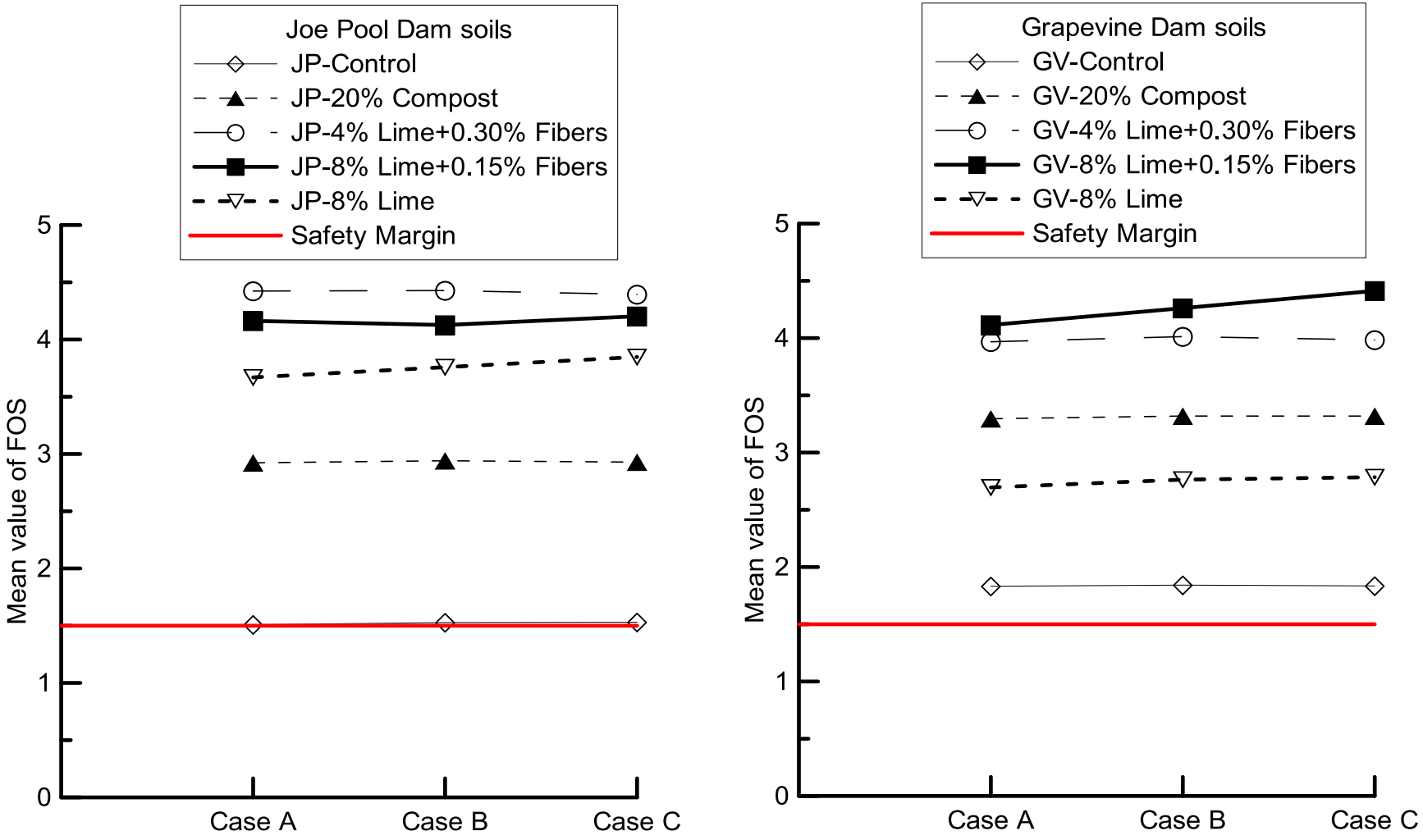

Figure 7.42. Mean Values of FOS in 3 cases for Joe Pool Dam and Grapevine Dam soils

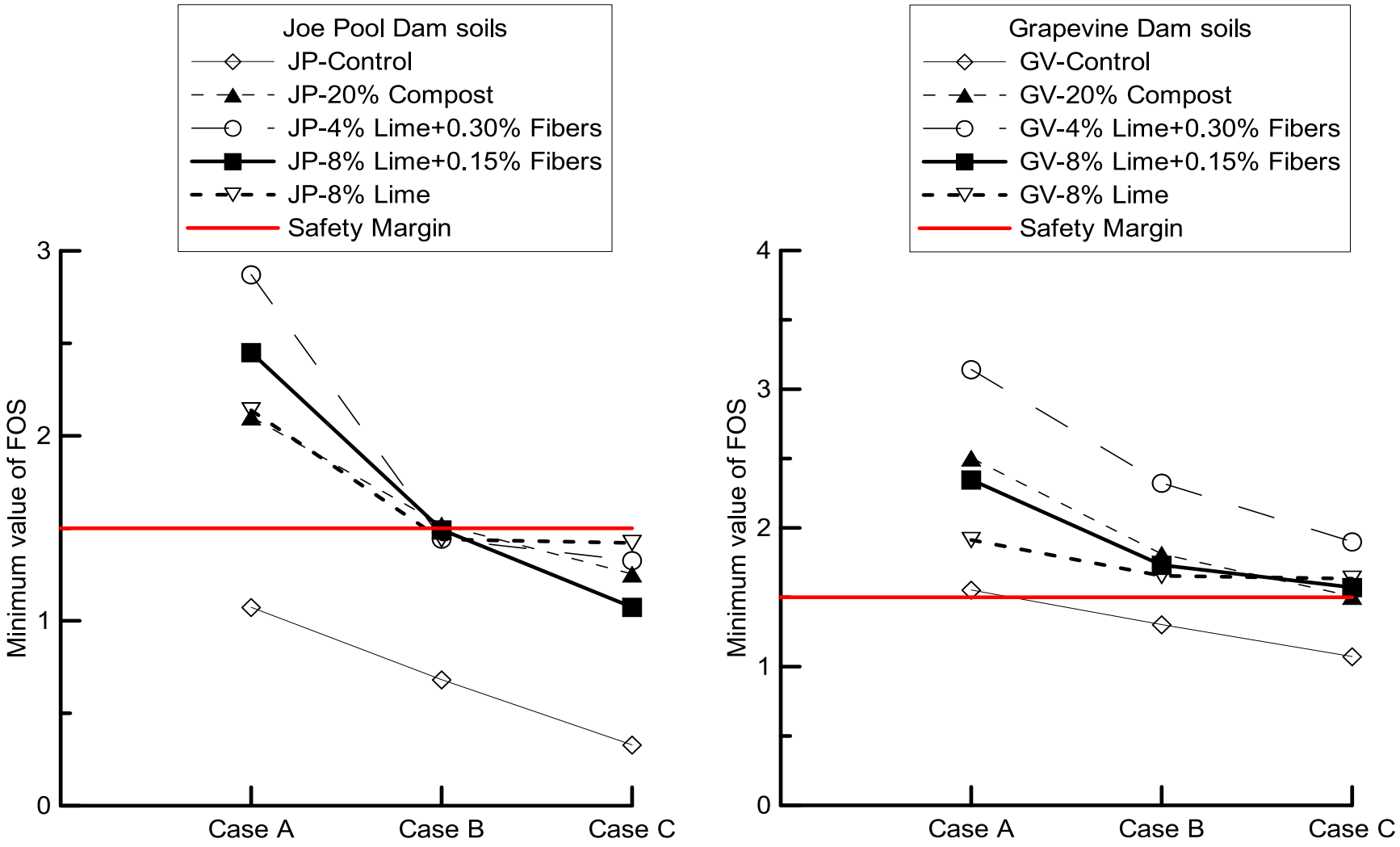

Figure 7.43. Minimum Values of FOS in 3 cases for Joe Pool Dam and Grapevine Dam soils

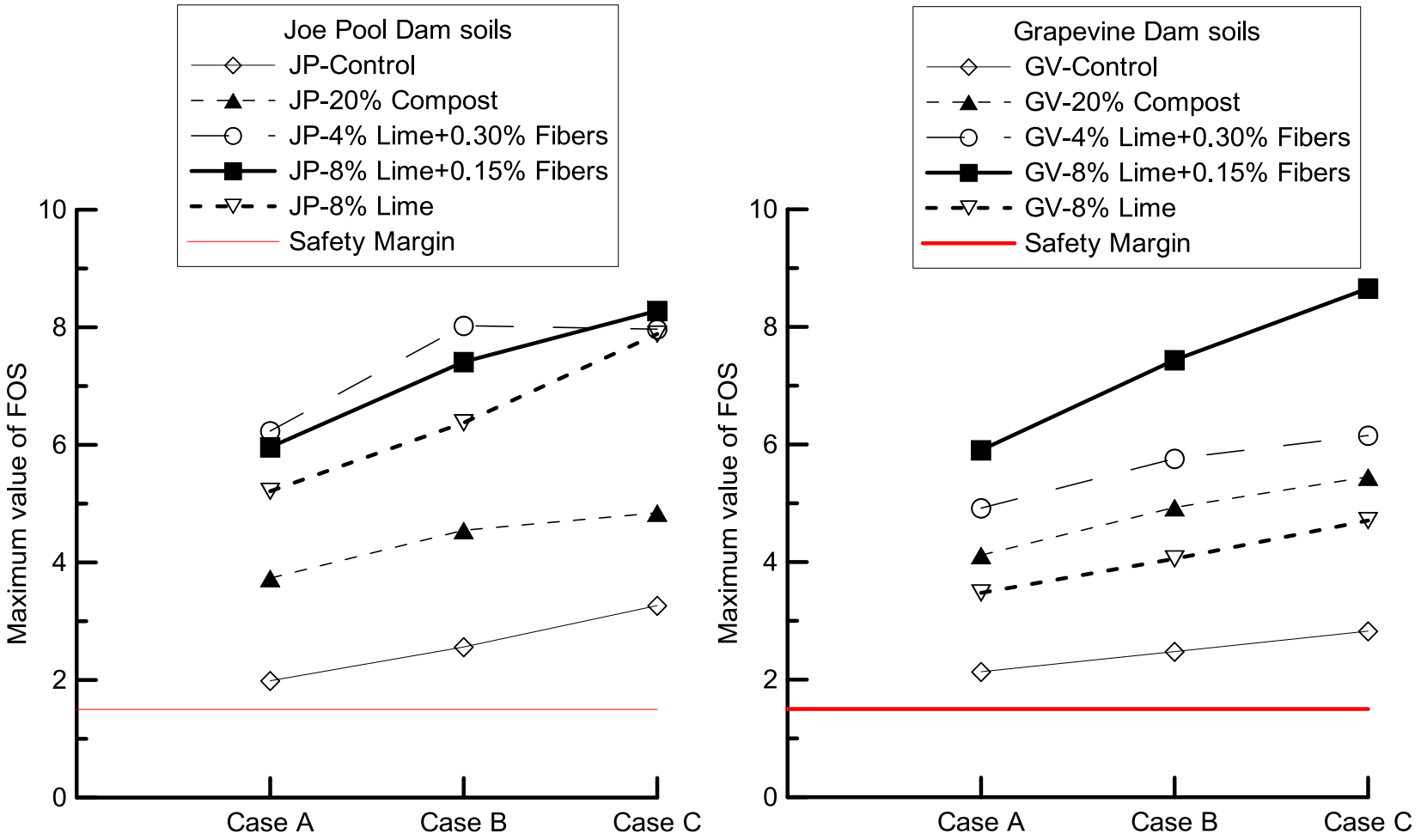

Figure 7.44. Maximum Values of FOS in 3 cases for Joe Pool Dam and Grapevine Dam soils

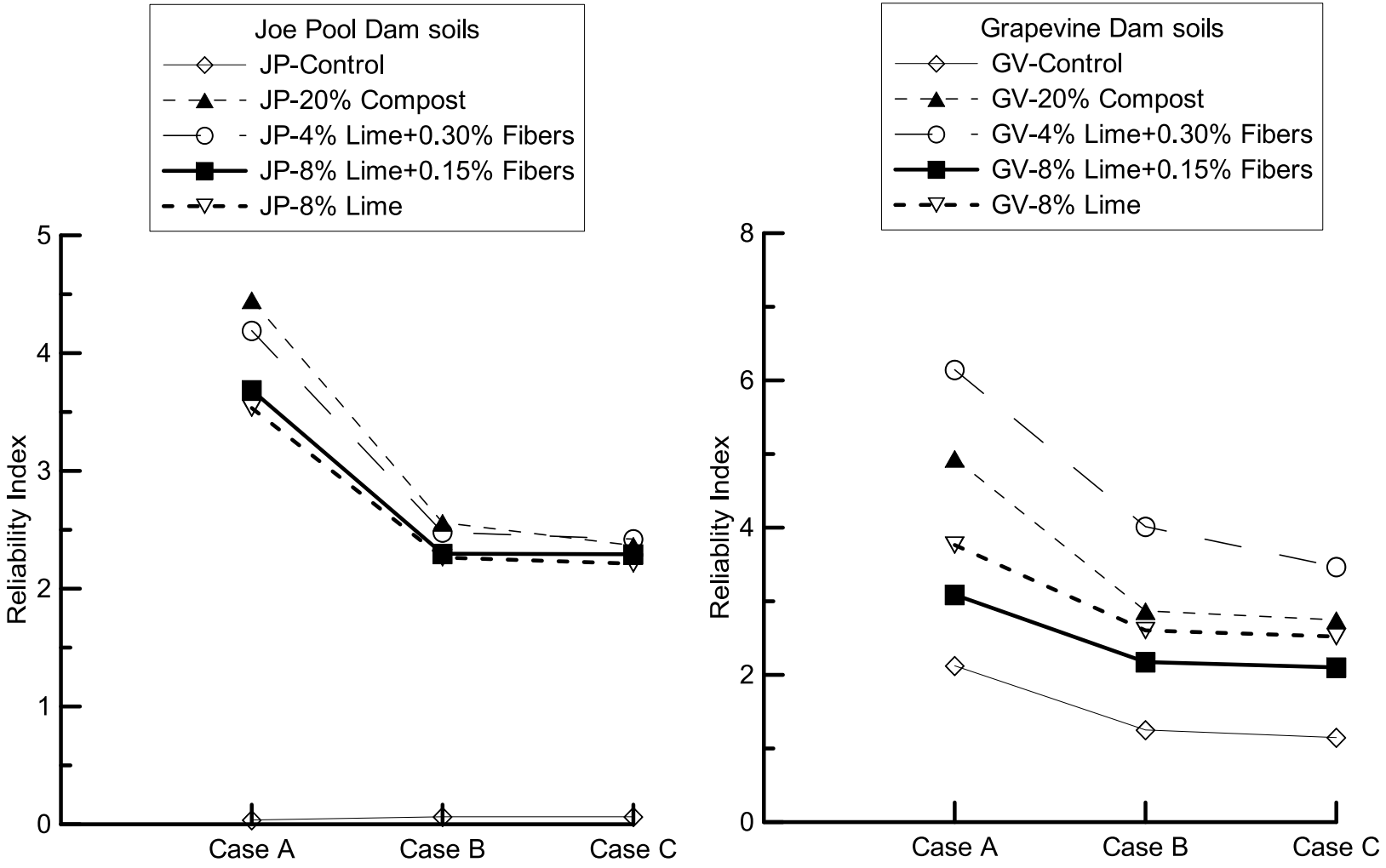

Figure 7.45. Reliability Indices of FOS in 3 cases for Joe Pool Dam and Grapevine Dam soils

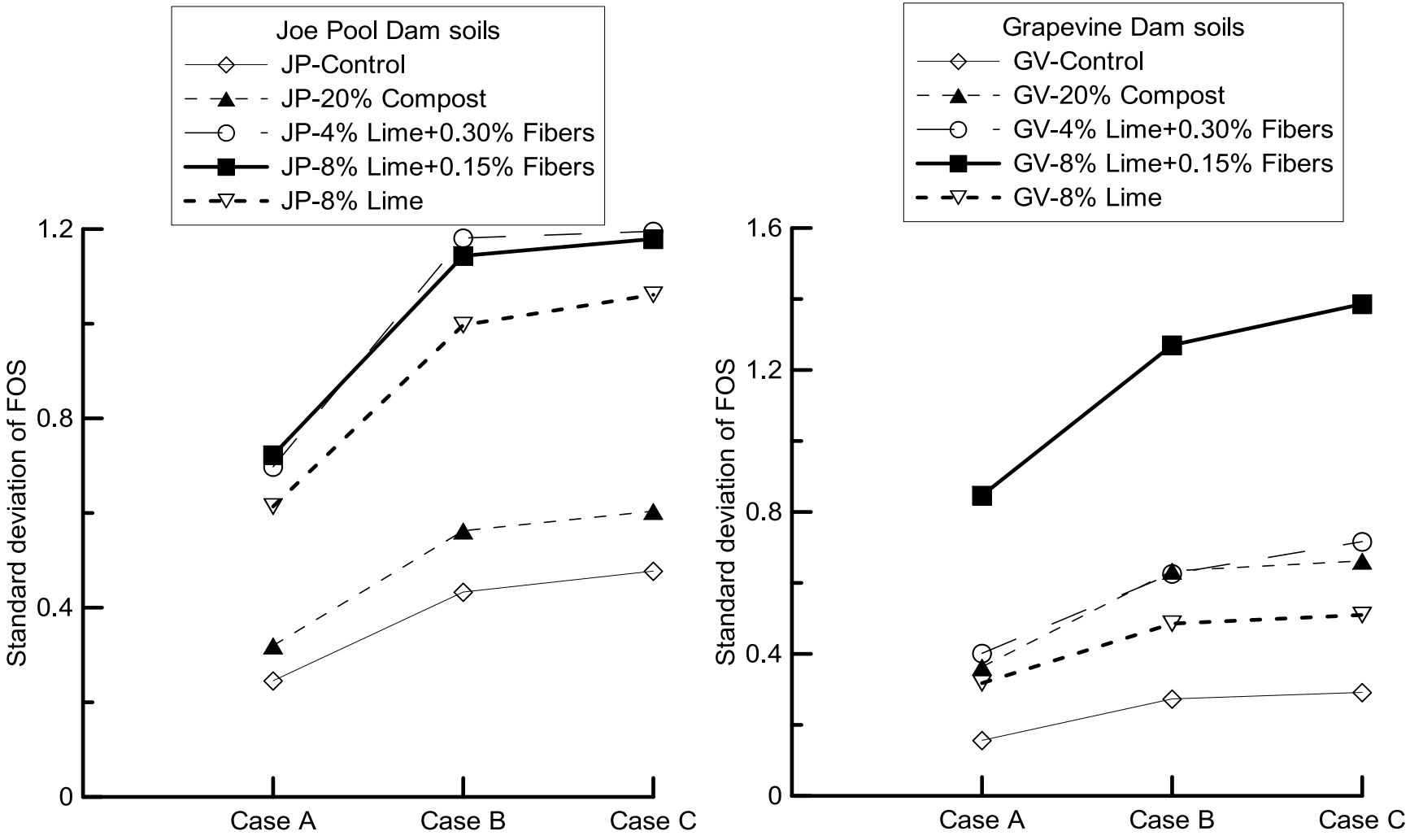

Figure 7.46. Standard Deviations of FOS in 3 cases for Joe Pool Dam and Grapevine Dam soils

Joe Pool Dam Soils

It can be inferred from the graphs that the mean values of FOS in all 3 cases remained stable, as the FOS distribution was considered to be normal. 4%lime+0.30%fibers treatment has the highest average values of FOS followed by 8%lime+0.15%fibers and 8%lime additive amendments. Mean values of FOS for control soil in all three cases were very near the safety margin line of 1.5 indicating, that failure was imminent with untreated soil layers.

Regarding the minimum values of FOS, all treatments obtained a least values of FOS in Cases B and C, below the safety margin line. This can be interpreted as probability of failure present in all soil amendments in these two cases. In particular, control soil had all minimum values of FOS lying below the safety margin line, showing the probability of failure was largest compared to other treatments.

Maximum value of FOS increased from Case A to Case C. This is explained by the nonlinearity relationship between FOS and cohesion and friction angle. As the span of variability enlarged from Case A to Case C, more critical combination of cohesion and friction angle could be generated.This may give a higher FOS as a consequence.

Reliability indices results reflected the treatment effects on FOS over the control soil. Control soil obtained the least reliability index signaling the probability of failure is prevalent. Overall, the reliability indices reduced from Case A to Case C as the soil parameters hit the lower values that resulted in the lower FOS.

Standard deviation of FOS appeared to increase from Case A to Case C. This is attributed to the fact that the outcome of FOS changes more upon the variability of its contributing components namely cohesion and friction angle of the soil.

Grapevine Dam Soils

The results of mean value of FOS of the Joe Pool Dam soils showed that the Grapevine Dam soils are less prone to failure as all mean values were above the safety line.

8%lime+0.15%fibers treated soil had the highest mean value of FOS followed by 4%lime+0.30%fibers and 20%compost treated soils.

From the results of minimum values of FOS, it can be seen that the control soil has the greatest risk of failure, as almost all minimum values of FOS lie below the safety margin. Results of the treated sections indicate that the probability of failure is close to zero, as all the minimum FOS values are positioned above the safety margin line of 1.5.

Maximum values of FOS results highlight the effectiveness of 8%lime+0.15%fibers treatment, as it achieved highest values of maximum FOS in all cases.

However, reliability indices and standard deviation of FOS, 8%lime+0.15%fibers amendment appeared to have the biggest variability in terms of FOS. Reliability obtained by 8%lime+0.15%fibers was second lowest after the control soil and its standard deviation of FOS was highest among all other treatment additives.

Table 7.20 and Table 7.21 present the probability of failure (when FOS is below 1.5) as shown by the results of Monte Carlo simulation in SLOPE/W. Zero probability of failure indicated that the minimum of FOS was well above value of 1.5. It should be noted that with the increase of variability of cohesion and friction angle, the probability of failure is increased as well. Among all the sections, control soil exhibited the highest probability of failure followed by the compost section for both Joe Pool Dam and Grapevine Dam soils. Reliability analysis results were incorporated into the ranking analysis showing the effectiveness of the soil stabilizers over the control soil.

Table 7.20. Probability of Failure for Joe Pool Dam Soils based on 1000 Trials Monte Carlo Simulation

Soils	Case A %	Case B %	Case C %
Control soil	51.4	52.6	53.4
20%compost treated soil	0	0.2	0.7
4%lime+0.30%fibers treated soil	0	0.25	0.51
8%lime+0.15 %fibers treated soil	0	0.12	0.58
8 %lime treated soil	0	0.32	0.32

Table 7.21. Probability of Failure for Grapevine Dam Soils based on 1000 Trials Monte Carlo Simulation

Soils	Case A %	Case B %	Case C %
Control soil	0	12.4	12.9
20%compost treated soil	0	0	0.1
4%lime+0.30%fibers treated soil	0	0	0
8%lime+0.15 %fibers treated soil	0	0	0
8 %lime treated soil	0	0	0

7.4 Ranking Analysis

Effectiveness of FSS soil parameters for the untreated and treated soil in the present slope stability assessments were ranked based on the results of the reliability analysis using the Monte Carlo simulation. To further explain the ranking results, the following rules and criteria were applied:

- Ranking points are given on a scale of 1 to 5 with 1 indicating the best and 5 the worst ranked section. Therefore, the test section that obtained the lowest total score was the best section and vice versa.
- Regarding the values of FOS, a section that yielded the highest value was termed the best one. This rule applies for the average value of FOS, the minimum value of FOS and the maximum value of FOS categories. The standard deviation of FOS, standard deviation and the mean value of FOS are parts of the reliability index as described in Eq. 7-7. Performance of soil sections was already ranked in the mean value of FOS and reliability index categories. Thus, ranking for standard deviation is not necessary.
- Regarding the reliability index, a section that has the higher value of reliability index is more reliable. In terms of probability of failure, soil that exhibits least probability of failure is given the best rank of 1.

Table 7.22 and Table 7.23 present the reliability performance ranking for the Joe Pool Dam and Grapevine Dam untreated and treated soils.

Table 7.22. Reliability Performance ranking for the Joe Pool Dam soils

Soil	Mean value of FOS	Minimum value of FOS	Maximum value of FOS	Reliability Index	Probability of Failure	Total
Control soil	5	5	5	5	5	5
20%compost treated soil	4	4	4	1	4	4
4%lime+0.30%fibers treated soil	1	1	1	2	3	1
8%lime+0.15 %fibers treated soil	2	3	2	3	2	2
8 %lime treated soil	3	2	3	4	1	3

Table 7.23. Reliability Performance ranking for the Grapevine Dam soils

Soil	Mean value of FOS	Minimum value of FOS	Maximum value of FOS	Reliability Index	Probability of Failure	Total
Control soil	5	5	5	5	5	5
20%compost treated soil	3	2	3	2	4	3
4%lime+0.30%fibers treated soil	2	1	2	1	1	1
8%lime+0.15 %fibers treated soil	1	3	1	4	2	2
8 %lime treated soil	4	4	4	3	3	4

Note: For Lime treated sections since probability of failure is zero for all cases. Safety of margin is increased to 3.3 for the sake of quantitative comparisons. Results are shown in Table 7.24 below:

Table 7.24. Probability of failure for safety margin of 3.3 for Lime Treated soil of Grapevine Dam

Soils	Case A	Case B	Case C
4%lime+0.30%fibers treated soil	4.4	14.3	18
8%lime+0.15 %fibers treated soil	21	26.1	25.2
8 %lime treated soil	98.7	85.8	86.5

7.5 Summary

Laboratory test results of FSS soil parameters were analyzed in a slope modeling using both deterministic and probabilistic approaches. The probabilistic approach is similar to reliability analysis. Factor of Safety was calculated based on the original FSS soil parameters obtained from Chapter 5 as well as from the additional FSS tests. Ranking analysis was incorporated to address the reliability of FSS properties results. Based on the ranking, 4%lime+0.30%fibers and 8%lime+0.15%fibers treatment amendments appear to be the most reliable stabilizers for both Joe Pool Dam and Grapevine Dam soils. The results of this chapter will be included in the final ranking analysis of untreated and treated soils based on all categories including field performance and laboratory testing.

CHAPTER 8

SUMMARY AND CONCLUSIONS

8.1 Introduction

The main objectives of this research were to study the long-term effects of different surficial soil stabilizers to mitigate the shallow slope failures and also to recommend the best performing additive(s) for surficial slopes. These objectives were assessed based on the continuous field monitoring studies, laboratory model studies, analytical and reliability model studies. More importantly the fully softened shear strength property and its implications with surficial slope stability are fully addressed in this research.

A literature review was first conducted and various aspects of slope stability were studied. Principles of design of earthfill dams were reviewed with the study of unsatisfactory slope performance case studies. The current state of the art in slope stability analysis was reviewed and highlighted with the focus on the limit equilibrium approach methods for stability assessments. Three-dimensional slope analysis methods were also studied and compared with the traditional two-dimensional slope stability assessment and design methodologies. Surficial slope failure concepts were reviewed and several related case studies in Texas were discussed. The effects of desiccation cracking and rainfall on surficial failures were studied. The concept of fully softened shear strength and its current practices were reviewed and discussed. Various slope stabilization methods were detailed with the emphasis on the use of chemical and physical stabilizers namely lime, fibers and compost materials to amend topsoils.

Field performance of the test sections from both Joe Pool Dam and Grapevine Dam sites was continuously monitored to examine the long-term effects of the applied admixtures.

Collected data from moisture and temperature sensors, inclinometer and elevation surveys over several years are presented and analyzed. Earlier work done by Dronamraju (2008) was added to current monitoring data of three years and all the compiled data was statistically analyzed to address stabilization methods in enhancing slope stability. Visual observation of desiccation cracks and vegetation growth were also monitored and reported. The ranking was conducted based on the collected data.

The laboratory testing program was conducted, with the main focus on fully softened shear strength (FSS) testing. FSS testing on both control and treated soils was conducted, using both Direct Shear (DS) and Torsional Ring Shear (TRS) devices. Sample preparation and testing procedures for both devices followed ASTM standards and the recommendations of the US Army Corps of Engineers (USACE) procedures.

Results of FSS testing and analysis were presented. FSS soil parameters, namely FSS cohesion and FSS friction angle were determined using the average linear strength envelope approach, as recommended by the past researchers (Tiwari, 2011; Wright, 2005). Difference of FSS soil parameters obtained from the DS and TRS apparatus was discussed. Obtained data was in good agreement with the work of previous researchers (Tiwari, 2011; Castellanos, 2013). The FSS test results from the DS device were adopted for the analytical and reliability analyses.

Statistical analysis was conducted on the filed monitoring data to study the significant differences between different field-related performance categories of untreated and treated soils. The Student's t-test, using the Dunnett's procedure was chosen as the comparison test to carry out the analysis. Field performance was ranked based on the results that showed statistically significant differences on both Joe Pool Dam and Grapevine Dam soils.

In addition, the analytical and reliability-based slope stability modeling studies were conducted. Three case studies were analyzed with different soil conditions, and these are: (1) No rainfall (2) Long-term rainfall and (3) Wetting and drying cycles (FSS condition). The combined effects of the FSS cohesion and FSS friction angle based on the outcomes of factor

of safety (FOS) calculations are discussed in the deterministic slope stability analysis. Probabilistic and reliability analyses of slope stability were carried out to address the variability of the FSS soil parameters. Monte Carlo simulation of SLOPE/W software was utilized to conduct the analysis. Ranking analysis of the untreated and treated soils was presented based on the analytical and reliability studies.

8.2 Summary and Conclusions

The findings of this dissertation research are summarized as follows:

- Based on the volumetric moisture content results, 20%compost treated section held higher volumetric moisture content than the other treated sections on both the Joe Pool Dam and the Grapevine Dam sites. This was apparent in the field observation, with better vegetation growth on the compost-treated section than other treated sections. However, the potential to reduce desiccation cracks of compost amendment was not observed due to limited strength enhancements from this amendment. This results in major desiccation cracks being found in the compost treated section during the drought season (2011).
- Temperature data have showed that the applied surficial soil treatments had little or no effect on the temperature of the soil as the results of student's t-test showed no significant difference in the performance of untreated and treated soils. This is in agreement with Dronamraju (2008) results which were based on the early post-construction field monitoring data. Thus, temperature is not recommended to be a factor for the field performance comparisons of the present treated and untreated soils.
- Elevation surveys showed the improvements of the treated soils over the control or untreated soils. Among the treatments, 8%lime+0.15%fibers and 8%lime treated soils were ranked the top two treaments in the present research as their sections exhibited 50 to 60% less vertical movement than the control untreated section.

- Regarding the horizontal movements (inclinometer surveys), all lime treated soil sections showed significant improvements over the control soil section. The maximum displacement was observed in the control section and followed by the 20%compost treated section. This explains the chemical effects of lime additive as it altered the soil and improved its properties.
- Major desiccation cracks were observed in the control section and 20%compost treated section at both Joe Pool Dam and Grapevine Dam sites. Particularly, a 24 ft. long and 4 ft. deep crack was found in the control section at Joe Pool Dam site during the driest months of summer 2011. No cracks were noticed in other treated sections.
- The FSS results tested on the Joe Pool Dam and Grapevine Dam soils displayed consistency in terms of numerical values for shear strength between all the treatment additives. The peak shear strength of soils from both sites was mobilized at a minimum shear displacement of 4 mm (0.16 in.) in the Direct Shear (DS) test and at 2 mm (0.08 in.) for the Torsionala Ring Shear (TRS) test. At higher effective normal stresses, the more horizontal displacement was required to achieve the plateau condition than at lower effective normal stresses. As the effective normal stresses for testing increased, changes of shear strength became more distinguishable between untreated and treated soil.
- Comparing the FSS testing results by two devices, the DS test results provided higher values of FSS soil strength parameters than those obtained by using the TRS device. This is in agreement with the majority of studies conducted by the past researchers. The variation could be attributed to the difference in sample thickness used for the two devices, the difference of soil-to-soil contact while shearing, the proximity of the failure plane in the TRS device, the roughness of the TRS platen, as well as the unequal and high shear strain induced by the TRS device on the soil specimens. Nevertheless,

improvements of the treated soils over the control soil were reported on the FSS soil parameters, namely FSS cohesion and FSS friction angle.

- Lime treated soils exhibited significant improvements in FSS cohesion intercept with a maximum value of 34.8 kPa (726.8 psf) obtained by 4%lime+0.30%fibers treatment on Joe Pool Dam soil. In terms of FSS friction angle, lime treated sections also showed the most improvements by enhancing the value by 20-35% when compared to the FSS friction angle of the control or untreated soil.
- Results of FSS testing from TRS device also revealed the absence of soil cohesion intercept that may cause the underestimation of the FSS of the soil as it reduces the FOS values for slopes under heavy rainfall condition. Overall, the DS device is believed to better depict the FSS condition of the soil; thus the results from DS device were used for the analytical and reliability-based slope modeling studies.
- The analytical model study using SLOPE/W indicated that the application of FSS soil parameters was appropriate for surficial failures on slopes subjected to wetting and drying cycles. The FOS values calculated from the deterministic slope stability analysis using FSS soil properties were in between those from two other distinguished conditions of no rainfall and long-term rainfall scenarios, where the peak undrained soil properties and the residual soil properties applied, respectively. This indicates that the use of the undrained strength parameters will overestimate the soil strength while using the residual strength parameters will underestimate the strength of the soil.
- The safety margin for FOS value was set at 1.5 as recommended by past researchers (Wright, 2005; USACE) to better address the surficial slope failures of embankment dams. Reliability analysis analyzed the improvements of the surficial soil treatments in terms of the FSS condition from a probabilistic point of view. Additional tests were conducted on both Joe Pool Dam and Grapevine Dam soils under identical conditions to address the variability of FSS cohesion and FSS friction angle. Monte Carlo

simulation in SLOPE/W was utilized to conduct the analysis based on the given average and standard deviation of FSS cohesion and FSS friction angle. Three cases were studied to cover different ranges of variability as 68%, 97% and 99% of the possible raw data. The results of the reliability analysis indicated that fibers-treated sections (4%lime+0.30%fibers and 8%lime+0.15%fibers) are the most reliable sections with the highest values of reliability index and the lowest probability of failure.

- Based on the comprehensive results of both long-term field performance and analytical/reliability analyses of FSS testing, 4%lime+0.30%fibers and 8%lime+0.15%fibers treatment additives are recommended to be implemented to address the surficial slope instability for both Joe Pool Dam and Grapevine Dam soils.

8.3 Future Research Recommendations

As a part of future research needs, it is recommended that the cost analysis be carried out to study treatments and comparisons. The analysis should also cover a large area to address treatments over the entire slope of the dam. Also, unsaturated slope stability assessments need to be carried out to further understand the slope stability assessments under unsaturated soil conditions.

APPENDIX A

NORMALITY CHECKS FOR FIELD MONITORING DATA

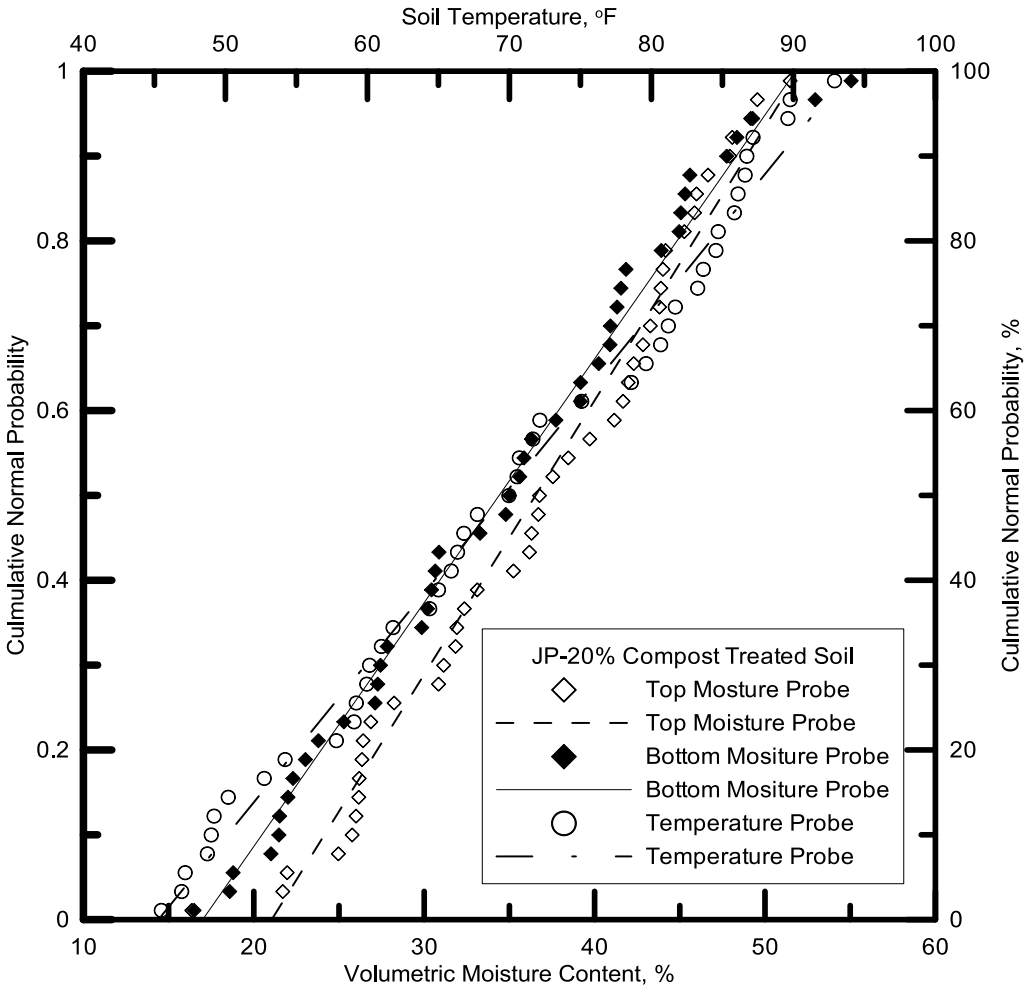

Fit Results

Top Moisture Probe
Equation Y = 0.03228637444 * X - 0.6795992889
Number of data points used = 45
Average X = 36.5355
Average Y = 0.5
Residual sum of squares = 0.0776201
Regression sum of squares = 3.67053
Coef of determination, R-squared = 0.979291
Residual mean square, sigma-hat-sq'd = 0.00180512

Fit Results

Bottom Mositure Probe
Equation Y = 0.0584862378 * X - 1.020060484
Number of data points used = 45
Average X = 25.9901
Average Y = 0.5
Residual sum of squares = 0.0433141
Regression sum of squares = 3.70483
Coef of determination, R-squared = 0.988444
Residual mean square, sigma-hat-sq'd = 0.0010073

Fit Results

Temperature Probe
Equation Y = 0.02136252803 * X - 0.990080139
Number of data points used = 45
Average X = 69.7521
Average Y = 0.5
Residual sum of squares = 0.0421898
Regression sum of squares = 3.70596
Coef of determination, R-squared = 0.988744
Residual mean square, sigma-hat-sq'd = 0.000981158

Figure 9.1 Normality check for soil moisture and temperature of the Joe Pool Dam 20%compost treated soil

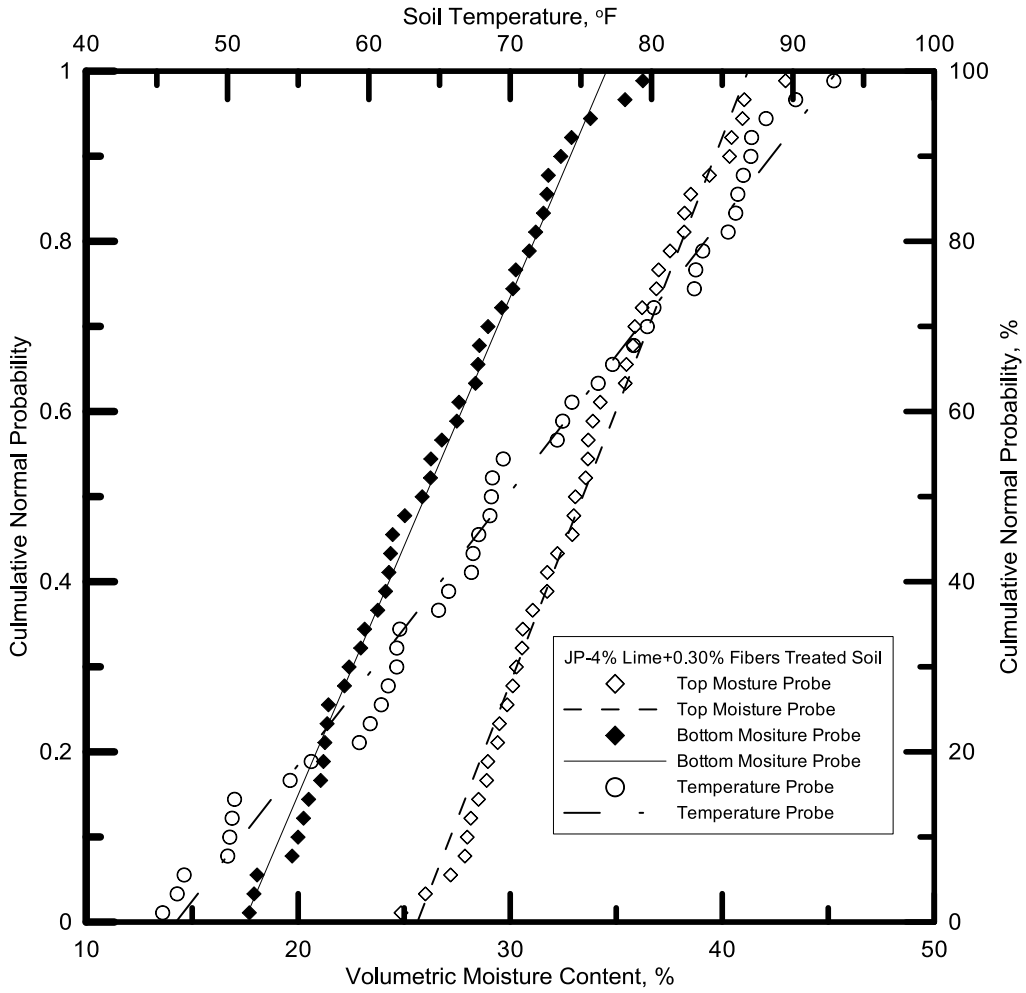

Fit Results

Top Moisture Probe
Equation Y = 0.06412492193 * X - 1.642918896
Number of data points used = 45
Average X = 33.4179
Average Y = 0.5
Residual sum of squares = 0.0613557
Regression sum of squares = 3.68679
Coef of determination, R-squared = 0.98363
Residual mean square, sigma-hat-sq'd = 0.00142688

Fit Results

Bottom Mositure Probe
Equation Y = 0.0584862378 * X - 1.020060484
Number of data points used = 45
Average X = 25.9901
Average Y = 0.5
Residual sum of squares = 0.0433141
Regression sum of squares = 3.70483
Coef of determination, R-squared = 0.988444
Residual mean square, sigma-hat-sq'd = 0.0010073

Fit Results

Temperature Probe
Equation Y = 0.02128296119 * X - 0.9316775542
Number of data points used = 45
Average X = 67.2687
Average Y = 0.5
Residual sum of squares = 0.0328893
Regression sum of squares = 3.71526
Coef of determination, R-squared = 0.991225
Residual mean square, sigma-hat-sq'd = 0.000764867

Figure 9.2 Normality check for soil moisture and temperature of the Joe Pool Dam 4%lime+0.30% Fibers treated soil

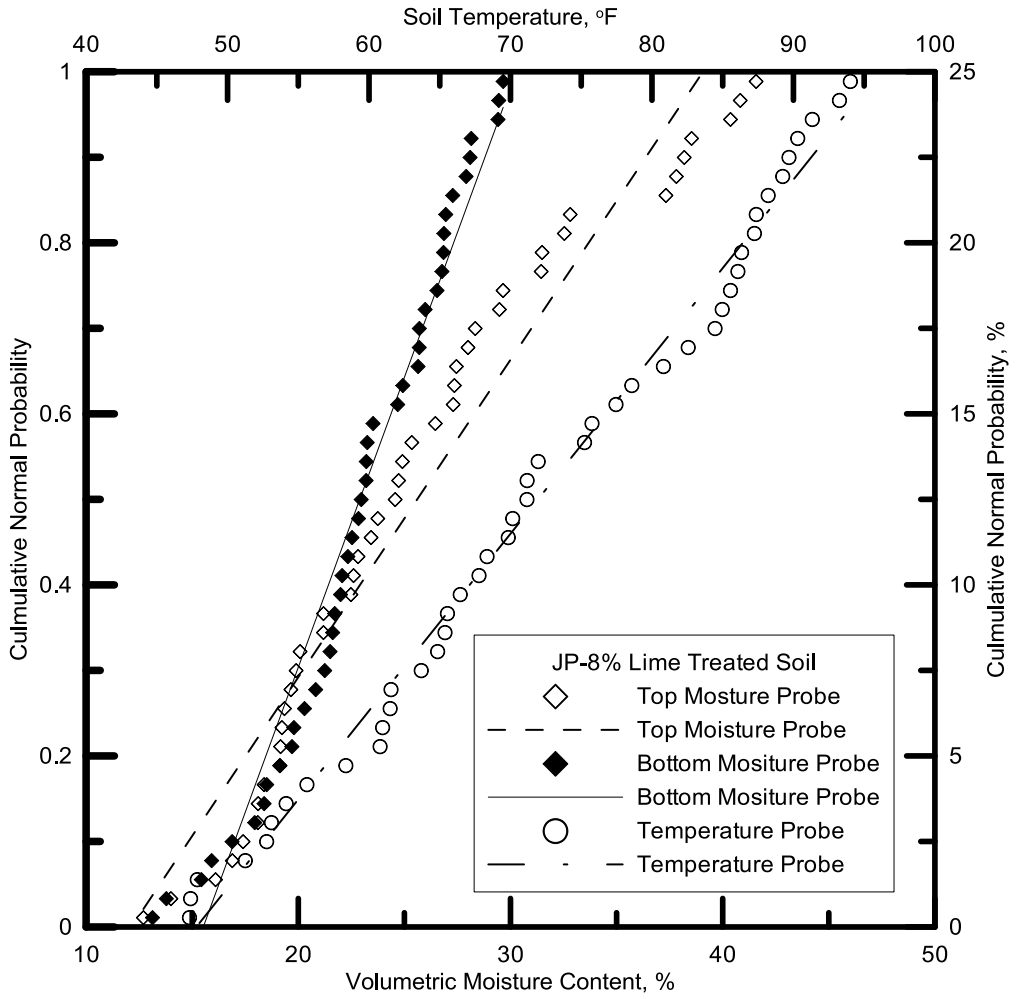

Fit Results

Top Moisture Probe
Equation Y = 0.03712275893 * X - 0.4504220499
Number of data points used = 45
Average X = 25.6021
Average Y = 0.5
Residual sum of squares = 0.195986
Regression sum of squares = 3.55216
Coef of determination, R-squared = 0.947711
Residual mean square, sigma-hat-sq'd = 0.00455781

Fit Results

Bottom Mositure Probe
Equation Y = 0.06780675872 * X - 1.052466457
Number of data points used = 45
Average X = 22.8955
Average Y = 0.5
Residual sum of squares = 0.139813
Regression sum of squares = 3.60834
Coef of determination, R-squared = 0.962698
Residual mean square, sigma-hat-sq'd = 0.00325146

Fit Results

Temperature Probe
Equation Y = 0.02070512575 * X - 0.9895377782
Number of data points used = 45
Average X = 71.9405
Average Y = 0.5
Residual sum of squares = 0.0361454
Regression sum of squares = 3.712
Coef of determination, R-squared = 0.990356
Residual mean square, sigma-hat-sq'd = 0.000840591

Figure 9.3 Normality check for soil moisture and temperature of the Joe Pool Dam 8%lime treated soil

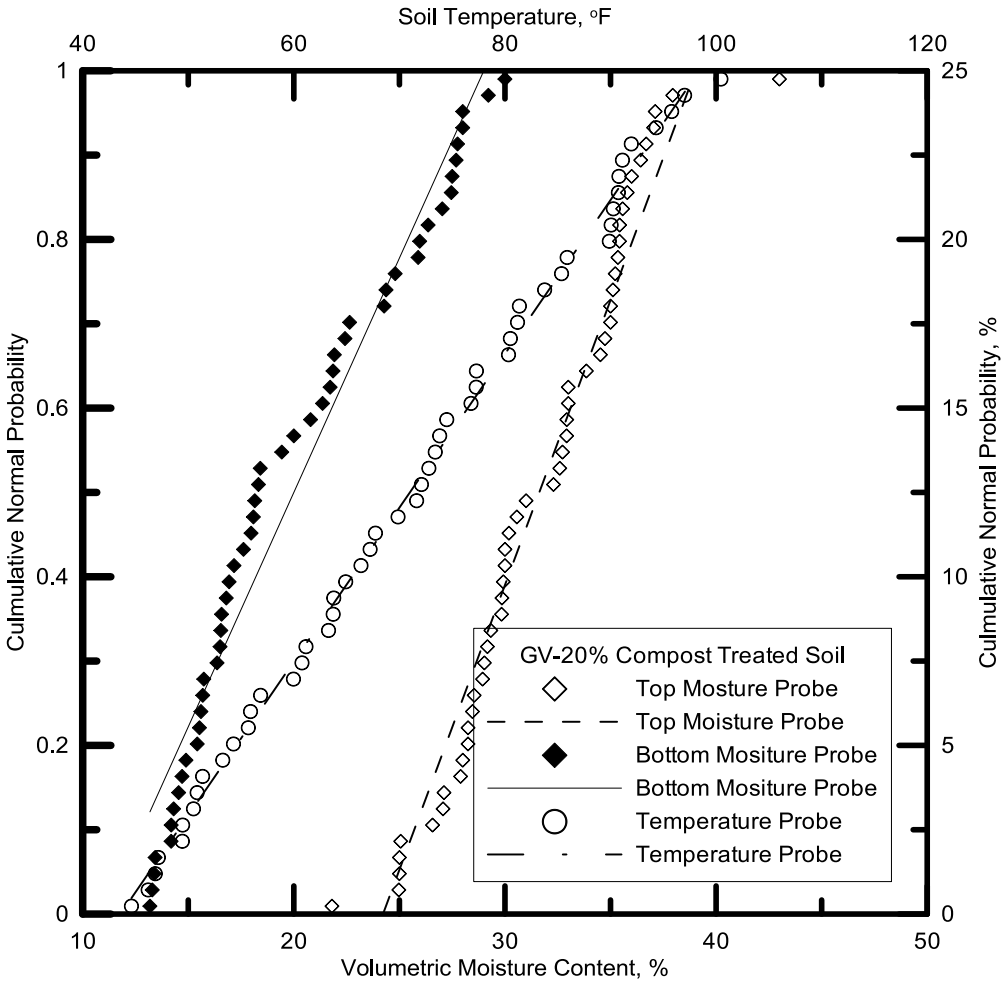

Fit Results

Top Moisture Probe
Equation Y = 0.06755179943 * X - 1.636351243
Number of data points used = 52
Average X = 31.6254
Average Y = 0.5
Residual sum of squares = 0.206242
Regression sum of squares = 4.12549
Coef of determination, R-squared = 0.952388
Residual mean square, sigma-hat-sq'd = 0.00412485

Fit Results

Bottom Mositure Probe
Equation Y = 0.05557495693 * X - 0.6115351426
Number of data points used = 52
Average X = 20.0006
Average Y = 0.5
Residual sum of squares = 0.167551
Regression sum of squares = 4.16418
Coef of determination, R-squared = 0.96132
Residual mean square, sigma-hat-sq'd = 0.00335103

Fit Results

Temperature Probe
Equation Y = 0.01823945283 * X - 0.7948664447
Number of data points used = 52
Average X = 70.9926
Average Y = 0.5
Residual sum of squares = 0.0151754
Regression sum of squares = 4.31656
Coef of determination, R-squared = 0.996497
Residual mean square, sigma-hat-sq'd = 0.000303508

Figure 9.4 Normality check for soil moisture and temperature of the Grapevine Dam 20%compost treated soil

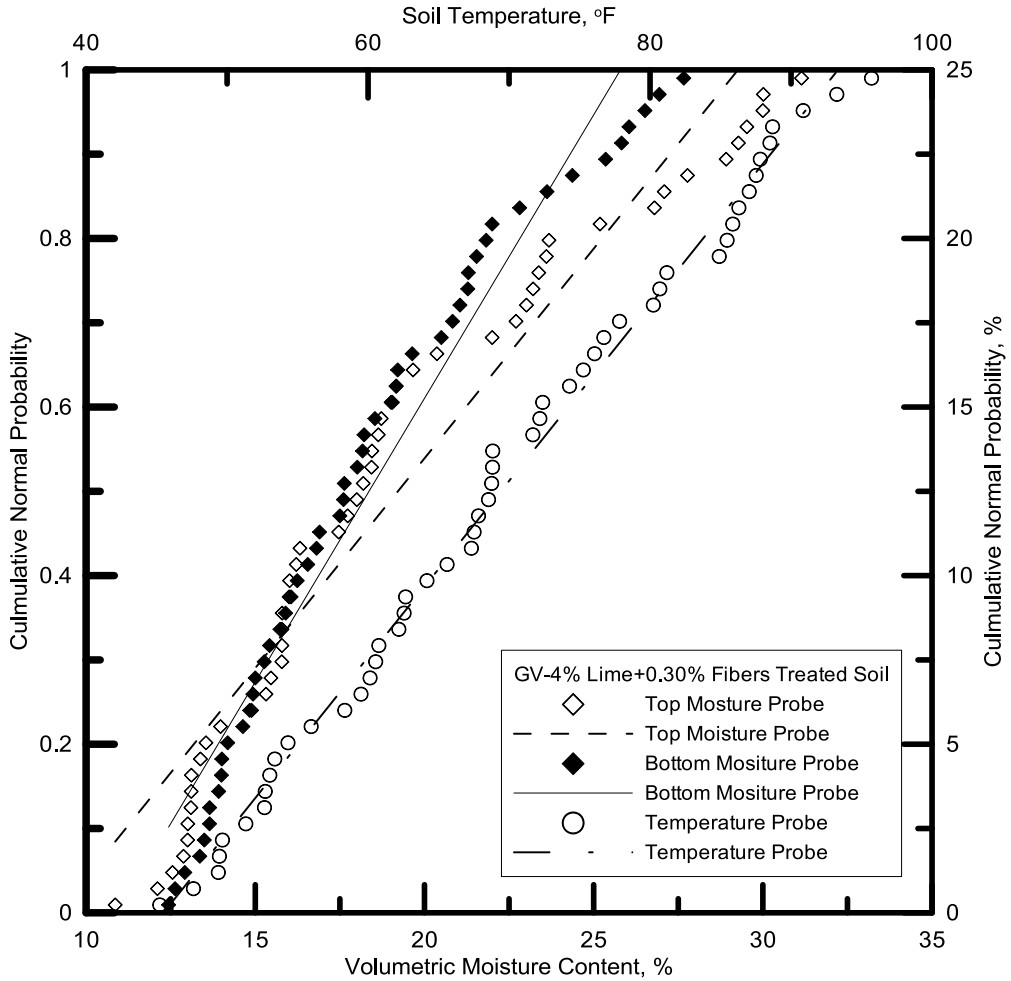

Fit Results

Top Moisture Probe
Equation Y = 0.04974454356 * X - 0.4557766659
Number of data points used = 52
Average X = 19.2137
Average Y = 0.5
Residual sum of squares = 0.263893
Regression sum of squares = 4.06784
Coef of determination, R-squared = 0.939079
Residual mean square, sigma-hat-sq'd = 0.00527785

Fit Results

Bottom Mositure Probe
Equation Y = 0.06726845917 * X - 0.7350637026
Number of data points used = 52
Average X = 18.3602
Average Y = 0.5
Residual sum of squares = 0.19685
Regression sum of squares = 4.13488
Coef of determination, R-squared = 0.954556
Residual mean square, sigma-hat-sq'd = 0.00393699

Fit Results

Temperature Probe
Equation Y = 0.02090014915 * X - 0.9506635175
Number of data points used = 52
Average X = 69.4092
Average Y = 0.5
Residual sum of squares = 0.0298662
Regression sum of squares = 4.30186
Coef of determination, R-squared = 0.993105
Residual mean square, sigma-hat-sq'd = 0.000597324

Figure 9.5 Normality check for soil moisture and temperature of the Grapevine Dam 4%lime+0.30%fibers treated soil

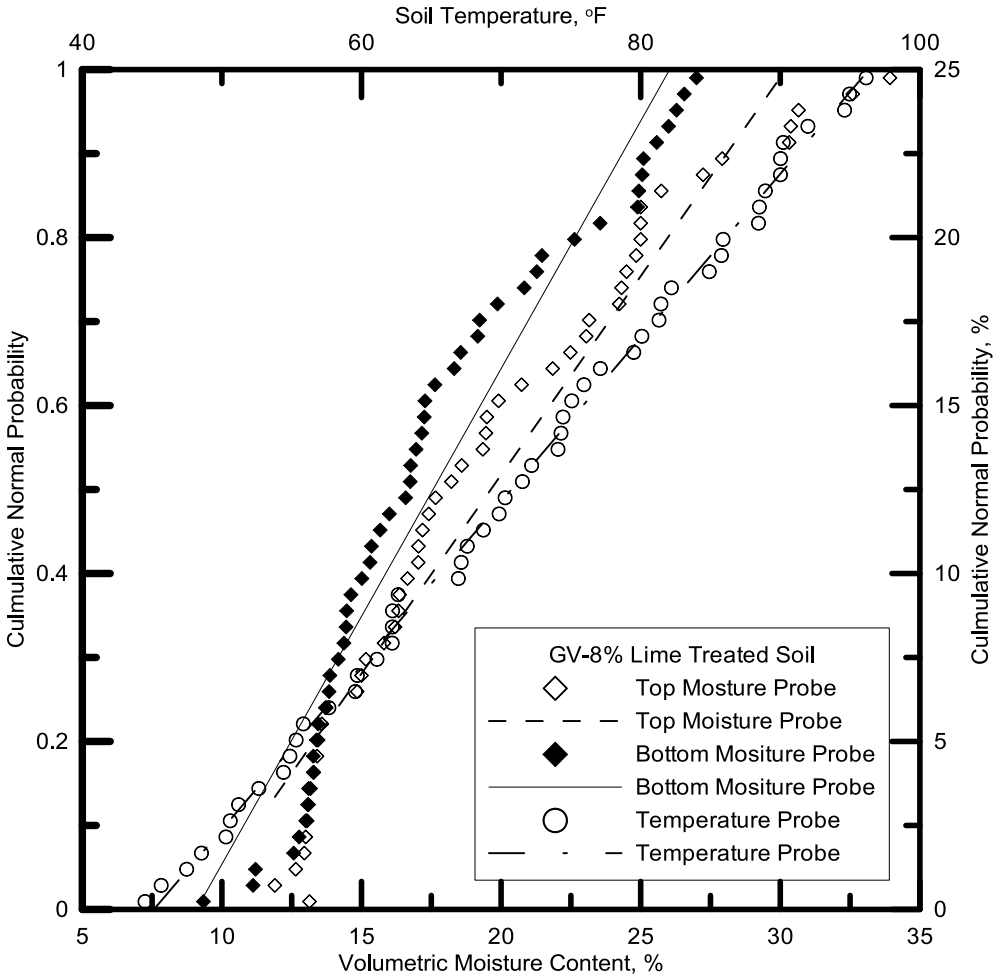

Fit Results

Top Moisture Probe
Equation Y = 0.04732412617 * X - 0.4290959533
Number of data points used = 52
Average X = 19.6326
Average Y = 0.5
Residual sum of squares = 0.264478
Regression sum of squares = 4.06725
Coef of determination, R-squared = 0.938944
Residual mean square, sigma-hat-sq'd = 0.00528956

Fit Results

Bottom Mositure Probe
Equation Y = 0.05898987251 * X - 0.535948432
Number of data points used = 52
Average X = 17.5615
Average Y = 0.5
Residual sum of squares = 0.288992
Regression sum of squares = 4.04274
Coef of determination, R-squared = 0.933285
Residual mean square, sigma-hat-sq'd = 0.00577983

Fit Results

Temperature Probe
Equation Y = 0.01951633127 * X - 0.8806767724
Number of data points used = 52
Average X = 70.7447
Average Y = 0.5
Residual sum of squares = 0.0115774
Regression sum of squares = 4.32015
Coef of determination, R-squared = 0.997327
Residual mean square, sigma-hat-sq'd = 0.000231549

Figure 9.6 Normality check for soil moisture and temperature of the Grapevine Dam 8%lime treated soil

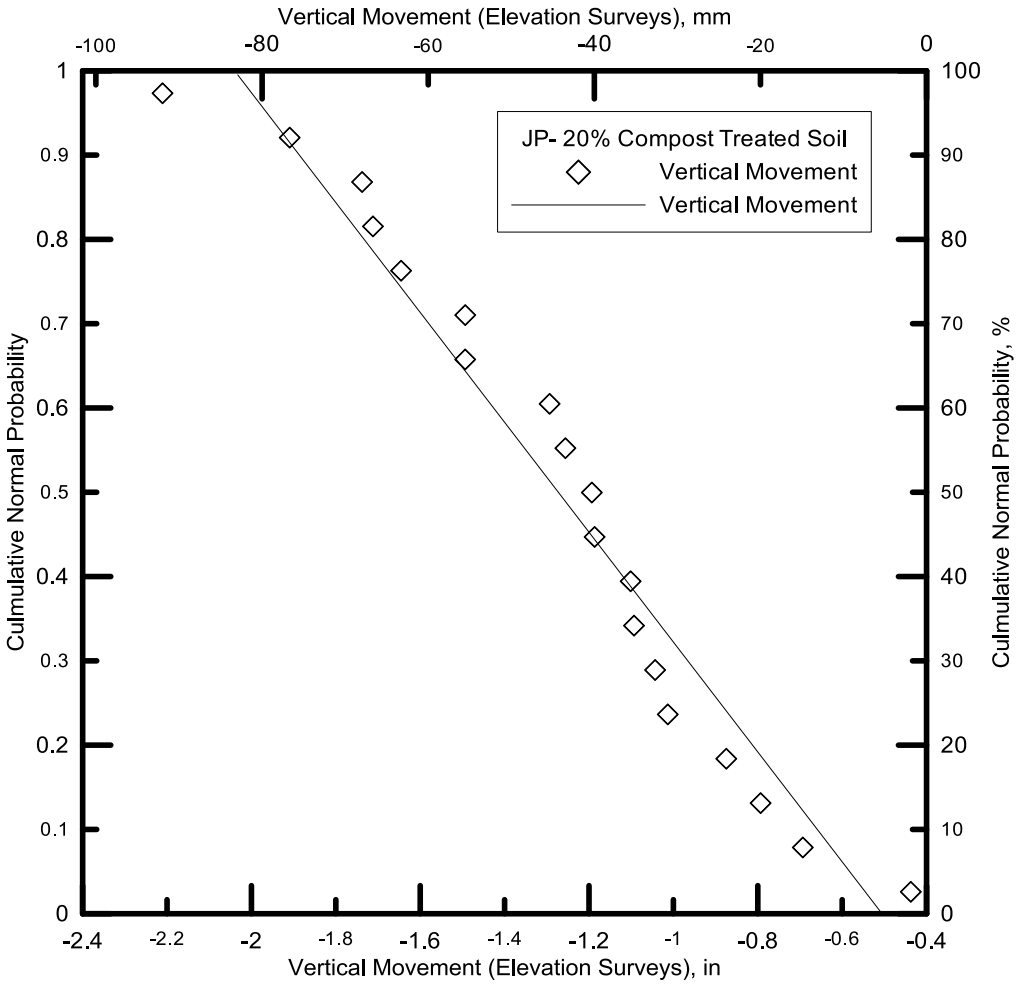

Fit Results

Vertical Movement
Equation Y = -0.651736171 * X - 0.3294581456
Number of data points used = 19
Average X = -1.27269
Average Y = 0.5
Residual sum of squares = 0.0718437
Regression sum of squares = 1.5071
Coef of determination, R-squared = 0.954499
Residual mean square, sigma-hat-sq'd = 0.0042261

Figure 9.7 Normality check for vertical movement of the Joe Pool Dam 20%compost Treated Soil

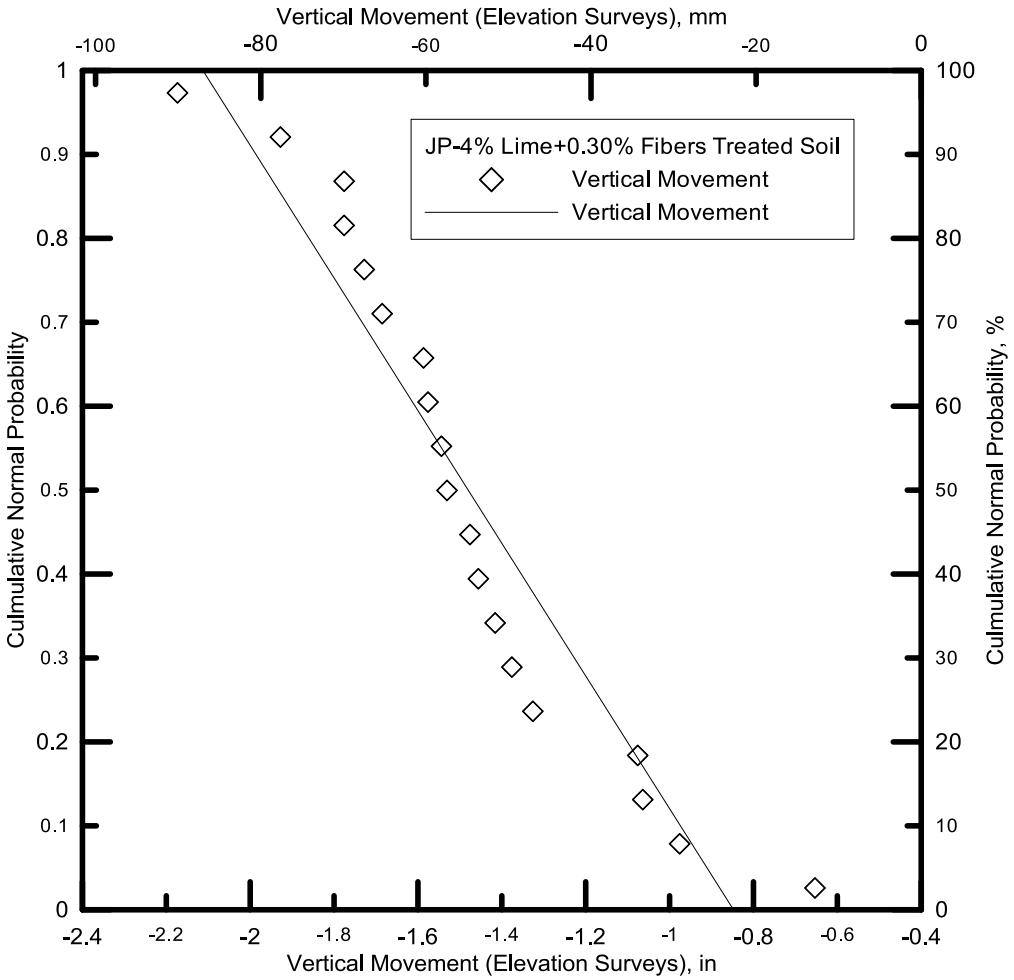

Fit Results

Vertical Movement
Equation Y = -0.7904004751 * X - 0.6699313698
Number of data points used = 19
Average X = -1.48018
Average Y = 0.5
Residual sum of squares = 0.141777
Regression sum of squares = 1.43717
Coef of determination, R-squared = 0.910208
Residual mean square, sigma-hat-sq'd = 0.00833985

Figure 9.8 Normality check for vertical movement of the Joe Pool Dam 4%lime+0.30%fibers Treated Soil

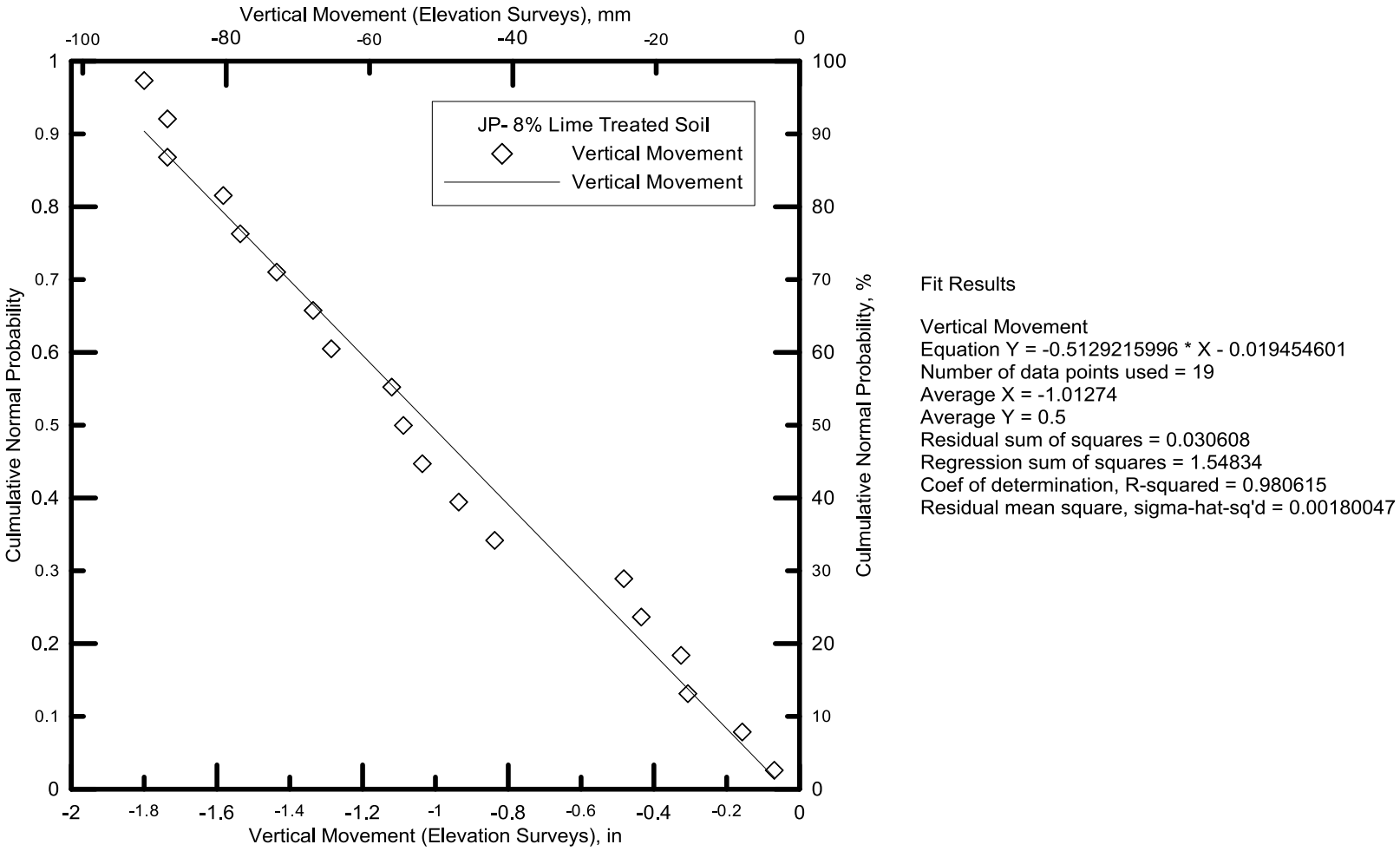

Fit Results

Vertical Movement
Equation Y = -0.5129215996 * X - 0.019454601
Number of data points used = 19
Average X = -1.01274
Average Y = 0.5
Residual sum of squares = 0.030608
Regression sum of squares = 1.54834
Coef of determination, R-squared = 0.980615
Residual mean square, sigma-hat-sq'd = 0.00180047

Figure 9.9 Normality check for vertical movement of the Joe Pool Dam 8%lime Treated Soil

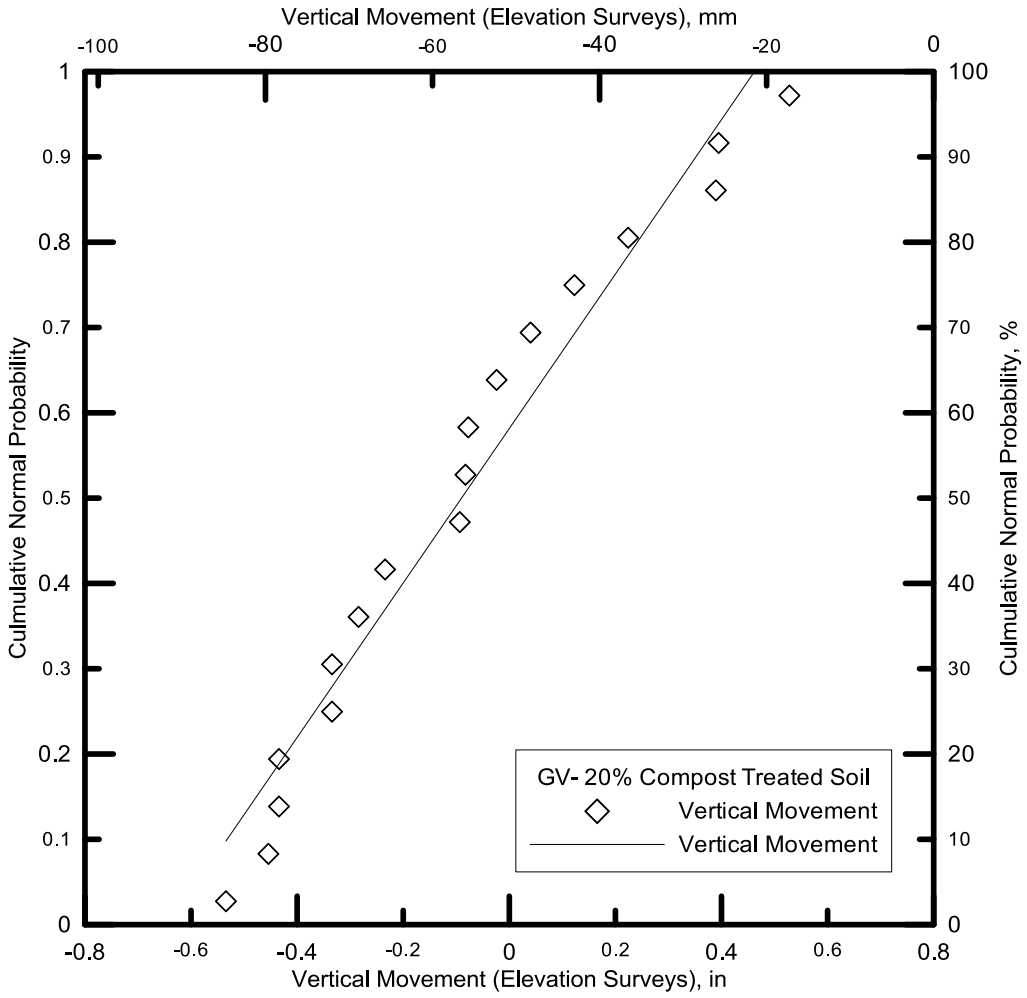

Fit Results

Vertical Movement
Equation Y = 0.9053074851 * X + 0.5816006166
Number of data points used = 18
Average X = -0.0901358
Average Y = 0.5
Residual sum of squares = 0.0556353
Regression sum of squares = 1.43974
Coef of determination, R-squared = 0.962795
Residual mean square, sigma-hat-sq'd = 0.00347721

Figure 9.10 Normality check for vertical movement of the Grapevine Dam 20%compost Treated Soil

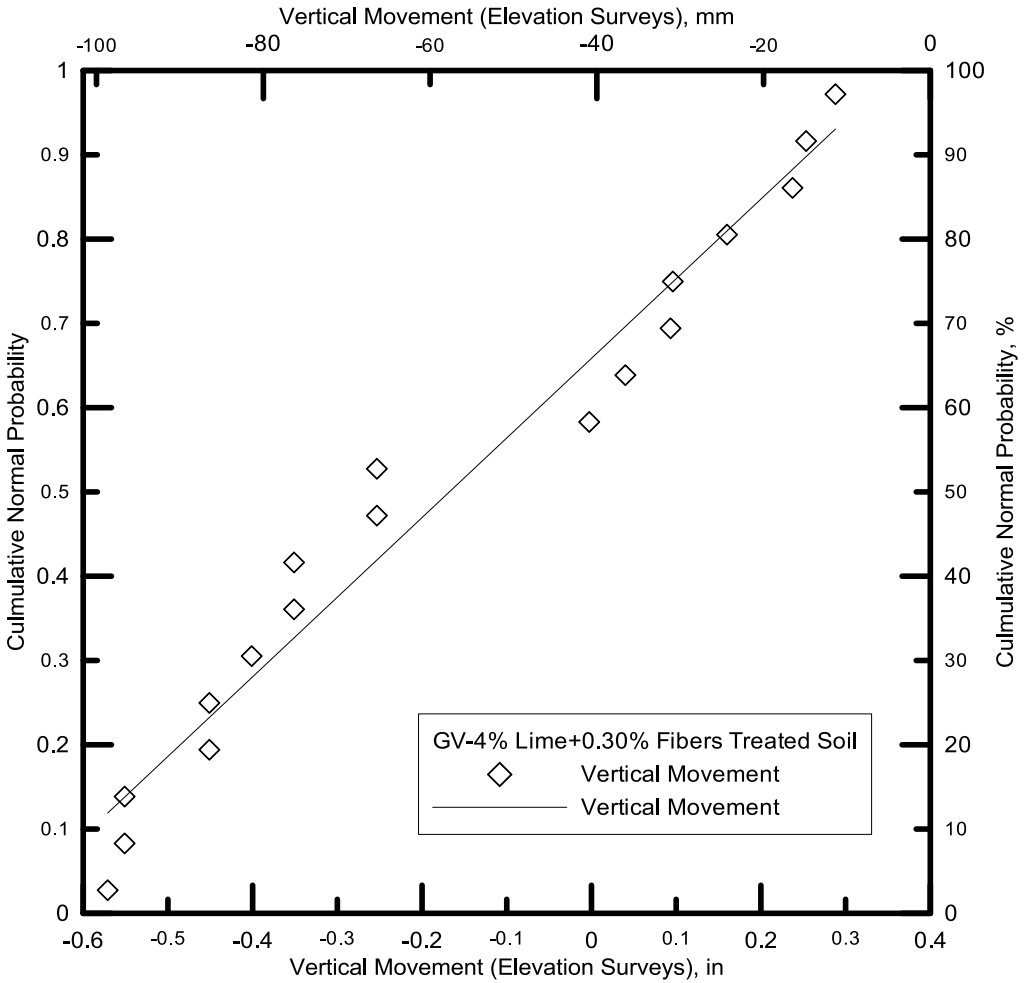

Fit Results

Vertical Movement
Equation Y = 0.94460535 * X + 0.6584954483
Number of data points used = 18
Average X = -0.16779
Average Y = 0.5
Residual sum of squares = 0.0514478
Regression sum of squares = 1.44392
Coef of determination, R-squared = 0.965595
Residual mean square, sigma-hat-sq'd = 0.00321549

Figure 9.11 Normality check for vertical movement of the Grapevine Dam 4%lime+0.30%fibers Treated Soil

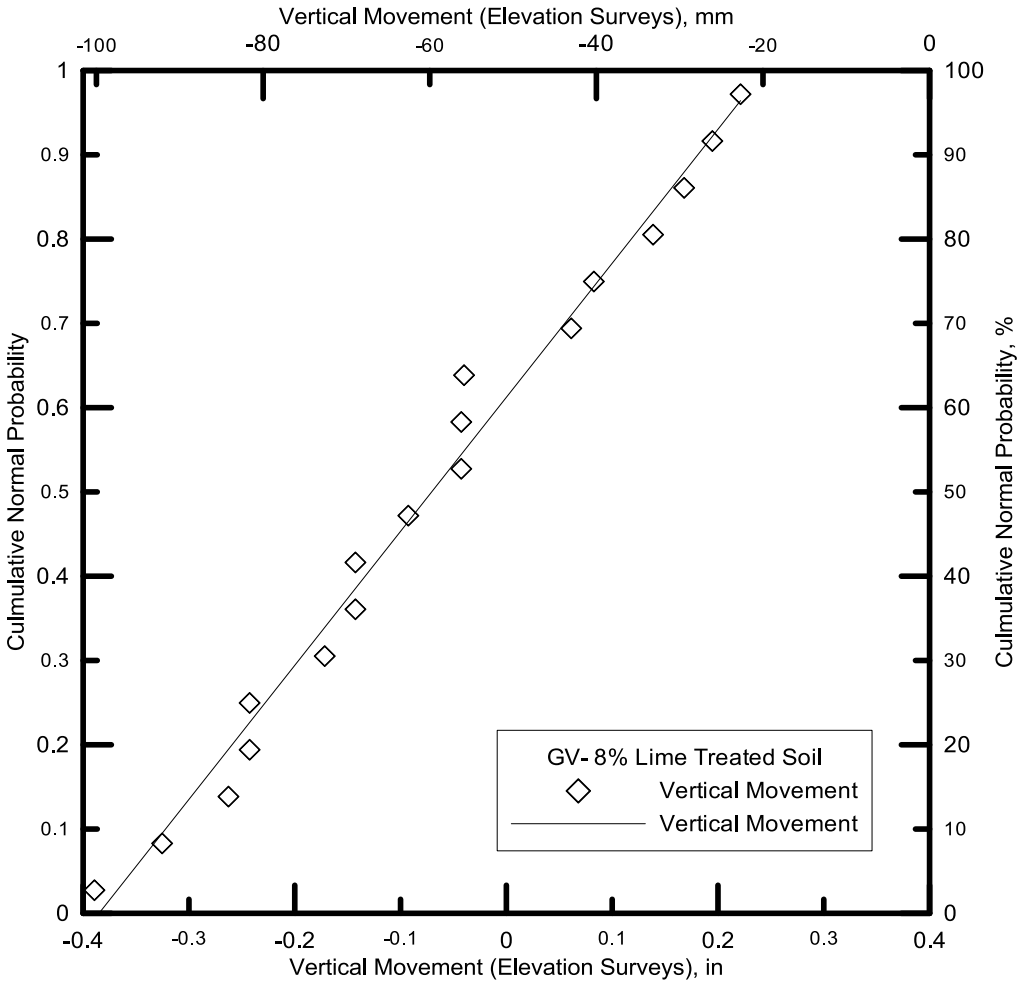

Fit Results

Vertical Movement
Equation Y = 1.590205965 * X + 0.6122862101
Number of data points used = 18
Average X = -0.0706111
Average Y = 0.5
Residual sum of squares = 0.0201451
Regression sum of squares = 1.47523
Coef of determination, R-squared = 0.986528
Residual mean square, sigma-hat-sq'd = 0.00125907

Figure 9.12 Normality check for vertical movement of the Grapevine Dam 8%lime Treated Soil

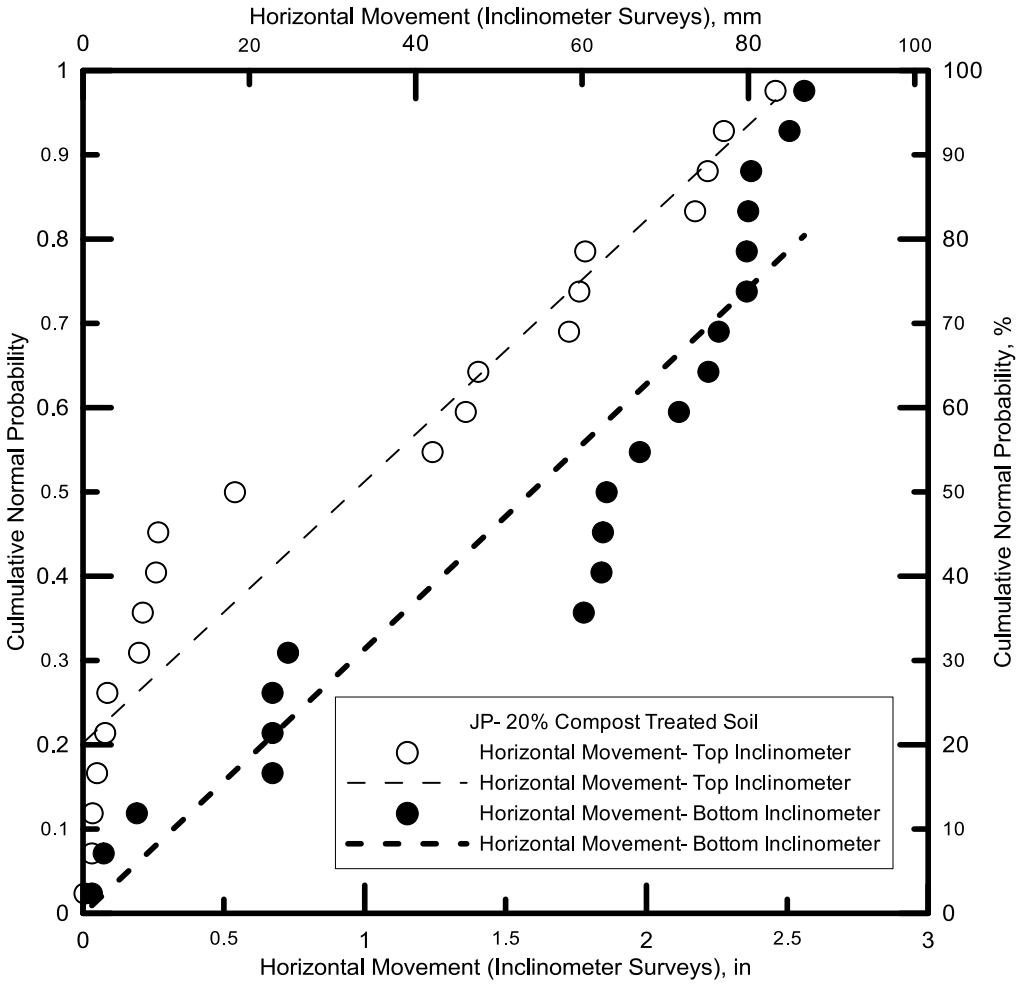

Fit Results

Horizontal Movement- Top Inclinometer
Equation Y = 0.3102883357 * X + 0.202166519
Number of data points used = 21
Average X = 0.95986
Average Y = 0.5
Residual sum of squares = 0.142875
Regression sum of squares = 1.60316
Coef of determination, R-squared = 0.918171
Residual mean square, sigma-hat-sq'd = 0.00751975

Fit Results

Horizontal Movement- Bottom Inclinometer
Equation Y = 0.7845583639 * X + 0.03179476344
Number of data points used = 21
Average X = 0.596776
Average Y = 0.5
Residual sum of squares = 0.0495131
Regression sum of squares = 1.69652
Coef of determination, R-squared = 0.971642
Residual mean square, sigma-hat-sq'd = 0.00260595

Figure 9.13 Normality check for horizontal movement of the Joe Pool Dam 20%compost Treated Soil

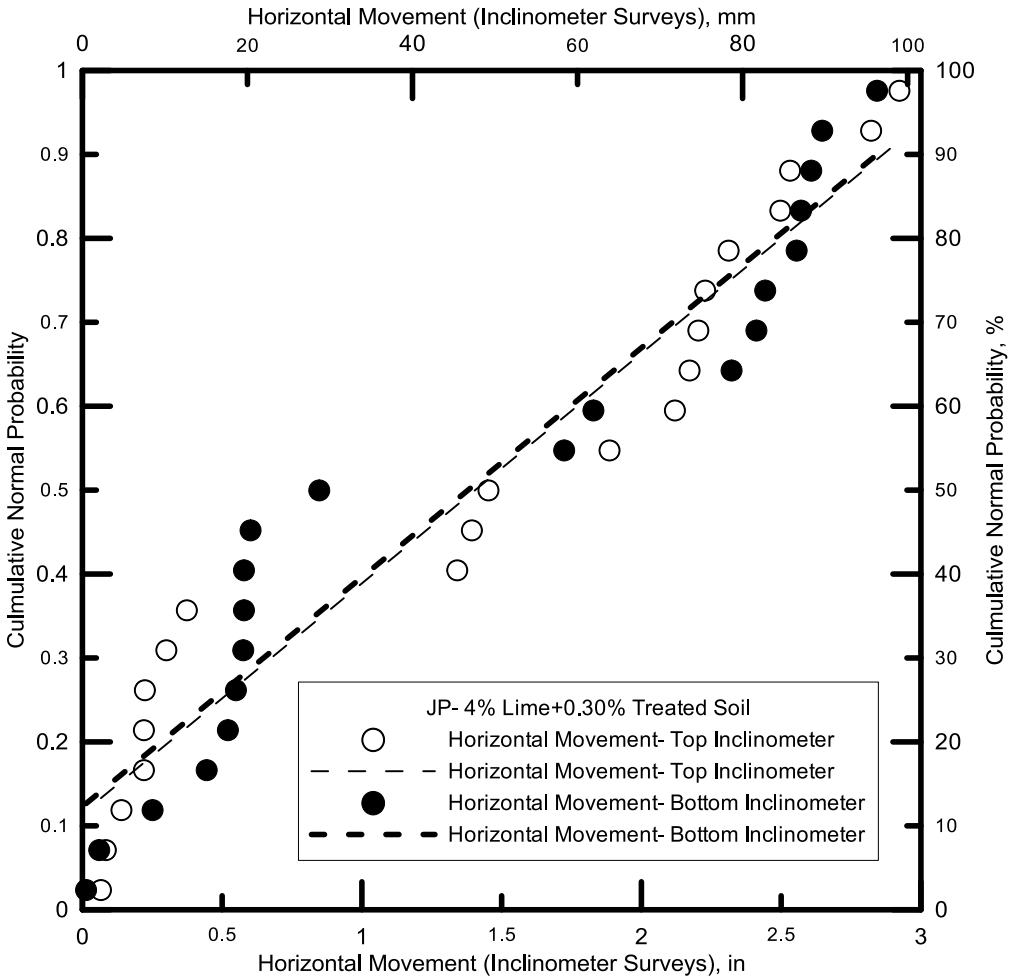

Fit Results

Horizontal Movement- Top Inclinometer
Equation Y = 0.2740857243 * X + 0.1148304723
Number of data points used = 21
Average X = 1.40529
Average Y = 0.5
Residual sum of squares = 0.10252
Regression sum of squares = 1.64351
Coef of determination, R-squared = 0.941284
Residual mean square, sigma-hat-sq'd = 0.0053958

Fit Results

Horizontal Movement- Bottom Inclinometer
Equation Y = 0.7845583639 * X + 0.03179476344
Number of data points used = 21
Average X = 0.596776
Average Y = 0.5
Residual sum of squares = 0.0495131
Regression sum of squares = 1.69652
Coef of determination, R-squared = 0.971642
Residual mean square, sigma-hat-sq'd = 0.00260595

Figure 9.14 Normality check for horizontal movement of the Joe Pool Dam 4%lime+0.30%fibers Treated Soil

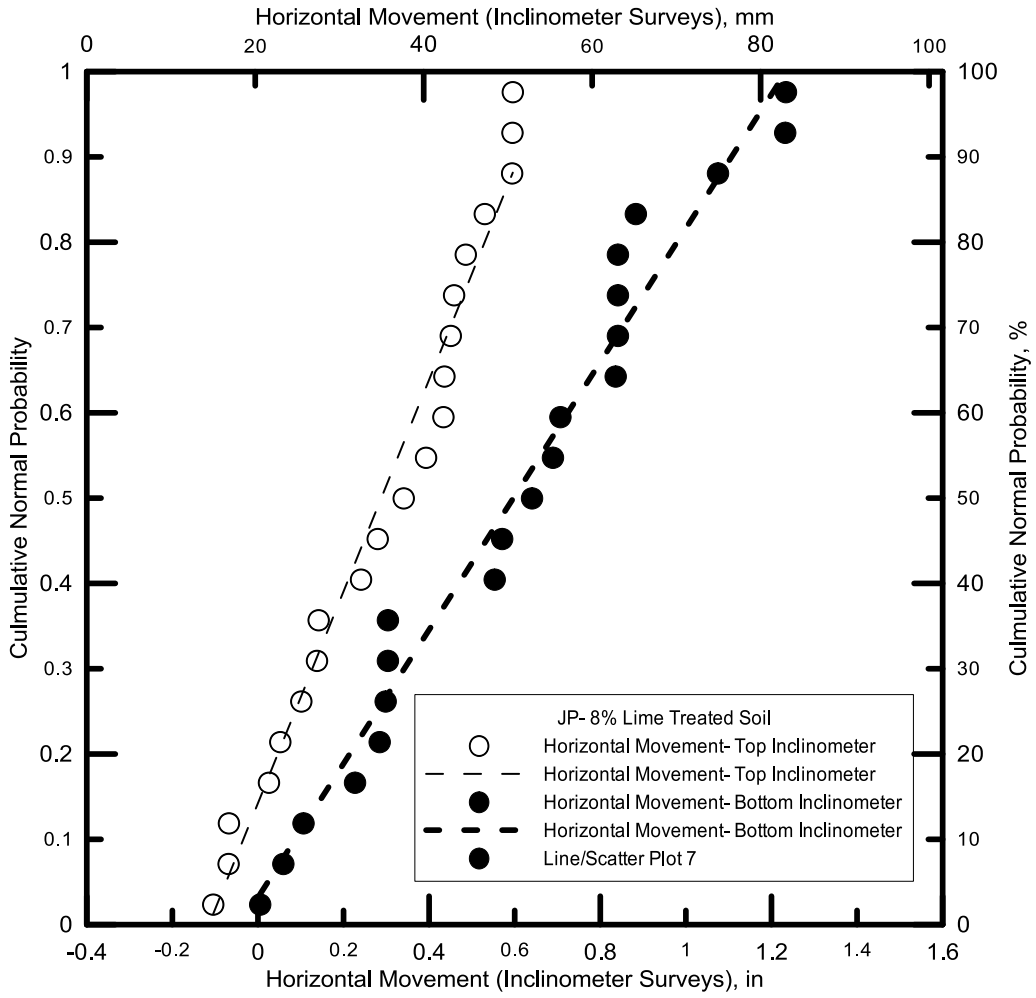

Fit Results

Horizontal Movement- Top Inclinometer
Equation Y = 1.241215115 * X + 0.1423789265
Number of data points used = 21
Average X = 0.288122
Average Y = 0.5
Residual sum of squares = 0.043162
Regression sum of squares = 1.70287
Coef of determination, R-squared = 0.97528
Residual mean square, sigma-hat-sq'd = 0.00227168

Fit Results

Horizontal Movement- Bottom Inclinometer
Equation Y = 0.7845583639 * X + 0.03179476344
Number of data points used = 21
Average X = 0.596776
Average Y = 0.5
Residual sum of squares = 0.0495131
Regression sum of squares = 1.69652
Coef of determination, R-squared = 0.971642
Residual mean square, sigma-hat-sq'd = 0.00260595

Figure 9.15 Normality check for horizontal movement of the Joe Pool Dam 8%lime Treated Soil

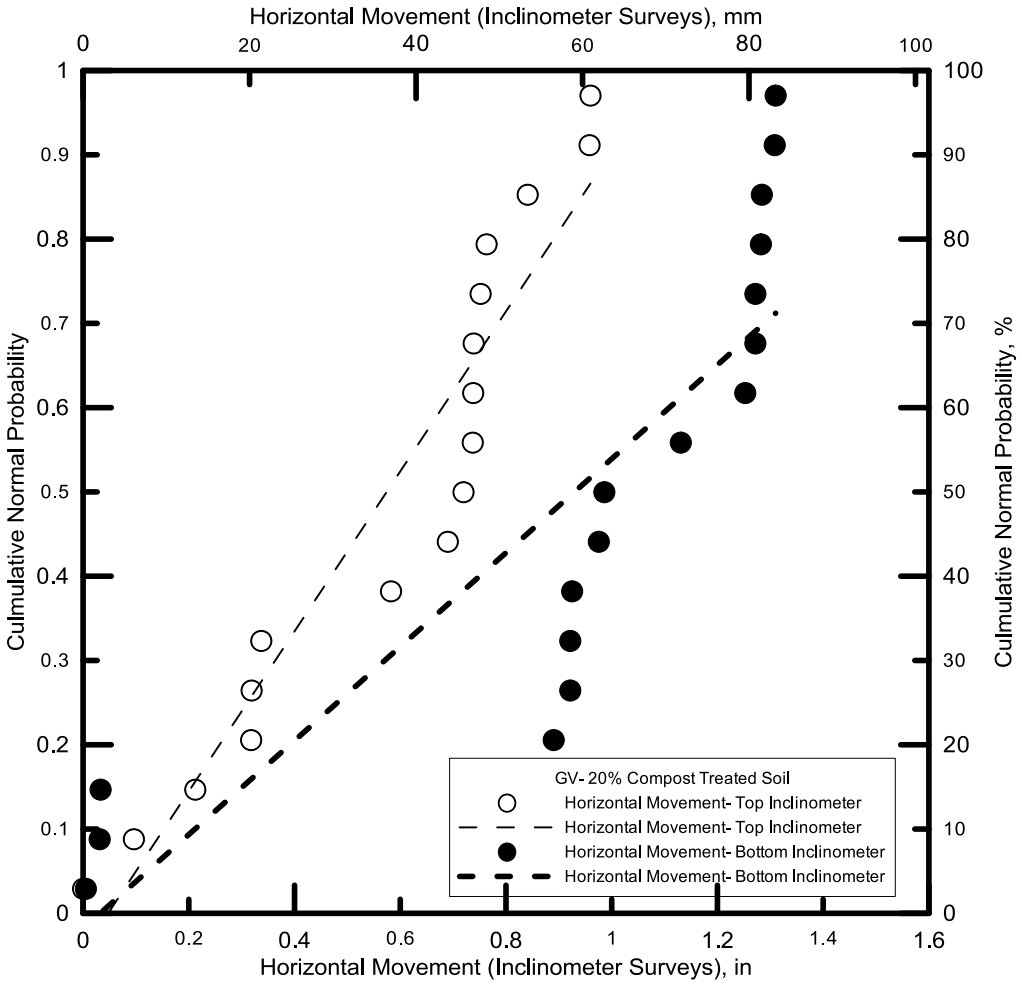

Fit Results

Horizontal Movement- Top Inclinometer
Equation Y = 0.9489753089 * X - 0.04495997957
Number of data points used = 17
Average X = 0.574261
Average Y = 0.5
Residual sum of squares = 0.127369
Regression sum of squares = 1.2844
Coef of determination, R-squared = 0.90978
Residual mean square, sigma-hat-sq'd = 0.00849129

Fit Results

Horizontal Movement- Bottom Inclinometer
Equation Y = 4.344743174 * X - 0.08273349321
Number of data points used = 17
Average X = 0.134124
Average Y = 0.5
Residual sum of squares = 0.140645
Regression sum of squares = 1.27112
Coef of determination, R-squared = 0.900376
Residual mean square, sigma-hat-sq'd = 0.00937635

Figure 9.16 Normality check for horizontal movement of the Grapevine Dam 20%compost Treated Soil

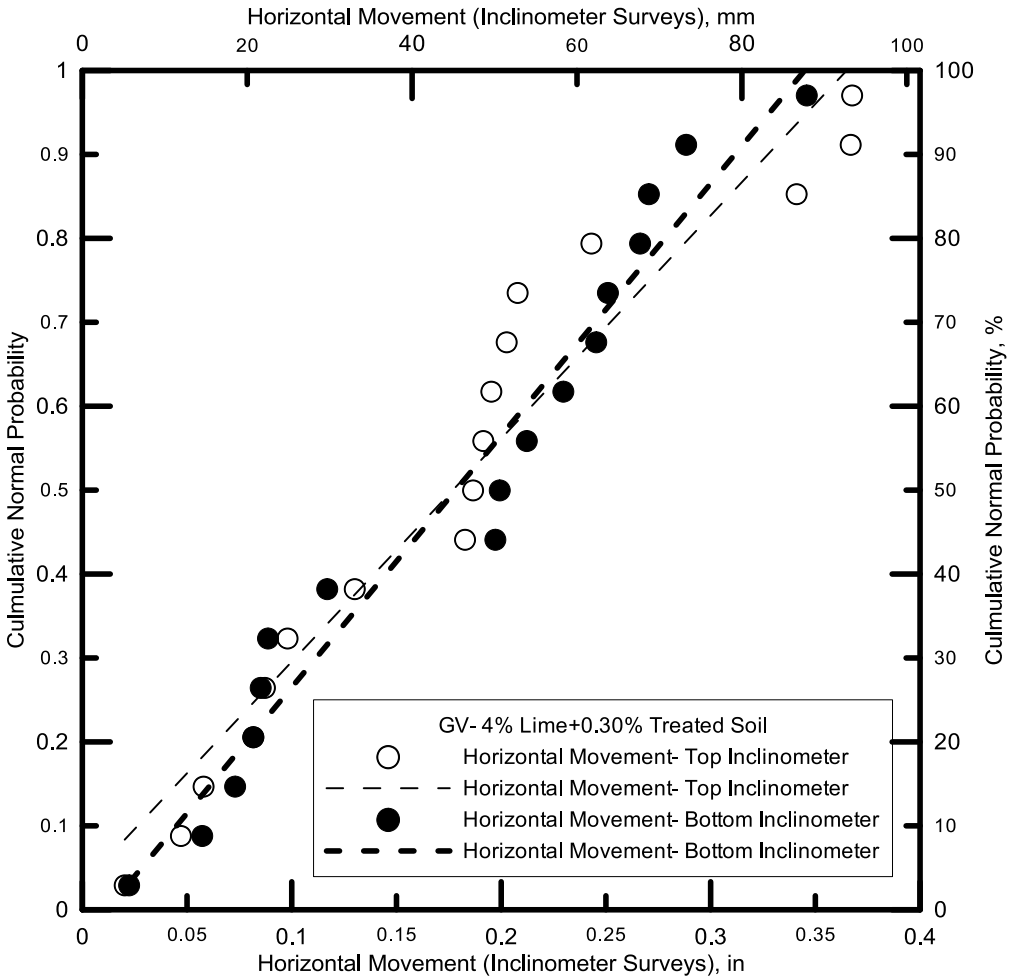

Fit Results

Horizontal Movement- Top Inclinometer
Equation Y = 2.658439088 * X + 0.02974572537
Number of data points used = 17
Average X = 0.176891
Average Y = 0.5
Residual sum of squares = 0.0889121
Regression sum of squares = 1.32285
Coef of determination, R-squared = 0.937021
Residual mean square, sigma-hat-sq'd = 0.00592747

Fit Results

Horizontal Movement- Bottom Inclinometer
Equation Y = 3.001086685 * X - 0.03502588416
Number of data points used = 17
Average X = 0.178277
Average Y = 0.5
Residual sum of squares = 0.0545132
Regression sum of squares = 1.35725
Coef of determination, R-squared = 0.961387
Residual mean square, sigma-hat-sq'd = 0.00363421

Figure 9.17 Normality check for horizontal movement of the Grapevine Dam 4%lime+0.30%fibers Treated Soil

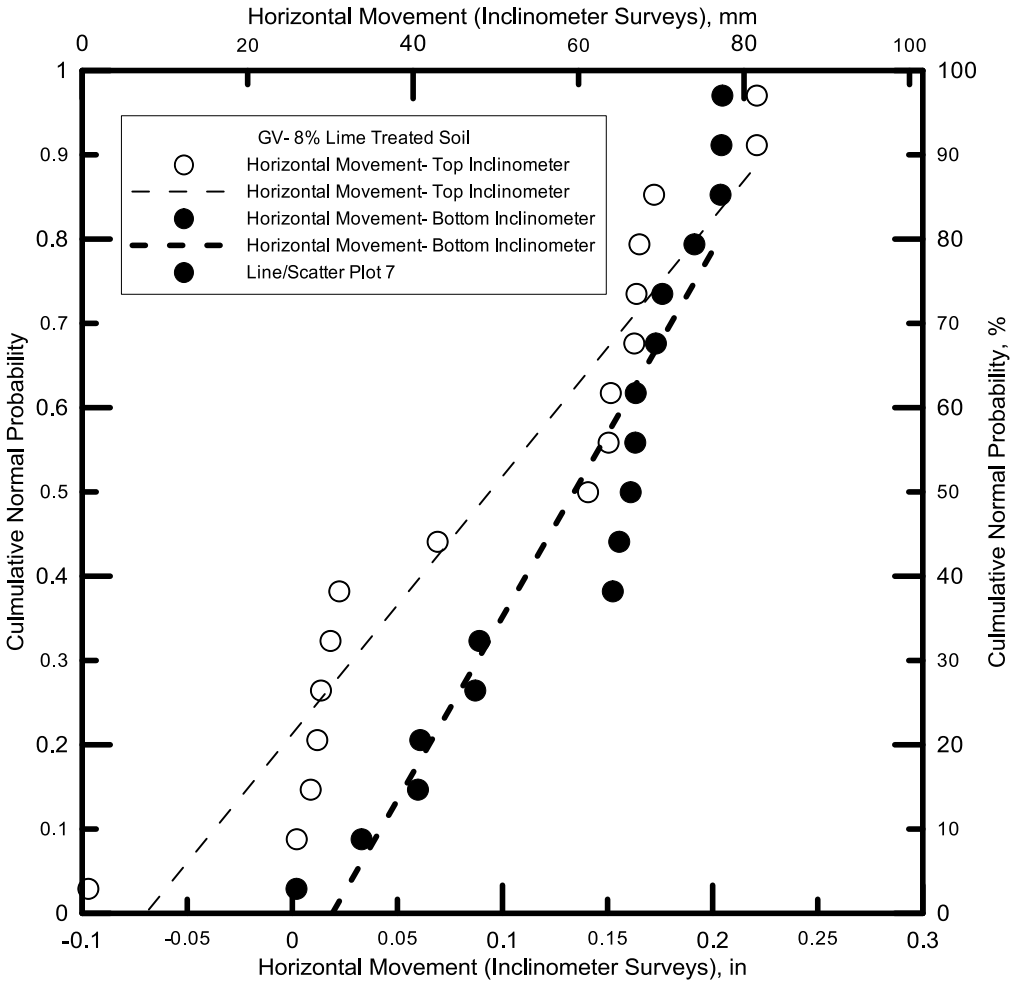

Fit Results

Horizontal Movement- Top Inclinometer
Equation Y = 3.053979289 * X + 0.2130308239
Number of data points used = 17
Average X = 0.0939657
Average Y = 0.5
Residual sum of squares = 0.118678
Regression sum of squares = 1.29309
Coef of determination, R-squared = 0.915936
Residual mean square, sigma-hat-sq'd = 0.0079119

Fit Results

Horizontal Movement- Bottom Inclinometer
Equation Y = 4.344743174 * X - 0.08273349321
Number of data points used = 17
Average X = 0.134124
Average Y = 0.5
Residual sum of squares = 0.140645
Regression sum of squares = 1.27112
Coef of determination, R-squared = 0.900376
Residual mean square, sigma-hat-sq'd = 0.00937635

Figure 9.18 Normality check for horizontal movement of the Grapevine Dam 8%lime Treated Soil

APPENDIX B

RESULTS OF ANALYTICAL AND RELIABLITY SLOPE MODELING STUDIES

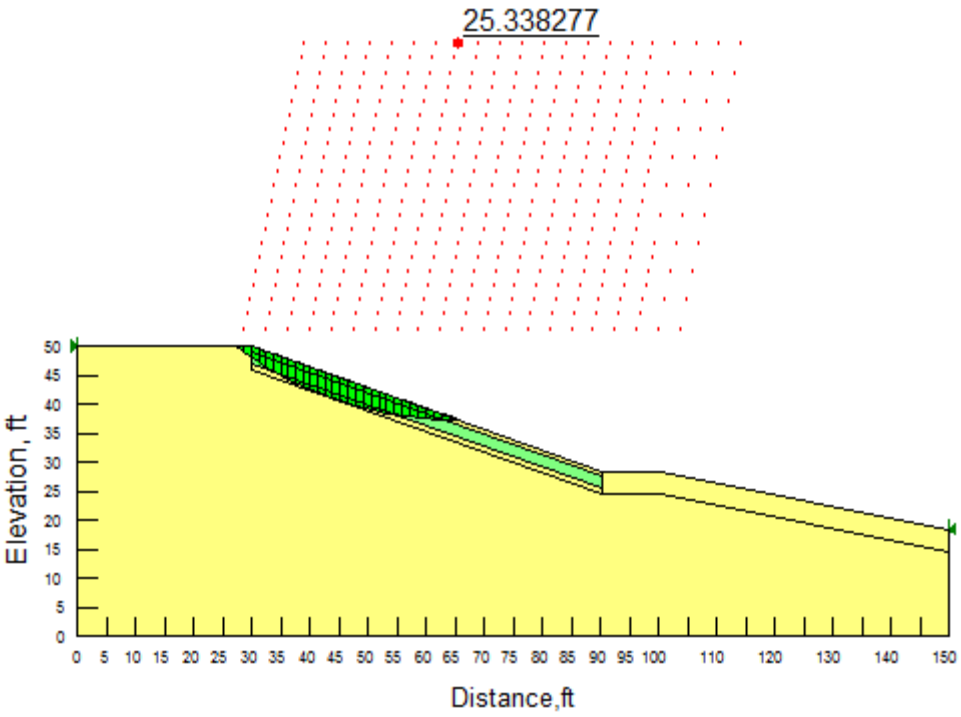

Figure 10.1. Case 1 results for Joe Pool Dam 20%compost treated soil

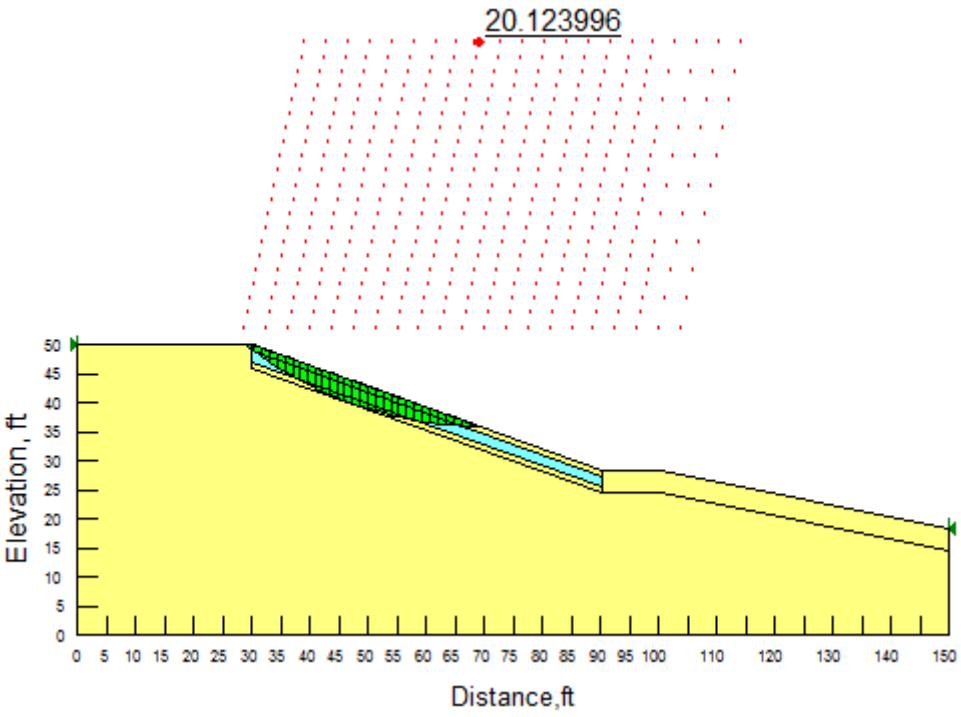

Figure 10.2. Case 1 results for Joe Pool Dam 4%lime+0.30%fibers treated soil

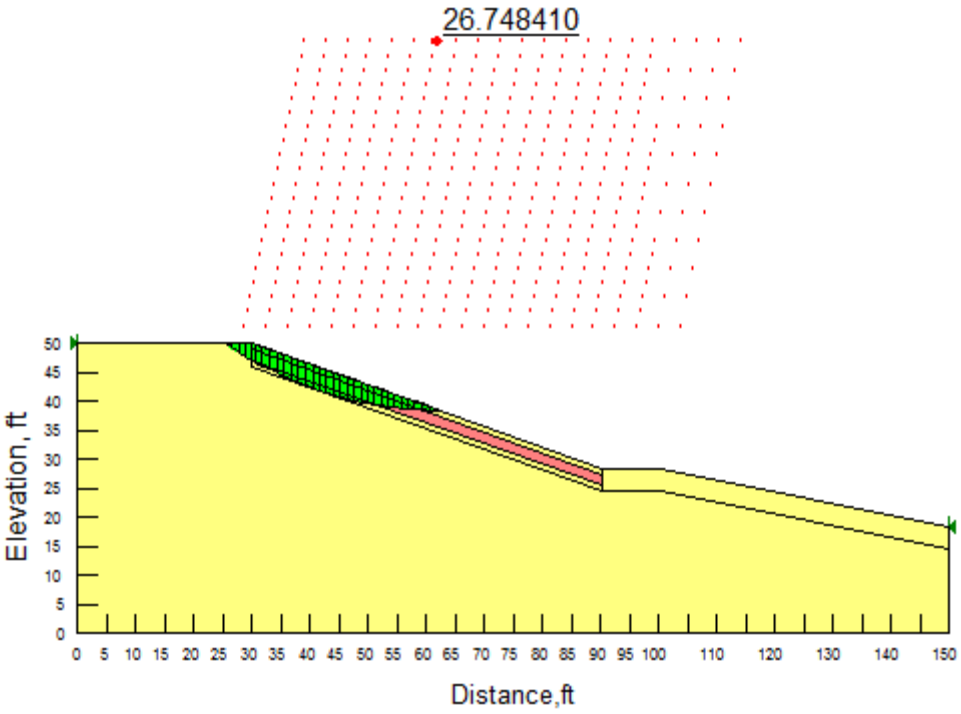

Figure 10.3. Case 1 results for Joe Pool Dam 8% Lime treated soil

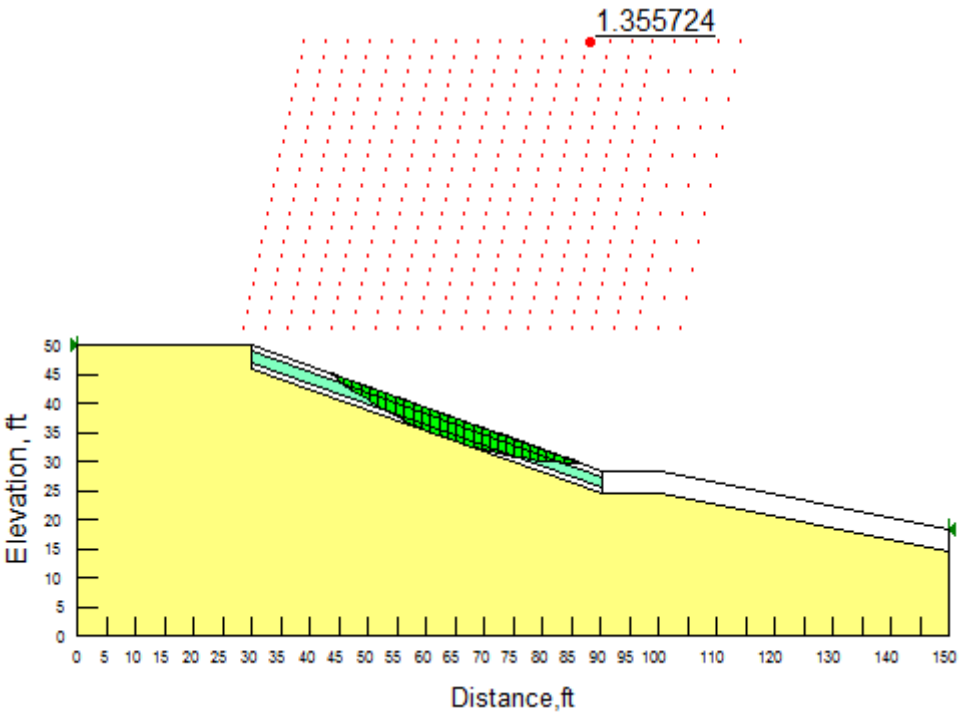

Figure 10.4. Case 2 results for Joe Pool Dam 20%compost treated soil

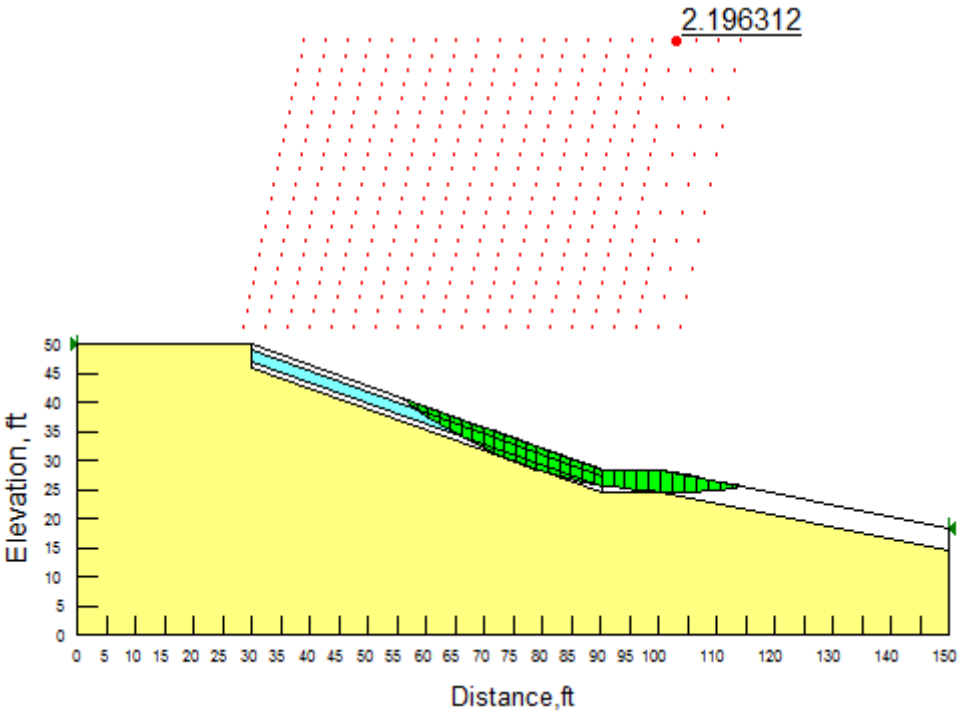

Figure 10.5. Case 2 results for Joe Pool Dam 4%lime+0.30%fibers treated soil

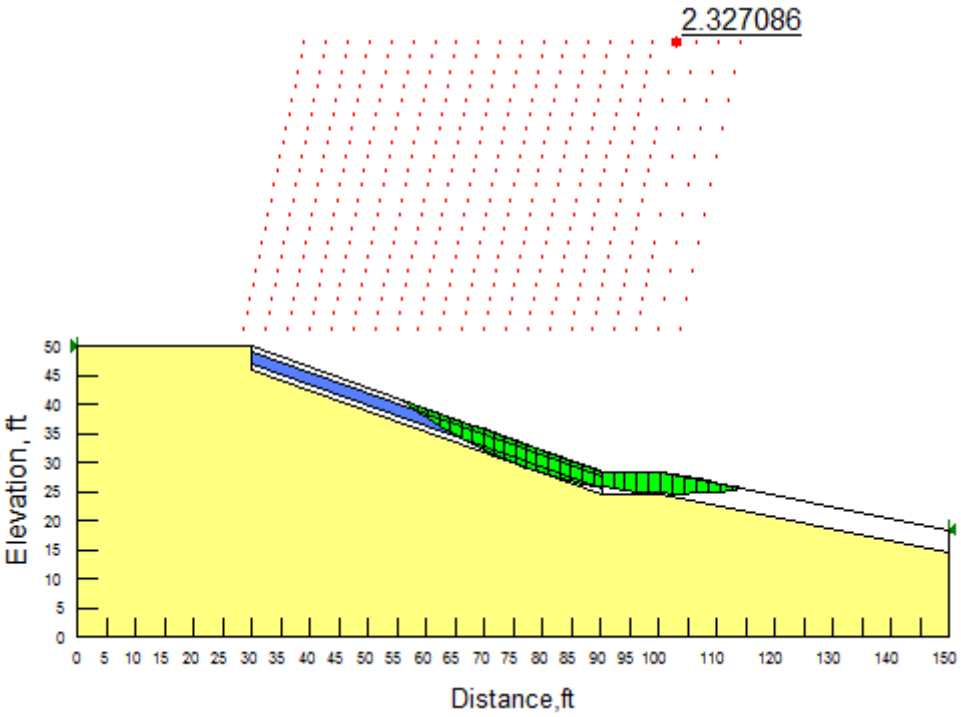

Figure 10.6. Case 2 results for Joe Pool Dam 8%lime treated soil

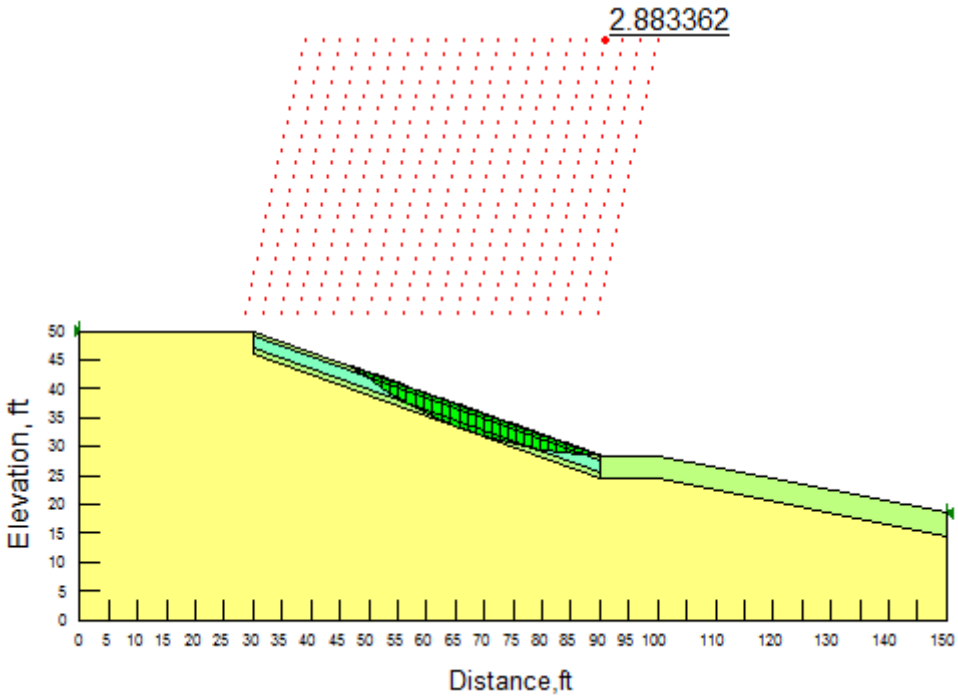

Figure 10.7. Case 3 results for Joe Pool Dam 20%compost treated soil

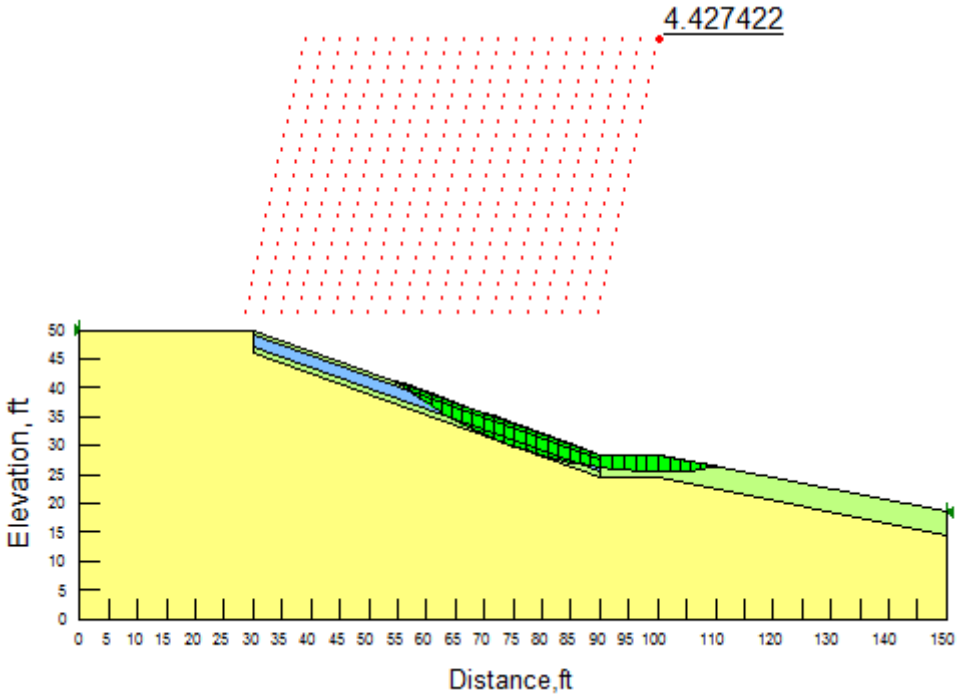

Figure 10.8. Case 3 results for Joe Pool Dam 4%lime+0.30%fibers treated soil

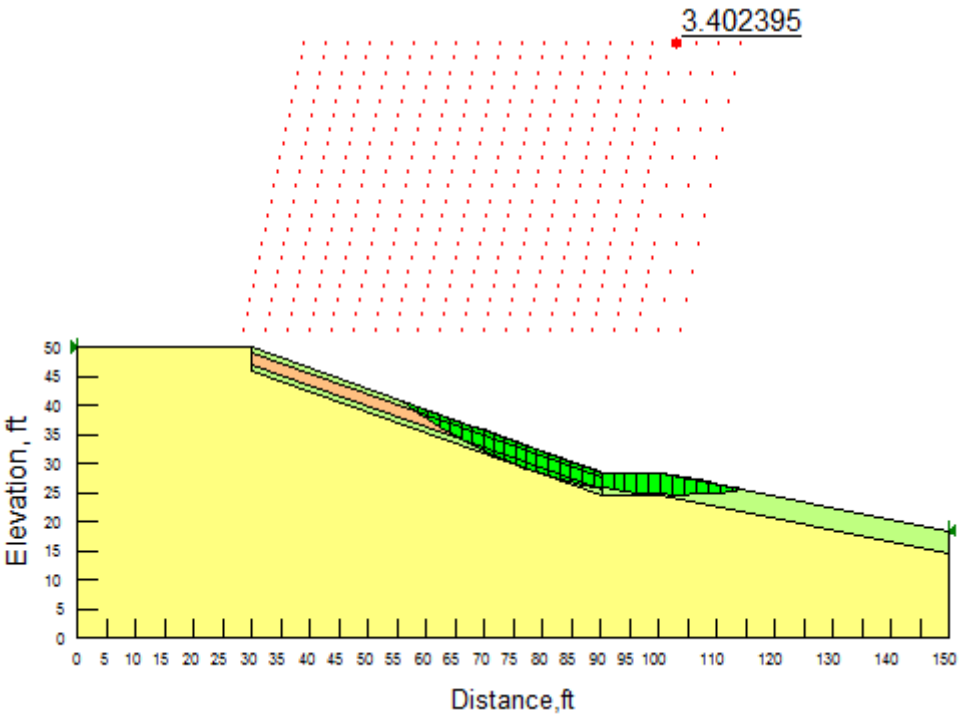

Figure 10.9. Case 3 results for Joe Pool Dam 8%lime treated soil

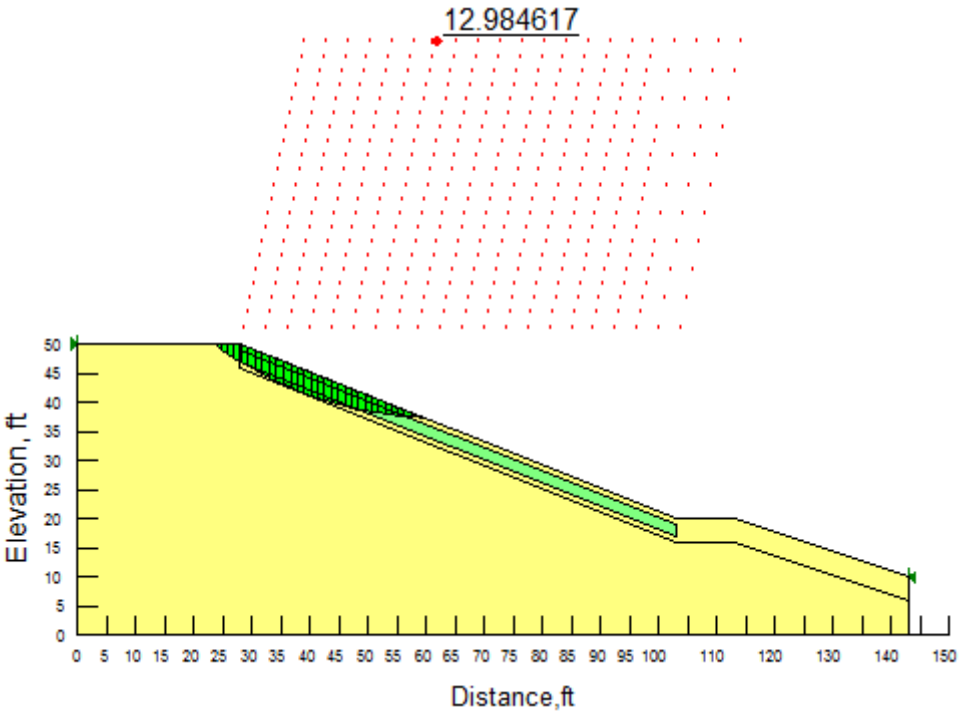

Figure 10.10. Case 1 results for Grapevine Dam 20%compost treated soil

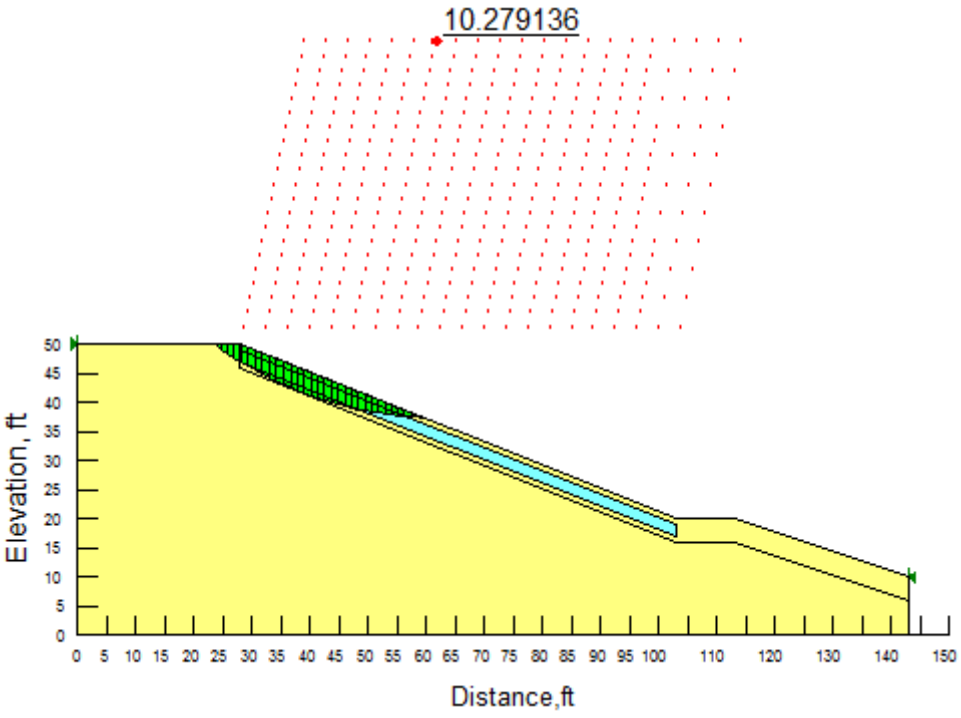

Figure 10.11. Case 1 results for Grapevine Dam 4%lime+0.30%fibers treated soil

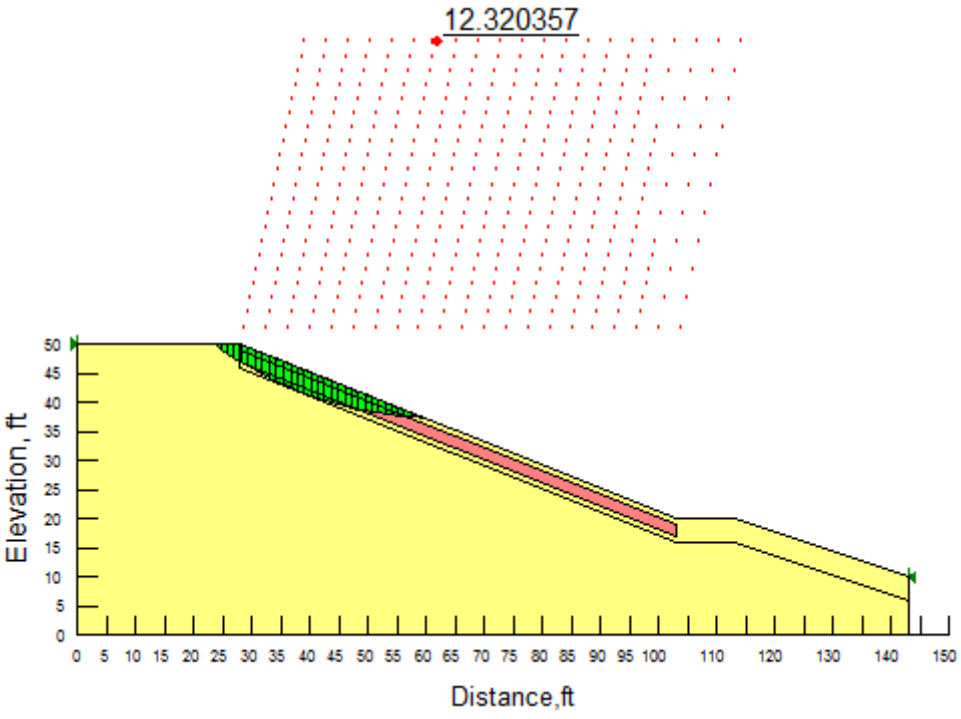

Figure 10.12. Case 1 results for Grapevine Dam 8%lime treated soil

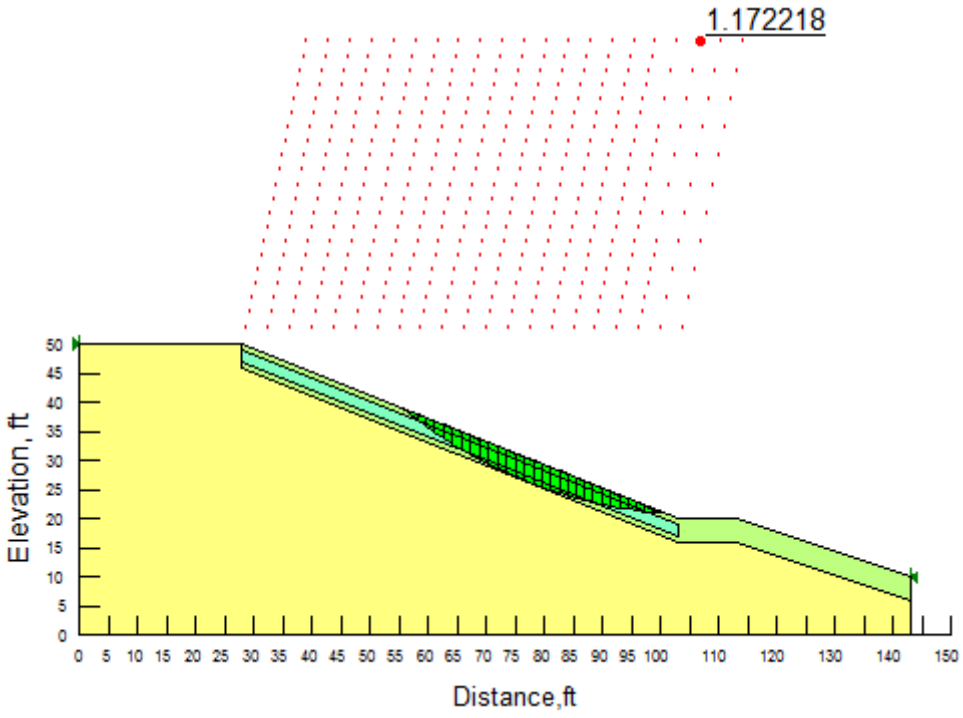

Figure 10.13. Case 2 results for Grapevine Dam 20%compost treated soil

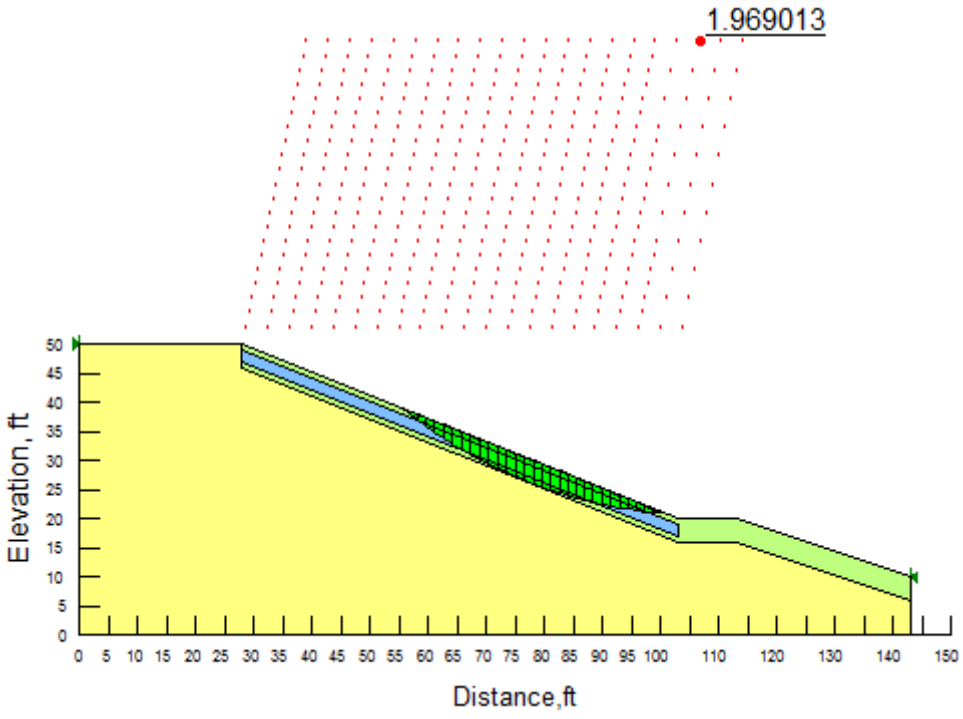

Figure 10.14. Case 2 results for Grapevine Dam 4%lime+0.30%fibers treated soil

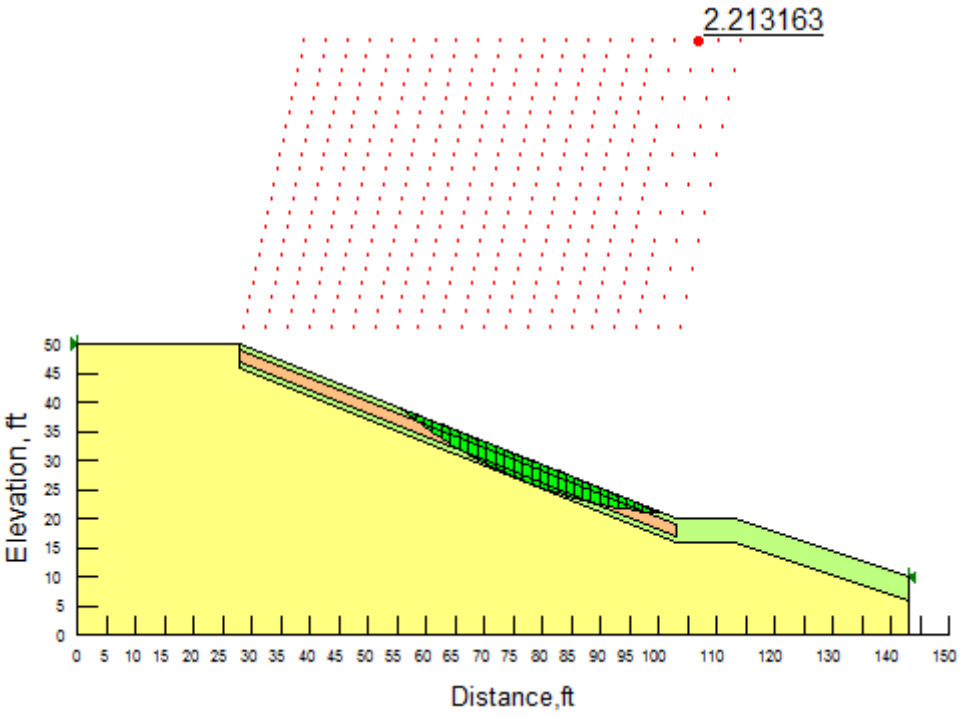

Figure 10.15. Case 2 results for Grapevine Dam 8%lime treated soil

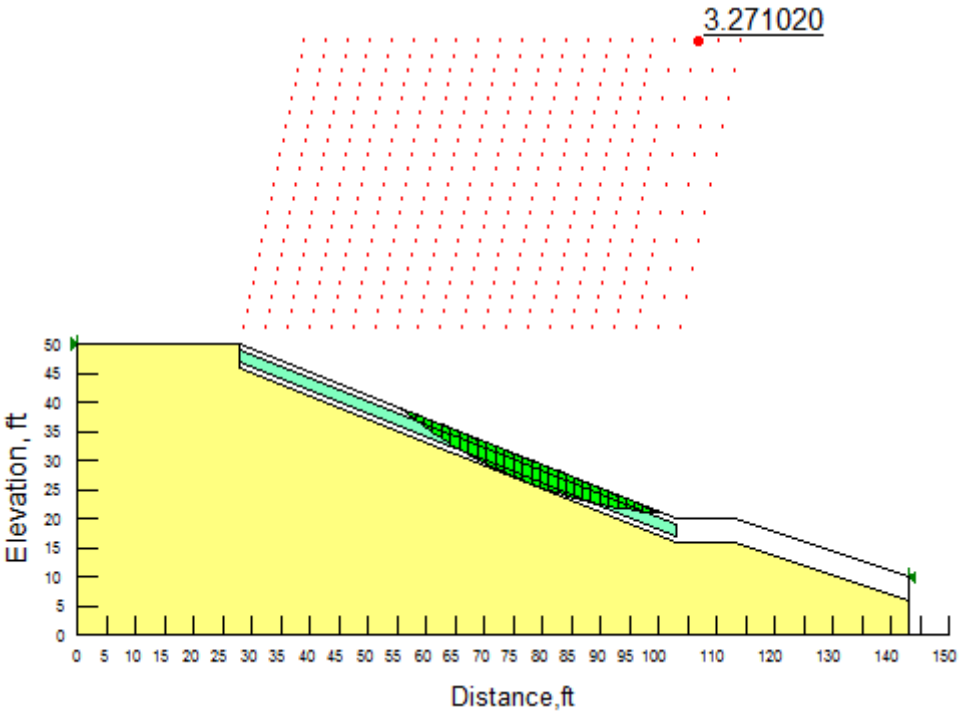

Figure 10.16. Case 3 results for Grapevine Dam 20%compost treated soil

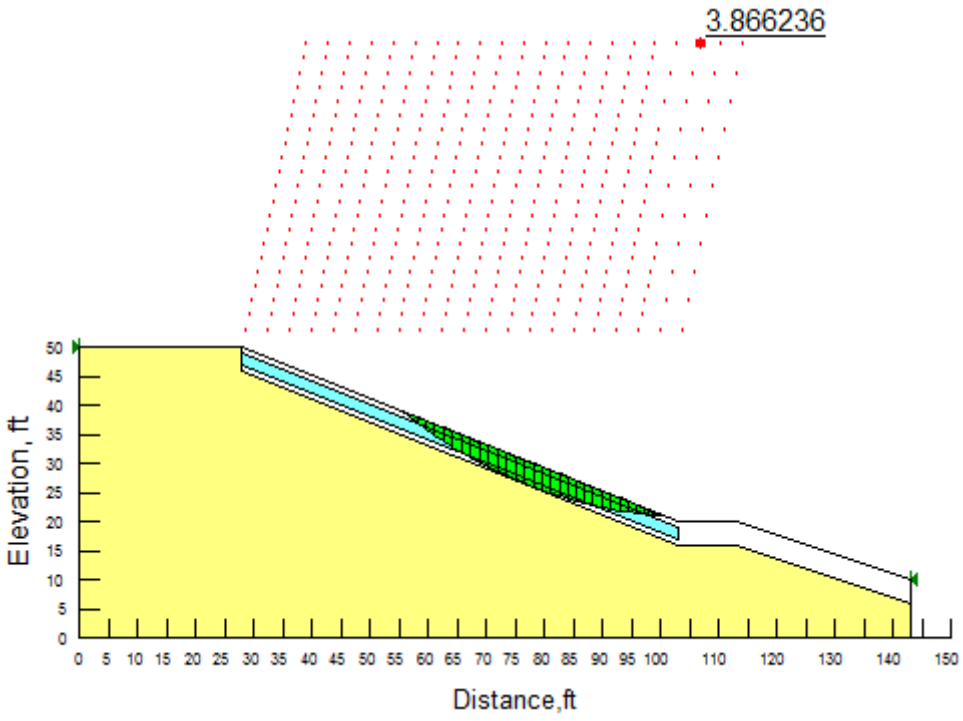

Figure 10.17. Case 3 results for Grapevine Dam 4%lime+0.30%fibers treated soil

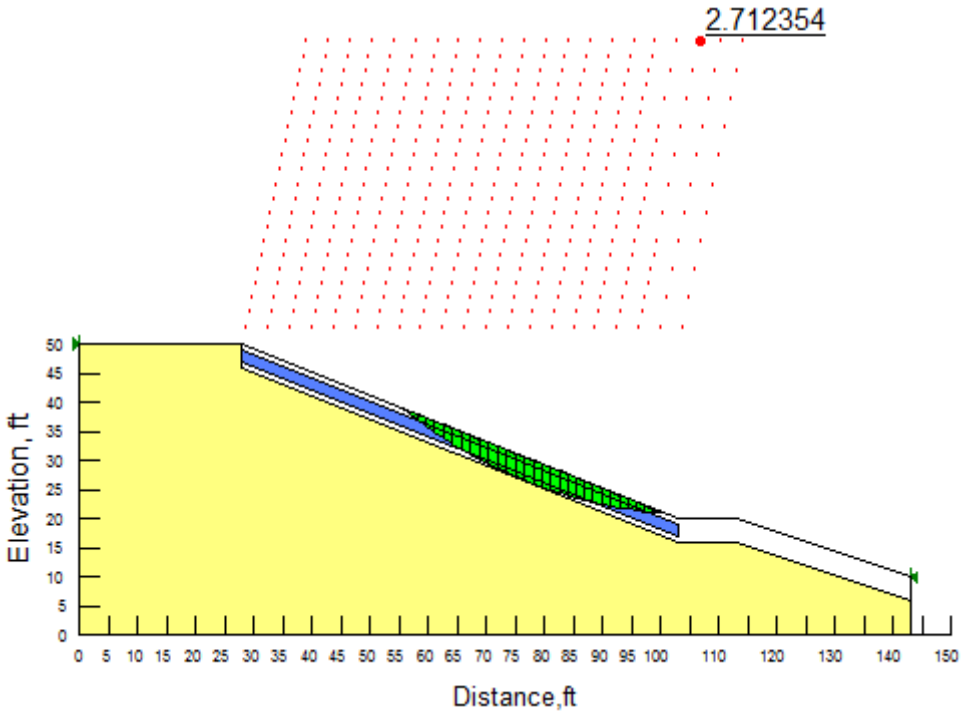

Figure 10.18. Case 3 results for Grapevine Dam 8%lime treated soil

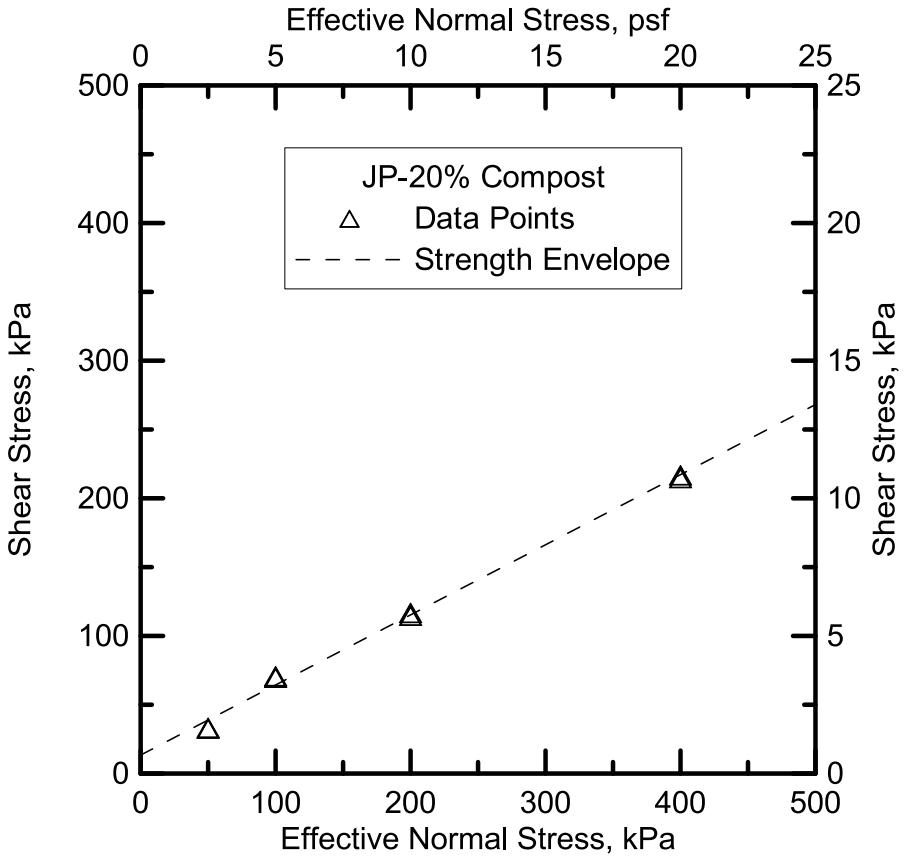

Fit Results

Strength Envelope
Equation Y = 0.5093478261 * X + 13.43478261
Number of data points used = 8
Average X = 187.5
Average Y = 108.938
Residual sum of squares = 147.408
Regression sum of squares = 37293.8
Coef of determination, R-squared = 0.996063
Residual mean square, sigma-hat-sq'd = 24.5679

Figure 10.19. Strength Envelope for Joe Pool Dam 20%compost Treated soil

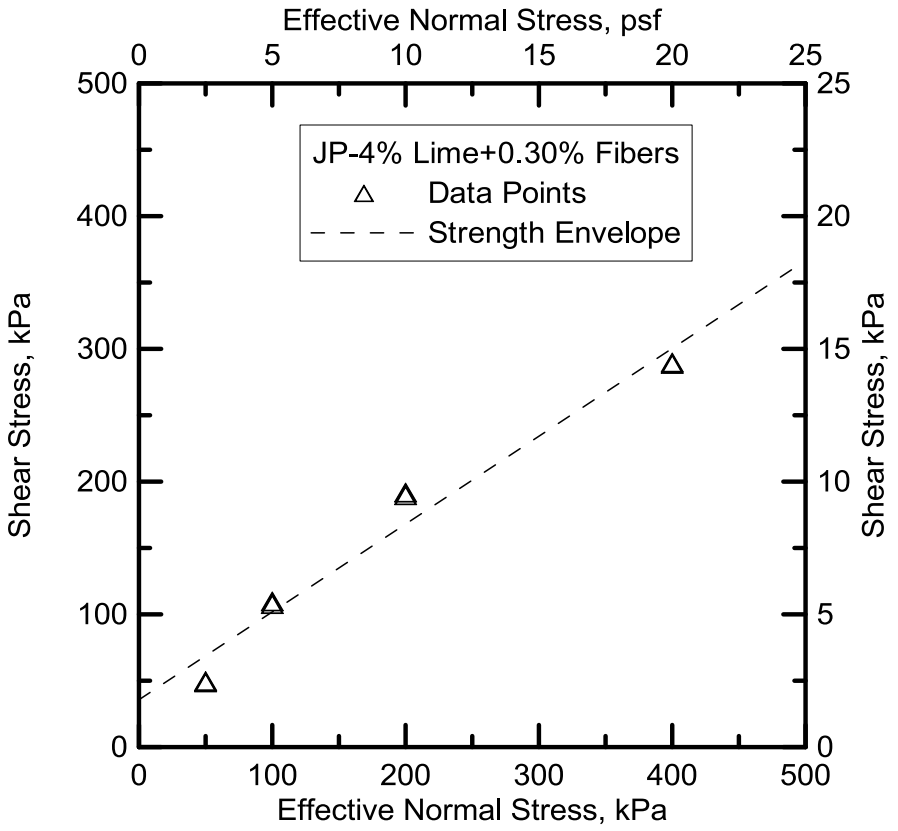

Fit Results

Strength Envelope
Equation Y = 0.6617391304 * X + 35.67391304
Number of data points used = 8
Average X = 187.5
Average Y = 159.75
Residual sum of squares = 2141.57
Regression sum of squares = 62947.9
Coef of determination, R-squared = 0.967098
Residual mean square, sigma-hat-sq'd = 356.928

Figure 10.20. Strength Envelope for Joe Pool Dam 4%lime+0.30%fibers Treated soil

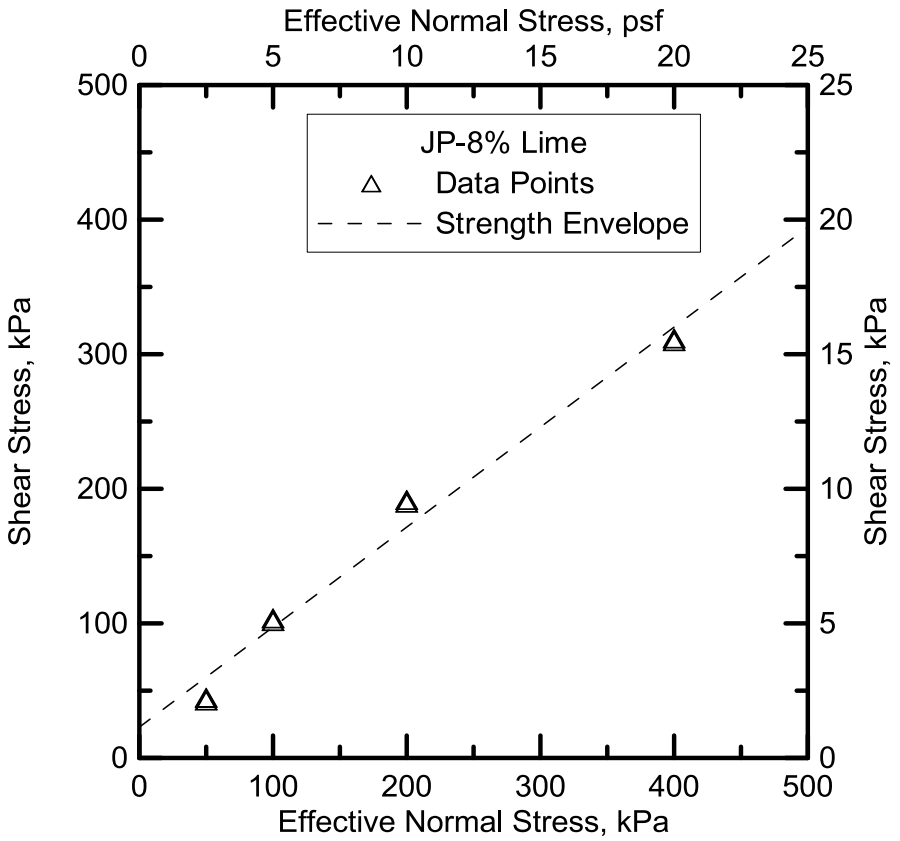

Fit Results

Strength Envelope
Equation Y = 0.7431304348 * X + 22.91304348
Number of data points used = 8
Average X = 187.5
Average Y = 162.25
Residual sum of squares = 1516.59
Regression sum of squares = 79384.9
Coef of determination, R-squared = 0.981254
Residual mean square, sigma-hat-sq'd = 252.765

Figure 10.21. Strength Envelope for Joe Pool Dam 8%lime Treated soil

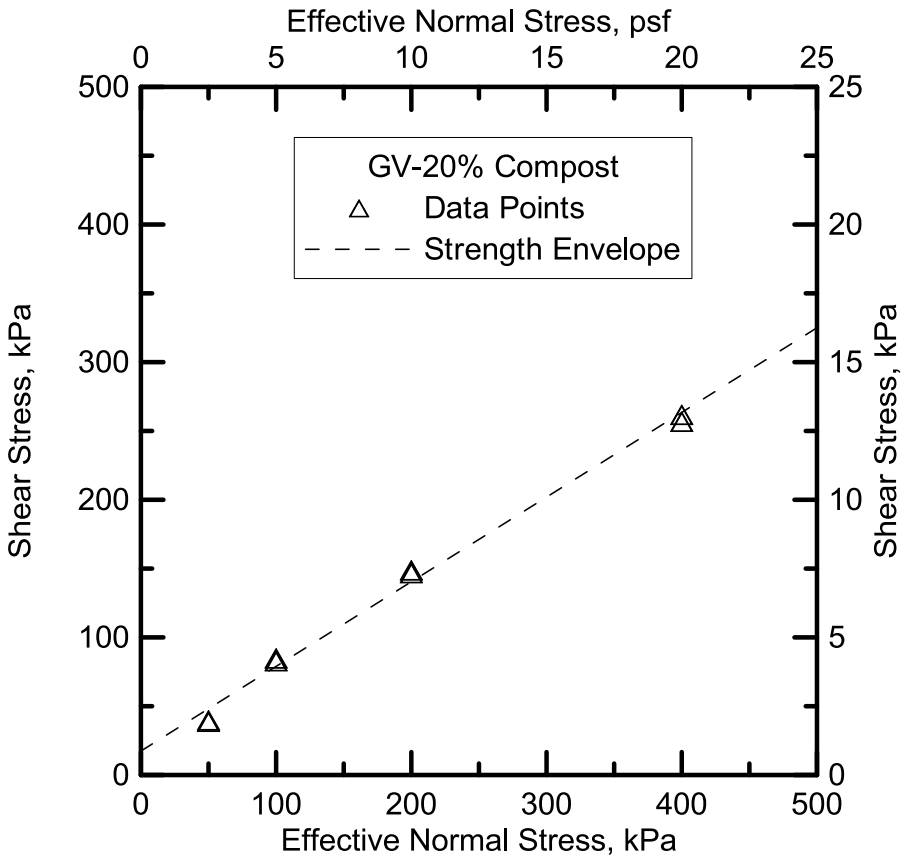

Fit Results

Strength Envelope
Equation Y = 0.6151304348 * X + 17.41304348
Number of data points used = 8
Average X = 187.5
Average Y = 132.75
Residual sum of squares = 364.591
Regression sum of squares = 54392.9
Coef of determination, R-squared = 0.993342
Residual mean square, sigma-hat-sq'd = 60.7652

Figure 10.22. Strength Envelope for Grapevine Dam 20%compost Treated soil

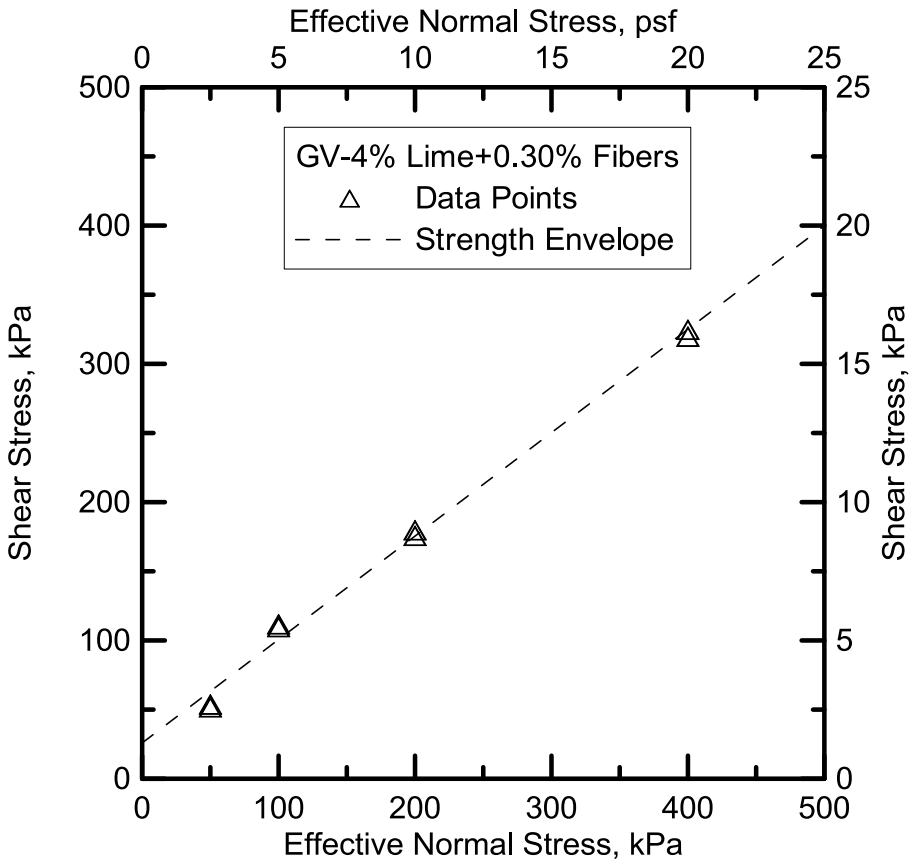

Fit Results

Strength Envelope
Equation Y = 0.7479130435 * X + 25.89130435
Number of data points used = 8
Average X = 187.5
Average Y = 166.125
Residual sum of squares = 474.874
Regression sum of squares = 80410
Coef of determination, R-squared = 0.994129
Residual mean square, sigma-hat-sq'd = 79.1457

Figure 10.23. Strength Envelope for Grapevine Dam 4%lime+0.30%fibers Treated soil

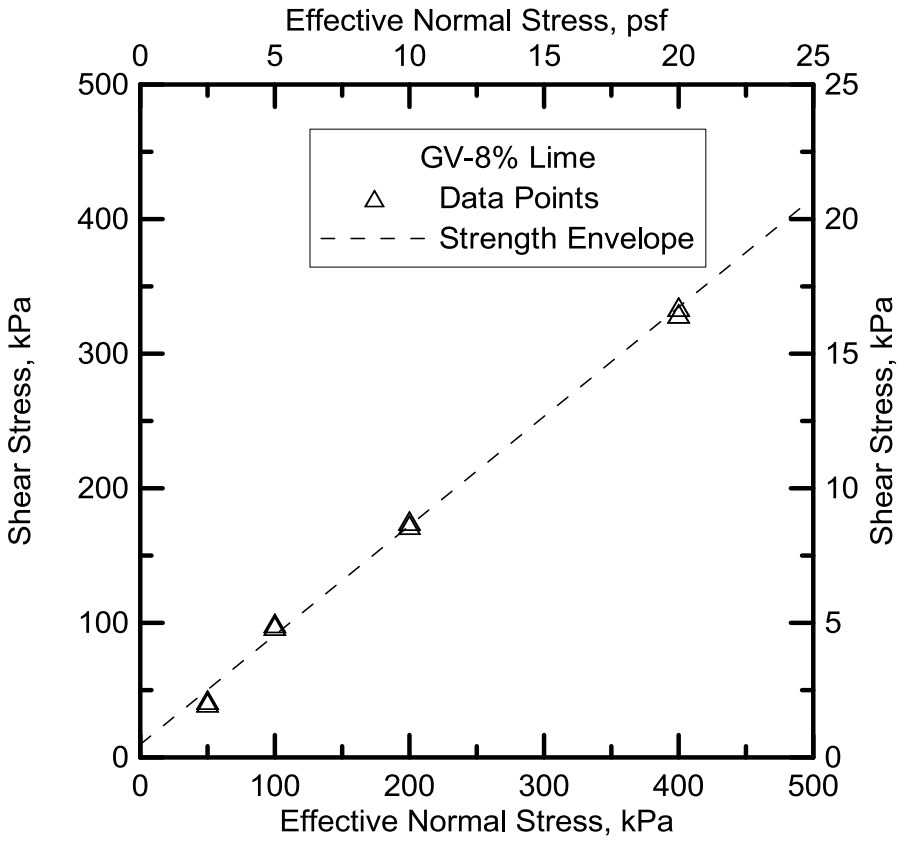

Fit Results

Strength Envelope
Equation Y = 0.8125217391 * X + 9.652173913
Number of data points used = 8
Average X = 187.5
Average Y = 162
Residual sum of squares = 309.461
Regression sum of squares = 94902.5
Coef of determination, R-squared = 0.99675
Residual mean square, sigma-hat-sq'd = 51.5768

Figure 10.24. Strength Envelope for Grapevine Dam 8%lime Treated soil

`

Table 10.1. Results of data interpretation for Joe Pool Dam 20%compost treated soil

Test No.	Effective Normal Stress σ'_{ni} kPa	FSS Shear Stress τ'_{fsi} kPa	FSS cohesion c'_{fsi} kPa	FSS friction angle φ'_{fsi} degree
1	50	33.5	8.03	21.87
2	50	33	7.53	21.37
3	100	70	19.07	29.49
4	100	71	20.07	29.93
5	200	115	13.13	26.92
6	200	117	15.13	27.38
7	400	215	11.26	26.74
8	400	217	13.26	26.97
$\varphi'_{fs} = tan^{-1}(0.5093) = 26.99^o$			$c'_{fs} = 13.43$	

Table 10.2. Results of data interpretation for Joe Pool Dam 4%lime+0.30%fibers treated soil

Test No.	Effective Normal Stress σ'_{ni} kPa	FSS Shear Stress τ'_{fsi} kPa	FSS cohesion c'_{fsi} kPa	FSS friction angle φ'_{fsi} degree
1	50	49	15.91	14.92
2	50	50	16.91	15.99
3	100	108	41.83	35.88
4	100	110	43.83	36.62
5	200	190	57.65	37.65
6	200	192	59.65	38.01
7	400	290	25.30	32.45
8	400	289	24.30	32.35

`

$\varphi'_{fs} = tan^{-1}(0.66173) = 33.49^o$	$c'_{fs} = 35.67$

Table 10.3. Results of data interpretation for Joe Pool Dam 8%lime treated soil

Test No.	Effective Normal Stress σ'_{ni} kPa	FSS Shear Stress τ'_{fsi} kPa	FSS cohesion c'_{fsi} kPa	FSS friction angle φ'_{fsi} degree
1	50	43	5.84	21.89
2	50	45	7.84	23.83
3	100	102	27.69	38.34
4	100	104	29.69	39.03
5	200	190	41.37	39.87
6	200	192	43.37	40.21
7	400	312	14.75	35.85
8	400	310	12.75	35.66
$\varphi'_{fs} = tan^{-1}(0.7431) = 36.61^o$			$c'_{fs} = 22.91$	

Table 10.4. Results of data interpretation for Grapevine Dam 20%compost treated soil

Test No.	Effective Normal Stress σ'_{ni} kPa	FSS Shear Stress τ'_{fsi} kPa	FSS cohesion c'_{fsi} kPa	FSS friction angle φ'_{fsi} degree
1	50	40	9.24	24.31
2	50	39	8.24	23.35
3	100	83	21.49	33.26
4	100	85	23.49	34.05
5	200	147	23.97	32.94

`

6	200	149	25.97	33.34
7	400	257	10.95	30.92
8	400	262	15.95	31.44
$\varphi'_{fs} = tan^{-1}(0.61513) = 31.59^o$			$c'_{fs} = 17.41$	

Table 10.5. Results of data interpretation for Grapevine Dam 4%lime+0.30%fibers treated soil

Test No.	Effective Normal Stress σ'_{ni} kPa	FSS Shear Stress τ'_{fsi} kPa	FSS cohesion c'_{fsi} kPa	FSS friction angle φ'_{fsi} degree
1	50	52	14.60	27.57
2	50	54	16.60	29.34
3	100	110	35.21	40.07
4	100	112	37.21	40.73
5	200	180	30.42	37.62
6	200	176	26.42	36.89
7	400	320	20.83	36.33
8	400	325	25.83	36.79
$\varphi'_{fs} = tan^{-1}(0.747913) = 34.79^o$			$c'_{fs} = 25.89$	

`

Table 10.6. Results of data interpretation for Grapevine Dam 8%lime treated soil

Test No.	Effective Normal Stress σ'_{ni} kPa	FSS Shear Stress τ'_{fsi} kPa	FSS cohesion c'_{fsi} kPa	FSS friction angle φ'_{fsi} degree
1	50	41	0.37	32.08
2	50	43	2.37	33.70
3	100	100	18.75	42.09
4	100	98	16.75	41.46
5	200	173	10.50	39.24
6	200	176	13.50	39.75
7	400	335	9.99	39.12
8	400	330	4.99	38.69
$\varphi'_{fs} = tan^{-1}(0.8125) = 39.09^o$			$c'_{fs} = 9.65$	

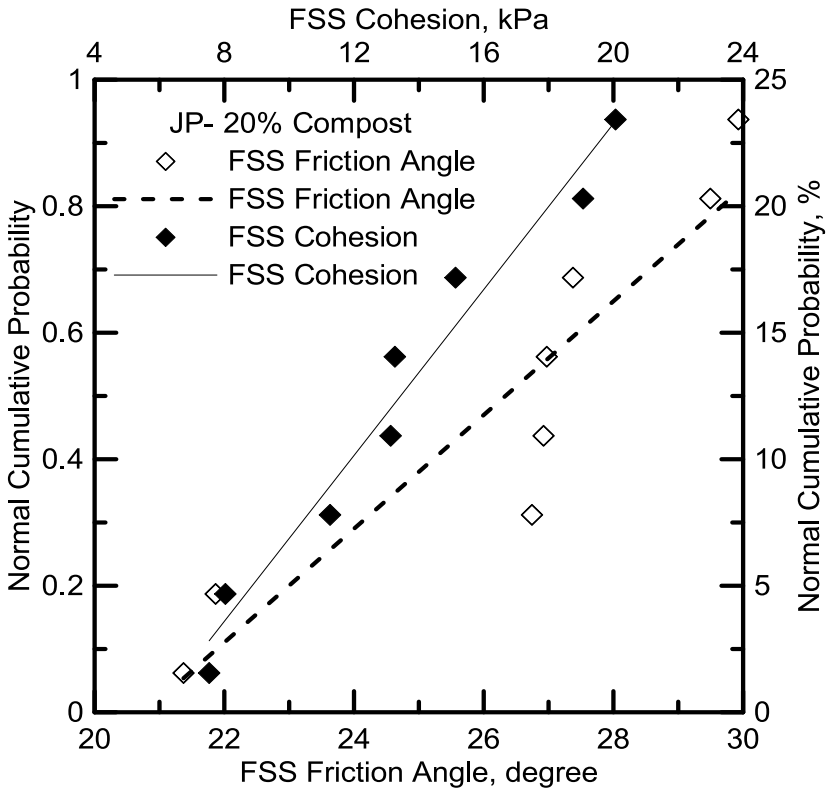

Fit Results

FSS Friction Angle
Equation Y = 0.08990431615 * X - 1.867555831
Number of data points used = 8
Average X = 26.3342
Average Y = 0.5
Residual sum of squares = 0.0944308
Regression sum of squares = 0.561819
Coef of determination, R-squared = 0.856105
Residual mean square, sigma-hat-sq'd = 0.0157385

Fit Results

FSS Cohesion
Equation Y = 0.06556243778 * X - 0.3808170989
Number of data points used = 8
Average X = 13.4348
Average Y = 0.5
Residual sum of squares = 0.0226282
Regression sum of squares = 0.633622
Coef of determination, R-squared = 0.965519
Residual mean square, sigma-hat-sq'd = 0.00377137

Figure 10.25. Normality check for FSS friction angle and FSS cohesion of Joe Pool Dam 20%compost Treated soil

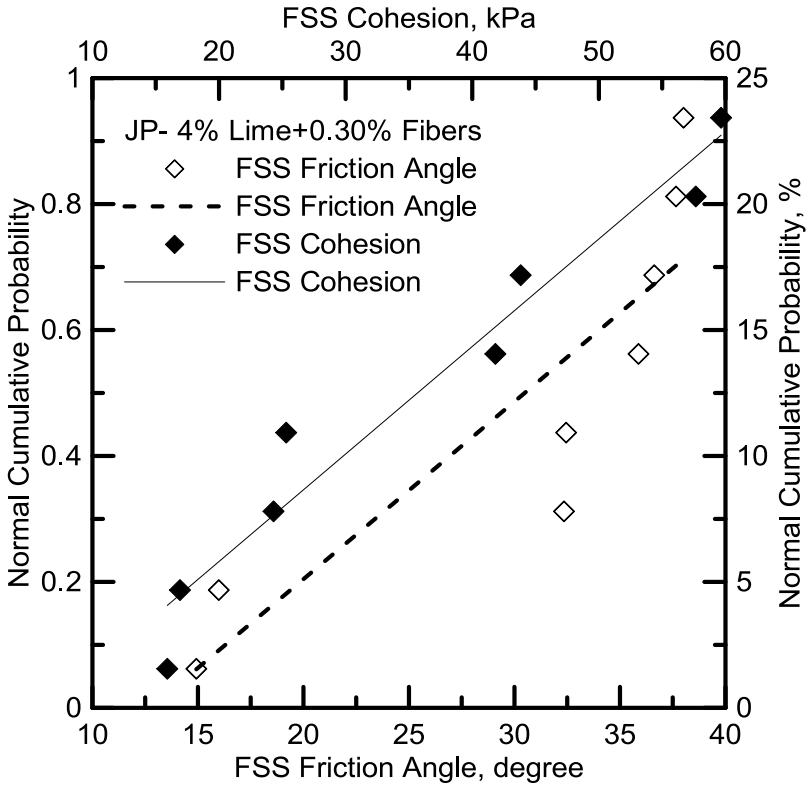

Fit Results

FSS Friction Angle
Equation Y = 0.02819506172 * X - 0.3595025112
Number of data points used = 8
Average X = 30.4842
Average Y = 0.5
Residual sum of squares = 0.151898
Regression sum of squares = 0.504352
Coef of determination, R-squared = 0.768537
Residual mean square, sigma-hat-sq'd = 0.0253163

Fit Results

FSS Cohesion
Equation Y = 0.02036317141 * X + 0.03341776803
Number of data points used = 8
Average X = 22.913
Average Y = 0.5
Residual sum of squares = 0.0273821
Regression sum of squares = 0.628868
Coef of determination, R-squared = 0.958275
Residual mean square, sigma-hat-sq'd = 0.00456369

Figure 10.26. Normality check for FSS friction angle and FSS cohesion of Joe Pool Dam 4%lime+0.30%fibers Treated soil

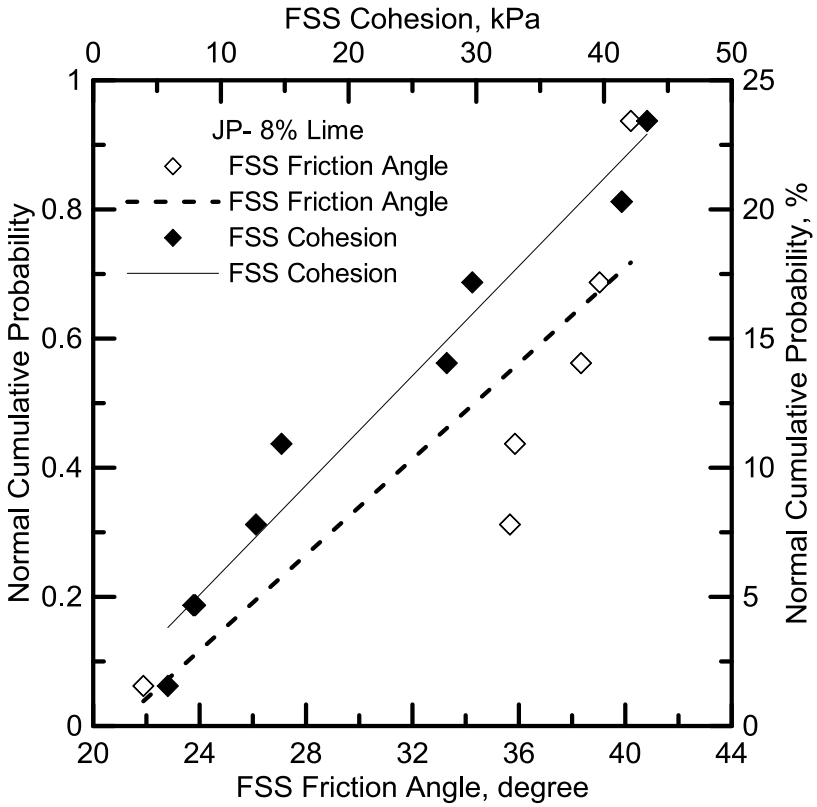

Fit Results

FSS Friction Angle
Equation Y = 0.03707577944 * X - 0.7730073941
Number of data points used = 8
Average X = 34.3353
Average Y = 0.5
Residual sum of squares = 0.143992
Regression sum of squares = 0.512258
Coef of determination, R-squared = 0.780584
Residual mean square, sigma-hat-sq'd = 0.0239987

Fit Results

FSS Cohesion
Equation Y = 0.02036317141 * X + 0.03341776803
Number of data points used = 8
Average X = 22.913
Average Y = 0.5
Residual sum of squares = 0.0273821
Regression sum of squares = 0.628868
Coef of determination, R-squared = 0.958275
Residual mean square, sigma-hat-sq'd = 0.00456369

Figure 10.27. Normality check for FSS friction angle and FSS cohesion of Joe Pool Dam 8%lime Treated soil

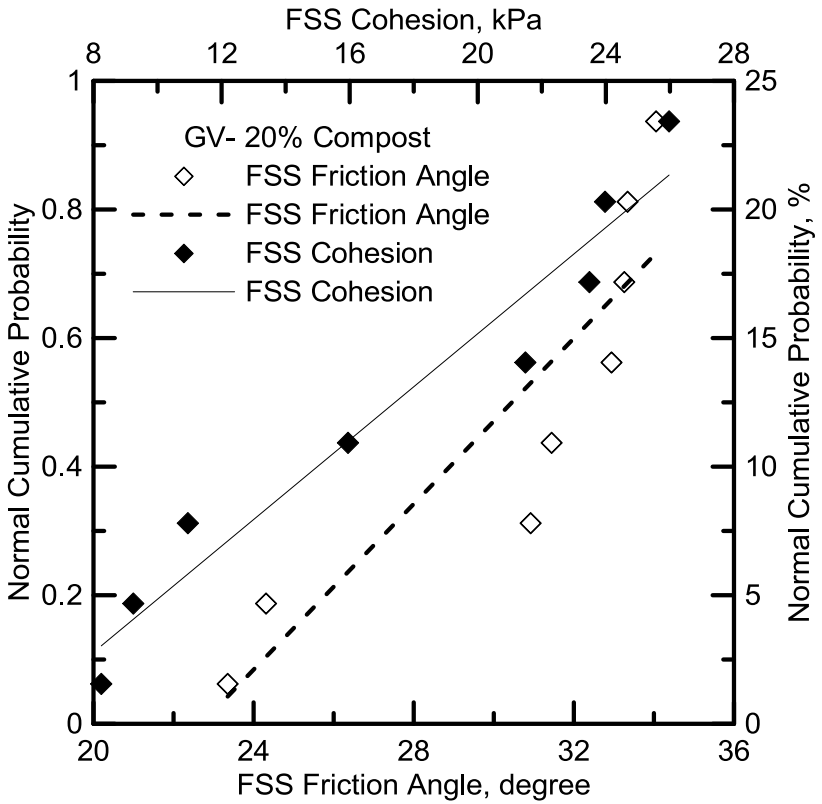

Fit Results

FSS Friction Angle
Equation Y = 0.06442888843 * X - 1.462045616
Number of data points used = 8
Average X = 30.4529
Average Y = 0.5
Residual sum of squares = 0.13846
Regression sum of squares = 0.51779
Coef of determination, R-squared = 0.789014
Residual mean square, sigma-hat-sq'd = 0.0230766

Fit Results

FSS Cohesion
Equation Y = 0.04129996661 * X - 0.2191581142
Number of data points used = 8
Average X = 17.413
Average Y = 0.5
Residual sum of squares = 0.0343713
Regression sum of squares = 0.621879
Coef of determination, R-squared = 0.947625
Residual mean square, sigma-hat-sq'd = 0.00572854

Figure 10.28. Normality check for FSS friction angle and FSS cohesion of Grapevine Dam 20%compost Treated soil

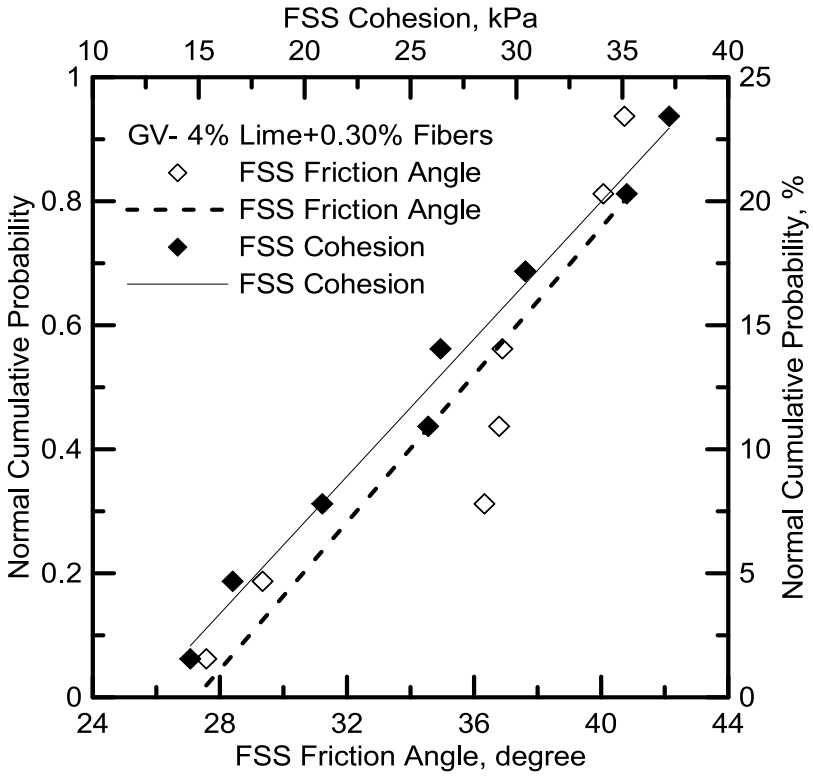

Fit Results

FSS Friction Angle
Equation Y = 0.05940535191 * X - 1.618793939
Number of data points used = 8
Average X = 35.6667
Average Y = 0.5
Residual sum of squares = 0.10044
Regression sum of squares = 0.55581
Coef of determination, R-squared = 0.846948
Residual mean square, sigma-hat-sq'd = 0.01674

Fit Results

FSS Cohesion
Equation Y = 0.03692856685 * X - 0.4561287635
Number of data points used = 8
Average X = 25.8913
Average Y = 0.5
Residual sum of squares = 0.0086554
Regression sum of squares = 0.647595
Coef of determination, R-squared = 0.986811
Residual mean square, sigma-hat-sq'd = 0.00144257

Figure 10.29. Normality check for FSS friction angle and FSS cohesion of Grapevine Dam 4%lime+0.30%fibers Treated soil

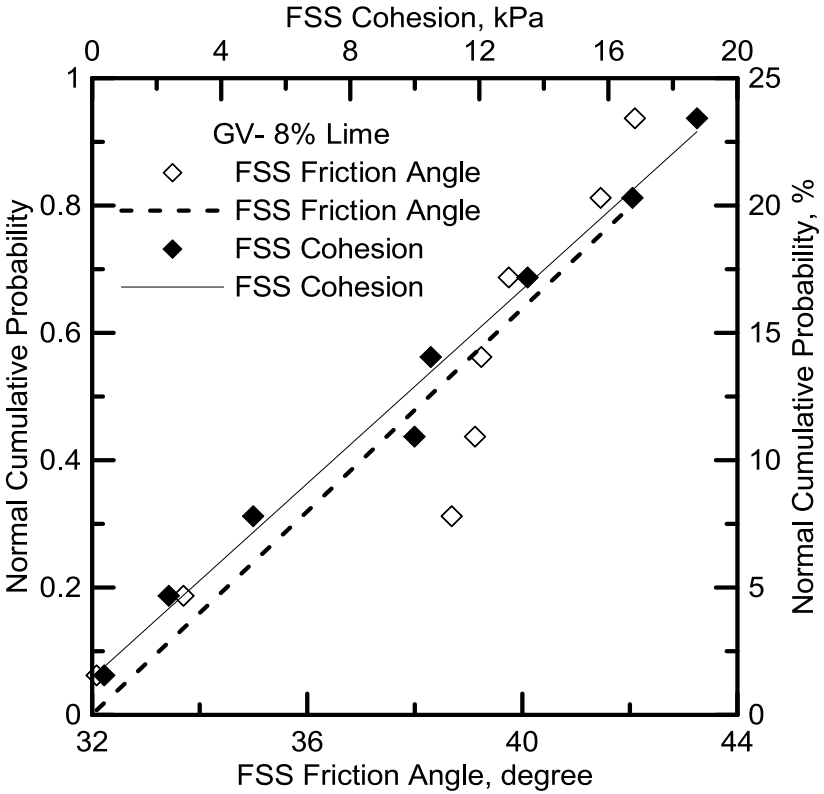

Fit Results

FSS Friction Angle
Equation Y = 0.07969519487 * X - 2.549528085
Number of data points used = 8
Average X = 38.2649
Average Y = 0.5
Residual sum of squares = 0.0975911
Regression sum of squares = 0.558659
Coef of determination, R-squared = 0.85129
Residual mean square, sigma-hat-sq'd = 0.0162652

Fit Results

FSS Cohesion
Equation Y = 0.045745757 * X + 0.05845399768
Number of data points used = 8
Average X = 9.65217
Average Y = 0.5
Residual sum of squares = 0.0086492
Regression sum of squares = 0.647601
Coef of determination, R-squared = 0.98682
Residual mean square, sigma-hat-sq'd = 0.00144153

Figure 10.30. Normality check for FSS friction angle and FSS cohesion of Grapevine Dam 8%lime treated Soil

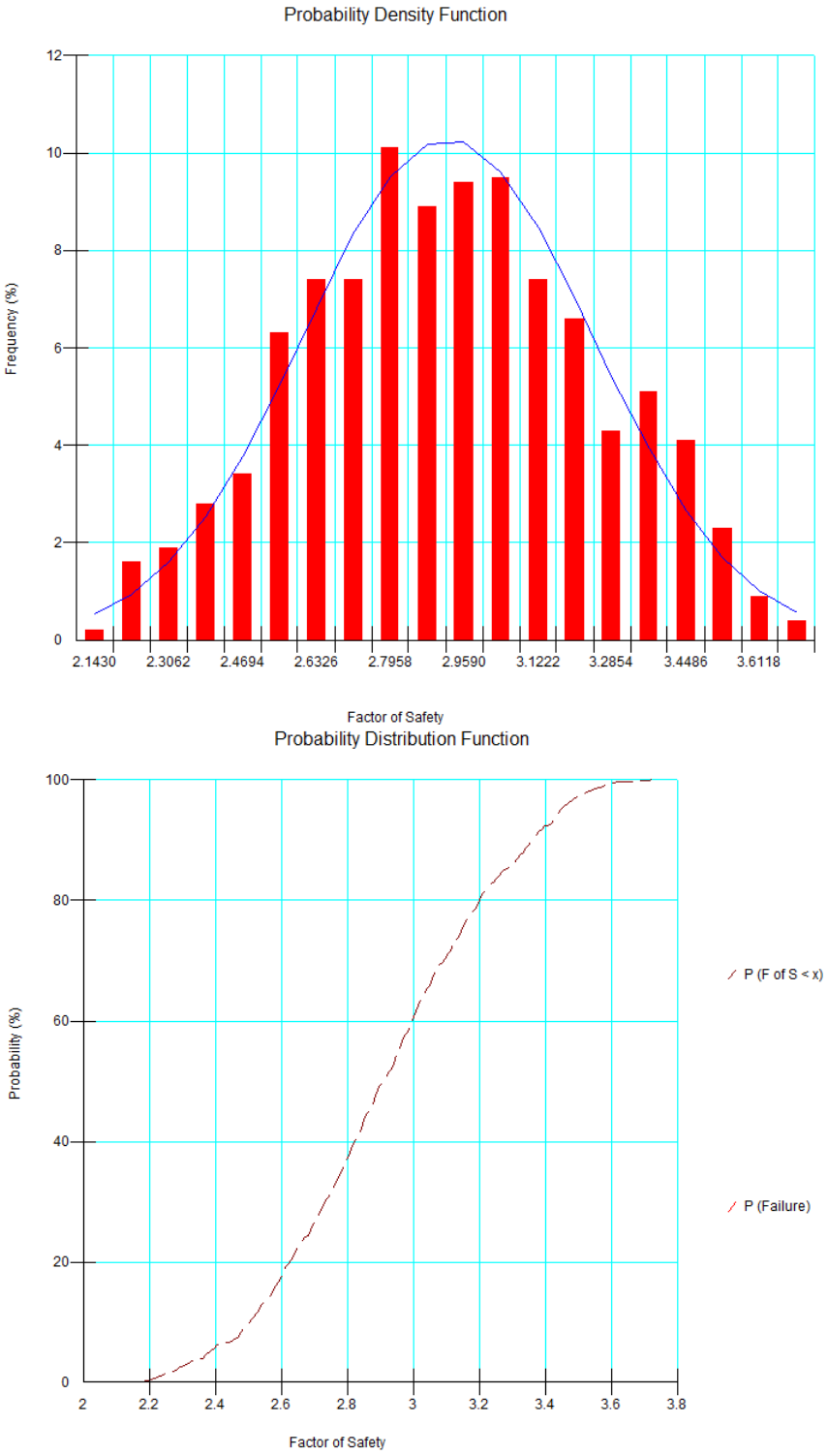

Figure 10.31. Probability Density Function (above) and Probability Distribution Function (below) of FOS for Joe Pool Dam 20%compost Soil (Case 1)

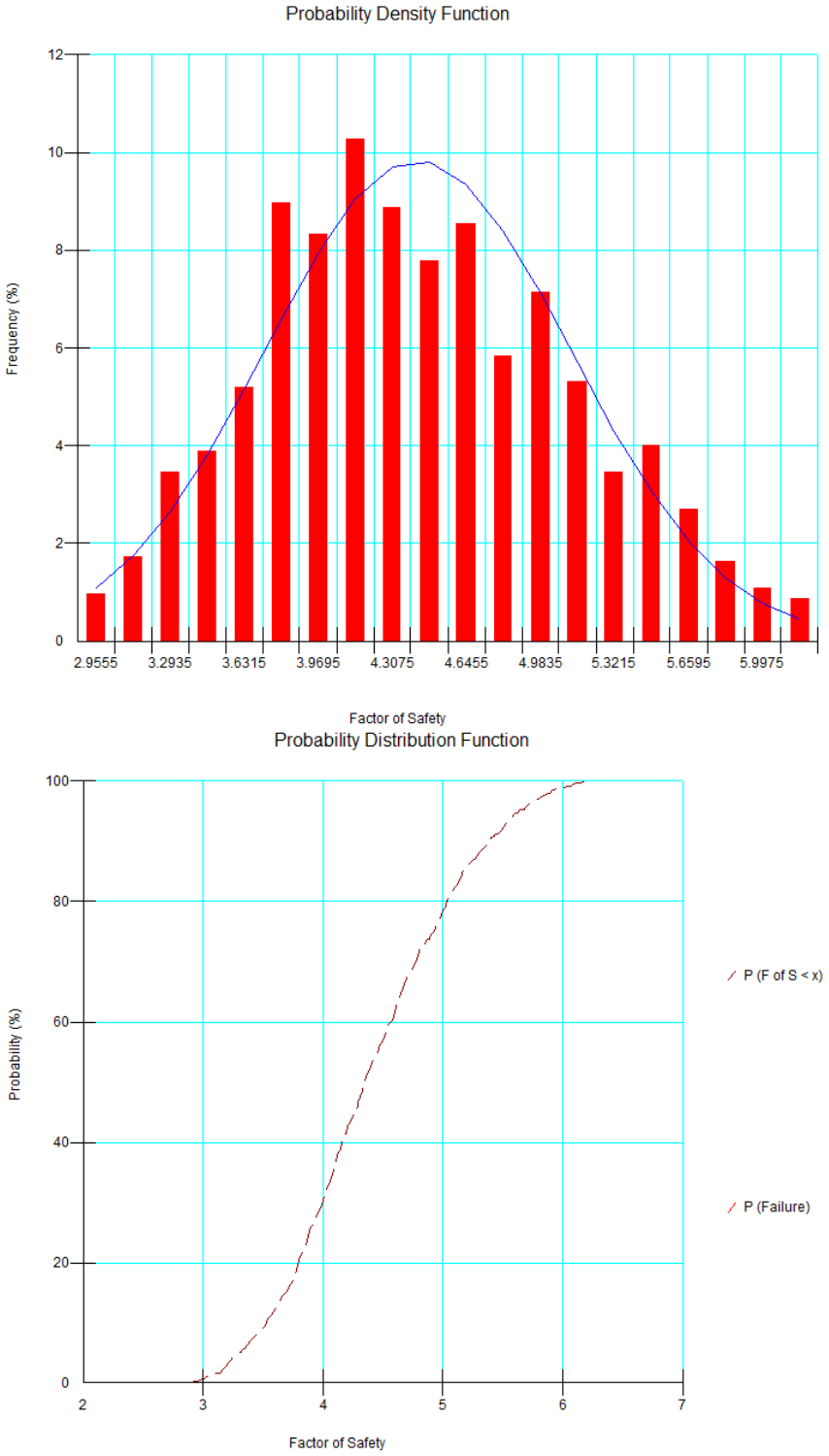

Figure 10.32. Probability Density Function (above) and Probability Distribution Function (below) of FOS for Joe Pool Dam 4%lime+0.30%fibers treated Soil (Case 1)

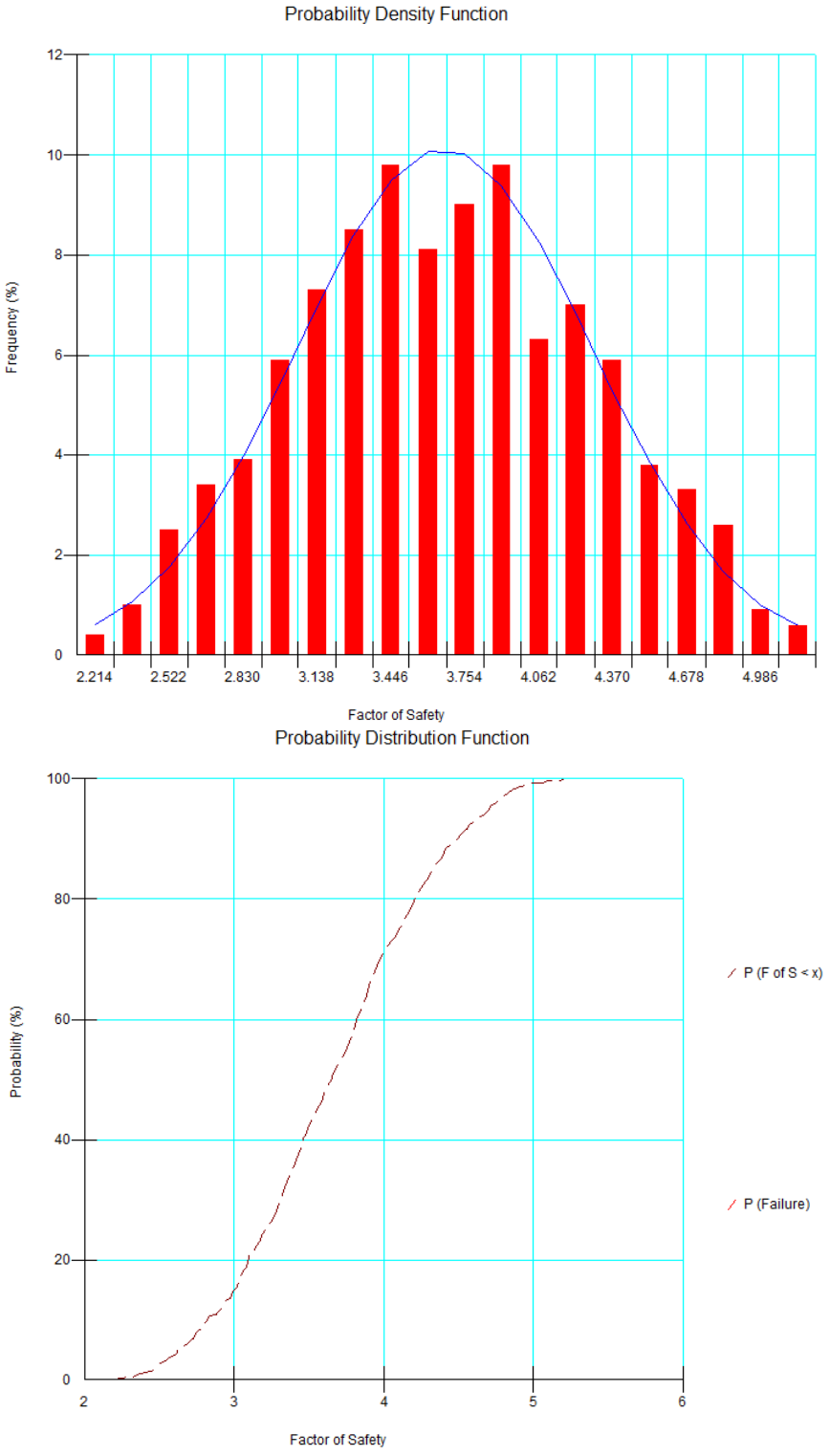

Figure 10.33. Probability Density Function (above) and Probability Distribution Function (below) of FOS for Joe Pool Dam 8%lime treated Soil (Case 1)

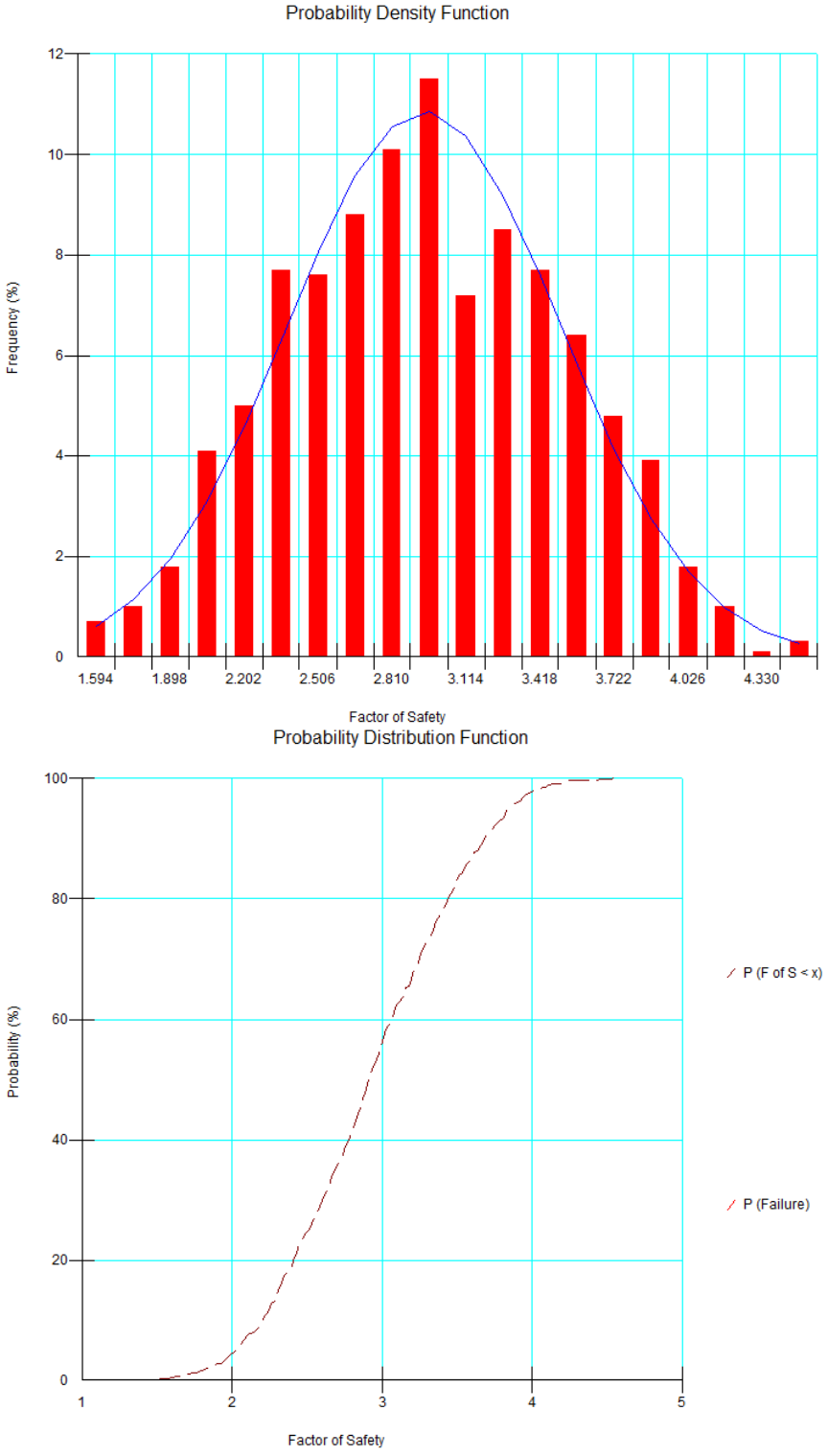

Figure 10.34. Probability Density Function (above) and Probability Distribution Function (below) of FOS for Joe Pool Dam 20%compost treated Soil (Case 2)

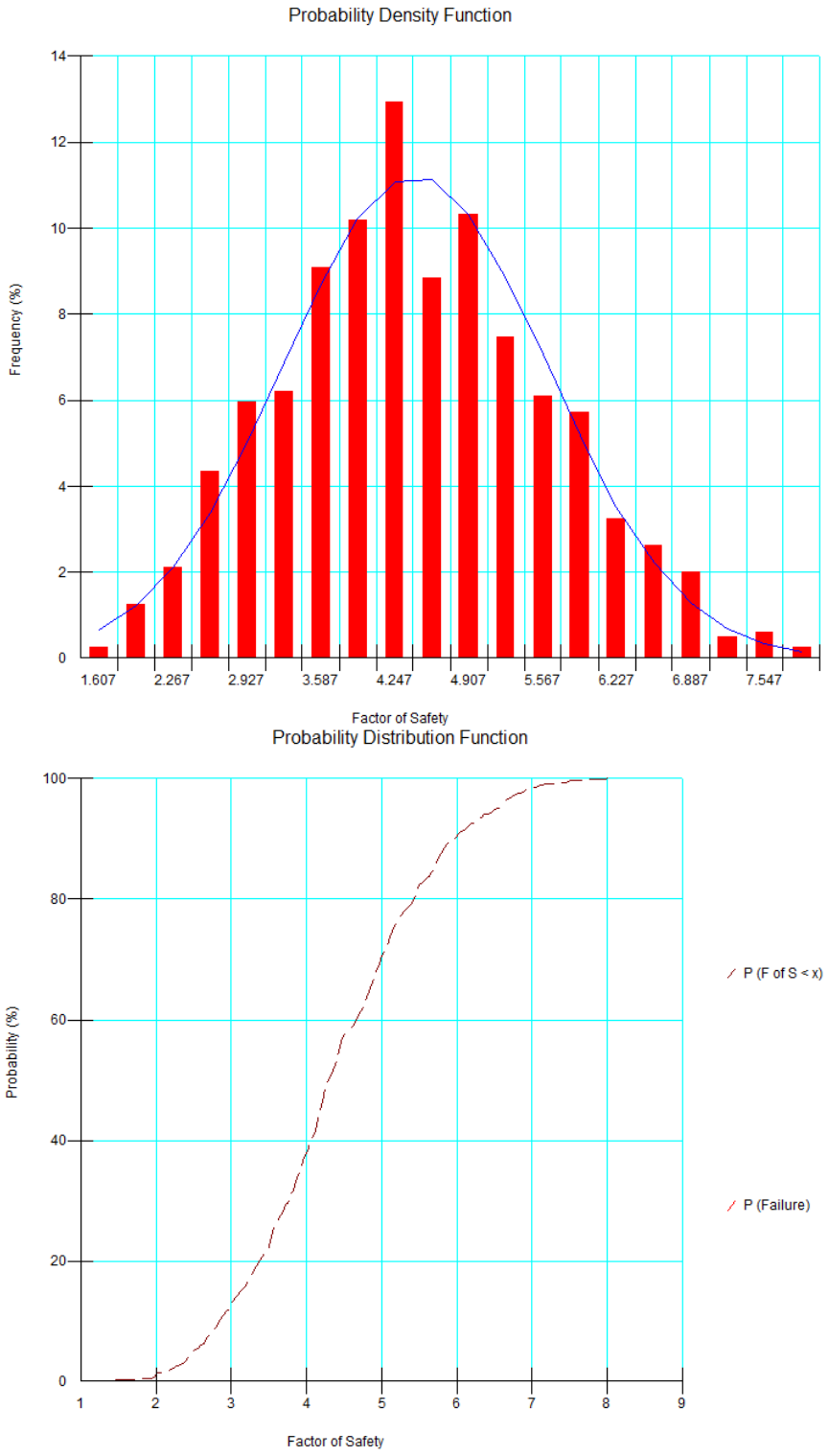

Figure 10.35. Probability Density Function (above) and Probability Distribution Function (below) of FOS for Joe Pool Dam 4%lime+0.30%fibers treated Soil (Case 2)

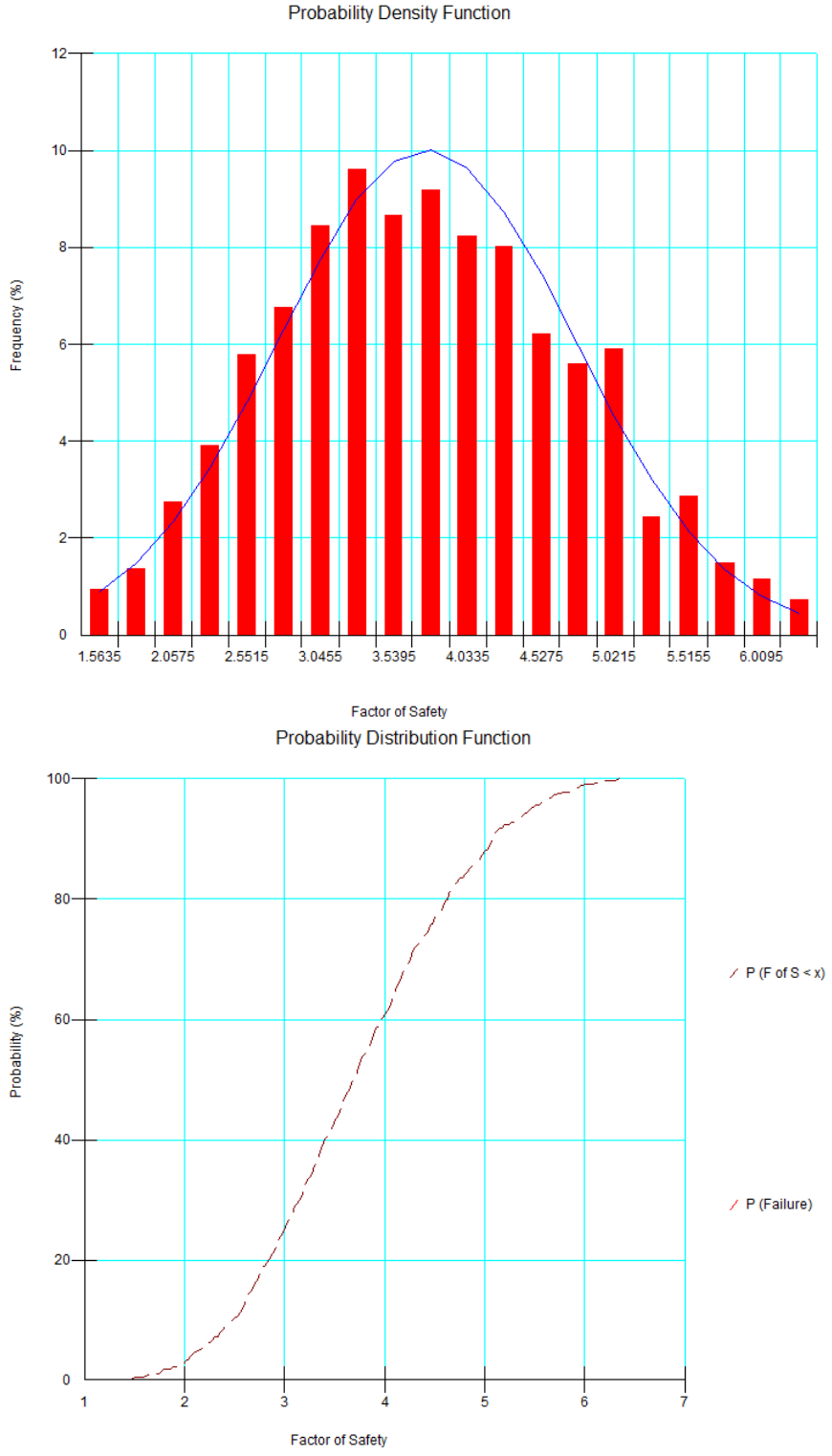

Figure 10.36. Probability Density Function (above) and Probability Distribution Function (below) of FOS for Joe Pool Dam 8%lime treated Soil (Case 2)

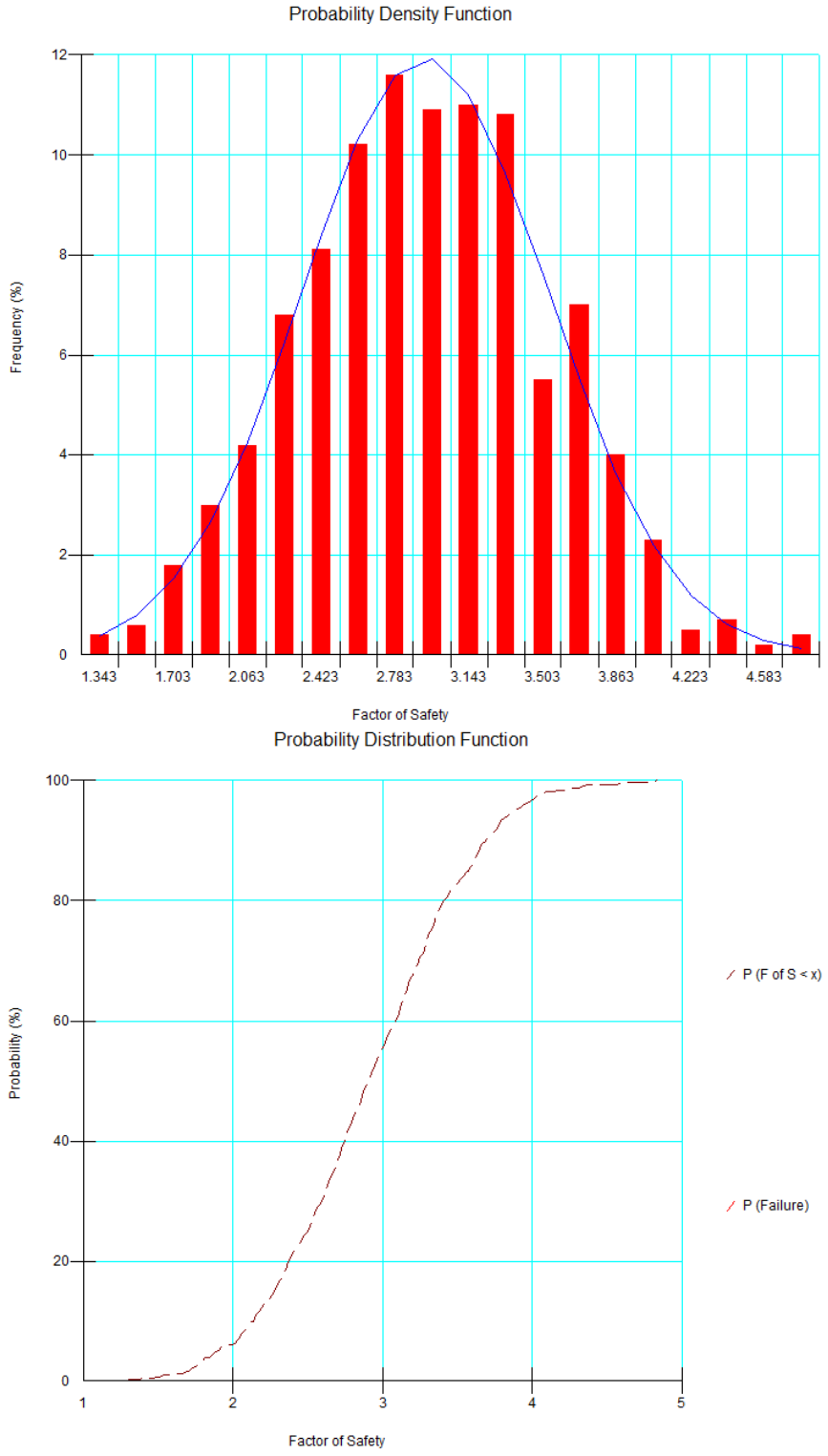

Figure 10.37. Probability Density Function (above) and Probability Distribution Function (below) of FOS for Joe Pool Dam 20%compost treated Soil (Case 3)

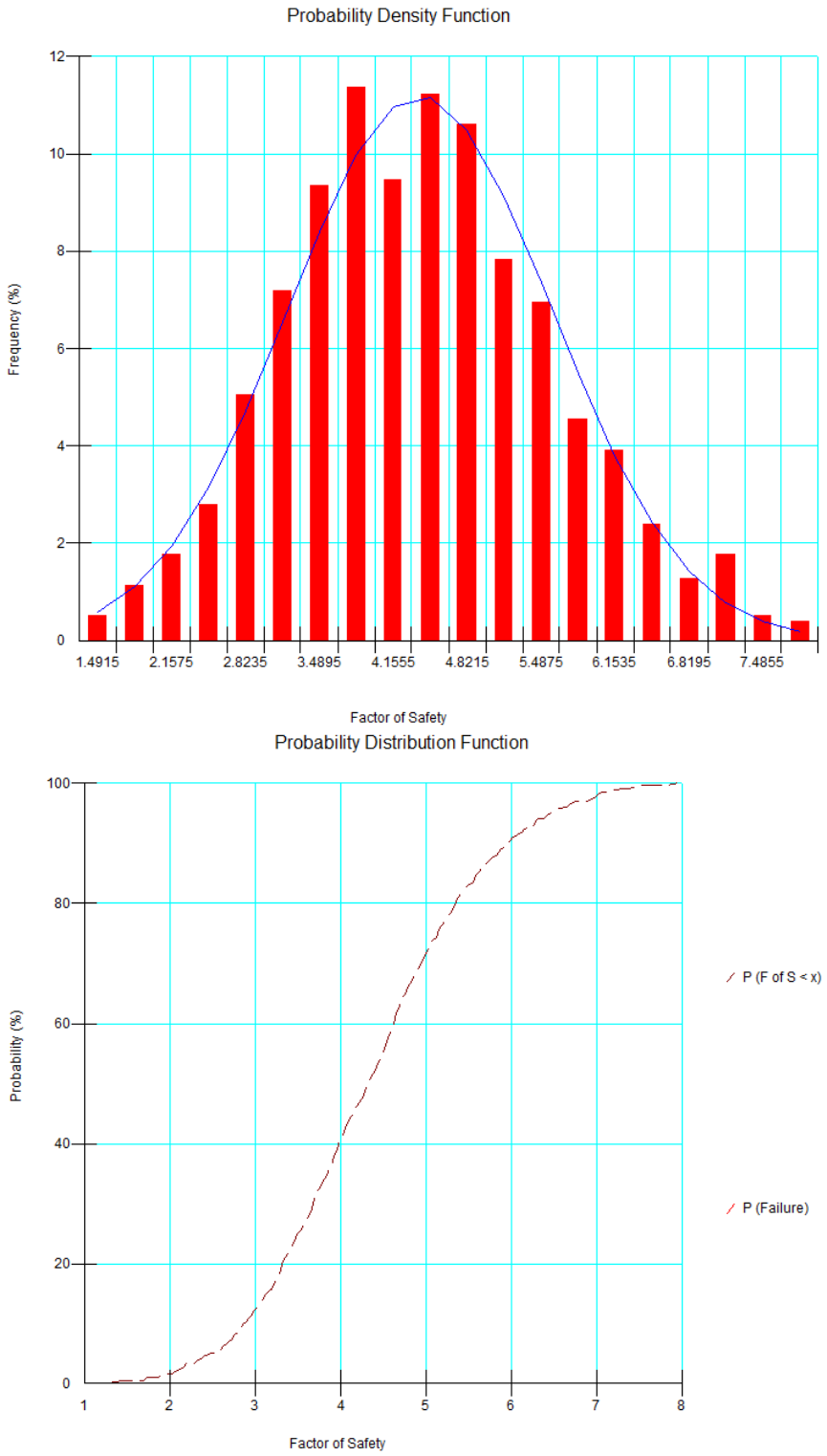

Figure 10.38. Probability Density Function (above) and Probability Distribution Function (below) of FOS for Joe Pool Dam 4%lime+0.30%fibers treated Soil (Case 3)

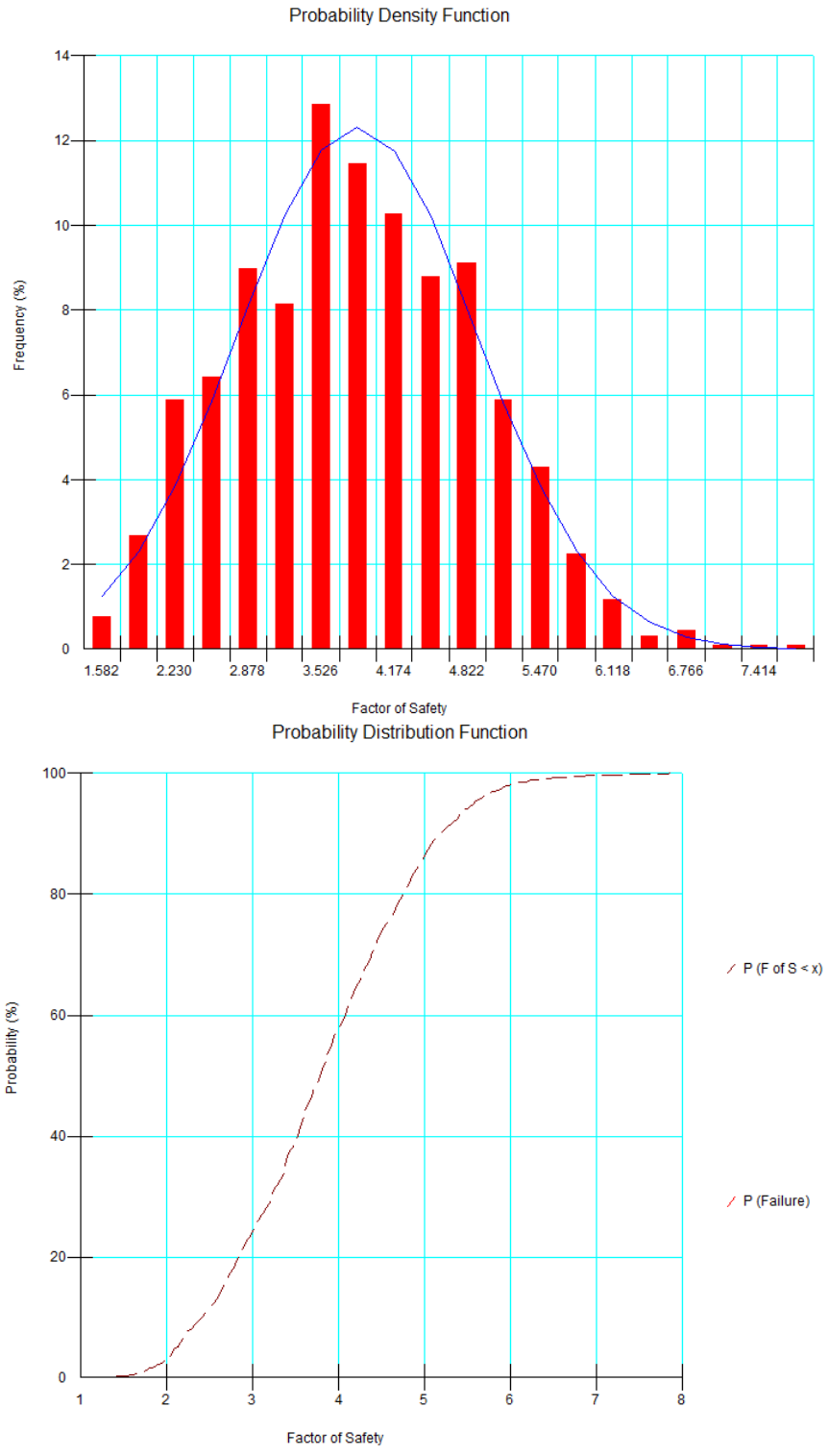

Figure 10.39. Probability Density Function (above) and Probability Distribution Function (below) of FOS for Joe Pool Dam 8%lime treated Soil (Case 3)

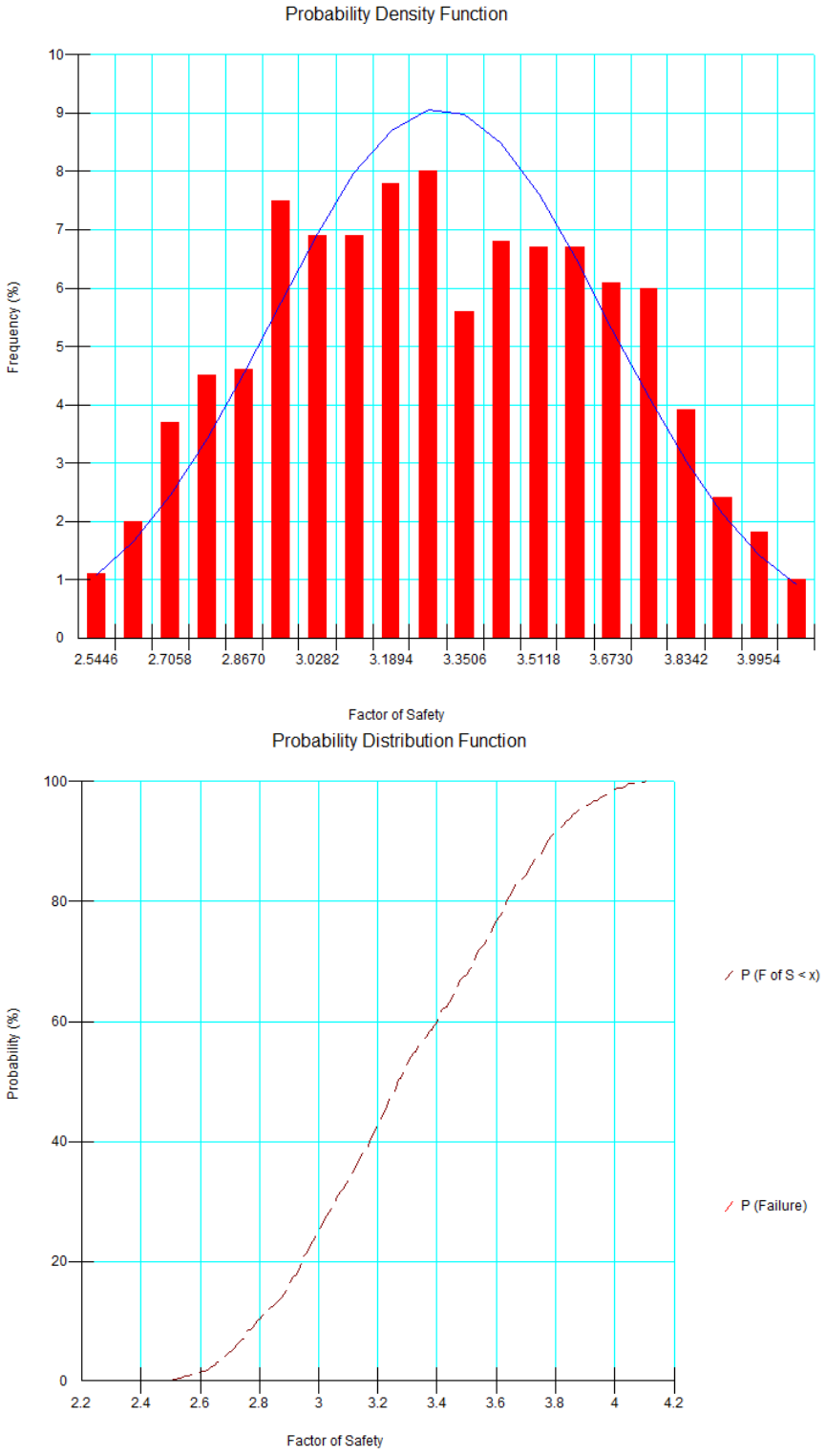

Figure 10.40. Probability Density Function (above) and Probability Distribution Function (below) of FOS for Grapevine Dam 20%compost treated Soil (Case 1)

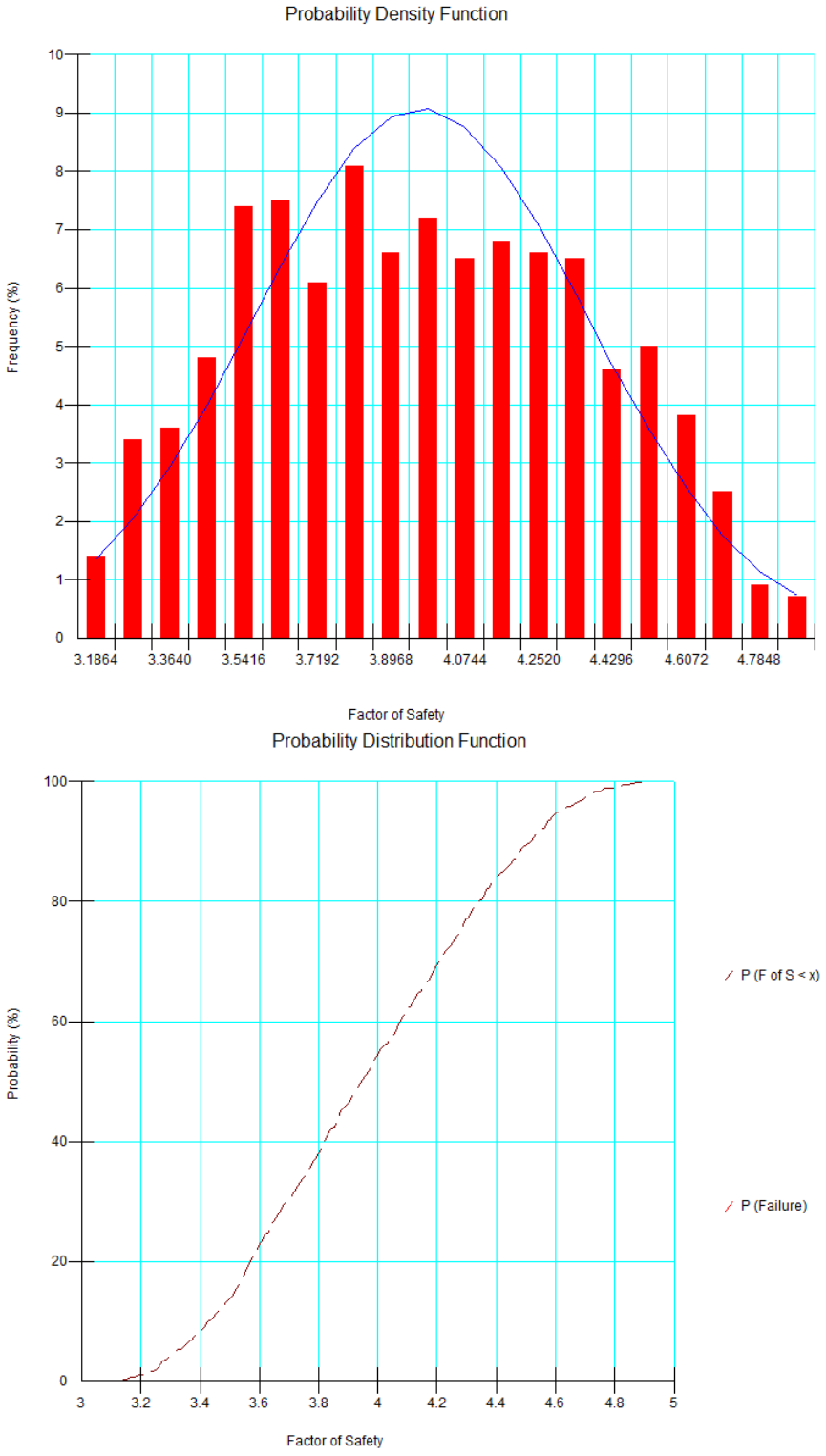

Figure 10.41. Probability Density Function (above) and Probability Distribution Function (below) of FOS for Grapevine Dam 4%lime+0.30%fibers treated Soil (Case 1)

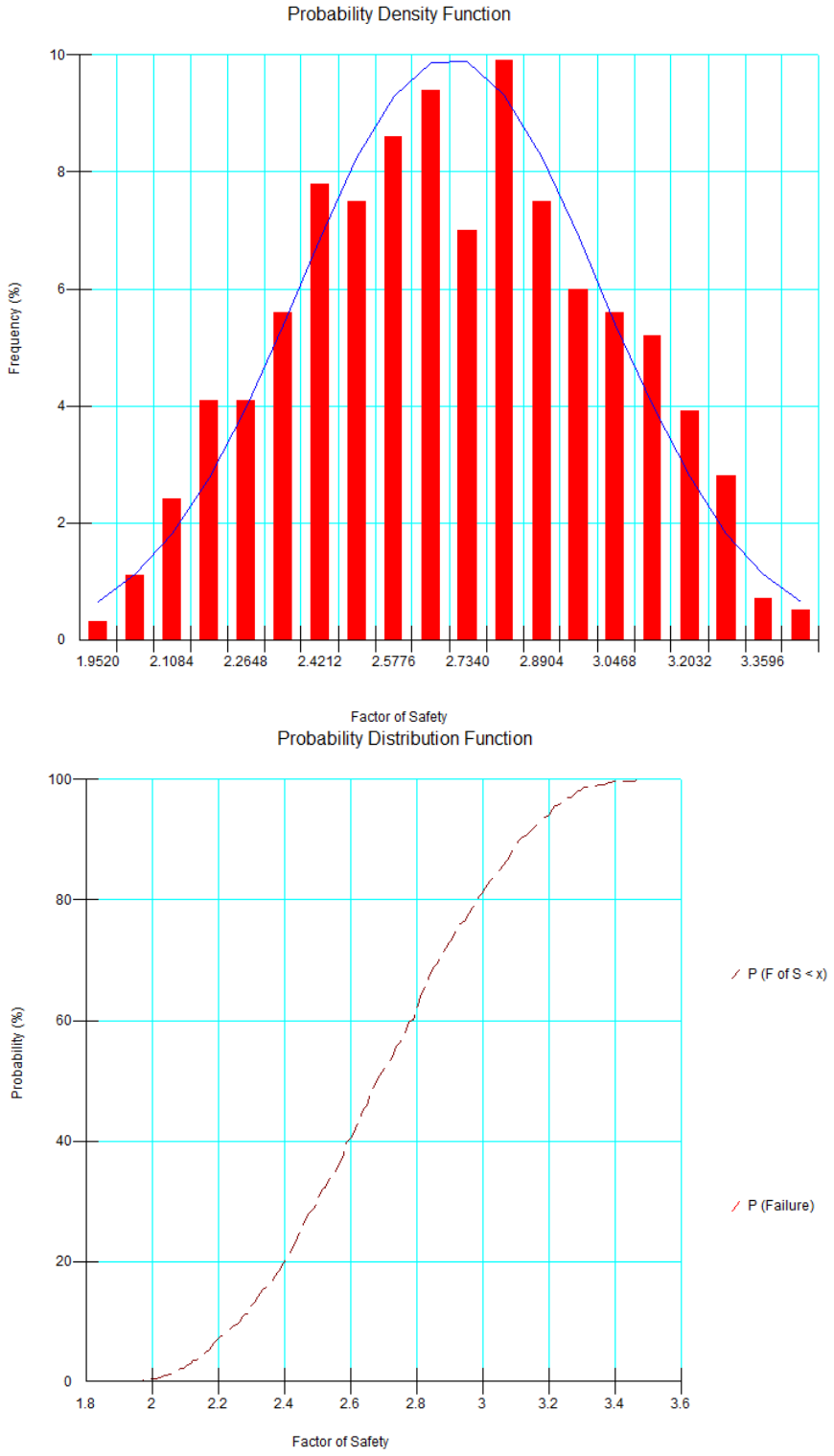

Figure 10.42. Probability Density Function (above) and Probability Distribution Function (below) of FOS for Grapevine Dam 8%lime treated Soil (Case 1)

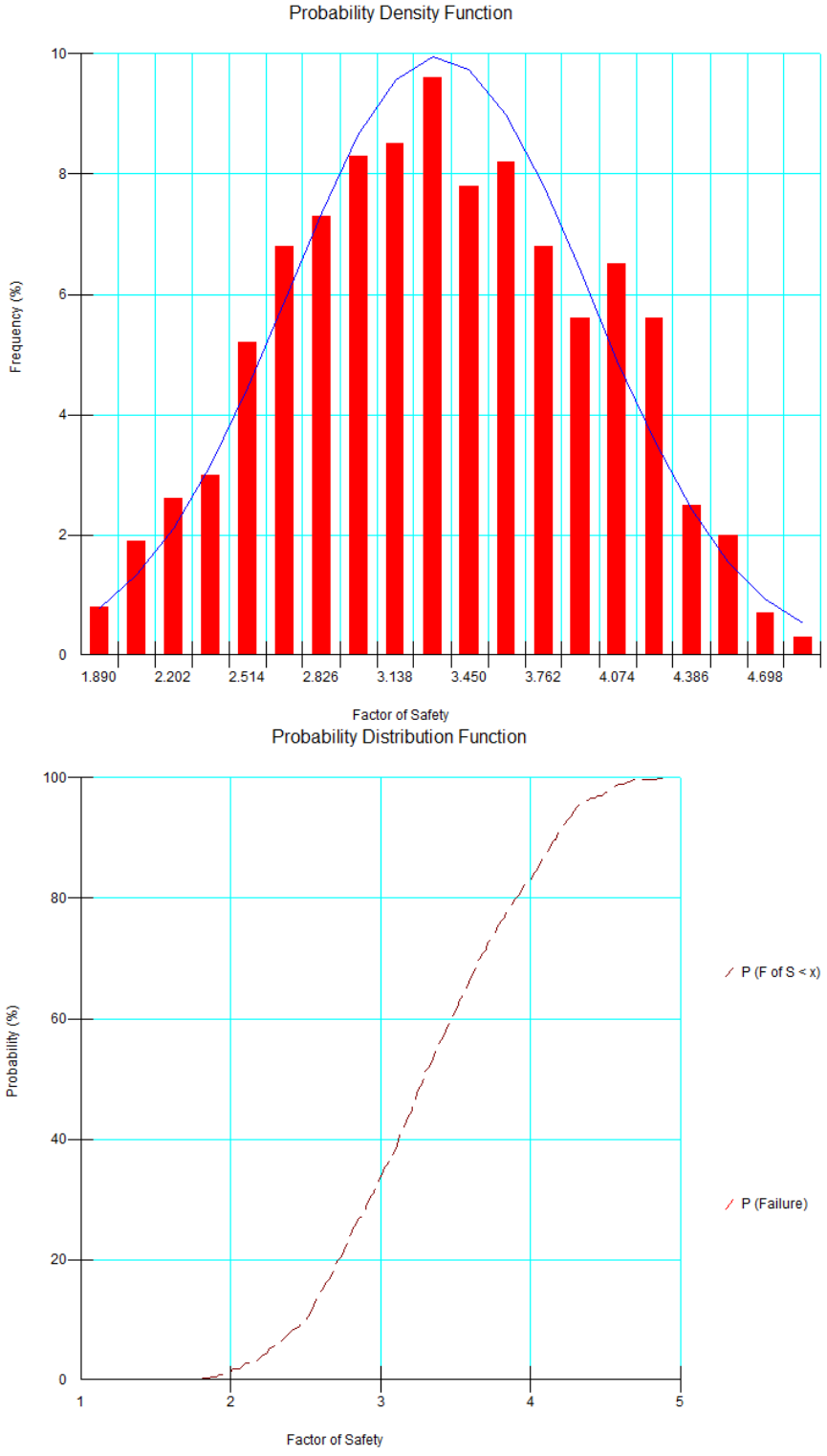

Figure 10.43. Probability Density Function (above) and Probability Distribution Function (below) of FOS for Grapevine Dam 20%compost treated Soil (Case 2)

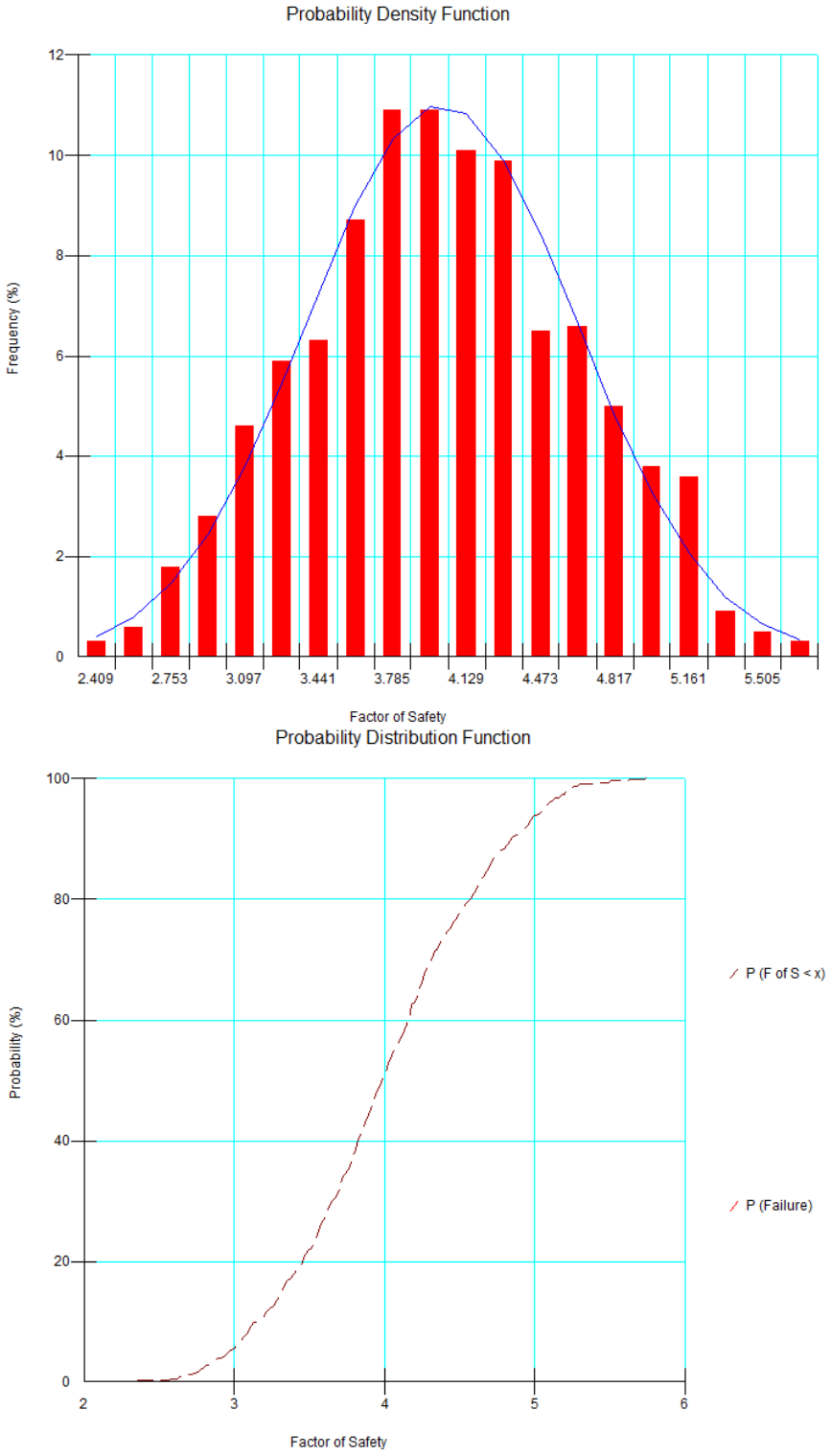

Figure 10.44. Probability Density Function (above) and Probability Distribution Function (below) of FOS for Grapevine Dam 4%lime+0.30%fibers treated Soil (Case 2)

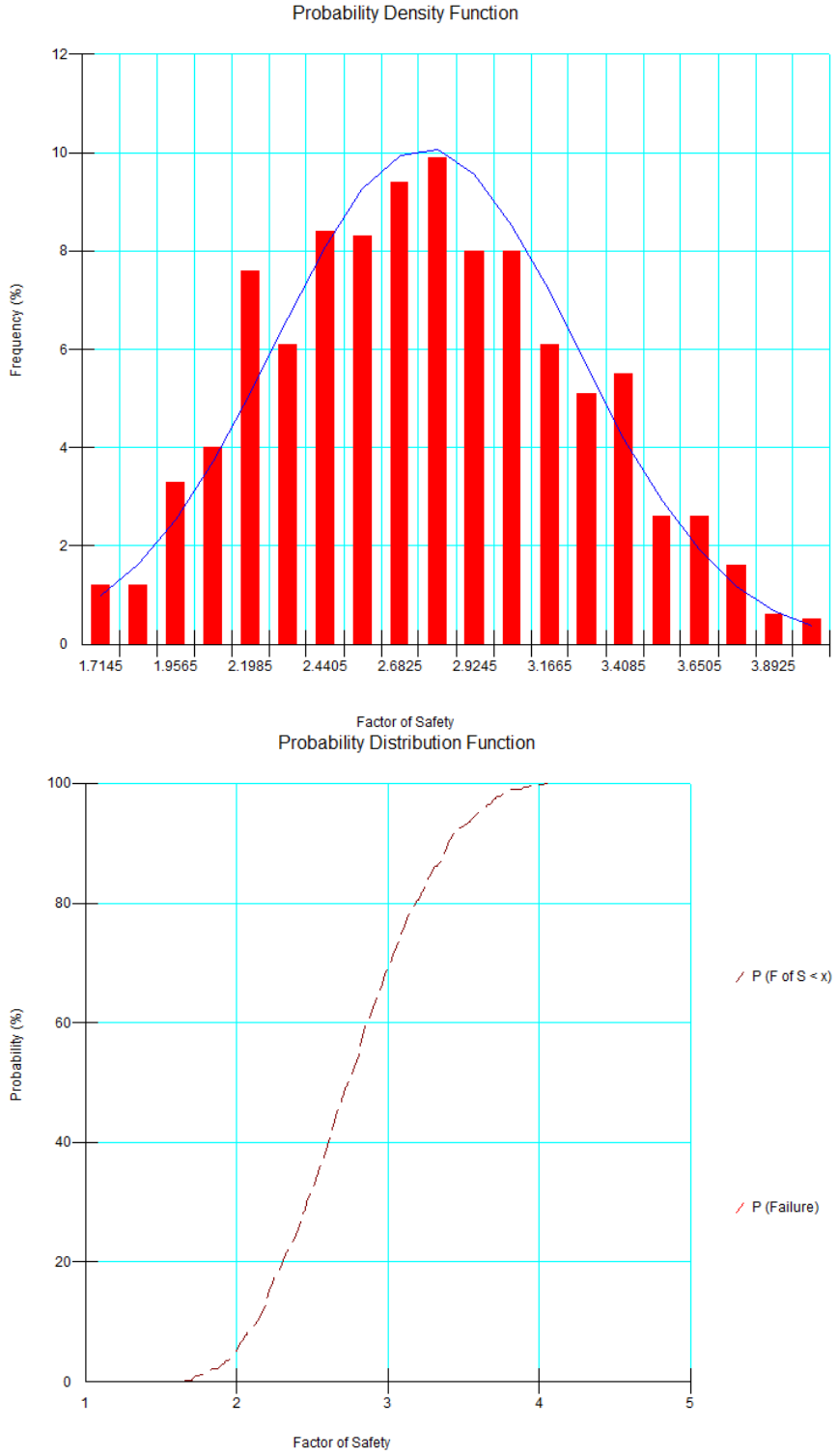

Figure 10.45. Probability Density Function (above) and Probability Distribution Function (below) of FOS for Grapevine Dam 8%lime treated Soil (Case 2)

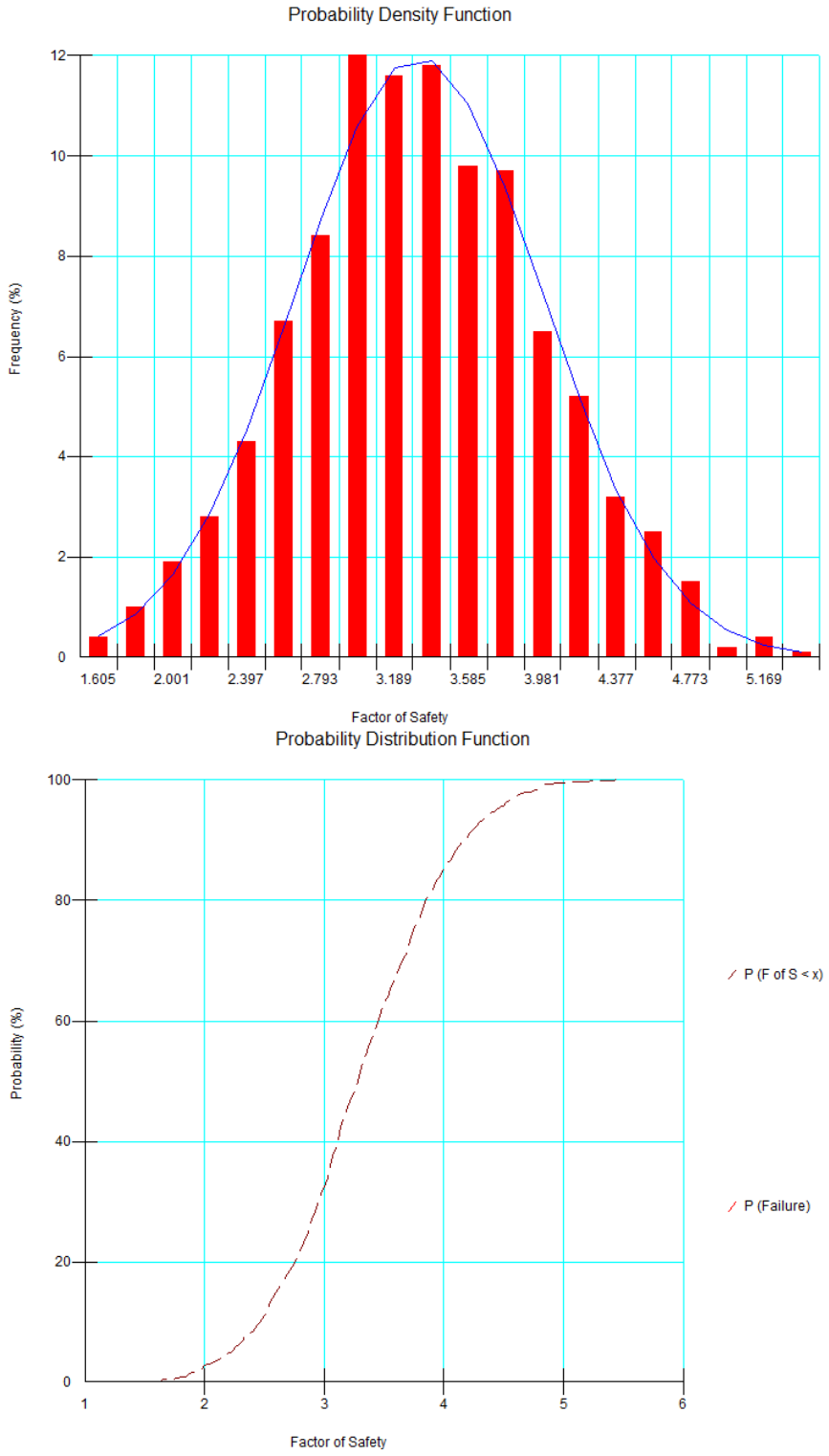

Figure 10.46. Probability Density Function (above) and Probability Distribution Function (below) of FOS for Grapevine Dam 20%compost treated Soil (Case 3)

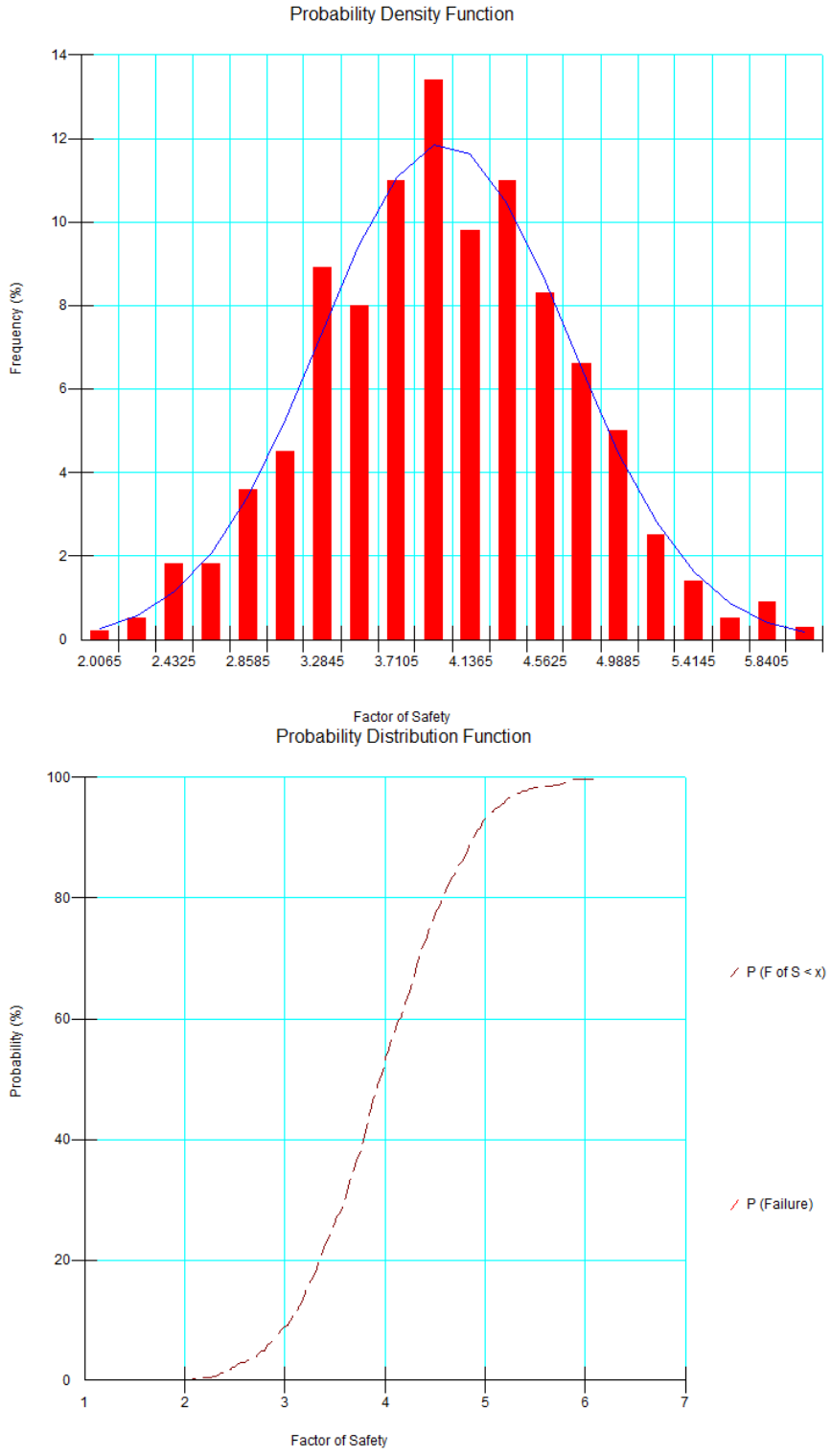

Figure 10.47. Probability Density Function (above) and Probability Distribution Function (below) of FOS for Grapevine Dam 4%lime+0.30%fibers treated Soil (Case 3)

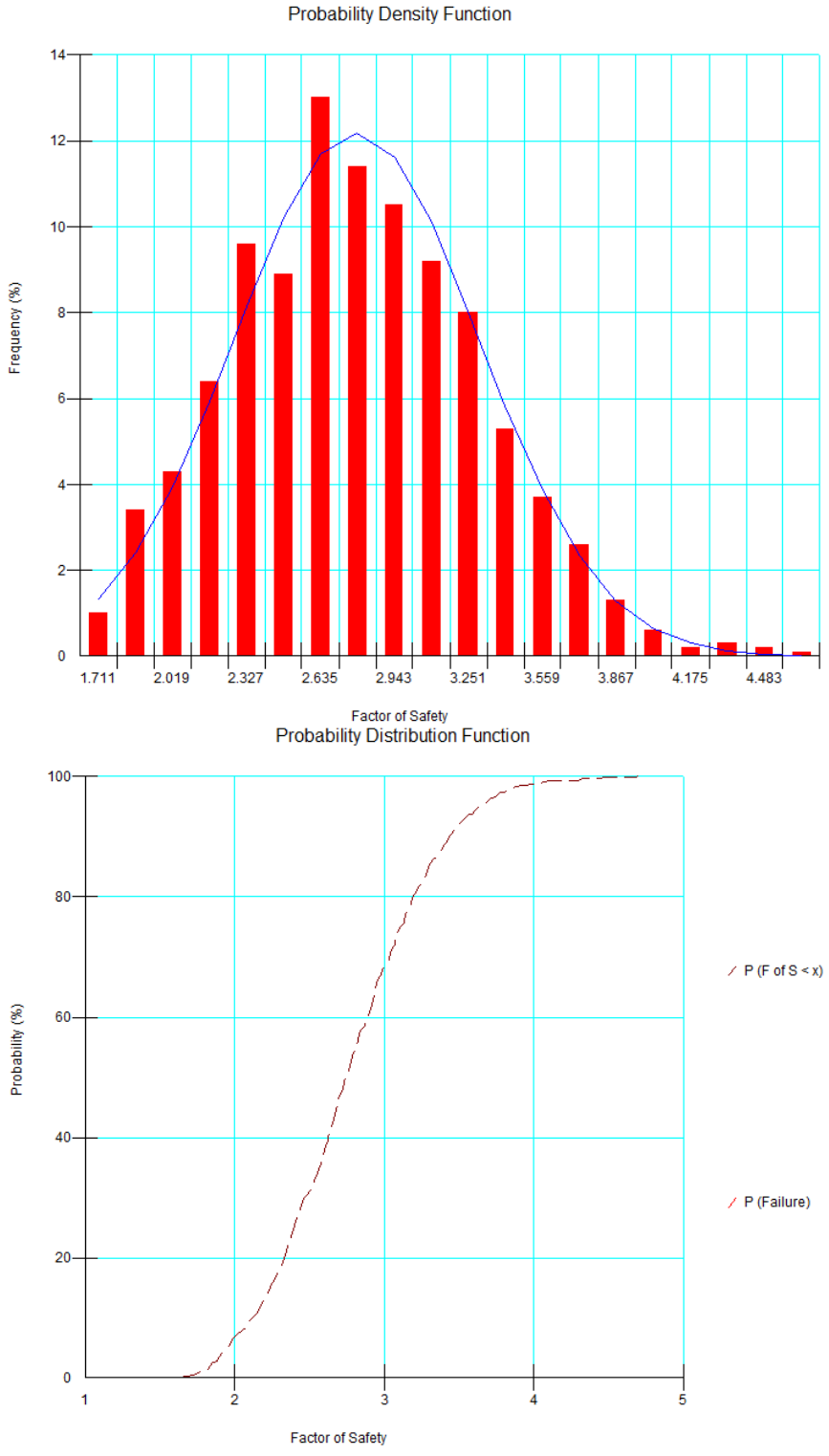

Figure 10.48. Probability Density Function (above) and Probability Distribution Function (below) of FOS for Grapevine Dam 8%lime treated Soil (Case 3)

`

REFERENCES

1. Abramson, L. W., Lee, T. S., Sharma,S., Boyce, G. M. “Slope Stability and Stabilization Methods”, second edition, 1996, 629 pg
2. Ajmera, B., Tiwari, B., Shrestha, D., “Effect of Mineral Composition and Shearing Rates on the Undrained Shear Strength of Expansive Clays”, Geo-Congress conference 2012, San-Francisco, California, 2012.
3. Albataineh, N., “Slope stability analysis using 2D and 3D methods”, The University of Akron, 2006.
4. Allen, J. R. (1982). “Sedimentary Structures: Their Character and Physical Basis Volume II”, Oxford: Elsevier Scientific Publishing Company.
5. Bishop, A.W., 1955. “The use of the slip circle in the stability analysis of slopes”, Geotehnique, 5:7-17.
6. Castellanos, B., Brandon, T.L., Stephens, I., Walshire, L., “Measurement of Fully Softened Shear Strength”, Geo-Congress Conference 2013, San-Diego, California, 2013.
7. Chen, R. H. (1981): “Three-dimensional slope stability analysis,” Joint Highway Research Project, Eng. Experiment station, Purdue University, Report JHRP-81-17.
8. Chen, R. H. and Chameau, J. L. (1983): “Three-dimensional limit equilibrium analysis of slopes,” Geotechnique, Vol. 32, No. 1, pp. 31-40.
9. Cho, S.E. and Lee, S.R. (2002), “Evaluation of Surficial Stability for Homogeneous Slopes Considering Rainfall Characteristics”, Journal of Geotechnical and Geoenvironmental Engineering, Vol. 128: No.9, September 2002, 756-763.
10. Chowdhury, R., Flentje, P. and Bhattacharya, G., “ Geotechnical Slope Analysis”, 2010

`

11. Conduto, D.P. “Foundation Design,” 2nd Edition, Prentice Hall (ADAMS Accession No. ML092040493)
12. Costa, S., Kodikara, J., Thusyanthan, N. I., “Modelling of Desiccation Crack Development in Clay Soils”, The 12th International Conference of International Association for Computer Methods and Advances in Geomechanics (IACMAG) 1-6 October, 2008 Goa, India
13. Dam Safety: Seepage Through Earthen Dams, Division of Soil and Water Resources, Ohio Department of Natural Resources, Fact Sheet 94-31,1994.
14. Day, R. “Foundation Engineering Handbook”, August 12,2010, ISBN-10:0071740090
15. Day, R. and Axten, G. (1989). ”Surficial Stability of Compacted Clay Slopes.” J. Geotech. Engrg., 115(4), 577–580. doi: 10.1061/(ASCE)0733-410(1989)115:4(577)
16. Day, R. W. (1996). “Design and Repair for Surficial Failures, Practice Periodical on Structural Design and Construction”, August 1996, 83-87.
17. Duncan, J.M. 1996. “State of the art: Limit equilibrium and finite element analysis of slopes”. Journal of Geotechnical Engineering. ASCE, **122**(7): 577–596.
18. Duncan, J.M., “Slope Stability Then and Now”, ASCE Geo-Congress conference 2013, San-Diego, California, 2013.
19. Duncan, J.M., Wright, G., “Soil Strength and Slope Stability”, 2005.
20. Evans, D. A. (1972). “Slope stability report”. Slope Stability Committee, Department of Building and Safety, Los Angeles, California, USA.
21. Fredlund, D.G and Krahn, J., “Comparision of slope stability methods of analysis”, 29th Canadian geotechnical Confreence, Vancouver, B.C, October 13-14, 1975.
22. General Design and Construction Considerations for Earth and Rock-Fill Dams, US Army Corps of Engineers.
23. Hovland, H. J. (1977). “Three-dimensional slope stability analysis method.” Journal of the Geotechnical Engineering Division, ASCE, Vol. 103, No. 9, pp. 971-986.

24. Kayyal, M.K and Wright, S.G, “Investigation of Long-Term Strength Properties of Paris and Beaumont Clays in Earth Embankments”, Research Report 1195-2F, Center of Transportation Research, The University of Texas at Austin, November 1991.
25. Krahn, J., “Stability Modeling with SLOPE/W: An engineering Methodology”, First edition, Revision 1, August 2004.
26. Lau, J.T.K, “Desiccation Cracking of Soils”, in partial fulfillment of the requirements for the degree of Master of Science in Civil Engineering, University of Saskatchewan, Saskatoon, Canada.
27. Liang, R.Y., Bodour, W.A., Yamin, M., Joorabchi, A.E., (2010). “Analysis Method for Drilled Shafts Stabilized Slopes using Arching Concept,” The 89th Annual Transportation Research Board Meeting in Washington, DC, 2010.
28. Loehr, E.J. and Bowders, J.J. (2007). “Slope Stabilization using Recycled Plastic Pins – Phase III, Final Report R198-007D”, Prepared by Missouri Transportation Institute and Missouri Department of Transportation, January 2007.
29. McCarthy, F. D. (2002). “Essentials of Soil Mechanics and Foundations”, Sixth Edition, Prentice Hall, Upper Saddle River, New Jersey, USA.
30. McCleskey, L. K Jr. (2005). “Experimental Investigations to Select Stabilization Methods to Mitigate Embankment Desiccation Cracks in order to Reduce Slope Failures.” report presented to University of Texas at Arlington, Texas, USA, in partial fulfillment of the requirements for the degree of Master of Science in Civil and Environmental Engineering.
31. McCook D. K. , “Discussion Of Modeling For Analyses Of Fully Softened Levees”, Innovative Dam and Levee Design and Construction for Sustainable Water Management, 32nd Annual USSD Conference New Orleans, Louisiana, April 23-27, 2012

32. Mesri, G., Shahien, M., " Residual Shear Strength Mobilized in First-Time Slope Failures", Journal of Geotechincal and Geoenvironmental Engineering, Jan 2013
33. Morris, P.H., Graham, J. and Williams, D.J. (1992). "Cracking in drying soils", Canadian Geotechnical Journal, Vol.29, pp.263-277.
34. Nelson, S.A, "Slope stability, Triggering Events, Mass Movement Hazards", EENS 2040, Tulane University, 2011
35. Omidi, G. H., Thomas, J. C., and Brown, K. W. (1996). "Effect of desiccation cracking on the hydraulic conductivity of a compacted clay liner. Water, Air and Soil Pollution", 89: 91-103, 1996.
36. Parra, J. R., Caskey, J.M., Marx, E. and Dennis, N. (2007) "Stabilization of Failing Slopes using Rammed Aggregate Pier Reinforcing Elements", Geo-Denver 2007, GSP 172,Soil Improvement, 1-10.
37. Pradel, D., and Raad, G. (1993). "Effect of Permeability on Surficial Stability of Homogeneous Slopes," Journal of Geotechnical Engineering, ASCE, Vol. 119, No. 2, pp. 315-332.
38. Rahardjo, H., LI, X.W., Toll, D. G. and Leong, E. C., "The effect of antecedent rainfall on slope stability", School of Civil & Structural Engineering, Nanyang Technological University, Singapore (Received 30 January 2001; revised 1 May 2001; accepted 23 May 2001)
39. Rahardjo, H., Lim, T. T., Chang, M. F., and Fredlund, D.G. (1994). "Shear-strength characteristics of a residual soil", Canadian Geotechnical Journal, 32: 60-67.
40. Rahardjo, H., Lim, T. T., Chang, M. F., and Fredlund, D.G. (1994). "Shear-strength characteristics of a residual soil", Canadian Geotechnical Journal, 32: 60-67.
41. Richards, K.S, "Internal Erosion-Potential Failure Modes", Federal Energy Regulatory Commision, Feb 2012.

42. Sadrekarimi, A., Olson, S.M., “A New Ring Shear Device to Measure the Large Displacement Shearing Behavior of Sands”, Geotechnical Testing Journal, Vol. 32, No. 3, 2009.
43. Saleh, A.A, Wright, S.G, “Shear Strength Correlations and Remedial Measure Guidelines for Long-Term Stability of Slopes Constructed of Highly Plastic Clay Soils”, Research Report 1435-2F, The University of Texas at Austin, Oct. 1997.
44. Samtani, N.C., Nowatzki, E.A, “Soils and Foundations”, Reference Manual-Vol.2., NHI Course No. 132012, US Department of Transportation, Federal Highway Administration, December 2006.
45. Short, R. Collins, B.D., Bray, J.D, and Sitar, N., “Testing and Evaluation of Driven Plate Piles in a Full Size Test Slope: A New Method for Stabilizing Shallow Landslides”
46. Skempton, A., and Delory, F., (1957). “Stability of Natural Slopes in London Clay,” Proceedings 4th International Conference on Soil Mechanics and Foundation Engineering, London, England, Butterworths, Vol. 2, pp. 378-381.
47. Skempton, A.W (1977), “Slope stability of cuttings in brown London Clay”, Proc. 9th International Conference on Soil Mechanics and Foundation Engineering, Tokyo, 3, 261-270.
48. Skempton, A.W, 1970, “First-time slides in over-consolidated clays”, Geotechnique, 20 (3) , 320-324
49. Skempton, A.W., 1977, “Slope stability of Cuttings in Brown London Clay”, Proceedings, 9th International Conference on Soil Mechanics and Foundation Engineering, Tokyo, Volume 3, 267-270.
50. Spencer, E., 1973. “The thrust line criterion in embankment stability analysis”, Geotechnique, 23: 85–101.
51. Stark, T.D and Vettel, J.J., “Bromhead Ring Shear Test Procedure”, Geotechnical Testing Journal, March 1992

52. Stephens, T. “Manual on small Earth Dams, A guide to siting, designing and construction”.
53. Stow, D. A. (2005). “Sedimentary Rocks in the Field”, London: Manson Publishing Ltd.
54. Tan, W., Qu, S. and Gao, D.,” Stability Analysis on Highway Slopes in Rainy Region”, Geotechnical Special Publication No.216, ASCE 2011.
55. Tennessee Department of Transportation Earth Retaining Structures Manual
56. Terzaghi,K., Peck, R. B., Mesri, G., “Soil Mechanics in Engineering Practice”, Feb 7, 1996 - 549 pages
57. Titi, H.H. and Helwany, S. , “Investigation of Vertical Members to Resist Surficial Slope Instabilities”, SPR #0092-05-09, Department of Civil Engineering and Mechanics, University of Wisconsin, 2009
58. Towner, G.D. (1987). “The mechanics of cracking of drying clay”, Journal of Agri. Engg. Res., Vol.36, pp.115-124.
59. US Army Corps of Engineers, “Design and Construction Considerations for Earth and Rock-Fill Dams”, EM 1110-2-2300, July 2004.
60. VandenBerge, D.R., Duncan, J.M., Brandon, T.L., “Fully Softened Strength of Natural and Compacted Clays for Slope Stability”, Geo-Congress Conference 2013, San-Diego, California, 2013.
61. Watn, A., Christensen, S., Emdal, A., Nordal,S.” Lime-cement stabilization of slopes-Experiences and a design approach,” Dry Mix Methods for Deep Soil Stabilization, Bredenberg, Holm & Broms (eds) , 1999 Balkema, Rotterdam, ISBN 90 5809 108 2.
62. Whitman, R. V., and Bailey, W. A. (1967). “Use of Computers for Slope Stability Analysis,” Journal of the Soil Mechanics and Foundations Division, ASCE, Vol. 93,No. SM4, pp 475-498
63. Wright, S.G, Evaluation of Soil Shear Strengths for Slope and Retaining Wall Stability Analyses with Emphasis on High Plasticity Clays, FHWA/TX-06/5-1874-

01-1, Center for Transportation Research, The University of Texas at Austin, August 2005

64. Wright, S.G.,Zornberg, J.G, Aguettant, J.E, The Fully Softened Shear Strength of High Plasticity Clays, FHWA/TX-07/0-5202-3, Center for Transportation Research, The University of Texas at Austin, February 2007
65. Zein El Abedine, A. and Robinson, G.H. 1971. " A study on Cracking in some Vetisols of the Sudan: Geoderman, 5, pp. 229-241.

`

BIOGRAPHICAL INFORMATION

Minh Tuan Le was born on 28th May 1984, in Hanoi, Vietnam. After successfully finishing his freshman year at The University of Water Resources in Hanoi, he was awarded a Russian Education Scholarship. He graduated from Saint-Petersburg State Polytechnical University, Saint-Petersburg, Russia in 2008 with a Bachelor's degree in Civil Engineering. He graduated from the same university in 2010 with a Master's degree in geotechnical engineering. He then joined the doctoral program at the Department of Civil Engineering at the University of Texas at Arlington, USA in fall 2010. He performed research under the guidance of Prof. Anand J. Puppala in the area of slope stabilization against surficial failures. He conducted his field and laboratory research on Joe Pool Dam and Grapevine Dam, which are owned and maintained by the United States Army Corps of Engineers. He successfully defended his dissertation in April 2013. During his course of study he submitted several technical papers and reports as author and co-author for domestic and international conferences.